frontiers | Research Topics

IgG4 autoantibodies in the context of IgG4 autoimmunity

Edited by
Inga Koneczny, Vuslat Yilmaz, Maartje G. Huijbers, Erdem Tüzün, Luis Querol and Pilar Martinez

Published in
Frontiers in Immunology

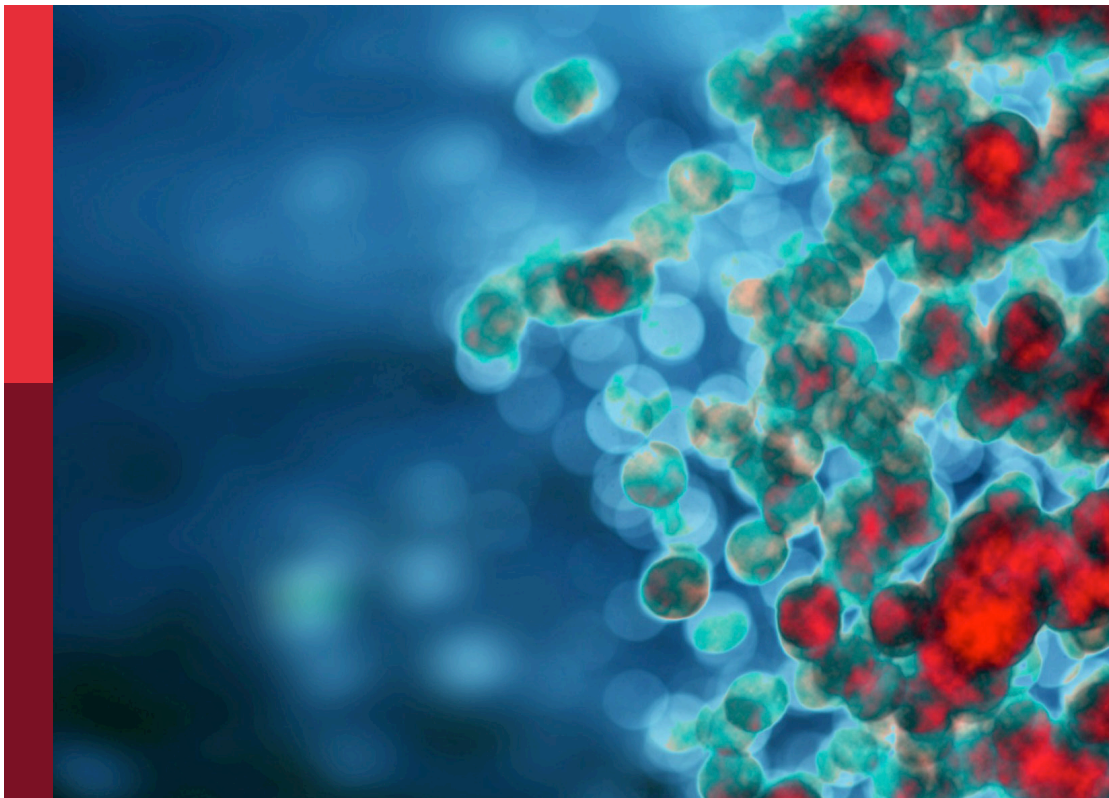

ISSN 1664-8714
ISBN 978-2-8325-5616-0
DOI 10.3389/978-2-8325-5616-0

About Frontiers

Frontiers is more than just an open access publisher of scholarly articles: it is a pioneering approach to the world of academia, radically improving the way scholarly research is managed. The grand vision of Frontiers is a world where all people have an equal opportunity to seek, share and generate knowledge. Frontiers provides immediate and permanent online open access to all its publications, but this alone is not enough to realize our grand goals.

Frontiers journal series

The Frontiers journal series is a multi-tier and interdisciplinary set of open-access, online journals, promising a paradigm shift from the current review, selection and dissemination processes in academic publishing. All Frontiers journals are driven by researchers for researchers; therefore, they constitute a service to the scholarly community. At the same time, the *Frontiers journal series* operates on a revolutionary invention, the tiered publishing system, initially addressing specific communities of scholars, and gradually climbing up to broader public understanding, thus serving the interests of the lay society, too.

Dedication to quality

Each Frontiers article is a landmark of the highest quality, thanks to genuinely collaborative interactions between authors and review editors, who include some of the world's best academicians. Research must be certified by peers before entering a stream of knowledge that may eventually reach the public - and shape society; therefore, Frontiers only applies the most rigorous and unbiased reviews. Frontiers revolutionizes research publishing by freely delivering the most outstanding research, evaluated with no bias from both the academic and social point of view. By applying the most advanced information technologies, Frontiers is catapulting scholarly publishing into a new generation.

What are Frontiers Research Topics?

Frontiers Research Topics are very popular trademarks of the *Frontiers journals series*: they are collections of at least ten articles, all centered on a particular subject. With their unique mix of varied contributions from Original Research to Review Articles, Frontiers Research Topics unify the most influential researchers, the latest key findings and historical advances in a hot research area.

Find out more on how to host your own Frontiers Research Topic or contribute to one as an author by contacting the Frontiers editorial office: frontiersin.org/about/contact

IgG4 autoantibodies in the context of IgG4 autoimmunity

Topic editors

Inga Koneczny — Medical University of Vienna, Austria
Vuslat Yilmaz — Istanbul University, Türkiye
Maartje G. Huijbers — Leiden University Medical Center (LUMC), Netherlands
Erdem Tüzün — Istanbul University, Türkiye
Luis Querol — Hospital de la Santa Creu i Sant Pau, Spain
Pilar Martinez — Maastricht University, Netherlands

Citation

Koneczny, I., Yilmaz, V., Huijbers, M. G., Tüzün, E., Querol, L., Martinez, P., eds. (2024). *IgG4 autoantibodies in the context of IgG4 autoimmunity*. Lausanne: Frontiers Media SA. doi: 10.3389/978-2-8325-5616-0

Table of contents

frontiers in Immunology

REVIEW
published: 24 March 2022
doi: 10.3389/fimmu.2022.834342

IgG4 Autoantibodies in Organ-Specific Autoimmunopathies: Reviewing Class Switching, Antibody-Producing Cells, and Specific Immunotherapies

Inga Koneczny[1], John Tzartos[2,3†], Marina Mané-Damas[4†], Vuslat Yilmaz[5†], Maartje G. Huijbers[6,7], Konstantinos Lazaridis[8], Romana Höftberger[1], Erdem Tüzün[5], Pilar Martinez-Martinez[4], Socrates Tzartos[2,9] and Frank Leypoldt[10]*

[1] Division of Neuropathology and Neurochemistry, Department of Neurology, Medical University of Vienna, Vienna, Austria, [2] Neuroimmunology, Tzartos NeuroDiagnostics, Athens, Greece, [3] 2nd Department of Neurology, "Attikon" University Hospital, School of Medicine, National and Kapodistrian University of Athens, Athens, Greece, [4] Research Group Neuroinflammation and Autoimmunity, Department of Psychiatry and Neuropsychology, Faculty of Health, Medicine and Life Sciences, Maastricht University, Maastricht, Netherlands, [5] Department of Neuroscience, Aziz Sancar Institute of Experimental Medicine, Istanbul University, Istanbul, Turkey, [6] Department of Human Genetics, Leiden University Medical Center, Leiden, Netherlands, [7] Department of Neurology, Leiden University Medical Center, Leiden, Netherlands, [8] Department of Immunology, Laboratory of Immunology, Hellenic Pasteur Institute, Athens, Greece, [9] Department of Neurobiology, Hellenic Pasteur Institute, Athens, Greece, [10] Neuroimmunology, Institute of Clinical Chemistry and Department of Neurology, UKSH Kiel/Lübeck, Kiel University, Kiel, Germany

OPEN ACCESS

Edited by:
Robert Eisenberg, University of Pennsylvania, United States

Reviewed by:
Katrina Louise Randall, Australian National University, Australia
Matteo Gastaldi, Neurological Institute Foundation Casimiro Mondino (IRCCS), Italy

***Correspondence:**
Inga Koneczny
inga.koneczny@meduniwien.ac.at

†These authors have contributed equally to this work

Specialty section:
This article was submitted to B Cell Biology, a section of the journal Frontiers in Immunology

Received: *13 December 2021*
Accepted: *28 February 2022*
Published: *24 March 2022*

Citation:
Koneczny I, Tzartos J, Mané-Damas M, Yilmaz V, Huijbers MG, Lazaridis K, Höftberger R, Tüzün E, Martinez-Martinez P, Tzartos S and Leypoldt F (2022) IgG4 Autoantibodies in Organ-Specific Autoimmunopathies: Reviewing Class Switching, Antibody-Producing Cells, and Specific Immunotherapies. Front. Immunol. 13:834342. doi: 10.3389/fimmu.2022.834342

Organ-specific autoimmunity is often characterized by autoantibodies targeting proteins expressed in the affected tissue. A subgroup of autoimmunopathies has recently emerged that is characterized by predominant autoantibodies of the IgG4 subclass (IgG4-autoimmune diseases; IgG4-AID). This group includes pemphigus vulgaris, thrombotic thrombocytopenic purpura, subtypes of autoimmune encephalitis, inflammatory neuropathies, myasthenia gravis and membranous nephropathy. Although the associated autoantibodies target specific antigens in different organs and thus cause diverse syndromes and diseases, they share surprising similarities in genetic predisposition, disease mechanisms, clinical course and response to therapies. IgG4-AID appear to be distinct from another group of rare immune diseases associated with IgG4, which are the IgG4-related diseases (IgG4-RLD), such as IgG4-related which have distinct clinical and serological properties and are not characterized by antigen-specific IgG4. Importantly, IgG4-AID differ significantly from diseases associated with IgG1 autoantibodies targeting the same organ. This may be due to the unique functional characteristics of IgG4 autoantibodies (e.g. anti-inflammatory and functionally monovalent) that affect how the antibodies cause disease, and the differential response to immunotherapies of the IgG4 producing B cells/plasmablasts. These clinical and pathophysiological clues give important insight in the immunopathogenesis of IgG4-AID. Understanding IgG4 immunobiology is a key step towards the development of novel, IgG4 specific treatments. In this review we therefore summarize current knowledge on

IgG4 regulation, the relevance of class switching in the context of health and disease, describe the cellular mechanisms involved in IgG4 production and provide an overview of treatment responses in IgG4-AID.

Keywords: IgG4 autoimmune disease, MHC, autoimmunity, IL-4, IL-10, Fab-arm exchange, memory B cells

INTRODUCTION

IgG4 autoimmune diseases (IgG4-AID) are an emerging group of autoimmune diseases caused by IgG4 subclass autoantibodies (1, 2). Autoantibodies are key pathogenic players in many autoimmunopathies, and cause disease by a range of different effector mechanisms, such as complement activation, antibody-dependent cellular cytotoxicity or cross-linking and endocytosis of antigen (3). These are pathogenic mechanisms that depend on the antibody Fc region of IgG1-3 subclass antibodies, such as acetylcholine receptor (AChR) antibodies in myasthenia gravis, NMDAR antibodies in autoimmune encephalitis or of antibodies against aquaporin 4 (AQP4) in neuromyelitis optica. These effector functions are not available to the IgG4 subclass which has a structurally distinct Fc region (4, 5). IgG4 is produced in response to prolonged or strong antigen stimulation, and thought to play a role as anti-inflammatory or tolerogenic antibody (discussed in more detail below). Despite IgG4's protective and tolerogenic role, in recent years two groups of rare diseases emerged, in which IgG4 takes the center stage: IgG4-AID that are caused directly by pathogenic IgG4 autoantibodies [such as MuSK myasthenia gravis (6, 7) or pemphigus vulgaris (8, 9), reviewed in more detail here (10)] and IgG4 related diseases [IgG4-RLD, such as IgG4-related pancreatitis (11) or IgG4-related periaortitis/periarteritis (12)]. IgG4-RLD are a rare multiorgan diseases that are characterized by tissue-destructive fibrotic lesions with lymphocyte and IgG4 plasma cell infiltrates and elevated serum IgG4 concentrations (13). Both IgG4-AID and IgG4-RLD are rare diseases of the immune system that may affect different target organs that are nevertheless most likely two unrelated groups of diseases (14). A key difference lies in the role of the IgG4 antibodies: In IgG4-RLD, increased serum concentrations of IgG4 are present in a majority of patients (15), but the antigenic targets of IgG4 and the role of IgG4 antibodies for pathogenicity is unclear [reviewed in detail here (16, 17)]. In contrast, IgG4-AID patients do not show the 10-fold increase in serum IgG4 levels as IgG4-RD patients (14), which otherwise– even though causing diverse symptoms and affecting different organs - all share one common feature: They are associated with antigen-specific, pathogenic IgG4 autoantibodies (1, 10).

Antibodies involved in IgG4-AID, known to date, target antigens in mainly four organ systems: 1) the central and peripheral nervous system with diseases such as MuSK myasthenia gravis (MG), anti-LGI1 and anti-Caspr2 encephalitis, anti-IgLON5 disease or chronic inflammatory demyelinating polyneuropathy (CIDP) with antibodies against NF155/contactin-1/CASPR1, 2) the skin and mucosa with skin blistering diseases such as pemphigus vulgaris (PV) and pemphigus foliaceus (PF), 3) the kidneys with PLA2R- and THSD7A- antibody positive membranous glomerulonephritis and 4) the haematological system with diseases such as thrombotic thrombocytopenic purpura (TTP, ADAMTS13) or GPIHBP1 autoantibody syndrome. Other unifying features of IgG4-AID are their low prevalence (10), their emerging strong genetic associations with specific HLA alleles such as HLA-DQB1*05 and HLA-DRB1*14 (18, 19), their clinical severity and chronicity and their good response to B cell depletion therapy.

How can the disease-overarching association of these common features be explained and which commonalities can we identify in the immune cells involved in the production of pathogenic IgG4 autoantibodies (2, 20)?

IgG4-ISOTYPE ANTIBODIES: THE FRIENDLY VILLAIN?

IgG is the main antibody class in the human body, with serum concentrations of 7-15g/L. However, the four IgG subclasses are numbered in descending order of their frequency, making IgG4 with an average of 5% (0.35-0.51g/L) of total IgG the rarest IgG subclass (21–23). Notably, IgG4 concentrations vary considerably between healthy individuals and throughout life (24), and may range from 0.01g/L to 1.4g/L (25), but may exceed these ranges in inflammatory conditions such as helminth infection to extreme levels such as 9g/L (26).

Normally IgG4 is produced after chronic exposure to antigen (27–31) or a strong antigenic stimulus such as in allergen immunotherapy (29–32), and it is usually induced by a class switch from IgE (or other antibody classes/subclasses) towards IgG4. IgG4 then competes with antibodies of other classes and subclasses for the antigen, and blocks the epitope so that the effector function of the competing antibody is abolished (30–38). Experiments using IgG4 derived from hyper-immune beekeepers show that it is protective in bee venom allergy patients (28, 39) and mice exposed to lethal africanised honey bee venom (40). IgG4 antibodies against the AChR protected experimental animals in a passive transfer model from the pathogenic effects of IgG1 antibodies against the AChR (20).

The four IgG subclasses share over 90% sequence homology, but single amino acid differences in IgG4 affect its structure and function substantially. IgG4 has anti-inflammatory properties (**Figure 1**), as it does not activate the complement system or engage activating Fcγ receptors on immune cells. A single amino acid difference in the hinge leads to increased stereometric flexibility and allows – under reducing conditions- the formation of intrachain disulphide bridges instead of

interchain disulphide bridges, which leads to a loss of covalent connection of the two antibody half-molecules (41–43). This allows for a dissociation of IgG4 into two half-molecules that may then recombine randomly with IgG4 half-molecules of other specificities, and generate bi-specific functionally monovalent antibodies. This process is termed "Fab-arm exchange" (20, 44–50). Fab-arm exchange and bi-specificity were also observed in IgG4 autoantibodies against MuSK (50, 51). Functionally monovalent antibodies cannot cross-link antigen and induce antibody-induced antigen-internalization (**Figure 1**). Furthermore antigen-antibody immune complexes cannot be formed (20, 52, 53). Single amino acid differences in the CH2 region also render IgG4 immunologically inert: 1) a serine instead of a proline at position 331 (P331S) prevents binding of C1q and activation of the classical complement pathway (54, 55), while 2) further differences in the CH2 (L234F, P331S, A327G) reduce IgG4 binding to activating Fcγ receptors, which prevents activation of immune cells (56–61).

Therefore, IgG4 autoantibodies do not hold classical effector functions such as complement- or immune cell- mediated tissue damage. Rather they exert their effects by direct steric interference with their target antigens. Since they are unable to form immune complexes, this interaction would be beneficial in situation where non pathogenic antigen needs to be cleared and eliminated without causing overt inflammation. However, in the setting of autoimmunity, this mechanism has the potential to act as pharmacological antagonism at its target antigen. Increasing antibody concentrations will increasingly compete with physiological interaction of the targeted protein with its partners. And indeed, this has been found to be the main effect in many IgG4-AID such as MuSK-MG, pemphigus vulgaris or anti-LGI1 encephalitis (62–67). For example, antibodies to MuSK interrupt a signal transduction pathway required for the functioning of the neuromuscular junction, therefore causing muscle weakness in patients with MuSK-MG (62, 63), antibodies against desmoglein 1 and/or 3 lead to loss of cell adhesion between keratinocytes, therefore causing blistering of the skin in pemphigus patients (65, 68, 69), and inhibitory antibodies against the protease ADAMTS13 lead to an accumulation of multimeric von Willebrand factor and vascular occlusion in patients with TTP (70–72).

The autoantibody isotype and subclass is thus a critical factor in the pathomechanism of antibody-mediated autoimmunity. Yet it remains a crucial question, why IgG4 subclass autoantibodies are produced in the first place. What causes B-cells to undergo class-switching towards IgG4 and which cells are involved in its production?

B CELLS IN IgG4-AID: THE GUN THAT SHOOTS THE BULLETS

B cells are the antibody-producing cells of the adaptive immune system and are responsible for humoral immunity. B cells are also powerful antigen presenting cells and provide critical costimulatory signals to T cells. Naive B cells can develop into distinct cytokine-producing subsets that influence CD4+ T cell responses. Various cytokine-producing B cell subsets (TNF-α, CCL3, IFN-γ, GM-CSF, IL-6, IL-17, IL-2) have now been identified to modulate the polarization of CD4+ T cell responses *in vivo* (73, 74).

During isotype switching, which is required for the formation of immunoglobulin subtypes, T helper cells stimulate the progeny of IgM– and IgD–expressing B lymphocytes to produce antibodies of different heavy-chain isotypes. Heavy chain isotype switching is induced by a combination of CD40L-mediated signals and cytokines. These signals act on antigen stimulated B cells and induce switching in some of the progeny of these cells. In the absence of CD40 or CD40L, B cells secrete only IgM and fail to switch to other isotypes, indicating the essential role of this ligand-receptor pair in isotype switching. Activated B cells in germinal centers may differentiate into long-lived plasma cells or memory cells. The antibody-secreting cells, called plasmablasts, enter the circulation and migrate to the bone marrow or mucosal tissues, where they may survive for years as plasma cells and continue to produce high-affinity antibodies, even after the antigen is eliminated (75, 76). In anti-LGI1-encephalitis, cloning of recombinant human antibodies from the CSF of three patients indeed showed that 84% of all antibody-secreting cells and 21% of memory B cells did produce LGI1-specific antibodies (77).

Considering the substantial progress in B cell targeting therapy approaches in recent years, understanding the role of effector B cells and B cell dysregulation in subgroup specific differences of IgG4-AID is crucial. Although the proportion of B cells in the peripheral blood is not altered, memory B cells are increased in both AChR- and MuSK-MG patients (78). Notably, immunosuppressive treatment appears to reduce regulatory B cell subsets and increase memory B cell proportions in the peripheral blood (78–80). CD40 or TLR9-mediated IL-10 production of isolated B cells is reduced in MuSK-MG, suggesting suppressed regulatory B cell functions (78). Rituximab, a monoclonal anti-CD20 antibody, is highly effective in treatment of MuSK-MG and PV and appears to show its beneficial effects, at least partially, through repopulation of diminished IL-10 producing B cells (81). Although rituximab is also successfully used in other IgG1-3-AIDs, the general consensus is that IgG4-AIDs seem particularly sensitive and more often remain in long term remission (82–90). In a recent study, treatment with a low dose of teriflunomide was shown to ameliorate muscle weakness in the mouse model of MuSK-MG, predominantly through suppression of memory B cells in the lymph nodes without significantly reducing effector T cell populations (80). MuSK-MG patients also exhibit defective IL-6 production after B cell stimulation (78). This may be a compensating counter-measure to regulate autoantibody production, since IL-6 is involved in IgG class-switching (91).

The importance of B cells has been shown in other IgG4-AID as well. In great likeness to MuSK-MG, PV patients show increased memory B cell pools and impaired regulatory B cell functions. Treatment induced amelioration of PV symptoms is associated with reduction of memory B cells and enhancement of

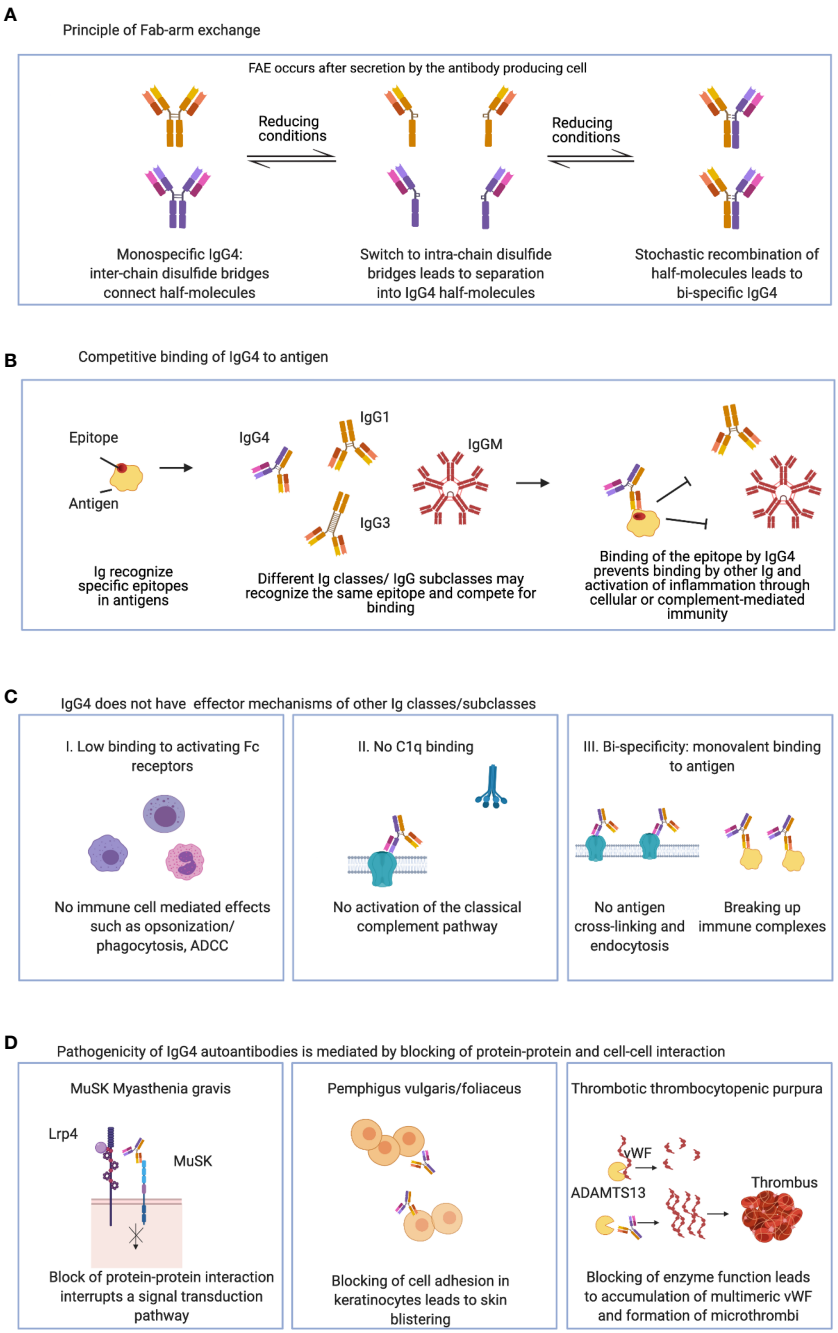

FIGURE 1 | Charactristics of IgG4: **(A)** IgG4 can undergo Fab-arm exchange and form functionally monovalent antibodies. **(B)** IgG4 may bind and compete for binding of other Ig classes and IgG subclasses. **(C)** IgG4 has anti-inflammatory properties and lacks typical IgG effector mechanisms. **(D)** IgG4 autoantibodies can be pathogenic by direct blocking of protein-protein and cell-cell interaction. ADCC, Antibody-dependent cellular cytotoxicity; MuSK, muscle-specific kinase; Lrp4, low density lipoprotein receptor-related protein 4; vWF, von Willebrand factor; ADAMTS13, a disintegrin and metalloprotease with thrombospondin type 1 motif 13.

IL-10 producing regulatory B cells (92–94). Memory B cell levels are also correlated with disease activity and rituximab-mediated reduction of memory B cells result in amelioration of symptoms in TTP (95).

In brief, the dysbalance between memory/regulatory B cell activities appears to be a determining factor in IgG4-AID. Treatment response appears to be more closely associated with those targeting the aforementioned B cell subsets than other cell types of adaptive and innate immunity. However, what makes antigen-secreting B cells undergo class switch to IgG4? Does IgG4 have a physiological role and which cytokine factors are inductors of IgG4?

PHYSIOLOGICAL REGULATION OF IgG4 CLASS SWITCH: A PATH TO TOLERANCE

Interestingly, IgE and IgG4 are both stimulated by the same Th2 cytokines, namely IL-4 and IL-13, and the determining factor, which induces the switch towards IgG4 production and IgE inhibition seems to be IL-10 (96–99). Among other cells, regulatory T cells (Tregs) secrete IL-10, which induces IgG4 production (100), and it is thought that this is mediated by signalling *via* glucocorticoid-induced tumour necrosis factor receptor-related protein (GITR) and GITR- ligand (GITR-L) (101). Regulatory B cells (Bregs) are mainly defined by their ability to secrete IL-10 *in vitro* (102–104). A common set of defining cell surface markers is not yet described, which may be due to the large variety of Breg subsets and the fact that every B cell subset has the ability to become an IL-10 producing Breg (103), even plasma cells (105). In one study, IL-10 producing Bregs were found to produce preferentially IgG4, in contrast to other B cell subsets (106). How exactly IL-10 promotes IgG4 and inhibits IgE production is not sufficiently understood. A recent study suggests that IL-10 directly increases the IL-4 induced IgG4 production in B cells over 20-fold, while the inhibition of IgE-production in B cells is indirect and requires the help of a further, yet unknown, cell population from PBMCs (107). In the context of allergy immunotherapy, the IgG4 response is also associated with a diversification and increased numbers of epitopes, while the number and diversity of IgE epitopes is reduced (108).

Taken together, IgG4 production is associated with anti-inflammatory tolerance mechanisms that is set in motion after prolonged or strong exposure to antigen and likely mediated *via* regulatory T and B cells *via* cytokines like IL-10 [discussed in more detail in (5)]. The induced switch towards the IgG4 subclass is thought to convey protection from chronic antigen exposure, including the potentially damaging effector mechanisms of other antibody classes and to save energy required to uphold a state of constant inflammation [**Figure 1** (30–38, 109)]. However, where does this tolerogenic mechanism get corrupted and skewed towards autoimmunity?

CLASS SWITCH TOWARDS IgG4 IN AUTOANTIBODY-ASSOCIATED DISEASES: GOOD INTENTION, BAD OUTCOME?

One of the key questions is why the autoantibodies in IgG4-AID are predominantly of the IgG4 subclass. Indeed, it is currently unclear, why and how a preferential class switch towards the "protective" IgG4 subclass in patients with IgG4-AID is achieved and whether this is cause or consequence of disease chronicity.

A major challenge currently hampers our understanding of the class switch in IgG4-AID, which is the lack of commercially available and CE/FDA approved diagnostic tests that include autoantibody isotyping. The IgG subclass profiles of the autoantibodies are rarely analysed, and if so mostly in the context of basic or translational research studies. Quantitative IgG subclass profiles can be determined e.g. using flow cytometry (62, 82, 110, 111) or ELISA (112–114), which are research-based methods that are technically challenging, therefore not available for many diagnostic laboratories. The option to quantify antigen-specific IgG subclass profiles with certified, commercially available diagnostic test kits would greatly improve diagnosis and clinical management, and further both translational and clinical research into IgG4-AID, including the correlation between serological concentrations of the four IgG subclasses with clinical outcomes in response to different types of immunosuppression or the timing of the IgG4 class switch in the patients. With the data available to date, three different (but not per se mutually exclusive) scenarios can be hypothesized:

(1) After initial breach of tolerance and dominant relative low dose IgG1-3-mediated disease including complement mediated tissue damage, chronic antigenic exposure together with regulatory T-cell influence leads to class switch to IgG4. While this prevents complement mediated tissue damage, high-titer IgG4 autoantibodies cause direct steric interference with their target antigens and thus disrupt their respective function, which accelerates chronic ongoing disease activity. In other words, IgG1-3 autoantibodies may be of lesser dose or less pathogenic than IgG4 autoantibodies to the same target antigen. In most IgG4-AIDs, IgG4 levels predominate at time of diagnosis but often considerable levels of IgG1-3 antibodies against the same antigenic target can (still) be detected. Very recently, cloned recombinant human antibodies isolated from cerebrospinal fluid of three patients with the IgG4-AID anti-LGI1 encephalitis were analysed. In all three patients, IgG1, IgG2 and IgG4 LGI1 antibodies were identified (77). The class switch from IgG1/3 to IgG4 could merely be difficult to be observed, because by the time the disease has manifested and serum was tested for antibodies, the class switch had already taken place. Indeed, in some patients with IgG4-AID, class switch has been observed: In CNTN1 antibody-associated neuropathy and membranous nephropathy with PLA2R antibodies or acute autoimmune paranodopathy, a class switch from complement-fixing IgG1 or IgG3 in the acute disease phase towards IgG4 in the chronic phase has been observed (115–118). In TTP with anti-ADAMT13, a class switch to IgG4 has been documented before relapse in patients (119).

(2) Individual predisposition for antigen-specific autoimmunity mediated by certain MHC II- antigen- T-cell receptor combinations could predispose to a "skewed" isotype profile towards IgG4, as supported by the strong genetic associations with specific HLA alleles such as HLA-DQB1*05 and HLA-DRB1*14 (18, 19). This would mean, that IgG4-predominance occurs already early during the disease in predisposed individuals and causes chronicity rather than being a consequence of it: A recent study by Ellebrecht et al. (120) has looked into the evolution of autoreactive B cells in PV. B cells normally undergo class switch in the order IgM > IgG3 > IgG1 > IgA1 > IgG2 > IgG4 > IgE > IgA2, therefore it is possible that from the initial IgM class, first anti-Dsg B cells of a different

antibody class or subclass (e.g. IgA) were generated before they switched to the IgG4 subclass. However, it was found that IgG4-specific B cells showed no clonal relationships to B cells with other subclasses and preferentially targeted desmoglein adhesion domains, while anti-Dsg B cells of other classes and subclasses also targeted other regions, suggesting that IgG4 anti-Dsg B cells evolve independent of other antibody classes and subclasses, perhaps by a direct switch from IgM to IgG4 (120). In line with this observation is the finding that IgG4, but not IgG1-3 antibodies against MuSK are able to block Lrp4-MuSK interaction, which suggests the recognition of different epitopes (62, 63). Another related possibility is a class switch first to IgG3, followed by an immediate switch to IgG4 due to unknown regulatory mechanisms. This possibility (and specifically IgG3) was not investigated in the Ellebrecht study (120), but another recent study suggested that a single amino acid replacement in IgG3, which increases its half-life, is associated with a risk to develop PV (121). This is interesting since the PV antibodies are not usually of the IgG3 subclass, but predominantly IgG4 and, to a lesser degree, IgG1 and IgA (122–125). Perhaps a switch to long-lived IgG3 leads to conditions where the immune system induces for yet unknown reasons an immediate and complete class switch towards IgG4. Still, one would expect remnant IgG3 to be present, yet in PV and MuSK MG this subclass is mostly absent in the antigen-specific IgG repertoire (62). Furthermore, some allergens e.g. food or tree pollen, seem especially inclined to induce IgG4 responses, as shown e.g. in response to banana, a lectin antigen (126) or increased IgG4 response to allergens in patients with IgG4-RLD (127).

(3) Aberrant B cell development in IgG4-AID may lead to individuals being more inclined to develop an IgG4 response. Serum IgG4 levels are generally normal or slightly elevated in IgG4-AID patients (14, 128, 129). Upon vaccination with a recall antigen, MuSK MG patients did not develop a disproportionately high IgG4 response (130). Moreover, circulating isotype-specific plasma cells and memory B cell numbers do not show large deviations from healthy individuals. Although many of these studies are challenged by the use of immunosuppressants by the patients, the data thus far does not suggests large B cell developmental problems in patients with IgG4-AID. Cells involved in regulation of the immune response do sometimes appear in abnormal levels. Especially lower Tregs and Breg numbers have been reported, but this is also found in other IgG1-IgG3 dominated AIDs.

Confirming or refuting one (or all) of these hypothesis is remarkably difficult in humans. Longitudinal analysis of patients starting at presymptomatic time points and including cell sampling from bone marrow and target organs would be required. Yet what translational insight can be gained from modelling IgG4-AID in model organisms? Are there suitable models and what are their limitations?

LESSONS LEARNED FROM ANIMAL MODELS

Some evidence – albeit to some degree conflicting - can be gleaned from animal models. It is important to mention that mice do not have a proper equivalent of human IgG4, meaning mouse IgG subclasses do not undergo Fab-arm exchange and all have some immunogenic capacity. That being said, mouse IgG1 is the closest homolog to human IgG4, as it does not fix complement by the classical pathway and is driven by Th2 cells, which allows for studying the effect of vaccination for example in rodent models. Furthermore, mice have two IgG2 isotypes, IgG2a and IgG2b, although B6 mice, and a few other strains, lack the IgG2a isotype and have IgG2c instead. In B6 mice with the same genetic background, both AChR and MuSK antibodies can be induced with full-blown symptoms of myasthenic muscle weakness. While AChR autoantibodies are IgG2-dominant, MuSK antibodies are IgG1-(human IgG4 equivalent) dominant in B6 mice, suggesting that the direction of immune response is at least partially mediated by the molecular characteristics of the target antigen in addition to genetic factors (131, 132). Notably, both MuSK and Dsg-immunized mice show IgG1-dominant antibody responses in both sera and the target tissue (muscle and skin, respectively), already shortly after the immunizations. However, respectable levels of anti-MuSK and anti-Dsg IgG2 and IgG3 antibodies are also present in sera of immunized mice at the same time point, implying that class switch may occur from other IgG isotypes to mouse IgG1/human IgG4 in IgG4-AID or that these responses develop in parallel and are not clonally related (131–134). Moreover, in MuSK experimental autoimmune myasthenia gravis (EAMG) models, IgG1 KO mice are capable of developing pathogenic IgG2 and IgG3 antibodies and MuSK-binding IgG2+ and IgG3+ peripheral blood B cells, further conforming that autoantigens of the IgG4-AID may induce antibody responses of all IgG isotypes (131, 132). Significantly enhanced IgG3 responses in IgG1 KO mice suggests that mouse IgG1 (and putatively human IgG4) might be suppressing production of complement-fixing IgG isotypes and this might be an additional underestimated anti-inflammatory mechanism of the human IgG4 isotype (131, 132). In AChR-EAMG, IgG1 deficiency causes increased EAMG incidence and severity in parallel to enhanced AChR-specific IgG2 and IgG3 production further supporting this assertion (135). To the best of our knowledge, IgG1 KO experiments have not been conducted for other IgG4-AID and thus it is not certain whether the abovementioned results can be generalized to all autoantigens associated with IgG4-AID.

Passive transfer of MuSK-MG and PV IgG into experimental animals induce the characteristic clinical and pathological features of the human disease, indicating the pathogenic action of serum IgGs in both disorders. Passive transfer of equal amounts of patient derived IgG4 and IgG1-3 to mice also showed that IgG4 was pathogenic, while IgG1-3 were not (136). However, MuSK antibody levels in the IgG1-3 injected mice were below detection level, while they were clearly detectable in the IgG4-injected mice probably due to low amounts of MuSK-specific IgG1-3 within the IgG1-3 fraction and has to be interpreted with caution. Removal of anti-Dsg IgG by immunoadsorption abolishes the pathogenic activity of PV sera (137). Moreover transfer of splenocytes of Dsg-3-immunized mice to Rag-2 deficient mice, which are not

capable of producing antigen-specific B cells, generated anti-Dsg-3 antibodies and induced PV in recipient mice (137). Similarly, administration of inhibitory monoclonal antibodies against human recombinant ADAMTS13, target antigen in TTP, resulted in reduced ADAMTS13 activity, severe thrombocytopenia and hemolytic anemia in baboons. Also, treatment of mice with anti-ADAMTS13 single-chain variable-region fragments generated fatal thrombocytopenia (138–140).

Immunization based-mouse models of PV show striking resemblance to MuSK-EAMG in terms of pathogenic factors and corroborate the significance of IL-4, IL-10 and IgG1 as major contributing factors of IgG4-AID pathogenesis. In the mouse model of PV, IL-4 and IL-10 producing Dsg-3-reactive T cells have been associated with pathogenicity and neutralization of IL-4 has led to suppression of anti-Dsg-3 production and reduced disease severity. Moreover, in the animal model of PV, IgG1 has been identified as the dominant isotype both in serum and on keratinocyte surfaces (134, 141, 142).

It is also possible that further antibody-mediated mechanisms may additionally contribute to disease. A relatively understudied common denominator might be antibody-mediated mitochondrial dysfunction and apoptotic cell death in IgG4-AID, which so far have been implicated in PV, membranous nephropathy/IgG4-related disease and anti-LGI1 encephalitis (143–147). For example, muscle samples of MuSK-MG patients often exhibit mitochondrial dysfunction. MuSK-immunized, but not AChR-immunized, mice show increased numbers of ragged red fibers (a histochemical sign of mitochondrial dysfunction) and decreased activity of mitochondrial enzymes indicating the role of MuSK-immunity in induction of mitochondrial dysfunction.

In this context, it should be considered that perhaps not all pathogenic effects in IgG4-AID are necessarily induced by directly antibody-mediated mechanisms. In resemblance to AChR-EAMG, where proinflammatory cytokines have been shown to induce muscle cell toxicity (148), non-antibody pathogenic factors causing IgG4-AID may also influence the functions of the target organs. For example, IL-4 has been shown to reduce ADAMTS13 expression thereby potentially contributing to pathogenesis of TTP (149).

The role of IgG4 antibodies is still unclear in anti-IgLON5 disease, where patients often show a rather "neurodegenerative" clinical phenotype, brain autopsies may present hyperphosphorylated tau-deposition (a marker of neurodegeneration) and anti-IgLON5 autoantibodies induce neurodegeneration *in vitro via* unknown intracellular mechanisms (150, 151).

Taken together, although it is possible that the production of IgG4-autoantibodies represents a "primary" phenomenon in IgG4-AID, and their ongoing production causes chronicity, for the time being, one cannot exclude that they are simply a "secondary" phenomenon and their ongoing production is a result of chronic antigenic "stimulation". Hopefully, future systematic approaches using sophisticated single cell based high throughput directly *ex vivo* analysis of transcriptomes and B/T cell receptors of lymphocytes together with animal experiments will provide the definite answer.

Yet how do these insights from human and animal studies contribute to "personalized therapies". Can IgG4-producing plasmablasts or downstream effects of IgG4 itself be targeted and what are potential side effects? Is the new subcategorization into IgG4-AID relevant from a therapeutical point of view or is their treatment identical to comparable IgG1-antibody mediated autoimmunopathies?

TREATMENTS OF IgG4 NEUROLOGICAL DISEASES

Overall, general or partially selective immunosuppression or immunomodulation is the major treatment applied to the autoimmune neurological diseases. Unfortunately, to date, there are almost no disease-specific therapies for neuroimmunological diseases. However, *in vitro* (cell cultures) and *in vivo* (animal, brain pathology and clinical) studies have suggested the presence of different pathophysiological mechanisms in patients with different antibody types and subtypes (152, 153). These findings suggest that special treatment requirements may apply to neuroimmunological diseases with different antibody subtypes, including patients with dominant IgG4 antibodies, and indeed IgG4-AID have a unique response pattern to conventional therapies for autoimmune diseases. Importantly, IgG4 is not the sole antibody present in IgG4-AID. IgG1 antibodies can be present, and may also contribute to disease. The patients are heterogenous and may react differently to treatments, perhaps due to the different involvement of immune cells. Distinct B-cell populations may predominate in different patients, IgG subclass profiles of autoantibodies may vary, which could explain the differences in clinical responsiveness towards different immunosuppressive drugs. As in most autoimmune conditions, steroids have - mostly empirically - been shown to be effective in IgG4-autoantibody mediated diseases. Most if not all treatment regimens at least initially contain corticosteroids (152, 154–157). Some physicians initially apply high-dose iv methylprednisolone and other start with oral steroids (1mg/kg bodyweight followed by tapering). However, in most instances, long-term steroids are needed as maintenance therapy to prevent relapses and oftentimes side-effects become a limiting factor. Even though many questions regarding steroid therapy in IgG4-antibody mediated diseases remain unclear, this review will focus on four specific therapies directly addressing IgG4 antibodies or their producing cells that we estimate to be the most relevant treatments across diseases.

Plasmapheresis

Plasmapheresis (plasma exchange, PLEX) and Ig-apheresis remove the majority of antibodies located in the patient's blood plasma [which does not extend to extravascular antibodies, which may account for up to 65% (158)]. Since autoantibodies directly cause disease, and are removed from the body, it is considered to provide immediate relief for patients and is utilized in cases of acute exacerbation. PLEX is the first line of treatment for TTP where it contributes significantly in survival

of acute episodes of the disease (159), possibly not only by removing ADAMTS13 inhibitory antibodies but also by replenishing active ADAMTS13. In MG, PLEX has long been used as a treatment option, especially during myasthenic crises or pre-operatively (160). It is especially effective in MuSK-MG, probably more effective than in AChR-MG (161). Plasmapheresis has been successfully performed in pemphigus for over thirty years, particularly in cases of severe or recalcitrant disease, and as a steroid-sparing agent (162, 163). More recently, there is growing evidence to the therapeutic value of plasmapheresis in AE, including patients with GABA, LGI1 and AMPA antibodies. In a single center prospective study, significant improvement of the modified Rankin scale was seen in patients with severe refractory AE after treatment with PLEX, steroids and IVIG compared to those that only received steroids and IVIG (164). Studies have shown that both plasmapheresis and Ig-apheresis are well tolerated with minimal adverse effects supporting their use in clinical practice (165). Taken together, plasmapheresis appears to be a safe and efficient escalation therapy for acute IgG4-AID.

IVIGs

Intravenous immunoglobulins (IVIGs) are pooled human IgG from many healthy donors, and as such comprised of a highly diverse antibody repertoire of human IgG1,2,3 and 4. IVIGs have a range of proposed mechanisms, of which some may be relevant and others irrelevant for IgG4-AID (166).

Possible mechanisms: A key mechanism of action of IVIGs may be the blocking of the neonatal Fc receptor (FcRn), which contributes to effective humoral immunity by recycling IgG and extending its half-life in the circulation to 3-4 weeks (167). IVIGs block and saturate these receptors, thereby increasing the degradation of IgG, reducing the half-life of IgG and ultimately leading to reduction of circulating IgG (168, 169) IgG1 and IgG4 both bind to the FcRn with similar efficiency (170), and blocking of the FcRn by a different drug led to reduction of both serum IgG1 and IgG4 (171). This mechanism of action is therefore available for IgG4 and may provide relief by enhancing IgG4 degradation.

In the highly diverse antibody repertoire of IVIGs, it is possible that antibodies against distinct autoantibodies, particularly against the antigen-binding part, termed anti-idiotype antibodies, can be present, and could neutralize the effects of autoantibodies (172–174). IVIGs may therefore also provide anti-idiotype antibodies that may bind to and neutralize pathogenic antibodies, but whether this applies to IgG4 autoantibodies is not clear.

Less likely mechanisms: Effect on proinflammatory cytokines: IVIGs may reduce the levels of proinflammatory cytokines that do not play a major role for IgG4-AID and induce anti-inflammatory cytokines (175–177). Effect on FcγRs: IgG4 has reduced binding affinity to activating FcγRs it does bind to FcγRIIB, which is an inhibitory IgG Fc receptor expressed on immune cells (170). IVIGs may bind and upregulate the receptors, therefore suppressing inflammation (178, 179), which is not essential in IgG4-AID. Furthermore, IVIGs have a range of inhibitory effects on other immune cells, e.g. monocytes, macrophages and dendritic cells (180–182).

Effect on complement: An important mechanism of IVIGs that is not relevant for IgG4 is the inhibition of complement activation, which is a main effector mechanism of IgG3 and IgG1, but not of IgG4 autoantibodies (183). Perhaps the degree of complement involvement in pathology is the determining factor for IVIG efficacy for the patients. In AChR-MG, complement-mediated damage is a key pathogenic mechanism, and IVIGs are considered as a short time treatment that provides immediate relief in AChR MG (160). In contrast, IVIG seems to be less efficient in MuSK MG, and particularly less effective than plasmapheresis (155), which could be due to the fact that MuSK IgG4 does not activate complement. A similar conclusion was drawn by Rodriguez et al. in a recent study with LGI1 encephalitis patients. In this large retrospective case series of 118 patients with LGI1 encephalitis patients, the authors observed that IVIGs were less efficient in comparison with corticosteroid treatment (184). Nevertheless, IVIGs did have an effect and fared better than placebo in a small randomized placebo-controlled trial, in which patients with anti-LGI1 antibody-associated epilepsy (all with predominantly IgG4 autoantibodies) showed response in 6 out of 8 patients in the IVIG group, compared to zero response in the 6 patients in the placebo group (185). In pemphigus, high dose IVIG treatment has been reported to be an efficient treatment in patients that are unresponsive to immunosuppression (186) most likely due to FcRn blocking by IVIGs and increased IgG degradation, as a rapid decrease of Dsg autoantibodies (IgG1 and IgG4) was observed following IVIg treatment (187).

While IVIGs are considered as short-term treatment for most IgG4-AID, it is also used as a long-term treatment in certain disorders such as inflammatory neuropathies (188). The underlying mechanism of action of IVIG in the treatment of CIDP remains unclear. Long-term IVIG treatment appears to decrease autoreactive CD4+ and CD8+ T effector memory cells (189) and enhance FcγRIIB expression on B cells thus reducing conversion of naïve B cells to memory B cells (176, 190).

Taken together, IVIGs have several potential mechanisms of action targeting different parts of the immune system, and depending on their respective role for disease, IVIGs may be more or less efficient. The effects on complement, cytokine production and cellular immunity may not have a major impact of IVIGs in most IgG4-AIDs. These anti-inflammatory actions may in theory also backfire in IgG4-AID: IVIGs upregulate regulatory T-cells (191, 192), which are known producers of IL-10, and induce production of IL-10 by macrophages (182). IL-10 is a regulator of IgG4 class switch and may as such even increase production of pathogenic IgG4. In contrast, FcRn blocking and increased degradation of IgG4 may provide therapeutic relief as e.g. observed in pemphigus.

Rituximab

Targeting B-cells, which are the cells producing autoantibodies, is a main focus of therapy for IgG4-AID. CD20 is a marker that is expressed on B-cells throughout development, but not on the antibody-secreting cells, short-lived plasmablasts or long-lived

plasma cells. Rituximab is an anti-CD20 monoclonal antibody and as such depletes B-cells expressing CD20, therefore the treatment efficacy of rituximab depends directly on the type of B-cells involved in the production of autoantibodies which also appears to be linked to the IgG subclass.

For example, in refractory AChR-MG, rituximab is usually the preferred treatment (193), but its efficacy is not conclusive, probably because AChR antibodies are secreted by long-lived plasma cells, e.g. residing in the thymus or bone marrow (194–196). In contrast, rituximab has a much more promising effect in the IgG4 associated form, MuSK MG where it was found to be very efficient (88, 197–201), leading to depletion of MuSK IgG4 (86). The generally accepted explanation to date is that the cells responsible for MuSK autoantibody secretion (such as plasmablasts) require constant replenishment by memory B cells that express CD20 and are therefore susceptible to rituximab treatment (202).

It has well been established that CIDP patients with neurofascin antibodies do not respond to steroid and IVIG treatment but to rituximab, which was found to enhance regulatory B cell responses and inhibit memory B cell and plasmablast populations (203). More importantly, rituximab suppresses short-lived plasma cells and their CD20+ precursors involved in IgG4 production (204). Rituximab is also considered as a very efficient treatment in TTP (205–207) and pemphigus (84, 85, 206, 208–212). Rituximab may be another efficient therapy in anti-LGI1 and CASPR2 encephalitis with predominantly IgG4 antibodies (213). Several studies suggest clinical usefulness of rituximab treatment for autoimmune encephalitis with antibodies against LGI1 and CASPR2, among these a large study from the GENERATE Registry with 62 patients with anti-LGI1 and 34 with anti-CASPR2 antibodies. The results suggest class IV evidence that early and short-term rituximab therapy could be an effective and safe treatment for these patients (214–216). An important limitation of these studies is that the IgG antibody subtype was not established. Future studies linking antigen-specific IgG-subtypes and specific immunotherapies are required to identify the best treatment for IgG4 of these patients.

However, because of its potential side effects and its high cost, in several countries rituximab is mostly used for the treatment of steroid-refractory MuSK-MG. In several cases, rituximab treatment was sufficient by itself, eliminating the need for other treatments or even leading to long term remission (201), and aggressive treatment strategies including rituximab led to better clinical outcomes of MuSK-MG patients in general (217). Clinical guidelines suggested the early use of rituximab when an initial standard immunosuppression treatment does not result in rapid remission (218). On another note, a study on cost of rituximab in patients with pemphigus vulgaris suggests that the initial higher cost of rituximab may be at least in part counterbalanced by reduced long-term treatment cost (219).

Bortezomib

Several preclinical studies have shown a potential benefit from proteasome inhibitors, which target long-lived plasma cells, a subset of cells that remains untouched with all the therapies previously mentioned (220). Due to their high antibody production rate, plasma cells are highly sensitive to the inhibition of the ubiquitin-proteasome pathway, resulting in the accumulation of misfolded proteins, leading to plasma cell death. *In vitro* treatment of thymocytes from AChR-MG patients with bortezomib resulted in marked depletion of long-lived plasma cells and inhibition of autoantibody production (221), and treatment of animals (active immunization model for MG, EAMG) resulted in an improvement of the symptoms (222). The TAVAB clinical trial (ClinicalTrials.gov Identifier: NCT02102594), aiming to assess the efficacy of bortezomib, a first generation proteasome inhibitor, in generalized AChR-MG among other antibody-mediated autoimmune diseases was unfortunately prematurely terminated due to difficulties in recruitment (ClinicalTrials.gov Identifier: NCT02102594). Interestingly, a case report presented a therapeutic benefit of a patient with refractory MuSK-MG after treatment with bortezomib (treated in combination with rituximab, aciclovir and cotrimoxazole after initial courses of IVIG and prednisone) (223). Treatment with bortezomib has also shown to be efficient in refractory cases of autoimmune encephalitis (224–226). Its efficacy and safety is currently being tested in severe cases of NMDAR, LGI1 and Caspr2 autoimmune encephalitis, of which the LGI1 and Caspr2 antibodies have IgG4 as the predominant isotype (227). Among IgG4-AID, bortezomib was described as a good therapeutic option for CIDP patients (228) with severe relapses or an acute progression who did not respond adequately to regular immunosuppression treatment and rituximab (228). Additionally, in a patient with anti-pan-NF-associated neuropathy (predominantly of the IgG4 isotype) with severe clinical manifestations, it has also being shown reduction in antibody titer leading to clinical improvement after receiving a combination of IVIG, PLEX, rituximab and bortezomib (229). Bortezomib was beneficial in patients with relapsed/refractory TTP with an acceptable adverse event profile (230). Together with rituximab, bortezomib has shown to induce long-lasting remission in an acute refractory subgroup of patients with TTP (231). Additionally, some case reports of TTP patients unresponsive to plasma exchange, immunosuppressive therapy and rituximab, presented with a reduction in autoantibody levels and an improvement in clinical condition after treatment with bortezomib alone (232) or in combination with plasma exchange and steroids (233). The authors attributed the improvement to an abolition of residual autoreactive plasma cells. A new clinical trial to investigate the efficacy and safety of bortezomib as a first line treatment for acquired TTP has been approved, but at the last update in November 2021, recruitment had not yet begun (ClinicalTrials.gov Identifier: NCT05135442). Among the IgG4-RD spectrum, hyper IgG4 syndrome is characterized by the lymphoplasmacytic infiltration with IgG4-positive cells and a pronounced fibrosis of different tissues. Interestingly, a patient suffering from recurrent and unresponsive hyper IgG4 disease, in this case characterized by IgG4 plasma cell infiltration in the lungs, was successfully treated with a combination of bortezomib, dexamethasone and cyclophosphamide (234).

Strategies for Novel and Specific Therapeutic Approaches

As described above, current treatments for IgG4- AIDs rely mostly on immunosuppression (corticosteroids or non-steroid immunosuppressants) and depletion of antibodies or B cell antigen-specific, which are non-specific. Therefore, they can be associated with side-effects, raising the need for novel, more targeted therapies.

Plasmapheresis or total IgG immunoadsorption is often beneficial in MuSK-MG, PV, TTP, CIDP, AIDP, Goodpasture's syndrome and anti-DPPX encephalitis (235–242). A targeted approach would be the selective adsorption of the IgG4 or antigen-specific antibodies, while leaving unaffected the majority of plasma IgGs, thus avoiding hypogammaglobulinemia. In addition, the removal of a very small percentage of the total IgGs could prolong the treatment effect, due to the slower rate of autoantibody reappearance after treatment (243, 244). This could be accomplished by passing the plasma through a suitable matrix before being returned to the patient. In the case of MuSK-MG, we have explored an antigen-specific approach by the generation of sepharose-immobilized recombinant MuSK extracellular domains. The efficiency and specificity of the method has been established by *in vitro* experiments, where immunoadsorption resulted in almost complete removal of the autoantibodies from all the patients' sera tested (245). In addition, *ex vivo* immunoadsorption in rats with EAMG, induced by immunization with human MuSK, resulted in a rapid and significant amelioration of symptoms, without the emergence of any adverse effects (246). Similarly, others have found that sepharose-immobilized Dsg-1 and 3 ectodomains successfully and specifically removed the Dsg antibodies and eliminated the pathogenic activity of PV patient sera (247). Although the demonstration of the proof of principle by these studies supports that similar strategies could be applied in other IgG4-associated diseases as well, it may be difficult and cost-prohibitive to optimize different matrices for each individual of these rare diseases. A similar but much more feasible solution could be the generation of matrices capable of binding only the IgG4 fraction of antibodies, thus removing the pathogenic autoantibodies, but not the majority of the IgGs (IgGs 1-3).

Another approach that gains ground as an antigen-specific therapy is the induction of tolerance towards the autoantigens, by administration of disease-relevant antigen derived domains and peptides. A recent study using MuSK-induced EAMG in mice demonstrated the potential for tolerance induction by oral administration of recombinant MuSK domains (248). However, MuSK administration took place prior to induction, so further studies are necessary to evaluate the actual therapeutic potential. Furthermore, it is not clear what IgG autoantibody subclasses were generated in the mouse model, so it is difficult to extrapolate the findings to IgG4-mediated MuSK-MG in humans. In fact, several lines of evidence support that tolerance induction works by diverting the immune response from a Th1 type to Th2/Th3 (249, 250). Furthermore, it appears that tolerance induction is accompanied by an increase in IL-10 levels, suggesting the diversion of the immune response towards IgG4 (251, 252). Therefore, it is still not clear how beneficial such an approach would be in the case of IgG4-associated autoimmune diseases, and further studies illuminating the underlying mechanisms are required.

IL-10 is essential in IgG4 class switch, however, it probably increases the production of IgG4 by enhancing IL-4 induced IgG4 switch (52, 99), making IL-4 also a key player in IgG4-RLD and, potentially, in IgG4-AID. Increased IL-4 levels have been associated with an increment in Th2 and plasmablast cell count and stimulation with IL-4 resulted in elevated IgG4 and IgG4: IgG ratios in patients with active untreated IgG4-RLD (253, 254), and lymph node cells and sera from MuSK immunized mice also showed upregulation of IL-4 and IL-10 (131).

Several drugs targeting soluble IL-4 or its receptor have been developed (**Figure 2**). Among those, dupilumab is an IgG4 monoclonal antibody that acts on the IL-4 receptor alpha (IL-4Rα), a receptor that can bind to both IL-4 and IL-13 (255).

In IgG4-RLD, the efficacy of dupilumab has been described in a few case reports. After refusing treatment with other immunosuppressants, a patient with a complex and acute clinical picture including allergies, asthma, atopic dermatitis and a borderline diagnosis for IgG4-RLD was treated with dupilumab. After 12 months, the patient's IgG and IgG4 levels decreased and most of the complaints resolved. Importantly, no relapses were observed and the patient did not suffer from any long-term side effects (256). Another case report described a patient with IgG4-RLD, who presented a good initial clinical response to steroid treatment. However, after suffering a relapse, rituximab was introduced, which helped initially to ameliorate disease, but could not prevent relapse one year later. Dupilumab treatment was started thereafter and led to rapid improvement accompanied by a biological reduction of all cells currently associated with IgG4-RLD (decrease of total T helper 2 cells, T follicular helper (Tfh) cells, Tfh2 cells and plasmablasts as well as serum IgE after 3 and 8 months of treatment). Interestingly, IgG4 levels remained stable. It is likely that the clinical improvement was not exclusively due to dupilumab treatment but perhaps due to combination therapy (with rituximab). The authors suggested that dupilumab could be a good treatment option for IgG4-RLD patients with relapses after an induction treatment (257). Another IL-4 targeting therapy known as dectrekumab (VAK-694), an IL-4 antagonist fully humanized monoclonal antibody, showed a decrease in the number of allergen-specific IL-4 producing cells in a clinical trial with patients with seasonal allergic rhinitis. However, VAK-694 did not show any extra benefit compared to patients treated only with the routine/standard therapy when looking at the symptoms (258).

Clinical trials are required to further investigate and validate the therapeutic benefit of anti-IL-4 therapies, but the initial data suggest that targeting the regulation of IgG4 production and IgG4 class switch *via* IL-4 may present a potential novel therapeutic strategy for IgG4-RLD, and perhaps also IgG4 autoimmune diseases (**Figure 2**).

CONCLUSIONS

IgG4-AID affect different organs, are characterized by IgG4 autoantibodies targeting specific antigens and mostly display a

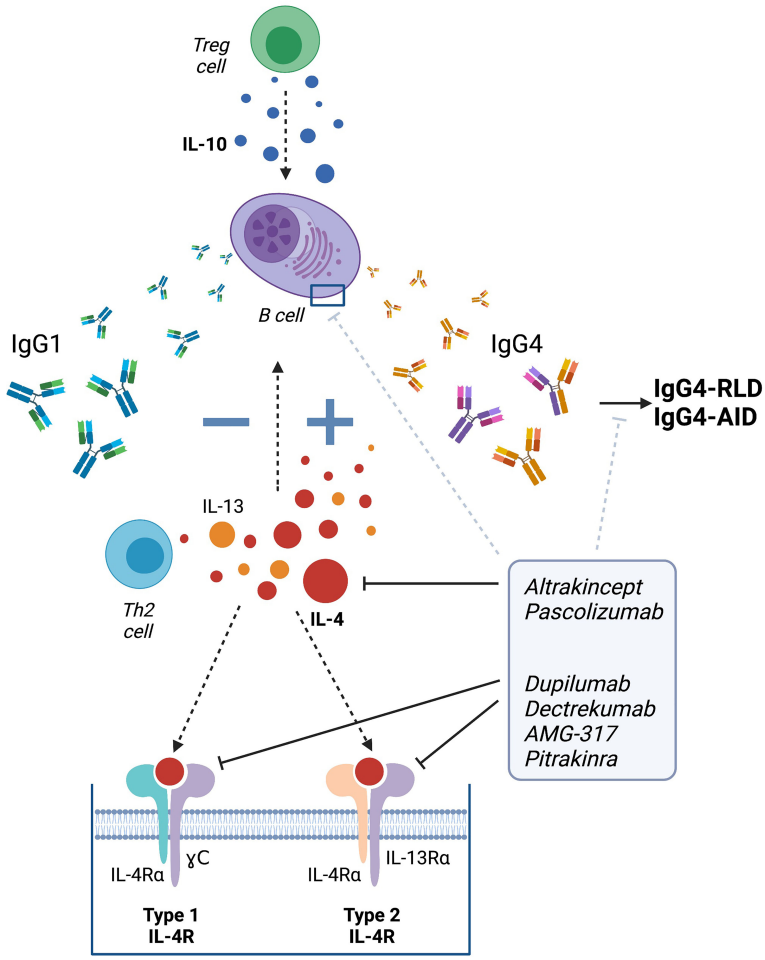

FIGURE 2 | Therapeutic strategies targeting IgG4 class switch *via* IL-4. Altrakincept, pascolizumab, dupilumab, dectrekumab, AMG-317 and pitrakinra have been developed to prevent the binding of IL-4 to its receptor by blocking the soluble IL-4 or targeting its receptor itself. Targeting IL-4 may help to avert IgG4 class switch and therefore, the development of IgG4-RLD and IgG4-AID. Figure created using Biorender.

strong genetic predisposition mediated by HLA-genes. IgG4-AID are distinct from IgG4-RLD which are characterized by fibrosis, elevated serum IgG4 concentrations and IgG4 positive plasma cell infiltrates in the affected tissue, but mostly lack antigen-specific IgG4. Hallmarks of IgG4 are the absence of complement activation, lack of bispecificity due to Fab arm exchange and inability to activate cells *via* Fc receptors. Instead, IgG4 autoantibodies are pathogenic by direct blocking mechanisms. Why and how IgG4 autoantibodies are produced is currently unknown, but we suspect that IL-4, IL-13 and IL-10 that are known regulators of IgG4 class switch may also play a role in the production of pathogenic IgG4, and a dysbalance between memory and regulatory B cells may determine the induction of IgG4-AID. Overall we propose three possible scenarios contributing to IgG4-AID immunopathogenesis: 1) initial disease includes antigen-specific IgG1-3 antibodies with low pathogenicity (e.g. *via* complement activation) or at low concentration, but chronic antigen exposure and influence from regulatory T cells induces class switch to IgG4, which then- either by increased dosis or pathogenicity- cause disease by steric hindrance. 2) Genetic predisposition, e.g. *via* distinct MHCII-antigen-T-cell receptor combinations may lead to a "skewed" isotype profile towards IgG4, or 3) aberrant B cell development in IgG4-AID may lead to individuals being more inclined to develop an IgG4 response. Further studies are necessary to investigate these different possibilities. Clinically, therapies targeting B cells have led to better clinical outcomes than general immunosuppression with corticosteroids in MuSK-MG and anti-LGI1 encephalitis, therefore we conclude that IgG4-AID may require different treatment strategies than classical antibody-mediated autoimmunity. We also discuss IgG4- or antigen-specific -apheresis and IL-4 receptor blockade as potential new treatment strategies for IgG4-AID. Finally, we think that the key to a better therapy lies in understanding the underlying immunopathogenesis and better diagnostics that also include the analysis of IgG subclasses to improve our assessment of treatment outcomes.

AUTHOR CONTRIBUTIONS

IK conceived the idea, wrote the manuscript, and provided figures. MM-D wrote the manuscript and provided a figure. VY, JT, KL, ST, ET and MH wrote the manuscript. IK, FL, RH, PM-M, and ET revised the final manuscript. All authors contributed to the article and approved the submitted version.

FUNDING

IK was funded by a Hertha Firnberg Fellowship by the Austrian Science Fund, Austria, project number: T996-B30. FL is supported by German Ministry of Education and Research (01GM1908A) and E-Rare Joint Transnationalresearch support (ERA-Net, LE3064/2-1). JT and ST were cofinanced by the EU and Greek national funds through the Operational Program Competitiveness, Entrepreneurship and Innovation (project: T1EDK-05024, MIS 5032815). MM-D was funded by a Kootstra Talent Fellowship awarded by the Maastricht University Medical Center+. PM-M was funded by NIH 18-003826 and NIH 4224868 grants. MH receives financial support from the LUMC (Gisela Thier Fellowship 2021), Top Sector Life Sciences & Health to Samenwerkende Gezondheidsfondsen via the Target to B! Consortium (LSHM18055-SGF), PPS-Match call LUMC – Topsector LSH 2021, Prinses Beatrix Spierfonds (W.OR-19.13), and the Dutch Science Organization NWO (VENI 0915016181 0040).

ACKNOWLEDGMENTS

Figures created with Biorender (License: IK).

REFERENCES

1. Huijbers MG, Querol LA, Niks EH, Plomp JJ, van der Maarel SM, Graus F, et al. The Expanding Field of IgG4-Mediated Neurological Autoimmune Disorders. *Eur J Neurol* (2015) 22(8):1151–61. doi: 10.1111/ene.12758
2. Koneczny I. A New Classification System for IgG4 Autoantibodies. *Front Immunol* (2018) 9:97. doi: 10.3389/fimmu.2018.00097
3. Ludwig RJ, Vanhoorelbeke K, Leypoldt F, Kaya Z, Bieber K, McLachlan SM, et al. Mechanisms of Autoantibody-Induced Pathology. *Front Immunol* (2017) 8:603. doi: 10.3389/fimmu.2017.00603
4. Davies AM, Rispens T, Ooijevaar-de Heer P, Gould HJ, Jefferis R, Aalberse RC, et al. Structural Determinants of Unique Properties of Human IgG4-Fc. *J Mol Biol* (2014) 426(3):630–44. doi: 10.1016/j.jmb.2013.10.039
5. Lighaam LC, Rispens T. The Immunobiology of Immunoglobulin G4. *Semin Liver Dis* (2016) 36(3):200–15. doi: 10.1055/s-0036-1584322
6. Cao M, Koneczny I, Vincent A. Myasthenia Gravis With Antibodies Against Muscle Specific Kinase: An Update on Clinical Features, Pathophysiology and Treatment. *Front Mol Neurosci* (2020) 13:159. doi: 10.3389/fnmol.2020.00159
7. Evoli A, Alboini PE, Damato V, Iorio R, Provenzano C, Bartoccioni E, et al. Myasthenia Gravis With Antibodies to MuSK: An Update. *Ann N Y Acad Sci* (2018) 1412(1):82–9. doi: 10.1111/nyas.13518
8. Schmidt E, Kasperkiewicz M, Joly P. Pemphigus. *Lancet* (2019) 394 (10201):882–94. doi: 10.1016/S0140-6736(19)31778-7
9. Kasperkiewicz M, Ellebrecht CT, Takahashi H, Yamagami J, Zillikens D, Payne AS, et al. Pemphigus. *Nat Rev Dis Primers* (2017) 3:17026. doi: 10.1038/nrdp.2017.26
10. Koneczny I. Update on IgG4-Mediated Autoimmune Diseases: New Insights and New Family Members. *Autoimmun Rev* (2020) 102646. doi: 10.1016/j.autrev.2020.102646
11. Watanabe T, Minaga K, Kamata K, Kudo M, Strober W. Mechanistic Insights Into Autoimmune Pancreatitis and IgG4-Related Disease. *Trends Immunol* (2018) 39(11):874–89. doi: 10.1016/j.it.2018.09.005
12. Akiyama M, Kaneko Y, Takeuchi T. Characteristics and Prognosis of IgG4-Related Periaortitis/Periarteritis: A Systematic Literature Review. *Autoimmun Rev* (2019) 18(9):102354. doi: 10.1016/j.autrev.2019.102354
13. Umehara H, Okazaki K, Kawa S, Takahashi H, Goto H, Matsui S, et al. Welfare: The 2020 Revised Comprehensive Diagnostic (RCD) Criteria for IgG4-RD. *Mod Rheumatol* (2021) 31(3):529–33. doi: 10.1080/14397595.2020.1859710
14. Endmayr V, Tunc C, Ergin L, De Rosa A, Weng R, Wagner L, et al. Anti-Neuronal IgG4 Autoimmune Diseases and IgG4-Related Diseases May Not Be Part of the Same Spectrum: A Comparative Study. *Front Immunol* (2022) 12:785247. doi: 10.3389/fimmu.2021.785247
15. Palazzo E, Palazzo C, Palazzo M. IgG4-Related Disease. *Joint Bone Spine* (2014) 81(1):27–31. doi: 10.1016/j.jbspin.2013.06.001
16. Umehara H, Okazaki K, Kawano M, Tanaka Y. The Front Line of Research Into Immunoglobin G4-Related Disease - Do Autoantibodies Cause Immunoglobin G4-Related Disease? *Mod Rheumatol* (2019) 29(2):214–8. doi: 10.1080/14397595.2018.1558519
17. Trampert DC, Hubers LM, van de Graaf SFJ, Beuers U. On the Role of IgG4 in Inflammatory Conditions: Lessons for IgG4-Related Disease. *Biochim Biophys Acta* (2018) 1864(4):1401–9. doi: 10.1016/j.bbadis.2017.07.038
18. Koneczny I, Yilmaz V, Lazaridis K, Tzartos J, Lenz TL, Tzartos S, et al. Common Denominators in the Immunobiology of IgG4 Autoimmune Diseases: What Do Glomerulonephritis, Pemphigus Vulgaris, Myasthenia Gravis, Thrombotic Thrombocytopenic Purpura and Autoimmune Encephalitis Have in Common? *Front Immunol* (2021) 11:605214(3609). doi: 10.3389/fimmu.2020.605214
19. Panhuber A, Lamorte G, Bruno V, Cetin H, Bauer W, Erber A, et al. A Systematic Review and Meta-Analysis of HLA-Class-II Associations in Patients With IgG4 Autoimmunity. *Res Square* (2021). doi: 10.21203/rs.3.rs-638050/v2
20. van der Neut Kolfschoten M, Schuurman J, Losen M, Bleeker WK, Martinez-Martinez P, Vermeulen E, et al. Anti-Inflammatory Activity of Human IgG4 Antibodies by Dynamic Fab Arm Exchange. *Science* (2007) 317(5844):1554–7. doi: 10.1126/science.1144603
21. Schur PH. IgG Subclasses. A Historical Perspective. *Monogr Allergy* (1988) 23:1–11.
22. French M. Serum IgG Subclasses in Normal Adults. *Monogr Allergy* (1986) 19:100–7.
23. Aucouturier P, Danon F, Daveau M, Guillou B, Sabbah A, Besson J, et al. Measurement of Serum IgG4 Levels by a Competitive Immunoenzymatic Assay With Monoclonal Antibodies. *J Immunol Methods* (1984) 74(1):151–62. doi: 10.1016/0022-1759(84)90376-4
24. Blanco E, Perez-Andres M, Arriba-Mendez S, Contreras-Sanfeliciano T, Criado I, Pelak O, et al. EuroFlow: Age-Associated Distribution of Normal B-Cell and Plasma Cell Subsets in Peripheral Blood. *J Allergy Clin Immunol* (2018) 141(6):2208–2219 e16. doi: 10.1016/j.jaci.2018.02.017
25. Nirula A, Glaser SM, Kalled SL, Taylor FR. What is IgG4? A Review of the Biology of a Unique Immunoglobulin Subtype. *Curr Opin Rheumatol* (2011) 23(1):119–24. doi: 10.1097/BOR.0b013e3283412fd4
26. Boctor FN, Peter JB. IgG Subclasses in Human Chronic Schistosomiasis: Over-Production of Schistosome-Specific and non-Specific Igg4. *Clin Exp Immunol* (1990) 82(3):574–8. doi: 10.1111/j.1365-2249.1990.tb05492.x
27. Lichtenstein LM, Holtzman NA, Burnett LS. A Quantitative *In Vitro* Study of the Chromatographic Distribution and Immunoglobulin Characteristics of Human Blocking Antibody. *J Immunol* (1968) 101(2):317–24.
28. Kemeny DM, MacKenzie-Mills M, Harries MG, Youlten LJ, Lessof MH. Antibodies to Purified Bee Venom Proteins and Peptides. II. A Detailed Study of Changes in IgE and IgG Antibodies to Individual Bee Venom Antigens. *J Allergy Clin Immunol* (1983) 72(4):376–85. doi: 10.1016/0091-6749(83)90503-1

29. Aalberse RC, van der Gaag R, van Leeuwen J. Serologic Aspects of IgG4 Antibodies. I. Prolonged Immunization Results in an IgG4-Restricted Response. *J Immunol* (1983) 130(2):722–6.
30. Nakagawa T, Miyamoto T. The Role of IgG4 as Blocking Antibodies in Asthmatics and in Bee Keepers. *Int Arch Allergy Appl Immunol* (1985) 77(1-2):204–5. doi: 10.1159/000233787
31. Platts-Mills T, Vaughan J, Squillace S, Woodfolk J, Sporik R. Sensitisation, Asthma, and a Modified Th2 Response in Children Exposed to Cat Allergen: A Population-Based Cross-Sectional Study. *Lancet* (2001) 357(9258):752–6. doi: 10.1016/S0140-6736(00)04168-4
32. James LK, Bowen H, Calvert RA, Dodev TS, Shamji MH, Beavil AJ, et al. Allergen Specificity of IgG(4)-Expressing B Cells in Patients With Grass Pollen Allergy Undergoing Immunotherapy. *J Allergy Clin Immunol* (2012) 130(3):663–670 e3. doi: 10.1016/j.jaci.2012.04.006
33. Van der Zee S, Aalberse RC. IgG4 and Hyposensitization. *N Engl Reg Allergy Proc* (1987) 8(6):389–91. doi: 10.2500/108854187778999667
34. van der Zee JS, van Swieten P, Aalberse RC. Inhibition of Complement Activation by IgG4 Antibodies. *Clin Exp Immunol* (1986) 64(2):415–22.
35. Margni RA, Perdigon G, Abatangelo C, Gentile T, Binaghi RA. Immunobiological Behaviour of Rabbit Precipitating and non-Precipitating (Co-Precipitating) Antibodies. *Immunology* (1980) 41 (3):681–6.
36. van Toorenenbergen AW, Aalberse RC. IgG4 and Release of Histamine From Human Peripheral Blood Leukocytes. *Int Arch Allergy Appl Immunol* (1982) 67(2):117–22. doi: 10.1159/000233000
37. Aalberse RC, Dieges PH, Knul-Bretlova V, Vooren P, Aalbers M, van Leeuwen J. IgG4 as a Blocking Antibody. *Clin Rev Allergy* (1983) 1 (2):289–302. doi: 10.1007/BF02991163
38. Santos AF, James LK, Bahnson HT, Shamji MH, Couto-Francisco NC, Islam S, et al. IgG4 Inhibits Peanut-Induced Basophil and Mast Cell Activation in Peanut-Tolerant Children Sensitized to Peanut Major Allergens. *J Allergy Clin Immunol* (2015) 135(5):1249–56. doi: 10.1016/j.jaci.2015.01.012
39. Kemeny DM, McKenzie-Mills M, Harries MG, Youlten LJ, Lessof MH. Changes in the Levels of Anti-Phospholipase A2 and Hyaluronidase Antibodies During Bee Venom Immunotherapy. *Monogr Allergy* (1983) 18:150–2.
40. Schumacher MJ, Egen NB, Tanner D. Neutralization of Bee Venom Lethality by Immune Serum Antibodies. *Am J Trop Med Hyg* (1996) 55(2):197–201. doi: 10.4269/ajtmh.1996.55.197
41. Schuurman J, Perdok GJ, Gorter AD, Aalberse RC. The Inter-Heavy Chain Disulfide Bonds of IgG4 are in Equilibrium With Intra-Chain Disulfide Bonds. *Mol Immunol* (2001) 38(1):1–8. doi: 10.1016/S0161-5890(01)00050-5
42. Bloom JW, Madanat MS, Marriott D, Wong T, Chan SY. Intrachain Disulfide Bond in the Core Hinge Region of Human Igg4. *Protein Sci Publ Protein Soc* (1997) 6(2):407–15. doi: 10.1002/pro.5560060217
43. Angal S, King DJ, Bodmer MW, Turner A, Lawson AD, Roberts G, et al. A Single Amino Acid Substitution Abolishes the Heterogeneity of Chimeric Mouse/Human (IgG4) Antibody. *Mol Immunol* (1993) 30(1):105–8. doi: 10.1016/0161-5890(93)90432-B
44. King DJ, Adair JR, Angal S, Low DC, Proudfoot KA, Lloyd JC, et al. Expression, Purification and Characterization of a Mouse-Human Chimeric Antibody and Chimeric Fab' Fragment. *Biochem J* (1992) 281(Pt 2):317–23. doi: 10.1042/bj2810317
45. Margni RA, Binaghi RA. Nonprecipitating Asymmetric Antibodies. *Annu Rev Immunol* (1988) 6:535–54. doi: 10.1146/annurev.iy.06.040188.002535
46. van der Zee JS, van Swieten P, Aalberse RC. Serologic Aspects of IgG4 Antibodies. II. IgG4 Antibodies Form Small, Nonprecipitating Immune Complexes Due to Functional Monovalency. *J Immunol* (1986) 137 (11):3566–71.
47. Petersen JG, Dorrington KJ. An *In Vitro* System for Studying the Kinetics of Interchain Disulfide Bond Formation in Immunoglobulin G. *J Biol Chem* (1974) 249(17):5633–41. doi: 10.1016/S0021-9258(20)79774-7
48. Colcher D, Milenic D, Roselli M, Raubitschek A, Yarranton G, King D, et al. Characterization and Biodistribution of Recombinant and Recombinant/Chimeric Constructs of Monoclonal Antibody B72.3. *Cancer Res* (1989) 49 (7):1738–45.
49. Rispens T, Davies AM, Ooijevaar-de Heer P, Absalah S, Bende O, Sutton BJ, et al. Dynamics of Inter-Heavy Chain Interactions in Human Immunoglobulin G (IgG) Subclasses Studied by Kinetic Fab Arm Exchange. *J Biol Chem* (2014) 289(9):6098–109. doi: 10.1074/jbc.M113.541813
50. Young E, Lock E, Ward DG, Cook A, Harding S, Wallis GL. Estimation of Polyclonal IgG4 Hybrids in Normal Human Serum. *Immunology* (2014) 142 (3):406–13. doi: 10.1111/imm.12265
51. Koneczny I, Stevens JAA, De Rosa A, Huda S, Huijbers MG, Saxena A, et al. IgG4 Autoantibodies Against Muscle-Specific Kinase Undergo Fab-Arm Exchange in Myasthenia Gravis Patients. *J Autoimmun* (2017) 77:104–15. doi: 10.1016/j.jaut.2016.11.005
52. Aalberse RC, Stapel SO, Schuurman J, Rispens T. Immunoglobulin G4: An Odd Antibody. *Clin Exp Allergy* (2009) 39(4):469–77. doi: 10.1111/j.1365-2222.2009.03207.x
53. Collins AM, Davies JM. Enhanced Cell-Binding by Allergen Multimers: How Complex is it? *Immunol Cell Biol* (2013) 91(2):115–7. doi: 10.1038/icb.2013.5
54. Lu Y, Harding SE, Michaelsen TE, Longman E, Davis KG, Ortega A, et al. Solution Conformation of Wild-Type and Mutant IgG3 and IgG4 Immunoglobulins Using Crystallohydrodynamics: Possible Implications for Complement Activation. *Biophys J* (2007) 93(11):3733–44. doi: 10.1529/biophysj.107.108993
55. Abe Y, Gor J, Bracewell DG, Perkins SJ, Dalby PA. Masking of the Fc Region in Human IgG4 by Constrained X-Ray Scattering Modelling: Implications for Antibody Function and Therapy. *Biochem J* (2010) 432(1):101–11. doi: 10.1042/BJ20100641
56. Tao MH, Smith RI, Morrison SL. Structural Features of Human Immunoglobulin G That Determine Isotype-Specific Differences in Complement Activation. *J Exp Med* (1993) 178(2):661–7. doi: 10.1084/jem.178.2.661
57. Brekke OH, Michaelsen TE, Aase A, Sandin RH, Sandlie I. Human IgG Isotype-Specific Amino Acid Residues Affecting Complement-Mediated Cell Lysis and Phagocytosis. *Eur J Immunol* (1994) 24(10):2542–7. doi: 10.1002/eji.1830241042
58. Canfield SM, Morrison SL. The Binding Affinity of Human IgG for its High Affinity Fc Receptor is Determined by Multiple Amino Acids in the CH2 Domain and is Modulated by the Hinge Region. *J Exp Med* (1991) 173 (6):1483–91. doi: 10.1084/jem.173.6.1483
59. Sondermann P, Huber R, Oosthuizen V, Jacob U. The 3.2-A Crystal Structure of the Human IgG1 Fc Fragment-Fc gammaRIII Complex. *Nature* (2000) 406(6793):267–73. doi: 10.1038/35018508
60. Shields RL, Namenuk AK, Hong K, Meng YG, Rae J, Briggs J, et al. High Resolution Mapping of the Binding Site on Human IgG1 for Fc Gamma RI, Fc Gamma RII, Fc Gamma RIII, and FcRn and Design of IgG1 Variants With Improved Binding to the Fc Gamma R. *J Biol Chem* (2001) 276 (9):6591–604. doi: 10.1074/jbc.M009483200
61. Radaev S, Motyka S, Fridman WH, Sautes-Fridman C, Sun PD. The Structure of a Human Type III Fcgamma Receptor in Complex With Fc. *J Biol Chem* (2001) 276(19):16469–77. doi: 10.1074/jbc.M100350200
62. Koneczny I, Cossins J, Waters P, Beeson D, Vincent A. MuSK Myasthenia Gravis IgG4 Disrupts the Interaction of LRP4 With MuSK But Both IgG4 and IgG1-3 can Disperse Preformed Agrin-Independent AChR Clusters. *PloS One* (2013) 8(11):e80695. doi: 10.1371/journal.pone.0080695
63. Huijbers MG, Zhang W, Klooster R, Niks EH, Friese MB, Straasheijm KR, et al. MuSK IgG4 Autoantibodies Cause Myasthenia Gravis by Inhibiting Binding Between MuSK and Lrp4. *Proc Natl Acad Sci U.S.A.* (2013) 110 (51):20783–8. doi: 10.1073/pnas.1313944110
64. Saito M, Stahley SN, Caughman CY, Mao X, Tucker DK, Payne AS, et al. Signaling Dependent and Independent Mechanisms in Pemphigus Vulgaris Blister Formation. *PloS One* (2012) 7(12):e50696. doi: 10.1371/journal.pone.0050696
65. Ishii K, Harada R, Matsuo I, Shirakata Y, Hashimoto K, Amagai M. *In Vitro* Keratinocyte Dissociation Assay for Evaluation of the Pathogenicity of Anti-Desmoglein 3 IgG Autoantibodies in Pemphigus Vulgaris. *J Invest Dermatol* (2005) 124(5):939–46. doi: 10.1111/j.0022-202X.2005.23714.x
66. Payne AS, Ishii K, Kacir S, Lin C, Li H, Hanakawa Y, et al. Genetic and Functional Characterization of Human Pemphigus Vulgaris Monoclonal

Autoantibodies Isolated by Phage Display. *J Clin Invest* (2005) 115(4):888–99. doi: 10.1172/JCI24185
67. Ohkawa T, Fukata Y, Yamasaki M, Miyazaki T, Yokoi N, Takashima H, et al. Autoantibodies to Epilepsy-Related LGI1 in Limbic Encephalitis Neutralize LGI1-ADAM22 Interaction and Reduce Synaptic AMPA Receptors. *J Neurosci* (2013) 33(46):18161–74. doi: 10.1523/JNEUROSCI.3506-13.2013
68. Rock B, Martins CR, Theofilopoulos AN, Balderas RS, Anhalt GJ, Labib RS, et al. The Pathogenic Effect of IgG4 Autoantibodies in Endemic Pemphigus Foliaceus (Fogo Selvagem). *N Engl J Med* (1989) 320(22):1463–9. doi: 10.1056/NEJM198906013202206
69. Spindler V, Eming R, Schmidt E, Amagai M, Grando S, Jonkman MF, et al. Mechanisms Causing Loss of Keratinocyte Cohesion in Pemphigus. *J Invest Dermatol* (2017) 138(1):32–7. doi: 10.1016/j.jid.2017.06.022
70. Thomas MR, de Groot R, Scully MA, Crawley JT. Pathogenicity of Anti-ADAMTS13 Autoantibodies in Acquired Thrombotic Thrombocytopenic Purpura. *EBioMedicine* (2015) 2(8):942–52. doi: 10.1016/j.ebiom.2015.06.007
71. Tsai HM, Lian EC. Antibodies to Von Willebrand Factor-Cleaving Protease in Acute Thrombotic Thrombocytopenic Purpura. *N Engl J Med* (1998) 339 (22):1585–94. doi: 10.1056/NEJM199811263392203
72. Schaller M, Vogel M, Kentouche K, Lammle B, Kremer Hovinga JA. The Splenic Autoimmune Response to ADAMTS13 in Thrombotic Thrombocytopenic Purpura Contains Recurrent Antigen-Binding CDR3 Motifs. *Blood* (2014) 124(23):3469–79. doi: 10.1182/blood-2014-04-561142
73. Pillai S. T and B Lymphocytes in Fibrosis and Systemic Sclerosis. *Curr Opin Rheumatol* (2019) 31(6):576–81. doi: 10.1097/BOR.0000000000000644
74. Milo R. Therapies for Multiple Sclerosis Targeting B Cells. *Croat Med J* (2019) 60(2):87–98. doi: 10.3325/cmj.2019.60.87
75. Karnell JL, Rieder SA, Ettinger R, Kolbeck R. Targeting the CD40-CD40L Pathway in Autoimmune Diseases: Humoral Immunity and Beyond. *Adv Drug Delivery Rev* (2019) 141:92–103. doi: 10.1016/j.addr.2018.12.005
76. Grewal IS, Flavell RA. The Role of CD40 Ligand in Costimulation and T-Cell Activation. *Immunol Rev* (1996) 153:85–106. doi: 10.1111/j.1600-065x.1996.tb00921.x
77. Kornau HC, Kreye J, Stumpf A, Fukata Y, Parthier D, Sammons RP, et al. Human Cerebrospinal Fluid Monoclonal LGI1 Autoantibodies Increase Neuronal Excitability. *Ann Neurol* (2020) 87(3):405–18. doi: 10.1002/ana.25666
78. Yilmaz V, Oflazer P, Aysal F, Parman YG, Direskeneli H, Deymeer F, et al. B Cells Produce Less IL-10, IL-6 and TNF-Alpha in Myasthenia Gravis. *Autoimmunity* (2015) 48(4):201–7. doi: 10.3109/08916934.2014.992517
79. Yilmaz V, Maillard S, Truffault F, Bolgert F, Behin A, Regnard JF, et al. Regulatory B Cells in Myasthenia Gravis are Differentially Affected by Therapies. *Ann Clin Transl Neurol* (2018) 5(11):1408–14. doi: 10.1002/acn3.645
80. Yilmaz V, Ulusoy C, Hajtovic S, Turkoglu R, Kurtuncu M, Tzartos J, et al. Effects of Teriflunomide on B Cell Subsets in MuSK-Induced Experimental Autoimmune Myasthenia Gravis and Multiple Sclerosis. *Immunol Invest* (2020) 50(6):1–14. doi: 10.1080/08820139.2020.1785491
81. Sun F, Ladha SS, Yang L, Liu Q, Shi SX, Su N, et al. Interleukin-10 Producing-B Cells and Their Association With Responsiveness to Rituximab in Myasthenia Gravis. *Muscle Nerve* (2014) 49(4):487–94. doi: 10.1002/mus.23951
82. De Simoni D, Ricken G, Winklehner M, Koneczny I, Karenfort M, Hustedt U, et al. Antibodies to Nodal/Paranodal Proteins in Paediatric Immune-Mediated Neuropathy. *Neurol Neuroimmunol Neuroinflamm* (2020) 7(4): e763. doi: 10.1212/NXI.0000000000000763
83. Martin-Aguilar L, Lleixa C, Pascual-Goni E, Caballero-Avila M, Martinez-Martinez L, Diaz-Manera J, et al. Clinical and Laboratory Features in Anti-NF155 Autoimmune Nodopathy. *Neurol Neuroimmunol Neuroinflamm* (2022) 9(1):e1098. doi: 10.1212/NXI.0000000000001098
84. Shimanovich I, Baumann T, Schmidt E, Zillikens D, Hammers CM. Long-Term Outcomes of Rituximab Therapy in Pemphigus. *J Eur Acad Dermatol Venereol* (2020) 34(12):1884–9. doi: 10.1111/jdv.16561
85. Frampton JE. Rituximab: A Review in Pemphigus Vulgaris. *Am J Clin Dermatol* (2020) 21(1):149–56. doi: 10.1007/s40257-019-00497-9
86. Marino M, Basile U, Spagni G, Napodano C, Iorio R, Gulli F, et al. Long-Lasting Rituximab-Induced Reduction of Specific-But Not Total-IgG4 in MuSK-Positive Myasthenia Gravis. *Front Immunol* (2020) 11:613. doi: 10.3389/fimmu.2020.00613
87. Topakian R, Zimprich F, Iglseder S, Embacher N, Guger M, Stieglbauer K, et al. High Efficacy of Rituximab for Myasthenia Gravis: A Comprehensive Nationwide Study in Austria. *J Neurol* (2019) 266(3):699–706. doi: 10.1007/s00415-019-09191-6
88. Hehir MK, Hobson-Webb LD, Benatar M, Barnett C, Silvestri NJ, Howard JF Jr, et al. Rituximab as Treatment for Anti-MuSK Myasthenia Gravis: Multicenter Blinded Prospective Review. *Neurology* (2017) 89(10):1069–77. doi: 10.1212/WNL.0000000000004341
89. Jestin M, Benhamou Y, Schelpe AS, Roose E, Provot F, Galicier L, et al. Preemptive Rituximab Prevents Long-Term Relapses in Immune-Mediated Thrombotic Thrombocytopenic Purpura. *Blood* (2018) 132(20):2143–53. doi: 10.1182/blood-2018-04-840090
90. Westwood JP, Thomas M, Alwan F, McDonald V, Benjamin S, Lester WA, et al. Rituximab Prophylaxis to Prevent Thrombotic Thrombocytopenic Purpura Relapse: Outcome and Evaluation of Dosing Regimens. *Blood Adv* (2017) 1(15):1159–66. doi: 10.1182/bloodadvances.2017008268
91. Arkatkar T, Du SW, Jacobs HM, Dam EM, Hou B, Buckner JH, et al. B Cell-Derived IL-6 Initiates Spontaneous Germinal Center Formation During Systemic Autoimmunity. *J Exp Med* (2017) 214(11):3207–17. doi: 10.1084/jem.20170580
92. Kabuto M, Fujimoto N, Tanaka T. Increase of Interleukin-10-Producing B Cells Associated With Long-Term Remission After I.V. Immunoglobulin Treatment for Pemphigus. *J Dermatol* (2016) 43(7):815–8. doi: 10.1111/1346-8138.13295
93. Pollmann R, Walter E, Schmidt T, Waschke J, Hertl M, Mobs C, et al. Identification of Autoreactive B Cell Subpopulations in Peripheral Blood of Autoimmune Patients With Pemphigus Vulgaris. *Front Immunol* (2019) 10:1375. doi: 10.3389/fimmu.2019.01375
94. Zhu HQ, Xu RC, Chen YY, Yuan HJ, Cao H, Zhao XQ, et al. Impaired Function of CD19(+) CD24(hi) CD38(hi) Regulatory B Cells in Patients With Pemphigus. *Br J Dermatol* (2015) 172(1):101–10. doi: 10.1111/bjd.13192
95. Becerra E, Scully MA, Leandro MJ, Heelas EO, Westwood JP, de la Torre I, et al. Effect of Rituximab on B Cell Phenotype and Serum B Cell-Activating Factor Levels in Patients With Thrombotic Thrombocytopenic Purpura. *Clin Exp Immunol* (2015) 179(3):414–25. doi: 10.1111/cei.12472
96. Punnonen J, Aversa G, Cocks BG, McKenzie AN, Menon S, Zurawski G, et al. Interleukin 13 Induces Interleukin 4-Independent IgG4 and IgE Synthesis and CD23 Expression by Human B Cells. *Proc Natl Acad Sci U.S.A.* (1993) 90(8):3730–4. doi: 10.1073/pnas.90.8.3730
97. Meiler F, Zumkehr J, Klunker S, Ruckert B, Akdis CA, Akdis M. *In Vivo* Switch to IL-10-Secreting T Regulatory Cells in High Dose Allergen Exposure. *J Exp Med* (2008) 205(12):2887–98. doi: 10.1084/jem.20080193
98. Meiler F, Klunker S, Zimmermann M, Akdis CA, Akdis M. Distinct Regulation of IgE, IgG4 and IgA by T Regulatory Cells and Toll-Like Receptors. *Allergy* (2008) 63(11):1455–63. doi: 10.1111/j.1398-9995.2008.01774.x
99. Jeannin P, Lecoanet S, Delneste Y, Gauchat JF, Bonnefoy JY. IgE Versus IgG4 Production can be Differentially Regulated by IL-10. *J Immunol* (1998) 160(7):3555–61.
100. Satoguina JS, Weyand E, Larbi J, Hoerauf A. T Regulatory-1 Cells Induce IgG4 Production by B Cells: Role of IL-10. *J Immunol* (2005) 174(8):4718–26. doi: 10.4049/jimmunol.174.8.4718
101. Satoguina JS, Adjobimey T, Arndts K, Hoch J, Oldenburg J, Layland LE, et al. Tr1 and Naturally Occurring Regulatory T Cells Induce IgG4 in B Cells Through GITR/GITR-L Interaction, IL-10 and TGF-Beta. *Eur J Immunol* (2008) 38(11):3101–13. doi: 10.1002/eji.200838193
102. Mizoguchi A, Mizoguchi E, Takedatsu H, Blumberg RS, Bhan AK. Chronic Intestinal Inflammatory Condition Generates IL-10-Producing Regulatory B Cell Subset Characterized by CD1d Upregulation. *Immunity* (2002) 16 (2):219–30. doi: 10.1016/S1074-7613(02)00274-1
103. Rosser EC, Mauri C. Regulatory B Cells: Origin, Phenotype, and Function. *Immunity* (2015) 42(4):607–12. doi: 10.1016/j.immuni.2015.04.005
104. Fillatreau S, Sweenie CH, McGeachy MJ, Gray D, Anderton SM. B Cells Regulate Autoimmunity by Provision of IL-10. *Nat Immunol* (2002) 3 (10):944–50. doi: 10.1038/ni833

105. Fillatreau S. Natural Regulatory Plasma Cells. *Curr Opin Immunol* (2018) 55:62–6. doi: 10.1016/j.coi.2018.09.012
106. van de Veen W, Stanic B, Yaman G, Wawrzyniak M, Sollner S, Akdis DG, et al. IgG4 Production is Confined to Human IL-10-Producing Regulatory B Cells That Suppress Antigen-Specific Immune Responses. *J Allergy Clin Immunol* (2013) 131(4):1204–12. doi: 10.1016/j.jaci.2013.01.014
107. Lin AA, Freeman AF, Nutman TB. IL-10 Indirectly Downregulates IL-4-Induced IgE Production by Human B Cells. *Immunohorizons* (2018) 2 (11):398–406. doi: 10.4049/immunohorizons.1800076
108. Vickery BP, Lin J, Kulis M, Fu Z, Steele PH, Jones SM, et al. Peanut Oral Immunotherapy Modifies IgE and IgG4 Responses to Major Peanut Allergens. *J Allergy Clin Immunol* (2013) 131(1):128–34.e1-3. doi: 10.1016/j.jaci.2012.10.048
109. Caubet JC, Lin J, Ahrens B, Gimenez G, Bardina L, Niggemann B, et al. Natural Tolerance Development in Cow's Milk Allergic Children: IgE and IgG4 Epitope Binding. *Allergy* (2017) 72(11):1677–85. doi: 10.1111/all.13167
110. Sabater L, Planaguma J, Dalmau J, Graus F. Cellular Investigations With Human Antibodies Associated With the Anti-IgLON5 Syndrome. *J Neuroinflamm* (2016) 13(1):226. doi: 10.1186/s12974-016-0689-1
111. Shelly S, Klein CJ, Dyck PJB, Paul P, Mauermann ML, Berini SE, et al. Neurofascin-155 Immunoglobulin Subtypes: Clinicopathologic Associations and Neurologic Outcomes. *Neurology* (2021) 97(24):e2392–403. doi: 10.1212/WNL.0000000000012932
112. McConville J, Farrugia ME, Beeson D, Kishore U, Metcalfe R, Newsom-Davis J, et al. Detection and Characterization of MuSK Antibodies in Seronegative Myasthenia Gravis. *Ann Neurol* (2004) 55(4):580–4. doi: 10.1002/ana.20061
113. Kadoya M, Kaida K, Koike H, Takazaki H, Ogata H, Moriguchi K, et al. IgG4 Anti-Neurofascin155 Antibodies in Chronic Inflammatory Demyelinating Polyradiculoneuropathy: Clinical Significance and Diagnostic Utility of a Conventional Assay. *J Neuroimmunol* (2016) 301:16–22. doi: 10.1016/j.jneuroim.2016.10.013
114. Pascual-Goni E, Fehmi J, Lleixa C, Martin-Aguilar L, Devaux J, Hoftberger R, et al. Antibodies to the Caspr1/contactin-1 Complex in Chronic Inflammatory Demyelinating Polyradiculoneuropathy. *Brain* (2021) 144 (4):1183–96. doi: 10.1093/brain/awab014
115. Appeltshauser L, Brunder AM, Heinius A, Kortvelyessy P, Wandinger KP, Junker R, et al. Antiparanodal Antibodies and IgG Subclasses in Acute Autoimmune Neuropathy. *Neurol Neuroimmunol Neuroinflamm* (2020) 7 (5):e817. doi: 10.1212/NXI.0000000000000817
116. Doppler K, Schuster Y, Appeltshauser L, Biko L, Villmann C, Weishaupt A, et al. Anti-CNTN1 IgG3 Induces Acute Conduction Block and Motor Deficits in a Passive Transfer Rat Model. *J Neuroinflamm* (2019) 16(1):73. doi: 10.1186/s12974-019-1462-z
117. Kanigicherla D, Gummadova J, McKenzie EA, Roberts SA, Harris S, Nikam M, et al. Anti-PLA2R Antibodies Measured by ELISA Predict Long-Term Outcome in a Prevalent Population of Patients With Idiopathic Membranous Nephropathy. *Kidney Int* (2013) 83(5):940–8. doi: 10.1038/ki.2012.486
118. Segawa Y, Hisano S, Matsushita M, Fujita T, Hirose S, Takeshita M, et al. IgG Subclasses and Complement Pathway in Segmental and Global Membranous Nephropathy. *Pediatr Nephrol* (2010) 25(6):1091–9. doi: 10.1007/s00467-009-1439-8
119. Sinkovits G, Szilagyi A, Farkas P, Inotai D, Szilvasi A, Tordai A, et al. Concentration and Subclass Distribution of Anti-ADAMTS13 IgG Autoantibodies in Different Stages of Acquired Idiopathic Thrombotic Thrombocytopenic Purpura. *Front Immunol* (2018) 9:1646. doi: 10.3389/fimmu.2018.01646
120. Ellebrecht CT, Mukherjee EM, Zheng Q, Choi EJ, Reddy SG, Mao X, et al. Autoreactive IgG and IgA B Cells Evolve Through Distinct Subclass Switch Pathways in the Autoimmune Disease Pemphigus Vulgaris. *Cell Rep* (2018) 24(9):2370–80. doi: 10.1016/j.celrep.2018.07.093
121. Recke A, Konitzer S, Lemcke S, Freitag M, Sommer NM, Abdelhady M, et al. The P.Arg435His Variation of IgG3 With High Affinity to FcRn Is Associated With Susceptibility for Pemphigus Vulgaris-Analysis of Four Different Ethnic Cohorts. *Front Immunol* (2018) 9:1788. doi: 10.3389/fimmu.2018.01788
122. Ayatollahi M, Joubeh S, Mortazavi H, Jefferis R, Ghaderi A. IgG4 as the Predominant Autoantibody in Sera From Patients With Active State of Pemphigus Vulgaris. *J Eur Acad Dermatol Venereol* (2004) 18(2):241–2. doi: 10.1111/j.1468-3083.2004.00708.x
123. Futei Y, Amagai M, Ishii K, Kuroda-Kinoshita K, Ohya K, Nishikawa T. Predominant IgG4 Subclass in Autoantibodies of Pemphigus Vulgaris and Foliaceus. *J Dermatol Sci* (2001) 26(1):55–61. doi: 10.1016/S0923-1811(00)00158-4
124. Bhol K, Mohimen A, Ahmed AR. Correlation of Subclasses of IgG With Disease Activity in Pemphigus Vulgaris. *Dermatology* (1994) 189 Suppl 1:85–9. doi: 10.1159/000246938
125. Spaeth S, Riechers R, Borradori L, Zillikens D, Budinger L, Hertl M. IgG, IgA and IgE Autoantibodies Against the Ectodomain of Desmoglein 3 in Active Pemphigus Vulgaris. *Br J Dermatol* (2001) 144(6):1183–8. doi: 10.1046/j.1365-2133.2001.04228.x
126. Koshte VL, Aalbers M, Calkhoven PG, Aalberse RC. The Potent IgG4-Inducing Antigen in Banana is a Mannose-Binding Lectin, BanLec-I. *Int Arch Allergy Immunol* (1992) 97(1):17–24. doi: 10.1159/000236090
127. Culver EL, Vermeulen E, Makuch M, van Leeuwen A, Sadler R, Cargill T, et al. Increased IgG4 Responses to Multiple Food and Animal Antigens Indicate a Polyclonal Expansion and Differentiation of Pre-Existing B Cells in IgG4-Related Disease. *Ann Rheum Dis* (2015) 74(5):944–7. doi: 10.1136/annrheumdis-2014-206405
128. Basile U, Marino M, Napodano C, Pocino K, Alboini PE, Gulli F, et al. Serological Immunoglobulin-Free Light Chain Profile in Myasthenia Gravis Patients. *J Immunol Res* (2018) 2018:9646209. doi: 10.1155/2018/9646209
129. Funakoshi T, Lunardon L, Ellebrecht CT, Nagler AR, O'Leary CE, Payne AS. Enrichment of Total Serum IgG4 in Patients With Pemphigus. *Br J Dermatol* (2012) 167(6):1245–53. doi: 10.1111/j.1365-2133.2012.11144.x
130. Strijbos E, Huijbers MG, van Es IE, Alleman I, van Ostaijen-Ten Dam MM, Bakker J, et al. A Prospective, Placebo Controlled Study on the Humoral Immune Response to and Safety of Tetanus Revaccination in Myasthenia Gravis. *Vaccine* (2017) 35(46):6290–6. doi: 10.1016/j.vaccine.2017.09.078
131. Ulusoy C, Kim E, Tuzun E, Huda R, Yilmaz V, Poulas K, et al. Preferential Production of IgG1, IL-4 and IL-10 in MuSK-Immunized Mice. *Clin Immunol* (2014) 151(2):155–63. doi: 10.1016/j.clim.2014.02.012
132. Kucukerden M, Huda R, Tuzun E, Yilmaz A, Skriapa L, Trakas N, et al. MuSK Induced Experimental Autoimmune Myasthenia Gravis Does Not Require IgG1 Antibody to MuSK. *J Neuroimmunol* (2016) 295–296:84–92. doi: 10.1016/j.jneuroim.2016.04.003
133. Takahashi H, Kuwana M, Amagai M. A Single Helper T Cell Clone is Sufficient to Commit Polyclonal Naive B Cells to Produce Pathogenic IgG in Experimental Pemphigus Vulgaris. *J Immunol* (2009) 182(3):1740–5. doi: 10.4049/jimmunol.182.3.1740
134. Ohyama M, Amagai M, Tsunoda K, Ota T, Koyasu S, Hata J, et al. Immunologic and Histopathologic Characterization of an Active Disease Mouse Model for Pemphigus Vulgaris. *J Invest Dermatol* (2002) 118(1):199–204. doi: 10.1046/j.0022-202x.2001.01643.x
135. Huda R, Strait RT, Tuzun E, Finkelman FD, Christadoss P. IgG1 Deficiency Exacerbates Experimental Autoimmune Myasthenia Gravis in BALB/c Mice. *J Neuroimmunol* (2015) 281:68–72. doi: 10.1016/j.jneuroim.2015.03.004
136. Klooster R, Plomp JJ, Huijbers MG, Niks EH, Straasheijm KR, Detmers FJ, et al. Muscle-Specific Kinase Myasthenia Gravis IgG4 Autoantibodies Cause Severe Neuromuscular Junction Dysfunction in Mice. *Brain J Neurol* (2012) 135(Pt 4):1081–101. doi: 10.1093/brain/aws025
137. Amagai M. Pemphigus Vulgaris and its Active Disease Mouse Model. *Curr Dir Autoimmun* (2008) 10:167–81. doi: 10.1159/000131453
138. Ostertag EM, Bdeir K, Kacir S, Thiboutot M, Gulendran G, Yunk L, et al. ADAMTS13 Autoantibodies Cloned From Patients With Acquired Thrombotic Thrombocytopenic Purpura: 2. Pathogenicity in an animal model. . *Transfusion* (2016) 56(7):1775–85. doi: 10.1111/trf.13583
139. Coppo P, Lammle B. Animal Models of Thrombotic Thrombocytopenic Purpura: The Tales From Zebrafish. *Haematologica* (2020) 105(4):861–3. doi: 10.3324/haematol.2019.245043
140. Vanhoorelbeke K, De Meyer SF. Animal Models for Thrombotic Thrombocytopenic Purpura. *J Thromb Haemost* (2013) 11 Suppl:1, 2–10. doi: 10.1111/jth.12255

141. Takahashi H, Amagai M, Nishikawa T, Fujii Y, Kawakami Y, Kuwana M. Novel System Evaluating *In Vivo* Pathogenicity of Desmoglein 3-Reactive T Cell Clones Using Murine Pemphigus Vulgaris. *J Immunol* (2008) 181 (2):1526–35. doi: 10.4049/jimmunol.181.2.1526
142. Cho MJ, Ellebrecht CT, Payne AS. The Dual Nature of Interleukin-10 in Pemphigus Vulgaris. *Cytokine* (2015) 73(2):335–41. doi: 10.1016/j.cyto.2014.11.002
143. Marchenko S, Chernyavsky AI, Arredondo J, Gindi V, Grando SA. Antimitochondrial Autoantibodies in Pemphigus Vulgaris: A Missing Link in Disease Pathophysiology. *J Biol Chem* (2010) 285(6):3695–704. doi: 10.1074/jbc.M109.081570
144. Buelli S, Perico L, Galbusera M, Abbate M, Morigi M, Novelli R, et al. Mitochondrial-Dependent Autoimmunity in Membranous Nephropathy of IgG4-Related Disease. *EBioMedicine* (2015) 2(5):456–66. doi: 10.1016/j.ebiom.2015.03.003
145. Kalantari-Dehaghi M, Chen Y, Deng W, Chernyavsky A, Marchenko S, Wang PH, et al. Mechanisms of Mitochondrial Damage in Keratinocytes by Pemphigus Vulgaris Antibodies. *J Biol Chem* (2013) 288(23):16916–25. doi: 10.1074/jbc.M113.472100
146. Ozkok E, Durmus H, Yetimler B, Tasli H, Trakas N, Ulusoy C, et al. Reduced Muscle Mitochondrial Enzyme Activity in MuSK-Immunized Mice. *Clin Neuropathol* (2015) 34(6):359–63. doi: 10.5414/NP300875
147. Aysit-Altuncu N, Ulusoy C, Ozturk G, Tuzun E. Effect of LGI1 Antibody-Positive IgG on Hippocampal Neuron Survival: A Preliminary Study. *Neuroreport* (2018) 29(11):932–8. doi: 10.1097/WNR.0000000000001055
148. Tuzun E, Li J, Wanasen N, Soong L, Christadoss P. Immunization of Mice With T Cell-Dependent Antigens Promotes IL-6 and TNF-Alpha Production in Muscle Cells. *Cytokine* (2006) 35(1-2):100–6. doi: 10.1016/j.cyto.2006.05.009
149. Shen L, Lu G, Dong N, Ma Z, Ruan C. Simvastatin Increases ADAMTS13 Expression in Podocytes. *Thromb Res* (2013) 132(1):94–9. doi: 10.1016/j.thromres.2013.05.024
150. Landa J, Gaig C, Plaguma J, Saiz A, Antonell A, Sanchez-Valle R, et al. Effects of IgLON5 Antibodies on Neuronal Cytoskeleton: A Link Between Autoimmunity and Neurodegeneration. *Ann Neurol* (2020) 88(5):1023–7. doi: 10.1002/ana.25857
151. Gaig C, Graus F, Compta Y, Hogl B, Bataller L, Bruggemann N, et al. Clinical Manifestations of the Anti-IgLON5 Disease. *Neurology* (2017) 88(18):1736–43. doi: 10.1212/WNL.0000000000003887
152. Borges LS, Richman DP. Muscle-Specific Kinase Myasthenia Gravis. *Front Immunol* (2020) 11:707. doi: 10.3389/fimmu.2020.00707
153. Dalmau J, Geis C, Graus F. Autoantibodies to Synaptic Receptors and Neuronal Cell Surface Proteins in Autoimmune Diseases of the Central Nervous System. *Physiol Rev* (2017) 97(2):839–87. doi: 10.1152/physrev.00010.2016
154. Porro AM, Seque CA, Ferreira MCC, Enokihara M. Pemphigus Vulgaris. *Bras Dermatol* (2019) 94(3):264–78. doi: 10.1590/abd1806-4841.20199011
155. Guptill JT, Sanders DB, Evoli A. Anti-MuSK Antibody Myasthenia Gravis: Clinical Findings and Response to Treatment in Two Large Cohorts. *Muscle Nerve* (2011) 44(1):36–40. doi: 10.1002/mus.22006
156. Thompson J, Bi M, Murchison AG, Makuch M, Bien CG, Chu K, et al. The Importance of Early Immunotherapy in Patients With Faciobrachial Dystonic Seizures. *Brain* (2018) 141(2):348–56. doi: 10.1093/brain/awx323
157. Yanovsky RL, McLeod M, Ahmed AR. Treatment of Pemphigus Vulgaris: Part 1 - Current Therapies. *Expert Rev Clin Immunol* (2019) 15(10):1047–60. doi: 10.1080/1744666X.2020.1672535
158. Dietzen DJ. 13 - Amino Acids, Peptides, and Proteins. In: E Rifai, AR Horvath and CT Wittwer, editors. *In: Principles and Applications of Molecular Diagnostics*. Elsevier (2018). Available at: 10.1016/B978-0-12-816061-9.00013-8
159. Bell WR, Braine HG, Ness PM, Kickler TS. Improved Survival in Thrombotic Thrombocytopenic Purpura-Hemolytic Uremic Syndrome. Clinical Experience in 108 Patients. *N Engl J Med* (1991) 325(6):398–403. doi: 10.1056/NEJM199108083250605
160. Gilhus NE, Tzartos S, Evoli A, Palace J, Burns TM, Verschuuren J. Myasthenia Gravis. *Nat Rev Dis Primers* (2019) 5(1):30. doi: 10.1038/s41572-019-0079-y
161. Deguchi K, Matsuzono K, Nakano Y, Kono S, Sato K, Deguchi S, et al. Anti-MuSK Antibody-Positive Myasthenia Gravis Successfully Treated With Outpatient Periodic Weekly Blood Purification Therapy. *Intern Med* (2018) 57(10):1455–8. doi: 10.2169/internalmedicine.9466-17
162. Eming R, Hertl M. Immunoadsorption in Pemphigus. *Autoimmunity* (2006) 39(7):609–16. doi: 10.1080/08916930600972040
163. Sagi L, Baum S, Gendelman V, Trau H, Barzilai A. The Role of Therapeutic Plasma Exchange in Pemphigus Vulgaris. *J Eur Acad Dermatol Venereol* (2011) 25(1):82–6. doi: 10.1111/j.1468-3083.2010.03703.x
164. Zhang Y, Huang HJ, Chen WB, Liu G, Liu F, Su YY. Clinical Efficacy of Plasma Exchange in Patients With Autoimmune Encephalitis. *Ann Clin Transl Neurol* (2021) 8(4):763–73. doi: 10.1002/acn3.51313
165. Dorst J, Fillies F, Dreyhaupt J, Senel M, Tumani H. Safety and Tolerability of Plasma Exchange and Immunoadsorption in Neuroinflammatory Diseases. *J Clin Med* (2020) 9(9):2874. doi: 10.3390/jcm9092874
166. Dalakas MC. IgG4-Mediated Neurologic Autoimmunities: Understanding the Pathogenicity of IgG4, Ineffectiveness of IVIg, and Long-Lasting Benefits of Anti-B Cell Therapies. *Neurol Neuroimmunol Neuroinflamm* (2022) 9(1): e1116. doi: 10.1212/NXI.0000000000001116
167. Nelke C, Spatola M, Schroeter CB, Wiendl H, Lunemann JD. Neonatal Fc Receptor-Targeted Therapies in Neurology. *Neurotherapeutics* (2022). doi: 10.1007/s13311-021-01175-7
168. Dalakas MC, Spaeth PJ. The Importance of FcRn in Neuro-Immunotherapies: From IgG Catabolism, FCGRT Gene Polymorphisms, IVIg Dosing and Efficiency to Specific FcRn Inhibitors. *Ther Adv Neurol Disord* (2021) 14:1756286421997381. doi: 10.1177/1756286421997381
169. Yu Z, Lennon VA. Mechanism of Intravenous Immune Globulin Therapy in Antibody-Mediated Autoimmune Diseases. *N Engl J Med* (1999) 340(3):227–8. doi: 10.1056/NEJM199901213400311
170. Vidarsson G, Dekkers G, Rispens T. IgG Subclasses and Allotypes: From Structure to Effector Functions. *Front Immunol* (2014) 5:520. doi: 10.3389/fimmu.2014.00520
171. Blumberg LJ, Humphries JE, Jones SD, Pearce LB, Holgate R, Hearn A, et al. Blocking FcRn in Humans Reduces Circulating IgG Levels and Inhibits IgG Immune Complex-Mediated Immune Responses. *Sci Adv* (2019) 5(12): eaax9586. doi: 10.1126/sciadv.aax9586
172. Sultan Y, Kazatchkine MD, Maisonneuve P, Nydegger UE. Anti-Idiotypic Suppression of Autoantibodies to Factor VIII (Antihaemophilic Factor) by High-Dose Intravenous Gammaglobulin. *Lancet* (1984) 2(8406):765–8. doi: 10.1016/s0140-6736(84)90701-3
173. Dalakas MC. Intravenous Immunoglobulin in Autoimmune Neuromuscular Diseases. *JAMA* (2004) 291(19):2367–75. doi: 10.1001/jama.291.19.2367
174. Kohler H, Pashov A, Kieber-Emmons T. The Promise of Anti-Idiotype Revisited. *Front Immunol* (2019) 10:808. doi: 10.3389/fimmu.2019.00808
175. Park-Min KH, Serbina NV, Yang W, Ma X, Krystal G, Neel BG, et al. FcgammaRIII-Dependent Inhibition of Interferon-Gamma Responses Mediates Suppressive Effects of Intravenous Immune Globulin. *Immunity* (2007) 26(1):67–78. doi: 10.1016/j.immuni.2006.11.010
176. Lunemann JD, Nimmerjahn F, Dalakas MC. Intravenous Immunoglobulin in Neurology–Mode of Action and Clinical Efficacy. *Nat Rev Neurol* (2015) 11(2):80–9. doi: 10.1038/nrneurol.2014.253
177. Le Pottier L, Sapir T, Bendaoud B, Youinou P, Shoenfeld Y, Pers JO. Intravenous Immunoglobulin and Cytokines: Focus on Tumor Necrosis Factor Family Members BAFF and APRIL. *Ann N Y Acad Sci* (2007) 1110:426–32. doi: 10.1196/annals.1423.044
178. Spellberg B. Mechanism of Intravenous Immune Globulin Therapy. *N Engl J Med* (1999) 341(1):57–8. doi: 10.1056/nejm199907013410115
179. Anthony RM, Kobayashi T, Wermeling F, Ravetch JV. Intravenous Gammaglobulin Suppresses Inflammation Through a Novel T(H)2 Pathway. *Nature* (2011) 475(7354):110–3. doi: 10.1038/nature10134
180. Bayry J, Lacroix-Desmazes S, Carbonneil C, Misra N, Donkova V, Pashov A, et al. Inhibition of Maturation and Function of Dendritic Cells by Intravenous Immunoglobulin. *Blood* (2003) 101(2):758–65. doi: 10.1182/blood-2002-05-1447
181. Bayry J, Lacroix-Desmazes S, Delignat S, Mouthon L, Weill B, Kazatchkine MD, et al. Intravenous Immunoglobulin Abrogates Dendritic Cell Differentiation Induced by Interferon-Alpha Present in Serum From

Patients With Systemic Lupus Erythematosus. *Arthritis Rheum* (2003) 48 (12):3497–502. doi: 10.1002/art.11346
182. Kozicky LK, Zhao ZY, Menzies SC, Fidanza M, Reid GS, Wilhelmsen K, et al. Intravenous Immunoglobulin Skews Macrophages to an Anti-Inflammatory, IL-10-Producing Activation State. *J Leukoc Biol* (2015) 98(6):983–94. doi: 10.1189/jlb.3VMA0315-078R
183. Jacob S, Rajabally YA. Current Proposed Mechanisms of Action of Intravenous Immunoglobulins in Inflammatory Neuropathies. *Curr Neuropharmacol* (2009) 7(4):337–42. doi: 10.2174/157015909790031166
184. Rodriguez A, Klein CJ, Sechi E, Alden E, Basso MR, Pudumjee S, et al. LGI1 Antibody Encephalitis: Acute Treatment Comparisons and Outcome. *J Neurol Neurosurg Psychiatry* (2021) 93(3):309–15. doi: 10.1136/jnnp-2021-327302
185. Dubey D, Britton J, McKeon A, Gadoth A, Zekeridou A, Lopez Chiriboga SA, et al. Randomized Placebo-Controlled Trial of Intravenous Immunoglobulin in Autoimmune LGI1/CASPR2 Epilepsy. *Ann Neurol* (2020) 87(2):313–23. doi: 10.1002/ana.25655
186. Amagai M, Ikeda S, Shimizu H, Iizuka H, Hanada K, Aiba S, et al. A Randomized Double-Blind Trial of Intravenous Immunoglobulin for Pemphigus. *J Am Acad Dermatol* (2009) 60(4):595–603. doi: 10.1016/j.jaad.2008.09.052
187. Green MG, Bystryn JC. Effect of Intravenous Immunoglobulin Therapy on Serum Levels of IgG1 and IgG4 Antidesmoglein 1 and Antidesmoglein 3 Antibodies in Pemphigus Vulgaris. *Arch Dermatol* (2008) 144(12):1621–4. doi: 10.1001/archdermatol.2008.503
188. Rajabally YA. Long-Term Immunoglobulin Therapy for Chronic Inflammatory Demyelinating Polyradiculoneuropathy. *Muscle Nerve* (2015) 51(5):657–61. doi: 10.1002/mus.24554
189. Klehmet J, Meisel C, Meisel A. Efficiency of Long-Term Treatment With Intravenous Immunoglobulins Correlates With Reduced Autoreactive T Cell Responses in Chronic Inflammatory Demyelinating Polyneuropathy Patients. *Clin Exp Immunol* (2014) 178 Suppl:1, 149–50. doi: 10.1111/cei.12549
190. Tackenberg B, Nimmerjahn F, Lunemann JD. Mechanisms of IVIG Efficacy in Chronic Inflammatory Demyelinating Polyneuropathy. *J Clin Immunol* (2010) 30 Suppl:1, S65–9. doi: 10.1007/s10875-010-9398-1
191. Massoud AH, Guay J, Shalaby KH, Bjur E, Ablona A, Chan D, et al. Intravenous Immunoglobulin Attenuates Airway Inflammation Through Induction of Forkhead Box Protein 3-Positive Regulatory T Cells. *J Allergy Clin Immunol* (2012) 129(6):1656–65 e3. doi: 10.1016/j.jaci.2012.02.050
192. Ephrem A, Chamat S, Miquel C, Fisson S, Mouthon L, Caligiuri G, et al. Expansion of CD4+CD25+ Regulatory T Cells by Intravenous Immunoglobulin: A Critical Factor in Controlling Experimental Autoimmune Encephalomyelitis. *Blood* (2008) 111(2):715–22. doi: 10.1182/blood-2007-03-079947
193. Tandan R, Hehir MK2nd, Waheed W, Howard DB. Rituximab Treatment of Myasthenia Gravis: A Systematic Review. *Muscle Nerve* (2017) 56(2):185–96. doi: 10.1002/mus.25597
194. Hill ME, Shiono H, Newsom-Davis J, Willcox N. The Myasthenia Gravis Thymus: A Rare Source of Human Autoantibody-Secreting Plasma Cells for Testing Potential Therapeutics. *J Neuroimmunol* (2008) 201–202:50–6. doi: 10.1016/j.jneuroim.2008.06.027
195. Shiono H, Wong YL, Matthews I, Liu JL, Zhang W, Sims G, et al. Spontaneous Production of Anti-IFN-Alpha and Anti-IL-12 Autoantibodies by Thymoma Cells From Myasthenia Gravis Patients Suggests Autoimmunization in the Tumor. *Int Immunol* (2003) 15(8):903–13. doi: 10.1093/intimm/dxg088
196. Fujii Y, Hashimoto J, Monden Y, Ito T, Nakahara K, Kawashima Y. Specific Activation of Lymphocytes Against Acetylcholine Receptor in the Thymus in Myasthenia Gravis. *J Immunol* (1986) 136(3):887–91.
197. Hain B, Jordan K, Deschauer M, Zierz S. Successful Treatment of MuSK Antibody-Positive Myasthenia Gravis With Rituximab. *Muscle Nerve* (2006) 33(4):575–80. doi: 10.1002/mus.20479
198. Diaz-Manera J, Martinez-Hernandez E, Querol L, Klooster R, Rojas-Garcia R, Suarez-Calvet X, et al. Long-Lasting Treatment Effect of Rituximab in MuSK Myasthenia. *Neurology* (2012) 78(3):189–93. doi: 10.1212/WNL.0b013e3182407982
199. Illa I, Diaz-Manera J, Rojas-Garcia R, Pradas J, Rey A, Blesa R, et al. Sustained Response to Rituximab in Anti-AChR and Anti-MuSK Positive Myasthenia Gravis Patients. *J Neuroimmunol* (2008) 201–202:90–4. doi: 10.1016/j.jneuroim.2008.04.039
200. Nowak RJ, DiCapua DB, Zebardast N, Goldstein JM. Response of Patients With Refractory Myasthenia Gravis to Rituximab: A Retrospective Study. *Ther Adv Neurol Disord* (2011) 4(5):259–66. doi: 10.1177/1756285611411503
201. Keung B, Robeson K, DiCapua DB, Rosen JB, O'Connor KC, Goldstein JM, et al. Long Term Efficacy of Rituximab in Patients With MuSK Autoantibody Myasthenia Gravis. *J Neurol Neurosurg Psychiatry* (2013) 84:1407–9. doi: 10.1136/jnnp-2012-303664
202. Zografou C, Vakrakou AG, Stathopoulos P. Short- and Long-Lived Autoantibody-Secreting Cells in Autoimmune Neurological Disorders. *Front Immunol* (2021) 12:686466. doi: 10.3389/fimmu.2021.686466
203. Jiao L, Xiang Y, Li S, Zhang F, Ruan X, Guo S. Efficacy of Low Dose Rituximab in Treatment-Resistant CIDP With Antibodies Against NF-155. *J Neuroimmunol* (2020) 345:577280. doi: 10.1016/j.jneuroim.2020.577280
204. Wallace ZS, Mattoo H, Mahajan VS, Kulikova M, Lu L, Deshpande V, et al. Predictors of Disease Relapse in IgG4-Related Disease Following Rituximab. *Rheumatol (Oxford)* (2016) 55(6):1000–8. doi: 10.1093/rheumatology/kev438
205. Uhl L, Kiss JE, Malynn E, Terrell DR, Vesely SK, George JN. Rituximab for Thrombotic Thrombocytopenic Purpura: Lessons From the STAR Trial. *Transfusion* (2017) 57(10):2532–8. doi: 10.1111/trf.14193
206. Chen H, Fu A, Wang J, Wu T, Li Z, Tang J, et al. Rituximab as First-Line Treatment for Acquired Thrombotic Thrombocytopenic Purpura. *J Int Med Res* (2017) 45(3):1253–60. doi: 10.1177/0300060517695646
207. Scully M, McDonald V, Cavenagh J, Hunt BJ, Longair I, Cohen H, et al. A Phase 2 Study of the Safety and Efficacy of Rituximab With Plasma Exchange in Acute Acquired Thrombotic Thrombocytopenic Purpura. *Blood* (2011) 118(7):1746–53. doi: 10.1182/blood-2011-03-341131
208. Mignard C, Maho-Vaillant M, Golinski ML, Balaye P, Prost-Squarcioni C, Houivet E, et al. Factors Associated With Short-Term Relapse in Patients With Pemphigus Who Receive Rituximab as First-Line Therapy: A Post Hoc Analysis of a Randomized Clinical Trial. *JAMA Dermatol* (2020) 156(5):545–52. doi: 10.1001/jamadermatol.2020.0290
209. Chen DM, Odueyungbo A, Csinady E, Gearhart L, Lehane P, Cheu M, et al. Rituximab is an Effective Treatment in Patients With Pemphigus Vulgaris and Demonstrates a Steroid-Sparing Effect. *Br J Dermatol* (2020) 182 (5):1111–9. doi: 10.1111/bjd.18482
210. Hamadah I, Chisti MA, Haider M, Binamer Y, Alajlan S, Aleyouni Y, et al. Rituximab/IVIG in Pemphigus - a 10-Year Study With a Long Follow-Up. *J Dermatol Treat* (2019) 30(2):170–5. doi: 10.1080/09546634.2018.1484873
211. Tavakolpour S, Mahmoudi H, Balighi K, Abedini R, Daneshpazhooh M. Sixteen-Year History of Rituximab Therapy for 1085 Pemphigus Vulgaris Patients: A Systematic Review. *Int Immunopharmacol* (2018) 54:131–8. doi: 10.1016/j.intimp.2017.11.005
212. Joly P, Maho-Vaillant M, Prost-Squarcioni C, Hebert V, Houivet E, Calbo S, et al. First-Line Rituximab Combined With Short-Term Prednisone Versus Prednisone Alone for the Treatment of Pemphigus (Ritux 3): A Prospective, Multicentre, Parallel-Group, Open-Label Randomised Trial. *Lancet* (2017) 389(10083):2031–40. doi: 10.1016/S0140-6736(17)30070-3
213. Keung B, Robeson KR, DiCapua DB, Rosen JB, O'Connor KC, Goldstein JM, et al. Long-Term Benefit of Rituximab in MuSK Autoantibody Myasthenia Gravis Patients. *J Neurol Neurosurg Psychiatry* (2013) 84(12):1407–9. doi: 10.1136/jnnp-2012-303664
214. Thaler FS, Zimmermann L, Kammermeier S, Strippel C, Ringelstein M, Kraft A, et al. Rituximab Treatment and Long-Term Outcome of Patients With Autoimmune Encephalitis: Real-World Evidence From the GENERATE Registry. *Neurol Neuroimmunol Neuroinflamm* (2021) 8(6):e1088. doi: 10.1212/NXI.0000000000001088
215. Irani SR, Gelfand JM, Bettcher BM, Singhal NS, Geschwind MD. Effect of Rituximab in Patients With Leucine-Rich, Glioma-Inactivated 1 Antibody-Associated Encephalopathy. *JAMA Neurol* (2014) 71(7):896–900. doi: 10.1001/jamaneurol.2014.463
216. Lee WJ, Lee ST, Byun JI, Sunwoo JS, Kim TJ, Lim JA, et al. Rituximab Treatment for Autoimmune Limbic Encephalitis in an Institutional Cohort. *Neurology* (2016) 86(18):1683–91. doi: 10.1212/WNL.0000000000002635
217. Tomschik M, Hilger E, Rath J, Mayer EM, Fahrner M, Cetin H, et al. Subgroup Stratification and Outcome in Recently Diagnosed Generalized

Myasthenia Gravis. *Neurology* (2020) 95(10):e1426–36. doi: 10.1212/WNL.0000000000010209
218. Sanders DB, Wolfe GI, Benatar M, Evoli A, Gilhus NE, Illa I, et al. International Consensus Guidance for Management of Myasthenia Gravis: Executive Summary. *Neurology* (2016) 87(4):419–25. doi: 10.1212/WNL.0000000000002790
219. Hebert V, Vermeulin T, Tanguy L, Tedbirt B, Mignard C, Benichou J, et al. Comparison of Real Costs in the French Healthcare System in Newly Diagnosed Patients With Pemphigus for First-Line Treatment With Rituximab vs. Standard Corticosteroid Regimen: Data From a National Multicentre Trial. *Br J Dermatol* (2019) 183(1):121–7. doi: 10.1111/bjd.18563
220. Gomez AM, Willcox N, Molenaar PC, Buurman W, Martinez-Martinez P, De Baets MH, et al. Targeting Plasma Cells With Proteasome Inhibitors: Possible Roles in Treating Myasthenia Gravis? *Ann N Y Acad Sci* (2012) 1274:48–59. doi: 10.1111/j.1749-6632.2012.06824.x
221. Gomez AM, Willcox N, Vrolix K, Hummel J, Nogales-Gadea G, Saxena A, et al. Proteasome Inhibition With Bortezomib Depletes Plasma Cells and Specific Autoantibody Production in Primary Thymic Cell Cultures From Early-Onset Myasthenia Gravis Patients. *J Immunol* (2014) 193(3):1055–63. doi: 10.4049/jimmunol.1301555
222. Gomez AM, Vrolix K, Martinez-Martinez P, Molenaar PC, Phernambucq M, van der Esch E, et al. Proteasome Inhibition With Bortezomib Depletes Plasma Cells and Autoantibodies in Experimental Autoimmune Myasthenia Gravis. *J Immunol* (2011) 186(4):2503–13. doi: 10.4049/jimmunol.1002539
223. Schneider-Gold C, Reinacher-Schick A, Ellrichmann G, Gold R. Bortezomib in Severe MuSK-Antibody Positive Myasthenia Gravis: First Clinical Experience. *Ther Adv Neurol Disord* (2017) 10(10):339–41. doi: 10.1177/1756285617721093
224. Schroeder C, Back C, Koc U, Strassburger-Krogias K, Reinacher-Schick A, Gold R, et al. Breakthrough Treatment With Bortezomib for a Patient With Anti-NMDAR Encephalitis. *Clin Neurol Neurosurg* (2018) 172:24–6. doi: 10.1016/j.clineuro.2018.06.005
225. Sveinsson O, Granqvist M, Forslin Y, Blennow K, Zetterberg H, Piehl F. Successful Combined Targeting of B- and Plasma Cells in Treatment Refractory Anti-NMDAR Encephalitis. *J Neuroimmunol* (2017) 312:15–8. doi: 10.1016/j.jneuroim.2017.08.011
226. Turnbull MT, Siegel JL, Becker TL, Stephens AJ, Lopez-Chiriboga AS, Freeman WD. Early Bortezomib Therapy for Refractory Anti-NMDA Receptor Encephalitis. *Front Neurol* (2020) 11:188. doi: 10.3389/fneur.2020.00188
227. Wickel J, Chung HY, Platzer S, Lehmann T, Pruss H, Leypoldt F, et al. Generate-Boost: Study Protocol for a Prospective, Multicenter, Randomized Controlled, Double-Blinded Phase II Trial to Evaluate Efficacy and Safety of Bortezomib in Patients With Severe Autoimmune Encephalitis. *Trials* (2020) 21(1):625. doi: 10.1186/s13063-020-04516-7
228. Pitarokoili K, Yoon MS, Kroger I, Reinacher-Schick A, Gold R, Schneider-Gold C. Severe Refractory CIDP: A Case Series of 10 Patients Treated With Bortezomib. *J Neurol* (2017) 264(9):2010–20. doi: 10.1007/s00415-017-8599-4
229. Fels M, Fisse AL, Schwake C, Motte J, Athanasopoulos D, Gruter T, et al. Report of a Fulminant Anti-Pan-Neurofascin-Associated Neuropathy Responsive to Rituximab and Bortezomib. *J Peripher Nerv Syst* (2021) 26 (4):475–80. doi: 10.1111/jns.12465
230. Eskazan AE. Bortezomib Therapy in Patients With Relapsed/Refractory Acquired Thrombotic Thrombocytopenic Purpura. *Ann Hematol* (2016) 95(11):1751–6. doi: 10.1007/s00277-016-2804-x
231. Patriquin CJ, Thomas MR, Dutt T, McGuckin S, Blombery PA, Cranfield T, et al. Bortezomib in the Treatment of Refractory Thrombotic Thrombocytopenic Purpura. *Br J Haematol* (2016) 173(5):779–85. doi: 10.1111/bjh.13993
232. Shortt J, Oh DH, Opat SS. ADAMTS13 Antibody Depletion by Bortezomib in Thrombotic Thrombocytopenic Purpura. *N Engl J Med* (2013) 368(1):90–2. doi: 10.1056/NEJMc1213206
233. Pandey MR, Vachhani P, Ontiveros EP. Remission of Severe, Relapsed, and Refractory TTP After Multiple Cycles of Bortezomib. *Case Rep Hematol* (2017) 2017:9681832. doi: 10.1155/2017/9681832
234. Khan ML, Colby TV, Viggiano RW, Fonseca R. Treatment With Bortezomib of a Patient Having Hyper IgG4 Disease. *Clin Lymphoma Myeloma Leuk* (2010) 10(3):217–9. doi: 10.3816/CLML.2010.n.034
235. Mazzi G, Raineri A, Zanolli FA, Da Ponte C, De Roia D, Santarossa L, et al. Plasmapheresis Therapy in Pemphigus Vulgaris and Bullous Pemphigoid. *Transfus Apher Sci* (2003) 28(1):13–8. doi: 10.1016/S1473-0502(02)00095-2
236. Hahn AF, Bolton CF, Pillay N, Chalk C, Benstead T, Bril V, et al. Plasma-Exchange Therapy in Chronic Inflammatory Demyelinating Polyneuropathy. A Double-Blind, Sham-Controlled, Cross-Over Study. *Brain* (1996) 119(Pt 4):1055–66. doi: 10.1093/brain/119.4.1055
237. Dyck PJ, Daube J, O'Brien P, Pineda A, Low PA, Windebank AJ, et al. Plasma Exchange in Chronic Inflammatory Demyelinating Polyradiculoneuropathy. *N Engl J Med* (1986) 314(8):461–5. doi: 10.1056/NEJM198602203140801
238. Didona D, Maglie R, Eming R, Hertl M. Pemphigus: Current and Future Therapeutic Strategies. *Front Immunol* (2019) 10:1418. doi: 10.3389/fimmu.2019.01418
239. Kremer Hovinga JA, Coppo P, Lammle B, Moake JL, Miyata T, Vanhoorelbeke K. Thrombotic Thrombocytopenic Purpura. *Nat Rev Dis Primers* (2017) 3:17020. doi: 10.1038/nrdp.2017.20
240. Liu S, Dong C, Ubogu EE. Immunotherapy of Guillain-Barre Syndrome. *Hum Vaccin Immunother* (2018) 14(11):2568–79. doi: 10.1080/21645515.2018.1493415
241. Hermetter C, Fazekas F, Hochmeister S. Systematic Review: Syndromes, Early Diagnosis, and Treatment in Autoimmune Encephalitis. *Front Neurol* (2018) 9:706. doi: 10.3389/fneur.2018.00706
242. Apaydin S. The Treatment of ANCA-Associated Rapidly-Progressive Glomerulonephritis and Goodpasture Syndrome With Therapeutic Apheresis. *Transfus Apher Sci* (2018) 57(1):8–12. doi: 10.1016/j.transci.2018.02.007
243. Aoyama Y, Moriya C, Kamiya K, Nagai M, Rubenstein D, Iwatsuki K, et al. Catabolism of Pemphigus Foliaceus Autoantibodies by High-Dose IVIg Therapy. *Eur J Dermatol* (2011) 21(1):58–61. doi: 10.1684/ejd.2011.1169
244. Roopenian DC, Akilesh S. FcRn: The Neonatal Fc Receptor Comes of Age. *Nat Rev Immunol* (2007) 7(9):715–25. doi: 10.1038/nri2155
245. Skriapa L, Zisimopoulou P, Trakas N, Grapsa E, Tzartos SJ. Expression of Extracellular Domains of Muscle Specific Kinase (MuSK) and Use as Immunoadsorbents for the Development of an Antigen-Specific Therapy. *J Neuroimmunol* (2014) 276(1-2):150–8. doi: 10.1016/j.jneuroim.2014.09.013
246. Lazaridis K, Baltatzidou V, Tektonidis N, Tzartos SJ. Antigen-Specific Immunoadsorption of MuSK Autoantibodies as a Treatment of MuSK-Induced Experimental Autoimmune Myasthenia Gravis. *J Neuroimmunol* (2020) 339:577136. doi: 10.1016/j.jneuroim.2019.577136
247. Langenhan J, Dworschak J, Saschenbrecker S, Komorowski L, Schlumberger W, Stocker W, et al. Specific Immunoadsorption of Pathogenic Autoantibodies in Pemphigus Requires the Entire Ectodomains of Desmogleins. *Exp Dermatol* (2014) 23(4):253–9. doi: 10.1111/exd.12355
248. Reuveni D, Aricha R, Souroujon MC, Fuchs S. MuSK EAMG: Immunological Characterization and Suppression by Induction of Oral Tolerance. *Front Immunol* (2020) 11:403. doi: 10.3389/fimmu.2020.00403
249. Souroujon MC, Maiti PK, Feferman T, Im SH, Raveh L, Fuchs S. Suppression of Myasthenia Gravis by Antigen-Specific Mucosal Tolerance and Modulation of Cytokines and Costimulatory Factors. *Ann N Y Acad Sci* (2003) 998:533–6. doi: 10.1196/annals.1254.069
250. Maiti PK, Feferman T, Im SH, Souroujon MC, Fuchs S. Immunosuppression of Rat Myasthenia Gravis by Oral Administration of a Syngeneic Acetylcholine Receptor Fragment. *J Neuroimmunol* (2004) 152(1-2):112–20. doi: 10.1016/j.jneuroim.2004.04.010
251. Consonni A, Sharma S, Schon K, Lebrero-Fernandez C, Rinaldi E, Lycke NY, et al. A Novel Approach to Reinstating Tolerance in Experimental Autoimmune Myasthenia Gravis Using a Targeted Fusion Protein, Mcta1-T146. *Front Immunol* (2017) 8:1133. doi: 10.3389/fimmu.2017.01133
252. Sheng JR, Quan S, Soliven B. IL-10 Derived From CD1dhiCD5(+) B Cells Regulates Experimental Autoimmune Myasthenia Gravis. *J Neuroimmunol* (2015) 289:130–8. doi: 10.1016/j.jneuroim.2015.10.023
253. Akiyama M, Suzuki K, Yamaoka K, Yasuoka H, Takeshita M, Kaneko Y, et al. Number of Circulating Follicular Helper 2 T Cells Correlates With IgG4 and Interleukin-4 Levels and Plasmablast Numbers in IgG4-Related Disease. *Arthritis Rheumatol* (2015) 67(9):2476–81. doi: 10.1002/art.39209
254. Akiyama M, Yasuoka H, Yoshimoto K, Takeuchi T. Interleukin-4 Contributes to the Shift of Balance of IgG Subclasses Toward IgG4 in IgG4-Related Disease. *Cytokine* (2018) 110:416–9. doi: 10.1016/j.cyto.2018.05.009

255. Kamisawa T, Zen Y, Pillai S, Stone JH. IgG4-Related Disease. *Lancet* (2015) 385(9976):1460–71. doi: 10.1016/S0140-6736(14)60720-0
256. Simpson RS, Lau SKC, Lee JK. Dupilumab as a Novel Steroid-Sparing Treatment for IgG4-Related Disease. *Ann Rheumat Dis* (2020) 79(4):549–50. doi: 10.1136/annrheumdis-2019-216368
257. Ebbo M, De Sainte-Marie B, Muller R, Piperoglou C, Grados A, Vely F, et al. Comment on Article: 'Dupilumab as a Novel Steroid-Sparing Treatment for IgG4-Related Disease' by Simpson Et al. *Ann Rheum Dis* (2020) 81(2). doi: 10.1136/annrheumdis-2020-217010
258. Chaker AM, Shamji MH, Dumitru FA, Calderon MA, Scadding GW, Makatsori M, et al. Short-Term Subcutaneous Grass Pollen Immunotherapy Under the Umbrella of Anti-IL-4: A Randomized Controlled Trial. *J Allergy Clin Immunol* (2016) 137(2):452–61.e9. doi: 10.1016/j.jaci.2015.08.046

Conflict of Interest: JT and ST have shares in the research and diagnostic laboratory Tzartos NeuroDiagnostics, Athens. FL discloses having received speaker honoraria from Grifols, Teva, Biogen, Bayer, Roche, Novartis, Fresenius, travel funding from Merck, Grifols and Bayer and serving on advisory boards for Roche, Biogen and Alexion. MH Is a member of the European Reference Network for Rare Neuromuscular Diseases and The Netherlands Neuromuscular Center. MH is a co-inventor on two patent applications on MuSK-related research. LUMC and MH receive license income from these patents. LUMC receives royalties on a MuSK ELISA.

The remaining authors declare that the research was conducted in the absence of any commercial or financial relationships that could be construed as a potential conflict of interest.

Publisher's Note: All claims expressed in this article are solely those of the authors and do not necessarily represent those of their affiliated organizations, or those of the publisher, the editors and the reviewers. Any product that may be evaluated in this article, or claim that may be made by its manufacturer, is not guaranteed or endorsed by the publisher.

GLOSSARY

AChEi	Acetylcholinesterase inhibitors
AChR	Acetylcholine receptor
ADAM22	ADAM metallopeptidase domain 22
ADAMTS13	A disintegrin and metalloprotease with thrombospondin type 1 motif 13
ADCC	Antibody-dependent cellular cytotoxicity
AIDP	Acute inflammatory demyelinating polyneuropathy
AMPAR	α-amino-3-hydroxy-5-methyl-4-isoxazolepropionic acid receptor
Bregs	Regulatory B-cells
Caspr2	Contactin associated protein 2
CCL3	C-c motif chemokine ligand 3
CIDP	Chronic inflammatory demyelinating polyneuropathy
CNTN1	Contactin 1
DPPX	Dipeptidyl-peptidase–like protein-6
Dsg-1 Dsg-3	Desmoglein-1, desmoglein-3
EAMG	Experimental autoimmune myasthenia gravis
FAE	Fab-arm exchange
GABAaR	Gamma-aminobutyric acid a receptor
GABAbR	Gamma-aminobutyric acid b receptor
GITR	Glucocorticoid-induced tumour necrosis factor receptor-related protein
GITR-L	GITR- ligand
GM-CSF	Granulocyte macrophage colony-stimulating factor
HLA	Human lymphocyte antigen
IFN-γ	Interferon gamma
IgG4-AID	IgG4 autoimmune diseases
IgG4-RLD	IgG4 related disease
IgLON5	Immunoglobulin-like cell adhesion molecule 5
IL	Interleukin (IL-4
IL-10	IL-13)
IL-4Rα	Interleukin 4 receptor alpha
IVIG	Intravenous immunoglobulin
KO	Knock out
LGI1	Leucine rich glioma inactivated 1
LRP4	Low density lipoprotein receptor-related protein 4
MG	Myasthenia gravis
MN	Membranous nephropathy
MuSK	Muscle specific kinase
NMDAR	N-methyl-D-aspartate receptor
PBMC	Peripheral blood mononuclear cell
PF	Pemphigus foliaceus
PLA2R	Phospholipase A2 receptor
PLEX	Plasmapheresis or plasma exchange
PV	Pemphigus vulgaris
TNF-α	Tumor necrosis factor alpha
Tregs	Regulatory T cells
THSD7A	Thrombospondin type 1 domain containing 7a
TTP	Thrombotic thrombocytopenic purpura
vWF	Von Willebrand factor

frontiers | Frontiers in Immunology

ORIGINAL RESEARCH
published: 07 July 2022
doi: 10.3389/fimmu.2022.952235

The Alternative Pathway Is Necessary and Sufficient for Complement Activation by Anti-THSD7A Autoantibodies, Which Are Predominantly IgG4 in Membranous Nephropathy

Pallavi Manral[1], *Tiffany N. Caza*[2], *Aaron J. Storey*[3], *Laurence H. Beck Jr*[4] *and Dorin-Bogdan Borza*[1]*

[1] Department of Microbiology, Immunology and Physiology, Meharry Medical College, Nashville, TN, United States, [2] Arkana Laboratories, Little Rock, AR, United States, [3] Department of Biochemistry and Molecular Biology, University of Arkansas for Medical Sciences, Little Rock, AR, United States, [4] Department of Medicine (Nephrology), Boston University School of Medicine and Boston Medical Center, Boston, MA, United States

OPEN ACCESS

Edited by:
Erdem Tüzün,
Istanbul University, Turkey

Reviewed by:
Liu Baoli,
Beijing Hospital of Traditional Chinese Medicine, Capital Medical University, China
Gunther Zahner,
University Medical Center Hamburg-Eppendorf, Germany
Andrey Cybulsky,
McGill University Health Centre, Canada

***Correspondence:**
Dorin-Bogdan Borza
dborza@mmc.edu

Specialty section:
This article was submitted to B Cell Biology, a section of the journal Frontiers in Immunology

Received: 24 May 2022
Accepted: 16 June 2022
Published: 07 July 2022

Citation:
Manral P, Caza TN, Storey AJ, Beck LH Jr and Borza D-B (2022) The Alternative Pathway Is Necessary and Sufficient for Complement Activation by Anti-THSD7A Autoantibodies, Which Are Predominantly IgG4 in Membranous Nephropathy. Front. Immunol. 13:952235. doi: 10.3389/fimmu.2022.952235

Membranous nephropathy (MN) is an immune kidney disease characterized by glomerular subepithelial immune complexes (ICs) containing antigen, IgG, and products of complement activation. Whereas proteinuria is caused by complement-mediated podocyte injury, the pathways of complement activation remain controversial due to the predominance of IgG4 in ICs, an IgG subclass considered unable to activate complement. THSD7A, a transmembrane protein expressed on podocytes, is the target autoantigen in ~3% of cases of primary MN. In this study, we analyzed sera from 16 patients with THSD7A-associated MN with regard to the anti-THSD7A IgG subclasses and their ability to fix complement *in vitro*. The serum concentration of anti-THSD7A IgG varied over two orders of magnitude (1.3-243 μg/mL). As a relative proportion of all IgG anti-THSD7A, IgG4 was by far the most abundant subclass (median 79%), followed by IgG1 (median 11%). IgG4 was the dominant subclass of anti-THSD7A antibodies in 14 sera, while IgG1 was dominant in one and co-dominant in another. One quarter of MN sera additionally contained low levels of anti-THSD7A IgA1. ICs formed by predominantly IgG4 anti-THSD7A autoantibodies with immobilized THSD7A were relatively weak activators of complement *in vitro*, compared to human IgG1 and IgG3 mAbs used as positive control. Complement deposition on THSD7A ICs was dose-dependent and occurred to a significant extent only at relatively high concentration of anti-THSD7A IgG. C3b fixation by THSD7A ICs was completely abolished in factor B-depleted sera, partially inhibited in C4-depleted sera, unchanged in C1q-depleted sera, and also occurred in Mg-EGTA buffer. These results imply that THSD7A ICs predominantly containing IgG4 activate

complement at high IgG4 density, which strictly requires a functional alternative pathway, whereas the classical and lectin pathways are dispensable. These findings advance our understanding of how IgG4 antibodies activate complement.

Keywords: complement activation, alternative pathway of complement, membranous nephropathy, THSD7A (thrombospondin type 1 domain-containing protein 7A), IgG4 antibodies

INTRODUCTION

Membranous nephropathy (MN), one of the leading causes of nephrotic syndrome in adults, is an antibody-mediated kidney disease clinically characterized by proteinuria, often heavy and persistent. MN is a disease of heterogeneous etiology, defined histologically by immune complexes (ICs) deposited on the subepithelial side of glomerular basement membrane (GBM), together with GBM thickening and podocyte foot process effacement, but without proliferative changes. The most prevalent form is the so-called "primary" MN, an autoimmune disease in which IgG autoantibodies (autoAbs) form subepithelial ICs with autoantigens expressed on podocyte cell surface (1, 2). About 70% of patients with primary MN have autoAbs targeting phospholipase A2 receptor (PLA2R), and an additional 3-5% have autoAbs targeting thrombospondin type-1 domain-containing 7A (THSD7A) (3, 4). Serologic assays established for both PLA2R and THSD7A show that circulating autoAb levels correlate to disease activity, are useful for therapeutic monitoring, and inform prognosis (5–8). Recent studies have identified additional autoantigens or biomarkers implicated in MN, including neural epidermal growth factor-like 1 (9), exostosin 1/2 (10), serine protease HTRA1 (11), neural cell adhesion molecule-1 (12), semaphorin 3B (13), protocadherin 7 (14), transforming growth factor beta receptor 3 (15), and contactin (16).

In the current paradigm for the pathogenesis of MN based on studies in passive Heymann nephritis, complement activation by subepithelial ICs leading to sublethal podocyte injury by C5b-9 is a major effector mechanism of proteinuria (17). In human MN, complement activation products are abundant in subepithelial deposits. Nonetheless, because the autoAbs implicated in PLA2R- and THSD7A-associated MN are predominantly of the IgG4 subclass (7, 17–20), how ICs activate complement in MN remains a conundrum (21). IgG4 does not bind C1q and is considered unable to activate complement, at least not *via* the classical pathway (22–24). Yet, ICs formed by model monoclonal human IgG4 antibodies are capable of activating complement *via* the alternative pathway under certain circumstances, i.e. at high IgG concentrations and high epitope density (25–27).

In PLA2R-associated MN, it has been reported that altered glycosylation (degalactosylation) of IgG4 autoAbs promotes the binding of mannose-binding lectin (MBL) and complement activation *via* the lectin pathway, which mediates injury of human podocytes in culture (28). One caveat is that MBL binding to IgG4 purified by acid elution may be artifactual, given that acid denaturation of human IgG was reported to increase MBL binding to an even greater extent than IgG degalactosylation (29). PLA2R-associated MN can in fact occur in individuals with complete MBL deficiency, in whom complement is activated solely *via* the alternative pathway, implying that the lectin pathway is dispensable (30). Another study has found that the classical pathway initiates and the alternative pathway amplifies complement activation by model immune complexes formed by anti-PLA2R1 autoAbs *in vitro*, suggesting a role for non-IgG4 autoAbs (31). Finally, a proteomic analysis of complement proteins in glomeruli from PLA2R1-associated MN suggests that both classical/lectin and alternative pathways drive and contribute to the activation of terminal pathway (32).

In THSD7A-associated MN, there is agreement that autoAbs are predominantly IgG4, but the relative proportion of other IgG subclasses is less clear. Some studies have shown low abundance of IgG1, IgG2 and IgG3 anti-THSD7A (4, 20), yet others have shown relatively intense staining for IgG1, IgG2 and IgG3, in addition to IgG4 (33). These differences are likely due to the use of qualitative assays, without standardization of subclass-specific secondary antibodies. Since the four IgG subclasses show wide variation in regard to their effector properties (23), the goal of this study was to quantitatively measure the serum levels of anti-THSD7A IgG subclasses and investigate the functional properties of anti-THSD7A autoAbs, i.e, their ability to activate complement *in vitro*.

MATERIALS AND METHODS

Materials

The recombinant human THSD7A was purchased from R&D (9524-TH, Minneapolis, Minnesota). Fresh-frozen normal human serum and complement C1q-, C4-, or factor B-depleted human sera in which more than 99% of the functional protein was depleted were from Complement Technologies (Tyler, Texas). Recombinant monoclonal human IgG1, IgG2, IgG3 and IgG4 anti-TNFα antibodies were purchased from InvivoGen (San Diego, California). Recombinant monoclonal human IgG1, IgG2, IgG3, IgG4, and IgA1 anti-GFP antibodies were from BioRad (Hercules, California). Recombinant human TNFα and *A. victoria* GFP were purchased from Millipore (Burlington, Massachusetts) and Abcam, respectively.

Abbreviations: AP, alternative pathway; FB, factor B; FP, properdin; GFP, green fluorescent protein; GVB, gelatin-veronal buffer; MBL, mannose binding lectin; MN, membranous nephropathy; NHS, normal human serum; PLA2R, phospholipase A2 receptor; TCC, terminal complement complex (C5b-9); THSD7A, thrombospondin type-1 domain-containing 7A.

Serum samples from THSD7A-associated MN patients had been collected Boston Medical Center, or obtained from banked residual sera from patients who underwent indirect immunofluorescence testing for anti-THSD7A antibodies at Arkana Laboratories. All serum samples were collected with informed consent under IRB-approved protocols at each institution. All included patients had a positive test of 1:10 or greater by the Euroimmun indirect immunofluorescence test (IIFT). The demographic and clinical characteristics are summarized in **Table 1**. The study cohort comprised 6 males and 10 females and included 7 Caucasians, 5 African-Americans and 2 Asians. The average age ± SD was 60 ± 20 years. The median values for proteinuria, serum albumin, and serum creatinine were 7.5 g/day, 2.7 g/dL, and 0.87 mg/dL, respectively. The results of routine IF staining in the biopsy were available for 12 cases, shown in **Table 2**. All biopsies showed positive staining for IgG and C3. IgA, IgM and C1q staining were negative, except for one case with weak IgM and another with weak IgA staining.

Quantitative Analysis of Serum Levels of Anti-THSD7A AutoAb Subclasses by ELISA

Serum antibodies binding to THSD7A were assayed by ELISA. Briefly, 96-well Nunc MaxiSorp microtiter plates (ThermoFisher Scientific, Waltham, Massachusetts) were coated overnight with THSD7A (150 ng per well) in carbonate-bicarbonate buffer, pH 9.6. After blocking with 1% bovine serum albumin (BSA), the wells were incubated for 1 hour with patient or control sera diluted 1/100. Some samples required further dilution (1/200-1/1,600) for IgG4 detection. Secondary antibodies were horseradish peroxidase-conjugated sheep anti-human IgG1-4 (The Binding Site, Birmingham, UK), goat anti-human IgA, and mouse anti-human IgA1 and IgA2 (Southern Biotech, Birmingham, Alabama). Plates were developed with TMB Microwell peroxidase substrate (VWR, Radnor, Pennsylvania), and absorbance was read at 650 nm with an ELISA plate reader (BioRad). A blank correction was applied to all values by subtracting the OD in antigen-coated wells incubated with buffer instead of serum. In parallel experiments, standard curves for human IgG1-IgG4 were generated by incubating known concentrations of recombinant human monoclonal IgG1-IgG4 anti-TNFα (2-500 ng/ml) in wells coated with recombinant TNFα (150 ng/well in carbonate buffer pH 9.6). A standard curve for IgA was generated by incubating human IgA1 anti-GFP mAb in wells coated with GFP. The serum concentration of anti-THSD7A IgG subclasses or IgA was interpolated from the standard curves by a non-linear regression assuming a one-site specific binding model.

In Vitro Complement Activation Assay

We developed a new functional assay to investigate the ability of anti-THSD7A autoAbs to fix complement. ELISA plates were coated with THSD7A protein (200 ng in 50 µl PBS), overnight at 4°C. The plates were next blocked with 1% BSA in phosphate-buffered saline (PBS) for 1 hour at room temperature, washed, and then incubated for 1 hour with sera from MN patients or non-MN controls (diluted 1/25 in PBS with 0.1% BSA and 0.05% Tween-20/PBS). Next, plates were washed again and incubated for 30 minutes at 37°C with fresh-frozen normal human serum (NHS) diluted 10% in gelatin-veronal buffer (GVB) containing 0.15 mM Ca^{2+} and 0.5 mM Mg^{2+}, in which all three complement activation pathways are functional. In some experiments, NHS was diluted in GVB with 5 mM MgEGTA (which inhibits the classical and lectin pathways), or in GVB with 10 mM EDTA (which inhibits all complement activation pathways). In other experiments, C1q-, C4-, and factor B-depleted sera were used instead of NHS. After a wash step, deposition of complement activation products was assayed. The deposition of C3b and its proteolytic inactivation product, iC3b, was detected with sheep anti-human C3c-HRP (BioRad, 2222-6604P) diluted 1:1000. C5b-9 (terminal complement complex, TCC) deposition was detected with mouse anti-human TCC mAb (HM 2167S, Hycult Biotech) diluted 1:500. Properdin (FP) was detected using mouse anti-human properdin mAb (Hycult Biotech, HM2283S) diluted 1:500. C1q and factor B (FB) were detected using goat anti-human C1q and goat anti-human FB antibodies (Quidel), diluted 1:2000. C4 was detected using goat anti-human C4 antibodies (Complement Technologies, A205) diluted 1:40000. The secondary antibodies were goat anti-mouse IgG-HRP diluted 1:2000 and donkey anti-goat IgG-HRP diluted 1:10000 (both from Invitrogen). The absorbance at 650 nm was read after color development with peroxidase substrate. In parallel assays, complement activation was also performed in wells coated with GFP (200 ng/50 µl in carbonate buffer, pH 9.6) and incubated with various concentrations (1-5 µg/mL) of human monoclonal anti-GFP IgG1κ, IgG3κ and IgG4ʎ.

TABLE 1 | Demographic and clinical characteristics of anti-THSD7A positive patients.

Patient characteristics	Result
Number of cases	16
Sex: M/F	6 (37.5%):10 (62.5%)
Age (yr)	61 (47 – 77)
Ethnicity: White:	7 (43.8%)
African-American:	5 (31.2%)
Asian:	2 (12.5%)
Unknown	2 (12.5%)
Proteinuria (g/day)	7.5 (2.8 – 10.4)
Serum albumin (g/dL)	2.7 (1.89 – 3.6)
Serum creatinine (mg/dL)	0.87 (0.80 – 1.47)

Values are median (interquartile range) or number (%).

TABLE 2 | The results of immunofluorescence staining in the MN renal biopsies.

Patient #	IgG	IgA	IgM	C3	C1q
MN-1	3+	0	0	1+	0
MN-2	4+	1+	0	3+	0
MN-3	4+	0	0	2+	0
MN-4	3+	0	0	1+	0
MN-5	3+	0	trace	1+	0
MN-6	2+	0	0	1+	0
MN-7	4+	0	0	2+	0
MN-8	1+	N.D.[a]	N.D.[a]	N.D.[a]	N.D.[a]
MN-9	positive	0	0	positive	0
MN-11	3+	0	1+	1+	0
MN-13	3+	0	0	1+	0
MN-14	3+	0	0	2+	N.D.
MN-15	4+	0	0	3+	0

[a]*N.D., Not determined; no glomeruli in IF sample.*

Statistical Analyses

Analyses were performed using GraphPad Prism 8.4 software (San Diego, CA). The significance of differences among groups was determined by one-way ANOVA followed by Bonferroni's test for pairwise comparisons, or by repeated measures ANOVA with the Geisser-Greenhouse correction, followed by Dunnet's multiple comparisons test. Other statistical analyses are described in the text or the figure legends. A multiplicity-adjusted value of $P < 0.05$ was considered statistically significant.

RESULTS

IgG4 Is the Dominant Subclass of Anti-THSD7A AutoAbs

Circulating autoAbs were analyzed in 16 sera from patients with THSD7A-associated MN along with four normal sera used as controls. To quantitatively measure the levels of anti-THSD7A subclasses, standard/calibration curves were generated using serial dilutions of anti-TNFα human IgG1-IgG4 mAbs bound to immobilized TNFα (**Figure 1A**). The total concentration of anti-THSD7A IgG varied over a broad range (1.3-243 μg/mL), spanning over two orders of magnitude (**Figure 1B**), consistent with previous reports (8). The anti-THSD7A IgG levels measured by ELISA and the anti-THSD7A titers measured by a commercial indirect immunofluorescence test (IIFT) were significantly correlated (**Figure 1C**). The mean ± SD for anti-THSD7A IgG in control sera was 0.14 ± 0.18 μg/ml. Among IgG autoAbs, the relative proportion of IgG4 was the highest (median 79%, interquartile range IQR 62%-88%), followed by IgG1 (median 11%, IQR 4.8%-31%), while the proportions of IgG2 (median 2.8%, IQR 1.8%-6.2%), and IgG3 (median 1.5%, IQR 0.7%-7%) were low (**Figure 1D**). Although IgG4 was the dominant subclass of anti-THSD7A in the majority of MN sera (14/16), IgG1 was dominant in one case (MN-8, diagnosed as secondary MN based on the EM findings in the biopsy), and co-dominant in another (MN-5). For four cases for which IgG subclass staining was performed on the kidney biopsy, the intensity of the staining showed a good correlation with the results of serologic assays for anti-THSD7A IgG subclasses (**Table 3**).

We further analyzed the possible presence of other isotypes of anti-THSD7A autoAbs. Interestingly, a quarter of MN sera (4/16) were positive for IgA anti-THSD7A (**Figure 2A**). However, the levels of IgA autoAbs were relatively low (0.26-1.03 μg/mL), corresponding to 0.2%-0.5% of the levels of IgG autoAbs in the respective sera. Further analysis of subclasses of anti-THSD7A IgA revealed the presence of IgA1 (**Figure 2B**) but not IgA2 (**Figure 2C**). IgM or IgE anti-THSD7A were not detected (data not shown).

Anti-THSD7A Antibodies Bound to THSD7A Antigen Activate Complement *In Vitro*

We developed a new functional assay to investigate the ability of serum anti-THSD7A autoAbs to activate complement *in vitro* (**Figure 3A**). First, immobilized THSD7A was incubated with diluted MN sera to form plate-bound ICs. In control experiments performed in parallel, human anti-GFP IgG3 and IgG4 mAbs were bound to immobilized GFP to prepare reference ICs. Next, 10% normal human serum diluted in buffer containing Ca^{2+} and Mg^{2+} was added as a source of complement, and then complement activation products deposited onto the ICs were detected using specific antibodies (**Figure 3B**). We assayed the binding of C3b/iC3b as a marker of overall complement activation *via* all pathways (**Figure 4A**), C5b-9 as a marker of terminal complement pathway activation (**Figure 4B**), properdin (FP; **Figure 4C**) and factor B (FB, **Figure 4D**) as markers of the alternative pathway activation, C4 as a marker of classical and lectin pathways activation (**Figure 4E**), and C1q as a marker of classical pathway activation (**Figure 4F**).

In general, the amount of C3b/iC3b, properdin, factor B and C4 bound to THSD7A ICs varied linearly with the concentration of anti-THSD7A IgG in each serum sample. Nonetheless, significant binding (i.e., above the cutoff value set at 4 SD above the mean of control sera) was only observed for MN sera in which the anti-THSD7A IgG concentration —adjusted for the dilution factor—was greater than 3.7 μg/mL (i.e. MN-1, MN-2, and MN-3). Complement deposition on THSD7A ICs

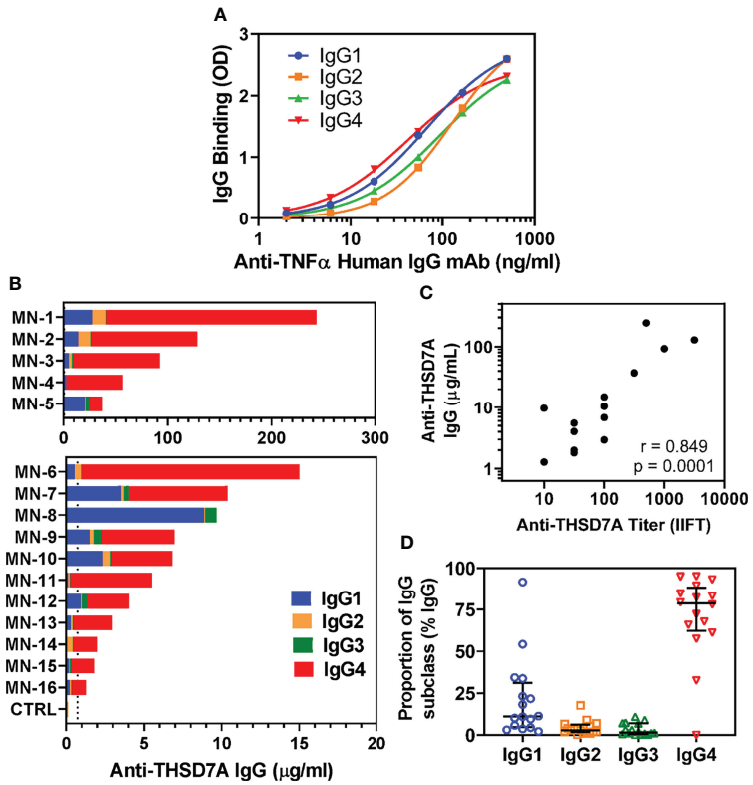

FIGURE 1 | Analysis of IgG subclasses of anti-THSD7A autoAbs. **(A)** Standard curves show the concentration dependence for the binding of recombinant human anti-TNFα IgG1 (blue), IgG2 (orange), IgG3 (green) and IgG4 (red) to wells coated with TNFα antigen. **(B)** Sera from 16 patients with THSD7A-associated MN were analyzed by ELISA for IgG autoAb subclasses binding to immobilized THSD7A. The serum concentrations of anti-THSD7A IgG1 (blue), IgG2 (orange), IgG3 (green) and IgG4 (red) in each MN serum were interpolated from standard curves using recombinant human IgG1-IgG4 mAbs anti-TNFα. Sera were designated MN-1 to MN-16 in decreasing order of their levels of anti-THSD7A IgG, calculated as the sum of the concentrations of all four IgG subclasses. **(C)** The correlation between serum levels of anti-THSD7A IgG measured by ELISA and the anti-THSD7A titers measured by indirect immunofluorescence test (IIFT) was significant (Pearson r=0.849, p=0.0001). **(D)** The relative proportion of IgG subclasses in MN sera was calculated by dividing the serum concentration of each subclass to sum of concentrations for all four IgG subclasses of autoAbs. The error bars show the median and the interquartile range.

formed by serum MN-4 (which contained 2.3 μg/mL anti-THSD7A IgG when diluted 1/25) was borderline. For all other MN sera with lower titers of anti-THSD7A IgG, complement fixation was negligible, comparable to control sera. Significant activation of the terminal pathway, as judged from C5b9 deposition, was only observed for serum MN-1, which had the highest titer of anti-THSD7A IgG (**Figure 4B**). This suggests that the activation of terminal complement pathway requires higher density of IgG4 in ICs that the activation at the level of C3. Finally, the binding of C1q to THSD7A ICs was negligible, which is consistent with the negative C1q staining in the MN patient biopsies. Overall, the deposition of factor B and properdin suggests the activation of the alternative pathway, while deposition of C4 in the absence of C1q suggests (but not prove) lectin pathway.

The Alternative Pathway Is Essential for Complement Activation by THSD7A ICs

We next investigated the contribution of specific pathways to complement activation by THSD7A ICs by measuring the deposition of C3b/iC3b from C1q-depleted serum (lacking a functional classical pathway), C4-depleted serum (lacking

TABLE 3 | The correlation between IgG subclasses in serum and in the renal biopsy.

Patient #	IgG1	IgG2	IgG3	IgG4
MN-3	2.5+ (5.3)	2+ (2.6)	1+ (1.7)	4+ (82.7)
MN-4	3+ (2.6)	0 (0.11)	0 (0.13)	3+ (53.9)
MN-6	1+ (0.55)	1+ (0.41)	0 (0.04)	2+ (14.0)
MN-8	1+ (8.9)	0 (0.08)	trace (0.71)	0 (0.0)
MN-9	ND (1.5)	ND (0.25)	ND (0.48)	3+ (4.7)

The values represent the intensity of IF staining (serum anti-THSD7A IgG subclass level in μg/ml).

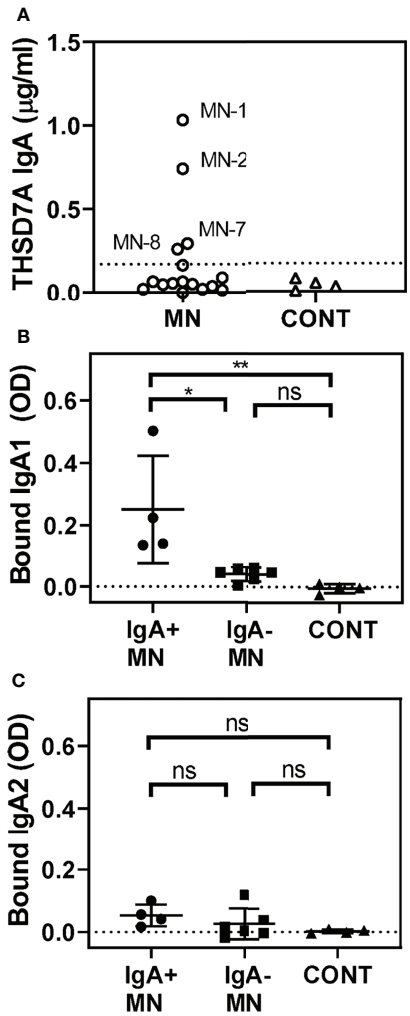

FIGURE 2 | Identification of IgA anti-THSD7A autoAbs. **(A)** Quantitative analysis of anti-THSD7A IgA in MN sera (circles). The threshold for positivity, depicted by the dotted line, was defined as the mean + 4SD of control sera (tringles). B-C. IgA-positive MN sera (circles) show significantly higher binding to THSD7A of IgA1 **(B)** but not IgA2 **(C)**, compared to IgA-negative MN sera (squares) or control sera (triangles). The significance of differences among groups was analyzed by one-way ANOVA follow by Bonferroni's test for multiple comparison (ns, not significant; *p<0.05; **p<0.01).

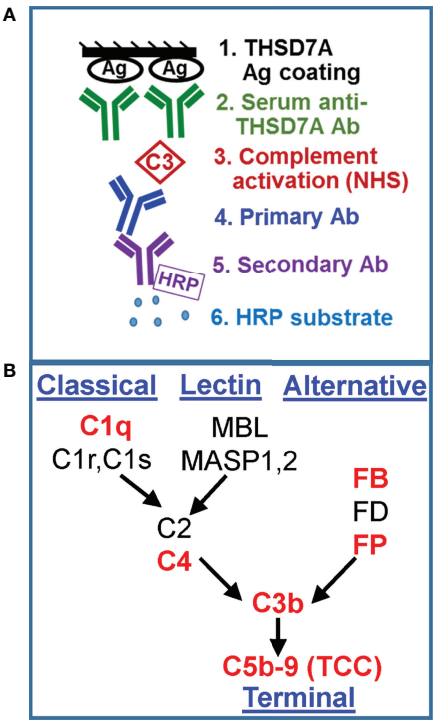

FIGURE 3 | Development of a functional assay for complement fixation by THSD7A ICs. **(A)** Schematic representation of the *in vitro* assay for complement activation. **(B)** Simplified diagram of the complement activation pathways. The complement proteins for which the binding to ICs was assayed in this study are shown in red.

functional classical and lectin pathways) and FB-depleted serum (lacking a functional alternative pathway), as compared to normal human serum as source of complement (**Figure 5A**). C3b/iC3b deposition was almost completely abolished in FB-deficient serum (88-95% inhibition), largely unaffected in C1q-depleted serum, and partially reduced (35-50% inhibition) in C4-depleted serum for some but not all MN sera (**Figure 5B**). This result indicates that the alternative pathway is essential for complement activation by IgG4-dominant THSD7A ICs, while the classical pathway is dispensable, and the lectin pathway may play a limited role. By contrast, in control experiments using reference ICs formed by human IgG1 and IgG3 mAbs, the C3b/iC3b deposition onto was completely abolished when complement activation was performed in C1q-depleted serum, as well as in C4-depleted serum or normal serum containing EDTA, but less affected in FB-depleted serum (**Figure 5C**). This indicates that the classical pathway is essential to initiate complement activation by human IgG1 and IgG3 ICs, while the alternative pathway may further amplify (but is not essential for) this activation.

The Alternative Pathway Is Sufficient for Complement Activation of THSD7A ICs

We further corroborated the role of the alternative pathway by performing complement activation in normal human serum containing MgEGTA, which inhibits the classical/lectin pathways while the alternative pathway remains active. Under these conditions, we observed concentration-dependent C3b/iC3b binding in direct proportion with the amount of anti-THSD7A IgG in ICs formed by MN1-MN3 sera (**Figure 6A**). Reference ICs formed by IgG1 and IgG4 anti-GFP mAbs bound to GFP exhibited a very similar concentration dependent C3b/iC3b binding in MgEGTA, suggesting that the major determinant of alternative pathway activation is the density of IgG4 in ICs rather than the IgG4 specificity for antigen. In control experiments, we further established that C3b/iC3b deposition onto IgG4-GFP ICs was not affected by inhibition of the classical/lectin pathways, while C3b/iC3b binding to IgG1-GFP ICs was inhibited by more

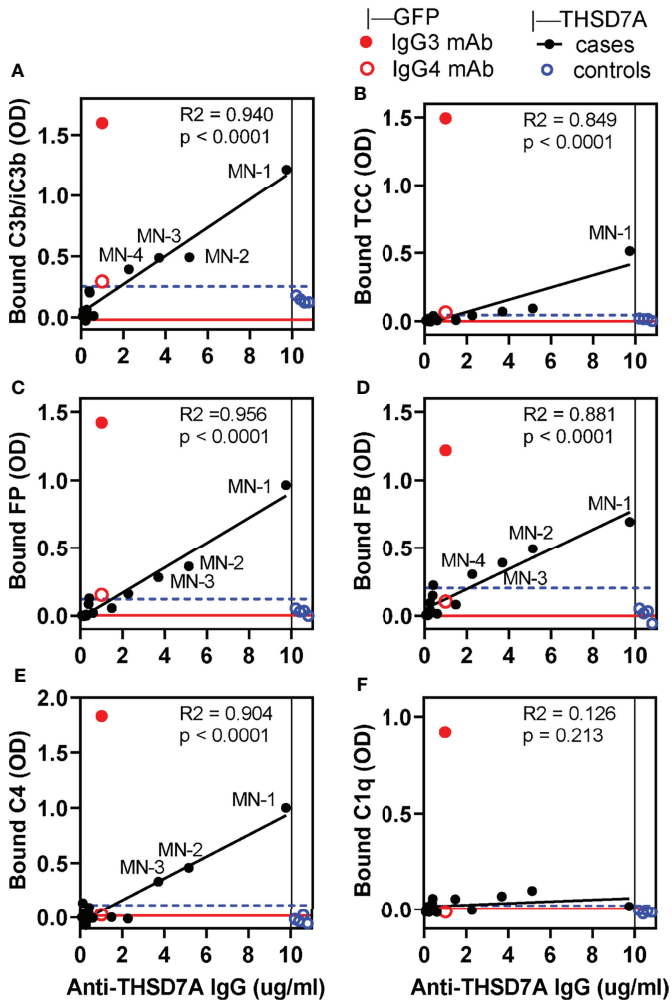

FIGURE 4 | *In vitro* complement activation by THSD7A ICs under conditions in which all activation pathways are active. Complement activation was performed using 10% normal human serum (NHS) diluted in GVB++ buffer containing Ca^{2+} and Mg^{2+} in wells coated with THSD7A (200 ng/well) and then incubated with sera MN-1 through MN-14 (solid black circles) or control sera (open blue circles), all diluted 1/25. For each sample, the x-coordinate indicates the concentration of anti-THSD7A IgG in the diluted MN serum. In parallel experiments, activation was performed on reference ICs prepared by incubating human IgG3 (1 µg/ml, solid red circle) and IgG4 (1 µg/ml, open red circle) anti-GFP mAbs in GFP-coated wells (200 ng/well). Graphs depict the binding of antibodies specific to C3b/iC3b **(A)**, C5b-9/TCC **(B)**, FP **(C)**, FB **(D)**, C4 **(E)**, and C1q **(F)**. A blank correction was performed by subtracting the OD value on immobilized antigen incubated with PBS from the OD value of immobilized antigen incubated with antibody. The threshold for positivity (blue dashed line) was calculated as the mean OD of the control sera + 4 SD. Labels indicate MN sera which showed complement deposition above the positivity threshold. The OD values for MN sera were fitted to the concentration of anti-THSD7A IgG in each sample (values taken from Figure 1 and divided by the dilution factor) by simple linear regression (black line). The red line indicates the baseline obtained by performing the complement activation assays using 10% heat-inactivated NHS in GVB++ as a source of complement.

than 80% (**Figure 6B**). Furthermore, when complement activation was performed in the presence of MgEGTA, the binding of C3b/iC3b, factor B and properdin to IgG4-GFP ICs was completely abolished in FB-deficient serum, but not affected in C4-deficient serum (**Figure 6C**). This result shows that a functional alternative pathway is necessary and sufficient for complement activation by IgG4.

Proteomic Identification of Complement Proteins in Microdissected Glomeruli

We also performed a preliminary LC-MS analysis of complement proteins in microdissected glomeruli from patients with THSD7A-associated MN, as compared to those from PLA2R1-associated MN (**Supplemental Figure 1A**). Whereas the average iBAQ intensity values were essentially the same for heavy chains of all four IgG subclasses, the average intensities for C3, C4A and C4B, and terminal pathway components (C5, C6, C7, C8, and C9) were consistently about 2-fold lower in THSD7A-MN (**Supplemental Figure 1B**), implying less complement activation occurs in THSD7A-associated MN compared to PLA2R1-associated MN. The alternative pathway component factor B and a specific inhibitor of this pathway, factor H, were detected with similar intensities in both forms of MN. Lectin pathway components e.g. MASP1, were detected sporadically and with low intensity.

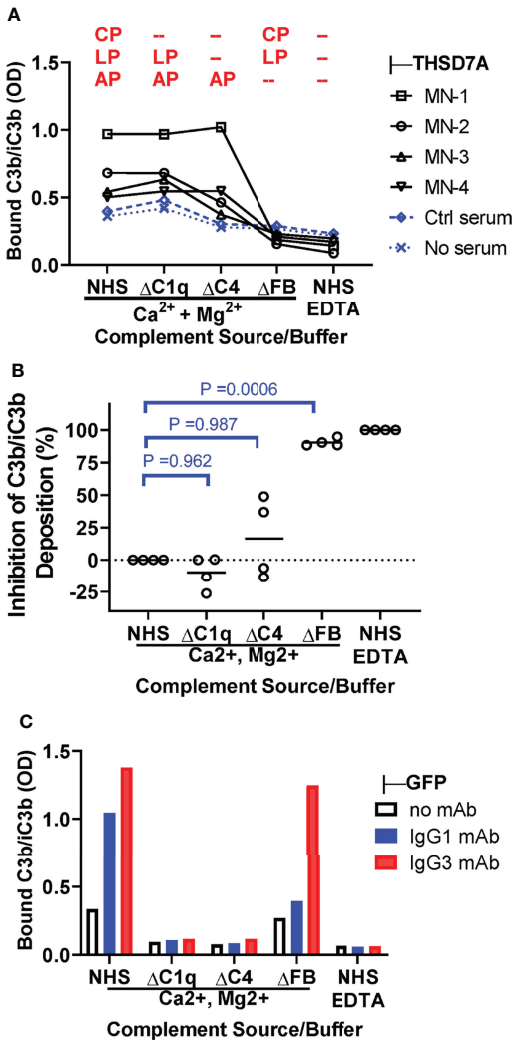

FIGURE 5 | The alternative pathway is essential for complement activation by THSD7A ICs. **(A)** Plot depicting the deposition of C3b/iC3b (expressed as OD) onto THSD7A ICs formed by MN1-MN4 sera (black symbols) or in THSD7A-coated wells incubated with buffer or control serum (blue symbols). Complement activation was performed in 10% normal human serum (NHS), C1q-depleted serum (ΔC1q), C4-depleted serum (ΔC4), and FB-depleted serum (ΔFB) in buffer containing Ca2+ and Mg2+, as well as 10% NHS in EDTA buffer. The complement activation pathway active under each condition are shown in red (CP, classical pathway; LP, lectin pathway, AP, alternative pathway). **(B)** The relative inhibition of C3b/iC3b deposition of onto THSD7A ICs formed by MN1-MN4 sera was calculated for C1q-, C4- and FB-depleted sera on a scale from 0% inhibition (10% NHS in buffer containing Ca2+ and Mg2+) to 100% inhibition (10% NHS in EDTA buffer). C3b/iC3b deposition was significantly inhibited in FB-depleted serum lacking a functional alternative pathway (p=0.0006, one-way repeated measures ANOVA followed by *post-hoc* Dunnet test). **(C)** Deposition of C3b/iC3b on human monoclonal IgG1 and IgG3 anti-GFP (1 μg/mL each) bound to TNFα was measured after incubation with 10% NHS or C1q-, C4 and FB-depleted sera in buffer containing Ca2+ and Mg2+ or in 10% NHS in EDTA-containing buffer as source of complement.

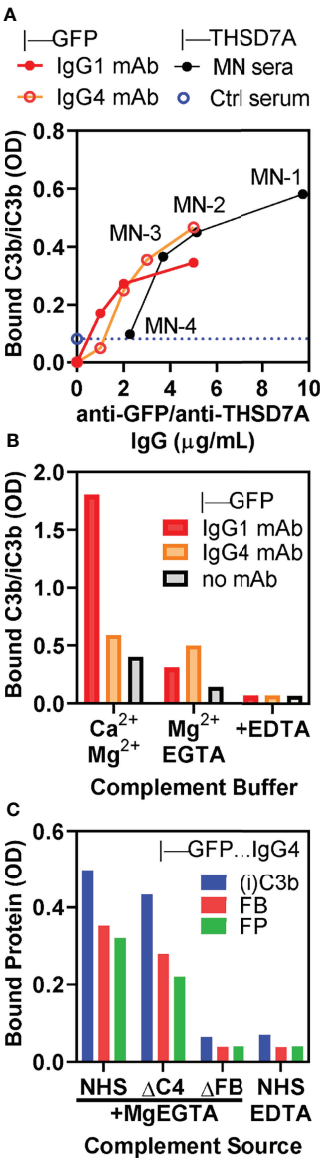

FIGURE 6 | *In vitro* complement activation by THSD7A ICs in MgEGTA buffer, which inhibits the classical and lectin pathways. **(A)** Concentration dependence of C3b/iC3b deposition on ICs formed by anti-THSD7A antibodies (black circles) from MN-1, MN-2, MN-3 and MN-4 sera (all diluted 1/25) bound to immobilized THSD7A or by anti-GFP human IgG1 (red circles) and anti-GFP IgG4 (orange circles) mAbs bound to immobilized GFP. **(B)** C3b/iC3b deposition on ICs formed by IgG1 mAb (1 μg/mL) and IgG4 mAbs (3 μg/mL) bound to immobilized GFP. Complement activation was performed using 10% NHS diluted in buffer containing Ca^{2+} and Mg^{2+}, MgEGTA, or EDTA. Inhibition of classical and lectin pathways by MgEGTA reduced C3b/iC3b binding to IgG1 ICs by >80% but had minimal effect on C3b binding to IgG4 ICs. **(C)** The deposition of C3b/iC3b (blue), factor B (FP, red) and properdin (FP, green) on ICs formed by anti-GFP IgG4 mAb (3 μg/mL) was completely abolished when using FB-depleted serum or normal serum containing EDTA as complement source, but largely unchanged in C4-depleted serum.

Curiously, classical pathway components— such as C1q subunits, C1r and C1s— were detected in almost all cases in both forms of MN. Proteomic identification of C1q, in apparent contradiction with the negative C1q staining in MN biopsies as well as with our results (**Figure 4F**). This suggests that C1q may in fact be bound to ICs but becomes "concealed" (undetectable by anti-C1q antibodies) due to C3b/iC3b deposition on ICs, as previously reported (34).

DISCUSSION

Whereas podocyte injury by C5b-9 is considered a major effector mechanism of ICs causing proteinuria in MN, there is less agreement about which subclasses of autoAbs and which complement activation pathways are involved. In this study, we have measured quantitatively the serum levels of anti-THSD7A subclasses and assessed their ability to fix complement *in vitro*.

For quantitative analyses of IgG subclasses, we generated calibration curves using recombinant human mAbs bound to their target antigen. Since this ensures oriented binding of the IgG mAbs, similar to binding of anti-THSD7A IgG to coated THSD7A, we propose that this assay format provides more accurate results than using human IgG1-4 myeloma proteins directly absorbed onto plastic wells, an approach previously used to quantify anti-PLA2R IgG subclasses (35). We found that IgG4 was the dominant class of anti-THSD7A autoAbs in the majority (14/16, 88%) of sera analyzed in this work. IgG4 antibodies feature several unusual properties (36). They undergo Fab arm exchange, which accounts for their functional monovalency and inability to form large precipitating ICs (37). With regard to its effector properties, IgG4 is generally considered unable to fix the complement since it cannot bind C1q to initiate the classical pathway (22–24). In addition, by competing with IgG1 and IgG3 for binding to (auto)antigen, IgG4 can inhibit the activation of classical complement pathway by other IgG subclasses (38).

Under the conditions used in our functional complement activation assay (MN sera diluted 1/25), we observed significant deposition of complement activation products only on ICs formed by three sera with the highest levels of THSD7A autoAbs (MN1-MN3), which were all dominant IgG4. Compared to reference ICs formed by IgG1 and IgG3 mAbs, THSD7A ICs activated complement to a lesser extent and only at relatively high concentrations of IgG autoAbs (at least 3.7 μg/mL). The detection of C3b, factor B and properdin bound to THSD7A ICs formed by MN1-MN3 sera is consistent the formation of a stabilized C3 convertase of the alternative pathway, C3bBbP. Bound C4 was also detected in the absence of C1q, which suggests that either the lectin pathway is activated, or that C3b/iC3b deposition conceals bound C1q (34). Finally, bound C5b-9 was detected in significant amounts only on THSD7A ICs formed by MN-1 serum, indicating that the downstream activation of the terminal pathway requires even higher concentrations of anti-THSD7A IgG (5-10 μg/ml) than complement activation at the level of C3.

For all complement-fixing MN sera, the C3b/iC3b binding to THSD7A-IgG4 complexes was completely abolished in FB-depleted serum but was largely unchanged in C1q-depleted sera, indicating that the alternative pathway is essential for complement activation, while the classical pathway is dispensable. For two sera (MN2 and MN3), C3b/iC3b deposition was partially inhibited (by about 35%-50%) in C4-depleted serum, which provides circumstantial evidence of lectin pathway activation. Nonetheless, the same sera supported C3b/iC3b fixation in the presence of MgEGTA, implying that the classical and lectin pathways are dispensable. Taken together, these results show that (a) the alternative pathway is necessary and sufficient for complement activation by THSD7A ICs, and (b) the lectin pathway may contribute to but is not critical for complement activation by anti-THSD7A IgG4. Prior studies using model recombinant human mAbs have shown that ICs formed at high IgG4 concentration and high epitope density can activate complement *via* the alternative pathway (25–27). Our results are the first to show that these findings further extend to naturally occurring human IgG4 autoAbs from patients.

Complement activation products are detected on biopsy in most cases of THSD7A-associated MN (39), although the intensity of staining is often weaker than what is typically seen in PLA2R-associated MN. While this is attributable to ICs formed to anti-THSD7A autoAbs, we cannot rule out that "second-wave" antibodies such as those to cytoplasmic neoantigens upregulated in disease also contribute complement activation (40). In addition, glomerular complement activation in MN may also occur independently of ICs because of local complement dysregulation. A putative mechanism is the impaired recruitment of factor H, a major regulator of the alternative pathway, secondary to the loss of heparan sulfate from the GBM in MN (41). Also, the dysregulation of the alternative pathway may be the result of autoAbs to factor H, which have been reported to occur in as many as 3% of patients with PLA2R-associated MN (42).

Given the relatively weak ability of anti-THSD7A autoAbs to activate complement (especially the terminal pathway) found in our study, we speculate that there may be additional mechanisms by which injury occurs in this form of MN. Anti-THSD7A may have direct function-blocking effects that directly lead to breakdown of the glomerular filtration barrier and consequent proteinuria, since THSD7A localizes directly basal to the slit diaphragm protein nephrin and may thereby stabilize podocyte adhesion and structure (43). Supporting this view, mice passively immunized with human anti-THSD7A autoAbs, as well as mice injected with rabbit anti-THSD7A IgG, developed proteinuria associated with subepithelial ICs and histologic features of MN in the absence of significant glomerular C3b/iC3b deposition (44, 45).

An unexpected finding was the detection of IgA1 anti-THSD7A in 4/16 (25%) of MN sera. To our knowledge, this is the first instance of a podocyte antigen implicated in MN being targeted by IgA autoAbs. Positive glomerular IgA staining has been reported in about 40% of biopsies from THSD7A-associated MN, compared to ~10% of cases of PLA2R-associated MN (15, 39). In our study cohort, positive (1+) glomerular IgA staining on the renal biopsy was found in only one patient, who had the

second highest serum titer of circulating IgA anti-THSD7A. This suggest that serum IgA anti-THSD7A autoAbs may deposit in glomeruli, at least in some cases of MN.

Our study has several limitations. With regard to complement activation, the ICs formed *in vitro* represent a simplified 2D model for subepithelial ICs, which may not fully reproduce the complex *in vivo* milieu, comprising the surrounding GBM and the adjacent podocytes. The essential role of the alternative pathway in complement activation by anti-THSD7A IgG4 remains to be corroborated *in vivo* using animal models. As discussed above, mice passively immunized with anti-THSD7A patient sera only exhibit IgG4 but not C3b/iC3b deposition in glomeruli, despite developing proteinuria and histologic features of MN. The lack of complement activation in this mouse model is likely due to insufficient surface density of human IgG4 deposited in mouse glomeruli and/or sub-optimal activation of mouse complement by human antibodies. Nonetheless, we have shown that the alternative pathway is essential for glomerular complement deposition and proteinuria in another mouse model of MN induced by active immunization with α3NC1 (46). This model features subepithelial ICs containing predominantly mouse IgG1, which recapitulates human IgG4 regarding its inability to bind C1q and activate the classical pathway (47).

In summary, our results show that predominantly IgG4 anti-THSD7A autoAbs have the ability to activate complement *via* the alternative pathway, albeit only at high IgG4 surface density. Additional mechanisms yet to be defined may contribute to pathogenic complement activation in THSD7A-associated MN. It is also possible that the pathogenicity of anti-THSD7A autoAbs may be independent of, or only partly mediated by their ability to fix complement. Further studies are required to determine the relative contribution of complement-independent and complement-dependent mechanisms of podocyte injury in THSD7A-associated MN.

DATA AVAILABILITY STATEMENT

The raw data supporting the conclusions of this article will be made available by the authors, without undue reservation.

ETHICS STATEMENT

The studies involving human participants were reviewed and approved by the respective Institutional Review Boards at each institution. The patients/participants provided their written informed consent to participate in this study.

AUTHOR CONTRIBUTIONS

D-BB conceived the idea, designed the research studies, performed data analysis, and wrote the original draft. PM, AS, and TC performed experiments and collected, assembled, analysed, and interpreted data. TC and LB provided critical reagents/samples and curated data. All authors contributed to editing, reviewed, and approved the final manuscript.

FUNDING

This work was supported by pilot grants funded by the Meharry Research Centers in Minorities Institutions grant U54MD007586 from the National Institute on Minority Health and Health Disparities of the National Institutes of Health (PM and D-BB). Support was also provided by the award W81XWH-20-1-0698 (grant number LR190150) from the Lupus Research Program of the US Department of Defense (D-BB) and institutional funding for the Glomerular Disease Center, Boston Medical Center (LB).

ACKNOWLEDGMENTS

Meharry core facilities used in this work are supported by Core Meharry RCMI Infrastructure Core (CRISALIS) grant U54MD007586. We thank Dr. Christopher Larsen for THSD7A and control serum samples from the Arkana Laboratories biorepository, which is supported in part by grant R43MD014110 from the National Institute on Minority Health and Health Disparities.

SUPPLEMENTARY MATERIAL

The Supplementary Material for this article can be found online at: https://www.frontiersin.org/articles/10.3389/fimmu.2022.952235/full#supplementary-material

REFERENCES

1. Beck LHJr., Salant DJ. Membranous Nephropathy: From Models to Man. *J Clin Invest* (2014) 124(6):2307–14. doi: 10.1172/JCI72270
2. Cattran DC, Brenchley PE. Membranous Nephropathy: Integrating Basic Science Into Improved Clinical Management. *Kidney Int* (2017) 91(3):566–74. doi: 10.1016/j.kint.2016.09.048
3. Beck LHJr., Bonegio RG, Lambeau G, Beck DM, Powell DW, Cummins TD, et al. M-Type Phospholipase A2 Receptor as Target Antigen in Idiopathic Membranous Nephropathy. *N Engl J Med* (2009) 361(1):11–21. doi: 10.1056/NEJMoa0810457
4. Tomas NM, Beck LH Jr., Meyer-Schwesinger C, Seitz-Polski B, Ma H, Zahner G, et al. Thrombospondin Type-1 Domain-Containing 7A in Idiopathic Membranous Nephropathy. *N Engl J Med* (2014) 371(24):2277–87. doi: 10.1056/NEJMoa1409354

5. Ruggenenti P, Debiec H, Ruggiero B, Chianca A, Pelle T, Gaspari F, et al. Anti-Phospholipase A2 Receptor Antibody Titer Predicts Post-Rituximab Outcome of Membranous Nephropathy. *J Am Soc Nephrol* (2015) 26 (10):2545–58. doi: 10.1681/ASN.2014070640
6. Hofstra JM, Beck LH Jr., Beck DM, Wetzels JF, Salant DJ. Anti-Phospholipase A(2) Receptor Antibodies Correlate With Clinical Status in Idiopathic Membranous Nephropathy. *Clin J Am Soc Nephrol* (2011) 6(6):1286–91. doi: 10.2215/CJN.07210810
7. Kanigicherla D, Gummadova J, McKenzie EA, Roberts SA, Harris S, Nikam M, et al. Anti-PLA2R Antibodies Measured by ELISA Predict Long-Term Outcome in a Prevalent Population of Patients With Idiopathic Membranous Nephropathy. *Kidney Int* (2013) 83(5):940–8. doi: 10.1038/ki.2012.486
8. Hoxha E, Beck LH Jr., Wiech T, Tomas NM, Probst C, Mindorf S, et al. An Indirect Immunofluorescence Method Facilitates Detection of Thrombospondin Type 1 Domain-Containing 7a-Specific Antibodies in Membranous Nephropathy. *J Am Soc Nephrol* (2017) 28(2):520–31. doi: 10.1681/ASN.2016010050
9. Sethi S, Debiec H, Madden B, Charlesworth MC, Morelle J, Gross L, et al. Neural Epidermal Growth Factor-Like 1 Protein (NELL-1) Associated Membranous Nephropathy. *Kidney Int* (2020) 97(1):163–74. doi: 10.1016/j.kint.2019.09.014
10. Sethi S, Madden BJ, Debiec H, Charlesworth MC, Gross L, Ravindran A, et al. Exostosin 1/Exostosin 2-Associated Membranous Nephropathy. *J Am Soc Nephrol* (2019) 30(6):1123–36. doi: 10.1681/ASN.2018080852
11. Al-Rabadi LF, Caza T, Trivin-Avillach C, Rodan AR, Andeen N, Hayashi N, et al. Serine Protease HTRA1 as a Novel Target Antigen in Primary Membranous Nephropathy. *J Am Soc Nephrol* (2021) 32(7):1666–81. doi: 10.1681/ASN.2020101395
12. Caza TN, Hassen SI, Kuperman M, Sharma SG, Dvanajscak Z, Arthur J, et al. Neural Cell Adhesion Molecule 1 is a Novel Autoantigen in Membranous Lupus Nephritis. *Kidney Int* (2021) 100(1):171–81. doi: 10.1016/j.kint.2020.09.016
13. Sethi S, Debiec H, Madden B, Vivarelli M, Charlesworth MC, Ravindran A, et al. Semaphorin 3B-Associated Membranous Nephropathy is a Distinct Type of Disease Predominantly Present in Pediatric Patients. *Kidney Int* (2020) 98(5):1253–64. doi: 10.1016/j.kint.2020.05.030
14. Sethi S, Madden B, Debiec H, Morelle J, Charlesworth MC, Gross L, et al. Protocadherin 7-Associated Membranous Nephropathy. *J Am Soc Nephrol* (2021) 32(5):1249-61. doi: 10.1681/ASN.2020081165
15. Caza TN, Hassen SI, Kenan DJ, Storey A, Arthur JM, Herzog C, et al. Transforming Growth Factor Beta Receptor 3 (TGFBR3)–Associated Membranous Nephropathy. *Kidney360* (2021) 2(8):1275–86. doi: 10.34067/KID.0001492021
16. Le Quintrec M, Teisseyre M, Bec N, Delmont E, Szwarc I, Perrochia H, et al. Contactin-1 Is a Novel Target Antigen in Membranous Nephropathy Associated With Chronic Inflammatory Demyelinating Polyneuropathy. *Kidney Int* (2021) 100(6):1240–9. doi: 10.1016/j.kint.2021.08.014
17. Ma H, Sandor DG, Beck LH Jr. The Role of Complement in Membranous Nephropathy. *Semin Nephrol* (2013) 33(6):531–42. doi: 10.1016/j.semnephrol.2013.08.004
18. Doi T, Mayumi M, Kanatsu K, Suehiro F, Hamashima Y. Distribution of IgG Subclasses in Membranous Nephropathy. *Clin Exp Immunol* (1984) 58(1):57–62.
19. Larsen CP, Messias NC, Silva FG, Messias E, Walker PD. Determination of Primary Versus Secondary Membranous Glomerulopathy Utilizing Phospholipase A2 Receptor Staining in Renal Biopsies. *Modern Pathol* (2013) 26(5):709–15. doi: 10.1038/modpathol.2012.207
20. Zaghrini C, Seitz-Polski B, Justino J, Dolla G, Payre C, Jourde-Chiche N, et al. Novel ELISA for Thrombospondin Type 1 Domain-Containing 7A Autoantibodies in Membranous Nephropathy. *Kidney Int* (2019) 95(3):666–79. doi: 10.1016/j.kint.2018.10.024
21. Borza DB. Alternative Pathway Dysregulation and the Conundrum of Complement Activation by IgG4 Immune Complexes in Membranous Nephropathy. *Front Immunol* (2016) 7:157. doi: 10.3389/fimmu.2016.00157
22. van der Zee JS, van Swieten P, Aalberse RC. Inhibition of Complement Activation by IgG4 Antibodies. *Clin Exp Immunol* (1986) 64(2):415–22.
23. Vidarsson G, Dekkers G, Rispens T. IgG Subclasses and Allotypes: From Structure to Effector Functions. *Front Immunol* (2014) 5:520. doi: 10.3389/fimmu.2014.00520
24. Tao MH, Canfield SM, Morrison SL. The Differential Ability of Human IgG1 and IgG4 to Activate Complement is Determined by the COOH-Terminal Sequence of the CH2 Domain. *J Exp Med* (1991) 173(4):1025–8. doi: 10.1084/jem.173.4.1025
25. Garred P, Michaelsen TE, Aase A. The IgG Subclass Pattern of Complement Activation Depends on Epitope Density and Antibody and Complement Concentration. *Scand J Immunol* (1989) 30(3):379–82. doi: 10.1111/j.1365-3083.1989.tb01225.x
26. Seino J, Eveleigh P, Warnaar S, van Haarlem LJ, van Es LA, Daha MR. Activation of Human Complement by Mouse and Mouse/Human Chimeric Monoclonal Antibodies. *Clin Exp Immunol* (1993) 94(2):291–6.
27. Dillman SL, Strelkauskas AJ, Su HR, Boackle RJ. Activation of Human Complement by Totally Human Monoclonal Antibodies. *Mol Immunol* (1995) 32(13):957–64. doi: 10.1016/0161-5890(95)00064-L
28. Haddad G, Lorenzen JM, Ma H, de Haan N, Seeger H, Zaghrini C, et al. Altered Glycosylation of IgG4 Promotes Lectin Complement Pathway Activation in Anti-PLA2R1-Associated Membranous Nephropathy. *J Clin Invest* (2021) 131(5):e140453. doi: 10.1172/JCI140453
29. Terai I, Kobayashi K, Vaerman JP, Mafune N. Degalactosylated and/or Denatured IgA, But Not Native IgA in Any Form, Bind to Mannose-Binding Lectin. *J Immunol* (2006) 177(3):1737–45. doi: 10.4049/jimmunol.177.3.1737
30. Bally S, Debiec H, Ponard D, Dijoud F, Rendu J, Faure J, et al. Phospholipase A2 Receptor-Related Membranous Nephropathy and Mannan-Binding Lectin Deficiency. *J Am Soc Nephrol* (2016) 27(12):3539-44. doi: 10.1681/ASN.2015101155
31. Borza DB, Rana T, Olaru F, Thurman JM, Tomlinson S, Beck LHJr., et al. Alternative Pathway Amplifies Complement Activation by Human Anti-PLA2R Antibodies in Membranous Nephropathy [Abstract: FR-Or087]. *J Am Soc Nephrol* (2014) 25:66A.
32. Ravindran A, Madden B, Charlesworth MC, Sharma R, Sethi A, Debiec H, et al. Proteomic Analysis of Complement Proteins in Membranous Nephropathy. *Kidney Int Rep* (2020) 5(5):618–26. doi: 10.1016/j.ekir.2020.01.018
33. von Haxthausen F, Reinhard L, Pinnschmidt HO, Rink M, Soave A, Hoxha E, et al. Antigen-Specific IgG Subclasses in Primary and Malignancy-Associated Membranous Nephropathy. *Front Immunol* (2018) 9:3035. doi: 10.3389/fimmu.2018.03035
34. Nilsson UR. Deposition of C3b/iC3b Leads to the Concealment of Antigens, Immunoglobulins and Bound C1q in Complement-Activating Immune Complexes. *Mol Immunol* (2001) 38(2-3):151–60. doi: 10.1016/S0161-5890(01)00039-6
35. Hofstra JM, Debiec H, Short CD, Pelle T, Kleta R, Mathieson PW, et al. Antiphospholipase A2 Receptor Antibody Titer and Subclass in Idiopathic Membranous Nephropathy. *J Am Soc Nephrol* (2012) 23(10):1735–43. doi: 10.1681/ASN.2012030242
36. Aalberse RC, Schuurman J. IgG4 Breaking the Rules. *Immunology* (2002) 105 (1):9–19. doi: 10.1046/j.0019-2805.2001.01341.x
37. van der Neut Kolfschoten M, Schuurman J, Losen M, Bleeker WK, Martinez-Martinez P, Vermeulen E, et al. Anti-Inflammatory Activity of Human IgG4 Antibodies by Dynamic Fab Arm Exchange. *Science* (2007) 317(5844):1554–7. doi: 10.1126/science.1144603
38. Zuo Y, Evangelista F, Culton D, Guilabert A, Lin L, Li N, et al. IgG4 Autoantibodies Are Inhibitory in the Autoimmune Disease Bullous Pemphigoid. *J Autoimmun* (2016) 73:111–9. doi: 10.1016/j.jaut.2016.06.019
39. Hara S, Tsuji T, Fukasawa Y, Hisano S, Morito S, Hyodo T, et al. Clinicopathological Characteristics of Thrombospondin Type 1 Domain-Containing 7A-Associated Membranous Nephropathy. *Virchows Arch* (2019) 474(6):735–43. doi: 10.1007/s00428-019-02558-0
40. Ghiggeri GM, Seitz-Polski B, Justino J, Zaghrini C, Payre C, Brglez V, et al. Multi-Autoantibody Signature and Clinical Outcome in Membranous Nephropathy. *Clin J Am Soc Nephrol* (2020) 15(12):1762–76. doi: 10.2215/CJN.02500220
41. Borza DB. Glomerular Basement Membrane Heparan Sulfate in Health and Disease: A Regulator of Local Complement Activation. *Matrix Biol* (2017) 57-58:299–310. doi: 10.1016/j.matbio.2016.09.002
42. Seikrit C, Ronco P, Debiec H. Factor H Autoantibodies and Membranous Nephropathy. *N Engl J Med* (2018) 379(25):2479–81. doi: 10.1056/NEJMc1805857

43. Herwig J, Skuza S, Sachs W, Sachs M, Failla AV, Rune G, et al. Thrombospondin Type 1 Domain-Containing 7a Localizes to the Slit Diaphragm and Stabilizes Membrane Dynamics of Fully Differentiated Podocytes. *J Am Soc Nephrol* (2019) 30(5):824–39. doi: 10.1681/ASN.2018090941
44. Tomas NM, Hoxha E, Reinicke AT, Fester L, Helmchen U, Gerth J, et al. Autoantibodies Against Thrombospondin Type 1 Domain-Containing 7A Induce Membranous Nephropathy. *J Clin Invest* (2016) 126(7):2519–32. doi: 10.1172/JCI85265
45. Tomas NM, Meyer-Schwesinger C, von Spiegel H, Kotb AM, Zahner G, Hoxha E, et al. A Heterologous Model of Thrombospondin Type 1 Domain-Containing 7a-Associated Membranous Nephropathy. *J Am Soc Nephrol* (2017) 28(11):3262–77. doi: 10.1681/ASN.2017010030
46. Luo W, Olaru F, Miner JH, Beck LH Jr., van der Vlag J, Thurman JM, et al. Alternative Pathway Is Essential for Glomerular Complement Activation and Proteinuria in a Mouse Model of Membranous Nephropathy. *Front Immunol* (2018) 9:1433. doi: 10.3389/fimmu.2018.01433
47. Zhang JJ, Malekpour M, Luo W, Ge L, Olaru F, Wang XP, et al. Murine Membranous Nephropathy: Immunization With Alpha3(IV) Collagen Fragment Induces Subepithelial Immune Complexes and FcgammaR-Independent Nephrotic Syndrome. *J Immunol* (2012) 188(7):3268–77. doi: 10.4049/jimmunol.1103368

Conflict of Interest: The authors declare a potential conflict of interest and state it below. LB reports being a co-inventor on the U.S. patent "Diagnostics for Membranous Nephropathy" and receives royalty income through Boston University. LB has served on advisory boards on the topic of MN and other glomerular diseases for Visterra, Ionis, Alexion, and Novartis, and receives royalties from UpToDate for topics related to MN. TC is employed by Arkana Laboratories, Little Rock, AR.

The remaining authors declare that the research was conducted in the absence of any commercial or financial relationships that could be construed as a potential conflict of interest.

Publisher's Note: All claims expressed in this article are solely those of the authors and do not necessarily represent those of their affiliated organizations, or those of the publisher, the editors and the reviewers. Any product that may be evaluated in this article, or claim that may be made by its manufacturer, is not guaranteed or endorsed by the publisher.

frontiers | Frontiers in Immunology

TYPE Original Research
PUBLISHED 12 October 2022
DOI 10.3389/fimmu.2022.1020459

OPEN ACCESS

EDITED BY
Erdem Tüzün,
Istanbul University, Turkey

REVIEWED BY
Tsukasa Ikeura,
Kansai Medical University, Japan
Satoshi Hara,
Kanazawa University, Japan

*CORRESPONDENCE
Min-Chan Park
mcpark@yuhs.ac
Yong-Gil Kim
bestmd2000@amc.seoul.kr

SPECIALTY SECTION
This article was submitted to B Cell Biology, a section of the journal Frontiers in Immunology

RECEIVED 16 August 2022
ACCEPTED 28 September 2022
PUBLISHED 12 October 2022

CITATION
Kwon OC, Park M-C and Kim Y-G (2022) Correlation between serologic parameters and disease activity of IgG4-related disease: Differences between patients with normal and elevated serum IgG4 concentrations. *Front. Immunol.* 13:1020459. doi: 10.3389/fimmu.2022.1020459

Correlation between serologic parameters and disease activity of IgG4-related disease: Differences between patients with normal and elevated serum IgG4 concentrations

Oh Chan Kwon[1], Min-Chan Park[1]* and Yong-Gil Kim[2,3]*

[1]Division of Rheumatology, Department of Internal Medicine, Yonsei University College of Medicine, Seoul, South Korea, [2]Division of Rheumatology, Department of Internal Medicine, University of Ulsan, College of Medicine, Asan Medical Center, Seoul, South Korea, [3]Convergence Medicine Research Center, Asan Institution for Life Science, Asan Medical Center, Seoul, South Korea

Objective: We aimed to identify serologic parameters that correlate with the disease activity of IgG4-related disease (IgG4-RD) in patients with normal and elevated serum IgG4 concentrations, respectively.

Methods: This retrospective cohort study included 148 patients with IgG4-RD. Patients were categorized into normal (≤201 mg/dL) and elevated (>201 mg/dL) serum IgG4 concentration groups. Disease activity was assessed using the IgG4-RD responder index (RI). The correlations between IgG4-RD RI and serologic parameters (erythrocyte sedimentation rate [ESR], C-reactive protein, C3, C4, IgG4 concentration, IgG concentration, and IgG4/IgG ratio) were evaluated in each group, using Spearman's correlation coefficient.

Results: Of the 148 patients with IgG4-RD, 38 (25.7%) and 110 (74.3%) patients were categorized into the normal and elevated serum IgG4 concentration groups, respectively. In the normal serum IgG4 concentration group, IgG concentration was the only serologic parameter that showed a significant correlation with IgG4-RD RI (rho=0.411, p=0.013). However, in the elevated serum IgG4 concentration group, ESR (rho=0.196, p=0.041), C3 (rho=-0.432, p<0.001), C4 (rho=-0.363, p=0.001), IgG4 concentration (rho=0.423, p<0.001), IgG concentration (rho=0.224, p=0.020), and IgG4/IgG ratio (rho=0.328, p=0.001) correlated with IgG4-RD RI. The combination of C3 and IgG4 concentration (rho=0.509, p<0.001) had the strongest correlation with IgG4-RD RI in this group.

Conclusion: Among the serologic parameters tested, IgG concentration was the only parameter that correlated with IgG4-RD RI in patients with normal serum IgG4 concentrations, whereas multiple parameters correlated with IgG4-RD RI in those with elevated serum IgG4 concentrations.

10.3389/fimmu.2022.1020459

The combination of C3 and IgG4 concentration had the strongest correlation coefficient in the latter group.

KEYWORDS

IgG4-related disease, disease activity, IgG4, serology, correlation

Introduction

Immunoglobulin G4-related disease (IgG4-RD) is an immune-mediated condition characterized by fibroinflammatory lesions that can affect virtually any organ (1–3). Although elevation of serum IgG4 concentrations was once considered a prerequisite for the diagnosis of IgG4-RD, it is now known that elevated serum IgG4 concentration is neither sufficiently sensitive nor specific for the diagnosis of IgG4-RD (2, 4). A substantial proportion of patients with IgG4-RD have normal serum IgG4 concentrations (4–6); in a cohort consisting of 125 patients with IgG4-RD, 48.5% of patients had normal serum IgG4 concentrations, even among patients with clinically active disease (6).

IgG4-RD responder index (RI) is a validated disease activity assessment tool widely used for IgG4-RD (7). The scoring system consists of 26 domains (24 standard organs, constitutional symptoms, and other organs) that are scored separately and then summed to calculate the IgG4-RD RI (7). Although reliable and valid as a disease activity assessment tool (7), it is difficult to accurately score the IgG4-RD RI if laboratory tests and imaging studies to assess organ involvement status are not fully completed. Full laboratory and imaging assessments at every visit are not feasible in routine clinical practice. Hence, identifying a simple serologic biomarker that is readily available in routine clinical practice and correlates well with the disease activity of IgG4-RD could be helpful. Serum IgG4 concentration has been traditionally suggested as a biomarker for the disease activity of IgG4-RD (8). However, data on the use of serum IgG4 concentration as a biomarker for disease activity of IgG4-RD has shown mixed results (9–11). Therefore, the validity of serum IgG4 concentration as a biomarker of disease activity, when universally applied to patients with IgG4-RD as a whole, is controversial. It is particularly uncertain whether serum IgG4 concentration could be used as a biomarker for disease activity of IgG4-RD in a subset of patients with normal serum IgG4 concentrations. Data on whether serum IgG4 concentration correlates stronger or weaker with disease activity of IgG4-RD in particular subsets of patients are lacking; to better assess this, it is necessary to analyze patients with normal serum IgG4 concentrations and those with elevated serum IgG4 concentrations separately.

In this study, using a cohort of patients with IgG4-RD, we categorized patients into those with normal serum IgG4 concentrations and those with elevated serum IgG4 concentrations and assessed the correlation between serum IgG4 concentration and disease activity in each group. We also tested other easily accessible serologic parameters, including erythrocyte sedimentation rate (ESR), C-reactive protein (CRP), complement 3 (C3), complement 4 (C4), IgG concentration, and IgG4/IgG ratio, as potential biomarkers for disease activity in each group.

Methods

Study population

Patients who were newly diagnosed with IgG4-RD between 2011 and 2021 at two referral hospitals were retrospectively included for analysis. All included patients fulfilled the 2019 American College of Rheumatology (ACR)/European League Against Rheumatism (EULAR) classification criteria for IgG4-RD (12). Data on the following variables at the time of IgG4-RD diagnosis were reviewed: age, sex, involved organs, ESR, CRP, C3, C4, serum IgG4 concentration, serum IgG concentration, and serum IgG4/IgG ratio. Serum IgG4 concentrations were measured by nephelometry using Siemens assay (Siemens Healthcare Diagnostics, Malburg, Germany). The manufacturer's reference range of serum IgG4 concentration was 3–201 mg/dL. Patients were categorized into the normal serum IgG4 concentration (≤ 201 mg/dL) and elevated serum IgG4 concentration (> 201 mg/dL) groups according to their serum IgG4 concentrations. This study was approved by the Institutional Review Board (IRB) of Gangnam Severance Hospital (IRB No: 3-2022-0247). Owing to the retrospective design of the study, the requirement for informed consent was waived.

Disease activity

We used the IgG4-RD responder index (RI) as the gold standard of disease activity assessment (7). All patients had

undergone laboratory and imaging studies for the diagnostic workup of IgG4-RD, and the scoring of each domain of IgG4-RD RI was assessed comprehensively based on the clinical, laboratory, and imaging findings at the time of diagnosis. Although the serum IgG4 concentration was included in the earlier version of IgG4-RD RI (13), this domain was removed in the latest version (7). As we used the latest version of IgG4-RD RI, serum IgG4 concentration was not included in the scoring of IgG4-RD RI.

Statistical analysis

Continuous variables following normal or non-normal distribution are expressed as mean (± standard deviation [SD]) or median (interquartile range [IQR]), respectively, and categorical variables are expressed as numbers with percentages. For comparison between the two groups (normal serum IgG4 concentration vs. elevated serum IgG4 concentration), we used the independent two-sample t-test or Mann–Whitney U test for continuous variables following normal or non-normal distribution, respectively. For comparison of categorical variables, the $\chi 2$ test or Fisher's exact test was used. Correlations between IgG4-RD RI and serologic parameters (ESR, CRP, C3, C4, IgG4 concentration, IgG concentration, and IgG4/IgG ratio) were evaluated using the Spearman's correlation coefficient. Correlations were assessed in the normal serum IgG4 concentration and elevated serum IgG4 concentration groups. Multivariable linear regression analysis with backward elimination was conducted to select a combination of serologic parameters that could potentially have a stronger correlation with IgG4-RD RI. All variables that significantly correlated with IgG4-RD RI in the correlation analysis were included in the multivariable model, except for the serum IgG4/IgG ratio, which was excluded due to multicollinearity with serum IgG4 concentration and serum IgG concentration. The variables selected in the multivariable analysis were combined by multiplying each variable by its respective β coefficient, and then summing them. A p-value of < 0.05 was considered statistically significant. All analyses were conducted using SPSS software (version 25.0; IBM Corp., Armonk, NY, USA). Figures were generated using GraphPad Prism (version 7.0; GraphPad Software Inc., San Diego, CA, USA).

Results

Baseline characteristics of the patients

A total of 148 patients with IgG4-RD who fulfilled the 2019 ACR/EULAR classification criteria for IgG4-RD were included for analysis. The median value of the total points of the 2019 ACR/EULAR classification criteria for IgG4-RD was 26.0 (23.0–34.0). The baseline characteristics of the patients are shown in Table 1. The mean age of the patients was 57.3 (± 11.5) years, and 68.2% were male. The organ most commonly involved was the lymph nodes (36.5%), followed by orbits and lacrimal glands (31.8%), salivary glands (29.1%), kidney (16.2%), retroperitoneum (15.5%), pancreas (13.5%), and lung (13.5%). According to the number of organs involved, 48.0%, 23.0%, and 29.1% of the patients had one, two, and three or more organs involved, respectively. The median (or mean) values of the serologic parameters were as follows: ESR, 34.0 (15.0–61.0) mm/h; CRP, 2.4 (0.5–10.4) mg/L; C3, 102.3 (± 31.9) mg/dL; C4, 23.5 (± 11.0) mg/dL; IgG4 concentration, 439.0 (179.3–

TABLE 1 Characteristics of the 148 patients diagnosed with IgG4-related disease.

	N = 148
Age, years, mean (± SD)	57.3 (± 11.5)
Male sex, n (%)	101 (68.2)
Organ involvement, n (%)	
Lymph nodes	54 (36.5)
Orbits and lacrimal glands	47 (31.8)
Salivary glands	43 (29.1)
Kidney	24 (16.2)
Retroperitoneal fibrosis	23 (15.5)
Pancreas	20 (13.5)
Lung	20 (13.5)
Aorta	12 (8.1)
Bile duct	8 (5.4)
Prostate	6 (4.1)
Sinusitis	6 (4.1)
Pituitary gland	4 (2.7)
Others*	25 (16.9)
Number of organs involved, n (%)	
1 organ involved	71 (48.0)
2 organs involved	34 (23.0)
≥3 organs involved	43 (29.1)
ESR, mm/h, median (IQR)	34.0 (15.0–61.0)
CRP, mg/L, median (IQR)	2.4 (0.5–10.4)
C3, mg/dL, mean (± SD)	102.3 (± 31.9)
C4, mg/dL, mean (± SD)	23.5 (± 11.0)
IgG4 concentration, mg/dL, median (IQR)	439.0 (179.3–1157.5)
Normal serum IgG4 concentration, n (%)	38 (25.7)
Elevated serum IgG4 concentration, n (%)	110 (74.3)
IgG concentration, mg/dL, median (IQR)	1535.9 (1251.8–1975.0)
IgG4/IgG ratio, median (IQR)	0.28 (0.13–0.61)
IgG4-RD RI, median (IQR)	5.0 (4.0–8.0)

ESR, erythrocyte sedimentation rate; CRP, C-reactive protein; IgG4-RD, IgG4-related disease; RI, responder index.
*Detailed numbers of patients with other organ involvement are as follows: pleura (n = 4), heart (n = 3), mesentery (n = 3), paraspinal mass (n = 3), pericardium (n = 3), testicle (n = 3), gallbladder (n = 2), pharynx (n = 2), adnexa (n = 1), bladder (n = 1), colon (n = 1), liver (n = 1), nasal cavity (n = 1), peritoneum (n = 1), skin (n = 1), and stomach (n = 1).

1157.5) mg/dL; IgG concentration, 1535.9 (1251.8–1975.0) mg/dL; and IgG4/IgG ratio, 0.28 (0.13–0.61). According to the serum IgG4 concentrations, 38 (25.7%) and 110 (74.3%) patients were categorized into the normal and elevated serum IgG4 concentration groups, respectively. The median value of IgG4-RD RI was 5.0 (4.0–8.0).

Comparison between patients with normal and elevated serum IgG4 concentrations

Compared with patients with normal serum IgG4 concentrations, those with elevated serum IgG4 concentrations were older (52.5 [± 13.4] years vs. 58.9 [± 10.3] years, p = 0.009), more commonly had salivary gland (7.9% vs. 36.4%, p = 0.001), pancreas (2.6% vs.17.3%, p = 0.023) and multiple organ involvement (p = 0.019), and had lower CRP levels (10.8 [0.9–27.7] mg/L vs. 1.6 [0.5–5.7] mg/L, p = 0.002) (Table 2). As per the definition of each group, serum IgG4 concentrations were significantly higher in the elevated serum IgG4 concentration group (122.5 [73.1–150.8] mg/dL vs. 668.0 [351.0–1362.5] mg/dL, p < 0.001). The serum IgG concentration (1243.0 [1106.3–1541.5] mg/dL vs. 1667.0 [1367.0–2033.4] mg/dL, p < 0.001) and serum IgG4/IgG ratio (0.09 [0.04–0.12] vs. 0.45 [0.23–0.72], p < 0.001) were also higher in the elevated serum IgG4 concentration group. With regard to disease activity, IgG4-RD RI was higher in the elevated serum IgG4 concentration group (4.0 [4.0–6.0] vs. 6.0 [4.0–8.0], p = 0.012).

TABLE 2 Comparison between patients with normal and elevated serum IgG4 concentration.

	Normal serum IgG4 concentration (N = 38)	Elevated serum IgG4 concentration (N = 110)	P-value
Age, years, mean (± SD)	52.5 (± 13.4)	58.9 (± 10.3)	0.009
Male sex, n (%)	22 (57.9)	79 (71.8)	0.112
Organ involvement, n (%)			
Lymph nodes	10 (26.3)	44 (40.0)	0.131
Orbits and lacrimal glands	8 (21.1)	39 (35.5)	0.100
Salivary glands	3 (7.9)	40 (36.4)	0.001
Kidney	5 (13.2)	19 (17.3)	0.553
Retroperitoneal fibrosis	7 (18.4)	16 (14.5)	0.570
Pancreas	1 (2.6)	19 (17.3)	0.023
Lung	5 (13.2)	15 (13.6)	0.941
Aorta	3 (7.9)	9 (8.2)	> 0.999
Bile duct	0 (0.0)	8 (7.3)	0.114
Prostate	2 (5.3)	4 (3.6)	0.647
Sinusitis	0 (0.0)	6 (5.5)	0.339
Pituitary gland	2 (5.3)	2 (1.8)	0.272
Others*	10 (26.3)	15 (13.6)	0.072
Number of organs involved			
1 organ involved, n (%)	25 (65.8)	46 (41.8)	0.019
2 organs involved, n (%)	8 (21.1)	26 (23.6)	
≥3 organs involved, n (%)	5 (13.2)	38 (34.5)	
ESR, mm/h, median (IQR)	37.5 (13.8–77.0)	32.0 (15.5–57.0)	0.868
CRP, mg/L, median (IQR)	10.8 (0.9–27.7)	1.6 (0.5–5.7)	0.002
C3, mg/dL, mean (± SD)	112.6 (± 23.5)	99.0 (± 33.7)	0.059
C4, mg/dL, mean (± SD)	27.2 (± 8.1)	22.4 (± 11.6)	0.053
IgG4 concentration, mg/dL, median (IQR)	122.5 (73.1–150.8)	668.0 (351.0–1362.5)	< 0.001
IgG concentration, mg/dL, median (IQR)	1243.0 (1106.3–1541.5)	1667.0 (1367.0–2033.4)	< 0.001
IgG4/IgG ratio, median (IQR)	0.09 (0.04–0.12)	0.45 (0.23–0.72)	< 0.001
IgG4-RD RI, median (IQR)	4.0 (4.0–6.0)	6.0 (4.0–8.0)	0.012

ESR, erythrocyte sedimentation rate; CRP, C-reactive protein; IgG4-RD, IgG4-related disease; RI, responder index.
*Detailed comparisons of other organ involvement are as follows: pleura (2.6% vs. 2.7%, p > 0.999), heart (2.6% vs. 1.8%, p > 0.999), mesentery (2.6% vs. 1.8%, p > 0.999), paraspinal mass (0.0% vs. 2.7%, p = 0.570), pericardium (2.6% vs. 1.8%, p > 0.999), testicle (5.3% vs. 0.9%, p = 0.162), gallbladder (0.0% vs. 1.8%, p > 0.999), pharynx (5.3% vs. 0.0%, p = 0.065), adnexa (2.6% vs. 0.0%, p = 0.257), bladder (2.6% vs. 0.0%, p = 0.257), colon (0.0% vs. 0.9%, p > 0.999), liver (0.0% vs. 0.9%, p > 0.999), nasal cavity (2.6% vs. 0.0%, p = 0.257), peritoneum (2.6% vs. 0.0%, p = 0.257), skin (0.0% vs. 0.9%, p > 0.999), and stomach (0.0% vs. 0.9%, p > 0.999).

10.3389/fimmu.2022.1020459

Correlation between IgG4-RD RI and serologic parameters

In the normal serum IgG4 concentration group, serum IgG4 concentration did not significantly correlate with IgG4-RD RI (rho = 0.162, p = 0.332) (Figure 1). However, serum IgG concentration significantly correlated with IgG4-RD RI (rho = 0.411, p = 0.013). When the correlations were tested in the patients with elevated serum IgG4 concentrations, serum IgG4 concentration significantly correlated with IgG4-RD RI (rho = 0.423, p < 0.001). Other serologic parameters including ESR (rho = 0.196, p = 0.041), C3 (rho = -0.432, p < 0.001), C4 (rho = -0.363, p = 0.001), IgG concentration (rho = 0.224, p = 0.020), and IgG4/IgG ratio (rho = 0.328, p = 0.001) also had a significant correlation with IgG4-RD RI (Figure 2). The combination of C3 and serum IgG4 concentration (-0.034*C3 [mg/dL] + 0.001*IgG4 concentration [mg/dL]) was selected as a composite parameter in the multivariable linear regression analysis, which had the strongest correlation with IgG4-RD RI (rho = 0.509, p < 0.001) (Figure 2H).

Discussion

In this study, we found that serologic parameters that correlate with the disease activity of IgG4-RD differ between patients with normal and elevated serum IgG4 concentrations. IgG concentration was the only serologic parameter that correlated with IgG4-RD RI in patients with normal serum IgG4 concentrations. On the other hand, several serologic parameters, including ESR, C3, C4, IgG4 concentration, IgG concentration, and IgG4/IgG ratio, correlated with IgG4-RD RI in patients with elevated serum IgG4 concentrations. This finding is meaningful because it provides better insights into how serologic parameters could be interpreted in regard to disease activity in patients with IgG4-RD who have normal and elevated serum IgG4 concentrations, respectively.

In our study population, 25.7% of the patients had normal serum IgG4 concentrations. Similarly, in previous studies, normal serum IgG4 concentrations have been reported in 9.7–48.5% of patients with IgG4-RD (4–6). Thus, it is important to be aware that a substantial fraction of patients with IgG4-RD have normal serum IgG4 concentrations. There were some significant differences in characteristics between patients with normal and elevated serum IgG4 concentrations. Patients with elevated serum IgG4 concentrations were older and had a greater prevalence of multiple organ involvement than those with normal serum IgG4 concentrations. The salivary glands and pancreas were more commonly involved in patients with elevated serum IgG4 concentrations than in those with normal serum IgG4 concentrations. This is consistent with a previous cohort study, in which most of the patients (76%) were non-Hispanic whites: patients with elevated serum IgG4 concentrations were older, the proportion of patients with multiple organ involvement was higher, and the pancreas was more commonly involved than in those with normal serum IgG4 concentrations (6). Our study adds to the previous knowledge that these characteristic differences between patients with normal and elevated serum IgG4 concentrations also apply to the Asian population.

Another significant difference between patients with normal and elevated serum IgG4 concentrations was the lower CRP level in patients with elevated serum IgG4 concentrations. A recent study has shown that patients with higher number of superficial organ involvement (i.e., orbits, lacrimal glands, salivary glands, sinus and skin) have significantly lower CRP levels than those with internal organ-dominant (i.e., all other organs except the lymph nodes) involvement (14). In our study, compared with patients with normal serum IgG4 concentrations, those with elevated serum IgG4 concentrations had higher number of superficial organ involvement (0 [0–1] vs. 1 [0–1], p = 0.001) (data not shown in the Results). The difference in organ involvement pattern between the two groups could be a possible explanation for the lower CRP level in patients with elevated serum IgG4 concentrations.

Our data revealed that serologic parameters that correlate with the disease activity of IgG4-RD differ between patients with normal and elevated serum IgG4 concentrations. In patients with normal serum IgG4 concentrations, IgG concentration (rho = 0.411, p = 0.013), but not IgG4 concentration (rho = 0.162, p = 0.332), significantly correlated with IgG4-RD RI. In contrast, in patients with elevated serum IgG4 concentrations, multiple serologic parameters including IgG4 concentration (rho = 0.423, p < 0.001) correlated with IgG4-RD RI. The precise role of IgG4 on the disease pathogenesis of IgG4-RD remains unclear; an adoptive transfer model has shown that injection of patient IgG4 in neonatal BALB/c mice results in pancreatic and salivary gland injuries, suggesting a pathogenic role of IgG4 (15); while an anti-inflammatory role of IgG4 has also been suggested (16). Further studies are needed to determine whether the serum IgG4 plays a different role in patients with normal and elevated serum IgG4 concentrations. Regardless, our study shows that serum IgG4 concentration correlates with disease activity only in patients with elevated serum IgG4 concentrations.

Similar to the correlations observed in patients with elevated serum IgG4 concentrations in our study, a previous study consisting of 72 patients with IgG4-RD (68 [94.4%] patients with elevated serum IgG4 concentrations) showed that serum IgG4 concentration, serum IgG concentration, C3, and C4 correlate with IgG4-RD RI (17). We further advanced this finding by investigating whether the combination of the serologic parameters could yield a stronger correlation with disease activity and found that a combination of C3 and IgG4 concentration (rho = 0.509) had a stronger correlation with IgG4-RD RI than C3 alone (rho = -0.432) or IgG4 concentration alone (rho = 0.423). A previous study on 8 patients with IgG4-RD suggested that serum IgG4 could be associated with complement activation (18). Subsequent study on 12 patients with IgG4-RD from the same group reported that serum IgG4, particularly that

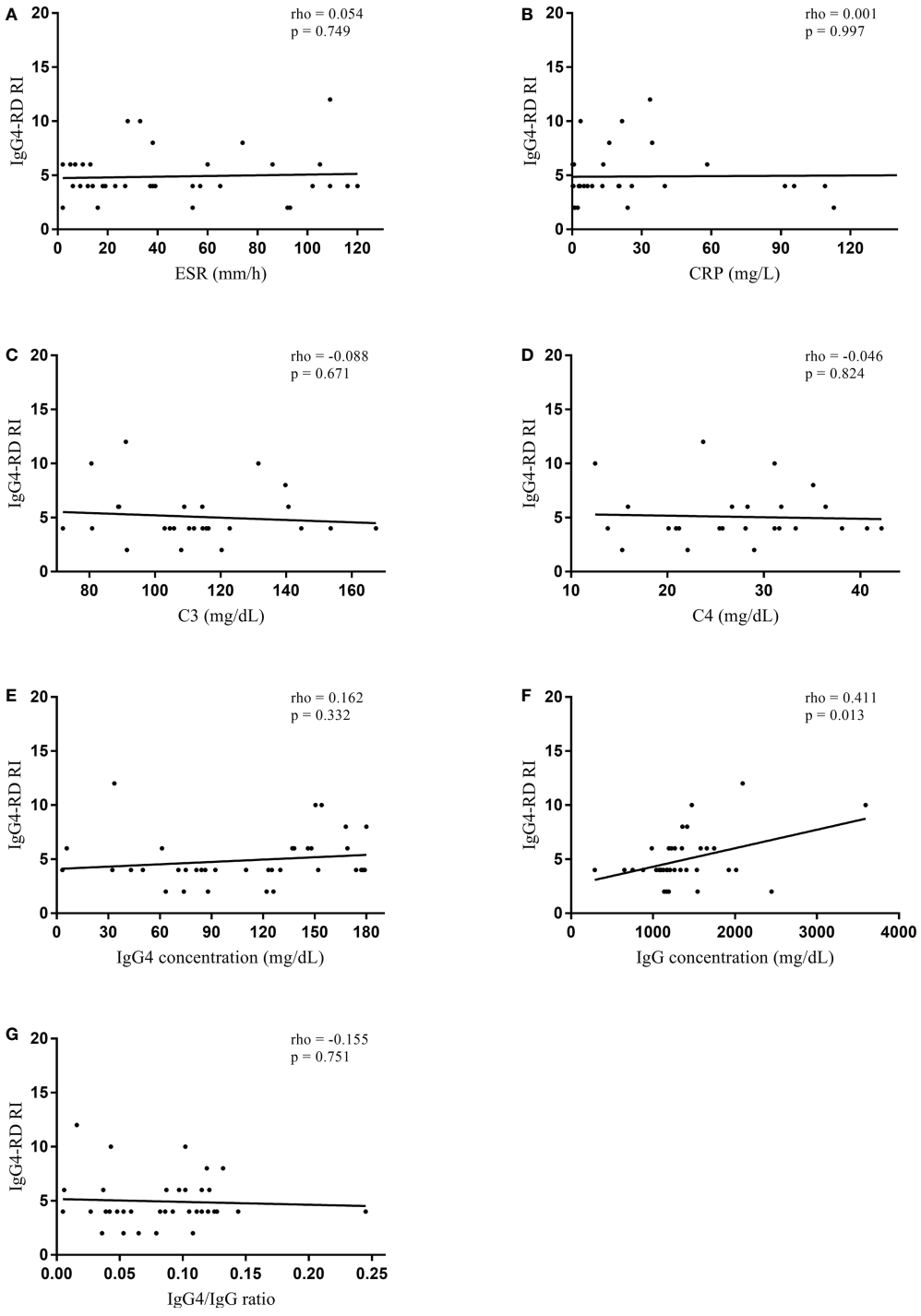

FIGURE 1
Spearman's correlation coefficient between serologic parameters and IgG4-RD RI in the normal serum IgG4 concentration group. **(A)** ESR, **(B)** CRP, **(C)** C3, **(D)** C4, **(E)** IgG4 concentration, **(F)** IgG concentration, and **(G)** IgG4/IgG ratio. IgG4-RD, IgG4-related disease; RI, responder index; ESR, erythrocyte sedimentation rate; CRP, C-reactive protein.

with flucosylation change, may be associated with complement activation (19). In contrast, more recent studies with larger number of patients (n = 85 (20); and n = 328 (21)) suggested that hypocomplementemia in IgG4-RD is associated with IgG subclasses other than IgG4. Indeed, immune complexes that contain IgG4 bind complement weakly; hypocomplementemia in IgG4-RD results from immune complexes containing IgG1 or IgG3 rather than IgG4 (2, 22, 23). The mechanistically independent

10.3389/fimmu.2022.1020459

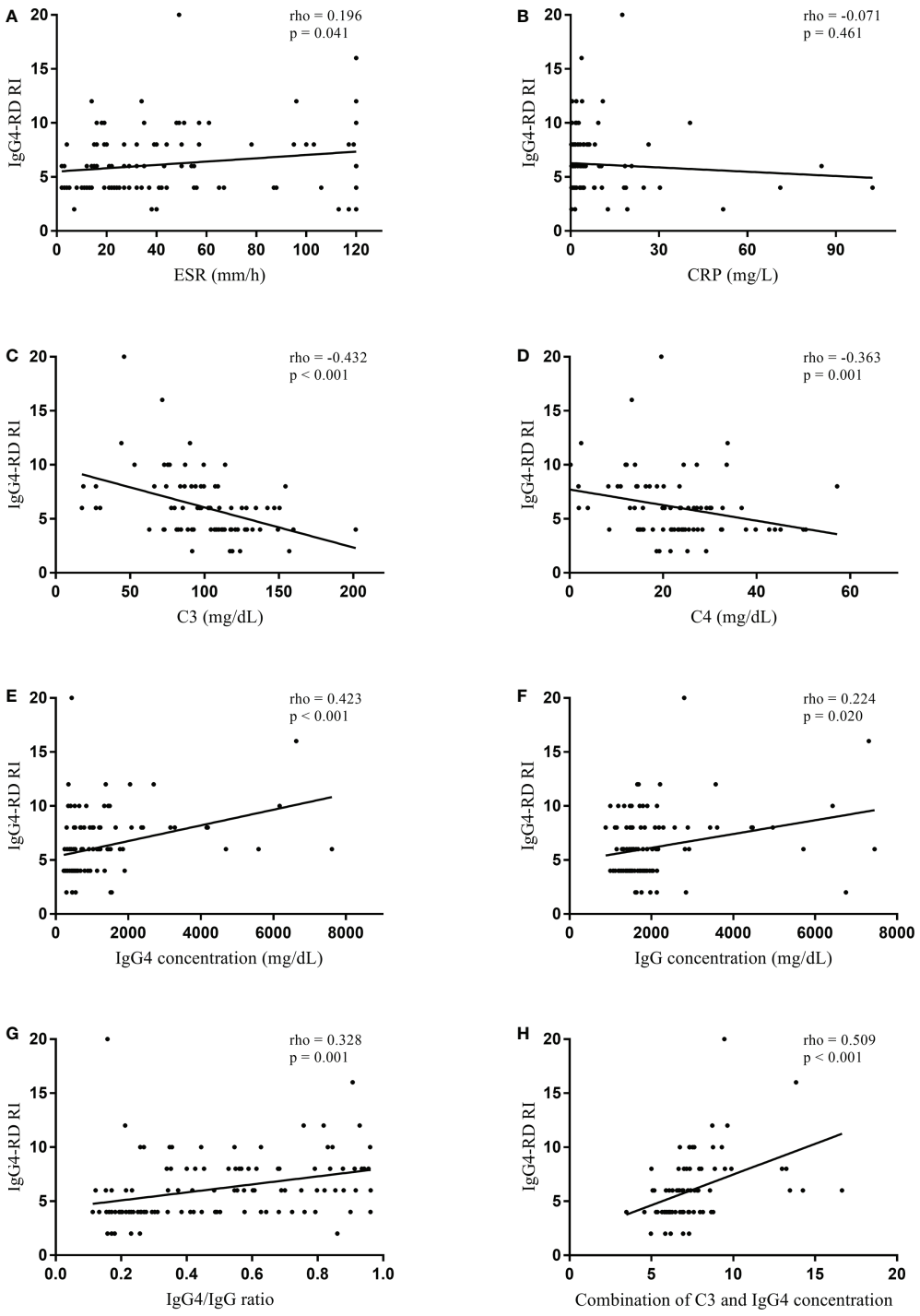

FIGURE 2
Spearman's correlation coefficient between serologic parameters and IgG4-RD RI in the elevated serum IgG4 concentration group. **(A)** ESR, **(B)** CRP, **(C)** C3, **(D)** C4, **(E)** IgG4 concentration, **(F)** IgG concentration, **(G)** IgG4/IgG ratio, and **(H)** combination of C3 and IgG4 concentration (-0.034*C3 [mg/dL] + 0.001*IgG4 concentration [mg/dL]). IgG4-RD, IgG4-related disease; RI, responder index; ESR, erythrocyte sedimentation rate; CRP, C-reactive protein.

action of C3 and serum IgG4 could explain why the combination of these two parameters showed a stronger correlation with disease activity.

We used a cut-off of 201 mg/dL to categorize patients into normal serum IgG4 concentration and elevated serum IgG4 concentration groups. Diagnostic criteria for IgG4-RD, established a decade ago, used a value of 135 mg/dL for the cut-off of elevated serum IgG4 concentration (24). One might argue that this cut-off value should be used for categorizing patients with normal and elevated serum IgG4 concentrations; however, this cut-off value was calculated in a study in which serum IgG4 concentrations were measured using a Binding Site assay (Binding Site, Birmingham, UK) (9). More recent studies have shown that the reference range of serum IgG4 concentration varies according to the measurement method; serum IgG4 concentrations are significantly higher when measured with the Siemens assay than with the Binding Site assay (25, 26). In line with these observations, the 2019 ACR/EULAR classification criteria for IgG4-RD did not state 135 mg/dL as the cut-off for the upper normal limit of serum IgG4 concentration but adopted the reference range of each assay as the cut-off for classification (12). As serum IgG4 concentrations were measured using Siemens assay in our study, we used the concentration of 201 mg/dL as the cut-off for the upper normal limit (25).

Our study had some limitations. First, the possibility of prozone phenomenon in the patients with normal serum IgG4 concentrations cannot be excluded (27). As this was a retrospective study using data obtained at the time of diagnosis of IgG4-RD, we are uncertain whether diluting method was appropriately performed to avoid the prozone phenomenon. Studies have shown that elevated serum IgG4 concentrations decrease during glucocorticoid treatment in all patients with IgG4-RD (28, 29). Therefore, if the normal serum IgG4 concentrations were the result of prozone phenomenon, the concentrations during the glucocorticoid treatment would increase initially and decrease subsequently. However, in the patients with normal serum IgG4 concentrations in our study, the increase in serum IgG4 concentrations during the early phase of glucocorticoid treatment was not observed in any of the patients (data not shown in the Results). This observation can be a clue to infer that the normal serum IgG4 concentrations were not likely the result of prozone phenomenon. Second, only the traditional serologic biomarkers were available, and we lacked several types of data, such as interleukin-6, soluble interleukin-2 receptor and CC-chemokine ligand 18, which have been more recently suggested as putative biomarkers of disease activity (8, 17, 30–32). However, considering that the recently suggested putative biomarkers are not as easily available as the traditional serologic biomarkers in routine clinical practice, our data are still clinically relevant for routine clinical practice. Third, although we found that serum IgG concentration, but not serum IgG4 concentration, correlated with disease activity in patients with normal serum IgG4 concentrations, an explanation for this correlation could not be drawn from our data. Further studies evaluating the mechanisms underlying this correlation would be helpful.

In conclusion, we demonstrated that serologic parameters correlate differently with disease activity depending on serum IgG4 concentrations. IgG concentration was the only serologic parameter that correlated with IgG4-RD RI in patients with normal serum IgG4 concentrations, while multiple serologic variables including ESR, C3, C4, IgG4 concentration, IgG concentration, and IgG4/IgG ratio correlated with IgG4-RD RI in patients with elevated serum IgG4 concentrations. In the latter group, a combination of C3 and IgG4 concentration as a composite parameter showed the strongest correlation with IgG4-RD RI. These findings could be useful for a more accurate serologic assessment of disease activity in patients with normal and elevated serum IgG4 concentrations, respectively.

Data availability statement

The original contributions presented in the study are included in the article/Supplementary Material. Further inquiries can be directed to the corresponding authors.

Ethics statement

The studies involving human participants were reviewed and approved by the Institutional Review Board (IRB) of Gangnam Severance Hospital (IRB No: 3-2022-0247). Written informed consent for participation was not required for this study in accordance with the national legislation and the institutional requirements.

Author contributions

OCK, M-CP and Y-GK contributed to the conception and design of the study. OCK, M-CP and Y-GK participated in acquisition of data, data analyses and data interpretation. OCK, M-CP and Y-GK wrote the manuscript. All authors contributed to the article and approved the submitted version.

Funding

Y-GK received grants from the National Research Foundation of Korea (NRF-2021M3A9G1026605).

Conflict of interest

The authors declare that the research was conducted in the absence of any commercial or financial relationships that could be construed as a potential conflict of interest.

Publisher's note

References

1. Perugino CA, Stone JH. IgG4-related disease: An update on pathophysiology and implications for clinical care. *Nat Rev Rheumatol* (2020) 16(12):702–14. doi: 10.1038/s41584-020-0500-7

2. Kamisawa T, Zen Y, Pillai S, Stone JH. IgG4-related disease. *Lancet* (2015) 385(9976):1460–71. doi: 10.1016/s0140-6736(14)60720-0

3. Koneczny I, Tzartos J, Mané-Damas M, Yilmaz V, Huijbers MG, Lazaridis K, et al. IgG4 autoantibodies in organ-specific autoimmunopathies: Reviewing class switching, antibody-producing cells, and specific immunotherapies. *Front Immunol* (2022) 13:834342. doi: 10.3389/fimmu.2022.834342

4. Carruthers MN, Khosroshahi A, Augustin T, Deshpande V, Stone JH. The diagnostic utility of serum IgG4 concentrations in IgG4-related disease. *Ann Rheum Dis* (2015) 74(1):14–8. doi: 10.1136/annrheumdis-2013-204907

5. Wallace ZS, Mattoo H, Carruthers M, Mahajan VS, Della Torre E, Lee H, et al. Plasmablasts as a biomarker for IgG4-related disease, independent of serum IgG4 concentrations. *Ann Rheum Dis* (2015) 74(1):190–5. doi: 10.1136/annrheumdis-2014-205233

6. Wallace ZS, Deshpande V, Mattoo H, Mahajan VS, Kulikova M, Pillai S, et al. IgG4-related disease: Clinical and laboratory features in one hundred twenty-five patients. *Arthritis Rheumatol* (2015) 67(9):2466–75. doi: 10.1002/art.39205

7. Wallace ZS, Khosroshahi A, Carruthers MD, Perugino CA, Choi H, Campochiaro C, et al. An international multispecialty validation study of the IgG4-related disease responder index. *Arthritis Care Res (Hoboken)* (2018) 70 (11):1671–8. doi: 10.1002/acr.23543

8. Tang J, Cai S, Ye C, Dong L. Biomarkers in IgG4-related disease: A systematic review. *Semin Arthritis Rheum* (2020) 50(2):354–9. doi: 10.1016/j.semarthrit.2019.06.018

9. Hamano H, Kawa S, Horiuchi A, Unno H, Furuya N, Akamatsu T, et al. High serum IgG4 concentrations in patients with sclerosing pancreatitis. *N Engl J Med* (2001) 344(10):732–8. doi: 10.1056/nejm200103083441005

10. Umemura T, Zen Y, Hamano H, Kawa S, Nakanuma Y, Kiyosawa K. Immunoglobin G4-hepatopathy: association of immunoglobin G4-bearing plasma cells in liver with autoimmune pancreatitis. *Hepatology* (2007) 46(2):463–71. doi: 10.1002/hep.21700

11. Nishino T, Toki F, Oyama H, Shimizu K, Shiratori K. Long-term outcome of autoimmune pancreatitis after oral prednisolone therapy. *Intern Med* (2006) 45 (8):497–501. doi: 10.2169/internalmedicine.45.1565

12. Wallace ZS, Naden RP, Chari S, Choi HK, Della-Torre E, Dicaire JF, et al. The 2019 American college of Rheumatology/European league against rheumatism classification criteria for IgG4-related disease. *Ann Rheum Dis* (2020) 79(1):77–87. doi: 10.1136/annrheumdis-2019-216561

13. Carruthers MN, Stone JH, Deshpande V, Khosroshahi A. Development of an IgG4-RD responder index. *Int J Rheumatol* (2012) 2012:259408. doi: 10.1155/2012/259408

14. Li J, Peng Y, Zhang Y, Zhang P, Liu Z, Lu H, et al. Identifying clinical subgroups in IgG4-related disease patients using cluster analysis and IgG4-RD composite score. *Arthritis Res Ther* (2020) 22(1):7. doi: 10.1186/s13075-019-2090-9

15. Shiokawa M, Kodama Y, Kuriyama K, Yoshimura K, Tomono T, Morita T, et al. Pathogenicity of IgG in patients with IgG4-related disease. *Gut* (2016) 65 (8):1322–32. doi: 10.1136/gutjnl-2015-310336

16. Aalberse RC, Stapel SO, Schuurman J, Rispens T. Immunoglobulin G4: An odd antibody. *Clin Exp Allergy* (2009) 39(4):469–77. doi: 10.1111/j.1365-2222.2009.03207.x

17. Kawashiri SY, Origuchi T, Umeda M, Nishino A, Shimizu T, Fukui S, et al. Association of serum levels of fibrosis-related biomarkers with disease activity in patients with IgG4-related disease. *Arthritis Res Ther* (2018) 20(1):277. doi: 10.1186/s13075-018-1777-7

18. Sugimoto M, Watanabe H, Asano T, Sato S, Takagi T, Kobayashi H, et al. Possible participation of IgG4 in the activation of complement in IgG4-related disease with hypocomplementemia. *Mod Rheumatol* (2016) 26(2):251–8. doi: 10.3109/14397595.2015.1076924

19. Konno N, Sugimoto M, Takagi T, Furuya M, Asano T, Sato S, et al. Changes in n-glycans of IgG4 and its relationship with the existence of hypocomplementemia and individual organ involvement in patients with IgG4-related disease. *PloS One* (2018) 13(4):e0196163. doi: 10.1371/journal.pone.0196163

20. Fujita Y, Fukui S, Umeda M, Tsuji S, Iwamoto N, Nakashima Y, et al. Clinical characteristics of patients with IgG4-related disease complicated by hypocomplementemia. *Front Immunol* (2022) 13:828122. doi: 10.3389/fimmu.2022.828122

21. Fujisawa Y, Mizushima I, Yamada K, Yamamoto M, Saeki T, Matsui S, et al. Hypocomplementemia is related to elevated serum levels of IgG subclasses other than IgG4 in IgG4-related kidney disease. *Mod Rheumatol* (2021) 31(1):241–8. doi: 10.1080/14397595.2019.1709942

22. Tao MH, Smith RI, Morrison SL. Structural features of human immunoglobulin G that determine isotype-specific differences in complement activation. *J Exp Med* (1993) 178(2):661–7. doi: 10.1084/jem.178.2.661

23. Canfield SM, Morrison SL. The binding affinity of human IgG for its high affinity fc receptor is determined by multiple amino acids in the CH2 domain and is modulated by the hinge region. *J Exp Med* (1991) 173(6):1483–91. doi: 10.1084/jem.173.6.1483

24. Umehara H, Okazaki K, Masaki Y, Kawano M, Yamamoto M, Saeki T, et al. Comprehensive diagnostic criteria for IgG4-related disease (IgG4-RD), 2011. *Mod Rheumatol* (2012) 22(1):21–30. doi: 10.1007/s10165-011-0571-z

25. Xia CS, Fan CH, Liu YY. Diagnostic performances of serum IgG4 concentration and IgG4/IgG ratio in IgG4-related disease. *Clin Rheumatol* (2017) 36(12):2769–74. doi: 10.1007/s10067-017-3685-7

26. Usami Y, Sugano M, Uehara T, Koinuma M, Ishimine N, Kawasaki K, et al. Cut-off values of serum IgG4 among three reagents, including a novel IgG4 reagent: A multicenter study. *Sci Rep* (2021) 11(1):7280. doi: 10.1038/s41598-021-86024-5

27. Khosroshahi A, Cheryk LA, Carruthers MN, Edwards JA, Bloch DB, Stone JH. Brief report: Spuriously low serum IgG4 concentrations caused by the prozone phenomenon in patients with IgG4-related disease. *Arthritis Rheumatol* (2014) 66 (1):213–7. doi: 10.1002/art.38193

28. Culver EL, Sadler R, Simpson D, Cargill T, Makuch M, Bateman AC, et al. Elevated serum IgG4 levels in diagnosis, treatment response, organ involvement, and relapse in a prospective IgG4-related disease UK cohort. *Am J Gastroenterol* (2016) 111(5):733–43. doi: 10.1038/ajg.2016.40

29. Kamisawa T, Shimosegawa T, Okazaki K, Nishino T, Watanabe H, Kanno A, et al. Standard steroid treatment for autoimmune pancreatitis. *Gut* (2009) 58 (11):1504–7. doi: 10.1136/gut.2008.172908

30. Akiyama M, Yasuoka H, Yoshimoto K, Takeuchi T. CC-chemokine ligand 18 is a useful biomarker associated with disease activity in IgG4-related disease. *Ann Rheum Dis* (2018) 77(9):1386–7. doi: 10.1136/annrheumdis-2017-212110

31. Kasashima S, Kawashima A, Kasashima F, Endo M, Matsumoto Y, Kawakami K. Inflammatory features, including symptoms, increased serum interleukin-6, and c-reactive protein, in IgG4-related vascular diseases. *Heart Vessels* (2018) 33(12):1471–81. doi: 10.1007/s00380-018-1203-8

32. Tsukuda S, Ikeura T, Ito T, Nakamaru K, Masuda M, Hori Y, et al. Clinical implications of elevated serum interleukin-6 in IgG4-related disease. *PloS One* (2020) 15(1):e0227479. doi: 10.1371/journal.pone.0227479

frontiers | Frontiers in Immunology

TYPE Original Research
PUBLISHED 14 March 2023
DOI 10.3389/fimmu.2023.1021513

OPEN ACCESS

EDITED BY
Gestur Vidarsson,
Sanquin Research, Netherlands

REVIEWED BY
T. Rispens,
Sanquin Research, Netherlands
Anja Lux,
University of Erlangen Nuremberg, Germany
Maartje G. Huijbers,
Leiden University Medical Center (LUMC), Netherlands

*CORRESPONDENCE
Jérôme J. Devaux
jerome.devaux@igf.cnrs.fr

†Deceased

SPECIALTY SECTION
This article was submitted to B Cell Biology, a section of the journal Frontiers in Immunology

RECEIVED 17 August 2022
ACCEPTED 02 March 2023
PUBLISHED 14 March 2023

CITATION
Taieb G, Jentzer A, Vegezzi E, Lleixà C, Illa I, Querol L and Devaux JJ (2023) Effect of monovalency on anti-contactin-1 IgG4. *Front. Immunol.* 14:1021513. doi: 10.3389/fimmu.2023.1021513

Effect of monovalency on anti-contactin-1 IgG4

Guillaume Taieb[1,2], Alexandre Jentzer[1,3], Elisa Vegezzi[4], Cinta Lleixà[5], Isabel Illa[5†], Luis Querol[5] and Jérôme J. Devaux[1*]

[1]Institut de Génomique Fonctionnelle, Université de Montpellier, CNRS, INSERM, Montpellier, France, [2]Department of Neurology, CHU Montpellier, Hôpital Gui de Chauliac, Montpellier, France, [3]Department of Immunology, CHU Montpellier, Hôpital Saint-Eloi, Montpellier, France, [4]Department of Brain and Behavioral Sciences, University of Pavia, Pavia, Italy, [5]Neuromuscular Diseases Unit, Hospital de la Santa Creu i Sant Pau, Universitat Autónoma de Barcelona, Barcelona, Spain

Introduction: Autoimmune nodopathies (AN) have been diagnosed in a subset of patients fulfilling criteria for chronic inflammatory demyelinating polyradiculoneuropathy (CIDP) who display no or poor response to intravenous immunoglobulins. Biomarkers of AN are autoantibodies, mainly IgG4, directed against the ternary paranodal complex composed by neurofascin-155, contactin-1 (CNTN1), and Contactin-associated-protein-1 (CASPR1) or against the nodal isoforms of neurofascin. IgG4 can undergo a Fab-arm exchange (FAE) which results in functionally monovalent antibody. This phenomenon differentially affects the pathogenicity of IgG4 depending on the target of autoantibodies. Here, we have evaluated this issue by examining the impact of valency on anti-CNTN1 IgG4 which induces paranodal destruction through a function blocking activity.

Methods: Sera were obtained from 20 patients with AN associated with anti-CNTN1 antibodies. The proportion of monospecific/bispecific anti-CNTN1 antibodies was estimated in each patient by ELISA by examining the ability of serum antibodies to cross-link untagged CNTN1 with biotinylated CNTN1. To determine the impact of monovalency, anti-CNTN1 IgG4 were enzymatically digested into monovalent Fab and tested *in vitro* on cell aggregation assay. Also, intraneural injections were performed to determine whether monovalent Fab and native IgG4 may penetrate paranode, and antibody infiltration was monitored 1- and 3-days post injection.

Results and discussion: We found that the percentage of monospecific antibodies were lower than 5% in 14 out of 20 patients (70%), suggesting that IgG4 have undergone extensive FAE *in situ*. The levels of monospecific antibodies correlated with the titers of anti-CNTN1 antibodies. However, no correlation was found with clinical severity, and patients with low or high percentage of monospecific antibodies similarly showed a severe phenotype. Native anti-CNTN1 IgG4 were shown to inhibit the interaction between cells expressing CNTN1/CASPR1 and cells expressing neurofascin-155 using an *in vitro* aggregation assay. Similarly, monovalent Fab significantly inhibited the interaction between CNTN1/CASPR1 and neurofascin-155. Intraneural

injections of Fab and native anti-CNTN1 IgG4 indicated that both mono- and bivalent anti-CNTN1 IgG4 potently penetrated the paranodal regions and completely invaded this region by day 3. Altogether, these data indicate anti-CNTN1 IgG4 are mostly bispecific in patients, and that functionally monovalent anti-CNTN1 antibodies have the pathogenic potency to alter paranode.

KEYWORDS

immunoglobulin, demyelination, GBS, auto-immune, myelin, Schwann, axon

Introduction

A subset of patients with autoimmune neuropathies displays acute or subacute onset, no overt macrophage-mediated demyelination on nerve biopsy, poor response to intravenous immunoglobulins, improvement after Rituximab, and specific autoantibodies directed against the paranodal proteins. Due to these characteristic features, these patients are currently classified under the autoimmune nodopathy diagnostic category (AN) (1). Autoantibodies associated with AN are mainly IgG4 and are directed against the ternary paranodal protein complex composed by neurofascin-155 (Nfasc155), contactin-1 (CNTN1), and Contactin-associated-protein-1 (CASPR1) or against the nodal isoforms of neurofascin (2). Nfasc155 is localized on Schwann cell surface and binds to CNTN1 and CASPR1 that are both localized on the surface of axon in septate-like junction at paranodes. This axoglial junction is important for the clustering/stabilization of voltage-gated sodium channels at the nodes of Ranvier and for myelin insulation (3–7). IgG4 are described as anti-inflammatory isotypes because they are unable to elicit both antibody-dependent cell-mediated cytotoxicity and complement-dependent cell-mediated cytotoxicity (8). However, passive transfer of purified IgG4 from patients with AN reproduces the disease in animals. While anti-Nfasc155 IgG4 promotes a cross-linking of transmembrane Nfasc155 leading to Nfasc155 depletion from the surface cell, anti-CNTN1 IgG4 induces a functional blockade of CNTN1/CASPR1-Nfasc155 interaction (9, 10). The first mechanism interferes on paranode formation and maintenance while the second elicits paranodal destruction. IgG4 is also unique because it exhibits labile disulfide connections between its heavy chains (11). Thus, IgG4 is able to undergo a dynamic swapping leading to half-molecule exchange, also termed Fab arm exchange (FAE) (12). FAE results in bispecific IgG4 that are monovalent to their target. This phenomenon appears to differentially affect the pathogenicity of IgG4 autoantibodies. Indeed, while FAE potentiates the pathogenicity of function blocking anti-Muscle-specific kinase (MuSK) IgG4, we recently demonstrated that FAE reduces the impact of anti-Nfasc155 antibodies which act *via* an antigen-crosslinking mechanism (13–15). Here, we examined whether the valency of anti-CNTN1 IgG4 has a beneficial or detrimental effect.

Material and methods

Patients

Sera were obtained from twenty patients with AN associated with anti-CNTN1 IgG4 antibodies, forty-three seronegative CIDP patients seen at CHU Montpellier, and twenty-three healthy donors (Etablissement Français du Sang, Montpellier, France). One sample was obtained from a patient included in the ADHERE trial and was collected prior to treatment. In patients presenting with AN, age, sex, time between sample and disease onset, disability (using the modified Rankin scale [mRS] and the Overall Neuropathy Limitation Scale [ONLS]), nerve conductions studies (according to the electrodiagnostic criteria of European Academy of Neurology/Peripheral Nerve Society guideline) (1), and the presence of nephrotic syndrome were assessed. Titers of anti-CNTN1 and isotype were determined in each patient by ELISA. Titers were defined as the greatest serum dilution resulting in a positive ELISA test. Written informed consent were obtained from all patients.

Antibody purification and cleavage

IgG1, IgG3 and IgG4 fractions were purified with CaptureSelect™ affinity matrix (191303005, 191304005, 2942902005, ThermoFisher scientific, Waltham, MA) on an AKTA Go (Cytiva, Marlborough, MA). Antibodies were desalted to artificial cerebrospinal fluid using HiTrap Desalting column (GE17-1408-01, Cytiva), concentrated at 10 mg/ml, filter sterilized and stored at -20°C until use. Fab fragments were generated using Pierce's Fab preparation kit (44985, Thermofisher) according to manufacturer's protocols. Fab fragments were dialyzed to artificial cerebrospinal fluid, concentrated at 10 mg/ml, and filter sterilized. Digestion was monitored by migration on 4-20% SDS-PAGE gels (Supplementary Figure 1).

Monospecificity ELISA assay

Recombinant human His-tagged CNTN1 (Met1-Ala993) was produced in HEK293T cells and purified with HisTrap HP column

(GE17-5247-01, Cytiva), then was biotinylated as previously described (14). MaxiSorp microtiter plates were coated overnight with 25 ng of untagged human CNTN1 at 4°C. Wells were blocked with 0.5% casein sodium 0.05% Tween 20 in PBS for 1 hour at 37°C, then incubated overnight at 4°C with patients' sera diluted 1:10 or with increasing concentration of purified IgG3 anti CNTN1 (ranging from 50 ng to 20 µg). The day after, wells were incubated with 25 ng of biotinylated-CNTN1 for 1 hour at 37°C, and the reactivity was revealed using peroxidase-conjugated streptavidin (1:2000; 18-152, Merck-Millipore, Burlington, MA) and SIGMAFAST OPD (P9187, Merck-Millipore). The percentage of monospecific antibodies was interpolated from the calibration curve obtained with anti-CNTN1 IgG3 as detailed in Supplementary Method and Supplementary Figure 2. The percentage of monospecific anti-Nfasc155 antibodies was measured in a similar manner against 50 ng of untagged human Nfasc155 as described in Supplementary Method.

Cell aggregation assay

HEK cells were plated in 6-well plates at a density of 500,000 cells/wells and transiently transfected using JetPEI (POL101-10N, Polyplus-transfection, Illkirch-Graffenstaden, France) with mcherry-conjugated (red) rat Nfasc155 or with both rat CNTN1 and GFP-conjugated (green) rat CASPR1, or with only peGFP-N1. The day after, cells were trypsinized using 0.25% trypsin in PBS and suspended in 1 mL of serum free Opti-MEM medium (11564506, ThermoFisher Scientific). Cells were then mixed together in a 1:1 ratio (400,000 cells/ml) in presence of 10 µg of purified antibodies (including either control IgG4 from healthy donors, native anti-CNTN1 IgG4, or monovalent Fab-reactive to CNTN1 from patients AN1 and AN2) and agitated at 100 rpm for 2 hours at 37°C. Fifty microliters of cell suspension were then mounted between slides and coverslips, and immediately observed using an ApoTome fluorescence microscope at the 10X objective. Aggregates were defined as clusters of cells of at least 4 cells. Aggregates showing interactions between green and red cells were considered as cell clusters with contacts. In addition, the percentage of green cells was quantified in each cell clusters. Four experiments were performed for each condition, and a minimum of 40 cell clusters were quantified per experiments.

Intraneural injections and quantification of antibody infiltration

Four adult Wistar rats (9 weeks old) were anesthetized with Isovet and received a subcutaneous injection of buprenorphine for pain relief. Since native IgG4 and Fab do not have the same molecular mass (150 kDa vs 50 kDa), 1 µl of native anti-CNTN1 IgG4 at 10 µg/µl or 1 µl anti-CNTN1 Fab at 3 µg/µl from patient AN1 were injected with a glass micropipette in the sciatic nerves at the level of the sciatic notch.

One or three days after surgery, injected nerves were dissected out, fixed in 2% paraformaldehyde in PBS for 1 hour at 4°C, then rinsed in PBS. Axons were gently teased, dried on glass slides, and stored at -20°C. Teased fibers were permeabilized by immersion in -20°C acetone for 10 min, blocked at RT for 1 hour with PBS containing 5% fish skin gelatin and 0.1% Triton X-100, then incubated overnight at 4°C with a goat antibody against CNTN1 (1:2000; AF904, R&D Systems, Mineapolis, MN). The slides were then washed several times and incubated with the following conjugated secondary antibodies (Jackson ImmunoResearch, West Grove, PA) diluted 1:500 in blocking solution: donkey anti-human IgG Alexa 488 (709-545-149) and donkey anti-goat Alexa 594 (705-585-147). Slides were mounted with Mowiol plus 2% DABCO, and examined using an ApoTome fluorescence microscope (ApoTome, AxioObserver and AxioCam MRm, Carl Zeiss MicroImaging GmbH). Antibody infiltration was quantified using ImageJ software (NIH). The length of IgG labeling (i.e. native anti-CNTN1 IgG4, monovalent Fab-reactive to CNTN1, or control IgG4) and the length of CNTN1 labeling were measured, then the ratio IgG length/paranode length was calculated. Digital images were manipulated into figures with CorelDraw and Corel Photo-Paint (Corel Corporation, Ottawa, Canada).

Statistics

Statistical significance was assessed by unpaired and paired two-tailed Student's t tests, Kolmogorov-Smirnov tests, or by one-way ANOVA followed by Bonferroni's *post-hoc* tests using GraphPad Prism (GraphPad Software, San Diego, CA). Linear regression and Spearman correlation were performed using GraphPad Prism. P values inferior to 0.05 were considered significant.

Standard protocol approvals, registrations, and patient consents

The study was approved by the Ethics Committee of Montpellier University Hospital (IRB-MTP-2020-01-20200339). All animal experiments were in lines with the European community's guiding principles on the care and use of animals (2010/63/EU) and were approved by the local ethical committee and by the "ministére de l'éducation nationale de l'enseignement supérieur et de la recherche" (APAFIS#3847-2016012610089856v5). Experiments were performed without blinding.

Results

Characteristics of patients with AN related to anti-CNTN1 IgG4

Twenty patients (19 males and 1 female) with AN associated with anti-CNTN1 IgG4 antibodies were enrolled. The median age of onset was 64 (IQR 55-75). Median values on disability scales were 4.5 (IQR 4-5) on mRS and 9.5 (IQR 8-12) on ONLS. According to the electrodiagnostic criteria of the European Academy of Neurology/Peripheral Nerve Society, motor nerve conduction

10.3389/fimmu.2023.1021513

studies showed demyelinating features in all patients (i.e. strongly supportive of demyelination). Nephrotic syndrome was present in 9 patients. The median anti-CNTN1 titers was 6200 (IQR 2700-8400) and isotypes were IgG4 in all patients; additionally, IgG3 was also detected in five, IgG1 in three, and IgG2 in one patient (Table 1).

Anti-CNTN1 IgG4 have majorly undergone FAE *in situ*

To determine whether anti-CNTN1 antibodies are predominantly mono- or bispecific *in situ*, we have examined the potency of anti-CNTN1 autoantibodies to cross-link untagged CNTN1 with biotinylated CNTN1. For that purpose, sera from 20 CNTN1+ AN patients were tested by sandwich-ELISA, as well as the sera from 23 healthy donors, 21 Nfasc155+ AN patients, and 43 seronegative CIDP patients (Figure 1). Those patients were tested for antibodies against biotin, and none were positive (Supplementary Figure 4). Anti-CNTN1 autoantibodies from AN patients were found to significantly cross-link CNTN1 with biotinylated CNTN1, albeit with variable degrees among the cohort. By contrast, healthy donors Nfasc155+ AN, and seronegative CIDP patients did not bind CNTN1. The percentages of monospecific antibodies were then calculated by interpolating the data to a standard curve obtained with increasing concentration of purified anti-CNTN1 IgG3 (Supplementary Material, Supplementary Figure 2). For comparison, the percentages of monospecific anti-Nfasc155 antibodies were calculated in a cohort of 21 Nfasc155+ AN patients. Sixteen out of the 20 CNTN1+ AN patients presented with less than 10% of monospecific anti-CNTN1 antibodies (Figure 1B). The mean percentage of monospecific anti-CNTN1 antibodies was 5.2 +/- 7.8, and was strongly inferior to that of monospecific anti-Nfasc155 antibodies in the Nfasc155+ cohort (31.4 +/- 36.9). In a preliminary study, the percentage of monospecific antibodies was also evaluated in the purified IgG4 fraction from 4 CNTN1+ AN patients (Supplementary Figure 3). In those patients, the percentage of monospecific anti-CNTN1 antibodies calculated in the IgG4

TABLE 1 Antibody titers and clinical features of CNTN1-reactive patients.

	Titers 1/x	Isotype	Monospecific anti-CNTN1 (%)	Gender	Age	Clinical score		Nephropathy	Response to treatment
						mRS	ONLS		
AN1	52700	IgG4,3,1	24,9	M	71	5	12	+	Plex +, Ritux +
AN2	20000	IgG4	5,1	M	59	NA	8	–	IVIg -
AN3	500	IgG4	0,1	M	39	5	12	–	IVIg -, Cx +
AN4	5000	IgG4	3,1	M	70	NA	8	+	IVIg -, Cx partial
AN5	4200	IgG4	1,5	M	75	5	9	+	IVIg -, Ritux +
AN6	6200	IgG4	3,2	M	58	4	4	+	NA
AN7	7500	IgG4	0,3	M	60	4	9	–	IVIg -, Cx -
AN8	1200	IgG4	0,6	M	79	5	12	–	IVIg -, Cx -
AN9	6500	IgG4,3	8,6	M	80	5	12	+	IVIg -, Cx -
AN10	2700	IgG4	1,9	F	40	2	3	–	IVIg -, Cx +
AN11	1900	IgG4,3	0,1	M	54	5	12	–	IVIg +, Cx -
AN12	2500	IgG4	0,7	M	66	5	10	+	IVIg -, Cx -
AN13	7000	IgG4,3,2,1	21,5	M	74	4	10	–	IVIg -, Cx -
AN14	8400	IgG4	0,3	M	37	NA	8	+	IVIg -, Cx +
AN15	7000	IgG4	0,2	M	52	4	6	–	Cx -
AN16	4400	IgG4	0,7	M	82	NA	10	–	IVIg -, Cx -
AN17	32000	IgG4	18,9	M	75	4	NA	–	IVIg -
AN18	900	IgG4,1	0,7	M	61	4	NA	–	Cx +, Aza +
AN19	16000	IgG4,3	11,3	M	71	5	NA	+	Cx -, IVIg -, PLEX +
AN20	2900	IgG4	0,3	M	62	4	NA	+	Cx-, IVIg –, Aza -, PLEX + RTX + Rituximab

Aza, azathioprine; Cx, corticosteroids; F, Female; IVIg, Intravenous Immunoglobulin; M, Male; mRS, modified Rankin Score; NA, not available; ONLS, Overall Neuropathy Limitation Score; Plex, Plasma Exchange; Ritux, Rituximab.
In the nephropathy column, +/- indicate the presence or absence of nephrophathy, respectively. In the response to treatment column, +/- indicate the responsiveness or lack of response to treatment, respectively.

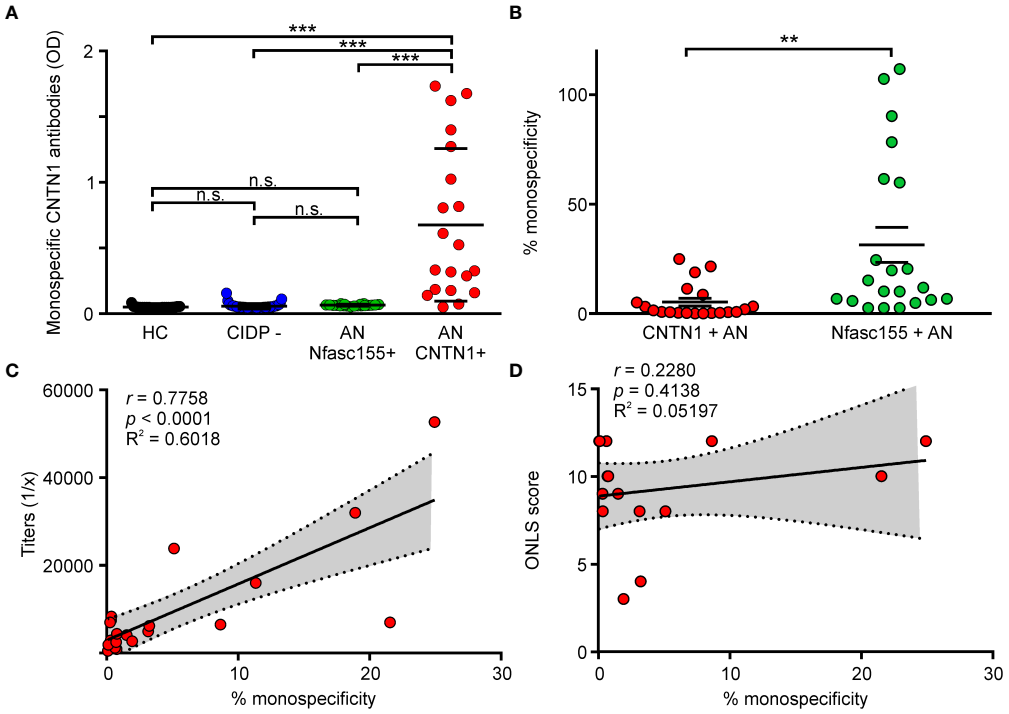

FIGURE 1
Fab-arm exchange occurs in patient with AN. **(A)** The capacity of serum antibodies to cross-link untagged CNTN1 with biotinylated CNTN1 was measured by sandwich ELISA in healthy controls (HC; n = 23), seronegative CIDP patients (CIDP -; n = 43), Nfasc155+ autoimmune nodopathy (AN Nfasc155 +; n = 21) and CNTN1+ autoimmune nodopathy (AN CNTN1+; n = 20). Antibodies from HC, seronegative patients or Nfasc155+ did not cross-link CNTN1. By contrast, CNTN1+ AN patients significantly cross-linked CNTN1 (*** $P<0.001$ by one-way ANOVA followed by Bonferroni's *post-hoc* tests). **(B)** The percentage of monospecific antibodies was calculated by interpolating the data from a calibration curve obtained with anti-CNTN1 IgG3. The percentage of monospecific anti-CNTN1 antibodies in CNTN1+ AN (n = 20) was significantly smaller compared to the percentage of monospecific anti-Nfasc155 antibodies in Nfasc155+ AN (n = 21) (** $P<0.005$ by unpaired two-tailed Student's t tests). **(C)** The titers of anti-CNTN1 IgG4 correlated with the percentage of monospecific CNTN1 antibodies calculated in each patient. **(D)** The clinical severity (ONLS) is plotted against the percentage of monospecific antibodies in each patient (n = 16). No significant correlation was found. P value, Spearman's correlation coefficient (r), R square (R^2) and 95% confidence band (dotted lines) are indicated on the graph. n.s.: non-significant, ONLS: Overall Neuropathy Limitation Score.

fraction were lower than those detected in serum. This further indicated that the majority of anti-CNTN1 IgG4 have undergone FAE *in situ*, and are less likely to cross-link their targets compared to anti-Nfasc155 IgG4.

We then investigated whether the levels of monospecific antibodies influenced clinical severity. The levels of monospecific anti-CNTN1 antibodies strongly correlated with antibody titers in AN patients (Figure 1C; $p < 0.001$). However, no correlation was found between the amount of monospecific anti-CNTN1 antibodies and clinical severity (Figure 1D; $p = 0.3322$). Most patients presented with a severe clinical presentation (Table 1; mean ONLS score = 9 +/- 3) irrespectively of the levels of monospecific antibodies. No significant correlation was detected between the levels of monospecific antibodies and any clinical features.

Monovalent anti-CNTN1 IgG4 blocks CNTN1/CASPR1-Nfasc155 interaction

Previous studies have shown that anti-CNTN1 IgG4 have a function blocking activity and block the interaction between CNTN1/CASPR1 and Nfasc155. In order to determine whether the valency of anti-CNTN1 influence its function blocking activity, the IgG4 from two CNTN1+ AN patients were purified and reduced into monovalent Fab by enzymatic cleavage. These patients presented with different percentages of monospecific antibodies of 24.9% (AN1) and 5.1% (AN2). The potency of native IgG4 or Fab fragment to inhibit the interaction between CNTN1/CASPR1 and Nfasc155 was tested using a cell aggregation assay. HEK cells transfected with CNTN1 and CASPR1-GFP were incubated for 2 hours with HEK cells transfected with mcherry-Nfasc155, then visualized under a microscope. The number of cell aggregates including green and red cells was then quantified in each visualization field (n = 4 experiments per condition, 10 visualization fields were examined by experiments). As negative controls, Nfasc155-transfected cells were incubated with GFP-transfected cells. In control condition, Nfasc155-transfected cells readily aggregated with CNTN1/CASPR1-transfected cells and an average of 8 to 12 aggregates were found in each visualization field (Figure 2). These aggregates were composed of nearly equal number of green and red cells (Figure 2B). The adjunction of native anti-CNTN1 IgG4 from both AN1 and AN2 strongly inhibited the capacity of Nfasc155-transfected cells to aggregates with CNTN1/CASPR1-transfected cells ($P<0.0001$ by one-way ANOVA followed

10.3389/fimmu.2023.1021513

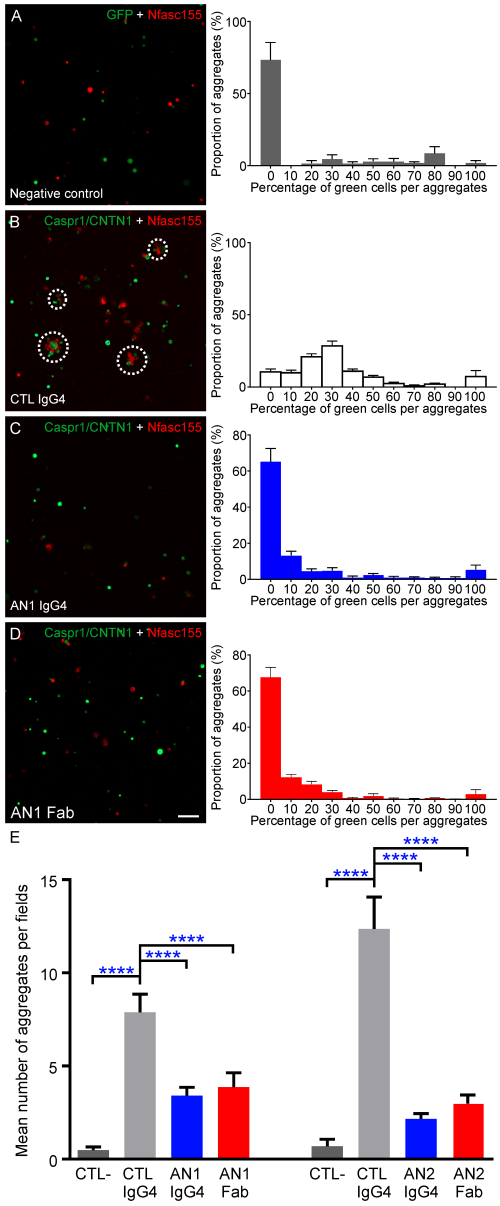

FIGURE 2
Monovalent Fab are sufficient to inhibit the interaction between CNTN1/CASPR1 and Nfasc155. **(A-D)** These are representative images of cell aggregation assays. HEK293T cells were transfected with CASPR1-GFP/CNTN1 (green) and were incubated with cells expressing mcherry tagged Nfasc155 (red) in presence of control IgG4 from a healthy donor (CTL; B), native CNTN1-reactive IgG4 from patient AN1 **(C)** or monovalent Fab-reactive to CNTN1 **(D)**. As negative controls, cells expressing GFP (green) were incubated with cells expressing mcherry tagged Nfasc155 **(A)**. The right panels represent the distribution of the percentage of green cells per aggregate in each aggregate (N = 4 distinct experiments for each condition). **(E)** The native IgG4 and monovalent Fab were tested from two AN patients reactive against CNTN1 (AN1 and AN2). The number of cell aggregates per visualization field was counted in ten images and averaged (N = 4 distinct experiments per condition). Both native IgG4 and monovalent Fab reactive against CNTN1 significantly inhibited the interaction between CASPR1/CNTN1 and Nfasc155 (**** $P<0.0001$ by one-way ANOVA followed by Bonferroni's *post-hoc* tests). No significant differences were observed between the effect of monovalent or native IgG4 for both patients. Native anti-CNTN1 IgG4 do not promote CNTN1/CASPR1 antigen clustering **(C)**. Bars represent mean +/- S.E.M. Scale bar: 10 µm.

by Bonferroni's *post-hoc* tests), and did not promote CNTN1/CASPR1-transfected cell clustering.

Monovalent Fab fragments induced similar effects and potently abrogated the interaction between Nfasc155 and CNTN1/CASPR1 *in vitro*. No significant difference was seen between the effect of native or monovalent anti-CNTN1 IgG4 ($P>0.05$ by one-way ANOVA followed by Bonferroni's *post-hoc* tests). As most IgG4 appears to have undergone FAE in CNTN1+ AN patients, these results suggested that bispecific (functionally monovalent) anti-CNTN1 IgG4 blocks CNTN1 function.

Anti-CNTN1 fab penetrates paranodal regions

Because Fab fragments inhibit CNTN1/CASPR1-Nfasc155 interaction, we next investigated whether the reduction of anti-CNTN1 IgG4 into monovalent Fab alters its potency to invade the paranodal regions. For that purpose, intraneural injections of native anti-CNTN1 IgG4 or Fab fragments from patient AN1 were performed in the sciatic nerves of adult rats. In order to inject equimolar amounts of antibodies (Fab fragment being three time smaller than native IgG), 10 µg of native IgG4 and 3 µg of Fab were injected. The penetration of antibodies within the paranodal region was monitored one- and three-days post-injection (Figure 3; Supplementary Figure 5). As previously described, by one day post-injection, anti-CNTN1 IgG4 were detected within the paranodal regions at the border of the nodes of Ranvier, then progressively invaded the entire paranode by three days (Figure 3; Supplementary Figure 5). Monovalent Fab fragment also readily penetrated the paranodes *in vivo* by one day. Fab fragment of anti-Nfasc155 IgG4 or unreactive IgG4 do not infiltrate paranodal regions (14). It thus seems unlikely that Fab infiltration is solely due to the small size of Fab and to unspecific diffusion across the paranode. At three days post-injection, the extent of diffusion of anti-CNTN1 Fab or IgG4 across the paranodes was significantly higher than that at one-day post injection ($P<0.0001$ and $P<0.01$, respectively by one-way ANOVA followed by Bonferroni's *post-hoc* tests). No significant difference was seen between monovalent Fab and native IgG4 at both time points, indicating that monovalent anti-CNTN1 Fab antibodies have the same capacity to invade paranode as native antibodies.

Discussion

In this study, the levels of mono/bispecific anti-CNTN1 IgG4 were estimated in AN patients as well as the pathogenic function of monovalent anti-CNTN1 IgG4. Our results suggest that most anti-CNTN1 IgG4 have already undergone FAE *in situ* since only 5% of these were bivalent and monospecific against CNTN1. In addition, the proteolytic digestion of these antibodies into monovalent Fab did not alter their function and monovalent Fab potently inhibited the interaction between CNTN1/CASPR1 and Nfasc155, and infiltrated paranodal regions. This suggested that bispecific antibodies may alter paranodal complex association.

10.3389/fimmu.2023.1021513

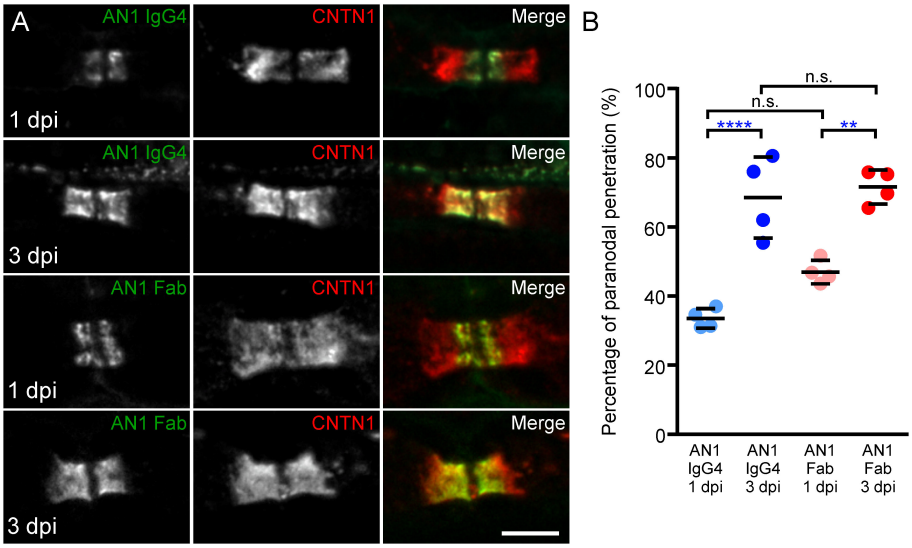

FIGURE 3
Mono- and bivalent IgG4 infiltrate paranodal regions. **(A)** These are teased sciatic nerve fibers from adult Lewis rats which have received a single intraneural injection of native CNTN1 reactive IgG4 (top panels; n = 4 at each time point) or monovalent Fab (lower panels; n = 4 at each time point). Nerves have been collected 1- or 3-days post-injection (dpi) and have been stained for CNTN1 (red) and IgG (green). **(B)** The percentage of IgG infiltration was measured in each animal at 1 and 3 dpi, and the mean percentage of infiltration was calculated (n = 4 for each condition). The paranodal infiltration of native IgG4 reactive to CNTN1 was significantly higher at 3 dpi compared to 1 dpi (**** $P<0.0001$, by one-way ANOVA followed by Bonferroni's *post-hoc* tests). The percentage of infiltration of monovalent Fab was also significantly higher at 3 dpi compared to 1 dpi (** $P<0.01$ by one-way ANOVA followed by Bonferroni's *post-hoc* tests). No significant difference was seen between monovalent Fab and native IgG4 infiltration at both times. Bars represent mean and S.D. Scale bar: 5 µm.

IgG4 are known to undergo FAE *in situ* and to coexist as functionally monovalent antibodies. This property is central for the physiological non-inflammatory function of IgG4. In addition, it appears to influence the pathogenicity of IgG4 autoantibodies in autoimmune diseases. In myasthenia gravis (MG) associated with anti-MuSK IgG4, FAE enhances the pathogenic function of these autoantibodies by generating monovalent bispecific antibodies unable to cluster MuSK but capable of blocking the interaction between MuSK and Low-density lipoprotein receptor related protein 4 (Lrp4) (15). In MuSK+ MG patients, circulating autoantibodies were reported to be majorly bispecific. By contrast, in Nfasc155+ AN, FAE was reported to have an opposite effect, and to decrease the potency of anti-Nfasc155 IgG4 to cluster Nfasc155 and to block paranode formation (14). Here and in a previous study, we found that 21-31% of the anti-Nfasc155 IgG4 were monospecific and that some patients showed nearly 100% monospecific antibodies. The reasons why the levels of bivalent monospecific anti-Nfasc155 IgG4 is high is uncertain, but could be due to a selection bias. Indeed, these autoantibodies were only tested when the neuropathic condition was declared or severe, thus when high levels of pathogenic monospecific bivalent anti-Nfasc155 IgG4 are circulating. Conversely, in anti-CNTN1+ AN, the proportion of monospecific antibodies was low (~ 5%) and most antibodies appeared bispecific. Like in anti-MuSK+ MG, IgG4 had a function blocking activity and monovalent Fab-reactive to CNTN1 could potently block the interaction between CNTN1/CASPR1-Nfasc155. As indicated in the Supplementary Material, one of the limitations of the study is that the percentage of monospecific antibodies were measured in patients' sera and may have been overestimated due to the coexistence of IgG1 and IgG3. The percentage of monospecific IgG4 in CNTN1+ AN patients may thus be lower.

Our results suggest that the impact of valency on pathogenicity strongly depend on the mode of action of the IgG4: function blocking or antigen-crosslinking mechanism. When IgG4 have a function blocking activity, monovalent antibodies can participate to the pathogenic mechanism. Conversely, if IgG4 act through an antigen clustering, then monovalency reduces the pathogenic mechanism, probably because antigen-crosslinking requires a monospecific and bivalent antibody. These differences may explain why patients with anti-CNTN1 IgG4 have a more severe presentation. While FAE naturally dampen the pathogenicity of anti-Nfasc155 IgG4, it may not preclude the action of anti-CNTN1 IgG4. However, this cannot be formally ascertained here, albeit our results suggest this pathophysiological mechanism. Indeed, the pathogenic action of pure monospecific bivalent anti-CNTN1 IgG4 has not been specifically investigated, neither the impact of FAE. Of course, this study has several limitations. The levels of monospecific IgG have been inferred from patients' sera and not from purified IgG4, thus the presence of other IgG isotypes may have led to an overestimation of the percentage of monospecificity. Also, those levels were interpolated from a calibration curve obtained with anti-CNTN1 IgG3, and thus are rough estimate rather than definite levels.

Although the inhibition of CNTN1 function seems to be the main pathogenic process leading to paranode alteration, antigen-crosslinking mechanism may also exist in other regions *in situ*. Besides paranodes, CNTN1 is also present on the surface of dorsal

root ganglia and on podocytes, which may explain sensory ataxia and nephrotic syndrome, respectively. Recently, Gruner and colleagues showed that anti-CNTN1 IgG1-3 and F(ab')$_2$ fragment decreased CNTN1 surface expression on dorsal root ganglia. As anti-CNTN1 Fab fragment abolished this effect, a cross-linking mechanism and subsequent internalization of CNTN1 have been suggested (16). It still remains to be demonstrated whether monospecific, and not bispecific, anti-CNTN1 IgG4 promote the same effect. In our study, 9 patients also displayed a nephrotic syndrome. Although CNTN1 is expressed by podocytes in normal kidney and is the target of anti-CNTN1 IgG4 in patients with nephrotic syndrome, it remains unknown whether the pathogenic mechanism in membranous nephropathy results from a function blocking, antigen-crosslinking or immune-complex deposition (17). Here, we did not find a correlation between the presence of a nephrotic syndrome and the percentage of circulating monospecific antibodies. However, we cannot exclude that IgG4 deposits in kidney are due to bivalent monospecific autoantibodies.

Immunotherapies classically used in autoimmune neuropathies, such as intravenous immunoglobulins, are usually ineffective in AN that, conversely, respond very well to B-cell depleting therapies such as Rituximab (1). However, axonal loss is sometimes already advanced before Rituximab fully exerts its effect. Because IgG4 has poor Fc-mediated effector functions, imlifidase (a therapeutic enzyme that cleaves Fc domain of IgG) and anti-complement therapy may be disregarded as useful options in anti-CNTN1+ AN. Finally, neonatal Fc receptor targeting agents may be a promising therapy for AN since this treatment seems to be effective in mouse model for IgG4 MuSK+ MG (18).

Our study underscores that the paranodopathy mechanism in anti-CNTN1+ AN is by the blockade of the CNTN1/CASPR1-Nfasc155 interactions by anti-CNTN1 antibodies and that anti-CNTN1 Fab fragments or bispecific antibodies can carry a function blocking activity. This may explain why patients with anti-CNTN1 IgG4 which have undergone extensive FAE still present a severe phenotype.

Data availability statement

The raw data supporting the conclusions of this article will be made available by the authors, without undue reservation.

Author contributions

All authors drafted and revised the manuscript. All authors were involved in the acquisition of data, analysis and interpretation of data. All authors contributed to the article and approved the submitted version.

Funding

Supported by the Agence Nationale pour la Recherche (NECCIN; GT and JD), from the Association Française contre les Myopathies (grant#23593; GT and JD) and ArgenX. The funders were not involved in the study design, collection, analysis, interpretation of data, the writing of this article or the decision to submit it for publication.

Acknowledgments

We thank the RAM-Neuro facility and Antoine Picot for technical assistance.

Conflict of interest

LQ received research grants from Instituto de Salud Carlos III – Ministry of Economy and Innovation Spain, Fundació La Marató, GBS-CIDP Foundation International, Novartis Pharma Spain, Roche, UCB and Grifols. LQ received speaker or expert testimony honoraria from CSL Behring, Novartis, Sanofi-Genzyme, Merck, Annexon, Biogen, Janssen, ArgenX, UCB, LFB, Octapharma and Roche. LQ serves at Clinical Trial Steering Committee for Sanofi Genzyme and Roche, and is Principal Investigator for UCB's CIDP01 trial. JD received a research grant from CSL Behring.

The remaining authors declare that the research was conducted in the absence of any commercial or financial relationships that could be construed as a potential conflict of interest.

Publisher's note

Supplementary material

The Supplementary Material for this article can be found online at: https://www.frontiersin.org/articles/10.3389/fimmu.2023.1021513/full#supplementary-material

References

1. Van den Bergh PYK, van Doorn PA, Hadden RDM, Avau B, Vankrunkelsven P, Allen JA, et al. European Academy of Neurology/Peripheral nerve society guideline on diagnosis and treatment of chronic inflammatory demyelinating polyradiculoneuropathy: Report of a joint task force-second revision. *J Peripher Nerv Syst* (2021) 26:242–68. doi: 10.1111/jns.12455

2. Querol L, Devaux J, Rojas-Garcia R, Illa I. Autoantibodies in chronic inflammatory neuropathies: Diagnostic and therapeutic implications. *Nat Rev Neurol* (2017) 13:533–47. doi: 10.1038/nrneurol.2017.84

3. Bhat MA, Rios JC, Lu Y, Garcia-Fresco GP, Ching W, St Martin M, et al. Axon-glia interactions and the domain organization of myelinated axons require neurexin IV/Caspr/Paranodin. *Neuron.* (2001) 30:369–83. doi: 10.1016/S0896-6273(01)00294-X

4. Boyle MET, Berglund EO, Murai KK, Weber L, Peles E, Ranscht B. Contactin orchestrates assembly of the septate-like junctions at the paranode in myelinated peripheral nerve. *Neuron.* (2001) 30:385–97. doi: 10.1016/S0896-6273(01)00296-3

5. Charles P, Tait S, Faivre-Sarrailh C, Barbin G, Gunn-Moore F, Denisenko-Nehrbass N, et al. Neurofascin is a glial receptor for the paranodin/Caspr-contactin axonal complex at the axoglial junction. *Curr Biol* (2002) 12:217–20. doi: 10.1016/s0960-9822(01)00680-7

6. Rasband MN, Peles E. Mechanisms of node of ranvier assembly. *Nat Rev Neurosci* (2021) 22:7–20. doi: 10.1038/s41583-020-00406-8

7. Sherman DL, Tait S, Melrose S, Johnson R, Zonta B, Court FA, et al. Neurofascins are required to establish axonal domains for saltatory conduction. *Neuron.* (2005) 48:737–42. doi: 10.1016/j.neuron.2005.10.019

8. Koneczny I. Update on IgG4-mediated autoimmune diseases: New insights and new family members. *Autoimmun Rev* (2020) 19:102646. doi: 10.1016/j.autrev.2020.102646

9. Manso C, Querol L, Lleixa C, Poncelet M, Mekaouche M, Vallat JM, et al. Anti-Neurofascin-155 IgG4 antibodies prevent paranodal complex formation *in vivo*. *J Clin Invest* (2019) 129:2222–36. doi: 10.1172/JCI124694

10. Manso C, Querol L, Mekaouche M, Illa I, Devaux JJ. Contactin-1 IgG4 antibodies cause paranode dismantling and conduction defects. *Brain.* (2016) 139:1700–12. doi: 10.1093/brain/aww062

11. Angal S, King DJ, Bodmer MW, Turner A, Lawson AD, Roberts G, et al. A single amino acid substitution abolishes the heterogeneity of chimeric mouse/human (IgG4) antibody. *Mol Immunol* (1993) 30:105–8. doi: 10.1016/0161-5890(93)90432-b

12. van der Neut Kolfschoten M, Schuurman J, Losen M, Bleeker WK, Martinez-Martinez P, Vermeulen E, et al. Anti-inflammatory activity of human IgG4 antibodies by dynamic fab arm exchange. *Science.* (2007) 317:1554–7. doi: 10.1126/science.1144603

13. Huijbers MG, Vergoossen DL, Fillie-Grijpma YE, van Es IE, Koning MT, Slot LM, et al. MuSK myasthenia gravis monoclonal antibodies: Valency dictates pathogenicity. *Neurol Neuroimmunol Neuroinflamm* (2019) 6:e547. doi: 10.1212/NXI.0000000000000547

14. Jentzer A, Attal A, Roue C, Raymond J, Lleixa C, Illa I, et al. IgG4 valency modulates the pathogenicity of anti-Neurofascin-155 IgG4 in autoimmune nodopathy. *Neurol Neuroimmunol Neuroinflamm* (2022) 9:e200014 doi: 10.1212/NXI.0000000000200014

15. Vergoossen DLE, Plomp JJ, Gstottner C, Fillie-Grijpma YE, Augustinus R, Verpalen R, et al. Functional monovalency amplifies the pathogenicity of anti-MuSK IgG4 in myasthenia gravis. *Proc Natl Acad Sci U S A* (2021) 118:e2020635118 doi: 10.1073/pnas.2020635118

16. Gruner J, Stengel H, Werner C, Appeltshauser L, Sommer C, Villmann C, et al. Anti-contactin-1 antibodies affect surface expression and sodium currents in dorsal root ganglia. *Neurol Neuroimmunol Neuroinflamm* (2021) 8. doi: 10.1212/NXI.0000000000001056

17. Le Quintrec M, Teisseyre M, Bec N, Delmont E, Szwarc I, Perrochia H, et al. Contactin-1 is a novel target antigen in membranous nephropathy associated with chronic inflammatory demyelinating polyneuropathy. *Kidney Int* (2021) 100:1240–9. doi: 10.1016/j.kint.2021.08.014

18. Huijbers MG, Plomp JJ, van Es IE, Fillie-Grijpma YE, Kamar-Al Majidi S, Ulrichts P, et al. Efgartigimod improves muscle weakness in a mouse model for muscle-specific kinase myasthenia gravis. *Exp Neurol* (2019) 317:133–43. doi: 10.1016/j.expneurol.2019.03.001

frontiers | Frontiers in Immunology

TYPE Original Research
PUBLISHED 21 March 2023
DOI 10.3389/fimmu.2023.1151574

OPEN ACCESS

EDITED BY
Hong Zan,
The University of Texas Health Science Center at San Antonio, United States

REVIEWED BY
Hui Yan,
The University of Texas Health Science Center at San Antonio, United States
Morten Blaabjerg,
University of Southern Denmark, Denmark

*CORRESPONDENCE
Lidia Sabater
lisabate@recerca.clinic.cat

SPECIALTY SECTION
This article was submitted to B Cell Biology, a section of the journal Frontiers in Immunology

RECEIVED 26 January 2023
ACCEPTED 28 February 2023
PUBLISHED 21 March 2023

CITATION
Landa J, Serafim AB, Gaig C, Saiz A, Koneczny I, Hoftberger R, Santamaria J, Dalmau J, Graus F and Sabater L (2023) Patients' IgLON5 autoantibodies interfere with IgLON5-protein interactions. *Front. Immunol.* 14:1151574. doi: 10.3389/fimmu.2023.1151574

Patients' IgLON5 autoantibodies interfere with IgLON5-protein interactions

Jon Landa[1], Ana Beatriz Serafim[1], Carles Gaig[2], Albert Saiz[2], Inga Koneczny[3,4], Romana Hoftberger[3,4], Joan Santamaria[2], Josep Dalmau[1,2,5,6], Francesc Graus[1] and Lidia Sabater[1]*

[1]Neuroimmunology Program, Fundació de Recerca Clínic Barcelona-Institut d'Investigacions Biomèdiques August Pi i Sunyer, Universitat de Barcelona, Barcelona, Spain, [2]Service of Neurology, Hospital Clinic de Barcelona, Barcelona, Spain, [3]Division of Neuropathology and Neurochemistry, Department of Neurology, Medical University of Vienna, Vienna, Austria, [4]Comprehensive Center for Clinical Neurosciences and Mental Health, Medical University of Vienna, Vienna, Austria, [5]Department of Neurology, University of Pennsylvania, Philadelphia, PA, United States, [6]Institució Catalana de Recerca i Estudis Avançats (ICREA), Barcelona, Spain

Background: Anti-IgLON5 disease is a rare neurological disorder characterized by autoantibodies against IgLON5, and pathological evidence of neurodegeneration. IgLON5 is a cell adhesion molecule but its physiological function is unknown. Our aim was to investigate the IgLON5 interactome and to determine if IgLON5 antibodies (IgLON5-abs) affect these protein interactions.

Methods: IgLON5 interactome was investigated by mass spectrometry sequencing of proteins immunoprecipitated by IgLON5 autoantibodies using cultures of rat cerebellar granular neurons (CGNs). Shedding of IgLON5 was explored using HEK cells transfected with human IgLON5 plasmid and in CGNs. Interactions of IgLON5 with identified binding partners and IgLON5-abs effects were confirmed by immunofluorescence in transfected HEK cells and rat hippocampal neurons.

Results: Patients' IgLON5 antibodies co-precipitated all members of the IgLON family and three 3 additional surface proteins. IgLON5 predominantly establishes homomeric and heteromeric *cis* (within the cell) and *trans* (between cells)-interactions with other IgLON family members and undergoes spontaneous ectodomain shedding. Antibodies from patients with anti-IgLON5 disease prevent trans-interactions in hippocampal neurons independently of the IgLON5 IgG subclass distribution.

Conclusions: We show a potentially novel pathogenic mechanism of IgLON5-abs that consists in blocking IgLON5 interactions with its binding partners. These findings extend our knowledge about the physiological role of IgLON5 and pave the way to future understanding of the pathological mechanisms of anti-IgLON5 disease.

KEYWORDS

anti-IgLON5 antibody encephalopathy, anti-IgLON5 disease, IgG4, interactome, neurons, IgLON5 antibodies

1 Introduction

Autoantibodies against IgLON5 (IgLON5-abs) are the hallmark of anti-IgLON5 disease, a recently identified clinical entity in which neurodegeneration and autoimmunity converge (1). Unlike other neurological disorders targeting neuronal cell surface antigens, the clinical progression of anti-IgLON5 disease is usually chronic with limited response to immunotherapy. Furthermore, neuropathological studies in a few patients show neuronal accumulation of hyperphosphorylated tau mainly involving the brainstem and hypothalamus supporting an underlying neurodegenerative process (2).

IgLON5 is the fifth member of the IgLON family that belongs to the immunoglobulin superfamily (IgSF) of cell adhesion molecules (CAMs). IgLONs contain 3-immunoglobulin-like (Ig-like) domains attached to the membrane by a glycosylphosphatidylinositol (GPI)-anchor protein without a transmembrane domain. Shedding of the ectodomain (soluble extracellular part of the protein) of GPI-anchored proteins has been described as an important post-translational mechanism involved in adhesion and cell signaling and has been shown to occur with other IgLON family members (3, 4).

IgLON5-abs belong to the IgG1 and IgG4 subclasses (rarely IgG2). The IgG1 subclass of IgLON5-abs cause an irreversible decrease of IgLON5 clusters on the neuronal surface by crosslinking and internalization, and after long-term exposure to total purified IgG *in vitro*, the architecture of the neuronal cytoskeleton is impaired (5, 6). Although IgG4 is the predominant subclass of IgLON5-abs, the role this subclass plays in the disease remains unclear (5), but in other diseases, the main pathogenic mechanism described for IgG4 antibodies is interference with protein-protein interactions (7). Thus, the aims of our study were to investigate if IgLON5 is shed from the cell surface in normal conditions, to analyze the interactome of IgLON5, and to explore the effects of IgLON5-abs on the interaction of IgLON5 with its binding partners.

2 Materials and methods

2.1 Patients' samples and IgG purification

Sera from two patients with anti-IgLON5 disease and 3 healthy blood donors were used for the studies of immunoprecipitation. Paired serum/CSF samples from another 4 patients with anti-IgLON5 disease, a patient with anti-NMDAR encephalitis and a patient with Alzheimer disease were used for the studies of interaction of IgLON5 with other cell surface proteins. Total IgG was purified from these 4 patients as previously described (6). The percentage of IgLON5-IgG subclass was measured as previously reported by flow cytometry (5).

2.2 Primary cell cultures

Primary cell cultures of rat hippocampal neurons were prepared from embryonic E18 day as previously reported (8). Briefly, dissected hippocampi were trypsinized with 0.25% trypsin (Thermo-Fisher Scientific, Waltham Massachusetts, USA) for 15 min at 37°C and mechanically dissociated. Single cell suspension was plated in P35 plates (100.000 cells) on coverslips coated with Poly-L-lysine and maintained in Neurobasal medium plus B27 (Thermo-Fisher Scientific).

Cerebellar granule neurons (CGN) were prepared from postnatal P8 Wistar rat pups following the same protocol as for hippocampal neurons but using a different plating media (Neurobasal-A plus B27 and KCl 25 mM). Cells were plated in P100 dishes at a density of $1{,}3x10^6$ cells/ml. Ara-C was added (10μm) 24 hours post-plating to arrest the glial cell growth.

2.3 Analysis of IgLON5 ectodomain shedding

HEK293 cells (HEK) were transfected with untagged human-IgLON5 plasmid (HEK-IgLON5; SC317071, Origene, Rockville, MA, USA) as reported (1) and 24 hours post-transfection, the culture medium was replaced by Opti-MEM medium (Thermo-Fisher). As a positive control of shedding, phosphoinositide-specific phospholipase C (PI-PLC) (1U/mL), which removes GPI-anchored proteins from the cell surface, was added to one HEK-IgLON5 plate. After 24 hours, the medium of HEK-IgLON5 cultures with and without PI-PLC was collected and concentrated 10-fold using Amicon Ultracentrifugal filters 30K (UFC903024, Millipore; Burlington, MA, USA). HEK-IgLON5 cells from P60 plates were lysed with cell lysis buffer (FNN0011, Thermo-Fisher) and membrane proteins were isolated with a commercial kit (A44390, Thermo-Fisher). Proteins from total cell lysate, membrane protein preparation, and culture medium were separated electrophoretically and transferred to a nitrocellulose membrane that was sequentially incubated with IgLON5 (ab122763, Abcam, Cambridge, UK, 1:500) overnight at 4°C and goat anti-rabbit HRP secondary antibody (1/1000 diluted) provided with a chemiluminescence kit (RPN2108, GE Healthcare, Chicago, IL, USA) and visualized in an ImageQuant LAS 4000 imager (GE Healthcare). The concentration of soluble IgLON5 was quantified by immunoblot comparing the signal with that produced by IgLON5 human recombinant protein Fc-tagged (rIgLON5-Fc; 9728-IG-050, R&D Systems, Minneapolis, MN, USA) of known concentration (data not shown). Similar experiments were done using cultures of CGN.

2.4 Identification of IgLON5 interactome using immunoprecipitation

Live CGNs were incubated with serum (dilution 1:100) containing IgLON5-abs or from healthy donors, for 1 hour at 37°C. After extensive washing, neurons were lysed and protein complexes were incubated overnight with protein A/G beads (20424, Thermo-Fischer Scientific) at 4°C. After on-beads digestion with trypsin, the beads were centrifuged and the supernatant was analyzed by mass spectroscopy at the Proteomic facility of Centre for Genomics Regulation (CRG, Barcelona) as

previously described (9). *Bona-fide* IgLON5 interactors were defined as proteins pulled-down by IgLON5-abs in two or more independent immunoprecipitations and in none of the negative controls.

2.5 Binding of IgLON5 with interactors in HEK cells and neurons

To validate *cis*-interactions (within the same cell) of IgLON5 with identified interactors, HEK cells were co-transfected in pairs: *IGLON5* (SC317071, Origene) plus: 1) *IGLON1* (RG213594, Origene), 2) *IGLON2* (RG226879, Origene), 3) *IGLON3* (RG207618, Origene), 4) *IGLON4* (RG216034 Origene), 5) *KIDINS220* (RC216441Origene), 6) *IGSF21* (RG203559, Origene), 7) *CACNA2D2* (RC219452, Origene) and 8) *CASPR2* (SC115167, Origene), as a non-binding control. Twenty hours post-transfection, immunoprecipitations were performed as indicated above with IgLON5-abs and pulled-down proteins were electrophoresed and transferred to a nitrocellulose membrane. The presence of the interacting proteins was detected by incubating the membrane with the following antibodies (dilution 1:500, overnight at 4°C): IgLON1 (STJ94590), IgLON2 (STJ94442), IgLON3 (STJ116461), IgLON4 (STJ94394, St. John's Laboratory, London, UK), KIDINS220 (21856-1-AP, Proteintech, Rosemont, IL, USA), IGSF21 (21465-1-AP; Proteintech), CACNA2D2 (SAB1401461, SIGMA) and CASPR2 (ab33994, Abcam) followed by incubation with appropriate secondary antibodies (dilution 1:1000) for 1 hour at room temperature. Results were developed by chemiluminescence as described above.

To investigate interactions in *trans* (between cells), non-transfected hippocampal neurons or HEK cells transfected with: IgLON1 to 5, KIDINS220, IGSF21, and CACNA2D2 were incubated with: 1) rIgLON5-Fc protein, 2) irrelevant Fc protein (rCtrl-Fc; 110-HG-100, R&D Systems), 3) soluble IgLON5 at 2.5µg/ml, or 4) conditioned medium of untransfected HEK cells during 30 minutes. Cells were washed with PBS and fixed with 4% paraformaldehyde for 10 minutes. Binding of Fc-tagged recombinant proteins was determined by incubation with Alexa Fluor 594 goat anti-human Fcγ-fragment specific (109-586-098; Jackson Immunoresearch, Newmarket, UK). Binding of soluble IgLON5 was detected with a rabbit IgLON5 antibody (ab122763, Abcam) and anti-rabbit Alexa Fluor 594 secondary antibody (Thermo-Fisher Scientific) during 1 hour. Results were visualized in a confocal microscope ZEISS (LSM710, Carl Zeiss, Jena, Germany).

2.6 Effects of IgLON5-ab on IgLON5-protein interactions

rIgLON5-Fc and rCtrl-Fc proteins were biotinylated at 500 µg/mL with biotin-(long arm)-NHS following the datasheet (SP-1200, Vector Laboratories, Burlingame, CA, USA). Biotinylated rIgLON5-Fc (biot-rIgLON5-Fc) or biot-rCtrl-Fc protein were added to the media of cultures of hippocampal neurons or HEK cells transfected with the plasmids indicated above at 2.5 ug/mL for 30 min. To visualize the interactions, after washing, coverslips were fixed with 4% paraformaldehyde in PBS and incubated for 1 hour with Alexa Fluor 488-streptavidin (S11223, Thermo-Fisher) which specifically binds to biotinylated proteins.

To investigate if IgLON5-abs block the interaction of IgLON5 with its binding partners, parallel studies were performed in which biot-rIgLON5-Fc or biot-rCtrl-Fc were preincubated for 2 hours at 37°C with: 1) CSF diluted 1:2, or total purified IgG (2mg/mL) from 4 patients with the following IgLON5-IgG4 percentage of total IgLON5-IgG (patient #1 = 76%; #2 = 83%; #3 = 0%, and #4 = 100%); 2) NMDAR-IgG or 3) control IgG from blood donors (Ctrl-IgG) or CSF from a patient with Alzheimer's disease.

3 Results

3.1 IgLON5 is released from the cell surface *via* ectodomain shedding

Immunoblot analysis showed that IgLON5 is present in the media of IgLON5-HEK cells indicating that is constitutively shed. When we treated IgLON5-HEK cells with the PI-PLC enzyme, which cleaves GPI-anchored proteins, we found that IgLON5 levels dramatically decreased from membrane preparations whereas IgLON5 in the culture media of PI-PLC-treated cells increased (Figure 1). Soluble IgLON5 had an approximate molecular weight of 60 kDa demonstrating that the protein shed is fully glycosylated and the cleavage site is close to the membrane, thus nearly a full-length fragment of the protein is released (Figure 1). Soluble IgLON5 was also found in the media of CGNs but in lower concentration (data not shown).

3.2 Interactome of IgLON5 and effect of IgLON5 antibodies on rat neurons

To gain insight into the physiological function of IgLON5 and to identify potential binding partners with transmembrane domain that could act as scaffolding proteins in the interaction of IgLON5 with the cytoskeleton, we investigated the IgLON5 interactome in CGN immunoprecipitated with IgLON5-abs. IgLON5 peptides were found in all the immunoprecipitations performed with IgLON5-abs and in none of the controls. In addition to other members of the IgLON family, cell membrane proteins that consistently co-precipitated with IgLON5 included two GPI-anchor proteins; immunoglobulin superfamily member 21 (IGSF21) and voltage-dependent calcium channel subunit alpha-2/delta-2 (CACN2D2A), and the transmembrane protein KIDINS220 (kinase D-interacting substrate of 220-kDa), also known as ARMS (ankyrin repeat-rich membrane spanning) (Table 1). These membrane proteins were specifically identified by mass-spectrometry as *bona-fide* interactors of IgLON5 and were selected for further analysis. To confirm *cis*-interactions, these proteins were co-transfected with IgLON5 in HEK cells and immunoprecipitated with IgLON5-abs. Immunoblots of the

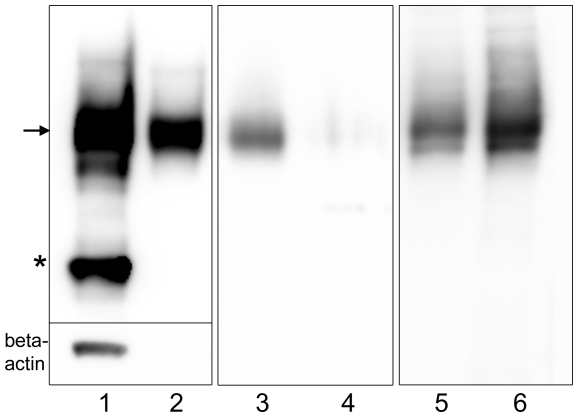

FIGURE 1
Immunoblots showing that IgLON5 is spontaneously shed and cleaved at the GPI-anchor. Immunoblots of different protein preparations from IgLON5-HEK probed with IgLON5 and actin antibodies: cell lysate (1); media obtained from 10 P60 plates with IgLON5-HEK cells (2); membrane preparations from one P60 plate untreated (3) and treated with PI-PLC (4); media from one P60 plate untreated (5) or treated with PI-PLC (6). Arrow indicates the glycosylated band of IgLON5 of approximately 60 kDa and the asterisk points the 37 kDa unglycosylated band. Only the lysate lane shows a beta-actin band, ruling out that the IgLON5 band detected in the other lanes is derived from dead IgLON5-HEK cells.

immunoprecipitates identified IgLON1 to 5 (Figure 2) but not any of the 3 additional proteins identified by mass-spectrometry (data not shown).

To search for the presence of self-trans-interactions of IgLON5 or trans-interactions with the identified binding partners, we incubated soluble IgLON5 or rIgLON5-Fc with HEK cells transfected with IgLON1 to 5, KIDINS220, IGSF21 or CACNA2D2. HEK cells transfected with IgLON5 were probed with rIgLON5-Fc as Fc-tag allowed us to discriminate between the added IgLON5 and the IgLON5 attached to the membrane. We observed robust IgLON5 immunoreactivity after HEK cells transfected with IgLON1 to 5 were incubated with soluble IgLON5 but not after incubation with controls; media from untransfected HEK cells or Ctrl-Fc protein (Figure 3A). Neither soluble IgLON5 nor rIgLON5-Fc was able to bind to HEK cells transfected with the other identified binding partners (data not shown).

To demonstrate that soluble IgLON5 binds to the cell-surface of neurons, we incubated rIgLON5-Fc or Ctrl-Fc protein in the medium of cultures of live rat hippocampal neurons and found that rIgLON5-Fc but not Ctrl-Fc protein bound to the neuronal membrane. To further investigate a potential effect of IgLON5-ab on interactions between IgLON5 and other IgLONs, we pre-incubated purified IgG or CSF from 4 patients with different IgLON5-IgG4 subclass percentage (from 0 to 100%) with biot-rIgLON5-Fc or biot-rCtrl-Fc. Samples from the four patients completely blocked the binding of biot-rIgLON5-Fc to IgLON1-5 expressed in HEK cells (data not shown) and to hippocampal neurons independent of the IgG4 content. Neither antibodies from healthy donors nor antibodies against the NMDA receptor were able to block IgLON5 interactions confirming specificity (Figure 3B).

4 Discussion

Although substantial progress has been made in describing the immunological and clinical features of anti-IgLON5 disease (10, 11), the physiological function of IgLON5, the target of patients' antibodies is largely unknown. Here we show that IgLON5 undergoes ectodomain shedding and interacts with the other members of the IgLON family, and IgLON5-abs disrupt this interaction. This effect represents a second potential pathogenic mechanism in addition to the irreversible internalization of IgLON5 clusters from the neuronal surface mediated by IgG1 IgLON5-abs that we previously described (5).

Our *in vitro* experiments in cultures of CGN and IgLON5-transfected HEK cells indicate that IgLON5 is spontaneously shed and that IgLON5 concentration in the media increases when cultures are exposed to PI-PLC enzyme that specifically cleaves GPI-anchored proteins. The molecular weight of the IgLON5 band that we detected in the media of untreated cells was similar to that observed after incubation with the PI-PLC enzyme indicating that in physiological conditions IgLON5 is cleaved at the level of the GPI anchor close to the membrane. These findings are in line with the previous

TABLE 1 Membrane proteins identified as *bona-fide* IgLON5 interactors.

Protein	Accession (NCBI)	Score	Coverage (%)	Peptides	IP*
IgLON5	XP_218634.5	277.6	38.69	11	5/5
IgLON3	NP_058938.1	160.4	23.67	7	4/5
IgLON2	XP_017451356.1	119.3	10.5	3	4/5
IgSF21	NP_001258383.1	62.9	6.41	3	2/5
IgLON1	XP_017450905.1	48.2	7.4	3	4/5
IgLON4	NP_067714.1	42.6	8.62	2	4/5
CACNA2D2	XP_006243799.1	34.3	0.87	1	3/5
KIDINS220	XP_017449472.1	28	0.47	1	2/5

* Number of immunoprecipitations where the protein is identified.
IgSF21: Immunoglobulin superfamily member 21 precursor; KIDINS220: Kinase D-interacting substrate of 220 kDa isoform X20; CACNA2D2: Voltage-dependent calcium channel subunit alpha-2/delta-2.

10.3389/fimmu.2023.1151574

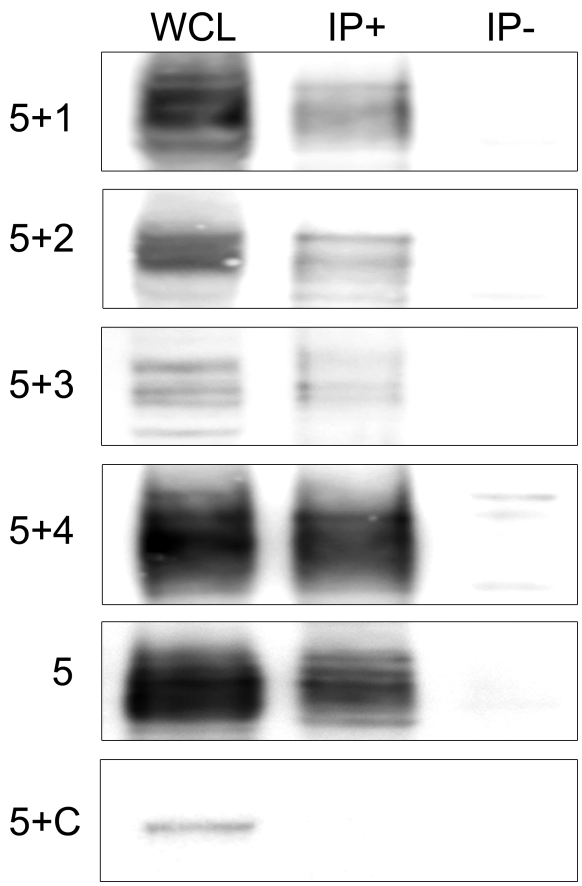

FIGURE 2
Immunoblots of co-tranfected HEK cells immunoprecipitated with patients' IgLON5 antibodies. HEK cells co-transfected with IgLON5 and each of the other IgLON family members: first row (IgLON5 + IgLON1), 2nd row IgLON2 (5+2), 3rd row (5+3), and 4th row (5+4). The 5th row corresponds to HEK cells transfected only with IgLON5, and the 6th row HEK cells co-transfected with IgLON5 and CASPR2 (5+C). Left column: Whole cell lysates (WCL); middle column: Immunoprecipitates of transfected HEK cells using patients' IgLON5-abs (IP+); right column: Immunoprecipitates of transfected cells using Ctrl-abs (IP). Each row was incubated with commercial antibodies against the corresponding proteins: IgLON1, 2,3,4,5 and CASPR2.

demonstration that other IgLON family members also undergo ectodomain shedding and are cleaved from the cell membrane by matrix metalloproteinases (3). Ectodomain shedding of several neuronal cell adhesion proteins (i.e., NCAM or N-Cadherin) has been implicated in neurobiological mechanisms such as neuronal plasticity, axonal guidance, or cell migration (12). In the case of IgLONs, *in vitro* studies have shown that cleaved heterodimers of IgLON1 and 2 inhibit initiation of neurite outgrowth from chick neurons through the interaction with the IgLONs expressed in the neuronal membrane (13). Our study also shows that soluble IgLON5 can establish intercellular interactions. Additional studies will be necessary to ascertain the final effects of this interaction and if the effects are mediated by IgLON5 alone or through the formation of heterodimers with other IgLON family members.

IgLONs do not have a transmembrane domain and how they initiate downstream signal transduction pathways is presently unknown. The most plausible explanation is that IgLONs interact with other transmembrane receptors. For example, the GPI-anchored protein cell adhesion molecule transient axonal glycoprotein-1 (TAG-1), forms part of a protein complex with contactin-associated protein-like 2 (CASPR2) and shaker-type voltage-gated potassium channels (Kv1.1 and Kv1.2) which have domains that initiate downstream signaling pathways (14). However, the transmembrane receptors for IgLONs remain largely unknown. In an *in vitro* model, IgLON4 interacted with receptor tyrosine kinase fibroblast growth factor receptor 2 (FGFR2) to form a molecular complex that regulates extracellular signal-regulated kinase (ERK) and protein kinase B (AKT) pathways which control neuronal migration and maturation (15).

Our immunoprecipitation studies confirm that IgLON5-abs co-precipitate IgLON5 along with the other members of the IgLON family forming a protein complex. This result was expected considering previous studies demonstrating that homophilic and heterophilic interactions between the other IgLON family members are necessary for the effects of IgLONs on neurite outgrowth during development (16). In addition to other IgLON family members, our unbiased mass spectrometry approach identified three membrane proteins, IGSF21, CACNA2D2, and KIDINS220, as *bona-fide* interactors. KIDINS220 is of particular interest because this membrane protein modulates the development and maturation of axons and dendrites and regulates the activity of components of the actin and microtubule cytoskeleton (17) and we have previously shown that IgLON5-abs disrupt the cytoskeletal organization in cultured rat hippocampal neurons resulting in dystrophic neurites and axonal swelling (6). However, unlike the IgLONs, IgLON5-abs failed to co-precipitate these 3 proteins when co-transfected with IgLON5 in HEK cells. Possible explanations are a higher sensitivity of the mass spectrometry technique or that the interactions are transient or only detectable in the neuronal membrane.

The predominant subclass of IgLON5-abs is IgG4 but the proportion of IgG1 and IgG4 IgLON5-abs varies among patients (5). We previously demonstrated that IgLON5-abs of the IgG1 subclass produce an irreversible decrease of IgLON5 clusters on the cell surface by cross-linking and internalization (5). Here we show another potential pathogenic mechanism in which patients' IgLON5-abs disrupt the interaction of the secreted IgLON5 ectodomain with its binding partners in the neuronal membrane. Disruption of protein-protein interactions is characteristic of IgG4-abs (18), however, we found that this phenomenon was not exclusively dependent of IgG4 IgLON5-abs as sera with only IgG1 antibodies produced the same effect. Our findings are in line with pathogenic mechanisms described for other autoimmune encephalitides associated with neuronal surface antibodies. For example, Leucine-rich glioma-inactivated 1 antibodies (LGI1-abs) block the interaction of soluble LGI1 to its binding partners ADAM22 and ADAM23 (19). Similarly, CASPR2-abs inhibit the interaction of CASPR2 with its ligand TAG1 resulting in a reduction of neuronal surface CASPR2 clusters without affecting TAG1, suggesting selective CASPR2 internalization (20). Neither model evaluated if the effects were mainly mediated by IgG1 or IgG4 antibodies.

Our results indicate that the physiological ectodomain shedding of IgLON5 and its interaction with the other members of the IgLON family likely mediate the effects of IgLON5 as has

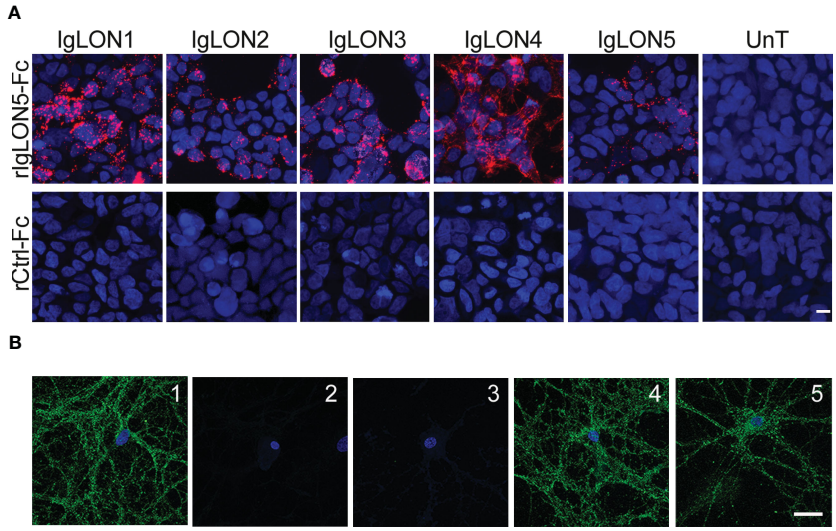

FIGURE 3
(A) Soluble IgLON5 is able to self-interact in trans and to bind to IgLON1-5. HEK cells, un-transfected (Unt) and transfected with IgLON1 to 5 incubated with rIgLON5-Fc protein (Top row) or rControl-Fc protein (second row). IgLON5 reactivity was detected with anti-Fc IgG-594 (Red fluorescence). The strongest IgLON5 interaction is observed with IgLON1, 3 and 4. No IgLON5 immunoreactivity was detected in untransfected HEK cells or when cells were incubated with rControl-Fc protein (bottom row). **(B)** Effect of IgLON5-abs on the binding of soluble IgLON5 to hippocampal neurons. IgLON5 immunofluorescence of live rat hippocampal neurons incubated with biotinylated rIgLON5-Fc (panel 1) or biotinylated rCtrl-Fc (2); Pre-incubation of biotinylated rIgLON5-Fc with CSF from patient 1 (100% IgLON5-IgG4) abolished the cell surface binding of IgLON5 (3), whereas pre-incubation with CSF from a patient with Alzheimer disease (4) or anti-NMDAR encephalitis (5) did not interfere with the binding of IgLON5 to the cell surface of neurons. Scale bar=20um.

been demonstrated for other IgLONs. The ability of patients' IgLON5-abs to interfere with these interactions represents another potential pathogenic mechanism in addition to the antibody-mediated irreversible internalization of IgLON5 (5).

Data availability statement

The data presented in the study about immunoprecipitation results are deposited in the dryad repository accession number: https://datadryad.org/stash/share/YX-zapxd15SZntbA3WSK7LpC0SSAIhKoosRcGE_ex2M.

Author contributions

1) Conception and design of the study LS, JL, FG, JD. 2) Acquisition and analysis of data LS, JL, CG, JS, FG, ABS, AS, IK, RH. 3) Drafting a significant portion of the manuscript or figures LS, FG, JL, JD. All authors contributed to the article and approved the submitted version.

Funding

This study has been funded by Instituto de Salud Carlos III through the project FIS21/00165 LS, CG (co-funded by the European Regional Development Fund "Investing in your future"). We thank the European Joint Programme on Rare Diseases (EJPRD) for funding a Networking event (contract number 463001015) on IgLON5 disease LS, CG, FG, JD from the European Union's Horizon 2020 research and innovation programme under the EJP RD COFUND-EJP N°825575. IDIBAPS belongs to CERCA (Centres de recerca de Calalunya). IK was funded by a Hertha Firnberg project grant by the Austrian Science Fund (FWF) (Grant No. T996-B30). RH was supported by grants from the Austrian Science Fund FWF: project I4685-B (SYNABS), and DOC 33-B27.The proteomics analyses were performed in the CRG/UPF Proteomics Unit which is part of the Proteored, PRB3 and is supported by grant PT17/0019, of the PE I+D+i 2013-2016, funded by ISCIII and ERDF. ABS thanks Fundação para a Ciência e Tecnologia (FCT) of Portugal for the doctoral fellowship grant number 2022.13121.BD.

Acknowledgments

We thank Mrs. Mercedes Alba for her excellent technical work. We thank Dr. Myrna R. Rosenfeld, for critical review of the manuscript and scientific advice.

Conflict of interest

FG: royalties, Euroimmun for the use of IgLON5 as an autoantibody test. JD: royalties, Athena Diagnostic for use of Ma2 as an autoantibody test; royalties and Euroimmun for use of NMDA receptor, GABAB receptor, GABAA receptor, DPPX, and IgLON5 as autoantibody tests.

The remaining authors declare that the research was conducted in the absence of any commercial or financial relationships that could be construed as a potential conflict of interest.

Publisher's note

References

1. Sabater L, Gaig C, Gelpi E, Bataller L, Lewerenz J, Torres–Vega E, et al. A novel non–rapid–eye movement and rapid–eye–movement parasomnia with sleep breathing disorder associated with antibodies to IgLON5: A case series, characterisation of the antigen, and post–mortem study. *Lancet Neurol* (2014) 13(6):575–86. doi: 10.1016/S1474–4422(14)70051–1

2. Gelpi E, Höftberger R, Graus F, Ling H, Holton JL, Dawson T, et al. Neuropathological criteria of anti–IgLON5–related tauopathy. *Acta Neuropathol* (2016) 132(4):531–43. doi: 10.1007/s00401–016–1591–8

3. Sanz R, Ferraro GB, Fournier AE. IgLON cell adhesion molecules are shed from the cell surface of cortical neurons to promote neuronal growth. *J Biol Chem* (2015) 290 (7):4330–42. doi: 10.1074/jbc.M114.628438

4. Pischedda F, Piccoli G. The IgLON family member Negr1 promotes neuronal arborization acting as soluble factor *via* FGFR2. *Front Mol Neurosci* (2015) 8:89. doi: 10.3389/fnmol.2015.00089

5. Sabater L, Planagumà J, Dalmau J, Graus F. Cellular investigations with human antibodies associated with the anti–IgLON5 syndrome. *J Neuroinflammation* (2016) 13 (1):226. doi: 10.1186/s12974–016–0689–1

6. Landa J, Gaig C, Plagumà J, Saiz A, Antonell A, Sanchez–Valle R, et al. Effects of IgLON5 antibodies on neuronal cytoskeleton: A link between autoimmunity and neurodegeneration. *Ann Neurol* (2020) 88(5):1023–7. doi: 10.1002/ana.25857

7. Koneczny I. Update on IgG4–mediated autoimmune diseases: New insights and new family members. *Autoimmun Rev* (2020) 19(10):102646. doi: 10.1016/j.autrev.2020.102646

8. Carceles–Cordon M, Mannara F, Aguilar E, Castellanos A, Planagumà J, Dalmau J. NMDAR antibodies alter dopamine receptors and cause psychotic behavior in mice. *Ann Neurol* (2020) 88(3):603–13. doi: 10.1002/ana.25829

9. Landa J, Guasp M, Míguez–Cabello F, Guimarães J, Mishima T, Oda F, et al. Encephalitis with autoantibodies against the glutamate kainate receptors GluK2. *Ann Neurol* (2021) 90(1):101–17. doi: 10.1002/ana.26098

10. Gaig C, Graus F, Compta Y, Högl B, Bataller L, Brüggemann N, et al. Clinical manifestations of the anti–IgLON5 disease. *Neurology* (2017) 88(18):1736–43. doi: 10.1212/WNL.0000000000003887

11. Grüter T, Möllers FE, Tietz A, Dargvainiene J, Melzer N, Heidbreder A, et al. Clinical, serological and genetic predictors of response to immunotherapy in anti–IgLON5 disease. *Brain* (2022) 8:awac090. doi: 10.1093/brain/awac090

12. Malinverno M, Carta M, Epis R, Marcello E, Verpelli C, Cattabeni F, et al. Cellular/Molecular synaptic localization and activity of ADAM10 regulate excitatory synapses through n–cadherin cleavage. *J Neurosci* (2010) 30(48):16343–55. doi: 10.1523/JNEUROSCI.1984-10.2010

13. Akeel M, McNamee CJ, Youssef S, Moss D. DIgLONs inhibit initiation of neurite outgrowth from forebrain neurons *via* an IgLON–containing receptor complex. *Brain Res* (2011) 1374:27–35. doi: 10.1016/j.brainres.2010.12.028

14. Patterson KR, Dalmau J, Lancaster E. Mechanisms of Caspr2 antibodies in autoimmune encephalitis and neuromyotonia. *Ann Neurol* (2018) 83(1):40–51. doi: 10.1002/ana.25120

15. Szczurkowska J, Pischedda F, Pinto B, Manago F, Haas CA, Summa M, et al. NEGR1 and FGFR2 cooperatively regulate cortical development and core behaviours related to autism disorders in mice. *Brain* (2018) 141(9):2772–94. doi: 10.1093/brain/awy190

16. Gil OD, Zhang L, Chen S, Ren YQ, Pimenta A, Zanazzi G, et al. Complementary expression and heterophilic interactions between igLON family members neurotrimin and LAMP. *J Neurobiol* (2002) 51(3):190–204. doi: 10.1002/neu.10050

17. Higuero AM, Sánchez–Ruiloba L, Doglio LE, Portillo F, Abad–Rodríguez J, Dotti CG, et al. Kidins220/ARMS modulates the activity of microtubule–regulating proteins and controls neuronal polarity and development. *J Biol Chem* (2010) 285 (2):1343–57. doi: 10.1074/jbc.M109.024703

18. Huijbers MG, Querol LA, Niks EH, Plomp JJ, van der Maarel SM, Graus F, et al. The expanding field of IgG4–mediated neurological autoimmune disorders. *Eur J Neurology* (2015) 22(8):1151–61. doi: 10.1111/ene.12758

19. Petit–Pedrol M, Sell J, Planagumà J, Mannara F, Radosevic M, Haselmann H, et al. LGI1 antibodies alter K v 1.1 and AMPA receptors changing synaptic excitability, plasticity and memory. *Brain* (2018) 141(11):3144–59. doi: 10.1093/brain/awy253

20. Joubert B, Petit–Pedrol M, Planagumà J, Mannara F, Radosevic M, Marsal M, et al. Human CASPR2 antibodies reversibly alter memory and the CASPR2 protein complex. *Ann Neurol* (2022) 91(6):801–13. doi: 10.1002/ana.26345

frontiers | Frontiers in Immunology

TYPE Original Research
PUBLISHED 14 June 2023
DOI 10.3389/fimmu.2023.1189734

OPEN ACCESS

EDITED BY
Inga Koneczny,
Medical University of Vienna, Austria

REVIEWED BY
Jérôme J Devaux,
INSERM U1191 Institut de Génomique Fonctionnelle (IGF), France
Jun-ichi Kira,
Kyushu University, Japan

*CORRESPONDENCE
Kathrin Doppler
Doppler_K@ukw.de

RECEIVED 19 March 2023
ACCEPTED 23 May 2023
PUBLISHED 14 June 2023

CITATION
Hecker K, Grüner J, Hartmannsberger B, Appeltshauser L, Villmann C, Sommer C and Doppler K (2023) Different binding and pathogenic effect of neurofascin and contactin–1 autoantibodies in autoimmune nodopathies. *Front. Immunol.* 14:1189734. doi: 10.3389/fimmu.2023.1189734

Different binding and pathogenic effect of neurofascin and contactin–1 autoantibodies in autoimmune nodopathies

Katharina Hecker[1], Julia Grüner[1], Beate Hartmannsberger[1,2], Luise Appeltshauser[1], Carmen Villmann[3], Claudia Sommer[1] and Kathrin Doppler[1]*

[1]Department of Neurology, University Hospital Würzburg, Würzburg, Germany, [2]Department of Anesthesiology, University Hospital Würzburg, Würzburg, Germany, [3]Institute of Clinical Neurobiology, University Hospital Würzburg, Würzburg, Germany

Introduction: IgG4 autoantibodies against paranodal proteins are known to induce acute-onset and often severe sensorimotor autoimmune neuropathies. How autoantibodies reach their antigens at the paranode in spite of the myelin barrier is still unclear.

Methods: We performed in vitro incubation experiments with patient sera on unfixed and unpermeabilized nerve fibers and in vivo intraneural and intrathecal passive transfer of patient IgG to rats, to explore the access of IgG autoantibodies directed against neurofascin-155 and contactin-1 to the paranodes and their pathogenic effect.

Results: We found that in vitro incubation resulted in weak paranodal binding of anti-contactin-1 autoantibodies whereas anti-neurofascin-155 autoantibodies bound to the nodes more than to the paranodes. After short-term intraneural injection, no nodal or paranodal binding was detectable when using anti-neurofascin-155 antibodies. After repeated intrathecal injections, nodal more than paranodal binding could be detected in animals treated with anti-neurofascin-155, accompanied by sensorimotor neuropathy. In contrast, no paranodal binding was visible in rats intrathecally injected with anti-contactin-1 antibodies, and animals remained unaffected.

Conclusion: These data support the notion of different pathogenic mechanisms of anti-neurofascin-155 and anti-contactin-1 autoantibodies and different accessibility of paranodal and nodal structures.

KEYWORDS

autoimmune nodopathy, IgG4, neurofascin, contactin, node of ranvier, inflammatory neuropathy, passive transfer

1 Introduction

Autoantibodies (abs) against proteins of the paranodal complex are detectable in a subgroup of patients with inflammatory neuropathies (1). These patients show distinct clinical features like acute onset, tremor and/or ataxia, and in contrast to the majority of patients with chronic inflammatory demyelinating polyradiculoneuropathy (CIDP), they mostly do not respond to treatment with intravenous immunoglobulins (2–4). Anti-pan-neurofascin (pan-NF) abs that bind to the nodal (neurofascin-186) and paranodal (neurofascin-155 (NF155)) isoform of neurofascin have been shown to induce an even more severe clinical phenotype with tetraplegia, cranial nerve involvement and respiratory insufficiency (5, 6). As there is evidence that the nodes of Ranvier are the site of the pathophysiological process, these disorders are called autoimmune nodopathies (7). Paranodal abs mainly belong to the IgG4 subclass and their pathogenicity has been proven in several studies (8–10). Abs against NF155 and contactin-1 (CNTN1) share several important features: They both bind to the paranodal axoglial complex, they are associated with a similar clinical phenotype and they mainly belong to the IgG4 subclass that does neither activate complement nor induce internalization by cross-linking of epitopes (1, 11). However, recent studies gave evidence that the pathomechanism of anti-NF155 and anti-CNTN1 abs differs in some respects: Anti-CNTN1 abs induce axoglial dysjunction, whereas anti-NF155 abs are supposed to impair the physiological protein turnover at the paranodal junction (8, 9, 12, 13). Differences of the access of abs to the paranodal complex that is protected by the myelin barrier (14) may account for different pathomechanisms.

In the current study, we aimed to compare the binding of anti-NF155 and anti-CNTN1 to paranodes and the pathogenicity of the antibodies *in-vivo* using two routes of application (intraneural and intrathecal injection). We first performed *in vitro* binding assays with a larger number of samples (n=12), followed by passive transfer of samples of one patient with each autoantibody that had shown clear binding patterns in the binding assays. The pathogenic effect as well as binding to the nodes/paranodes was directly compared between anti-CNTN1 and anti-NF155 and between chronic (intrathecal) and short-term (intraneural) exposure.

2 Material and methods

2.1 Patient material

Serum of five patients with anti-NF155, two patients with anti-pan-NF, and five patients with anti-CNTN1 abs was used for *in vitro* incubation of unpermeabilized and unfixed murine nerves. Paranodal abs and IgG subclasses were detected as previously described (15). Only patients with a distinct paranodal binding to permeabilized and fixed teased nerve fibers were included. For passive transfer experiments, IgG was purified from plasma exchange material using ion exchange chromatography with DEAE Sepharose fast flow (GE Healthcare, Chicago, Illinois, USA) as previously described (16). For intraneural injection, IgG of one patient with anti-NF155 IgG4 abs (patient 1) and one patient with anti-pan-NF IgG3 abs (patient 2) was used. We did not perform intraneural injection with IgG of a patient with anti-CNTN1 abs in this study as this was performed in a previous study using exactly the same protocol and material of patient 4 (10). For intrathecal injection, IgG of patient 2 and another patient with mainly IgG4 anti-NF155 (patient 3), and a patient with mainly IgG4 anti-CNTN1 abs (patient 4) was taken. IgG of three individuals who had undergone plasma exchange due to multiple sclerosis or optic neuritis and who were negatively screened for abs was used as a control. Autoantibody titers of purified IgG were determined by enzyme-linked immunosorbent assay (ELISA) as previously described (17). Demographic and serological data of all patients are presented in Table 1, and data of some patients have been described in detail in previous studies (5, 12, 18). All patients gave informed consent to participate in the study and the project was approved by the Ethics Committee of the University of Würzburg Medical Faculty (number 278/13 and 222/20).

2.2 Binding assays on murine nerves *in vitro*

Binding assays on permeabilized and fixed teased nerve fiber preparations were performed as previously described using either patient/control serum or purified IgG (12). For the detection of the IgG subclass in binding assays, subclass specific FITC-conjugated secondary antibodies were used (anti-human IgG3: Merck, Darmstadt, Germany; anti-human IgG1, IgG2, IgG4: Abcam, Cambridge, UK). To investigate the accessibility of the paranodal complex for patient abs, we performed *in vitro* nerve incubation experiments on unfixed and unpermeabilized mouse and rat sciatic nerves: Sciatic nerves were dissected from B6/NCrl mice and Lewis rats, the epi- and perineurium was removed and 1 cm long segments of unpermeabilized and unfixed sciatic nerves were incubated with patient or control serum diluted in artificial cerebrospinal fluid (Ecocyte Bioscience, Austin, Texas, USA) at a dilution of 1:250, for 3 h at 37°C. After incubation, nerves were fixed in 2% paraformaldehyde, teased onto slides, and blocked with 4% normal goat serum, 4% fetal calf serum and 0.3% Triton-X-100 in phosphate-buffered saline (PBS) for 1 h, before being incubated with a Cy3-conjugated anti-human IgG secondary antibody (1:100; Jackson Immuno Reseach) for 2 h. All samples were analyzed using a fluorescence microscope with appropriate filter settings (Zeiss Ax10 and Axio Imager M2 with an Apotome2 device, Zeiss, Oberkochen, Germany).

2.3 Animals, injections and study design

Eight- to twelve-week-old female Lewis rats were purchased from Charles River (Sulzfeld, Germany). Animals were housed in plexiglass cages in a light (day)/dark (night) cycle of 12:12 h and with water and food ad libitum. Animal experiments and housing and breeding of mice to obtain nerve tissue for binding assays were approved by the Bavarian State authorities (Regierung von Unterfranken, license

TABLE 1 Serological characteristics of patients and controls. *results from a previous study (10).

Patient no.	autoantigen	Serum titer	Purified IgG titer (dominant subclass)	Age, sex	IgG subclass	*In-vitro* incubation of unpermeabilized nerves	In- vivo binding	
							i.th.	i.n.
1	NF155	1:6,000	1:5,000 (IgG4: 1:500)	29, m	IgG4	weak nodal	n/a	none
2	Pan-NF	1:4,000	1:1,000 (IgG3: 1:500)	71, m	IgG3>2	nodal	weak nodal	weak nodal
3	NF155	1:14,000	1:10,000 (IgG4: 1:1,000)	78, m	IgG4>2,1	nodal >> paranodal	nodal >> paranodal	n/a
4	CNTN	1:2,000	1:15,000 (IgG4: 1:15,000)	71, f	IgG4>2	weak paranodal	none	paranodal*
5	NF155	1:2,500	n/a	18, m	IgG4	none	n/a	n/a
6	NF155	1:5,000	n/a	52, f	IgG4>2,1	nodal	n/a	n/a
7	NF155	1:5,000	n/a	33, m	IgG4>2	none	n/a	n/a
8	Pan-NF	1:200	n/a	52, m	IgG4>3	none	n/a	n/a
9	CNTN	1:19,000	n/a	62, m	IgG4>2	Strong paranodal	n/a	n/a
10	CNTN	1:7,500	n/a	76, m	IgG3>4	paranodal	n/a	paranodal*
11	CNTN	1:2,000	n/a	69, m	IgG4>3	none	n/a	none*
12	CNTN	1:1000	n/a	72, m	IgG4>2,1	none	n/a	n/a
13 (control)	–		–	37, f	–	none	none	none
14 (control)	–		–	38, f	–	none	none	n/a
15 (control)	–		–	37, f	–	none	none	n/a

number: 55.2.2-2532-2-593-17). Rats were anesthetized with isoflurane. For intrathecal injections, catheters were placed into the spinal subarachnoid space (19): A polyethylene catheter (6.5 cm intrathecal length, Instech Laboratories, BTPU-27) was inserted by incision of the atlanto-occipital membrane. After placement of intrathecal catheters, animals recovered for at least one week. Catheters were flushed daily with 20 µl NaCl using a 30G Hamilton syringe or 10 µl of patient or control IgG (100 mg/ml) followed by 10 µl NaCl, respectively. Injections were performed over a period of three weeks, timepoints are illustrated in Figure 1A. Intraneural injection of 10 µl of patient or control IgG (100 mg/ml) was performed under anesthesia with isoflurane as previously described (10): The left sciatic nerve was dissected at the sciatic notch and intraneural injection was performed at two time-points (Figure 1B). Tissue dissection was performed 48 hours after the second injection.

2.4 Scoring and behavioral testing

To monitor phenotypic abnormalities, animals were observed daily walking freely on a table. Symptoms were classified as followed: 0, no impairment; 1: reduced tone of the tail; 2: limp tail; 3: tail paralysis; 4: gait ataxia; 5: mild paraparesis; 6: moderate paraparesis; 7: severe paraparesis or paraplegia; 8: tetraparesis; 9: moribund; 10: death (20). All experimenters performing scoring, behavioral testing, and nerve conduction studies were blinded until all experiments and tissue dissections were finished. For experiments with intrathecal injection of anti-NF abs, ten control animals, twelve animals injected with anti-NF155 abs and four animals injected with anti-pan-NF abs were included. For intrathecal injection of anti-CNTN abs, twelve patient animals and 16 controls were measured. For intraneural injection of anti-NF abs, 18 control animals, 12 rats injected with anti-pan-NF and 5 animals injected with anti-NF155 were included.

The RotaRod performance test (TSE Systems, Bad Homburg, Germany) was used to assess motor function. Rats were placed on an accelerating RotaRod and the mean fall latency of five trials was measured for each animal. For the analysis of gait parameters (paw print area, maximum intensity, standing time), the Catwalk™ XT (Noldus, Emmerich am Rhein, Germany) was performed. Rats were placed on a transparent glass runway and footprints were detected by a video camera from below. Three runs per animal were recorded. To assess mechanical sensitivity, the hindpaws were tested with von-Frey filaments (Stoelting, Wood Dale, Illinois, USA) six times each and were analyzed using Dixon's staircase system (21). To assess thermal sensitivity, the Hargreaves test (Ugo Basile, Gemonio, Italy) was performed. A radiant heat stimulus was applied to the hindpaws, and the withdrawal latency was measured by a fiber optic sensor. The mean value of three measurements was calculated. To obtain baseline values, behavioral testing performed before the onset of IgG injections. During the experiment, behavioral testing was performed on day 4, 9, 16 and 20 of intrathecal injection and on day 4 after intraneural injection (Figure 1).

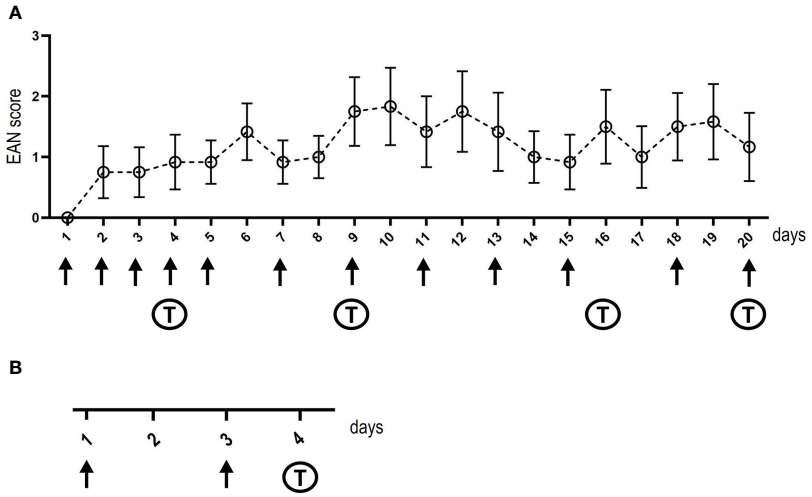

FIGURE 1
Timelines of intrathecal and intraneural injections. The days of injections (intrathecal in **A** and intraneural in **B**) are shown at the x-axis, arrows mark injections, "T" indica/tes the days of behavioral testing. Baseline behavioral testing and nerve conduction studies were performed before starting injections, post-injection nerve conduction studies and tissue dissection was performed on the day after the last intrathecal injection or two days after the second intraneural injection. The y-axis in **(A)** demonstrates the EAN score of rats treated with IgG of the anti-NF155-IgG4-positive patient, whiskers indicate standard errors.

2.5 Nerve conduction studies

Nerve conduction studies of the sciatic/tibial nerves were performed under anesthesia with ketamine/xylazine. Surface body temperature was maintained at 34-36°C with a heating lamp. In animals that underwent intraneural injection, both sciatic/tibial nerves were measured whereas in animals that were intrathecally injected, only the right sciatic/tibial nerve was recorded using Neurosoft-Evidence 3102 electromyograph (Schreiber and Zholen Medizintechnik GmbH, Stade, Germany) and needle electrodes as previously described (10). For motor neurography, the active electrode was inserted between the third and fourth toe, the inactive electrode lateral to the first toe. The stimulation electrodes were placed above the ankle (distal) and the sciatic notch (proximal). Amplitudes of compound muscle action potentials (CMAP) were recorded after supramaximal stimulation at the proximal and distal sites. F-waves and H-reflexes were recorded by ten stimuli with a frequency of 0.3 Hz, 1 Hz, and 10 Hz at the distal stimulation site. Minimum F-wave latency and persistence were determined for each frequency. For the analysis of mixed afferents, the recording electrodes were placed at the sciatic notch and the stimulation electrodes above the ankle. Electromyography was performed in the gastrocnemius muscles. Nerve conduction studies were performed at baseline and at the end of the experiment immediately prior to tissue dissection.

2.6 Tissue dissection, immunohistochemistry and microscopy

Tissue dissection after intrathecal injection included spinal cord, dorsal, and ventral nerve roots of segments L3, L4 and L5 and the sciatic nerves for immediate cryoconservation. Additionally, teased fiber preparations of the nerve roots and sciatic nerves were done as previously described (17). Intrathecal catheters were checked for correct placement during tissue dissection. After intraneural injection, only sciatic nerves were dissected, including cryoconservation for cross sections and teased fiber preparation.

To detect binding of patient or control IgG to the spinal cord or dorsal root ganglia, 10 µm thick longitudinal sections (spinal cord) or cross sections (dorsal root ganglia) were cut, fixed in 10% acetone for 10 minutes and blocked with 10% bovine serum albumin (BSA)/PBS for 1 h at room temperature (RT). Afterwards, sections were incubated with Cy3-conjugated anti-human IgG (1:100; Dianova, Hamburg, Germany) for 2 h.

Teased fiber samples were incubated with Cy3-conjugated anti-human IgG (1:100; Dianova, Hamburg, Germany) as previously described (10). For the investigation of complement deposition, nerve root teased fibers were incubated with primary antibody against the complement component C1q (mouse, 1:50, abcam) followed by secondary antibody (Alexa-Fluor488-conjugated anti-mouse, 1:200).

Nodal architecture was analyzed by immunofluorescence of spinal and sciatic teased nerve fibers with anti-Caspr1 (NeuroMab UC Davis, 1:100), anti-pan NF (R&D systems, 1:1000), anti-pan-sodium-channel (Sigma Aldrich, 1:250) at 4°C overnight and appropriate secondary antibodies (Alexa-Fluor488-conjugated anti-mouse, Jackson Immuno Research, 1:200 or Cy3-conjugated anti-chicken, Jackson Immuno Research, 1:300) for 2 h at RT. Microscopy was performed as described above. Nodes and paranodes were measured using ImageJ (Rasband, W.S., ImageJ, U. S. National Institutes of Health, Bethesda, Maryland, USA). All nodes within a field of view were measured. In the sciatic nerves of animals that were intraneurally injected, 100 nodes and 200 hemiparanodes were analyzed in control and patient animals

each, in the spinal nerves of animals that were intrathecally injected, 78 nodes of controls and 87 nodes of patients were assessed. Nodal length was defined as the gap between the paranodes stained with anti-Caspr1. Hemiparanodal length was measured as the length of Caspr1 staining on one side of the nodal gap.

2.7 Statistical analysis

Statistical testing was performed using Graph Pad Prism, version 9.5.0. Data of behavioral testing were compared between patient animals intrathecally injected with IgG of the anti-NF155, anti-pan-NF or anti-CNTN1-positive patients and control animals using two-way analysis of variance for repeated measure and with Kruskal-Wallis test in animals that were intraneurally injected. Nodal and hemiparanodal lengths were compared using Mann-Whitney-U-test. A significance level of 0.05 was applied in all tests.

3 Results

3.1 Binding of patient IgG to the nodo-paranodal complex *in vitro*

Binding assays of patient serum and purified IgG on fixed and permeabilized mouse and rat teased fibers showed distinct binding to the paranodes but not to the nodes. These binding patterns did not differ between anti-CNTN and anti-NF-155 positive patients (Figures 2 A, B). Patients with anti-NF-155 abs additionally showed strong binding to the Schmidt-Lanterman incisures (Figure 2B, arrows). Binding to the nodes and paranodes was detectable in the patients with anti-pan-NF IgG3 abs (Figure 2C). No binding was observed in controls (Figure 2D). For IgG of patients 1-4 that was used for passive transfer experiments, IgG4 was identified as the dominant IgG subclass binding at the nodes/paranodes in patients 1, 3 and 4, whereas IgG3 was the main subclass in patient 2 (Figures 2E-H). No binding of the other IgG subclasses was detectable.

To investigate the accessibility of abs to the paranodal/nodal region, *in vitro* incubation of unpermeabilized and unfixed nerves with patient sera was performed. Paranodal binding was detectable after incubation with serum of 3 of 5 patients with anti-CNTN IgG 4 abs (patients 4, 9 and 10, example in Figure 2I). Binding was weaker and often only comprised the node-adjacent half of the paranode and was more prominent and broader on small-diameter myelinated fibers. We did not detect any distinct binding to the nodes. In two patients (both with high anti-CNTN titers) we did not detect any binding to unpermeabilized and unfixed fibers. When performing these experiments using serum of anti-NF155 IgG4 positive patients, a completely different pattern of staining was detected: Binding was found at the nodal area in 3 of 5 patients with anti-NF155 abs (patients 1,3 and 6, example in Figure 2J), in one of these patients (patient 3) weak paranodal binding was also detectable (data not shown). In some binding assays of these patients, weak binding to the Schwann cell surface was observed (data not shown). In two patients (both with high titers) no nodal or paranodal binding was detectable. Serum of one of two patients with anti-pan-NF abs also showed distinct binding to the nodal region (Figure 2K) similar to the binding pattern of the commercial pan-NF control antibody (Figure 2L). We did not detect any binding in control sera. The same binding patterns were found in mouse and rat teased nerve fibers.

3.2 No *in vivo* binding or pathogenic effect after intraneural injection of anti-NF155 IgG

Teased sciatic nerve fibers were prepared and pre-fixed two days after intraneural injection of purified IgG of patients with anti-NF-155 IgG4 abs (patient 1) or controls (controls 13 and 14). In contrast to a previous study using IgG of patients with anti-CNTN1 abs where a small band of paranodal autoantibody binding was observed (10), no binding to the paranodes or nodes was detectable after injection of anti-NF155 IgG. When using IgG of a patient with anti-pan-NF abs (patient 2), only weak nodal binding was detectable in 50% of the animals (Figure 3A). Respectively – in contrast to our previous study performing intraneural injection of anti-CNTN1 abs – none of the rats injected with IgG of the patient with anti-NF155 abs or anti-pan-NF abs developed any motor or sensory symptoms as measured by RotaRod, von Frey, Hargreaves (Figure 3B) and Catwalk testing (data not shown). Nerve conduction studies did not give any evidence of a conduction block (data not shown) - in contrast to a recent study from our group using anti-CNTN1 abs where we observed conduction blocks and loss of F waves two days after injection (10). Immunofluorescence staining of teased sciatic nerves was performed to assess nodal architecture (Figure 3C). Nodal and hemiparanodal length did not differ between patient and control animals (Figure 3D).

3.3 Nodal binding and motor and sensory deficits after intrathecal injection of anti-NF155 IgG

Teased sciatic as well as ventral and dorsal lumbar root nerve fibers of animals that were intrathecally injected with patient or control IgG were assessed for autoantibody binding by staining with anti-human IgG. While no binding was detected in rats treated with control IgG (Figure 4A), animals treated with IgG of the anti-NF155 -positive patient showed distinct nodal more than paranodal binding in ventral roots (10/12 animals) and in dorsal nerve roots (7/12 animals) (Figure 4B) but not in teased sciatic nerve fibers (data not shown). The median percentage of positive nodes was 17.0% (0-40.2%) in the ventral roots and 10.2% in dorsal roots (0-51.0%). In rats treated with IgG of the anti-pan-NF -positive patient only weak binding at the nodes and/or adjacent to the nodes was observed in the ventral roots of all animals (median 18.0% (14.7-21.4%) and in the dorsal roots of three animals (median 5.4% (0-16.1%) (Figure 4C). In contrast to our recent study with intraneural injection of anti-CNTN1 (10), no deposition of complement (C1q)

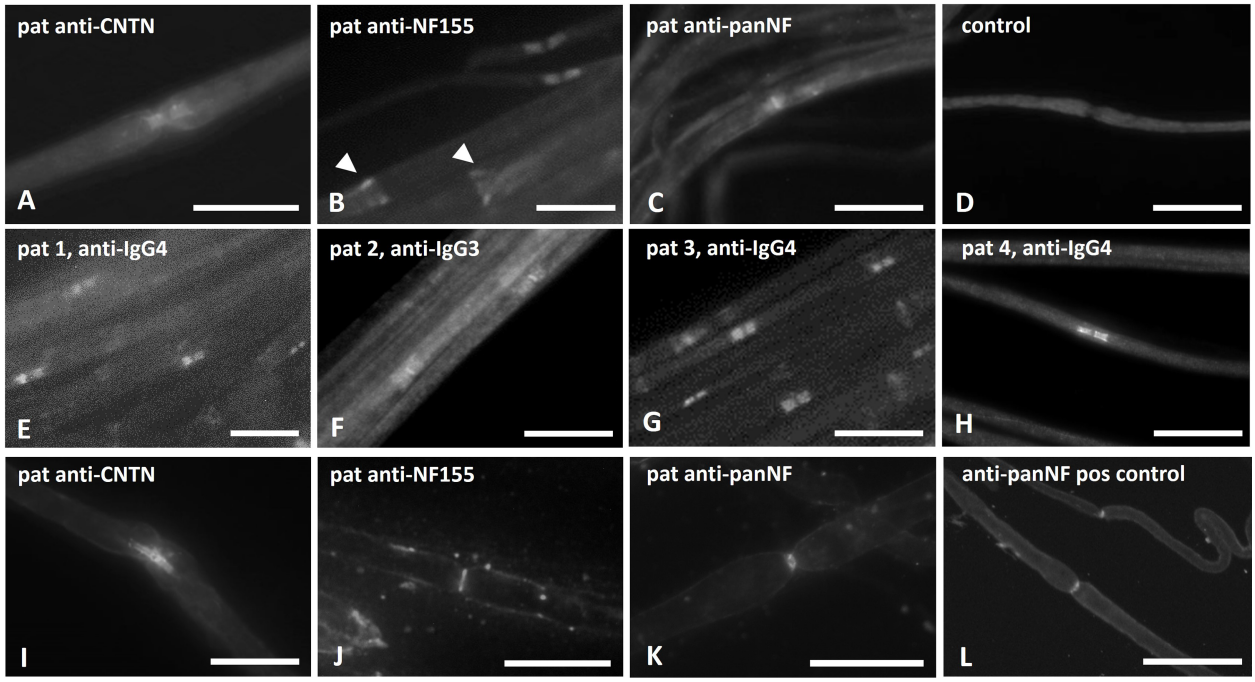

FIGURE 2
Photomicrographs of binding assays on teased nerve fibers. Binding assays of patient sera/IgG on teased sciatic nerve/rat fibers **(A–D)**, binding assays with purified IgG that was used for passive transfer experiments and staining with subclass specific anti-human IgG **(E–H)** and *in vitro* incubation of unfixed and unpermeabilized mouse nerves with patients' sera **(I–L)** were performed. Paranodal binding was detectable in binding assays of patients with anti-NF155 and anti-CNTN1 abs **(A, B)**, additional binding to the Schmidt-Lanterman incisures was found in patients with anti-NF155 (B, arrow heads). Strong binding to the nodal and weaker binding to the paranodal region was found in binding assays with IgG of an anti-pan-NF-positive patient **(C)**. No binding was seen when using serum of a healthy control **(D)**. IgG4 was identified as the major subclass in patients 1, 3 and 4 **(E, G, H)**, IgG3 in patient 2 **(F)**. After *in-vitro* incubation of unpermeabilized and unfixed nerve fibers, paranodal binding was found in some of the anti-contactin positive patients **(I)**, but only nodal binding in nerve fibers incubated with serum of patients with anti-neurofascin-155 **(J)** or anti-pan-NF **(K)** and after incubation with a commercial anti-pan-NF antibody **(L)** Scale bar = 20 µm.

was detectable by immunofluorescence. In animals injected with IgG of the anti-CNTN1 positive patient (patient 4), we did not observe any binding to the paranodes or nodes (Figure 4D).

We did further not observe any motor or sensory symptoms in animals intrathecally injected with IgG of the anti-CNTN1-positive patient and control IgG and could not detect any relevant motor or sensory deficits in the von-Frey, RotaRod, Hargreaves (Figure 4E, lower graphs) and Catwalk tests (data not shown). There was just a trend to an increased thermal threshold in patient animals, but without statistical significance (p=0.09, Figure 4E). Nerve conduction studies of the sciatic nerve including F waves were completely normal (data not shown).

In contrast, 8 of 12 (67%) of the animals injected with IgG of the anti-NF155 patient developed motor and sensory symptoms, mostly starting one or two days after starting injections (Figure 1). Half of the symptomatic animals (n=4) showed mild symptoms, like paresis of the tail (EAN scores 1-2) whereas in the other half paresis of the hind limbs was observed (EAN scores 4-6). We did not observe any paresis in animals treated with anti-pan-NF IgG. Motor testing revealed a decrease of the fall latency on the RotaRod in rats injected with IgG of the anti-NF155 positive patient (F=4.516, p=0.046; mean difference from baseline: 3%(-9s) (controls) and 31%(-44s) (NF155); Figure 4E). Sensory testing demonstrated increased latency in Hargreaves testing in anti-NF-155 patient animals compared to controls (F=12.97, p=0.002; mean difference from baseline: 8% (0.6s) (controls) and 42% (3.4s) (NF155)) and an increased threshold in the von-Frey testing (F=7.25, p=0.014; mean difference from baseline: 7% (1.2g) (controls) and 17% (2.9g) (NF155)) (Figure 4E). Nerve conduction studies of the sciatic nerve did not show any abnormalities including normal F wave persistence and latency in animals injected with anti-NF155 IgG/anti-panNF IgG. Immunofluorescence staining of the paranodal/nodal proteins Caspr1 and pan-NF at teased nerve roots did not show any dispersion to the juxtaparanodes or any destruction of nodal architecture or any obvious nodal or paranodal elongation. We did not find any difference of hemiparanodal or nodal length between dorsal and ventral roots within groups. Quantitative analysis of hemiparanodal and nodal length of dorsal and ventral nerve roots revealed a decrease of the hemiparanodal length in rats injected with IgG of the anti-NF155-positive patient (p=0.018) and an increase of nodal length in rats injected with IgG of the pan-NF-positive patient (p=0.0026) (Figure 4F).

4 Discussion

By directly comparing binding patterns of anti-CNTN1, anti-NF155 and anti-panNF *in vitro* and after passive transfer, we could demonstrate clear differences of binding: Weak paranodal binding

10.3389/fimmu.2023.1189734

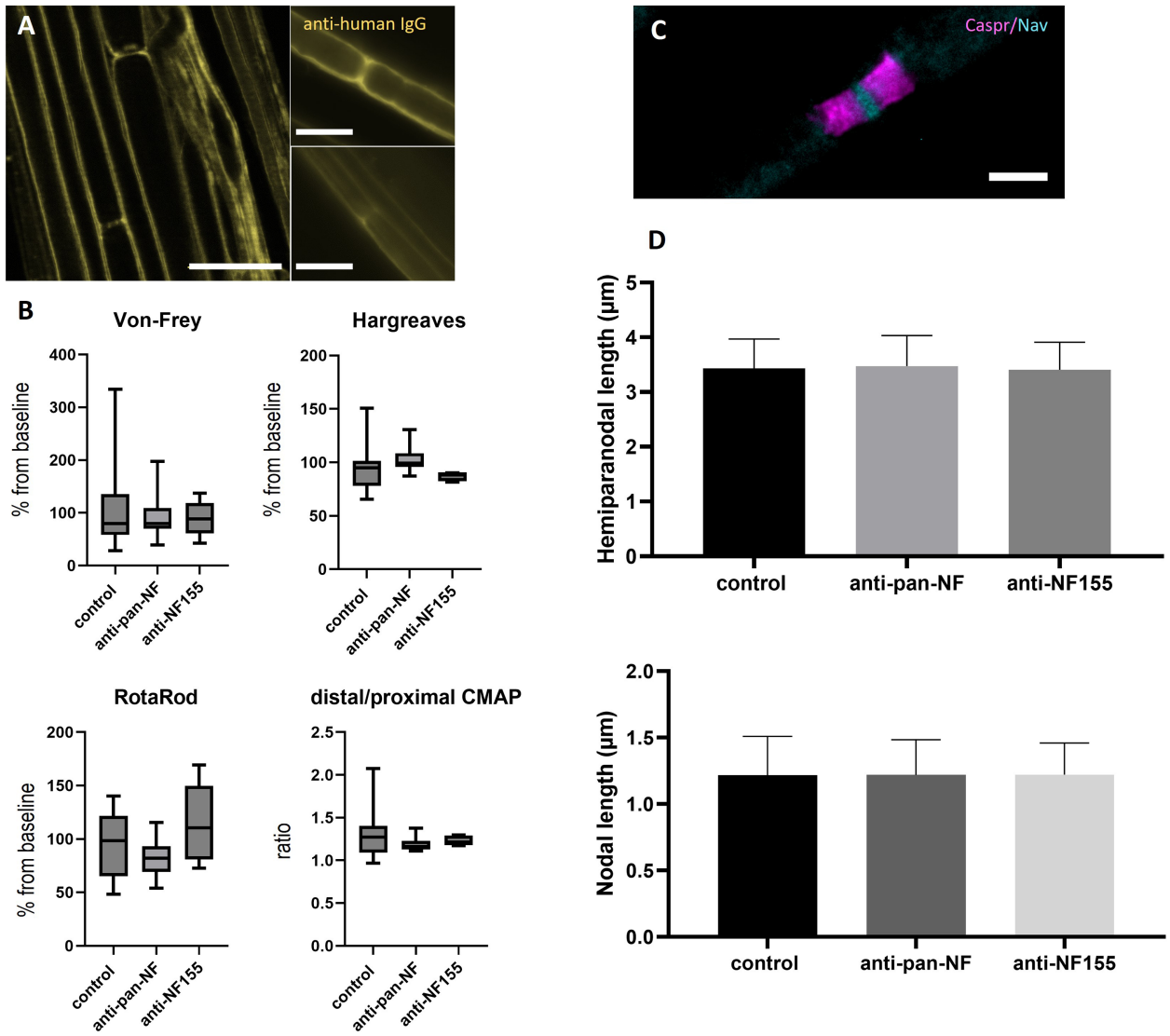

FIGURE 3
Effects of intraneural injection of anti-NF abs. Photomicrographs of teased sciatic nerve fibers after intraneural injection of IgG of a patient with anti-NF155 or anti-pan-NF abs and staining with anti-human IgG: Weak nodal binding was detectable at some nodes after injection of anti-pan-NF (A, left image, arrows), but not after injection of control IgG (A, right two images). Sensory and motor testing did not show any differences between patient and control animals and also no differences of the distal-to-proximal ratio of the compound muscle action potential of neurography of the sciatic nerve was found **(B)** (horizontal lines, boxes and whiskers mark medians, quartiles and ranges). Immunofluorescence staining of the nodes of Ranvier was performed to analyze hemiparanodal (Caspr1, magenta) and nodal (pan-Nav, cyan) length **(C)** No differences were found between patient and control animals (n = 100 nodes/200 hemiparanodes) **(D)**. **(A)** Scale bars = 20 µm, **(B)** Scale bar = 5 µm.

was detectable after incubation with anti-CNTN1 whereas anti-NF155 and anti-panNF bound to the nodes more than to the paranodes. No binding and no pathogenic effect was found after short-term intraneural injection of anti-NF155 – in contrast to a recent study applying purified IgG of patients with anti-CNTN1 IgG3 and IgG4 abs using the same protocol (10). By long-term intrathecal injection, nodal binding accompanied by motor and sensory symptoms was seen in animals injected with purified IgG of a patient with anti-NF155 IgG4 abs, not after injection of IgG of an anti-CNTN1 positive patient. Results are summarized in Figure 5. Even though NF155 and CNTN1 both are part of the paranodal protein complex forming the axoglial junction and abs against both proteins are associated with very similar clinical symptoms of a severe sensorimotor autoimmune neuropathy, our data further strengthen the notion of different pathogenic effects of both abs: Paranodal binding after incubation of mouse and rat sciatic nerve with anti-CNTN1 gives evidence that abs against CNTN1 are at least partly able to cross the myelin barrier and to bind to paranodal autoantigens. Our data are in accordance with a previous study that could also show paranodal binding of anti-CNTN1 IgG4 but not IgG1 (8). In our *in vitro* study, patients with anti-CNTN1 IgG4 and IgG3 abs were included and paranodal binding could be shown for both subclasses, similar to a recent study from our laboratory that could demonstrate paranodal binding after intraneural injection of anti-CNTN1 abs (10). However, interindividual differences of paranodal binding after *in vitro* incubation of unpermeabilized

10.3389/fimmu.2023.1189734

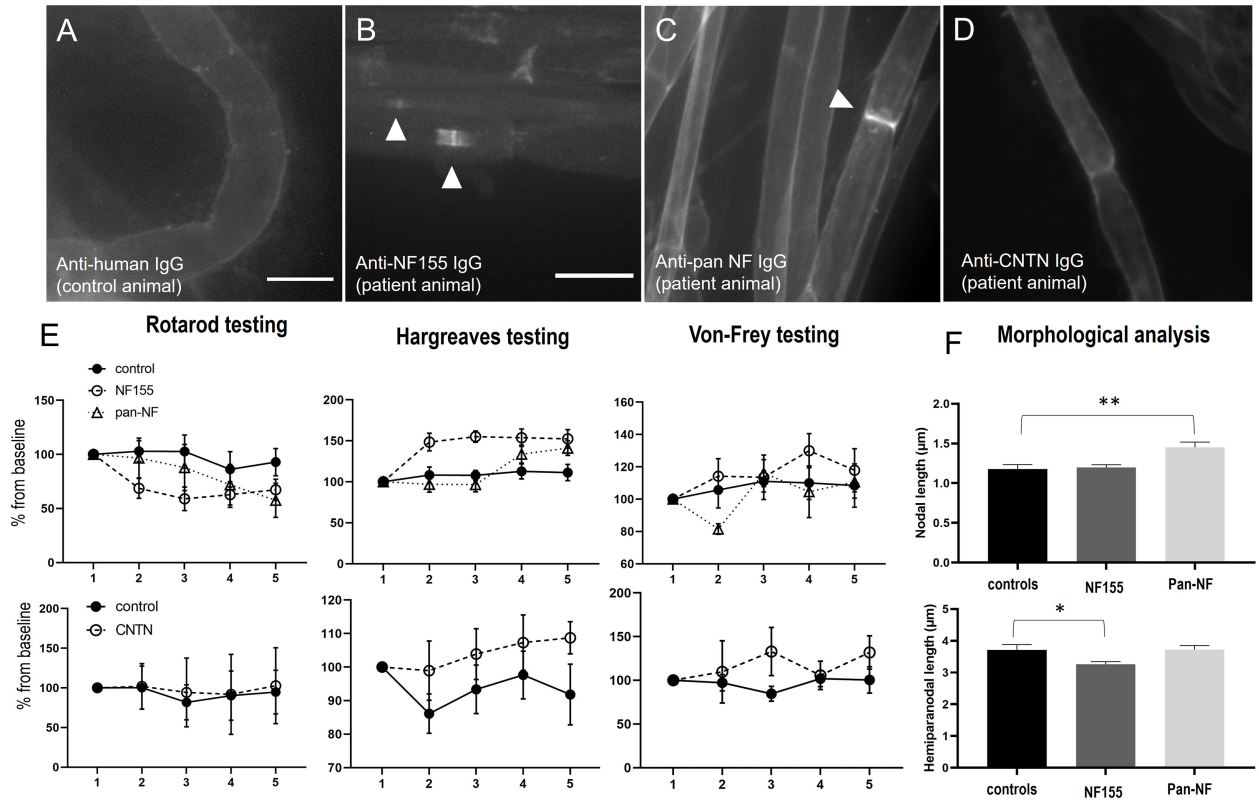

FIGURE 4
Photomicrographs of teased nerve roots of animals intrathecally injected with IgG of a control **(A)**, a patient with anti-NF155 **(B)**, anti-pan-NF **(C)** or anti-CNTN1 **(D)** abs. No binding is detectable after injection of control and anti-CNTN1 IgG **(A, D)**, nodal more than paranodal binding after injection of anti-NF155-positive IgG **(B)** and weak nodal and juxtanodal binding after injection of anti-pan-NF-IgG **(C)**. Behavioral testing revealed a decrease of fall latency in the RotaRod testing, increased thermal and mechanical sensory thresholds by Hargreaves and Von-Frey testing in animals treated with anti-NF155 IgG (upper images), not in animals injected with anti-CNTN1-IgG (lower images), just a trend towards increased thermal thresholds in patient animals but without statistical significance **(E)**. Morphological analysis of nodal and hemiparanodal length revealed increased nodal length in anti-pan-NF-IgG injected animals and a decrease of hemiparanodal length in animals treated with anti-NF155-IgG (n = 78 nodes (controls), 145 (NF155), 87 (pan-NF) **(F)**. Graphs show mean values and standard errors, *p<0.01, **p<0.001. Scale bars = 20 µm.

nerve fibers were observed that were not explained by different IgG subclasses and could only be partly explained by autoantibody titers. Different affinities of abs or different epitopes with various grades of accessibility may be an explanation, considering that such different epitopes have been described for patients with anti-CNTN1 abs (22, 23). Therefore larger studies are needed to draw a definite conclusion.

In contrast to anti-CNTN1 abs, where conduction blocks and pareses have been described after intraneural injection (10), high local concentrations of abs, as induced by intraneural injection, did not seem to be sufficient to access the paranodes in cases with anti-NF155 and anti-pan-NF. For these antibodies, no binding to the paranodes was observed in teased sciatic nerve fibers of animals that were intraneurally injected. In contrast to intrathecal injection, no binding to the nodes was detectable after intraneural injection of anti-NF155 and only weak nodal binding of anti-pan-NF, but without clinical effects. As anti-pan-NF abs were of the IgG3 subclass, lack of complement may account for the absence of an effect on nerve conduction. However, in a recent study with anti-CNTN1 abs, complement deposition and conduction blocks could be detected, also without the addition of human complement (10).

Upon intrathecal injection, we found clear differences between anti-NF155 and anti-CNTN1 abs: Similar to a recent study (9), motor symptoms were induced by anti-NF155 and distinct binding to the nodes but only weak and incomplete binding to the paranodes was observed. These results indicate that continuous exposure to anti-NF155 abs - in contrast to anti-CNTN1 where focally high concentrations seem to be effective - is required to induce clinical symptoms. Devaux and colleagues proposed impairment of the protein turnover by binding to NF155 that is expressed at the nodal Schwann cell surfaces as a potential pathogenic mechanism in anti-NF155 associated neuropathy, concordant with the necessity of continuous exposure to abs (8). Indeed, this may also explain the findings of our study, since we could not find evidence supporting other explanations like binding to the spinal cord or dorsal root ganglia. However, symptoms occurred after one to two days of injection, which would be early for such a mechanism. Another explanation for differences between intraneural and intrathecal injection may be a higher vulnerability of nerve roots compared to peripheral nerves like the sciatic nerve. As nerve roots originate at the transition between central and peripheral nervous system, the

10.3389/fimmu.2023.1189734

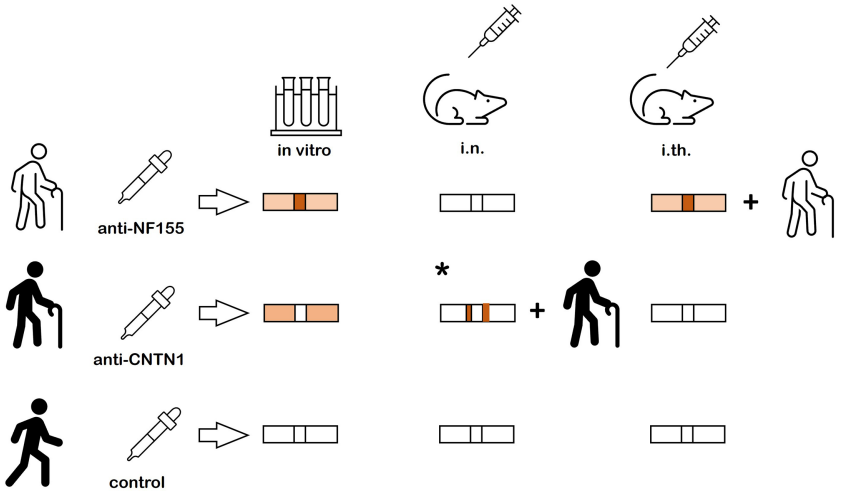

FIGURE 5
Summary of the results. Nodal more than paranodal binding is found after *in vitro* incubation of nerve fibers and after intrathecal passive transfer of anti-NF155 abs and clinical symptoms are induced by intrathecal passive transfer. No binding and no symptoms are detectable after intraneural injection of anti-NF155. Weak paranodal binding is found after *in vitro* incubation of unfixed and unpermeabilized nerve fibers with anti-CNTN, but neither binding nor symptoms are detectable after intrathecal passive transfer. A previous study could demonstrate paranodal binding adjacent to the nodal gap and clinical symptoms after intraneural injection (* = result from previous study (10)). *In vitro* incubation and intraneural and intrathecal passive transfer of control IgG does not induce any binding or symptoms.

the density of nodes may be increased and alterations of the ultrastructure may occur (24, 25) and thus, the myelin barrier may be easier to penetrate. Remarkably, polyradiculitis is a prominent feature in patients with anti-NF155 abs as demonstrated by MRI studies (26). However, we could not measure any loss of F waves as a potential correlate of conduction block of ventral roots. An explanation may be that the intrathecal catheters end at L3/L4 and other nerve roots that contribute to the sciatic nerve (L4-L6) are not sufficiently affected. Morphological analysis of nerve roots did not reveal any obvious damage to the nodes. Quantitative assessment found a mild decrease of hemiparanodal length in animals injected with anti-NF155 IgG that may be explained by a slightly decreased expression of NF155 at the paranodes, mostly affecting the marginal area of the hemiparanodes. In contrast to the recent study by Manso and colleagues (9), our animals did not only show motor but also sensory symptoms. This is in line with the clinical picture of the patients and is supported by binding of patient IgG to ventral as well as dorsal nerve roots and decreased paranodal length in ventral and dorsal nerve roots. Different autoantibody titers and/or epitopes may explain these differences. Due to the rareness of the disease and the complexity of the experiments, only a small number of patients can be tested in passive transfer experiments and samples of different patients were used for intraneural and intrathecal injection of anti-NF155. Interindividual differences of epitopes, autoantibody affinity and titers therefore need to be taken into account when interpreting results. Another limitation are different titers of abs that may reduce the comparability between different patients and the limited number of patients. Another barrier that may contribute to the accessibility of autoantibodies to nerve fibers is the blood nerve barrier that needs to be addressed in future studies using systemic administration of autoantibodies.

In summary, our data demonstrate different capabilities of paranodal abs to access their targets and support the notion of different pathogenic mechanisms of anti-CNTN1 and anti-NF155 abs, but also indicate interindividual differences of abs targeting the same protein that may explain different courses of disease and should be addressed in future studies.

Data availability statement

The original contributions presented in the study are included in the article/supplementary material. Further inquiries can be directed to the corresponding author.

Ethics statement

The studies involving human participants were reviewed and approved by Ethikkommission der Universität Würzburg. The patients/participants provided their written informed consent to participate in this study. The animal study was reviewed and approved by Regierung von Unterfranken.

Author contributions

KH: acquisition and analysis of data, JG: acquisition and analysis of data, BH: acquisition and analysis of data, LA: analysis of data, CV: study design and conception, CS: study design and conception, KD: study design and conception, analysis of data, writing of manuscript draft. All authors contributed to the article and approved the submitted version.

Funding

The study was supported by a grant of the Interdisciplinary Center of Clinical Research of the University Hospital Würzburg to KD and CV (N356). KD was supported by a grant of the German Research Foundation (DO2219/1-1). This publication was supported by the Open Access Publication Fund of the University of Wuerzburg.

Acknowledgments

We thank Lydia Biko, Antonia Kohl, Maria Gallant, Susanne Hellmig and Helga Brünner for expert technical assistance and animal care.

Conflict of interest

The authors declare that the research was conducted in the absence of any commercial or financial relationships that could be construed as a potential conflict of interest.

Publisher's note

References

1. Vural A, Doppler K, Meinl E. Autoantibodies against the node of ranvier in seropositive chronic inflammatory demyelinating polyneuropathy: diagnostic, pathogenic, and therapeutic relevance. *Front Immunol* (2018) 9:1029. doi: 10.3389/fimmu.2018.01029

2. Querol L, Nogales-Gadea G, Rojas-Garcia R, Martinez-Hernandez E, Diaz-Manera J, Suarez-Calvet X, et al. Antibodies to contactin-1 in chronic inflammatory demyelinating polyneuropathy. *Ann Neurol* (2013) 73(3):370–80. doi: 10.1002/ana.23794

3. Querol L, Nogales-Gadea G, Rojas-Garcia R, Diaz-Manera J, Pardo J, Ortega-Moreno A, et al. Neurofascin Igg4 antibodies in cidp associate with disabling tremor and poor response to ivig. *Neurology* (2014) 82(10):879–86. doi: 10.1212/WNL.0000000000000205

4. Doppler K, Appeltshauser L, Villmann C, Martin C, Peles E, Kramer HH, et al. Auto-antibodies to contactin-associated protein 1 (Caspr) in two patients with painful inflammatory neuropathy. *Brain* (2016) 139(Pt 10):2617–30. doi: 10.1093/brain/aww189

5. Stengel H, Vural A, Brunder AM, Heinius A, Appeltshauser L, Fiebig B, et al. Anti-Pan-Neurofascin Igg3 as a marker of fulminant autoimmune neuropathy. *Neurol Neuroimmunol Neuroinflamm* (2019) 6(5):e063. doi: 10.1212/NXI.0000000000000603

6. Appeltshauser L, Junghof H, Messinger J, Linke J, Haarmann A, Ayzenberg I, et al. Anti-Pan-Neurofascin antibodies induce subclass-related complement activation and nodo-paranodal damage. *Brain* (2022) 146(5):1932–1949. doi: 10.1093/brain/awac418

7. Van den Bergh PYK, van Doorn PA, Hadden RDM, Avau B, Vankrunkelsven P, Allen JA, et al. European Academy of Neurology/Peripheral nerve society guideline on diagnosis and treatment of chronic inflammatory demyelinating polyradiculoneuropathy: report of a joint task force-second revision. *Eur J Neurol* (2021) 28(11):3556–83. doi: 10.1111/ene.14959

8. Manso C, Querol L, Mekaouche M, Illa I, Devaux JJ. Contactin-1 Igg4 antibodies cause paranode dismantling and conduction defects. *Brain* (2016) 139(Pt 6):1700–12. doi: 10.1093/brain/aww062

9. Manso C, Querol L, Lleixa C, Poncelet M, Mekaouche M, Vallat JM, et al. Anti-Neurofascin-155 Igg4 antibodies prevent paranodal complex formation in vivo. *J Clin Invest* (2019) 129(6):2222–36. doi: 10.1172/JCI124694

10. Doppler K, Schuster Y, Appeltshauser L, Biko L, Villmann C, Weishaupt A, et al. Anti-Cntn1 Igg3 induces acute conduction block and motor deficits in a passive transfer rat model. *J Neuroinflamm* (2019) 16(1):73. doi: 10.1186/s12974-019-1462-z

11. Vidarsson G, Dekkers G, Rispens T. Igg subclasses and allotypes: from structure to effector functions. *Front Immunol* (2014) 5:520. doi: 10.3389/fimmu.2014.00520

12. Doppler K, Appeltshauser L, Wilhelmi K, Villmann C, Dib-Hajj SD, Waxman SG, et al. Destruction of paranodal architecture in inflammatory neuropathy with anti-Contactin-1 autoantibodies. *J Neurol Neurosurg Psychiatry* (2015) 86(7):720–8. doi: 10.1136/jnnp-2014-309916

13. Koike H, Kadoya M, Kaida KI, Ikeda S, Kawagashira Y, Iijima M, et al. Paranodal dissection in chronic inflammatory demyelinating polyneuropathy with anti-Neurofascin-155 and anti-Contactin-1 antibodies. *J Neurol Neurosurg Psychiatry* (2017) 88(6):465–73. doi: 10.1136/jnnp-2016-314895

14. Reinhold AK, Rittner HL. Barrier function in the peripheral and central nervous system-a review. *Pflugers Arch* (2017) 469(1):123–34. doi: 10.1007/s00424-016-1920-8

15. Appeltshauser L, Brunder AM, Heinius A, Kortvelyessy P, Wandinger KP, Junker R, et al. Antiparanodal antibodies and igG subclasses in acute autoimmune neuropathy. *Neurol Neuroimmunol Neuroinflamm* (2020) 7(5):e817. doi: 10.1212/NXI.0000000000000817

16. Sommer C, Weishaupt A, Brinkhoff J, Biko L, Wessig C, Gold R, et al. Paraneoplastic stiff-person syndrome: passive transfer to rats by means of igg antibodies to amphiphysin. *Lancet* (2005) 365(9468):1406–11. doi: 10.1016/S0140-6736(05)66376-3

17. Doppler K, Appeltshauser L, Kramer HH, Ng JK, Meinl E, Villmann C, et al. Contactin-1 and neurofascin-155/-186 are not targets of auto-antibodies in multifocal motor neuropathy. *PloS One* (2015) 10(7):e0134274. doi: 10.1371/journal.pone.0134274

18. Appeltshauser L, Messinger J, Starz K, Heinrich D, Brunder AM, Stengel H, et al. Diabetes mellitus is a possible risk factor for nodo-paranodopathy with antiparanodal autoantibodies. *Neurol Neuroimmunol Neuroinflamm* (2022) 9(3):e1163. doi: 10.1212/NXI.0000000000001163

19. Malkmus SA, Yaksh TL. Intrathecal catheterization and drug delivery in the rat. *Methods Mol Med* (2004) 99:109–21. doi: 10.1385/1-59259-770-X:011

20. Mausberg AK, Meyer Zu Horste G, Dehmel T, Stettner M, Lehmann HC, Sheikh KA, et al. Erythropoietin ameliorates rat experimental autoimmune neuritis by inducing transforming growth factor-beta in macrophages. *PloS One* (2011) 6(10):e26280. doi: 10.1371/journal.pone.0026280

21. Chaplan SR, Bach FW, Pogrel JW, Chung JM, Yaksh TL. Quantitative assessment of tactile allodynia in the rat paw. *J Neurosci Methods* (1994) 53(1):55–63. doi: 10.1016/0165-0270(94)90144-9

22. Labasque M, Hivert B, Nogales-Gadea G, Querol L, Illa I, Faivre-Sarrailh C. Specific contactin n-glycans are implicated in neurofascin binding and autoimmune targeting in peripheral neuropathies. *J Biol Chem* (2014) 289(11):7907–18. doi: 10.1074/jbc.M113.528489

23. Miura Y, Devaux JJ, Fukami Y, Manso C, Belghazi M, Wong AH, et al. Contactin 1 Igg4 associates to chronic inflammatory demyelinating polyneuropathy with sensory ataxia. *Brain* (2015) 138:1484–91. doi: 10.1093/brain/awv054

24. Fraher J. Node distribution and packing density in the rat cns-pns transitional zone. *Microsc Res Tech* (1996) 34(6):507–21. doi: 10.1002/(SICI)1097-0029(19960815)34:6<507::AID-JEMT3>3.0.CO;2-G

25. Fraher JP, Kaar GF. The transitional node of ranvier at the junction of the central and peripheral nervous systems: an ultrastructural study of its development and mature form. *J Anat* (1984) 139(Pt 2):215–38.

26. Shelly S, Klein CJ, Dyck PJB, Paul P, Mauermann ML, Berini SE, et al. Neurofascin-155 immunoglobulin subtypes: clinicopathologic associations and neurologic outcomes. *Neurology* (2021) 97(24):e2392–e403. doi: 10.1212/WNL.0000000000012932

frontiers | Frontiers in Immunology

TYPE Review
PUBLISHED 26 July 2023
DOI 10.3389/fimmu.2023.1212757

OPEN ACCESS

EDITED BY
Luis Querol,
Hospital de la Santa Creu i Sant Pau, Spain

REVIEWED BY
Judith Fraussen,
University of Hasselt, Belgium
Fubin Li,
Shanghai Jiao Tong University, China

*CORRESPONDENCE
John Tzartos
jtzartos@gmail.com

†These authors have contributed equally to this work

RECEIVED 26 April 2023
ACCEPTED 05 July 2023
PUBLISHED 26 July 2023

CITATION
Vakrakou AG, Karachaliou E, Chroni E, Zouvelou V, Tzanetakos D, Salakou S, Papadopoulou M, Tzartos S, Voumvourakis K, Kilidireas C, Giannopoulos S, Tsivgoulis G and Tzartos J (2023) Immunotherapies in MuSK-positive Myasthenia Gravis; an IgG4 antibody-mediated disease. *Front. Immunol.* 14:1212757. doi: 10.3389/fimmu.2023.1212757

Immunotherapies in MuSK-positive Myasthenia Gravis; an IgG4 antibody-mediated disease

Aigli G. Vakrakou[1†], Eleni Karachaliou[2†], Elisabeth Chroni[3], Vasiliki Zouvelou[1], Dimitrios Tzanetakos[2], Stavroula Salakou[2], Marianna Papadopoulou[2,4], Socrates Tzartos[5,6,7], Konstantinos Voumvourakis[2], Constantinos Kilidireas[1,8], Sotirios Giannopoulos[2], Georgios Tsivgoulis[2,9] and John Tzartos[2*]

[1]First Department of Neurology, Medical School, National and Kapodistrian University of Athens, Athens, Greece, [2]Second Department of Neurology, Attikon University Hospital, National and Kapodistrian University of Athens, Athens, Greece, [3]Department of Neurology, School of Medicine, University of Patras, Patras, Greece, [4]Department of Physiotherapy, University of West Attica, Athens, Greece, [5]Tzartos NeuroDiagnostics, Athens, Greece, [6]Department of Neurobiology, Hellenic Pasteur Institute, Athens, Greece, [7]Department of Pharmacy, University of Patras, Patras, Greece, [8]Department of Neurology, Henry Dunant Hospital Center, Athens, Greece, [9]Department of Neurology, The University of Tennessee Health Science Center, Memphis, TN, United States

Muscle-specific kinase (MuSK) Myasthenia Gravis (MG) represents a prototypical antibody-mediated disease characterized by predominantly focal muscle weakness (neck, facial, and bulbar muscles) and fatigability. The pathogenic antibodies mostly belong to the immunoglobulin subclass (Ig)G4, a feature which attributes them their specific properties and pathogenic profile. On the other hand, acetylcholine receptor (AChR) MG, the most prevalent form of MG, is characterized by immunoglobulin (Ig)G1 and IgG3 antibodies to the AChR. IgG4 class autoantibodies are impotent to fix complement and only weakly bind Fc-receptors expressed on immune cells and exert their pathogenicity *via* interfering with the interaction between their targets and binding partners (e.g. between MuSK and LRP4). Cardinal differences between AChR and MuSK-MG are the thymus involvement (not prominent in MuSK-MG), the distinct HLA alleles, and core immunopathological patterns of pathology in neuromuscular junction, structure, and function. In MuSK-MG, classical treatment options are usually less effective (e.g. IVIG) with the need for prolonged and high doses of steroids difficult to be tapered to control symptoms. Exceptional clinical response to plasmapheresis and rituximab has been particularly observed in these patients. Reduction of antibody titers follows the clinical efficacy of anti-CD20 therapies, a feature implying the role of short-lived plasma cells (SLPB) in autoantibody production. Novel therapeutic monoclonal against B cells at different stages of their maturation (like plasmablasts), or against molecules involved in B cell activation, represent promising therapeutic targets. A revolution in autoantibody-mediated diseases is pharmacological interference with the neonatal Fc receptor, leading to a rapid reduction of circulating IgGs (including autoantibodies), an approach already suitable for AChR-MG and promising for MuSK-MG. New precision medicine approaches involve Chimeric autoantibody receptor T (CAAR-T) cells that are engineered to target antigen-specific B cells in MuSK-MG and represent a milestone in the development of targeted

immunotherapies. This review aims to provide a detailed update on the pathomechanisms involved in MuSK-MG (cellular and humoral aberrations), fostering the understanding of the latest indications regarding the efficacy of different treatment strategies.

KEYWORDS

Myasthenia Gravis, MuSK, IgG4, anti-CD20, FcRn, CAAR-T cells

1 Introduction

Myasthenia Gravis (MG) is the most extensively studied and best-understood autoantibody-mediated autoimmune neurological disease; it affects the endplate region of the postsynaptic neuromuscular junction. MG is diagnosed based on clinical, electrophysiological, and serological findings (1). In approximately 80% of patients with generalized MG, it is characterized by increased levels of circulating immunoglobulin G1 (IgG1) and IgG3 autoantibodies against the acetylcholine receptor (AChR) (2, 3). Less frequently, patients who lack detectable serum AChR antibodies mainly demonstrate IgG4 antibodies against muscle-specific tyrosine kinase (MuSK) or IgG1 antibodies against low-density lipoprotein receptor-related protein 4 (LRP4). A small subgroup of patients (approximately 7%) with MG has no detectable circulating antibodies (4, 5).

MuSK belongs to the receptor tyrosine kinases enriched at the neuromuscular junction (NMJ) and is important for its differentiation and development (6, 7). The ectodomain of MuSK is comprised of three immunoglobulin (Ig) -like and one cysteine-rich/Frizzled domain, while the cytosolic compartment is mainly composed of a tyrosine kinase domain (8). Agrin, a heparan sulfate proteoglycan, released from motor neurons, binds to MuSK coreceptor LRP4 (located in the muscle membrane) and this interaction leads to the generation of a hetero-tetramerized complex consisting of 2 LRP4 and 2 MuSK molecules. The 2 MuSK molecules are dimerized, and the intracellular kinase domains are activated through autophosphorylation (transphosphorylation of tyrosine residues in the cytoplasmic domains like the Y553 site) (9–11). This phosphorylation leads to the recruitment of downstream kinase-7 (Dok-7), located in the cytosol of myofibers, which is phosphorylated and activated. Dimerization of Dok-7 leads to juxtaposition of the 2 MuSK molecules required for the full activation of MuSK (10, 12). Downstream of Dok-7 activation are the adaptor proteins Crk and Crk-L that recruit further proteins like Sorb1 and Sorb-2 finally leading to the activation of the scaffold protein rapsyn that is responsible for the proper AchR clustering in the muscle membrane (13, 14). Other downstream pathways of Dok-7 activation involved in AchR clustering are the activation of Rac and Rho proteins, or disheveled 1(Dvl1) and tumorous imaginal discs protein (Tid1) (15, 16). Moreover, the overactivation of Musk is regulated by various mechanisms involving the Wnt pathway leading to endocytosis, by Dok-7 ubiquitination and degradation, or a stringent process involving the juxta membrane and the autoactivation loop autoinhibition (17, 18). Constitutively active MuSK has been shown to induce ectopic NMJ-like structures independent of Agrin *in vivo* (19). In the research area of MuSK-MG, the activation of the agrin-LRP4-MuSK pathway is of importance as the patients circulating antibodies targeting MuSK affect MuSK phosphorylation and/or Agrin-dependent AChR clustering with complex mechanisms explained below.

In MuSK-MG, unprovoked disease exacerbations and myasthenic crises frequently occur even despite high doses of immunosuppression (20, 21). Nevertheless, in recent years, the early diagnosis of these patients and the administration of rituximab has led to a noticeable reduction in treatment-refractory cases (22). Very rare cases with mild ocular symptoms and spontaneous remission have been described (23, 24). Approximately, 10–15% of MuSK- MG patients have a refractory disease or suffer from relapses on tapering immunosuppressive medication (25). It is frequently difficult to manage this subset of individuals who do not respond favorably to steroids or standard immunosuppressants. Classical treatments for MuSK-MG include nonspecific immunomodulation (corticosteroids and plasmapheresis) in the condition of myasthenic crisis or an acute exacerbation of MG symptoms, and nonsteroidal immunosuppressants that serve as steroid-sparing agents for long-term remission. There is an urgent need for novel and more efficient therapies for MG due to devastating side effects and treatment resistance. Novel and upcoming immunotherapies for MuSK-MG include molecules that target B cells, specific B cells that recognize the MuSK antigen, plasmablasts, cytokines involved in B cell maturation, and neonatal fragment-crystallizable antagonists Receptors (FcRn) involved in the synthesis and recycling of immunoglobulins. In this review, we wanted to have an overview of these innovative therapies. In light of this, we will initially emphasize on the cellular and humoral mechanisms involved in the pathophysiology of the disease, as accomplishing this will enable researchers to create new, highly targeted medications.

2 General clinical aspects of MuSK-MG

MuSK-MG is a rare subtype of MG that affects 5–8% of MG patients. It usually appears alongside more severe clinical signs and has an initial start with quick progression within weeks affecting predominantly bulbar muscles and causing symptoms of jaw muscle fatigue, difficulty swallowing or speaking as well as diplopia and ptosis (26). Best clinical practice guidelines suggest

that in suspicion of MG, we should test AChR antibodies first and if negative, then MuSK antibodies should be evaluated (4). Clinicians should have in mind that during the course of AchR-MG, reassessment of antibody status is advisable when there is an unexpected change of pattern of clinical involvement and alterations in therapeutic response as there are emerging cases with double positivity with MuSK at the beginning (rarer) and especially years after disease onset (27–32). Double positivity has also been observed in a drug-associated MG case under d-penicillamine treatment (33).

MuSK-MG is considered to emerge during the fourth decade of life in contrast to AChR-MG which exhibits a more bimodal appearance with many patients diagnosed before the fourth decade and many others after the sixth decade. MuSK-MG more frequently affects women, whereas AChR-MG affects young women but also older men (34, 35). The pattern of muscle involvement in MuSK-MG is more directed to the facial, bulbar, and respiratory muscles (36). Many MuSK-positive patients experience a head drop owing to neck extensor weakness, whereas AChR-MG individuals suffer neck flexor weakness. Limb weakness is usually milder and less frequent than in AChR-MG (26, 37). A characteristic of MuSK-MG is the variably observed tongue, masseter, buccinators, orbicularis oculi muscle atrophy, as well as the occasionally seen shoulder and girdle muscle atrophy (38). Significantly, early initiation of immunosuppressive treatment could restore atrophy in designated muscles (39, 40). A cardinal difference between AChR-MG and MuSK-MG is the rare participation of the thymus with either thymoma or hyperplasia, in the latter that points to the different key immunological mechanisms underlying each subgroup (41). An intriguing aspect of MuSK-MG is that the emergence of MuSK Abs along with disease clinical features can appear years after the AChR-MG onset and thymectomy (30, 42, 43). In these unusual yet existing cases, a possible explanation might be the immunological changes following thymectomy in AChR-MG. HLA alleles that are associated with the two subtypes of MG are distinct. MuSK-MG has been associated with the risk alleles belonging to HLA-DRB1, DQ1, and DQ5 locus (44–47).

Most AChR and low-density lipoprotein receptor-related protein 4 (LRP4) antibodies are of the IgG1 subtype, while MuSK antibodies are typically of the IgG4 subtype. One of their main differences is that IgG1 antibodies can activate the complement, while IgG4 affects the neuromuscular junction without complement activation or induction of antigen internalization, but involved pathogenetic mechanisms include direct inhibition of MuSK protein interaction with other proteins and particularly LRP4 (48, 49).

The levels of IgG4 MuSK antibodies, particularly targeting the Ig-like-1 domain, have been found to correlate with disease severity in MuSK-MG, something that is not evident in AChR-MG (49). Notably, titers of antigen-specific IgG4, which outnumbered IgG1, were substantially associated with indices of disease severity (50). Furthermore, it is important to emphasize that, while IgG4 is predominant at the time of diagnosis, considerable concentrations of IgG1-3 antibodies can be detected, and are less thoroughly studied (51). In recombinant human antibodies isolated from the peripheral blood of MuSK-MG, all subclasses IgG1, IgG2, and IgG4 antibodies were identified, and part of them have pathogenic potential in *in-vitro* models (52).

3 MuSK-MG - pathogenetic mechanisms

3.1 Specific role of the B-cell lineage (memory B cells, plasmablast, plasma cells)

Based on their function, B-cells and plasma cells are in the foreground of the mechanisms that orchestrate the pathophysiology of MG. New insights into their importance and their mechanistic role have emerged after MG-related immunotherapies have been developed targeting autoantibody production and silencing of other B-cell functions that seem to have equal pathophysiological importance. Specifically, regulatory B cells, also known as B10 cells because they are responsible for producing IL-10 and direct CD4 T cell differentiation and growth, appear to have an essential part in the advancement of AChR-MG and MuSK-MG. An impaired B10 population or function has been correlated with enhanced disease severity. A CD20-specific antibody treatment (rituximab; CD20 is only expressed in immature B-cells or during their differentiation and is not expressed in plasma cells) that depletes B-cells in autoimmune diseases, revealed that early recovery of the B10 population post-treatment is beneficial for patients with MG and leads to disease recession, indicating that B10-targeted treatments can possess clinical importance (53). CD27+ memory B-cells are also involved in MG, as this memory B-cell branch was suppressed in patients with AChR-MG after rituximab (RTX) treatment (54). Plasmablasts are also important for the progression of MG and represent an in-between differentiation step of B-cells (mature B-cells that have not completely become mature plasma cells). These ephemeral cells are responsible for producing high levels of autoantibodies (55, 56). The clinical importance of CD20-expressing cells, such as B-cells and plasmablasts, has been linked with drastically diminished MuSK antibody levels after B-cell depletion due to RTX treatment (52, 57). It has also been revealed that most patients with MuSK-MG who received B-cell depletion therapy (BCDT) achieved complete and stable remission, followed by subtle levels of plasma autoantibodies. In contrast, other reports have shown that patients with MG can relapse after several years (24–42 months depending on the study and the protocol used) or not respond to BCDT therapy (58, 59). In line with previous insights, in 2020, Jiang et al. revealed that a proportion of B-cell clones actually dodge and survive the BCDT, with most of them being recognized as CD20-low memory B-cells and antibody-secreting cells (ASCs). The plasmablast implication in MG progression was also confirmed by the fact that the levels of plasma MuSK autoantibodies were enhanced in patients who had relapsed. Following the previous findings, several studies have attempted to shed light on the exact population that produces the detrimental MuSK-specific antibodies. Surprisingly, B-cells and plasmablasts producing anti-MuSK autoantibodies represent almost a nugatory proportion of cells that produce these pathogenic autoantibodies. One study showed that a specific clone (2E6) of plasmablasts with CD20-low expression could be responsible for the plasma anti-MuSK

antibodies. Nevertheless, taking into account that plasma anti-MuSK antibodies are polyclonal, it is currently unclear if a single antibody clone is responsible for these plasma anti-MuSK antibodies (60).

According to another study, people with MuSK-MG who relapse had marginally higher levels of CD19+ CD27hi CD38hi plasmablasts. Furthermore, patients with MG who relapsed after BCDT possessed a large percentage (25%) of plasmablasts not expressing CD20 but had a high abundance of transmembrane activator calcium modulator (TACI) and B-cell maturation antigen (BCMA) receptors and low levels of the B-cell activating factor (BAFF) receptor. This outcome might be in line with the finding that high plasma BAFF levels (a cytokine that promotes B-cell survival and differentiation into ASC) were found in patients with AChR-MG and MuSK-MG without differences in BAFF receptor levels (61–63) (Table 1).

Collectively, it seems that MuSK-MG tolerance defects (both in peripheral and central checkpoints) lead to the generation of autoreactive B cells (81). Moreover, apart from these aberrations in the immature and new emigrant B cells (assessed by tolerance assays and self-reactivity of produced antibodies), short-lived CD20-expressing, MuSK-specific plasmablasts seem to account in part for the autoantibody production (82). Apart from plasmablasts, memory antigen-specific B cells (recognized as CD20low memory B cells) also produce autoantibodies and these clones persist or even reemerge in the post-rituximab period (60).

3.2 Autoantibodies in MuSK-MG – pathogenetic role

3.2.1 Emphasis on IgG4: its properties

The pathology of MuSK-MG is mainly mediated by IgG4-subclass antibodies that exert their pathogenetic action *via* the

TABLE 1 Cells of B cell lineage and antibodies in MuSK-Myasthenia Gravis.

		References
New immigrant and Naïve B cells	Autoreactvity due to defects in central and peripheral immune tolerance mechanisms	(64, 65)
Regulatory B cells/B10	Lower percentages in MuSK-MG	(53, 66)
	Correlate with disease severity	
	Early recovery after rituximab associated with clinical improvement	
Memory B cell	MuSK-specific memory B cells identified in MuSK- MG patients	(52)
Plasmablasts	Mildly elevated especially during disease exacerbation/relapse	(52, 56)
	Rare MuSK-specific plasmablasts	(52, 56, 57)
	Rituximab-induced incomplete depletion	(57, 67)
	MuSK-specific IgG4 plasmablasts persist in relapse after a BCDT-induced remission	(60)
	Express high levels of the receptors TACI and BCMA, low levels of BAFF-R	(60)
IgGs		
Patient serum IgG	IgG4 anti-MuSK abs: functionally monovalent due to Fab exchange, inhibit MuSK phosphorylation (*in vitro*)	(51, 68–70)
	IgG4 subclass mediates pathology by inhibiting the interaction between MuSK and LRP4 (*in vivo*)	(49, 71–74)
	IgG4 binds to the collagen tail subunit (ColQ) of acetylcholinesterase and blocks the binding of ColQ to MuSK	(48, 50)
	Unable to bind to C1q to activate the complement cascade	(69)
	Unable to bind to FcγR to activate immune cells	(69)
	Passive transfer of IgG4, but not IgG1-3, into mice induces experimental gravis	(73)
	IgG1-3 induce complement activation ad MuSK endocytosis	(75, 76)
Recombinant Abs from memory B or ASC cells	Belong to various subclasses, MuSK IgG1-3s exhibit pathogenesis *in-vitro*	(52, 73, 75–77)
	MuSK-specific rAbs recognized epitopes within the first Ig- like domain of MuSK	(78)
	Bispecific MuSK-rAbs stimulated MuSK phosphorylation *in vitro*, while still inhibiting AChR clustering	(77)
	Rabs with pathogenic capacity derived from clonal MuSK-specific B cell clones reemerged after BCDT-mediated remission, predating disease relapse	(60)
	Exceptionally high affinities through the process of affinity maturation	(79)
	Monovalency increases the pathogenic effect of MuSK antibodies	(77, 80)

ASC, antibody-secreting cells; Abs, antibodies; MuSK, muscle-specific kinase; BCMA, B-Cell Maturation Antigen; TACI, Transmembrane activator calcium modulator, and cyclophilin ligand interactor; BAFF-R, B-cell activating factor receptor; BCDT, B cell depletion therapy; Rabs, recombinant antibodies.

inhibition of interactions between MuSK and collagen Q or LRP4. This is achieved *via* binding to the first Ig-like domain of MuSK, leading to decreased levels of phosphorylated MuSK and subsequent reduction of both agrin-induced and agrin-independent AChR clustering and signaling (48–50). Specific high-affinity maturation processes should be performed for anti-MuSK IgG4 to reach its pathogenic potential. More specifically, MuSK recognition by the anti-MuSK antibodies allows their structural maturation and functional monovalency that stimulates their pathogenicity (79, 83). Two possible mechanisms that affect MuSK-mediated AChR clustering have been proposed; a. bivalent IgG cross-links and auto-phosphorylates MuSK rendering its activation, b. functionally monovalent IgG4 directly inhibits MuSK autophosphorylation (84). Additionally, *in vitro* experiments in C2C12 cells revealed that MuSK antibodies, Fab fragments, and IgG4, but not IgG1-3, promoted the frailty of the MuSK/LRP4 complex, reducing AChR clustering (51). Another likely explanation is that MuSK antibodies disrupt the LRP4-mediated retrograde cascade, justifying enhanced AChR dissemination and acetylcholine levels (85). This is also supported by *in vivo* experiments where MuSK-MG mice failed to exhibit presynaptic acetylcholine increase that is phenotypical in AChR-MG mice (86). The effect of enhanced pathogenicity of these autoantibodies can also be documented by the isolation of two novel MuSK monoclonal antibodies that are produced from plasmablasts detected in BCDT relapse and can bind to the Ig1-like domain of MuSK (79). The MuSK Ig-like 1 domain is known as the main immunogenic epitope when challenged with polyclonal IgG4 fractions and serum derived from MG patients (87). The Ig-like domain 2 of MuSK, which can be observed by different IgG4 and IgG3 antibodies also leads to AChR cluster inhibition, surprisingly coupled with augmented MuSK phosphorylation, signifying multiple compensatory pathways (52).

MuSK-specific autoantibodies dictate the pathogenic effect and can be valuable prognostic biomarkers to predict post-BCDT relapse, as they can be identified alongside MuSK-positive B-cells prior to relapse (88). Additionally, anti-MuSK autoantibodies can abrogate the formation of the complex between MuSK and the subunit (ColQ) of acetyl-cholinesterase on the presynaptic muscle membrane by binding to the latter (89). In addition, this complex formation interaction has been reported to reduce AChE at the synapse and promote ACh accumulation within the synapse (48). This biochemical cascade has been proposed to be responsible for the hypersensitivity that patients with MuSK-MG exhibit after treatment with AChE inhibitors (90). Several other reports have well described the ability of anti-MuSK antibodies to disrupt the NMJ (68, 71). This has been accompanied by the fact that functional and structural synapse homeostasis is being disrupted because of inactivated MuSK at the NMJ (72) (Table 1 and Figure 1).

3.2.2 Evidence of pathogenicity from animal models (immunization and passive transfer models) and recombinant Abs from patient memory B or plasma cells

The importance of anti-MuSK IgG4 antibody pathogenicity has been documented during experiments where MG was induced in mice who passively received IgG4 antibodies derived from patients with MG. The same study also implicated that the pathogenesis of MG is not mediated *via* complement-related mechanisms, as the IgG4 subclass cannot activate the complement per se (73). Two reports, where placental transfer of antibodies was able to induce transient MG in the neonate, also strengthen this hypothesis (91). Of note, interspecies mechanistic studies revealed that only the extracellular part of human MuSK protein can induce myasthenic phenotypes in both murine and rabbit NMJs, whereas murine MuSK phosphorylation is reduced when purified antibodies obtained from patients with MuSK-MG, were inoculated (49, 74, 92). More mechanistic studies on anti-MuSK IgG4 CH2-amino substitutions have revealed that these constructs failed to activate immune cells or the complement through FcγR or C1q, respectively (69). Furthermore, monoclonal MuSK antibodies derived from B-cells and plasma cells of patients with MG are able to increase MuSK phosphorylation and inhibit AChR clustering in C2C12 myotubes as expected (52, 77). Furthermore, monovalent Fab fragments produced from patient-derived bivalent monospecific MuSK antibodies can diminish MuSK phosphorylation and AChR clustering (93).

4 MuSK-MG as part of neurological autoimmune disorders with the characteristic presence of IgG4

MuSK-MG belongs to a wider family of neurological autoimmune disorders characterized by the presence of IgG4 autoantibodies directed against different antigenic targets, specific to each disease (IgG4-AID). It is important to discriminate these neurological autoimmune diseases from IgG4-related diseases (IgG4-RLD) that comprise multiorgan diseases hallmarked by tissue-destructive fibrotic lesions along with lymphocyte and IgG4 plasma cell infiltrates and elevated serum IgG4 concentrations (94) (Perugino CA, 2020). It is unknown if IgG4-AID and IgG4-RLD share pertinent clinical and immunopathological characteristics, but more recent data indicate that they are separate disease entities (95). Some typical examples of IgG4-AID, apart from MuSK-MG, include LGI1 (leucine-rich, glioma-inactivated-1) autoimmune encephalitis in which the autoimmune response is directed against a secreted protein that stabilizes the trans-synaptic complex (LGI1), Caspr2 (Contactin-associated protein-like 2) associated encephalitis and/or peripheral nerve hyperexcitability, nodal/paranodal chronic inflammatory demyelinating polyradiculoneuropathy with antibodies to neurofascin-155, contactin-1/caspr-1, and anti-IgLON5 (immunoglobulin-like cell adhesion molecule 5) disorder with antibodies against an adhesive protein (IgLON5) in the Central Nervous System (CNS). Specific autoantigen has not been described in IgG4-RLD. *Via* novel single-cell immunoglobulin sequencing techniques and subsequent cloning, galectin-3 was identified as an autoantigen in patients with IgG4-RLD. Anti-galectin-3 autoantibodies were found in 28% of a variety of patients with IgG4-RLD, albeit their pathogenetic function is uncertain (96).

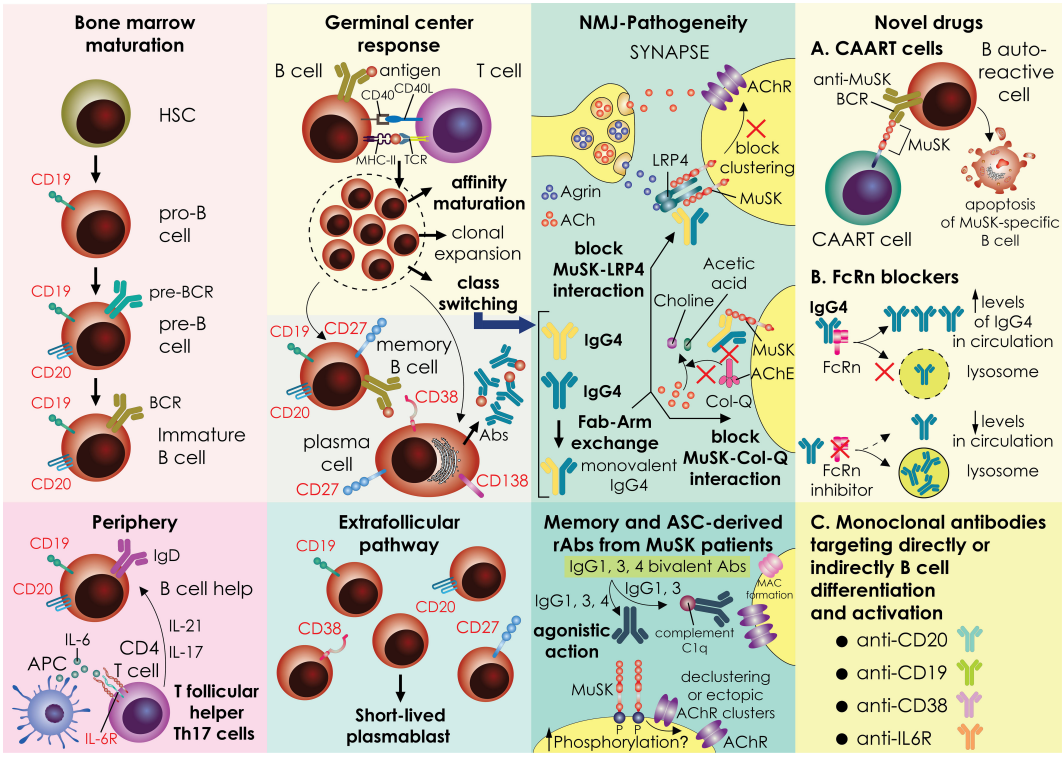

FIGURE 1
A graphical representation of a mechanistic theory for how MuSK autoantibodies are produced. The stages of B-cell development and differentiation are depicted in the image. In the bone marrow, the development process progresses through the pro-B-cell, pre-B-cell and immature-B-cell stages, and then gives rise to naïve B cells in the periphery. Naive B cells can take messages for cell proliferation and activation by CD4 T cells. specially in MuSK-MG patients, the expanded circulating T follicular CD4 T cells expressing IL-17 (Tfh17) secrete cytokines fostering B cell activation. B cells enter the germinal centers where are likely to encounter an antigen and receive support from T cells. Active germinal centers (GC) give rise to memory B cells and LLPCs, whereas the extrafollicular pathway of B cells activation ends up with the generation of SLPBs that enter the periphery (other pathways that also exist, but are not shown here, are less studied pathways). Important processes inside the germinal centers are B cell clonal expansion and affinity maturation. In MuSK-MG, a pool of memory B specific for MuSK, as well as SLPB have been recognized as projectors of cells secreting pathogenic IgG4 antibodies. In MuSK-MG, a specific cytokine milieu and other unknown factors foster IgG4 class-switching. An inherent property of IgG4 is the Fab-arm exchange that generates monovalent IgG4 antibodies that cause neuromuscular junction dysfunction by interfering with MuSK interaction with other proteins like LRP4 and ColQ. Recombinant antibodies produced by MuSK-MG patient memory or antibody-producing cells have exhibited also a pathogenicity profile with a different pattern of action (agonistic action, complement activation) from antibodies isolated from the serum of patients. A subset of recombinant antibodies produced in-vitro exhibit agonist action and enhance phosphorylation of MuSK. Nevertheless, some of them inhibit agrin-induced AchR clustering (agrin not shown). These effects need further in vivo studies for assessing antibody pathogenicity. Novel therapeutic strategies involve Chimeric autoantibody receptor (CAAR) T cells that are endogenous T cells from patients engineered in vitro to target B cells that produce autoantibodies against MuSK leading them to apoptotic cell death. MuSK-CAART is designed to specifically eliminate anti-MuSK B cell receptor (BCR) expressing B cells MuSK CAAR T cells efficiently kill various anti-MuSK BCR expressing cells but not control B cells. To achieve this, the CAAR comprises the native MuSK ectodomain tethered to tandem CD137-CD3ζ signaling domains. Another novel treatment approach currently in clinical trials for MuSK-MG is the targeting of the FcRn with inhibitors. FcRn functions as a protector of IgG from lysosomal degradation through the recycling and transcytosis of IgG within specific cells. Antagonism of this receptor promotes IgG degradation, leading to reduced overall IgG and pathogenic autoantibody levels. Finally, various monoclonals are being tested in clinical trials directly or indirectly targeting the activation and differentiation of B cells like anti-CD19, anti-CD38, and anti-IL6R. The surface expression of the proteins targeted by monoclonal is depicted in the picture. MG, MG; LLPCs; long-lived plasma cells; SLPBs, short-lived plasmablasts; ColQ, collagen-like tail subunit of Asymmetric Acetylcholinesterase; CAAR-T, Chimeric autoantibody receptor T cells; MuSK, muscle-specific kinase; BCR, B cell receptor; FcRn, neonatal Fc receptor; NMJ, neuromuscular-junction.

The exact cytokine milieu permitting class switch to IgG4 in MuSK-MG is still unknown. It is known that a TH2 milieu supported by IL-4 and IL-3 cytokines along with a synergistic action of IL-10 is a significant factor for the IgG4 class switch (97–99). Nevertheless, this simplified scenario has not been verified in MuSK-MG, as IL-10 production has been found to be diminished especially by stimulated B cells. Nevertheless, other cell sources of IL-10 have not been examined especially inside the germinal centers. Previous studies have shown that IL-10, IL-6, and TNF-alpha produced by B cells are down-regulated in MG, regardless of the kind of antibodies produced (100). Therefore, B cells' inefficient cytokine production solely cannot explain the propensity to IgG4 which is usually fueled by IL-10 and IL-6. A specific cytokine or cellular network (T helper cells, dendritic cells, etc.) in the germinal centers or in the extrafollicular compartment of MuSK-MG patients could be responsible for fostering IgG4 production. Indeed, in an animal model of MG after MuSK immunization, it was noticed the predominance of a Th2 milieu, that cannot be easily translated to human MuSK-MG (101). T-cells from MuSK-MG patients showed a higher Th1/17 versus Th2 response compared to healthy controls (102, 103). CD4+ T cells had higher IL-2, TNF-alpha, and IL-17. Patients with MuSK-MG exhibited a greater proportion of CD4+ T

cells that produced combinations of IFN-gamma/IL-2/TNF-gamma, TNF-alpha/IL-2, and IFN-gamma/TNF-alpha. Interestingly, Treg numbers and CD39 expression were not different from control values. Moreover, a higher Tfh/Tfr ratio was found in MuSK-MG patients along with increased frequencies of Th17-producing Tfh cells and higher Tfh-fostered IgG synthesis (104). Indeed, MuSK patients tend to have mildly elevated levels of immunoglobulin production (IgG) compared to controls (p=0,057), something however also observed in AChR-MG (105).

One theory is that the type of antigen (time of exposure) and the specific genetic pre-disposition as mainly determined by HLA alleles, could generate the appropriate environment -genetic conditions for predisposing to a "skewed" isotype profile towards IgG4 (69, 106). Indeed, patients with DQ5+ MuSK-MG appear to have a limited oligoclonal T-cell response that is specific for MuSK, showing a shared among patients repertoire that persists even under current immunosuppressive therapies (107). Future studies will delineate if specific T-cell receptor (TCR) rearrangement under exposure to a specific antigen (MuSK or another), favors specifically IgG4 B cell production.

It is not known in MuSK-MG when during disease evolution the class switch occurs. Moreover, it is not known exactly which is the precursor subclass from which the switch begins. In-depth sequencing analysis of different B cells and antibody screening could reveal similarities (shared lineages) and common progenitors, explaining the exact route followed for the final IgG4 class switch.

On the other hand, in some of the patients with IgG4-related autoimmune neurological disorders, the IgG4 possesses pathogenic potential especially in blocking protein-protein interactions, whereas in IgG4-RLD the role of the elevated IgG4 is unclear and no specific antigenic targets have been described so far. Usually IgG4-AID serum IgG4 levels are within the normal range (a small proportion of MuSK-MG patients have elevated IgG4 levels), and the suspected HLA risk loci are unique and not shared with IgG4-RLD. Common clinical characteristics among IgG4-AID and IgG4-RLD are the moderate response to corticosteroid treatment, whereas both diseases display exceptional response to B cell depletion, especially when other immunosuppressants have failed (108). Initial therapy with glucocorticoids, and subsequent additional immunosuppressive or a biologic agent, particularly RTX, is required in most patients. Variable decrease of antibody titers after RTX therapy has been observed in autoimmune neurological disorders with antibodies against LGI1, Contactin1, NF155 (neurofascin155), DPPX (dipeptidyl-peptidase-like protein-6), and Caspr2 (contactin-associated glycoprotein2) that share the common features of the presence of IgG4 antibodies (109–114). The presence of short (SLPB)- or long-lived plasma cells (LLPB) is not widely studied, as most studies are lacking due to the rarity of these diseases in the general population. The response to RTX is variable and in most of these disorders, a considerable number of patients exhibit a favorable response (like DPPX encephalitis, LGI1, caspr2 encephalitis), whereas in some the response is less profound (like in IgLON5) (115–117). Current evidence suggests that early and short-term RTX therapy could be an effective treatment option specifically for LGI1, and caspr2 encephalitis, albeit larger studies are needed to confirm this finding (64, 118, 119). RTX therapy resulted in a substantial decrease in autoantibody titer that was associated with clinical improvement in patients with Chronic inflammatory demyelinating polyneuropathy (CIDP) with primarily IgG4 autoantibodies against NF155, contactin-1, or Caspr1 (113).

Intravenous immunoglobin (IVIG) as a therapeutic option is not widely studied in these disorders. On the other hand, more evidence exists in IgG4-AID. For example, in patients with pemphigus, high doses of IVIG have been shown to be effective, and one mechanism was postulated to be the blockage of FcR by IVIGs and increased IgG degradation including IgG4 (120). IgG4 neurofascin antibody (NF-155)-mediated CIDP is less responsive to IVIG and predominantly responsive to anti-CD20 treatment (121). Nevertheless, in MuSK-MG, as analyzed below in detail, there is a variable response in IVIG with clinical efficacy observed in 11-60% of patients (20, 21, 122–127).

IgG4 antibodies, apart from their autoreactivity displayed in specific IgG4-AID are also part of an anti-inflammatory response related to Th2-driven IgE (allergic) responses. Indeed, a considerable number of patients belonging to the IgG4 RLD have increased IgE apart from IgG4. This is not the rule in most IgG4-AID, as only mild elevations have been observed. Chronic exposure to allergens leads to upregulation of IgG4, a clinical phenomenon seen in beekeepers (128). Antigen-specific IgG4 limits IgE-mediated allergy as IgG4 competes with IgE for the same antigen having at the same time weaker effector functions such as complement mobilization, antibody-dependent cellular cytotoxicity, and inability to crosslink the antigen or engage activating Fcγ receptors on immune cells. In the case of a passive transfer mouse model of AChR-MG, IgG4 antibodies against the AChR acted in a protected mode as counterbalanced the pathogenic effects of IgG1 antibodies against the AChR (129).

5 Diagnostic tools for MuSK Myasthenia Gravis (electrophysiological studies and antibody testing)

The aberrant neuromuscular transmission in MG can be confirmed using two electrophysiological procedures; first, a compound muscle action potential (CMAP) amplitude/area reduction of more than 10% on low-rate repeated nerve stimulation (RNS) and second an increased jitter on single-fiber electromyography (SF-EMG) (130). The sensitivity of the RNS for MG diagnosis is less in MuSK-MG compared to AChR-MG, and this is more relevant when testing distal limb muscles (only 12%–57% of MuSK patients exhibited decrement) (21). Thus, clinicians should be aware that RNS should be applied in more proximal muscles, facial muscles, and especially to the orbicularis oculi. RNS testing of this group of muscles could increase the diagnostic sensitivity (sensitivity of 75%–85% in MuSK). Similar to RNS in MuSK-MG, SFEMG when performed on more proximal muscles, including the deltoid, frontalis, orbicularis oculi, or cervical para-

spinals, is most often abnormal (reaching 100% sensitivity in facial muscles), in contrast to the regularly seen normal findings in peripheral muscles such as extensor digitorum communis (26, 130). In routine needle EMG in MuSK-MG more frequently may detect myopathic changes with scattered fibrillation potentials, whereas in AChR these features occurred after long-term treatment with corticosteroids (87, 131).

Regarding laboratory methods to detect MuSK antibodies the radioimmunoassay (RIA) which involves the immunoprecipitation of the extracellular domain of 125I-MuSK incubated with patient sera, represents the current gold standard for antibody identification in MG (132). RIA is positive for antibodies to muscle AChR in 80-85% of patients and for antibodies to MuSK in 5-7% of patients (38). To avoid radioactivity and increase sensitivity, cell-based assays (CBA) have been even more sensitive than RIA, as the antigen is expressed in a more native conformational form and more easily recognizable (133, 134). An international study examining sera from 633 SNMG (seronegative MG) patients from 13 European countries, revealed a prevalence of 13% for MuSK antibodies (5–22% depending on the country) although most of the antibodies detected were predominantly of the IgM type (135). A very recent study has shown that 8% (95% CI 2.9-16.6) of patients without MuSK (tested by RIA) or other antibodies have detectable binding to MuSK detected by CBA (performed in the human embryonic kidney, HEK293, cell line) (136). The live cell-based assay (CBA) can identify low-affinity antibodies against MuSK in a considerable subset of seronegative individuals with greater sensitivity and specificity than the RIA (133, 137). When compared to RIA, commercially available fixed CBA appears to have a stronger capacity to identify AChR and MuSK-Ab and may be beneficial as a serological test or a first diagnostic test in patients with double seronegative MG (137). Live CBA may be useful for serological evaluation of RIA and fixed CBA-negative samples (136). Although MuSK-ELISA (Enzyme-linked immunosorbent assay) is easier to be performed in a diagnostic lab, it has been shown that lacks sensitivity and specificity compared to RIA and CBA and therefore it is not highly recommended (69, 138).

6 Therapeutic options in MuSK Myasthenia Gravis

One of the challenges of MG is the development of effective, targeted therapies. In MuSK-MG, acetylcholinesterase inhibitors are less effective and induce frequent side effects. Therapies that target the complement are not suitable for IgG4 diseases since IgG4 antibodies do not activate the complement. That excludes eculizumab, ravulizumab, and zilucoplan from potential MuSK-MG treatments.

6.1 Acute treatment

Corticosteroids are the standard treatment for MG, and most patients usually respond within 2-3 weeks. MuSK-MG patients need higher doses to respond. However, about 15% of patients treated with high-dose corticosteroids respond poorly, a condition called refractory disease. This value is slightly higher than comparable data for AChR-MG (139).

Acetylcholinesterase inhibitors (AChEIs), which include pyridostigmine bromide are not well tolerated by MuSK-MG patients (causing increased side effects like fasciculations, and bronchial and oropharyngeal secretions), and in general show less effectiveness compared to AChR-MG. The intolerance of AChEIs has been shown in animal models of MuSK+experimental autoimmune MG (EAMG), in which administration of AChEIs led to denervation in the masseter muscle and neuromuscular hypersensitivity (spontaneous fibrillations) (140). Evidence from neurophysiological and histopathological findings in MuSK + EAMG mice, administration of AChEIs suggest that an excess of Ach in the synaptic cleft along with a reduction of postsynaptic AChRs due to fragmentation of AChRs and the observed down-regulation of AChE mainly affecting bulbar muscles would cause nicotinic adverse effects. Pyridostigmine clinical usage could be narrowed to a small group of patients with benign disease and without severe bulbar or respiratory symptoms (141, 142).

Plasmapheresis and IVIG are used to treat MuSK-MG with severe disease. A considerable variable response to IVIG has been observed in MuSK-MG (favorable response in 11%–61% of patients) that renders it not the preferable option in severe cases and in cases of myasthenic crisis (6, 7, 95–100). Plasmapheresis is a treatment that consists usually of 5 sessions over 1-2 weeks where the patients' plasma is removed and replaced with healthy plasma from a donor. It is mainly used as a rescue therapy in a myasthenic crisis. IVIG infusion and plasmapheresis are considered similarly effective and fast-acting treatments for active AChR-MG. Contrary to AChR-MG, IVIG appears to be less effective than plasmapheresis in MuSK-MG; this is mostly related to the characteristics of pathogenic IgG4 antibodies and the inherent characteristics of IVIG itself (143). Of note, the VNTR2/3 genotype is suggested as a genetic risk factor for determining endogenous IgG levels and stands for poor responses to IVIG in MG patients (144). Nevertheless, this polymorphism has not yet been tested in MuSK-MG in relation to the low response to IVIG.

6.2 Chronic treatment

Most non-steroidal immunosuppressive therapies (NSISTs) like azathioprine, cyclosporine, methotrexate, mycophenolate mofetil, and tacrolimus have been extensively studied in AChR-MG mostly as steroid-sparing agents during prednisone tapering. Regarding their use in MuSK-MG there is less evidence and in general are more often less effective (20, 37, 90, 122, 145). Evoli et al., 2008, examined 57 MuSK-positive patients and showed that approximately 70% of patients responded well to conventional therapy with prednisone alone or along with azathioprine or cyclosporine, but 30% of them were left with permanent muscle weakness. MuSK-MG patients exhibit a lower rate of disease remission upon immunosuppressive therapy and a higher proportion of treatment dependency compared to AChR-MG (90, 122, 146). Importantly, clinicians should pay vigilance and early

assess patients with MuSK-MG for poor response to initial immunotherapy, in which case they should without delay treat patients with anti-CD20, as recommended in the recently published international consensus guidelines.

6.3 Novel treatments

6.3.1 Monoclonal and other agents affecting B cells either directly or indirectly
6.3.2 Anti-CD20 agents

Rituximab is a genetically modified chimeric mouse/human IgG1-kappa monoclonal immunoglobulin. It targets CD20, a transmembrane phosphoprotein on the surface of B lymphocytes that is essential for B cell activation, differentiation, and expansion. RTX binds to CD20 and recruits immune effector cells that lead to B-cell lysis and therefore reduction of circulating CD20+ B-cells. Under normal conditions, CD20 is unique to B-cells in both humans and animals. It is first expressed by late pre-B cells in the bone marrow, mostly after Ig-heavy chain rearrangement, and its expression is reduced in plasmablasts and cells that have terminally differentiated (but not in early plasmablasts) (147).

In AChR-MG, long-lived plasma cells (not expressing CD20) are implicated in anti-AChR antibody production (148–150). Moreover, thymus-derived cells that produce pathogenic anti-AChR antibodies have been identified (151, 152); autoantibody-producing plasmablasts may possibly survive in the thymus by constitutive stimulation by autoreactive T cells. The response to RTX in AChR-MG appears to be significantly more delayed, and the autoantibody titer decline is less pronounced compared to MuSK-MG (57, 153, 154).

Most patients with MuSK-MG receiving RTX show sustained clinical improvement and a marked decline in MuSK autoantibody titer (Table 2). The quick and prolonged response to RTX suggests that MuSK Abs are mostly produced by short-lived Ab-secreting cells (52, 160). In contrast, bone marrow long-lived plasma cells are known to be scarcely affected by RTX (161). According to Marino et al. (2020), distinct patterns of decrease between MuSK-IgG4 and total IgG4 following RTX support the hypothesis that the majority of MuSK antibodies are produced by short-lived antibody-secreting cells (58). In particular, patients with refractory MuSK-MG that exhibited long-term remission upon RTX initiation displayed undetectable or low levels of MuSK IgG4 antibody titers, whereas total IgG and IgG4 levels transiently decreased at 2–7 months after RTX. A prior study found MuSK autoantibody-producing plasmablasts (CD27hiCD38hi B cells) upon disease recurrence in previously rituximab-induced remission patients (56). The markedly diminished MuSK autoantibody titer approximately 3 months after RTX-mediated B cell depletion suggests that RTX depletes MuSK-specific $CD20^+$ memory cells and, hence, indirectly reduces short-lived autoantibody-producing $CD20^-$ plasmablasts. The essential role of memory B cells in MuSK-MG is further illustrated by experiments in a mouse model of MuSK-MG, in which treatment with a low dose of teriflunomide showed to ameliorate muscle weakness, largely attributed to the suppression of memory B cells in the lymph nodes leaving unaffected the effector T cell populations (162). However, it could not be excluded the possibility that a fraction of plasmablasts could be $CD20^+$ (early plasmablast, $CD20^+CD27^{high}$) and thus directly depleted by RTX. This model, supported by consistent findings in other IgG4-mediated diseases (163, 164), proposes that the therapeutic effect of RTX would be mostly related to the depletion of plasmablast precursors (55, 56). The effect of RTX on T-cell responses may also be relevant, with an increase in regulatory T cells observed after RTX administration in refractory MuSK-positive patients but not in AChR-positive patients (129).

Litchmann et al. (2020) conducted a single-center, retrospective cohort study comparing responses to RTX between patients with AchR-MG (n = 17) and MuSK-MG (n = 16) (165). The response was evaluated using the Myasthenia Gravis Foundation of America (MGFA) classification which aims to divide patients into categories based on disease severity and symptom localization. This study found significant clinical responses in both study groups, with MuSK-MG showing a greater benefit. The proportion of patients who achieved MGFA post-intervention status of minimal manifestations or better 12 months after initiating RTX was 58.8% in AChR-MG (n = 17), compared to 68.8% in MuSK-MG. Both groups managed to lower the mean prednisone dose at 12 months at the final follow-up compared to baseline (i.e., before RTX), with MuSK-MG displaying the lowest mean levels of prednisolone. The mean number of disease exacerbations in AchR-MG (n = 17) was 1.7 (SD = 1.2) and in MuSK-MG (n = 16),1.4 (SD = 1.1).

Topakian et al. (2019) (166) evaluated the efficacy and safety of RTX in patients with refractory MG (N = 56, 39 patients were anti-AChR antibody positive, 14 patients were anti-MuSK antibody positive, and 3 patients were seronegative). The authors discovered that patients with MuSK antibodies had a higher rate of remission than those with AChR antibodies (71.4% vs. 35.9%, p = 0.022) and reported no major safety concerns about RTX. Another multicenter, blinded prospective review research investigated the effectiveness of RTX in 55 individuals with MuSK-MG, 24 of whom were treated with RTX and 31 of whom were not. Primary objectives were attained by 58% of MuSK-MG patients treated with RTX compared to 16% of the control group (those untreated with RTX). Furthermore, at the completion of the study, 29% of the RTX-treated patients were using steroids at an average dose of 4.5 mg/day, but 74% of the controls required larger doses (prednisone mean dose of 13 mg per day) and used more immunosuppressants (159).

Marino et al. (2020) (58) performed a single-center, cohort study that investigated the effect of rituximab treatment in patients (N = 9) with refractory MuSK-MG. This study found that RTX is safe and has a long-term benefit associated with a strong steroid- and immunosuppressant-sparing effect, with 66.9% of patients achieving an optimal response with MGFA post-intervention status of minimal manifestations or better along with a 50% reduction of steroid dose, withdrawal of immunosuppressants, and no need for plasma exchange or IV immunoglobulins. A significant reduction in MuSK-IgG4 antibody levels in RTX-treated patients that were in clinical remission with sustained improvement was observed (58). This is not observed with RTX treatment in AChR-MG (167, 168).

TABLE 2 Studies demonstrating the effectiveness of rituximab in MuSK and AChR MG.

Study	Type of study	N of patients (AChR, MuSK, seronegative)	Type of disease	Protocol	Follow-up duration	MGFA-PIS at the end of follow-up	AChR compared to MuSK	Abs and B/T cells after treatment	Adverse events
Stathopoulos et al., 2017 (56)	Prospective study	12 (8 AChR, 4 MuSK)	MGFA class I–IIIb	375 mg/m^2 weeks 1, 2, 3, and 4, repeat in 6 months (cycle). Repeat cycle in the case of relapse.	25–96 months	CSR, MM (3 relapsed)	In AChR MG the RTX response is more delayed and the ab titer decline is less pronounced than MuSK MG	Marked decrease of MuSK Abs titers post RTX	N/a
Zebardast et al., 2010 (155)	Retrospective study	6 (2 AChR, 4 MuSK)	Refractory MG	375 mg/m^2 weeks 1, 2, 3, 4, 5, and 6 (1 cycle); repeat after 1 year (weeks 1, 2, 3, 4, and 5)	13-27 months	CSR, PR, MM (0 relapsed)	Both groups reduced the need for multiple- and/or high-dose immunotherapy with dramatic clinical improvement	AChR patients had a decrease in Ab titers	None
Diaz-Manera et al., 2012 (57)	Prospective study	17 patients (6 MuSK and 11 AChR)	resistant to previous therapies and MGFA class III to V	375 mg/m^2 weeks 1, 2, 3, and 4, repeat every 2 months for 2 months, retreat if symptomatic	mean follow-up 31 months (4 – 60 months)	CSR, PR, MM (0 relapsed)	10 of the AChR patients improved but 6 of them needed reinfusions. In contrast, all MuSK patients achieved remission (4/6) or MM (2/6) status and no reinfusions were needed	Day 15 of first anti-CD20 infusion: B completely deleted, T cells unchanged Month 3: 20% decrease in IgM, no change in IgG MuSK-MG Ab titers decreased during follow-up, as early as 3 months after administration of the first dose	facial flushing and a generalized skin rush during the infusion in 2 patients
Guptill et al., 2011 (20)	Prospective multicenter review	110 MuSK (6 received RTX)	mostly MGFA III or higher	375 mg/m^2 weeks 1, 2, 3, and 4, then repeat every 1 month for 1–2 months. Repeat in the case of relapse	average 11 years for the Rome patients, and 5.3 years for the Duke patients (range 0.5–33 years)	MM, PR, I (All 6 patients who received RTX were able to taper or discontinue all oral IS medications)	Long-term outcomes in MuSK patients are generally favorable and comparable to those of patients with AChR MG	N/a	None
Nowak et al., 2011 (156)	Retrospective study	14 (6 AChR; 8 MuSK)	Refractory generalized MG	375 mg/m^2 weekly for 4 weeks, repeat after 6 months (2 or more cycles)	Not reported	MM or asymptomatic	Both groups respond similarly to RTX with a reduction of immunotherapy and clinical improvement	AChR Abs titers decreased a mean of 52.1% (p=0.0046) post-cycle 2.	pruritus, flushing, dyspnea, chills/rigors, leukopenia

(Continued)

10.3389/fimmu.2023.1212757

TABLE 2 Continued

Study	Type of study	N of patients (AChR, MuSK, seronegative)	Type of disease	Protocol	Follow-up duration	MGFA-PIS at the end of follow-up	AChR compared to MuSK	Abs and B/T cells after treatment	Adverse events
Keung et al., 2013 (67)	Retrospective study	9 MuSK refractory	refractory MuSK-MG	375 mg/m2 weeks 1, 2, 3, and 4 (cycle), repeat every 6 months, stop at 2–5 cycles	20–66 months with a mean of 41 months	CSR, MM (0 relapsed)	N/a	Post-treatment MuSK ab status was reported negative in two patients, borderline in two patients, positive in four patients, and not available in one patient	flushing, pruritus, chills, rigors
Choi et al., 2019 (157)	retrospective study	17 (9 AChR, 6 MuSK, 2 seronegative)	Refractory MG	375 mg/m^2 twice with a 2-week interval, followed by retreatment (375 mg/m^2 once)	median 24 months (range 7–49 months)	11 (65%) achieved the primary endpoint, defined as the MM or better status	RTX treatment tended to be more effective in patients with MuSK MG compared with AChR MG	substantial B-cell depletion in the peripheral blood from all patients tested	infusion reactions, chest discomfort, skin rash, herpes zoster, one patient died due to thymoma
Anderson et al., 2016 (158)	Prospective, open-label study	14 (5 AChR, 6 MuSK, 3 seronegative)	Refractory MG	375 mg/m^2 weeks 1,2,3,4 then once a month for 2 months or at a dose of 750 mg/m^2 every 2 weeks for 1 month	(22.6 ± 2.4 months)	MMT score was greatly reduced from a baseline of 13.1 ± 1.9 (range 5–27) to 3.5 ± 0.8 (range 0–5) at the end of the study ($P < 0.001$)	All patients markedly improved	T-cell counts were unchanged throughout the study. CD19/CD20 cell counts were typically depleted after the first infusion of RTX (range = 6–17 days)	Post-infusion headaches
Hehir et al., 2017 (159)	Prospective multicenter review	55 MuSK (24 RTX treated, 31 control)	MuSK MGFA 3,4 or 5 in 83,4% RTX-treated and 93,6% control group	375 mg/m^2 weekly x 4 doses. 13 were re-treated with the standard 375 mg/m^2 weekly x 4 doses. 2 patients were treated with 1,000 mg weekly x 2	RTX-treated: 45 months (6–64, 68, 69, 71–74, 77, 79, 81–124) Control: 54 months (6–64, 68, 69, 71–74, 77, 79, 81–154, 159–196)	MGFA-PIS MM or better in final visit: RTX 67% (16/24 patients), control 26% (8/31 patients)	N/a	4 weeks after RTX cycle: B cells reached nadir 24 and 31 weeks post-RTX infusion: begin to rise	one non-responder had a side effect
Topakian et al., 2019 (166)	Retrospective study	56 (39 AChR, 14 MuSK, 3 seronegative)	Generalized MG, 14% thymoma, Severe disease defined by an MGFA-Class of IIIb or higher was present in	Majority 2 × 375 mg/m^2 within 1–2 weeks	10-53 months (median 20)	10 Remission	Remission was more frequent in patients with MuSK vs. AchR (71.4% vs. 35.9%, $p = 0.022$)	65% slight decline of Abs levels (unrelated to outcome)	infusion reactions, respiratory tract infections, chronic pain syndromes, enteritis, herpes zoster, erysipelas, cholecystitis, unspecified mental disorder, alopecia areata

(Continued)

10.3389/fimmu.2023.1212757

TABLE 2 Continued

Study	Type of study	N of patients (AChR, MuSK, seronegative)	Type of disease	Protocol	Follow-up duration	MGFA-PIS at the end of follow-up	AChR compared to MuSK	Abs and B/T cells after treatment	Adverse events
			33 (58.9%) patients, Occular (13%)						
Dos Santos et al., 2020 (197)	Retrospective multicenter study	29 (20 AchR, 5 MuSK, 4 seronegative)	MGFA > II: Refractory or steroid dependent, generalized	Various protocols	Mean 20.06 (0.17–68.93) months	In all: R 42% MM 25% Total 86%	MuSK vs AChR 75% vs. 93% had 'improved' response or better (CSR, PR, or MM)	N/a	infections (21.4% of patients); infusion reaction (7%); bradycardia (3.7%); and cytopenia (7%)
Meng et al., 2022 (172)	Retrospective observational study	8 MuSK	MGFA II, III, or IV	Low sose protocol: 375mg/m^2×2 with 2 week-interval or 375 mg/m^2 as a single infusion (1-4 cycles)	8-29 months (median 25,5)	CSR had been achieved in one patient, PR in three patients, MM in three patients and I in one patient based on the MGFA-PIS criteria	1 Improvement, 3 PR, 3 MMS, 1 CSR (Steroid dose reduction 50-100%)	at 1 month: CD19+ B-cell depletion, CD19+CD27+ B cells < 0.05% at 3 months: CD19+ B-cell < 1%, CD19+CD27+ B cells; 0% at 6 months: CD19+ decreased to 0.300%, CD19+CD27+ B cells reappeared in 3 patients	1 patient reported minor post-infusion malaise.
Heckmann et al., 2022 (198)	Prospective study	17 (5 MuSK, 10 AChR, 2 seronegative	Refractory MG, MGFA II, III, IV, V. 65% MGFA class III or IV. 3 patients MGFA class I	Single infusion: 375 mg/m^2	Median 18 months (IQR 12; 27)	Thirteen individuals responded to a single RTX infusion including all five MuSK, 7 of 10 AChR, and one of two seronegative	Three (60%) MuSK-MG and three (30%) AchR-MG achieved asymptomatic status.	4,2 months after infusion: successful depletion of CD19+ cells in 15 from 17 patients (including 4 clinical non-responders)	No adverse effects
Zhou et al., 2021 (173)	prospective, open-label, self-controlled pilot study	12 MuSK	MGFA Class IIIb-Ivb	Single infusion: 600mg over 2 consecutive days, 100 mg on day 1 and 500 mg on day 2	6 months	6/12 asymptomatic	N/a	circulating CD19+ B cells, CD19+CD27− naïve, and CD19+CD27+ memory B cells declined by 92.0%, 90.8% and 93.9%, respectively CD3+ T, CD4+ T, CD8+ T, and natural killer cells; no difference before and after RTX CD19+ B cells, CD19+ CD27− naïve B cells, and CD19+ CD27+ B cells correlated positively with clinical scale scores The titers of MuSK abs mildly decreased	No serious side effects

(Continued)

10.3389/fimmu.2023.1212757

TABLE 2 Continued

Study	Type of study	N of patients (AChR, MuSK, seronegative)	Type of disease	Protocol	Follow-up duration	MGFA-PIS at the end of follow-up	AChR compared to MuSK	Abs and B/T cells after treatment	Adverse events
								after 6 mo. IgG1, IgG2, IgG3, and IgG4 levels were not significantly altered. Slight increase in three clinically improved patients.	
Marino et al., 2020 (58)	Retrospective study	9 MuSK refractory	Refractory, MGFA IIIb or V	375 mg/m^2 once a week for four consecutive weeks, plus a single dose of 375 mg/m^2 after 3 months.	17 months - 13 years	1 patient did not respond. Optimal response(MM, CSR, PR) to RTX was recorded in 6 of 9 patients (66.6%). Prednisone was tapered off in 2 patients and was reduced by 75% to 87.5% of the pretreatment dosage in the others	N/a	at 2–7 and at 12–30 months post-RTX: marked reduction of MuSK Abs at 2–7 months post-RTX: total IgG and IgG4 transiently decreased Non-responsive patients, MuSK-IgG and MuSK-IgG4 remained unchanged	No infusion reactions or long-term side effects
Litchman et al., 2020 (165)	Single-center retrospective study	33 (17 AChR, 16 MuSK)	Generalized MG median baseline MGFA Clinical Class was II	4 weekly infusions of 375 mg/m^2 (one cycle). The interval between cycles was 6 months. Majority received 2-4 cycles	mean follow-up of 1861 ± 953.4 days.	21 patients achieved clinical remission (12/17 AChR, 9/16 MuSK) improved from a median baseline class of II to asymptomatic	MM or better at last visit: AChR 11(65%), MuSK 12 (75%)	N/a	none reported
Caballero-Ávila et al., 2022 (199)	Retrospective, observational study	30 patients (18 AChR, 12 MuSK)	Refractory MG	375 mg/m^2 weekly for 4 weeks and then monthly for 2 months. Additional infusions in patients who relapsed	mean 85.5 (SD=48) months	18 patients achieved MM or remission	All 12 MuSK patients but only 6 (33%) AChR patients achieved MM or remission	24–48 months of follow-up: 37% of patients; hypogammaglobulinemia, 70%; mild and 30%; moderate. Median pre-treatment IgG levels: 10.7 and 9.1 g/L at 3–15 months after treatment initiation and 8.5 g/L at 24–48 months post-treatment.	Severe infections

(Continued)

10.3389/fimmu.2023.1212757

TABLE 2 Continued

Study	Type of study	N of patients (AChR, MuSK, seronegative)	Type of disease	Protocol	Follow-up duration	MGFA-PIS at the end of follow-up	AChR compared to MuSK	Abs and B/T cells after treatment	Adverse events
Castiglione et al., 2022 (200)	Retrospective study	16 patients with MG (8 AChR and 8 MuSK)	refractory generalized MG MGFA clinical class III or higher	(1) 3 weekly cycles [dose = 375 mg/m^2, (2) 2 cycles (dose = 375 mg/m^2) separated by a 2-week interval, and (3) 2 cycles (500 mg/m^2) separated by 2 weeks.	mean 39.1 ± 25.1 months	All 16 went into clinical remission, MGSTI level 2 or better (MM or PR either with low-dose dual therapy or high-dose monotherapy	Goal was reached significantly faster in the MuSK group although baseline MGFA was higher	6 and 12 months after induction: CD19+ and CD20+ B-cell counts remained undetectable 24 months after induction: 5 patients; undetectable counts, 6 patients; normal levels	No serious adverse effects were reported
Afanasiev et al., 2017 (201)	Retrospective, monocentric study	28 (21 AChR, 3 MuSK, 4 seronegatives)	Refractory MG	1000 mg on day 1 (D1) and D15, or 375 mg/m^2 on D1, D7, D15 and D21. The regime is followed by a maintenance treatment, 1000 mg or 375 mg/m^2 infusion, every 6 months	mean follow-up 27.2 months (range: 6–60 months).	At M12 (month 12), only 2 patients remained in class IV and 12 were in class II. At M36, among 12 patients, only one was in class IV	Among the 21 AChR+ patients, 12 were I, 8 were U and 1 patient was W according to the PIS. At M18, 2 AChR patients presented an exacerbation. All 3 MuSK patients did not respond to RTX (U PIS status). 3 seronegative were considered improved and 1 did not respond to RTX	N/a	11 patients (39%) had benign side effects: bronchitis, flu-like syndrome, immediate hot flashes, and paresthesia. 4 patients (14%) presented severe side effects: 1 transient aseptic neutropenia, 1 episode of paroxystic atrial fibrillation,1 infectious pneumonia, 1 histologically confirmed cerebral PML 5 years after the end of the study follow-up
Cortes-Vicente et al., 2018 (59)	retrospective, observational, multicenter study	25 MuSK	Patients with MGFA IV or V and no response to prednisone	1: 375 mg/m^2 for 4 weeks, then monthly for 2 months, 2: two 1g doses 2 weeks apart, 3: 375 mg/m^2 for 4 weeks	5.0 years (SD 3.3)	All patients achieved MM or a better MGFA PIS and a long-lasting response after an extended follow-up	N/a	N/a	No patient presented severe adverse events
Beecher et al., 2018 (202)	Prospective, open-label study	22 patients (10 AChR, 9 MuSK, 3 seronegative)	refractory MG	Various dosages as induction and maintenance doses if relapse occurred	mean follow-up of 28.8 ± 19.0 months (range, 6–66)	MMT scores demonstrated a reduction from a mean of 10.3 ± 5.6 to 3.3 ± 3.1 (P < 0.0001).	AChR patients showed mean MMT reduction from 10.3 ± 5.1 to 5.5 ± 2.6 (P = 0.018), whereas MuSK patients demonstrated	4 of 10 relapses were predicted by CD19/CD20 recovery 3 patients showed prolonged CD19+	No serious adverse events occurred

(Continued)

10.3389/fimmu.2023.1212757

TABLE 2 Continued

Study	Type of study	N of patients (AChR, MuSK, seronegative)	Type of disease	Protocol	Follow-up duration	MGFA-PIS at the end of follow-up	AChR compared to MuSK	Abs and B/T cells after treatment	Adverse events
							mean MMT reduction from 10.0 ± 3.6 to 1.1 ± 2.0 ($P < 0.0001$).	depletion (range, 24–45 months) after just 1 cycle	
Chan et al.f, 2019 (203)	Retrospective study	38 patients (AChR: 28, MuSK: 6, seronegative 4)	mostly refractory MG with MGFA class II, III, IV, V	cycles of 1000 mg, 500 mg, or 2000 mg	mean 55 months (range 1–131 months, median 49 months)	28 patients experienced clinical improvement (10 patients CSR, 7 patients MM, and 11 patients I). 5 patients were U or W. 5 patients were deceased.	N/a	N/a	5 patients died due to malignancy, infection, and asystole

Abs, antibodies; AChR+, acetyl choline receptor antibody positive; CSR, complete stable remission; I, improved; IQR, interquartile range; MGFA, MG Foundation of America clinical classification; MGSTI, Myasthenia gravis status and treatment intensity; MuSK, muscle specific kinase antibody positive; MM, minimal manifestations; MMT, Manual muscle testing; N/a, non-applicable; PIS, postintervention status classification; PR, pharmacologic remission; RTX, rituximab; SD, standard deviation; U, unchanged; W, worse; PML, Progressive multifocal leukoencephalopathy; SD, standard deviation; D, days; M, months.

Evidence from meta-analyses favors the use of RTX in all MG subtypes, particularly in MuSK-MG. A recent metanalysis including a total of 24 studies involving 417 patients (242 were AChR-IgG positive, 155 were MuSK-IgG positive, and 20 were defined as "double seronegative") showed that 64% (95% confidence interval, 49-77%) of patients under treatment with RTX achieved minimal manifestation status or improved quantitative MG (QMG) score. QMG score measures the severity of MG based on clinical findings and symptoms. The estimated reduction of the QMG score was 1.55 (95% confidence interval, 0.88-2.22). Approximately 81% of patients discontinued oral immunosuppressants and this was relatively independent of the dosing. Subgroup analyses showed that the group of patients with the greater benefit belonged to the MuSK-MG group. Pooled analysis showed that 10.7% of patients experienced infusion reactions, 5.8% developed infections, and 1.9% developed hematological disorders. Only one patient (0.2%) was histologically diagnosed with progressive multifocal leukoencephalopathy (PML) (169). Another systematic review evaluated the effectiveness and safety of RTX in 99 patients who had AChR positivity and 57 patients who had MuSK positivity. The results revealed that MuSK-positive patients responded better (72% attained mild manifestation status or remission) than AChR-positive patients (30%) (168).

The most generally used rituximab administration regimens include 2 doses of 1 g 2 weeks apart or 375 mg/m^2 infusions repeated weekly for 4 weeks. According to published data to date, there is no guideline for the proper timing for reinfusion and this is mainly based on clinical symptoms and less frequently on B cell repopulation kinetics. One study comparing various treatment protocols of RTX administration showed that patients treated with a sole induction regimen of RTX following the protocol 4 + 2 (375 mg/m^2 every week for 4 consecutive weeks and then monthly for the next 2 months) displayed a minimal rate of clinical relapse and long-lasting response. Authors suggested re-treating patients with RTX in cases of clinical relapse or remaining symptoms e.g. after 4 to 6 months in order to avoid adverse events (59). Other studies tried to identify risk factors for relapse and found that CD27 memory B cells rise during relapse and this knowledge could be used for determining anti-CD20 re-administration (170). Therefore, in patients at high risk of relapses, the RTX frequency can be narrowed by monitoring the re-emerging CD27+ memory B cells (mainly CD19+CD27+), in combination with clinical assessment. The cut-off value of 0.05% CD27+ memory B cells in peripheral blood was arbitrarily used according to the experience from another autoantibody-mediated disease especially neuromyelitis optica (NMO) (171). Re-emergence of CD27+ cells was noticed with a mean time of detection for memory B cells to be 7.5 months (3 – 12). We should have in mind that a small proportion of patients may have depleted memory B cells for longer time than 12 months. The need for multiple re-doses of rituximab in MuSK-MG was assessed by Hehir, et al., in a multicenter, blinded, prospective study that include 54 MuSK patients with a median follow-up duration of 3.5 years. Importantly, 73% of patients who received multiple courses of RTX achieved the primary outcome vs 33% who received a single course. So, this study was the first to demonstrate the need for

repeated doses for long-term remission (159). This is important as this implies that there is a heterogeneity in response to RTX implying district B cell pathologies in various patients.

Low-dose alternative regimens of 375 mg/m^2 given 2 weeks apart or 600 mg single-dose inductions have been tested with satisfactory results, but these studies did not include many patients, and no control arm with a high dose was included. Nevertheless, these approaches could be applied to high-risk patients for adverse effects from prolonged B cell depletion. In the study of Meng X., et al., 2022 8 MuSK-MG patients were included, and low-dose RTX (375 mg/m^2 for 1 or 2 infusions) was administrated and after a follow-up of 8 to 29 months found to be effective and safe. The authors noticed that three patients with CD19+CD27+ B-cell counts of >0.05%, but CD19+ B-cell counts <1% at 6 months, did not relapse. One patient relapsed among three patients whose CD27+ B-cell counts were >0.05% at 6 months. On the other hand, clinical relapses occurred even though B cells were depleted (172). Collectively, we could not reach a definite conclusion regarding the B lymphocytes number in patients and the recurrence of clinical symptoms. Another study assessing low-dose rituximab was performed by Zhou et al., 2021 (600 mg over 2 consecutive days, 100 mg on day 1 and 500 mg on day 2) (173). The titers of MuSK antibody decreased after 6 months, yet the levels of immunoglobulins, including IgG1, IgG2, IgG3, and IgG4, were not significantly altered by RTX. Interestingly, the MuSK antibody titer showed even a slight increase in three clinically improved patients. This was not in line with the previous reports possibly reflecting differences in dosage but also pointing out that in some patients other antibody-independent mechanisms of B cells could account for clinical remission (57, 58).

Rituximab should be used as soon as possible to treat MuSK+ individuals who do not react well to first immunosuppressive therapy, according to current consensus advice. In refractory AChR-MG patients, it is recommended only if other immunosuppressants resulted to be ineffective or scarcely tolerated since its efficacy is uncertain. In contrast to the common view formed by clinical practice, a phase 2 Trial of RTX in AChR - Generalized MG (The BeatMG Study), showed that RTX (every 6 months for 2 cycles) as an add-on treatment in mild to moderate AChR-MG failed to confer a significant steroid-sparing effect on chronic immunotherapy at 1 year. Additionally, no noticeable shifts in the severity of disease outcomes were found (174). However, the authors of the BeatMG study admitted that the relapse rate was reduced in the RTX group and that no conclusion can be drawn for more severe disease or MuSK-MG. According to retrospective cohort research that examined the role of RTX in patients with recently diagnosed generalized MG, RTX (usually 500 mg every six months) was associated with longer-lasting remissions than conventional immunotherapies. The RINOMAX randomized clinical trial evaluating the efficacy and safety of RTX as an adjunct to standard of care for MG patients with short onset (less than 12 months) and a Quantitative MG (QMG) score of 6 or greater recently announced that the proportion of patients with minimal disease manifestation who required only low doses of corticosteroids (a single 500 mg intravenous infusion) and did not require rescue therapy at 4 months was 71% on RTX versus 29% on placebo, showing a significant difference (175). So, the future guidelines for AChR-MG may be adapted according to new studies that have emerged. An unanswered question remains its role as an initial agent in AChR-MG, and the definition of preferred induction and maintenance doses. All studies with a considerable number of patients assessing the role of RTX in MuSK-MG, as well as the differential response among MuSK-MG and AChR-MG, are depicted in Table 2.

6.3.3 Anti-CD19

Monoclonal antibodies targeting CD19 (like inebilizumab, a humanized IgG1κis, glycoengineered, afucosylated antibody) that are expressed in pre-B and mature B cells are promising in autoantibody-mediated diseases. CD19 is also expressed in late-stage memory B cells and circulating plasma cells. An ongoing trial, NCT04524273, tested its efficacy in moderate to severe AchR-MG or MuSK-MG (Table 3). Inebilizumab (MEDI-551) has been approved in neuromyelitis optica spectrum disorder (NMOSD) an antibody-mediated demyelinating disease following a phase II/III placebo-controlled clinical trial (NCT02200770). Of note, anti-CD20 treatment exhibits good clinical efficacy in NMOSD, although the therapeutic benefit does not correlate with a decrease in NMO-IgG levels in the blood of all patients that are mainly of the IgG1 subtype (176). It is important to point out that in NMOSD SLPB has been reported to be augmented during relapses, as shown in MuSK-MG, but LLPB—not found so far in MuSK-MG—is thought to participate in NMOSD pathophysiology (177–179).

6.3.4 Anti-CD38

By directly targeting antibody-secreting phenotypes (plasma cells) with the anti-CD38 antibody daratumumab, novel treatment approaches aim to bypass the limitations of depletion of only CD20-expressing B cell subsets. Mezagitamab, a fully humanized anti-CD38 monoclonal (NCT04159805, ongoing), is currently being tested in MuSK-MG and the trial is ongoing.

6.3.5 Proteasomal inhibitors

Proteasomal inhibitors like Bortezomib. Only one case report exists with the response of a refractory MuSK-MG patient to bortezomib (180). Nevertheless, no clinical studies are ongoing and the trial in AChR-MG was terminated due to recruitment failure.

6.3.6 Others BAFFR, CD40, IL-6

Studies on belimumab (Benlysta, GSK), Iscalimab (anti-CD40) on MuSK-MG failed to show benefit in phase II trials, whereas studies on IL-6 pathway blockage are ongoing.

6.4 Monoclonal antibodies against FcRn receptors: rozanolixizumab, efgartigimod

FcRn inhibitors, which prevent FcRn from interacting with IgG, influence IgG breakdown and clearance and thus are used as treatments for IgG-mediated disorders (181). The principle of action of FcRn, the neonatal Fc receptor, is that it binds to the Fc region and rescues IgG from lysosomal acidic degradation, thus

TABLE 3 Novel treatment in MuSK-MG ongoing or with preliminary results.

Agents (general categories)	Targeted pathway	Product type	Study name	Reference (were available)	Number of participants with MG in general (MuSK positive were available)	Results	Study type	Study stauts	Adverse events
Abs blocking B cell lineages									
Inebilizumab anti-CD19 (MEDI-551)	pro-B cells, pre-B cells, and some plasmablasts and plasma cells.	a humanized, afucosylated IgG1κ monoclonal antibody	NCT04524273	N/A	82 MuSK-Ab+	pending	Phase III trial	ongoing	pending
Abs blocking plasma cells									
Mezagitamab anti-CD38 (Tak-079)	plasma cells, plasmablasts, and natural killer cells, some activated T and B cells, CD38 is an integral membrane glycoprotein, present in early B and T cell lineages and activated B and T cells but not in mature resting peripheral lymphocytes	humanized, IgG1	NCT04159805	N/A	36 total	pending	Phase II	Completed (no post of results)	pending
Tolebrutinib (SAR442168)	BTK inhibitor (Bruton's tyrosine kinase)	irreversible selective inhibitor of Bruton's tyrosine kinase (BTK)	NCT05132569	N/A		pending	Phase III	Recruiting	pending
Bortezomid	26S proteasome complex inhibitor	reversible inhibitor of the 26S proteasome complex in mammalian cells	N/A	Schneider-Gold C, et al., 2017 (180)	1 MuSK-Ab+	in combination with RTX, an effect strong enough to achieve long-term stabilization of MG	Case report	N/A	sensorimotor polyneuropathy
Indericter B cell targeting									
Satralizumab anti-IL-6	Block IL-6 promoting B cells activation and proliferation	humanized monoclonal antibody	NCT04963270	N/A	240 total	pending	Phase III	Recruiting	pending
Tocilizumab	Block IL-6 promoting B cells activation and proliferation	IgG1 humanized monoclonal antibody	NCT05067348	N/A	64 total	pending	Phase II	Recruiting	pending
Belimumab anti-BAFF	Block BAFF promoting B cells activation and proliferation	fully-humanized monoclonal antibody	NCT01480596	Karen Hewett, et al., 2018 (204)	40 total (2 MuSK-Ab+, placebo group)	completed	Phase II	completed	infections, gastrointestinal side effects nausea,

(Continued)

10.3389/fimmu.2023.1212757

TABLE 3 Continued

Agents (general categories)	Targeted pathway	Product type	Study name	Reference (were available)	Number of participants with MG in general (MuSK positive were available)	Results	Study type	Study stauts	Adverse events
									influenza, and post-infusion systemic reactions
Telitacicept (RC18)	Inhibition of BAFF and APRIL	fully human TACI-Fc fusion protein	NCT04302103	N/A	29 total	pending	Phase II	Active, not recruiting	pending
T cell activation targeting									
Iscalimab anti-CD40	Fc-silenced, IgG1 mAb that blocks the CD40 signaling pathway by binding with its ligand (CD154)	IGg1, fully-human, pathway-blocking, non-depleting ab	NCT02565576	N/A	44 total	unpublished results indicate that the outcome measure of significant improvement in MG scores was not reached, although there were no safety concerns	Phase II	completed	pending no safety concerns till now
FcRn blocking abs									
Efgartigimod	FcRn inhibitor	antibody fragment that binds to the neonatal Fc receptor (FcRn)	NCT03669588), NCT04735432	Howard et al., 2021 (184)	6 MuSK-Ab+ (3 on placebo)	All six patients were MG ADL responders in cycle 1. Approved in the US and Europe for the treatment of anti-AChR+ gMG (Vyvgart®).	Phase II, Phase III	completed	upper respiratory tract infections (>1/10) and urinary infections, bronchitis, myalgia, and procedural headache (≥1/100 to <1/10)
Efgartigimod PH20 SC	FcRn inhibitor	antibody fragment that binds to the neonatal Fc receptor (FcRn)	NCT04735432	N/A	111 total	pending	Phase III	Completed (pending results)	pending
Rozanolixizumab	FcRn blocker	a humanized high-affinity anti-human neonatal Fc receptor (FcRn) monoclonal antibody (IgG4)	NCT03052751, NCT03971422, NCT04124965, NCT04650854	Bril et al., 2021 (185), Bril et al,. 2023 (187)	From published studies: 43 (1 MuSK-Ab+), 200 (21 MuSK+), respectively.	Phase III: all five (100%) MuSK autoantibody-positive patients in the rozanolixizumab 7 mg/kg group and all seven (100%) patients in the rozanolixizumab 10 mg/kg group were MG-ADL responders, compared to one (14%) of seven in the placebo group	Phase II, III	completed phase III and ongoing phase III	headache, back pain, diarrhea, pyrexia

(Continued)

10.3389/fimmu.2023.1212757

TABLE 3 Continued

Agents (general categories)	Targeted pathway	Product type	Study name	Reference (were available)	Number of participants with MG in general (MuSK positive were available)	Results	Study type	Study stauts	Adverse events
Nipocalimab (or M281)	FcRn blocker	aglycosylated immunoglobulin (Ig)G1 monoclonal antibody (mAb)	NCT04951622	N/A	190 total	pending	Phase III	Recruiting	pending
Batoclimab	FcRn blocker	fully human anti-FcRn mAb blocking FcRn-IgG interactions	NCT05403541	N/A	210 total	pending	Phase III	Recruiting	pending
CAR T cells									
MuSK-CAART	targets MuSK expressing B cells	Autologous Muscle-specific Tyrosine Kinase Chimeric Autoantibody Receptor T Cells (MuSK-CAART)	NCT05451212	Oh S,et al., 2023 (205)	24 total	pending	Phase I	Ongoing	cytokine release syndrome
Descartes-08 CAR T-cells	targets B-Cell Maturation Antigen (BCMA)	Autologous T-Cells Expressing A Chimeric Antigen Receptor Directed to BCMA In patients With generalized MG	NCT04146051	N/A	30 total	pending	Phase Iib	Ongoing	pending
Haemapoietic stem cell therapy (HSCT)									
HSCT	Haemapoietic stem cell therapy	Infusing autologous stem cells to reconstitute a more tolerant immune system	N/A	Beland B, et al., 2023, (206) Burt R, et al., 2004 (207)	4 MuSK-Ab+	The average worst MG-ADL scores improved from 14.7 before to 0.3 after HSCT. The mean worst MG-QoL15 scores improved from 26.7 to 0.	Case series	completed	a tolerable side effect profile

ab, antibody; APRIL, a proliferation-inducing ligand; AChR+, acetylcholine receptor antibody positive; BAFF, B-cell activating factor, CAAR, chimeric autoantibody receptor; CAR, Chimeric antigen receptor; FcRn neonatal Fc receptor; HSCT, haematopoietic stem cell transplantation; IL-6, interleukin 6; MG, MG; MuSK+, muscle-specific kinase antibody positive; BTK, Bruton's tyrosine kinase; BCMA, B-Cell Maturation Antigen; TACI, Transmembrane activator calcium modulator and cyclophilin ligand interactor; MG-ADL. Myasthenia gravis Activities of Daily Living; MG-QoL15, Myasthenia Gravis Quality of Life 15-item Scale; BCMA, B-Cell Maturation Antigen; RTX, rituximab (207)

10.3389/fimmu.2023.1212757

promoting recycling. The mechanism of action is highly reminiscent of the action of IVIG as it is known that IVIG, apart from providing anti-idiotypic antibodies and thus protecting against the action of pathogenic ones, it saturates FcRn binding and directs the autoantibodies into the degradation pathway (143, 182). Likewise, FcRn inhibitors lower IgG levels, as seen with plasmapheresis.

Efgartigimod a human IgG1 antibody Fc fragment, is the first FcRn inhibitor approved for AChR-MG (183, 184).

The initial phase 2 trial of efgartigimod, which did not include MuSK-positive patients and recruited 24 AChR-MG (1:1 randomized to IV efgartigimod or placebo), showed a rapid onset and strong clinical improvement assessed by efficacy scales [patient reported MG-ADL and physician-reported (QMG) scales]. The drug was well tolerated, with the most common adverse events being headache and mild hematological changes in the monocyte number. Importantly, clinical improvement lasted at least 6 weeks in a high proportion of patients, reminiscent of the effectiveness of Plex, which peaked at around 6 weeks. A rapid and large decrease in total IgG and IgG subtype levels was observed in all 12 efgartigimod-treated patients, peaking 1 week after the fourth infusion (approximately 70%).

A phase 3 study of the efficacy and safety of efgartigimod (ARGX-113) generalized MG included 129 (77%) AChR-positive and 38 (23%) AChR-negative patients, six of whom (4%) were MuSK antibody positive. Efgartigimod (10 mg/kg) was compared to a matched placebo and initially administered as four infusions per cycle (one infusion per week), with the option to repeat the same cycle based on the observed clinical response. All six enrolled patients were responders as assessed by the MG Activities of Daily Living (MG-ADL) scale in Cycle 1. Extension of this ongoing open-label extension study will provide more conclusive results. In general, treatment with efgartigimod was well tolerated and effective in all patients with generalized MG. Over 50% of patients responded well from Cycle 1 within 2 weeks of treatment (2-point MG-ADL improvement sustained for 4 weeks). As expected, efgartigimod resulted in a similar reduction in acetylcholine receptor autoantibodies as IgG (without effect on other immunoglobulins), and most importantly this was accompanied by concomitant improvements in symptoms. This mode of action resembles that of plasma exchange, a treatment that removes autoantibodies and is considered highly efficacious in MuSK-MG, rendering FcR blockers a highly promising treatment modality for MuSK-MG (184). Vyvgart™ received the first U.S. Food and Drug approval for AChR-MG in 2021.

Forty-three patients with gMG enrolled in a phase 2 randomized controlled trial to evaluate the efficacy and tolerability of subcutaneous (sc) rozanolixizumab (7 mg/kg), another humanized monoclonal antibody to neonatal Fc receptors. Subcutaneous administration proved to be safer compared to iv. This study included only one MuSK-positive patient, so it is underpowered due to the low number of patients. The primary endpoint (change in Quantitative MG (QMG) score from baseline to Day 29) showed no significant improvement, but when all predefined efficacy parameters (QMG, MG-ADL, and MGC) are taken into account, the data suggest that rozanolixizumab may offer clinical benefit to patients with moderate to severe gMG. There was a higher frequency of headaches (57.1%) compared to placebo (13.6%) (185). Again, this treatment led to a reduction in IgG concentration in one week that returned to baseline by 2 months, as shown in the phase I study of the drug (186).

The Phase III clinical study NCT0397142, a randomized, double-blind, placebo-controlled study evaluating the efficacy and safety of rozanolixizumab in adult patients with generalized MG, has been completed and enrolled patients with confirmed positive records of AChR or MuSK at screening (200 total MG participants). In the primary endpoint, rozanolixizumab significantly reduced MG-ADL from baseline to Day 43 (185). Very recently the results from a randomized, double-blind, placebo-controlled, adaptive phase 3 study, named MycarinG were published. 200 patients were enrolled, among which 21 MuSK-positive were included. Patients were stratified into the placebo group (12% MuSK+), 8% received rozanolizizumab 7 mg/kg and 12% received rozanolixizumab 10 mg/kg (subcutaneous infusions). With the available data, all five (100%) MuSK autoantibody-positive patients in the rozanolizizumab 7 mg/kg group and all seven (100%) patients in the rozanolizizumab 10 mg/kg group were MG-ADL responders compared with one (14%) in seven in the placebo group. More specifically, participants who received a placebo reported a decrease in MG-ADL of 2.28 points, while those who received rozanolixizumab reported increases of 7.28 points at a dose of 7 mg/kg and 4.16 points at a dose of 10 mg/kg. As early as day 8, rozanolixizumab caused a rapid decrease in IgG levels that was associated with improvements in efficacy results. Headache, diarrhea, fever, and nausea were the most commonly reported treatment-associated adverse events (187).

All these encouraging results have led to a priority review of the FDA's Biologic License Application (BLA) and advance efforts to approve rozanolizizumab for the treatment of adults with generalized MG (gMG) who are AChR or MuSK antibody positive. All ongoing studies on the use of FcRn inhibitors in MuSK-MG are summarized in Table 3.

6.5 Chimeric autoantibody receptor T cells

The novel technology of chimeric auto-antibody receptor T (CAAR-T) cells involves genetically engineered endogenous T cells and subsequent expansion. The patient is then given autologous T cells, which detect antigen-specific B cells that are carrying the BCR against the MuSK antigens and cause pathogenic B cells to undergo apoptosis.

Phase I and II studies employing CD8-positive CAR T immunotherapy against plasma cells that express BCMA are currently being conducted.

Another ongoing clinical study is investigating the different dosing regimens of MuSK-CAART alone, in combination with cyclophosphamide (CY), and in combination with CY and fludarabine (FLU) under number NCT05451212 and is still recruiting patients. Recent findings showed that in an EAMG animal model, MuSK-CAART lowered anti-MuSK IgG without affecting B-cell or total IgG levels, indicating MuSK-specific B-cell

depletion (161). MuSK-CAART is considered a cellular precision immunotherapy in the field of autoantibody-mediated neurological autoimmune diseases (Table 3).

7 Pregnancy in MuSK Myasthenia Gravis

Evidence for the emergence of MuSK-MG during pregnancy is sparse and most information comes from case reports. Severe MG exacerbations have been reported during pregnancy, especially in newly diagnosed patients and not being stable under treatment (188, 189). In general, short disease duration and severe disease have been recognized as risk factors for MG worsening during pregnancy, whereas previous thymectomy is protective (190, 191). One Portuguese study looked back at the pregnancy history of 17 MuSK-positive women, 13 of whom had more than one pregnancy (27 total pregnancies studied) (192). Upon the time of conception, all were on steroids, with one on azathioprine and another on IVIg maintenance infusions. Only mild pregnancy-related changes were noted, some requiring dosage adjustments. No changes were counted as recurrences.

Pregnancy studies using mycophenolate mofetil, methotrexate, and cyclosphasmamide in animals or humans have revealed fetal malformations. As a result, the possible benefit to pregnancy is exceeded by the danger (193). Regarding azathioprine, the benefit may outweigh the risk and could be used with close monitoring of the fetus. Corticosteroids are recommended to be used at the lowest possible dose during pregnancy (194). Existing data on pregnancy outcomes following RTX can frequently be affected by the use of possibly teratogenic medications and other underlying medical problems (195). According to the prescribing information, women of childbearing potential and non-sterile men should be encouraged to use effective contraception for 12 months after the last dose of RTX.

Plasmapheresis might be used to treat severe disease exacerbations during pregnancy. Plasmapheresis is considered to create fluid changes that might cause hypotension and potentially jeopardize the pregnancy; hence the mother and fetus must be closely monitored. In cases refractory to steroids and when plasmapheresis is unavailable, IVIG can be used during pregnancy; with this approach, MuSK patients have shown a favorable response and, based on current evidence, mothers can continue breastfeeding. A large Italian study examined the consequences of 936 plasmapheresis procedures performed during 57 pregnancies; treatment rationale varied and among others included some for MG etiologies. Just 2% had serious adverse effects, and none required hospitalization or continued hospitalization (196).

8 Final considerations

Even though great progress has been made in the field of MuSK immunopathology, unanswered questions still exist. Are IgG4 B cells effective in producing LLPCs? The inadequate response to rituximab in specific cases could suggest that some LLPCs most probably do exist in MuSK-MG patients. Whether the dominance of IgG4 antibodies targeting MuSK is caused by a genetic predisposition to generate ubiquitously IgG4 responses is unknown. We currently do not know when during the clinical course of the disease there is an active MuSK-IgG subclass switch, especially towards IgG4, and whether there is a longitudinal germinal center activity. A MuSK-MG patient was described to undergo a class switch from IgG4 antibodies to IgG1 MuSK antibodies whilst entering stable remission and we currently don't know what drives this conversion, a knowledge that could open new therapeutic strategies (50). Future studies are needed to assess the role of post-translational modifications such as galactosylation on the pathogenic profile of IgG4 antibodies (activate complement, Fab arm exchange capacity).

The pathogenetic role of antibodies against MuSK has been demonstrated in a passive transfer animal model with immunoglobulins isolated from the serum of MG patients or with recombinant antibodies isolated from B or plasma cells isolated from the periphery of MG patients. *In vitro* studies of IgG pathogenicity have also been performed but animal models provide a more complex picture of the role of these antibodies *in vivo*. Recent studies revealed that the functional monovalency of IgG4 MuSK MG antibodies is crucial for inducing myasthenia (77). In-vitro-produced recombinant antibodies (all subclasses) usually possess bivalent forms (monospecific and have not undergone Fab-arm exchange) and act as partial MuSK agonists, as they induce MuSK kinase activity through phosphorylation, dimerize MuSK, promote AChR clustering and, variable responses in mice causing no or a mild myasthenic phenotype (less pathogenic profile) (80). When compared to the natural agonist agrin, the agonistic bivalent patient-derived MuSK monoclonal antibodies did not induce AChR clustering in the C2C12 myotube assay to the extent as agrin (52, 77). Mice exposed to bivalent 13–3B5 monoclonal antibody exhibited a mild clinical phenotype, with substantial loss of AChR in the NMJs and subclinical myasthenia. The 13–3B5 also induced smaller clusters compared with 11–3F6, another bivalent antibody (80).

One study produced recombinant antibodies that bound the Ig-like 2 of MuSK and promoted MuSK activation and interestingly displayed an inhibitory effect on MuSK signaling (52). This alternative mechanism for inhibiting AChR clustering with recombinant bivalent antibodies needs further studies and animal models could further elucidate the ensuing pathogenetic mechanisms (129). On the other hand, bispecific, functionally monovalent IgG4 anti-MuSK antibodies diminished MuSK signaling and subsequent AchR clustering. These antibodies are mainly found in their native conformation in patient peripheral blood, whereas recombinant produced monovalent IgG4 are produced *in vitro* with either controlled Fab-arm exchange (cFAE) methodology or by papain digestion (production of Fabs —simulating Fab-arm exchanged IgG4), something that makes it difficult to assess the circulating pathogenic autoantibodies in the serum of MG patients (77, 80). *In vitro*, these Fab fragments inhibited agrin-dependent MuSK phosphorylation and AChR clustering similar to patient serum-derived MuSK IgG4 (80).

Patient MuSK IgG1–3 antibodies (not recombinant antibodies) do not affect MuSK-Lrp4 interaction, but reduce agrin-induced

AchR clustering in cultured myotubes (51). Collectively, MG exacerbation and clinical severity will rely on combined action of antagonistic and agonistic effects, that are determined to a significant proportion by antibody monovalency. We cannot rule out that complement activation could occur and lead to pathogenicity but this seems less likely and needs further studies with IgG1-3 bivalent monoclonal antibodies.

Interestingly, outside MG pathology, the promotion of MuSK activation constitutes a promising therapeutic strategy for other diseases such as amyotrophic lateral sclerosis (ALS) (208). A recent study developed different agonist antibodies binding the MuSK Ig-like 1 domain that even though *in vitro* experimental settings exhibited a beneficial effect associated with MuSK activation, in mice models this effect was not found (sudden death due to urologic syndrome) (209). Of interest, forced activation of MuSK signaling holds therapeutic promise in neuromuscular disorders characterized by NMJ deficits. So, in MuSK MG some bivalent antibodies that stimulate MuSK signaling may have a protective role towards others with pathogenic profiles and the balance among them may determine the clinical severity and exacerbation.

It seems that antibodies with different effector mechanisms may coexist and agonistic or blocking functions apart from valency and antigen binding avidity could be also controlled by the IgG subclasses, the corresponding Fc-FcγR interactions, and the ability for complement activation. Of note, an IgG4 monoclonal antibody targeting acetylcholine receptor (AChR) diminished subsequent complement-mediated tissue damage induced by IgG1 directed to AChR in a passive transfer model of MG (129). Nevertheless, this is not the case for all diseases with implicated IgG4 antibodies. A recent study showed that while IgG switching to IgG4 subclass is a protective mechanism in IgG4-mediated autoimmune diseases with anti-ADAMTS13 autoantibodies (TTP; thrombotic thrombocytopenic purpura), this is not relevant for Pemphigus foliaceus (PF) in which anti-Dsg1 (desmoglein-1) IgG4 subclass exacerbates the pathogenicity in anti-Dsg1 autoantibodies (210). These differences were attributed to the magnitude of IgG subclass and Fc-FcγR interaction, leading to different functions regarding the clearance of autoantibody-Ag complexes.

Most evidence exists to support the presence of specific memory and short-lived plasma cells (SLPB) as the main producers of MuSK IgG. B- cell or plasma cell infiltrates were not infiltrating the neuromuscular junctions of intercostal muscles in MuSK-MG patients and germinal center-like structures are not found in the thymus of MuSK patients (41, 89, 211, 212). Nevertheless, there are still some patients refractory to anti-CD20 treatment. On the other hand, little evidence exists for drugs targeting LLPCs such as bortezomib, which was found effective in difficult-to-treat MuSK-MG patients, not responding to RTX. Knowledge of anti-CD19 treatment efficacy, which has been approved for NMOSD, is still lacking for MuSK-MG, and ongoing trials are assessing this promising treatment option. Another difficult question not entirely answered is the proper time for re-treating MuSK patients with anti-CD20 therapies for long-term remission and after how many re-doses a patient is considered refractory. Assessing the reemergence of CD19+ or CD27+ cells has been proposed as a peripheral biomarker for helping clinicians to proper disease control minimizing the cumulative dose of RTX. For all above, further studies are needed before reaching definite conclusions.

It seems that, in contrast to autoimmune disorders caused by IgG1 or 3 antibodies, neurological IgG4-antibody-mediated diseases share a particular/common disease mechanism. Rituximab, a monoclonal antibody that targets CD20 with the exception of stem cells, pro-B cells, and plasma cells, has been demonstrated to exhibit favorable effects on the treatment of LGI1 limbic encephalitis, MuSK-MG, CIDP, and pemphigus. Novel treatment strategies are being developed and bring hope, especially for patients refractory to anti-CD20 agents. The current knowledge of MuSK-MG pathophysiology with the expanding role of specific B cells in the pathogenetic process opened the way for more targeted approaches (anti-CD19, CD38). Ongoing clinical trials are currently recruiting patients and assessing the efficacy of BTK inhibitors (tolebrutinib) and humanized mAb targeting both cells- surface-bound and soluble IL6 receptor agents (satralizumab, tocilizumab). Novel agents may in the future lower the need for plasmapheresis in difficult-to-treat patients and subcutaneous injections of FcrN blockers could bring a revolution in daily clinical practice. IgG, for a number of additional neurological conditions, such as autoimmune encephalopathies, NMOSD, and inflammatory neuropathies, FcRn-targeted treatments are now being investigated in clinical studies. One limitation of the blockage of FcRn receptors is the non-specific elimination of pathogenic.

An innovative method that has been tried on animal models of EAMG utilizes an absorber column to selectively remove antigen-specific antibodies and then depleted blood is reinfused (213, 214). Significant portions of the autoantibodies are being removed, resulting in significant symptom relief. In the decade that precision medicine is the optimal goal in treatment options, the specific targeting of pathogenic cells expressing the autoantigen and leaving alive all other B cells could become a revolutionary treatment choice, and we are not far away from this.

Author contributions

AV and EK: first drafting and editing. AV: image making. JT: concept, design, drafting, and editing. All authors contributed to the article and approved the submitted version.

Acknowledgments

The authors would like to thank Meletios Verras for their professional assistance in the graphical presentation of Figure 1.

Conflict of interest

The authors declare that the research was conducted in the absence of any commercial or financial relationships that could be construed as a potential conflict of interest.

Publisher's note

References

1. Drachman DB. Myasthenia Gravis. *Semin Neurol* (2016) 36(5):419–24. doi: 10.1055/s-0036-1586265

2. Lefvert AK, Cuénoud S, Fulpius BW. Binding properties and subclass distribution of anti-acetylcholine receptor antibodies in myasthenia gravis. *J Neuroimmunol* (1981) 1(1):125–35. doi: 10.1016/0165-5728(81)90015-1

3. Rødgaard A, Nielsen FC, Djurup R, Somnier F, Gammeltoft S. Acetylcholine receptor antibody in myasthenia gravis: predominance of IgG subclasses 1 and 3. *Clin Exp Immunol* (1987) 67(1):82–8.

4. Evoli A, Iorio R, Bartoccioni E. Overcoming challenges in the diagnosis and treatment of myasthenia gravis. *Expert Rev Clin Immunol* (2016) 12(2):157–68. doi: 10.1586/1744666X.2016.1110487

5. Hehir MK, Silvestri NJ. Generalized Myasthenia Gravis: Classification, Clinical Presentation, Natural History, and Epidemiology. *Neurol Clin* (2018) 36(2):253–60. doi: 10.1016/j.ncl.2018.01.002

6. DeChiara TM, Bowen DC, Valenzuela DM, Simmons MV, Poueymirou WT, Thomas S, et al. The receptor tyrosine kinase MuSK is required for neuromuscular junction formation in vivo. *Cell* (1996) 85(4):501–12. doi: 10.1016/S0092-8674(00)81251-9

7. Li L, Xiong WC, Mei L. Neuromuscular Junction Formation, Aging, and Disorders. *Annu Rev Physiol* (2018) 80:159–88. doi: 10.1146/annurev-physiol-022516-034255

8. Lemmon MA, Schlessinger J. Cell signaling by receptor tyrosine kinases. *Cell* (2010) 141(7):1117–34. doi: 10.1016/j.cell.2010.06.011

9. Miyoshi S, Tezuka T, Arimura S, Tomono T, Okada T, Yamanashi Y. DOK7 gene therapy enhances motor activity and life span in ALS model mice. *EMBO Mol Med* (2017) 9(7):880–9. doi: 10.15252/emmm.201607298

10. Bergamin E, Hallock PT, Burden SJ, Hubbard SR. The cytoplasmic adaptor protein Dok7 activates the receptor tyrosine kinase MuSK *via* dimerization. *Mol Cell* (2010) 39(1):100–9. doi: 10.1016/j.molcel.2010.06.007

11. Herbst R, Burden SJ. The juxtamembrane region of MuSK has a critical role in agrin-mediated signaling. *EMBO J* (2000) 19(1):67–77. doi: 10.1093/emboj/19.1.67

12. Okada K, Inoue A, Okada M, Murata Y, Kakuta S, Jigami T, et al. The muscle protein Dok-7 is essential for neuromuscular synaptogenesis. *Sci (New York NY)* (2006) 312(5781):1802–5. doi: 10.1126/science.1127142

13. Hallock PT, Chin S, Blais S, Neubert TA, Glass DJ. Sorbs1 and -2 Interact with CrkL and Are Required for Acetylcholine Receptor Cluster Formation. *Mol Cell Biol* (2016) 36(2):262–70. doi: 10.1128/MCB.00775-15

14. Burden SJ, Yumoto N, Zhang W. The role of MuSK in synapse formation and neuromuscular disease. *Cold Spring Harbor Perspect Biol* (2013) 5(5):a009167. doi: 10.1101/cshperspect.a009167

15. Weston C, Gordon C, Teressa G, Hod E, Ren XD, Prives J. Cooperative regulation by Rac and Rho of agrin-induced acetylcholine receptor clustering in muscle cells. *J Biol Chem* (2003) 278(8):6450–5. doi: 10.1074/jbc.M210249200

16. Luo ZG, Wang Q, Zhou JZ, Wang J, Luo Z, Liu M, et al. Regulation of AChR clustering by Dishevelled interacting with MuSK and PAK1. *Neuron* (2002) 35(3):489–505. doi: 10.1016/S0896-6273(02)00783-3

17. Komiya Y, Habas R. Wnt signal transduction pathways. *Organogenesis* (2008) 4 (2):68–75. doi: 10.4161/org.4.2.5851

18. Chen A, Bai L, Zhong K, Shu X, Wang A, Xiao Y, et al. APC2(CDH1) negatively regulates agrin signaling by promoting the ubiquitination and proteolytic degradation of DOK7. *FASEB J* (2020) 34(9):12009–23. doi: 10.1096/fj.202000485R

19. Jones G, Moore C, Hashemolhosseini S, Brenner HR. Constitutively active MuSK is clustered in the absence of agrin and induces ectopic postsynaptic-like membranes in skeletal muscle fibers. *J Neurosci Off J Soc Neurosci* (1999) 19 (9):3376–83. doi: 10.1523/JNEUROSCI.19-09-03376.1999

20. Guptill JT, Sanders DB, Evoli A. Anti-MuSK antibody myasthenia gravis: clinical findings and response to treatment in two large cohorts. *Muscle Nerve* (2011) 44(1):36–40. doi: 10.1002/mus.22006

21. Oh SJ. Muscle-specific receptor tyrosine kinase antibody positive myasthenia gravis current status. *J Clin Neurol* (2009) 5(2):53–64. doi: 10.3988/jcn.2009.5.2.53

22. Veltsista D, Kefalopoulou Z, Tzartos J, Chroni E. Autoantibody profile in myasthenia gravis patients with a refractory phase. *Muscle Nerve* (2022) 65(5):607–11. doi: 10.1002/mus.27521

23. Zouvelou V, Papathanasiou A, Koros C, Rentzos M, Zambelis T, Stamboulis E. Pure ocular anti-musk myasthenia under no immunosuppressive treatment. *Muscle Nerve* (2013) 48(3):464. doi: 10.1002/mus.23847

24. Hosaka A, Takuma H, Ohta K, Tamaoka A. An ocular form of myasthenia gravis with a high titer of anti-MuSK antibodies during a long-term follow-up. *Intern Med* (2012) 51(21):3077–9. doi: 10.2169/internalmedicine.51.8196

25. Rodolico C, Bonanno C, Toscano A, Vita G. MuSK-Associated Myasthenia Gravis: Clinical Features and Management. *Front Neurol* (2020) 11:660. doi: 10.3389/fneur.2020.00660

26. Evoli A, Tonali PA, Padua L, Monaco ML, Scuderi F, Batocchi AP, et al. Clinical correlates with anti-MuSK antibodies in generalized seronegative myasthenia gravis. *Brain* (2003) 126(Pt 10):2304–11. doi: 10.1093/brain/awg223

27. Zouvelou V. Double Seropositive Myasthenia Gravis: A 5-Year Follow-Up. *Muscle Nerve* (2018) 57(5):E129. doi: 10.1002/mus.26040

28. Zouvelou V, Psimenou E. AChR-and MuSK-positive myasthenia gravis: Double trouble. *J Neuroimmunol* (2020) 348:577364. doi: 10.1016/j.jneuroim.2020.577364

29. Zouvelou V, Kyriazi S, Rentzos M, Belimezi M, Micheli MA, Tzartos SJ, et al. Double-seropositive myasthenia gravis. *Muscle Nerve* (2013) 47(3):465–6. doi: 10.1002/mus.23645

30. Zouvelou V, Zisimopoulou P, Psimenou E, Matsigkou E, Stamboulis E, Tzartos SJ. AChR-myasthenia gravis switching to double-seropositive several years after the onset. *J Neuroimmunol* (2014) 267(1-2):111–2. doi: 10.1016/j.jneuroim.2013.12.012

31. Jordan B, Schilling S, Zierz S. Switch to double positive late onset MuSK myasthenia gravis following thymomectomy in paraneoplastic AChR antibody positive myasthenia gravis. *J Neurol* (2016) 263(1):174–6. doi: 10.1007/s00415-015-7982-2

32. Meriggioli MN, Sanders DB. Muscle autoantibodies in myasthenia gravis: beyond diagnosis? *Expert Rev Clin Immunol* (2012) 8(5):427–38. doi: 10.1586/eci.12.34

33. Poulas K, Koutsouraki E, Kordas G, Kokla A, Tzartos SJ. Anti-MuSK- and anti-AChR-positive myasthenia gravis induced by d-penicillamine. *J Neuroimmunol* (2012) 250(1-2):94–8. doi: 10.1016/j.jneuroim.2012.05.011

34. Sanders DB, El-Salem K, Massey JM, McConville J, Vincent A. Clinical aspects of MuSK antibody positive seronegative MG. *Neurology* (2003) 60(12):1978–80. doi: 10.1212/01.WNL.0000065882.63904.53

35. Tsiamalos P, Kordas G, Kokla A, Poulas K, Tzartos SJ. Epidemiological and immunological profile of muscle-specific kinase myasthenia gravis in Greece. *Eur J Neurol* (2009) 16(8):925–30. doi: 10.1111/j.1468-1331.2009.02624.x

36. Lavrnic D, Losen M, Vujic A, De Baets M, Hajdukovic LJ, Stojanovic V, et al. The features of myasthenia gravis with autoantibodies to MuSK. *J Neurol Neurosurg Psychiatry* (2005) 76(8):1099–102. doi: 10.1136/jnnp.2004.052415

37. Sanders DB, Juel VC. MuSK-antibody positive myasthenia gravis: questions from the clinic. *J Neuroimmunol* (2008) 201-202:85–9. doi: 10.1016/j.jneuroim.2008.05.032

38. Vincent A, Newsom-Davis J. Acetylcholine receptor antibody as a diagnostic test for myasthenia gravis: results in 153 validated cases and 2967 diagnostic assays. *J Neurol Neurosurg Psychiatry* (1985) 48(12):1246–52. doi: 10.1136/jnnp.48.12.1246

39. Kitamura E, Takiyama Y, Nakamura M, Iizuka T, Nishiyama K. Reversible tongue muscle atrophy accelerated by early initiation of immunotherapy in anti-MuSK myasthenia gravis: A case report. *J Neurol Sci* (2016) 360:10–2. doi: 10.1016/j.jns.2015.11.032

40. Takahashi H, Kawaguchi N, Ito S, Nemoto Y, Hattori T, Kuwabara S. Is tongue atrophy reversible in anti-MuSK myasthenia gravis? Six-year observation. *J Neurol Neurosurg Psychiatry* (2010) 81(6):701–2. doi: 10.1136/jnnp.2009.171793

41. Lauriola L, Ranelletti F, Maggiano N, Guerriero M, Punzi C, Marsili F, et al. Thymus changes in anti-MuSK-positive and -negative myasthenia gravis. *Neurology* (2005) 64(3):536–8. doi: 10.1212/01.WNL.0000150587.71497.B6

42. Suhail H, Vivekanandhan S, Singh S, Behari M. Coexistent of muscle specific tyrosine kinase and acetylcholine receptor antibodies in a myasthenia gravis patient. *Neurol India* (2010) 58(4):668–9. doi: 10.4103/0028-3886.68687

43. Rajakulendran S, Viegas S, Spillane J, Howard RS. Clinically biphasic myasthenia gravis with both AChR and MuSK antibodies. *J Neurol* (2012) 259 (12):2736–9. doi: 10.1007/s00415-012-6661-9

44. Bartoccioni E, Scuderi F, Augugliaro A, Chiatamone Ranieri S, Sauchelli D, Alboino P, et al. HLA class II allele analysis in MuSK-positive myasthenia gravis suggests a role for DQ5. *Neurology* (2009) 72(2):195–7. doi: 10.1212/01.wnl.0000339103.08830.86

45. Niks EH, Kuks JB, Roep BO, Haasnoot GW, Verduijn W, Ballieux BE, et al. Strong association of MuSK antibody-positive myasthenia gravis and HLA-DR14-DQ5. *Neurology* (2006) 66(11):1772–4. doi: 10.1212/01.wnl.0000218159.79769.5c

46. Huijbers MG, Lipka AF, Plomp JJ, Niks EH, van der Maarel SM, Verschuuren JJ. Pathogenic immune mechanisms at the neuromuscular synapse: the role of specific antibody-binding epitopes in myasthenia gravis. *J Intern Med* (2014) 275(1):12–26. doi: 10.1111/joim.12163

47. Koneczny I, Yilmaz V, Lazaridis K, Tzartos J, Lenz TL, Tzartos S, et al. Common Denominators in the Immunobiology of IgG4 Autoimmune Diseases: What Do Glomerulonephritis, Pemphigus Vulgaris, Myasthenia Gravis, Thrombotic Thrombocytopenic Purpura and Autoimmune Encephalitis Have in Common? *Front Immunol* (2020) 11:605214. doi: 10.3389/fimmu.2020.605214

48. Kawakami Y, Ito M, Hirayama M, Sahashi K, Ohkawara B, Masuda A, et al. Anti-MuSK autoantibodies block binding of collagen Q to MuSK. *Neurology* (2011) 77 (20):1819–26. doi: 10.1212/WNL.0b013e318237f660

49. Huijbers MG, Zhang W, Klooster R, Niks EH, Friese MB, Straasheijm KR, et al. MuSK IgG4 autoantibodies cause myasthenia gravis by inhibiting binding between MuSK and Lrp4. *Proc Natl Acad Sci USA* (2013) 110(51):20783–8. doi: 10.1073/pnas.1313944110

50. Niks EH, van Leeuwen Y, Leite MI, Dekker FW, Wintzen AR, Wirtz PW, et al. Clinical fluctuations in MuSK myasthenia gravis are related to antigen-specific IgG4 instead of IgG1. *J Neuroimmunol* (2008) 195(1-2):151–6. doi: 10.1016/j.jneuroim.2008.01.013

51. Koneczny I, Cossins J, Waters P, Beeson D, Vincent A. MuSK myasthenia gravis IgG4 disrupts the interaction of LRP4 with MuSK but both IgG4 and IgG1-3 can disperse preformed agrin-independent AChR clusters. *PloS One* (2013) 8(11):e80695. doi: 10.1371/journal.pone.0080695

52. Takata K, Stathopoulos P, Cao M, Mané-Damas M, Fichtner ML, Benotti ES, et al. Characterization of pathogenic monoclonal autoantibodies derived from muscle-specific kinase myasthenia gravis patients. *JCI Insight* (2019) 4(12):e127167. doi: 10.1172/jci.insight.127167

53. Yi JS, Russo MA, Massey JM, Juel V, Hobson-Webb LD, Gable K, et al. B10 Cell Frequencies and Suppressive Capacity in Myasthenia Gravis Are Associated with Disease Severity. *Front Neurol* (2017) 8:34. doi: 10.3389/fneur.2017.00034

54. Muto K, Matsui N, Unai Y, Sakai W, Haji S, Udaka K, et al. Memory B cell resurgence requires repeated rituximab in myasthenia gravis. *Neuromuscul Disord* (2017) 27(10):918–22. doi: 10.1016/j.nmd.2017.06.012

55. Stathopoulos P, Kumar A, Heiden JAV, Pascual-Goñi E, Nowak RJ, O'Connor KC. Mechanisms underlying B cell immune dysregulation and autoantibody production in MuSK myasthenia gravis. *Ann N Y Acad Sci* (2018) 1412(1):154–65. doi: 10.1111/nyas.13535

56. Stathopoulos P, Kumar A, Nowak RJ, O'Connor KC. Autoantibody-producing plasmablasts after B cell depletion identified in muscle-specific kinase myasthenia gravis. *JCI Insight* (2017) 2(17):e94263. doi: 10.1172/jci.insight.94263

57. Díaz-Manera J, Martínez-Hernández E, Querol L, Klooster R, Rojas-García R, Suárez-Calvet X, et al. Long-lasting treatment effect of rituximab in MuSK myasthenia. *Neurology* (2012) 78(3):189–93. doi: 10.1212/WNL.0b013e3182407982

58. Marino M, Basile U, Spagni G, Napodano C, Iorio R, Gulli F, et al. Long-Lasting Rituximab-Induced Reduction of Specific-But Not Total-IgG4 in MuSK-Positive Myasthenia Gravis. *Front Immunol* (2020) 11:613. doi: 10.3389/fimmu.2020.00613

59. Cortés-Vicente E, Rojas-Garcia R, Díaz-Manera J, Querol L, Casasnovas C, Guerrero-Sola A, et al. The impact of rituximab infusion protocol on the long-term outcome in anti-MuSK myasthenia gravis. *Ann Clin Transl Neurol* (2018) 5(6):710–6. doi: 10.1002/acn3.564

60. Fichtner ML, Hoehn KB, Ford EE, Mane-Damas M, Oh S, Waters P, et al. Reemergence of pathogenic, autoantibody-producing B cell clones in myasthenia gravis following B cell depletion therapy. *Acta neuropathologica Commun* (2022) 10(1):154. doi: 10.1186/s40478-022-01454-0

61. Kang S-Y, Kang C-H, Lee K-H. B-cell–activating factor is elevated in serum of patients with myasthenia gravis. *Muscle Nerve* (2016) 54(6):1030–3. doi: 10.1002/mus.25162

62. Scuderi F, Alboini PE, Bartoccioni E, Evoli A. BAFF serum levels in myasthenia gravis: effects of therapy. *J Neurol* (2011) 258(12):2284–5. doi: 10.1007/s00415-011-6092-z

63. Guptill JT, Yi JS, Sanders DB, Guidon AC, Juel VC, Massey JM, et al. Characterization of B cells in muscle-specific kinase antibody myasthenia gravis. *Neurol Neuroimmunol Neuroinflamm* (2015) 2(2):e77. doi: 10.1212/NXI.0000000000000077

64. Lee WJ, Lee ST, Byun JI, Sunwoo JS, Kim TJ, Lim JA, et al. Rituximab treatment for autoimmune limbic encephalitis in an institutional cohort. *Neurology* (2016) 86 (18):1683–91. doi: 10.1212/WNL.0000000000002635

65. Cotzomi E, Stathopoulos P, Lee CS, Ritchie AM, Soltys JN, Delmotte FR, et al. Early B cell tolerance defects in neuromyelitis optica favour anti-AQP4 autoantibody production. *Brain* (2019) 142(6):1598–615. doi: 10.1093/brain/awz106

66. Sun F, Ladha SS, Yang L, Liu Q, Shi SX, Su N, et al. Interleukin-10 producing-B cells and their association with responsiveness to rituximab in myasthenia gravis. *Muscle Nerve* (2014) 49(4):487–94. doi: 10.1002/mus.23951

67. Keung B, Robeson KR, DiCapua DB, Rosen JB, O'Connor KC, Goldstein JM, et al. Long-term benefit of rituximab in MuSK autoantibody myasthenia gravis patients. *J Neurol Neurosurg Psychiatry* (2013) 84(12):1407–9. doi: 10.1136/jnnp-2012-303664

68. Farrugia ME, Bonifati DM, Clover L, Cossins J, Beeson D, Vincent A. 2007 Effect of sera from AChR-antibody negative myasthenia gravis patients on AChR and MuSK in cell cultures. *J Neuroimmunol* (2007) 185(1-2):136–44. doi: 10.1016/j.jneuroim.2007.01.010

69. Koneczny I, Stevens JA, De Rosa A, Huda S, Huijbers MG, Saxena A, et al. IgG4 autoantibodies against muscle-specific kinase undergo Fab-arm exchange in myasthenia gravis patients. *J Autoimmun* (2017) 77:104–15. doi: 10.1016/j.jaut.2016.11.005

70. Hoch W, McConville J, Helms S, Newsom-Davis J, Melms A, Vincent A. Auto-antibodies to the receptor tyrosine kinase MuSK in patients with myasthenia gravis without acetylcholine receptor antibodies. *Nat Med* (2001) 7(3):365–8. doi: 10.1038/85520

71. Cole RN, Reddel SW, Gervásio OL, Phillips WD. Anti-MuSK patient antibodies disrupt the mouse neuromuscular junction. *Ann Neurology* (2008) 63(6):782–9. doi: 10.1002/ana.21371

72. Viegas S, Jacobson L, Waters P, Cossins J, Jacob S, Leite MI, et al. Passive and active immunization models of MuSK-Ab positive myasthenia: electrophysiological evidence for pre and postsynaptic defects. *Exp Neurol* (2012) 234(2):506–12. doi: 10.1016/j.expneurol.2012.01.025

73. Klooster R, Plomp JJ, Huijbers MG, Niks EH, Straasheijm KR, Detmers FJ, et al. Muscle-specific kinase myasthenia gravis IgG4 autoantibodies cause severe neuromuscular junction dysfunction in mice. *Brain* (2012) 135(Pt 4):1081–101. doi: 10.1093/brain/aws025

74. Jha S, Xu K, Maruta T, Oshima M, Mosier DR, Atassi MZ, et al. Myasthenia gravis induced in mice by immunization with the recombinant extracellular domain of rat muscle-specific kinase (MuSK). *J Neuroimmunol* (2006) 175(1-2):107–17. doi: 10.1016/j.jneuroim.2006.03.016

75. Tüzün E, Yılmaz V, Parman Y, Oflazer P, Deymeer F, Saruhan-Direskeneli G. Increased complement consumption in MuSK-antibody-positive myasthenia gravis patients. *Med Princ Pract* (2011) 20(6):581–3. doi: 10.1159/000330031

76. Cole RN, Ghazanfari N, Ngo ST, Gervásio OL, Reddel SW, Phillips WD. Patient autoantibodies deplete postsynaptic muscle-specific kinase leading to disassembly of the ACh receptor scaffold and myasthenia gravis in mice. *J Physiol* (2010) 588(Pt 17):3217–29. doi: 10.1113/jphysiol.2010.190298

77. Huijbers MG, Vergoossen DL, Fillié-Grijpma YE, van Es IE, Koning MT, Slot LM, et al. MuSK myasthenia gravis monoclonal antibodies: Valency dictates pathogenicity. *Neurology(R) neuroimmunology neuroinflammation* (2019) 6(3):e547. doi: 10.1212/NXI.0000000000000547

78. Jiang R, Fichtner ML, Hoehn KB, Pham MC, Stathopoulos P, Nowak RJ, et al. Single-cell repertoire tracing identifies rituximab-resistant B cells during myasthenia gravis relapses. *JCI Insight* (2020) 5(14):e136471. doi: 10.1172/jci.insight.136471

79. Fichtner ML, Vieni C, Redler RL, Kolich L, Jiang R, Takata K, et al. Affinity maturation is required for pathogenic monovalent IgG4 autoantibody development in myasthenia gravis. *J Exp Med* (2020) 217(12):e20200513. doi: 10.1084/jem.20200513

80. Vergoossen DLE, Plomp JJ, Gstöttner C, Fillié-Grijpma YE, Augustinus R, Verpalen R, et al. Functional monovalency amplifies the pathogenicity of anti-MuSK IgG4 in myasthenia gravis. *Proc Natl Acad Sci United States America* (2021) 118(13):e2020635118. doi: 10.1073/pnas.2020635118

81. Lee JY, Stathopoulos P, Gupta S, Bannock JM, Barohn RJ, Cotzomi E, et al. Compromised fidelity of B-cell tolerance checkpoints in AChR and MuSK myasthenia gravis. *Ann Clin Trans neurology* (2016) 3(6):443–54. doi: 10.1002/acn3.311

82. Fichtner ML, Jiang R, Bourke A, Nowak RJ, O'Connor KC. Autoimmune Pathology in Myasthenia Gravis Disease Subtypes Is Governed by Divergent Mechanisms of Immunopathology. *Front Immunol* (2020) 11:776. doi: 10.3389/fimmu.2020.00776

83. Koneczny I, Herbst R. Myasthenia Gravis: Pathogenic Effects of Autoantibodies on Neuromuscular Architecture. *Cells* (2019) 8(7):671. doi: 10.3390/cells8070671

84. Mori S, Yamada S, Kubo S, Chen J, Matsuda S, Shudou M, et al. Divalent and monovalent autoantibodies cause dysfunction of MuSK by distinct mechanisms in a rabbit model of myasthenia gravis. *J Neuroimmunol* (2012) 244(1-2):1–7. doi: 10.1016/j.jneuroim.2011.12.005

85. Patel V, Oh A, Voit A, Sultatos LG, Babu GJ, Wilson BA, et al. Altered active zones, vesicle pools, nerve terminal conductivity, and morphology during experimental MuSK myasthenia gravis. *PloS One* (2014) 9(12):e110571. doi: 10.1371/journal.pone.0110571

86. Mori S, Kubo S, Akiyoshi T, Yamada S, Miyazaki T, Hotta H, et al. Antibodies against muscle-specific kinase impair both presynaptic and postsynaptic functions in a murine model of myasthenia gravis. *Am J Pathol* (2012) 180(2):798–810. doi: 10.1016/j.ajpath.2011.10.031

87. Huijbers MG, Vink AF, Niks EH, Westhuis RH, van Zwet EW, de Meel RH, et al. Longitudinal epitope mapping in MuSK myasthenia gravis: implications for disease severity. *J Neuroimmunol* (2016) 291:82–8. doi: 10.1016/j.jneuroim.2015.12.016

88. Triplett JD, Hardy TA, Riminton DS, Chu SYK, Reddel SW. Association between musk antibody concentrations and the myasthenia gravis composite score in 3 patients: A marker of relapse? *Muscle Nerve* (2019) 60(3):307–11. doi: 10.1002/mus.26609

89. Niks EH, Kuks JB, Wokke JH, Veldman H, Bakker E, Verschuuren JJ, et al. Pre- and postsynaptic neuromuscular junction abnormalities in musk myasthenia. *Muscle Nerve* (2010) 42(2):283–8. doi: 10.1002/mus.21642

90. Evoli A, Bianchi MR, Riso R, Minicuci GM, Batocchi AP, Servidei S, et al. Response to therapy in myasthenia gravis with anti-MuSK antibodies. *Ann N Y Acad Sci* (2008) 1132:76–83. doi: 10.1196/annals.1405.012

91. Murray EL, Kedar S, Vedanarayanan VV. Transmission of maternal muscle-specific tyrosine kinase (MuSK) to offspring: report of two cases. *J Clin Neuromuscul Dis* (2010) 12(2):76–9. doi: 10.1097/CND.0b013e3181f8a9aa

92. Shigemoto K, Kubo S, Maruyama N, Hato N, Yamada H, Jie C, et al. Induction of myasthenia by immunization against muscle-specific kinase. *J Clin Invest* (2006) 116 (4):1016–24. doi: 10.1172/JCI21545

93. Huijbers MG, Marx A, Plomp JJ, Le Panse R, Phillips WD. Advances in the understanding of disease mechanisms of autoimmune neuromuscular junction disorders. *Lancet Neurol* (2022) 21(2):163–75. doi: 10.1016/S1474-4422(21)00357-4

94. Perugino CA, Stone JH. IgG4-related disease: an update on pathophysiology and implications for clinical care. *Nat Rev Rheumatol* (2020) 16(12):702–14. doi: 10.1038/s41584-020-0500-7

95. Endmayr V, Tunc C, Ergin L, De Rosa A, Weng R, Wagner L, et al. Anti-Neuronal IgG4 Autoimmune Diseases and IgG4-Related Diseases May Not Be Part of the Same Spectrum: A Comparative Study. *Front Immunol* (2021) 12:785247. doi: 10.3389/fimmu.2021.785247

96. Perugino CA, AlSalem SB, Mattoo H, Della-Torre E, Mahajan V, Ganesh G, et al. Identification of galectin-3 as an autoantigen in patients with IgG(4)-related disease. *J Allergy Clin Immunol* (2019) 143(2):736–45.e6. doi: 10.1016/j.jaci.2018.05.011

97. Punnonen J, Aversa G, Cocks BG, McKenzie AN, Menon S, Zurawski G, et al. Interleukin 13 induces interleukin 4-independent IgG4 and IgE synthesis and CD23 expression by human B cells. *Proc Natl Acad Sci USA* (1993) 90(8):3730–4. doi: 10.1073/pnas.90.8.3730

98. Meiler F, Zumkehr J, Klunker S, Rückert B, Akdis CA, Akdis M. *In vivo* switch to IL-10-secreting T regulatory cells in high dose allergen exposure. *J Exp Med* (2008) 205 (12):2887–98. doi: 10.1084/jem.20080193

99. Jeannin P, Lecoanet S, Delneste Y, Gauchat JF, Bonnefoy JY. IgE versus IgG4 production can be differentially regulated by IL-10. *J Immunol* (1998) 160(7):3555–61. doi: 10.4049/jimmunol.160.7.3555

100. Yilmaz V, Oflazer P, Aysal F, Parman YG, Direskeneli H, Deymeer F, et al. B cells produce less IL-10, IL-6 and TNF-α in myasthenia gravis. *Autoimmunity* (2015) 48(4):201–7. doi: 10.3109/08916934.2014.992517

101. Ulusoy C, Kim E, Tüzün E, Huda R, Yılmaz V, Poulas K, et al. Preferential production of IgG1, IL-4 and IL-10 in MuSK-immunized mice. *Clin Immunol* (2014) 151(2):155–63. doi: 10.1016/j.clim.2014.02.012

102. Yi JS, Guidon A, Sparks S, Osborne R, Juel VC, Massey JM, et al. Characterization of CD4 and CD8 T cell responses in MuSK myasthenia gravis. *J Autoimmun* (2014) 52:130–8. doi: 10.1016/j.jaut.2013.12.005

103. Yilmaz V, Oflazer P, Aysal F, Durmus H, Poulas K, Yentur SP, et al. Differential Cytokine Changes in Patients with Myasthenia Gravis with Antibodies against AChR and MuSK. *PloS One* (2015) 10(4):e0123546. doi: 10.1371/journal.pone.0123546

104. Li Y, Guptill JT, Russo MA, Howard JFJr., Massey JM, Juel VC, et al. Imbalance in T follicular helper cells producing IL-17 promotes pro-inflammatory responses in MuSK antibody positive myasthenia gravis. *J Neuroimmunol* (2020) 345:577279. doi: 10.1016/j.jneuroim.2020.577279

105. Vergoossen DLE, Ruiter AM, Keene KR, Niks EH, Tannemaat MR, Strijbos E, et al. Enrichment of serum IgG4 in MuSK myasthenia gravis patients. *J Neuroimmunol* (2022) 373:577978. doi: 10.1016/j.jneuroim.2022.577978

106. Panhuber A, Lamorte G, Bruno V, Cetin H, Bauer W, Höftberger R, et al. A systematic review and meta-analysis of HLA class II associations in patients with IgG4 autoimmunity. *Sci Rep* (2022) 12(1):9229. doi: 10.1038/s41598-022-13042-2

107. Marino M, Maiuri MT, Di Sante G, Scuderi F, La Carpia F, Trakas N, et al. T cell repertoire in DQ5-positive MuSK-positive myasthenia gravis patients. *J Autoimmun* (2014) 52:113–21. doi: 10.1016/j.jaut.2013.12.007

108. Narayanaswami P, Sanders DB, Wolfe G, Benatar M, Cea G, Evoli A, et al. International Consensus Guidance for Management of Myasthenia Gravis: 2020 Update. *Neurology* (2021) 96(3):114–22. doi: 10.1212/WNL.0000000000011124

109. Ye L, Schnegelsberg M, Obermann M. Dipeptidyl-peptidase-like protein 6 encephalitis treated with immunotherapy. *Proc (Bayl Univ Med Cent)* (2020) 34 (1):114–5. doi: 10.1080/08998280.2020.1822132

110. Markovic I, Basic S, Devedjija S. Aggressive anti-LGI1 encephalitis defeated by one cycle of intravenous rituximab-a case report. *Neurol Sci* (2020) 41(7):1949–50. doi: 10.1007/s10072-020-04264-1

111. Kornau HC, Kreye J, Stumpf A, Fukata Y, Parthier D, Sammons RP, et al. Human Cerebrospinal Fluid Monoclonal LGI1 Autoantibodies Increase Neuronal Excitability. *Ann Neurol* (2020) 87(3):405–18. doi: 10.1002/ana.25666

112. Querol L, Rojas-García R, Diaz-Manera J, Barcena J, Pardo J, Ortega-Moreno A, et al. Rituximab in treatment-resistant CIDP with antibodies against paranodal proteins. *Neurol Neuroimmunol Neuroinflamm* (2015) 2(5):e149. doi: 10.1212/NXI.0000000000000149

113. Delmont E, Brodovitch A, Kouton L, Allou T, Beltran S, Brisset M, et al. Antibodies against the node of Ranvier: a real-life evaluation of incidence, clinical features and response to treatment based on a prospective analysis of 1500 sera. *J Neurol* (2020) 267(12):3664–72. doi: 10.1007/s00415-020-10041-z

114. Ong E, Viaccoz A, Ducray F, Pérol M, Cavillon G, Rogemond V, et al. Dramatic improvement after rituximab in a patient with paraneoplastic treatment-refractory Morvan syndrome associated with anti-CASPR2 antibodies. *Eur J Neurol* (2013) 20(7): e96–7. doi: 10.1111/ene.12164

115. Cabezudo-García P, Mena-Vázquez N, Estivill Torrús G, Serrano-Castro P. Response to immunotherapy in anti-IgLON5 disease: A systematic review. *Acta Neurol Scand* (2020) 141(4):263–70. doi: 10.1111/ane.13207

116. Hara M, Ariño H, Petit-Pedrol M, Sabater L, Titulaer MJ, Martinez-Hernandez E, et al. DPPX antibody-associated encephalitis: Main syndrome and antibody effects. *Neurology* (2017) 88(14):1340–8. doi: 10.1212/WNL.0000000000003796

117. van Sonderen A, Thijs RD, Coenders EC, Jiskoot LC, Sanchez E, de Bruijn MA, et al. Anti-LGI1 encephalitis: Clinical syndrome and long-term follow-up. *Neurology* (2016) 87(14):1449–56. doi: 10.1212/WNL.0000000000003173

118. Thaler FS, Zimmermann L, Kammermeier S, Strippel C, Ringelstein M, Kraft A, et al. Rituximab Treatment and Long-term Outcome of Patients With Autoimmune Encephalitis: Real-world Evidence From the GENERATE Registry. *Neurol Neuroimmunol Neuroinflamm* (2021) 8(6):e1088. doi: 10.1212/NXI.0000000000001088

119. Irani SR, Gelfand JM, Bettcher BM, Singhal NS, Geschwind MD. Effect of rituximab in patients with leucine-rich, glioma-inactivated 1 antibody-associated encephalopathy. *JAMA Neurol* (2014) 71(7):896–900. doi: 10.1001/jamaneurol.2014.463

120. Green MG, Bystryn JC. Effect of intravenous immunoglobulin therapy on serum levels of IgG1 and IgG4 antidesmoglein 1 and antidesmoglein 3 antibodies in pemphigus vulgaris. *Arch Dermatol* (2008) 144(12):1621–4. doi: 10.1001/archdermatol.2008.503

121. Jiao L, Xiang Y, Li S, Zhang F, Ruan X, Guo S. Efficacy of low dose rituximab in treatment-resistant CIDP with antibodies against NF-155. *J Neuroimmunol* (2020) 345:577280. doi: 10.1016/j.jneuroim.2020.577280

122. Pasnoor M, Wolfe GI, Nations S, Trivedi J, Barohn RJ, Herbelin L, et al. Clinical findings in MuSK-antibody positive myasthenia gravis: a U. *S. experience. Muscle Nerve* (2010) 41(3):370–4. doi: 10.1002/mus.21533

123. Zinman L, Ng E, Bril V. IV immunoglobulin in patients with myasthenia gravis: a randomized controlled trial. *Neurology* (2007) 68(11):837–41. doi: 10.1212/01.wnl.0000256698.69121.45

124. Barth D, Nabavi Nouri M, Ng E, Nwe P, Bril V. Comparison of IVIg and PLEX in patients with myasthenia gravis. *Neurology* (2011) 76(23):2017–23. doi: 10.1212/WNL.0b013e31821e5505

125. Takahashi H, Kawaguchi N, Nemoto Y, Hattori T. High-dose intravenous immunoglobulin for the treatment of MuSK antibody-positive seronegative myasthenia gravis. *J Neurol Sci* (2006) 247(2):239–41. doi: 10.1016/j.jns.2006.05.065

126. König N, Stetefeld HR, Dohmen C, Mergenthaler P, Kohler S, Schönenberger S, et al. MuSK-antibodies are associated with worse outcome in myasthenic crisis requiring mechanical ventilation. *J Neurol* (2021) 268(12):4824–33. doi: 10.1007/s00415-021-10603-9

127. Wolfe GI, Trivedi JR, Oh SJ. Clinical Review of Muscle-Specific Tyrosine Kinase-Antibody Positive Myasthenia Gravis. *J Clin Neuromuscular Disease* (2007) 8 (4):217–24. doi: 10.1097/CND.0b013e318137a24b

128. Aalberse RC, van der Gaag R, van Leeuwen J. Serologic aspects of IgG4 antibodies. *I. Prolonged immunization results an IgG4-restricted response. J Immunol* (1983) 130(2):722–6.

129. van der Neut Kolfschoten M, Schuurman J, Losen M, Bleeker WK, Martínez-Martínez P, Vermeulen E, et al. Anti-inflammatory activity of human IgG4 antibodies by dynamic Fab arm exchange. *Sci (New York NY)* (2007) 317(5844):1554–7. doi: 10.1126/science.1144603

130. Evoli A, Padua L. Diagnosis and therapy of myasthenia gravis with antibodies to muscle-specific kinase. *Autoimmun Rev* (2013) 12(9):931–5. doi: 10.1016/j.autrev.2013.03.004

131. Rostedt Punga A, Ahlqvist K, Bartoccioni E, Scuderi F, Marino M, Suomalainen A, et al. Neurophysiological and mitochondrial abnormalities in MuSK antibody seropositive myasthenia gravis compared to other immunological subtypes. *Clin Neurophysiol* (2006) 117(7):1434–43. doi: 10.1016/j.clinph.2006.03.028

132. Matthews I, Chen S, Hewer R, McGrath V, Furmaniak J, Rees Smith B. Muscle-specific receptor tyrosine kinase autoantibodies–a new immunoprecipitation assay. *Clin Chim Acta* (2004) 348(1-2):95–9. doi: 10.1016/j.cccn.2004.05.008

133. Huda S, Waters P, Woodhall M, Leite MI, Jacobson L, De Rosa A, et al. IgG-specific cell-based assay detects potentially pathogenic MuSK-Abs in seronegative MG. *Neurol Neuroimmunol Neuroinflamm* (2017) 4(4):e357. doi: 10.1212/NXI.0000000000000357

134. Kim MJ, Kim SW, Kim M, Choi YC, Kim SM, Shin HY. Evaluating an In-House Cell-Based Assay for Detecting Antibodies Against Muscle-Specific Tyrosine Kinase in Myasthenia Gravis. *J Clin Neurol* (2021) 17(3):400–8. doi: 10.3988/jcn.2021.17.3.400

135. Tsonis AI, Zisimopoulou P, Lazaridis K, Tzartos J, Matsigkou E, Zouvelou V, et al. MuSK autoantibodies in myasthenia gravis detected by cell based assay–A multinational study. *J Neuroimmunol* (2015) 284:10–7. doi: 10.1016/j.jneuroim.2015.04.015

136. Spagni G, Gastaldi M, Businaro P, Chemkhi Z, Carrozza C, Mascagna G, et al. Comparison of Fixed and Live Cell-Based Assay for the Detection of AChR and MuSK Antibodies in Myasthenia Gravis. *Neurol Neuroimmunol Neuroinflamm* (2023) 10(1): e200038. doi: 10.1212/NXI.0000000000200038

137. Damato V, Spagni G, Monte G, Woodhall M, Jacobson L, Falso S, et al. Clinical value of cell-based assays in the characterisation of seronegative myasthenia gravis. *J Neurol Neurosurg Psychiatry* (2022) 93(9):995–1000. doi: 10.1136/jnnp-2022-329284

138. Kwon YN, Woodhall M, Sung JJ, Kim KK, Lim YM, Kim H, et al. Clinical pitfalls and serological diagnostics of MuSK myasthenia gravis. *J Neurol* (2023) 270 (3):1478–86. doi: 10.1007/s00415-022-11458-4

139. Suh J, Goldstein JM, Nowak RJ. Clinical characteristics of refractory myasthenia gravis patients. *Yale J Biol Med* (2013) 86(2):255–60.

140. Chroni E, Punga AR. Neurophysiological characteristics of MuSK antibody positive myasthenia gravis mice: focal denervation and hypersensitivity to acetylcholinesterase inhibitors. *J Neurol Sci* (2012) 316(1-2):150–7. doi: 10.1016/j.jns.2011.12.016

141. Hatanaka Y, Hemmi S, Morgan MB, Scheufele ML, Claussen GC, Wolfe GI, et al. Nonresponsiveness to anticholinesterase agents in patients with MuSK-antibody-positive MG. *Neurology* (2005) 65(9):1508–9. doi: 10.1212/01.wnl.0000183145.91579.74

142. Shin HY, Park HJ, Lee HE, Choi YC, Kim SM. Clinical and Electrophysiologic Responses to Acetylcholinesterase Inhibitors in MuSK-Antibody-Positive Myasthenia Gravis: Evidence for Cholinergic Neuromuscular Hyperactivity. *J Clin Neurol* (2014) 10 (2):119–24. doi: 10.3988/jcn.2014.10.2.119

143. Dalakas MC. Update on Intravenous Immunoglobulin in Neurology: Modulating Neuro-autoimmunity, Evolving Factors on Efficacy and Dosing and Challenges on Stopping Chronic IVIg Therapy. *Neurotherapeutics* (2021) 18 (4):2397–418. doi: 10.1007/s13311-021-01108-4

144. Su S, Liu Q, Zhang X, Wen X, Lei L, Shen F, et al. VNTR2/VNTR3 genotype in the FCGRT gene is associated with reduced effectiveness of intravenous immunoglobulin in patients with myasthenia gravis. *Ther Adv Neurol Disord* (2021) 14:1756286420986747. doi: 10.1177/1756286420986747

145. Sanders DB, Wolfe GI, Benatar M, Evoli A, Gilhus NE, Illa I, et al. International consensus guidance for management of myasthenia gravis: Executive summary. *Neurology* (2016) 87(4):419–25. doi: 10.1212/WNL.0000000000002790

146. Guptill JT, Sanders DB. Update on muscle-specific tyrosine kinase antibody positive myasthenia gravis. *Curr Opin Neurol* (2010) 23(5):530–5. doi: 10.1097/WCO.0b013e32833c0982

147. Leandro MJ. B-cell subpopulations in humans and their differential susceptibility to depletion with anti-CD20 monoclonal antibodies. *Arthritis Res Ther* (2013) 15(Suppl 1):S3. doi: 10.1186/ar3908

148. Fujii Y, Monden Y, Hashimoto J, Nakahara K, Kawashima Y. Acetylcholine receptor antibody production by bone marrow cells in a patient with myasthenia gravis. *Neurology* (1985) 35(4):577–9. doi: 10.1212/WNL.35.4.577

149. Willcox HN, Newsom-Davis J, Calder LR. Cell types required for anti-acetylcholine receptor antibody synthesis by cultured thymocytes and blood lymphocytes in myasthenia gravis. *Clin Exp Immunol* (1984) 58(1):97–106.

150. Graus YF, de Baets MH, Parren PW, Berrih-Aknin S, Wokke J, van Breda Vriesman PJ, et al. Human anti-nicotinic acetylcholine receptor recombinant Fab fragments isolated from thymus-derived phage display libraries from myasthenia gravis patients reflect predominant specificities in serum and block the action of pathogenic serum antibodies. *J Immunol* (1997) 158(4):1919–29. doi: 10.4049/jimmunol.158.4.1919

151. Fujii Y, Monden Y, Nakahara K, Hashimoto J, Kawashima Y. Antibody to acetylcholine receptor in myasthenia gravis: production by lymphocytes from thymus or thymoma. *Neurology* (1984) 34(9):1182–6. doi: 10.1212/WNL.34.9.1182

152. Gomez AM, Willcox N, Vrolix K, Hummel J, Nogales-Gadea G, Saxena A, et al. Proteasome inhibition with bortezomib depletes plasma cells and specific autoantibody production in primary thymic cell cultures from early-onset myasthenia gravis patients. *J Immunol* (2014) 193(3):1055–63. doi: 10.4049/jimmunol.1301555

153. Illa I, Diaz-Manera J, Rojas-Garcia R, Pradas J, Rey A, Blesa R, et al. Sustained response to Rituximab in anti-AChR and anti-MuSK positive Myasthenia Gravis patients. *J Neuroimmunol* (2008) 201-202:90–4. doi: 10.1016/j.jneuroim.2008.04.039

154. Robeson KR, Kumar A, Keung B, DiCapua DB, Grodinsky E, Patwa HS, et al. Durability of the Rituximab Response in Acetylcholine Receptor Autoantibody-Positive Myasthenia Gravis. *JAMA Neurol* (2017) 74(1):60–6. doi: 10.1001/jamaneurol.2016.4190

155. Zebardast N, Patwa HS, Novella SP, Goldstein JM. Rituximab in the management of refractory myasthenia gravis. *Muscle Nerve* (2010) 41(3):375–8. doi: 10.1002/mus.21521

156. Nowak RJ, Dicapua DB, Zebardast N, Goldstein JM. Response of patients with refractory myasthenia gravis to rituximab: a retrospective study. *Ther Adv Neurol Disord* (2011) 4(5):259–66. doi: 10.1177/1756285611411503

157. Choi K, Hong YH, Ahn SH, Baek SH, Kim JS, Shin JY, et al. Repeated low-dose rituximab treatment based on the assessment of circulating B cells in patients with refractory myasthenia gravis. *Ther Adv Neurol Disord* (2019) 12:1756286419871187. doi: 10.1177/1756286419871187

158. Anderson D, Phan C, Johnston WS, Siddiqi ZA. Rituximab in refractory myasthenia gravis: a prospective, open-label study with long-term follow-up. *Ann Clin Transl Neurol* (2016) 3(7):552–5. doi: 10.1002/acn3.314

159. Hehir MK, Hobson-Webb LD, Benatar M, Barnett C, Silvestri NJ, Howard JFJr., et al. Rituximab as treatment for anti-MuSK myasthenia gravis: Multicenter blinded prospective review. *Neurology* (2017) 89(10):1069–77. doi: 10.1212/WNL.0000000000004341

160. Yi JS, Guptill JT, Stathopoulos P, Nowak RJ, O'Connor KC. B cells in the pathophysiology of myasthenia gravis. *Muscle Nerve* (2018) 57(2):172–84. doi: 10.1002/mus.25973

161. Hofmann K, Clauder AK, Manz RA. Targeting B Cells and Plasma Cells in Autoimmune Diseases. *Front Immunol* (2018) 9:835. doi: 10.3389/fimmu.2018.00835

162. Yilmaz V, Ulusoy C, Hajtovic S, Turkoglu R, Kurtuncu M, Tzartos J, et al. Effects of Teriflunomide on B Cell Subsets in MuSK-Induced Experimental Autoimmune Myasthenia Gravis and Multiple Sclerosis. *Immunol Invest* (2021) 50 (6):671–84. doi: 10.1080/08820139.2020.1785491

163. Khosroshahi A, Bloch DB, Deshpande V, Stone JH. Rituximab therapy leads to rapid decline of serum IgG4 levels and prompt clinical improvement in IgG4-related systemic disease. *Arthritis Rheumatol* (2010) 62(6):1755–62. doi: 10.1002/art.27435

164. Khosroshahi A, Carruthers MN, Deshpande V, Unizony S, Bloch DB, Stone JH. Rituximab for the treatment of IgG4-related disease: lessons from 10 consecutive patients. *Med (Baltimore)* (2012) 91(1):57–66. doi: 10.1097/MD.0b013e3182431ef6

165. Litchman T, Roy B, Kumar A, Sharma A, Njike V, Nowak RJ. Differential response to rituximab in anti-AChR and anti-MuSK positive myasthenia gravis patients: a single-center retrospective study. *J neurological Sci* (2020) 411:116690. doi: 10.1016/j.jns.2020.116690

166. Topakian R, Zimprich F, Iglseder S, Embacher N, Guger M, Stieglbauer K, et al. High efficacy of rituximab for myasthenia gravis: a comprehensive nationwide study in Austria. *J Neurol* (2019) 266(3):699–706. doi: 10.1007/s00415-019-09191-6

167. Di Stefano V, Lupica A, Rispoli MG, Di Muzio A, Brighina F, Rodolico C. Rituximab in AChR subtype of myasthenia gravis: systematic review. *J Neurol Neurosurg Psychiatry* (2020) 91(4):392–5. doi: 10.1136/jnnp-2019-322606

168. Tandan R, Hehir MK2nd, Waheed W, Howard DB. Rituximab treatment of myasthenia gravis: A systematic review. *Muscle Nerve* (2017) 56(2):185–96. doi: 10.1002/mus.25597

169. Zhao C, Pu M, Chen D, Shi J, Li Z, Guo J, et al. Effectiveness and Safety of Rituximab for Refractory Myasthenia Gravis: A Systematic Review and Single-Arm Meta-Analysis. *Front Neurol* (2021) 12:736190. doi: 10.3389/fneur.2021.736190

170. Lebrun C, Bourg V, Bresch S, Cohen M, Rosenthal-Allieri MA, Desnuelle C, et al. Therapeutic target of memory B cells depletion helps to tailor administration frequency of rituximab in myasthenia gravis. *J neuroimmunology* (2016) 298:79–81. doi: 10.1016/j.jneuroim.2016.07.009

171. Kim SH, Huh SY, Lee SJ, Joung A, Kim HJ. A 5-year follow-up of rituximab treatment in patients with neuromyelitis optica spectrum disorder. *JAMA neurology* (2013) 70(9):1110–7. doi: 10.1001/jamaneurol.2013.3071

172. Meng X, Zeng Z, Wang Y, Guo S, Wang C, Wang B, et al. Efficacy and Safety of Low-Dose Rituximab in Anti-MuSK Myasthenia Gravis Patients: A Retrospective Study. *Neuropsychiatr Dis Treat* (2022) 18:953–64. doi: 10.2147/NDT.S358851

173. Zhou Y, Yan C, Gu X, Zhou L, Lu J, Zhu W, et al. Short-term effect of low-dose rituximab on myasthenia gravis with muscle-specific tyrosine kinase antibody. *Muscle Nerve* (2021) 63(6):824–30. doi: 10.1002/mus.27233

174. Nowak RJ, Coffey CS, Goldstein JM, Dimachkie MM, Benatar M, Kissel JT, et al. Phase 2 Trial of Rituximab in Acetylcholine Receptor Antibody-Positive Generalized Myasthenia Gravis: The BeatMG Study. *Neurology* (2021) 98(4):e376–89. doi: 10.1212/WNL.0000000000013121

175. Piehl F, Eriksson-Dufva A, Budzianowska A, Feresiadou A, Hansson W, Hietala MA, et al. Efficacy and Safety of Rituximab for New-Onset Generalized Myasthenia Gravis: The RINOMAX Randomized Clinical Trial. *JAMA Neurol* (2022) 79(11):1105–12. doi: 10.1001/jamaneurol.2022.2887

176. Barreras P, Vasileiou ES, Filippatou AG, Fitzgerald KC, Levy M, Pardo CA, et al. Long-term Effectiveness and Safety of Rituximab in Neuromyelitis Optica Spectrum Disorder and MOG Antibody Disease. *Neurology* (2022) 99(22):e2504–e16. doi: 10.1212/WNL.0000000000201260

177. Guo Y, Weigand SD, Popescu BF, Lennon VA, Parisi JE, Pittock SJ, et al. Pathogenic implications of cerebrospinal fluid barrier pathology in neuromyelitis optica. *Acta neuropathologica* (2017) 133(4):597–612. doi: 10.1007/s00401-017-1682-1

178. Chihara N, Aranami T, Sato W, Miyazaki Y, Miyake S, Okamoto T, et al. Interleukin 6 signaling promotes anti-aquaporin 4 autoantibody production from plasmablasts in neuromyelitis optica. *Proc Natl Acad Sci United States America* (2011) 108(9):3701–6. doi: 10.1073/pnas.1017385108

179. Bennett JL, Lam C, Kalluri SR, Saikali P, Bautista K, Dupree C, et al. Intrathecal pathogenic anti-aquaporin-4 antibodies in early neuromyelitis optica. *Ann neurology* (2009) 66(5):617–29. doi: 10.1002/ana.21802

180. Schneider-Gold C, Reinacher-Schick A, Ellrichmann G, Gold R. Bortezomib in severe MuSK-antibody positive myasthenia gravis: first clinical experience. *Ther Adv Neurol Disord* (2017) 10(10):339–41. doi: 10.1177/1756285617721093

181. Zuercher AW, Spirig R, Baz Morelli A, Rowe T, Käsermann F. Next-generation Fc receptor-targeting biologics for autoimmune diseases. *Autoimmun Rev* (2019) 18 (10):102366. doi: 10.1016/j.autrev.2019.102366

182. Roopenian DC, Akilesh S. FcRn: the neonatal Fc receptor comes of age. *Nat Rev Immunol* (2007) 7(9):715–25. doi: 10.1038/nri2155

183. Howard JFJr., Bril V, Burns TM, Mantegazza R, Bilinska M, Szczudlik A, et al. Randomized phase 2 study of FcRn antagonist efgartigimod in generalized myasthenia gravis. *Neurology* (2019) 92(23):e2661–e73. doi: 10.1212/WNL.0000000000007600

184. Howard JFJr., Bril V, Vu T, Karam C, Peric S, Margania T, et al. Safety, efficacy, and tolerability of efgartigimod in patients with generalised myasthenia gravis (ADAPT): a multicentre, randomised, placebo-controlled, phase 3 trial. *Lancet Neurol* (2021) 20(7):526–36. doi: 10.1016/S1474-4422(21)00159-9

185. Bril V, Benatar M, Andersen H, Vissing J, Brock M, Greve B, et al. Efficacy and Safety of Rozanolixizumab in Moderate to Severe Generalized Myasthenia Gravis: A Phase 2 Randomized Control Trial. *Neurology* (2021) 96(6):e853–e65. doi: 10.1212/WNL.0000000000011108

186. Kiessling P, Lledo-Garcia R, Watanabe S, Langdon G, Tran D, Bari M, et al. The FcRn inhibitor rozanolixizumab reduces human serum IgG concentration: A randomized phase 1 study. *Sci Transl Med* (2017) 9(414):eaan1208. doi: 10.1126/scitranslmed.aan1208

187. Bril V, Drużdż A, Grosskreutz J, Habib AA, Mantegazza R, Sacconi S, et al. Safety and efficacy of rozanolixizumab in patients with generalised myasthenia gravis (MycarinG): a randomised, double-blind, placebo-controlled, adaptive phase 3 study. *Lancet Neurology* (2023) 22(5):383–94. doi: 10.1016/S1474-4422(23)00077-7

188. Terrero A, Ramírez-Rivera J. "Seronegative" anti-MUSK positive myasthenia gravis presenting during pregnancy. *Bol Asoc Med P R* (2006) 98(3):210–2.

189. Neves AR, Monteiro P, Matos A, Santos Silva I. Anti-MuSK-positive myasthenia gravis diagnosed during pregnancy: new challenges for an old disease? *BMJ Case Rep* (2015) 2015:bcr2014207708. doi: 10.1136/bcr-2014-207708

190. Alharbi M, Menon D, Barnett C, Katzberg H, Sermer M, Bril V. Myasthenia Gravis and Pregnancy: Toronto Specialty Center Experience. *Can J Neurol Sci* (2021) 48 (6):767–71. doi: 10.1017/cjn.2021.2

191. Su M, Liu X, Wang L, Song J, Zhou Z, Luo S, et al. Risk factors for pregnancy-related clinical outcome in myasthenia gravis: a systemic review and meta-analysis. *Orphanet J Rare Dis* (2022) 17(1):52. doi: 10.1186/s13023-022-02205-z

192. Santos E, Braga A, Gabriel D, Duarte S, Martins da Silva A, Matos I, et al. MuSK myasthenia gravis and pregnancy. *Neuromuscul Disord* (2018) 28(2):150–3. doi: 10.1016/j.nmd.2017.11.014

193. Gilhus NE. Treatment considerations in myasthenia gravis for the pregnant patient. *Expert Rev Neurother* (2023) 23(2):169–77. doi: 10.1080/14737175.2023.2178302

194. Bansal R, Goyal MK, Modi M. Management of myasthenia gravis during pregnancy. *Indian J Pharmacol* (2018) 50(6):302–8. doi: 10.4103/ijp.IJP_452_17

195. Chakravarty EF, Murray ER, Kelman A, Farmer P. Pregnancy outcomes after maternal exposure to rituximab. *Blood* (2011) 117(5):1499–506. doi: 10.1182/blood-2010-07-295444

196. Colpo A, Marson P, Pavanello F, Tison T, Gervasi MT, Zambon A, et al. Therapeutic apheresis during pregnancy: A single center experience. *Transfus Apher Sci* (2019) 58(5):652–8. doi: 10.1016/j.transci.2019.07.009

197. Dos Santos A, Noury JB, Genestet S, Nadaj-Pakleza A, Cassereau J, Baron C, et al. Efficacy and safety of rituximab in myasthenia gravis: a French multicentre real-life study. *Eur J Neurol* (2020) 27(11):2277–85. doi: 10.1111/ene.14391

198. Heckmann JM. A single low-dose rituximab infusion in severe chronic refractory myasthenia gravis in resource-limited settings. *J Neurol Sci* (2022) 442:120394. doi: 10.1016/j.jns.2022.120394

199. Caballero-Ávila M, Álvarez-Velasco R, Moga E, Rojas-Garcia R, Turon-Sans J, Querol L, et al. Rituximab in myasthenia gravis: efficacy, associated infections and risk of induced hypogammaglobulinemia. *Neuromuscul Disord* (2022) 32(8):664–71. doi: 10.1016/j.nmd.2022.06.006

200. Castiglione JI, Rivero AD, Barroso F, Brand P, Lautre A, Kohler AA. Long-Term Remission With Low-Dose Rituximab in Myasthenia Gravis: A Retrospective Study. *J Clin Neuromuscul Dis* (2022) 24(1):18–25. doi: 10.1097/CND.0000000000000420

201. Afanasiev V, Demeret S, Bolgert F, Eymard B, Laforêt P, Benveniste O. Resistant myasthenia gravis and rituximab: A monocentric retrospective study of 28 patients. *Neuromuscul Disord* (2017) 27(3):251–8. doi: 10.1016/j.nmd.2016.12.004

202. Beecher G, Anderson D, Siddiqi ZA. Rituximab in refractory myasthenia gravis: Extended prospective study results. *Muscle Nerve* (2018) 58(3):452–5. doi: 10.1002/mus.26156

203. Chan F, Swayne A, Gillis D, Walsh M, Henderson RD, McCombe PA, et al. Long-term follow-up of patients with myasthenia gravis treated with low-dose rituximab. *J Neurol Neurosurg Psychiatry* (2019) 90(8):955–6. doi: 10.1136/jnnp-2018-319410

204. Hewett K, Sanders DB, Grove RA, Broderick CL, Rudo TJ, Bassiri A, et al. Randomized study of adjunctive belimumab in participants with generalized myasthenia gravis. *Neurology* (2018) 90(16):e1425–e34. doi: 10.1212/WNL.0000000000005323

205. Oh S, Mao X, Manfredo-Vieira S, Lee J, Patel D, Choi EJ, et al. Precision targeting of autoantigen-specific B cells in muscle-specific tyrosine kinase myasthenia gravis with chimeric autoantibody receptor T cells. *Nat Biotechnol* (2023). doi: 10.1038/s41587-022-01637-z

206. Beland B, Hahn C, Jamani K, Chhibber S, White C, Atkins H, et al. Autologous hematopoietic stem cell transplant for the treatment of refractory myasthenia gravis with anti-muscle specific kinase antibodies. *Muscle nerve* (2023) 67(2):154–7. doi: 10.1002/mus.27772

207. Burt R, Statkute L, Gourineni R, et al. Treatment of refractory myasthenia gravis with high dose chemotherapy and autologous hematopoietic stem cell transplantation. *Neurology* (2004) 62:A497.

208. Cantor S, Zhang W, Delestrée N, Remédio L, Mentis GZ, Burden SJ. Preserving neuromuscular synapses in ALS by stimulating MuSK with a therapeutic agonist antibody. *eLife* (2018) 7:e34375. doi: 10.7554/eLife.34375

209. Lim JL, Augustinus R, Plomp JJ, Roya-Kouchaki K, Vergoossen DLE, Filliié-Grijpma Y, et al. Development and characterization of agonistic antibodies targeting the Ig-like 1 domain of MuSK. *Sci Rep* (2023) 13(1):7478. doi: 10.1038/s41598-023-32641-1

210. Bi Y, Su J, Zhou S, Zhao Y, Zhang Y, Zhang H, et al. Distinct impact of IgG subclass on autoantibody pathogenicity in different IgG4-mediated diseases. *eLife* (2022) 11. doi: 10.7554/eLife.76223

211. Leite MI, Ströbel P, Jones M, Micklem K, Moritz R, Gold R, et al. Fewer thymic changes in MuSK antibody-positive than in MuSK antibody-negative MG. *Ann Neurol* (2005) 57(3):444–8. doi: 10.1002/ana.20386

212. Selcen D, Fukuda T, Shen XM, Engel AG. Are MuSK antibodies the primary cause of myasthenic symptoms? *Neurology* (2004) 62(11):1945–50. doi: 10.1212/01.WNL.0000128048.23930.1D

213. Lazaridis K, Baltatzidou V, Tektonidis N, Tzartos SJ. Antigen-specific immunoadsorption of MuSK autoantibodies as a treatment of MuSK-induced experimental autoimmune myasthenia gravis. *J Neuroimmunol* (2020) 339:577136. doi: 10.1016/j.jneuroim.2019.577136

214. Skriapa L, Zisimopoulou P, Trakas N, Grapsa E, Tzartos SJ. Expression of extracellular domains of muscle specific kinase (MuSK) and use as immunoadsorbents for the development of an antigen-specific therapy. *J Neuroimmunol* (2014) 276(1-2):150–8. doi: 10.1016/j.jneuroim.2014.09.013

frontiers | Frontiers in Immunology

TYPE Original Research
PUBLISHED 15 November 2023
DOI 10.3389/fimmu.2023.1268986

OPEN ACCESS

EDITED BY
Lidia Sabater,
August Pi i Sunyer Biomedical Research Institute (IDIBAPS), Spain

REVIEWED BY
Hui Yan,
The University of Texas Health Science Center at San Antonio, United States
Luís F Ribeiro,
University of Coimbra, Portugal

*CORRESPONDENCE
Nihan Çarçak
nihan.carcak@istanbul.edu.tr
Erdem Tüzün
drerdem@yahoo.com

†These authors have contributed equally to this work

RECEIVED 28 July 2023
ACCEPTED 30 October 2023
PUBLISHED 15 November 2023

CITATION
Pişkin ŞA, Korkmaz HY, Ulusoy CA, Şanlı E, Küçükali CI, Onat F, Tüzün E and Çarçak N (2023) Antibody induced seizure susceptibility and impaired cognitive performance in a passive transfer rat model of autoimmune encephalitis.
Front. Immunol. 14:1268986.
doi: 10.3389/fimmu.2023.1268986

Antibody induced seizure susceptibility and impaired cognitive performance in a passive transfer rat model of autoimmune encephalitis

Şura Akat Pişkin[1†], Hande Yüceer Korkmaz[2†], Canan Aysel Ulusoy[3], Elif Şanlı[2], Cem Ismail Küçükali[3], Filiz Onat[4,5], Erdem Tüzün[3*] and Nihan Çarçak[5,6*]

[1]Department of Pharmacology, Faculty of Pharmacy, Institute of Health Sciences, Istanbul University, Istanbul, Türkiye, [2]Department of Neuroscience, Aziz Sancar Institute of Experimental Medicine, Institute of Health Sciences, Istanbul University, Istanbul, Türkiye, [3]Department of Neuroscience, Aziz Sancar Institute of Experimental Medicine, Istabul University, Istanbul, Türkiye, [4]Department of Medical Pharmacology, Acibadem Mehmet Ali Aydinlar University Faculty of Medicine, Istanbul, Türkiye, [5]Deparment of Neuroscience, Acibadem Mehmet Ali Aydinlar University Health Sciences Institute, Istanbul, Türkiye, [6]Department of Pharmacology, Faculty of Pharmacy, Istanbul University, Istanbul, Türkiye

Objective: Autoimmune encephalitis (AE) is a distinct neuro-immunological disorder associated with the production of autoantibodies against neuronal proteins responsible for pharmacoresistant seizures, cognitive decline and behavioral problems. To establish the causal link between leucine-rich glioma inactivated 1 (LGI1) antibody and seizures, we developed an *in-vivo* antibody-mediated AE rat model in which serum antibodies (IgG) obtained from blood samples of leucine-rich glioma inactivated 1 (LGI1) protein antibody (IgG) positive encephalitis patients were passively transferred into non-epileptic Wistar rats. Serum IgG of N-methyl-d-aspartate receptor (NMDAR) antibody positive patients were used as positive control since the pathogenicity of this antibody has been previously shown in animal models.

Methods: Total IgG obtained from the pooled sera of NMDAR and LGI1-IgG positive patients with epileptic seizures and healthy subjects was applied chronically every other day for 11 days into the cerebral lateral ventricle. Spontaneous seizure development was followed by electroencephalography. Behavioral tests for memory and locomotor activity were applied before and after the antibody infusions. Then, pentylenetetrazol (PTZ) was administered intraperitoneally to evaluate seizure susceptibility. Immunohistochemistry processed for assessment of hippocampal astrocyte proliferation and expression intensity of target NMDAR and LGI1 antigens.

Results: No spontaneous activity was observed during the antibody infusions. PTZ-induced seizure stage was significantly higher in the NMDAR-IgG and LGI1-IgG groups compared to control. Besides, memory deficits were observed in the NMDAR and LGI1-IgG groups. We observed enhanced astrocyte proliferation in NMDAR- and LGI1-IgG groups and reduced hippocampal NMDAR expression in NMDAR-IgG group.

Significance: These findings suggest that neuronal surface auto-antibody administration induces seizure susceptibility and disturbed cognitive performance in the passive transfer rat model of LGI1 AE, which could be a potential *in-vivo* model for understanding immune-mediated mechanisms underlying epileptogenesis and highlight the potential targets for immune-mediated seizures in AE patients.

KEYWORDS

autoimmune encephalitis, NMDAR antibody, Epilepsy, LGI1, Wistar, PTZ, animal model

Introduction

Autoimmune Encephalitis (AE) is recently identified immune-mediated disorder apparently accounting for 10-15% of all encephalitis cases (1). According to recent hypotheses, seizures occurring in the context of AEs could be provoked by the direct effect of auto-antibodies (auto-Abs) on neuronal surface antigens (e.g., ion channels, receptor proteins) involved in synaptic transmission (2, 3). Auto-Abs against N-methyl-d-aspartate receptor (NMDAR) and leucine-rich glioma inactivated 1 (LGI1) proteins expressed on the neuronal surface resulting in hyperexcitability and impairment of synaptic function are considered to be pathogenic in patients with AE that is characterized by a wide range of neurological and psychiatric clinical features including cognitive impairment, behavioral changes, movement disorders and epileptic seizures (4). Although immunotherapy improves clinical outcomes, some individuals may experience deficiencies that result in lifelong disability, such as pharmacoresistant epilepsy and persistent cognitive impairment (3). The detection of particular auto-Abs found in serum and/or cerebrospinal fluid (CSF) of patients in conjunction with an appropriate clinical presentation is required for the diagnosis of AE. However, in a considerable number of patients no auto-Abs expressed and presumably not all antibodies are known (4). Experimental studies conducted with antibodies from patients with NMDAR encephalitis also suggest that antibodies against neuronal cell-surface may contribute to epileptogenesis (5–8). However, it remains unknown in what extend the LGI1-directed antibodies contribute to seizure generation and the exact effect of LGI1 antibodies on AE remains largely unexplored. In recent research, LGI1 antibodies were found to be pathogenic in a passive transfer mouse model where patient- or control-derived IgG was transferred into the cerebral ventricle (9). Mice infused with LGI1-IgG exhibited memory impairment which partially reversed after stopping the infusion. Notably, no spontaneous seizures were observed in this model (9) However, LGI1-IgG did lead to significant reductions in the density of both total and synaptic Kv1.1 potassium channels and α-amino-3-hydroxy-5-methyl-4-isoxazolepropionic acid receptor (AMPAR) clusters resulted from the interference of LGI1 interactions with presynaptic ADAM23 and postsynaptic ADAM22 proteins. This disruption also led to increased presynaptic excitability and glutamatergic transmission, as evidenced by *in-vitro* experiments (10) but not sufficient to cause spontaneous seizures *in-vivo*. Further investigations are needed to delve into this aspect and its relevance to the clinical phenotype of LGI1- antibody associated disorders.

In this study, we attempted to determine the role of human anti-LGI1 auto-Abs in epileptogenesis by developing a translational rodent model for LGI-1-IgG that would allow for studying pathophysiology with clinical relevance and to compare it to the pathogenic consequences of anti-NMDAR-auto-Abs that had earlier been shown to contribute to the epileptogenesis (5–8). To test the hypothesis that, LGI1-antibodies may lead to increased seizure susceptibility *in-vivo*, we developed an antibody-mediated AE rat model for LGI-1gG; in which either anti-LGI1 or NMDAR auto-Ab containing total IgG obtained from blood samples of AE patients were passively transferred into the rat brain. The functional impact of each purified neuronal-surface auto-Ab on the development of a validated animal model of AE was evaluated in terms of electroencephalographical (EEG) changes, seizure susceptibility following pentylenetetrazole (PTZ) administration and behavioral manifestations.

Materials and methods

We used non-epileptic Wistar rats (n=34) that were 3–6 months old (weighed 250-350 g) from breeding colony of Aziz Sancar Institute of Experimental Medicine. Animals were maintained under standard laboratory conditions on a 12/12-h light/dark cycle, with ad libitum access to food and water. The study was approved by the Animal Ethics Committee of Istanbul University (Ethics number:1107593) conforming with the EU Directive 2010/63/EU for animal experiments. Every effort has been made to reduce the number of animals for experimentation and minimize pain and distress in animals.

Patient characteristics and purification of IgG

Serum samples containing anti-NMDAR (n=3) and anti-LGl1 (n=3) auto-Abs were obtained from blood samples of patients with

autoimmune encephalitis. Three healthy individual (age range 28-55; 1 man/2 women) sera were used as negative controls. Both NMDAR and LGI1 encephalitis patients fulfilled the clinical criteria for definite autoimmune encephalitis and NMDAR-IgG positive patients also fulfilled the criteria for definite NMDAR encephalitis (4).

NMDAR and LGI1 antibodies were detected in both serum (end-point titers 1:400-1600) and cerebrospinal fluid (CSF) samples of NMDAR (age range 25-52; 1 man/2 women) and LGI1-encephalitis (age range 32-61; 2 men/1 woman) patients, respectively. Serum and CSF samples were tested for other well-characterized AE antibodies (anti-CASPR2, -AMPAR, -GABABR, -glutamic acid decarboxylase, -Hu, -CV2, -Ma2, -Ri and -amphiphysin) and found negative. Healthy control (HC) sera did not show any well-characterized antibodies, as well. Antibody tests were conducted by commercial cell based, immunofluorescence or immunoblot assays, as required (Euroimmun, Luebeck, Germany). All autoimmune encephalitis patients had focal and/or generalized tonic clonic seizures. Other clinical features were short-term memory loss, delusions, hallucinations, autonomic symptoms, disorientation and coma. In all patients, CSF analysis showed increased protein concentration and lymphocyte counts and EEG examination showed focal or generalized slow waves. Cranial MRI was normal in 1 each patient with NMDAR and LGI1 encephalitis, whereas the remaining patients showed bilateral medial temporal lobe hyperintensity. None of the patients showed a tumor in whole-body CT imaging. Sera were obtained within the first week of the onset of clinical episode and stored at −80°C freezer until use. None of the patients or healthy controls were under any sort of treatment during sampling. Patients with coexisting neurological/systemic disorders or pregnancy were not included. Pooled IgG obtained from healthy individuals and sterile 0.9% NaCl solution (normal saline) were used as controls. Written consent was obtained from the patients to collect blood samples, and ethical approval was obtained from the Istanbul University Faculty of Medicine Clinical Research Ethics committee in order for the serum samples prepared from blood to be used for research purposes in the future (Ethical Approval Details - Project name: Investigation of autoantibodies in autoimmune subgroups of epilepsy patients. Issue: 408/2013).

Three pooled serum samples were obtained for NMDAR encephalitis, LGI1 encephalitis patients and healthy controls. IgG was isolated from pooled sera using a protein A-Sepharose CL-4B column (Sigma-Aldrich, St. Louis, Missouri, USA), as previously reported (11, 12). The IgG-containing solution was then dialyzed against PBS and filter sterilized. IgG isolation was confirmed by demonstration of IgG bands at the expected molecular weight range by gel electrophoresis. Protein concentrations of purified IgG solutions were measured by Bradford method. NMDAR- and LGI1-immunoreactivity of purified IgG was confirmed by cell-based assays (Euroimmun) (Supplementary Figure 1) and characteristic IgG-binding pattern of these samples was shown by indirect immunohistochemistry using frozen rat brain sections, as described previously (13, 14) (Supplementary Figure 2).

Stereotaxic surgery

Rats were anesthetized with ketamine; (100 mg/kg; i.p.) plus xylazine (10 mg/kg; i.p.) and placed into a stereotaxic frame. A guide cannula (C313G, Plastic's One Inc., Roanoke, VA), into the lateral ventricle, (AP:-0.8, ML:-1.5, V:-4.1 mm) (15) and recording electrodes over the left frontal (AP:+2, ML: ± 3.5mm) and occipital cortex (AP:-6, ML: ± 4 mm) were implanted then fixed in position by applying dental cement around. Rats were allowed a one-week recovery period before the start of the antibody infusions.

Intracerebroventricular (ICV) infusions

Animals were habituated for 20 min before infusions were performed through an internal cannula (C313I, Plastic's One Inc., Roanoke, VA) attached to a 10-µl Hamilton syringe then EEG was recorded for 2 hours following the antibody infusions. 5 µl of purified IgG from either NMDAR antibody-positive, LGI1 antibody-positive patients or healthy controls was slowly injected over 20 min into the right cerebral ventricle via a microinfusion pump. To ensure that the antibodies were fully delivered into the ventricle, the internal cannula was kept at the injection site for at least 10 min. An equal volume of sterile saline was also delivered at a rate of 5 µl/20min to another group of rats as negative control. Infusions were continued once every two days for ten days (Figure 1). At the end of the tenth day, each animal was delivered with a total of 25 µl of antibody pool, which was equivalent to approximately 150-225 µg of antibodies. Appropriate ventricular placement was assessed in randomly selected rats injecting 5 µl of 1% methylene blue through the internals inserted into the guide cannula. The methylene blue traces were examined in the ventricles system to confirm the injection locations (Figure 1D).

Seizure induction

To test seizure susceptibility, a subconvulsive (45 mg/kg) dose of pentylenetetrazol (PTZ; Sigma) was given intra-peritoneally (5, 16) and the rats were observed for 60 min while recording and observing PTZ-induced acute seizures. Seizures were classified according to the Racine scale (16) as follows: stage 1, behavioral arrest, chewing, and eye blinking; stage 2, stage 1 plus rhythmic head movements and head nodding; stage 3, unilateral forelimb clonus; stage 4, bilateral forelimb clonus and rearing; stage 5, falling and clonic convulsion. Seizure stage, stage 2 seizure duration, motor seizure duration and total seizure score were analyzed; the total seizure score was calculated at the end of the 10-min observation period, with a score of 2, 3, 4 or 5 given for each stage 2, 3, 4 or 5 seizure. The observation period was video recorded to allow subsequent video-EEG matching of observed events with EEG signatures.

10.3389/fimmu.2023.1268986

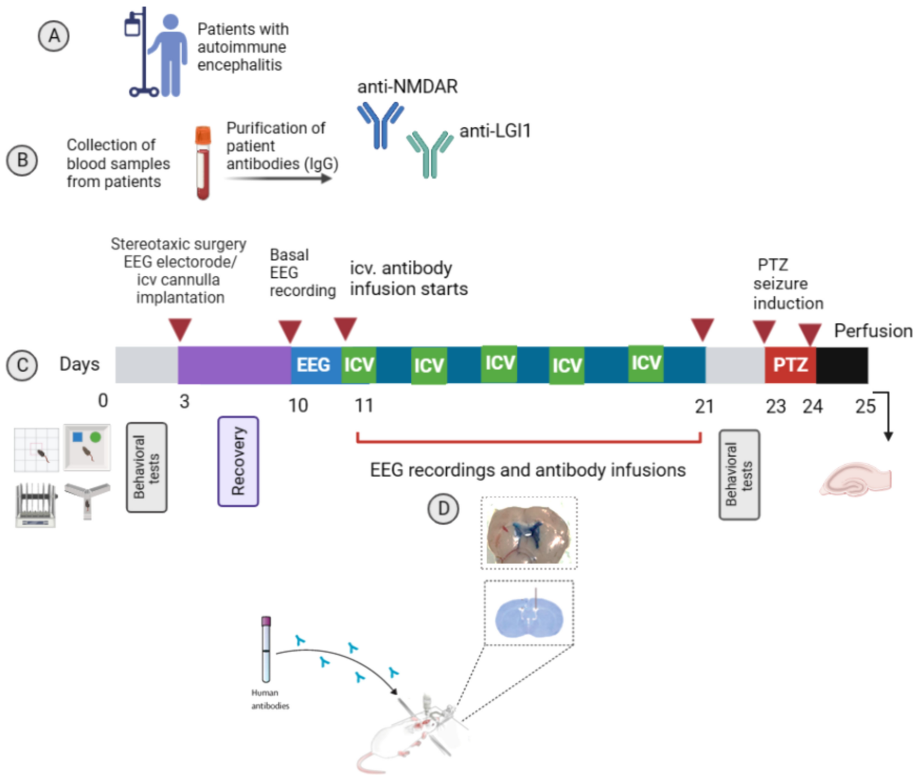

FIGURE 1
Experimental design. Experimental protocol to assess the role of NMDAR and LGI1 antibodies in in a passive transfer rat model of autoimmune encephalitis (AE). Model based on the autoantibodies obtained from blood samples of AE patients **(A)**. Total IgG obtained from the pooled sera of NMDAR and LGI1 antibody positive patients with epileptic seizures and healthy subjects was purified **(B)** and applied chronically every other day for 11 days into the cerebral lateral ventricle. Antibody infusions were performed on day 11, 13, 15 and 17 and 19 (as presented green labelled ICV). On days without infusion (10, 12, 14, 16, 18, 20th days, as presented blue). **(C)**. Spontaneous seizure development was followed by recording cortical electroencephalography (EEG) on consecutive days and after infusion administration for 2h. Behavioral tests for memory (novel object recognition test (NOR) and Y-maze) and locomotor activity (open field and rotarod tests) were applied to the animals before the antibody infusions started and at the end of the infusions. Then, pentylenetetrazole (PTZ) was administered at a convulsive dose (45 mg/kg) intraperitoneally in order to detect possible changes in seizure susceptibility. Immunohistochemistry was done for assessment of hippocampal astrocyte proliferation and expression intensity of target NMDAR and LGI1 antigens. Coronal brain section showing the appropriate ventricular placement of the guide cannullae **(D)**. Created with Biorender.com.

EEG acquisition and analysis of seizure patterns

EEG signals from the subdural screw electrodes were amplified through a BioAmp ML 136 amplifier, with band pass filter settings at 1–40 Hz, using Chart v7 program (PowerLab8S ADI Instruments, Oxfordshire, U.K). EEG was analyzed by observing the EEG trace and video recordings simultaneously to identify electrographic and behavioral seizures. Seizures were defined as rhythmic EEG activity lasting at least 5s or longer that exceeds the baseline amplitude by at least threefold.

Behavioral assays

Behavioral tests for memory (novel object recognition test (NOR) and Y-maze) and locomotor activity (open field and rotarod tests) were applied to the animals before the antibody infusions started (on day 0) and at the end (on days 21-23) of the ICV infusions (Figure 1; See Supplementary Method for detailed description). For all variables obtained by behavioral tests, percentage change of each variable after IgG infusion was calculated using the formula (after infusion – before infusion * 100). The percentage change values were compared among treatment arms by statistical analysis.

Immunohistochemistry

Immunohistochemical analysis was done to investigate whether LGI1 autoantibodies reduce the expression of their target antigen in a similar fashion as the NMDAR autoantibodies. Astrocytic activity was also assessed since previous studies have shown enhanced glial activity upon administration of AE samples (17, 18). At the end of the seizure induction protocol, rats were deeply anesthetized with sevoflurane and transcardially perfused with 0.1M phosphate-buffered saline (PBS). Isolated brains were post-fixed by immersion in 4% PFA for 1 h at 4°C, cryoprotected with 30%

sucrose for 24 h at 4°C before sectioning at 7 µm on cryostat. First, peroxidase blocking was performed with 0.3% H_2O_2 to brain sections for NMDAR and GFAP assays. After washing with PBS, the sections were blocked with 10% normal goat serum (NGS) in PBS for 1 hour. Then, sections were incubated in +4°C with anti-NMDAR-NR1 subunit (PA3-102, Thermo Fisher Scientific, US; 1:250), anti-LGI1 (ab30868, Abcam, US; 1:200); GFAP (GTX40996, GeneTex, US; 1:200) primary antibodies diluted in 5% NGS in PBS. Immunoreactivity of the commercial LGI1 antibody was tested by cell-based and immunofluorescence assays (Supplementary Figures 2, 3). After incubation, the sections were washed with PBS and incubated at room temperature with HRP-conjugated secondary antibodies for NMDAR and GFAP (ab6721, Abcam; 1:1000 and ab6789, Abcam; 1:500, respectively) and Alexa Fluor 488-conjugated secondary antibody for LGI1 (ab150077, Abcam, 1:500) assays diluted again in 5% NGS in PBS. After PBS washing, diaminobenzidine was added to the tissues to examine the immunoreactivity under microscope for NMDAR and GFAP assays. Counter-staining was done with hematoxylin (NMDAR and GFAP) or DAPI (4',6-diamidino-2-phenylindole) (LGI1). The images were processed using Image J (National Institutes of Health, Bethesda, MD). To ensure the diffusion of human antibodies in the hippocampus, frozen rat brain sections were incubated with biotinylated anti-human-IgG antibodies (Vector Laboratories, Newark, CA, USA), followed by the avidin-peroxidase and diaminobenzidine (19–21) (Supplementary Figure 4).

Statistical analysis

Statistical analysis was performed using Graphpad Prism 9.3 (GraphPad, La Jolla, CA). All quantitative data in the text and figures are expressed as mean ± SEM. The statistical tests were chosen alternatively depending on parametric distribution. Groups were compared by Mann-Whitney U or one-way analysis of variance (ANOVA) tests, as required. The percentage changes of behavioral parameters were evaluated between groups by one-way ANOVA or Kruskal-Wallis test. Tukey's or Dunn's multiple comparison test was used to compare the inter-group differences. For correlation analysis Pearson or Spearman correlation tests were used, as required. *p* values of < 0.05 were considered statistically significant.

Results

To determine whether patient-derived LGI1-IgG have a pathogenic role in epileptogenesis, we developed a passive transfer rat model in which we infused either pooled anti-LGI1 positive IgG (LGI1-IgG group, n=9) or pooled anti-NMDAR positive IgG (NMDAR-IgG group, n=8) containing total IgG obtained from blood samples of AE patients into the rat brain (Figure 1). We considered NMDAR group as positive control groups since the pathogenic effects are previously established (5, 8). Animals receiving total IgG collected form healthy individuals (HC-IgG, n=10) and saline (n=7) were considered as negative control groups. The animal model protocol is described in Methods and Figure 1. Briefly, total IgG obtained from the pooled sera of NMDAR and LGI1-IgG positive patients with epileptic seizures and healthy subjects was applied chronically every other day for 11 days into the cerebral lateral ventricle. Spontaneous seizure development was followed by electroencephalography. Behavioral tests for memory and locomotor activity were applied before and after the antibody infusions. PTZ was administered intraperitoneally to evaluate seizure susceptibility. Immunohistochemistry was performed for assessment of hippocampal astrocyte proliferation and expression intensity of target NMDAR and LGI1 antigens.

Seizure susceptibility increased upon administration of purified IgG in both LGI1-IgG and NMDAR-IgG groups

No spontaneous seizure activity was recorded during the antibody infusions as well as the 10 days of observation period of non-epileptic Wistar rats treated with anti-NMDAR and anti-LGI1 IgG containing total IgG, as reported in previous studies (5). 45 mg/kg PTZ injection produced seizures (stage 2 to stage 5) in all animals which were manually scored by a blinded observer. Seizure stage was significantly higher in the LGI1-IgG and NMDAR-IgG groups compared to HC-IgG and saline infused control groups ($F(2, 22) = 9.57$ $p<0.0001$; Figure 2A). One-way ANOVA followed by Tukey's multiple comparison test revealed that more severe stage 4 and 5 seizures were observed in the both antibody infused groups equally (mean seizure stage was 4.2 ± 0.27 for LGI1-IgG group; n=9 and 4.6 ± 0.18 for NMDAR-IgG group; n=8) compared to the HC (3.5 ± 0.22; n=10) and saline (2.8± 0.26; n=7) groups in which stage 3 seizures per animal was higher (Figure 2A). Motor seizure duration was higher in the NMDAR-IgG group (23.96 ± 1.8 s; n=8; Mann Whitney U $p = 0.017$) compared to the saline group (15.76± 1.4 s; Figure 2B). The total number of stage 2 seizures were higher in LGI1-IgG and NMDAR-IgG groups compared to negative control groups. This was significantly different in LGI1-IgG group (23.29 ± 4.8, Mann-Whitney U $p=0.04$) compared to HC-IgG group (11.38 ± 2.7; Figure 2C). Finally, the average seizure score calculated for the 10-min observation period following PTZ was higher in the LGI1 group (51.14 ± 9.7 Mann Whitney Figure p= 0.03) compared to saline group (versus 23.0 ± 6.0; Figure 2D). As shown in the traces sub-convulsive dose of PTZ induced more severe (stage 4 and 5) seizures with a higher number of brief stage 2 seizures consisting of spike-and-wave activity on the EEG that precedes convulsive seizures in NMDAR-IgG and LGI1-IgG groups (Figure 2E). This pattern was not observed in control animals those having mild stage 3 and 4 seizures.

Memory deficits were observed in animals treated with NMDAR and LGI1 auto-antibodies

In the open field test performed to measure motor functions, no significant difference was found between the groups in the parameters of distance, mean speed, max speed, time mobile, time immobile, time active and vertical activity ($p>0.05$)

10.3389/fimmu.2023.1268986

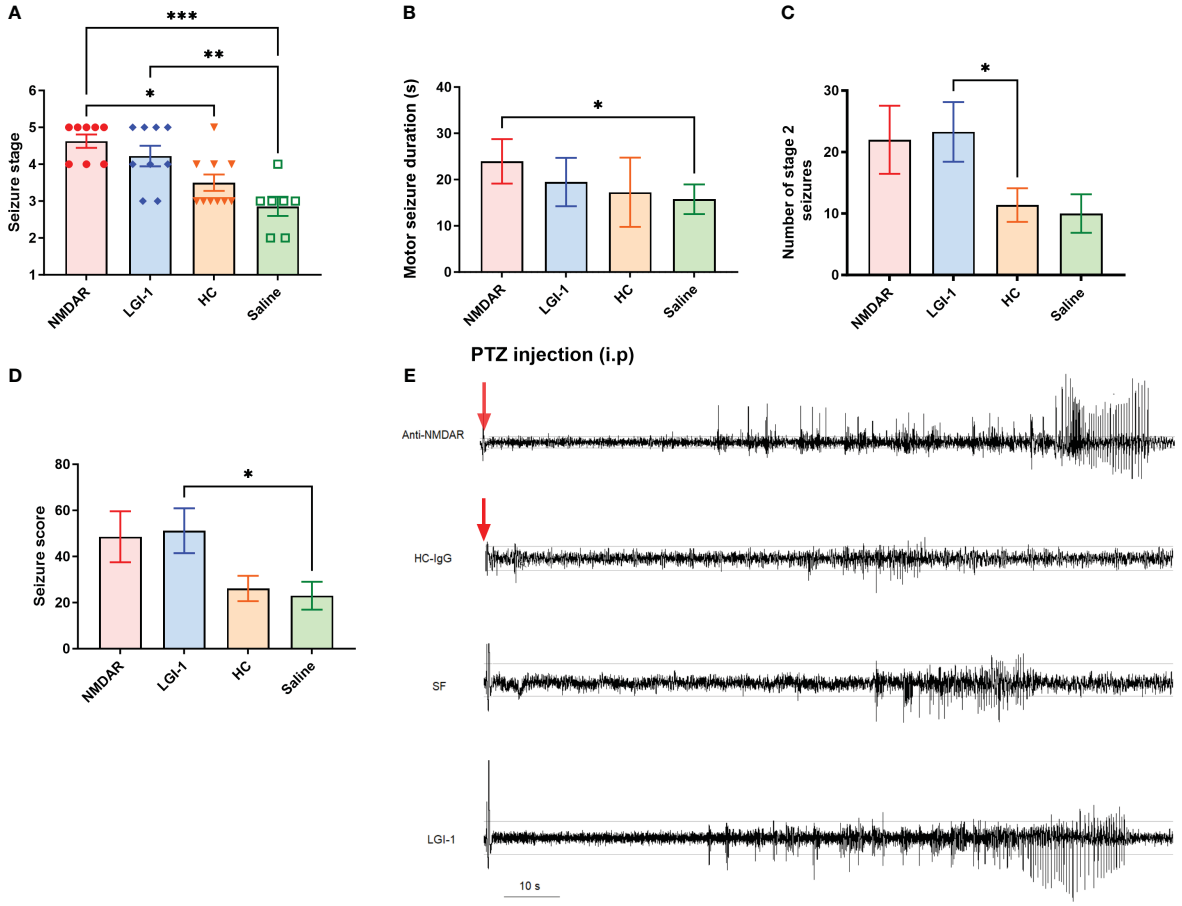

FIGURE 2
Administration of pooled IgG obtained from NMDAR and LGI1 encephalitis patients increased seizure susceptibility. Following i.p. injection of PTZ, seizure stage **(A)** was significantly higher in the NMDAR (n=8) and LGI1 (n=9) groups compared to healthy control- IgG (HC) (n=10) and saline infused control groups (n=7). Motor seizure duration **(B)** induced by acute PTZ administration was higher in NMDAR group compared to the saline infused control group. The total number of stage 2 seizures **(C)** were higher in auto-Ab groups compared to control groups. A higher total seizure score **(D)** was seen in the LGI1 group compared to saline group. **(E)** Representative EEG of ictal events recorded from a cortical electrode in animals receiving anti-NMDAR containing IgG, HC-IgG, saline and anti-LGI1 containing IgG. PTZ induced convulsive stage 4 and 5 seizures with a higher number of brief stage 2 seizures consisting of spike-and-wave activity on the EEG that precedes convulsive seizures in NMDAR and LGI1 Auto-Abs infused groups. Red arrow shows the PTZ injection time point. Horizontal guide lines show the 0.1 mV and -0.1 mV amplitude values of the EEG signal. Data were expressed as mean ± SEM. *p<0.05; **p<0.01; ***p<0.001.

(Figures 3A–G). Similarly, there was no difference in latency between groups in rotarod (Figure 3H) and total entries in Y-maze (Figure 4A) suggesting that the motor performance between groups did not differ (p>0.05). In addition, no difference was observed in the open field test in terms of anxiety parameters, time spent in the corner and time spent in center (p>0.05) (Figures 3I, J). However, the percentage of spontaneous alternation (Figure 4B) in the Y-maze test, which measures spatial memory, was statistically significantly lower in the NMDAR and LGI1 groups compared to the HC (p=0.0025; p=0.0063) and saline groups (p=0.0002; p=0.0005). Likewise, the time spent with the familiar object in the novel object recognition test, which measures recognition memory, was significantly higher in the NMDAR-IgG and LGI1-IgG groups than in the HC-IgG (p=0.0019; p=0.0024) and saline (p=0.0012; p=0.0015) groups, indicating poor memory (Figure 4C). Also, the time spent with the novel object was lower in the LGI1-IgG group than in both HC-IgG (p=0.0026) and saline groups (p=0.0264) (Figure 4D). Although the time spent with the novel object was found to be lower in NMDAR-IgG group compared to HC-IgG and saline groups, the significance could be only obtained for the HC-IgG group (p=0.0345). In addition, discrimination index indicating good memory performance, was found to be lower in NMDAR-IgG and LGI1-IgG groups than in the HC-IgG group (p=0.0253; p=0.0317, respectively) (Figure 4E). There was no significant difference between the saline group and the NMDAR/LGI1-IgG groups in terms of discrimination index (p>0.05) (Figure 4E). Moreover, a negative correlation was found between the seizure stage and the percentage of spontaneous alternation in the NMDAR-IgG group (r=-0.778; p=0.0394). No other significance could be obtained in the correlation analysis.

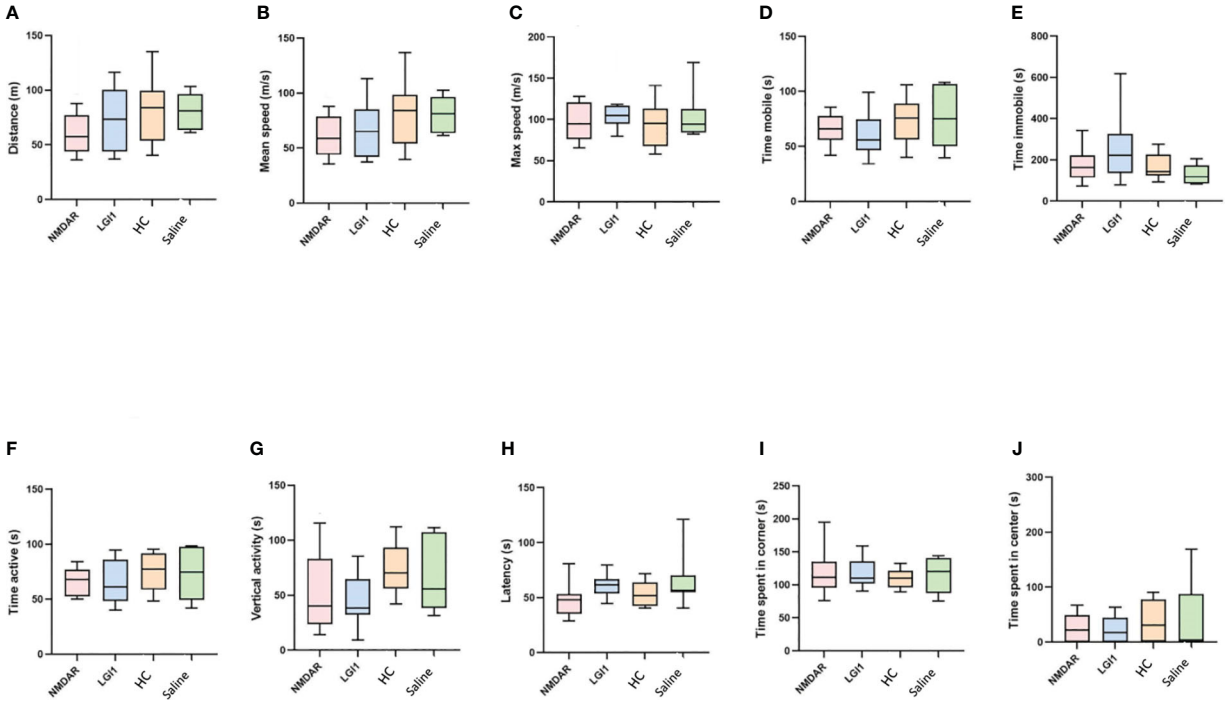

FIGURE 3
Motor functions did not change in the open field test following auto-antibody administration. In the open field test performed to measure motor functions, no significant difference was found between the groups in the parameters of distance **(A)**, mean speed **(B)**, max speed **(C)**, time mobile **(D)**, time immobile **(E)**, time active **(F)**, vertical activity **(G)** and latency **(H)** in rotarod test. In addition, no difference was observed in the open field test in terms of anxiety parameters, time spent in the corner **(I)** and time spent in center **(J)**. Data were expressed as mean ± SEM.

Antibody treatment induced astrocyte proliferation and NMDAR loss in the hippocampus

NMDAR- and LGI1-IgG-groups displayed robust human IgG binding on hippocampal sections as opposed to saline injected rat brains, which did not show appreciable human IgG staining (Supplementary Figure 4). Sections of hippocampus were stained for GFAP immunoreactivity and assessed for typical signs of astrocyte proliferation by morphological appearance (i.e. presence of thick tortuous processes and more intense staining) (Figure 5A). Such staining was observed only in hippocampus of rats treated with NMDAR- and LGI1 auto-Abs (Figure 5A, upper row). The intensity of hippocampal GFAP staining (as assessed by Image J software) was significantly higher in NMDAR- and LGI1 groups as compared to HC-IgG group (Figure 5B). The intensity of

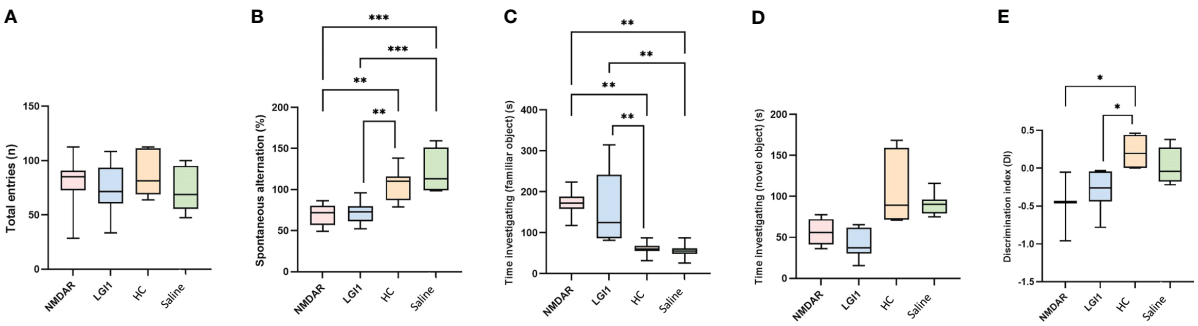

FIGURE 4
Memory deficits were observed in animals treated with NMDAR and LGI1 auto-antibodies. In the Y-maze test, total entries **(A)** was not different between groups. However, the percentage of spontaneous alternation **(B)** in the Y-maze test, which measures spatial memory, was statistically significantly lower in the NMDAR and LGI1 groups compared to the healthy control (HC) groups. In the open field test, time spent investigating familiar object **(C)** was lower however time spent investigating novel object **(D)** were significantly higher in NMDAR and LGI1 groups. Discrimination index **(E)** indicating good memory performance, was found to be lower in NMDAR and LGI1 groups. Data were expressed as mean ± SEM. *p<0.05; **p<0.01; ***p<0.001.

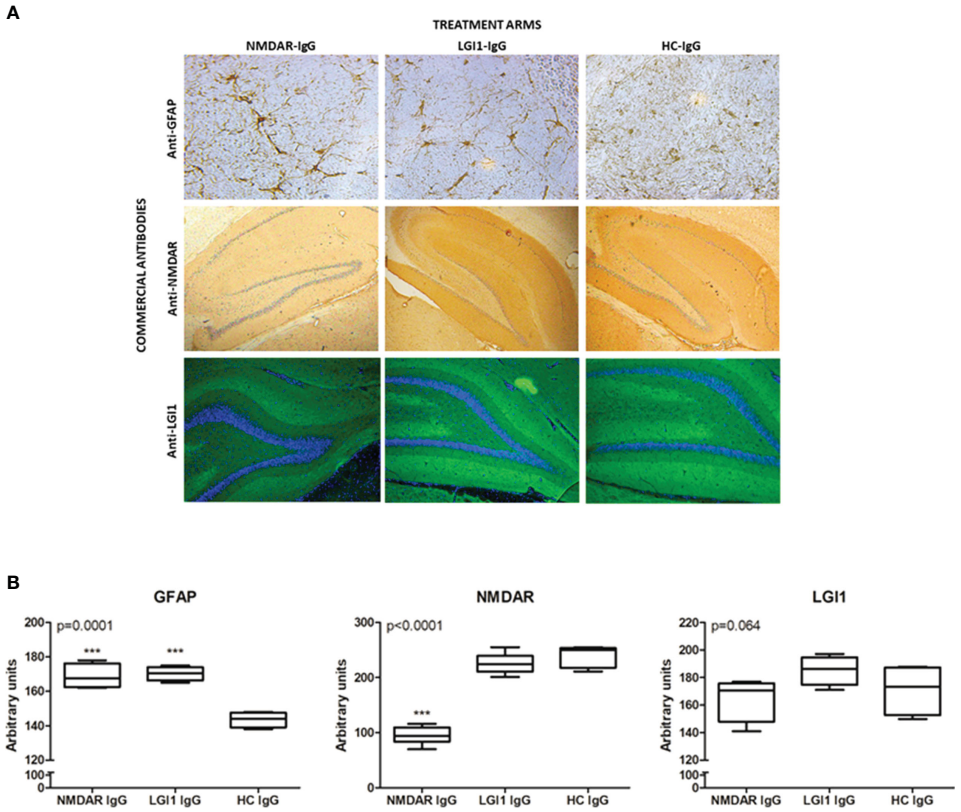

FIGURE 5
Antibody treatment induced astrocyte proliferation and NMDAR loss in the hippocampus Immunohistochemical staining of frozen sections **(A)** of rats treated icv with NMDAR-IgG (left column), LGI1-IgG (middle column) containing total serum IgG and healthy control (HC)-IgG (right column) using commercial antibodies directed against glial fibrillary acidic protein (anti-GFAP, upper row, brown color), anti-NMDAR (middle row, brown color) and anti-LGI1 (lower row, green color). Counter-staining was done with hematoxylin (blue color) in GFAP and NMDAR assays and DAPI (blue color) in LGI1 assays. Original magnification is 20x for upper row and 4x for middle and lower rows. Quantification of immunohistochemical stainings by Image J analysis **(B)**: GFAP, NMDAR and LGI1. Data were expressed as mean ± SEM p value denoted on the upper left corner of the panel is obtained by ANOVA; ***p<0.001 by Tukey's *post-hoc* test.

commercial anti-NMDAR antibody staining in the hippocampus was significantly decreased in rats injected with NMDAR-IgG, as compared to those injected with LGI1- IgG and HC-IgG, as expected (Figure 5A, middle row; Figure 5B). The intensity of commercial LGI1 antibody staining in the hippocampus was not significantly different among different treatment arms. However, LGI1-IgG group showed trends towards exhibiting increased hippocampal LGI1 expression than NMDAR-IgG and HC-IgG groups (Figure 5A, lower row; Figure 5B).

Discussion

In this study, we showed that passive transfer of purified IgG solutions containing NMDAR and LGI1 antibodies by ventricular infusion causes seizure susceptibility as well as memory deficits in rats. Our immunohistochemistry studies suggest that these clinical effects are likely mediated by reduced hippocampal NMDAR expression and enhanced astrocyte proliferation in the NMDAR-IgG group. Although astrocyte proliferation is also observed in the LGI1-IgG group exact molecular impact of LGI1 antibodies on the hippocampal synapses remain to be elucidated.

Several seizure-associated parameters depicted in Figure 2 were comparable among HC-IgG and saline groups suggesting that these findings represent the background impact of the sub-convulsive dose of PTZ. Seizure severity was significantly higher in the NMDAR-IgG and LGI1-IgG groups as compared to HC-IgG and saline groups only after PTZ treatment. Our findings are congruent with several animal model studies, which have shown that single or chronic injection of NMDAR-IgG and LGI1-IgG obtained from sera or CSF of AE patients does not cause seizures in the absence of an additional seizure precipitating agent (5, 23). Therefore, at least in our rat model, NMDAR-IgG and LGI1-IgG appear to reduce the threshold for seizure induction rather than directly influencing the occurrence of seizures. In other animal model studies, infusion of mice with patient-derived anti-NMDAR monoclonal antibodies (mAb), which exhibit very high epitope binding specificity, has caused seizures (but no behavioral symptoms) without PTZ administration (17, 18). Seizures have also been induced in mice treated with NMDAR-IgG containing CSF without PTZ (6). These

reports indicate that the seizure outcome in antibody-mediated animal models is determined by epitopes recognized by IgG of individual patients, the animal species used (mouse vs rat) and probably also the method by which IgG is administered.

AE associated with both NMDAR and LGI1 antibodies is typified with very high seizure prevalence (24). The seizure-inducing capacity of NMDAR- and LGI1-IgG might partially explain this seizure propensity. Clinical manifestations of AE are largely attributed to the intrathecally produced antibodies. Our study has shown that serum NMDAR/LGI1 auto-Abs generated in the secondary lymphoid organs may also contribute to the clinical symptoms if they gain access to the brain. Endogenous factors such as cytokines and inflammatory mediators found in circulation may putatively play role in fine-tuning and expression of cell-surface receptors thus leading to susceptibility to seizures and cognitive impairment in AE patients. Use of purified IgG in animal model induction largely excludes these putative non-IgG factors and emphasizes serum IgG as an important contributor of CNS findings of AE.

Our results confirm previous studies which have shown that administration of NMDAR-IgG positive serum and CSF may cause memory impairment, as demonstrated by maze and NOR experiments (8). We showed spatial and recognition memory impairment in rats in the absence of a significant alteration in motor activity and anxiety, suggesting that poor performance of NMDAR-IgG-administered rats in memory tests is not a bystander effect of the dysfunction of other cognitive and behavioral networks. Motor activity has been reported to remain intact in several previous animal models established by NMDAR-IgG (6, 17). Motor hyperactivity, seizures and lethargy have been reported in a single model using active immunization of immune competent mice with conformationally-stabilized, native-like NMDA receptors (25).

An intriguing finding was the correlation between spontaneous alternation scores and seizure stage, which cannot be attributed to PTZ that was administered after behavioral tests. This finding might be explained by affliction of common neuron groups (possibly located in the hippocampus) involved in both spatial memory and seizure induction. This argument is supported by the observation that intra-hippocampal kainate injection impairs both spatial memory and induces seizures in parallel in an animal model of epilepsy (26).

It has been well established that intrathecal administration of NMDAR-IgG reduces NMDAR expression (8). Treatment of hippocampal slices with NMDAR-IgG has been shown to diminish long-term potentiation (LTP) and increase neuronal excitability through reduced excitatory but not inhibitory neurotransmission. This finding suggests that NMDAR-IgG precipitates seizures by reducing NMDAR expression on inhibitory interneuronal populations (7). LGI1-IgG could also be inducing seizures via a similar mechanism since it is known to reduce AMPAR expression (9) However, in LGI1$^{-/-}$ mice, increased seizure activity has been linked to increased pre-synaptic glutamate release rather than altered post-synaptic AMPAR expression (27). Likewise, an ex vivo murine brain slice study has shown that LGI1-IgG treatment leads to increased glutamate release by hippocampal neurons (28). Increased glutamergic neurotransmission has also been shown in a passive transfer model of LGI1 encephalitis (9).

LGI1 encephalitis patients present quite frequently with seizures (24). Nevertheless, the precise pathogenic mechanisms of seizures remain understudied. In two former studies utilizing intraventricular or intracerebral infusions, administration of LGI1-IgG has failed to exert spontaneous motor seizures in the absence of PTZ administration (9, 23). Thus, the most novel finding of our study was induction of seizures in Wistar rats infused with anti-LGI1 bearing IgG solution and PTZ, which to the best of our knowledge has not been reported previously. Our results also corroborate previous electrophysiological experiments demonstrating neuronal hyperexcitability with increased glutamatergic transmission, higher presynaptic release probability and reduced synaptic failure rate upon minimal stimulation and severe impairment of long-term potentiation upon intracerebral administration of anti-LG11 IgG (23).

Our study also shows that both spatial and recognition memory are impaired in rats infused with anti-LGI1 containing IgG solution. This finding confirms a single study, which has shown impaired recognition memory by NOR in LGI1-IgG administered mice (9). As indicated in two previous studies, motor functions are not altered following anti-LGI1 treatment (9, 23).

Epileptic seizure is a common manifestation of both LGI1-antibody positive encephalitis and LGI1 mutations (29). Both inborn deficiency of LGI1 and downregulation of LGI1 by short-hair pin RNA (shRNA) lead to increased neuronal network hyperexcitability and impaired synaptic plasticity in rodents (27, 29). Moreover, LGI1 encephalitis patients and experimental animals with dendrotoxin-induced Kv1.1 inhibition show remarkably similar EEG features (22). However, our immunochemistry results suggest that anti-LGI1 containing IgG does not reduce hippocampal LGI1 expression and reduced LGI1 expression is not the underlying cause of seizures in our model. Patient serum-derived LGI1-IgG might facilitate seizures putatively through increased internalization of Kv1.1 potasium channels or impaired interaction between LGI1 and ADAM22/23 proteins. It is also possible that reduction of LGI1 expression in a relatively small but functionally critical number of hippocampal neurons might be causing seizures in IgG-injected mice.

Increased GFAP reactivity was the most striking pathological feature of both anti-NMDAR and anti-LGI1 administered rats, in our study. Mild glial activation and increased GFAP reactivity have been reported in passive transfer models conducted with infusion of anti-NMDAR containing IgG or patient-derived mAbs (6, 18). Given that NMDAR-IgG reduces cerebral NMDAR expression, these findings bring forward the question whether reduced astrocytic NMDAR expression might contribute to seizure induction and memory loss. As a matter of fact, astrocytic NMDAR expression has been linked to astrocyte activation in two former studies (30, 31). In our study, we show for the first time that LGI1-IgG infusion may also lead to astrocyte activation. Astrocytic glioma cells are known to express LGI1 (32). A recent combined immunofluorescence and mass spectrometry analyses has shown that LGI1 is putatively expressed by astrocytes in mouse hippocampus (33). Thus, the impact of LGI1-IgG on glial activation pends to be further studied.

PTZ is believed to act as an antagonist to $GABA_A$ receptor by directly blocking ionophores (34). PTZ increases seizure susceptibility in auto-Ab-injected rats putatively via this antagonistic activity. In support of our findings, dynamic causal modeling-mediated in depth analysis of EEG recordings of anti-NMDAR positive IgG administered animals suggests that NMDAR-Abs potentiate PTZ-induced effects in cortical microcircuitry (35). Similarly, several naturally occurring inflammatory factors that may be increased in AE (e.g. pro-inflammatory cytokines and chemokines) may putatively act as $GABA_A$ receptor antagonists and reduce seizure threshold. For example, TNF-α and CCL2 have been shown to reduce neuronal $GABA_A$ receptor expression (36, 37). Anti-GABAergic activity may also enhance cytotoxic T cell and macrophage responses (38). Therefore, $GABA_A$ receptor agonists may potentially be used in treatment of AE as seizure-preventing and anti-inflammatory agents (39).

A limitation of our study is that it does not exclude the impact of auto-Abs directed against non-NMDAR and non–LGI1 targets that may putatively exist in the patient-derived total IgG pools administered to rats. To overcome this limitation patient-derived mAbs interacting exclusively with the target epitopes of the NMDAR have already been produced and shown to induce seizures in animal models (17). A similar approach is recommended for LGI1 antibodies in future studies.

In brief, results of our passive transfer studies conducted in rats confirm the previously established pathogenic effects of anti-NMDAR-IgG and further shows for the first time that anti-LGI1-IgG positive total IgG solution is equally capable of inducing seizures with the additive assistance of PTZ. We have also shown that anti-LGI1 auto-Abs may be involved in spatial and recognition memory impairment and astrocyte proliferation. These findings provide *in vivo* pathogenic insights into neuronal dysfunction in LGI1 encephalitis. Furthermore, our results lend support for the putative ameliorative effects of agents preventing auto-Ab-LGI1 interaction and GABAergic agonists in autoimmune encephalitis.

Data availability statement

The original contributions presented in the study are included in the article/Supplementary Material. Further inquiries can be directed to the corresponding authors.

Ethics statement

The studies involving humans were approved by the Istanbul University Faculty of Medicine Clinical Research Ethics committee (Issue: 408/2013). The studies were conducted in accordance with the local legislation and institutional requirements. The participants provided their written informed consent to participate in this study.

The animal study was approved by the Animal Ethics Committee of Istanbul University (Ethics number:1107593). The study was conducted in accordance with the local legislation and institutional requirements.

Author contributions

ŞP: Formal Analysis, Investigation, Methodology, Project administration, Resources, Writing – original draft, Data curation. HY: Data curation, Formal Analysis, Investigation, Methodology, Software, Writing – original draft. CU: Data curation, Methodology, Writing – original draft, Resources. EŞ: Data curation, Formal Analysis, Software, Visualization, Writing – original draft. CK: Funding acquisition, Project administration, Writing – review & editing. FO: Conceptualization, Supervision, Writing – review & editing. ET: Conceptualization, Project administration, Resources, Supervision, Writing – original draft, Writing – review & editing. NÇ: Conceptualization, Supervision, Writing – review & editing, Formal Analysis, Funding acquisition, Investigation, Methodology, Project administration, Resources, Writing – original draft.

Funding

The author(s) declare financial support was received for the research, authorship, and/or publication of this article. This study was funded by Scientific Research Projects Coordination Unit of Istanbul University, Turkey (Grant number: TOA-2019-33449). The authors wish to thank Maya Jansis, Zerrin Kararaslan and Selen Çırak for their assistance during the data collection.

Conflict of interest

The authors declare that the research was conducted in the absence of any commercial or financial relationships that could be construed as a potential conflict of interest.

Publisher's note

Supplementary material

The Supplementary Material for this article can be found online at: https://www.frontiersin.org/articles/10.3389/fimmu.2023.1268986/full#supplementary-material.

References

1. Vora NM, Holman RC, Mehal JM, Steiner CA, Blanton J, Sejvar J. Burden of encephalitis-associated hospitalizations in the United States, 1998-2010. *Neurology* (2014) 82(5):443–51. doi: 10.1212/WNL.0000000000000086

2. Titulaer MJ, McCracken L, Gabilondo I, Armangué T, Glaser C, Iizuka T, et al. Treatment and prognostic factors for long-term outcome in patients with anti-NMDA receptor encephalitis: an observational cohort study. *Lancet Neurol* (2013) 12(2):157–65. doi: 10.1016/S1474-4422(12)70310-1

3. Dalmau J, Graus F. Antibody-mediated encephalitis. *N Engl J Med* (2018) 378 (9):840–51. doi: 10.1056/NEJMra1708712

4. Graus F, Titulaer MJ, Balu R, Benseler S, Bien CG, Cellucci T, et al. A clinical approach to diagnosis of autoimmune encephalitis. *Lancet Neurol* (2016) 15(4):391–404. doi: 10.1016/S1474-4422(15)00401-9

5. Wright S, Hashemi K, Stasiak L, Bartram J, Lang B, Vincent A, et al. Epileptogenic effects of NMDAR antibodies in a passive transfer mouse model. *Brain* (2015) 138(Pt 11):3159–67. doi: 10.1093/brain/awv257

6. Taraschenko O, Fox HS, Pittock SJ, Zekeridou A, Gafurova M, Eldridge E, et al. A mouse model of seizures in anti-N-methyl-d-aspartate receptor encephalitis. *Epilepsia* (2019) 60(3):452–63. doi: 10.1111/epi.14662

7. Wright SK, Rosch RE, Wilson MA, Upadhya MA, Dhangar DR, Clarke-Bland C, et al. Multimodal electrophysiological analyses reveal that reduced synaptic excitatory neurotransmission underlies seizures in a model of NMDAR antibody-mediated encephalitis. *Commun Biol* (2021) 4(1):1106. doi: 10.1038/s42003-021-02635-8

8. Planagumà J, Leypoldt F, Mannara F, Gutiérrez-Cuesta J, Martín-García E, Aguilar E, et al. Human N-methyl D-aspartate receptor antibodies alter memory and behaviour in mice. *Brain* (2015) 138(Pt 1):94–109. doi: 10.1093/brain/awu310

9. Petit-Pedrol M, Sell J, Planagumà J, Mannara F, Radosevic M, Haselmann H, et al. LGI1 antibodies alter Kv1.1 and AMPA receptors changing synaptic excitability, plasticity and memory. *Brain* (2018) 141(11):3144–59. doi: 10.1093/brain/awy253

10. Lalic T, Pettingill P, Vincent A, Capogna M. Human limbic encephalitis serum enhances hippocampal mossy fiber-CA3 pyramidal cell synaptic transmission. *Epilepsia* (2011) 52(1):121–31. doi: 10.1111/j.1528-1167.2010.02756.x

11. Cattoretti G, Schiró R, Orazi A, Soligo D, Colombo MP. Bone marrow stroma in humans: anti-nerve growth factor receptor antibodies selectively stain reticular cells *in vivo* and *in vitro*. *Blood* (1993) 81(7):1726–38. doi: 10.1182/blood.V81.7.1726.1726

12. Erdağ E, Şahin C, Küçükali C, Bireller S, Küçükerden M, Kürtüncü M, et al. Effects of *in vivo* and *in vitro* administration of neuro-Behcet's disease IgG. *Neurol Sci* (2017) 38(5):833–43. doi: 10.1007/s10072-017-2856-2

13. Vural B, Sehitoğlu E, Cavuş F, Yalçınkaya N, Haytural H, Küçükerden M, et al. Mitochondrial carrier homolog 1 (Mtch1) antibodies in neuro-Behçet's disease. *J Neuroimmunol* (2013) 263(1-2):139–44. doi: 10.1016/j.jneuroim.2013.08.007

14. Erdağ E, Emekli AS, Gündüz T, Küçükali C, Kürtüncü M, Tüzün E. Serum IgG of patients with relapsing inflammatory optic neuropathy immunoreacts with Sox2-positive glial cells of the optic nerve. *Mult Scler Relat Disord* (2023) 73:104694. doi: 10.1016/j.msard.2023.104694

15. Paxinos G, Watson C. *The rat brain in stereotaxic coordinate. 4 ed*. New York: Academic Press (1998).

16. Lüttjohann A, Fabene PF, van Luijtelaar G. A revised Racine's scale for PTZ-induced seizures in rats. *Physiol Behav* (2009) 98(5):579–86. doi: 10.1016/j.physbeh.2009.09.005

17. Taraschenko O, Fox HS, Eldridge E, Wang W, Dowd SW, Al-Saleem F, et al. Monoclonal antibodies from anti-NMDA receptor encephalitis patient as a tool to study autoimmune seizures. *Front Neurosci* (2021) 15:710650. doi: 10.3389/fnins.2021.710650

18. Taraschenko O, Fox HS, Zekeridou A, Pittock SJ, Eldridge E, Farukhuddin F, et al. Seizures and memory impairment induced by patient-derived anti-N-methyl-D-aspartate receptor antibodies in mice are attenuated by anakinra, an interleukin-1 receptor antagonist. *Epilepsia* (2021) 62(3):671–82. doi: 10.1111/epi.16838

19. Ekizoglu E, Tuzun E, Woodhall M, Lang B, Jacobson L, Icoz S, et al. Investigation of neuronal autoantibodies in two different focal epilepsy syndromes. *Epilepsia* (2014) 55(3):414–22. doi: 10.1111/epi.12528

20. Niehusmann P, Dalmau J, Rudlowski C, Vincent A, Elger CE, Rossi JE, et al. Diagnostic value of N-methyl-D-aspartate receptor antibodies in women with new-onset epilepsy. *Arch Neurol* (2009) 66(4):458–64. doi: 10.1001/archneurol.2009.5

21. Brenner T, Sills GJ, Hart Y, Howell S, Waters P, Brodie MJ, et al. Prevalence of neurologic autoantibodies in cohorts of patients with new and established epilepsy. *Epilepsia* (2013) 54(6):1028–35. doi: 10.1111/epi.12127

22. Baudin P, Whitmarsh S, Cousyn L, Roussel D, Lecas S, Lehongre K, et al. Kv1.1 channels inhibition in the rat motor cortex recapitulates seizures associated with anti-LGI1 encephalitis. *Prog Neurobiol* (2022) 213:102262. doi: 10.1016/j.pneurobio.2022.102262

23. Baudin P, Roussel D, Mahon S, Charpier S, Navarro V. *In vivo* injection of anti-LGI1 antibodies into the rodent M1 cortex and hippocampus is ineffective in inducing seizures. *eNeuro* (2023) 10(3). doi: 10.1523/ENEURO.0267-22.2023

24. Spatola M, Dalmau J. Seizures and risk of epilepsy in autoimmune and other inflammatory encephalitis. *Curr Opin Neurol* (2017) 30(3):345–53. doi: 10.1097/WCO.0000000000000449

25. Jones BE, Tovar KR, Goehring A, Jalali-Yazdi F, Okada NJ, Gouaux E, et al. Autoimmune receptor encephalitis in mice induced by active immunization with conformationally stabilized holoreceptors. *Sci Transl Med* (2019) 11(500). doi: 10.1126/scitranslmed.aaw0044

26. Kiasalari Z, Khalili M, Shafiee S, Roghani M. The effect of Vitamin E on learning and memory deficits in intrahippocampal kainate-induced temporal lobe epilepsy in rats. *Indian J Pharmacol* (2016) 48(1):11–4. doi: 10.4103/0253-7613.174394

27. Boillot M, Lee CY, Allene C, Leguern E, Baulac S, Rouach N. LGI1 acts presynaptically to regulate excitatory synaptic transmission during early postnatal development. *Sci Rep* (2016) 6:21769. doi: 10.1038/srep21769

28. Romoli M, Krashia P, Sen A, Franciotta D, Gastaldi M, Nobili A, et al. Hippocampal epileptogenesis in autoimmune encephalitis. *Ann Clin Transl Neurol* (2019) 6(11):2261–9. doi: 10.1002/acn3.50919

29. Lugarà E, Kaushik R, Leite M, Chabrol E, Dityatev A, Lignani G, et al. LGI1 downregulation increases neuronal circuit excitability. *Epilepsia* (2020) 61(12):2836–46. doi: 10.1111/epi.16736

30. Montes de Oca Balderas P, Aguilera P. A metabotropic-like flux-independent NMDA receptor regulates Ca2+ Exit from endoplasmic reticulum and mitochondrial membrane potential in cultured astrocytes. *PloS One* (2015) 10(5):e0126314. doi: 10.1371/journal.pone.0126314

31. Sühs KW, Gudi V, Eckermann N, Fairless R, Pul R, Skripuletz T, et al. Cytokine regulation by modulation of the NMDA receptor on astrocytes. *Neurosci Lett* (2016) 629:227–33. doi: 10.1016/j.neulet.2016.07.016

32. Besleaga R, Montesinos-Rongen M, Perez-Tur J, Siebert R, Deckert M. Expression of the LGI1 gene product in astrocytic gliomas: downregulation with Malignant progression. *Virchows Arch* (2003) 443(4):561–4. doi: 10.1007/s00428-003-0874-3

33. Ramirez-Franco J, Debreux K, Extremet J, Maulet Y, Belghazi M, Villard C, et al. Patient-derived antibodies reveal the subcellular distribution and heterogeneous interactome of LGI1. *Brain* (2022) 145(11):3843–58. doi: 10.1093/brain/awac218

34. Kalueff AV. Mapping convulsants' binding to the GABA-A receptor chloride ionophore: a proposed model for channel binding sites. *Neurochem Int* (2007) 50 (1):61–8. doi: 10.1016/j.neuint.2006.07.004

35. Rosch RE, Wright S, Cooray G, Papadopoulou M, Goyal S, Lim M, et al. NMDA-receptor antibodies alter cortical microcircuit dynamics. *Proc Natl Acad Sci U S A.* (2018) 115(42):E9916–e25. doi: 10.1073/pnas.1804846115

36. Gosselin RD, Varela C, Banisadr G, Mechighel P, Rostene W, Kitabgi P, et al. Constitutive expression of CCR2 chemokine receptor and inhibition by MCP-1/CCL2 of GABA-induced currents in spinal cord neurones. *J Neurochem* (2005) 95(4):1023–34. doi: 10.1111/j.1471-4159.2005.03431.x

37. Pribiag H, Stellwagen D. TNF-α downregulates inhibitory neurotransmission through protein phosphatase 1-dependent trafficking of GABA(A) receptors. *J Neurosci* (2013) 33(40):15879–93. doi: 10.1523/JNEUROSCI.0530-13.2013

38. Tian J, Kaufman DL. The GABA and GABA-receptor system in inflammation, anti-tumor immune responses, and COVID-19. *Biomedicines* (2023) 11(2). doi: 10.3390/biomedicines11020254

39. Bouwman BM, Suffczynski P, Midzyanovskaya IS, Maris E, van den Broek PL, van Rijn CM. The effects of vigabatrin on spike and wave discharges in WAG/Rij rats. *Epilepsy Res* (2007) 76(1):34–40. doi: 10.1016/j.eplepsyres.2007.06.006

frontiers | Frontiers in Immunology

TYPE Case Report
PUBLISHED 22 December 2023
DOI 10.3389/fimmu.2023.1285822

OPEN ACCESS

EDITED BY
Luis Querol,
Hospital de la Santa Creu i Sant Pau, Spain

REVIEWED BY
Keigo Ikeda,
Juntendo University Urayasu Hospital, Japan
Satoshi Hara,
Kanazawa University, Japan

*CORRESPONDENCE
Hongju Zhang
zhangcally@126.com

RECEIVED 30 August 2023
ACCEPTED 23 November 2023
PUBLISHED 22 December 2023

CITATION
Wei Q, Qi H, Wei H, Wang X and Zhang H (2023) IgG4-related disease with massive pericardial effusion diagnosed clinically using FDG-PETCT: a case report. *Front. Immunol.* 14:1285822. doi: 10.3389/fimmu.2023.1285822

IgG4-related disease with massive pericardial effusion diagnosed clinically using FDG-PETCT: a case report

Qiaofeng Wei[1], Huili Qi[1], Hongmei Wei[2], Xiuhua Wang[3] and Hongju Zhang[1]*

[1]Department of Rheumatology, Zibo Central Hospital, Shandong, Zibo, China, [2]Huaqiaocheng Clinic, Zibo Central Hospital, Shandong, Zibo, China, [3]Department of Rheumatology and Autoimmunology, The First Affiliated Hospital of Shandong First Medical University, Shandong Provincial Qianfoshan Hospital, Jinan, Shandong, China

Background: IgG4-related disease (IgG4-RD) is a systemic inflammatory disease which involves various organs such as the pancreas, lacrimal gland, salivary gland, retroperitoneum, and so on. These organs can be affected concomitantly. 18-Fluorodeoxyglucose positron emission tomography computed tomography (FDG-PETCT) is a systemic examination which can identify active inflammation and detect multiple organ involvement simultaneously. Pericardial involvement is rare in IgG4-RD, early detection and treatment can greatly improve the prognosis of patients.

Case summary: We reported a 82-year-old female patient referred to our department complaining of chest tightness and abdominal fullness for 8 months and massive pericardial effusion for 2 months. A large amount of pericardial effusion was found during the hospitalization of Gastroenterology. Then she was transferred to cardiology. Although infectious, tuberculous, and neoplastic pericardial effusions were excluded, there was still no diagnosis. The patients were examined by FDG-PETCT which considered IgG4-RD. After coming to our department, the results of the patient's laboratory tests showed that immunoglobulin subgroup IgG4 was 14.0 g/L. Then we performed a biopsy of the right submandibular gland. Pathological morphology and immunohistochemistry suggested IgG4-RD. Combined with level of IgG4, clinical, pathological and immunohistochemical results, we determined the final diagnosis of IgG4 related diseases. Then we gave glucocorticoid and immunosuppressant treatment. At the end, pericardial effusion was completely absorbed. As prednisone acetate was gradually reduced, no recurrence of the disease has been observed.

Conclusion: Pericardial effusion can be the initial presentation in IgG4-RD. For patients with massive pericardial effusion of unknown cause, early detection of IgG4 is recommended, and PETCT may be helpful for obtaining the diagnosis.

KEYWORDS

pericardial effusion, IgG4-related disease, FDG-PETCT, prognosis, treatment

1 Introduction

IgG4-related disease (IgG4-RD) is a systemic autoimmune disease with unknown etiology (1–3). The main characteristics of the disease are elevated serum IgG4 concentrations, marked lymphoplasmacytic infiltration, storiform fibrosis, and organ infiltration by IgG4-positive plasma cells. IgG4-RD may be present in a certain percentage of patients with various diseases including autoimmune pancreatitis, Mikuliçz's disease (MD), Küttner's tumor (KT), retroperitoneal fibrosis, Riedel's thyroiditis, hypophysitis, interstitial pneumonitis, interstitial nephritis, prostatitis, lymphadenopathy, inflammatory aortic aneurysm, and inflammatory pseudotumor (4). Although there are some reports about IgG4-RD cases complicated with cardiovascular system, it is rare to have pericardial effusion as the main manifestation (5–7). We herein report a case of IgG4-RD that mainly manifested as massive pericardial effusion, and 18-Fluorodeoxyglucose positron emission tomography computed tomography (FDG-PETCT) first suggested that it was IgG4-RD.

2 Case presentation

2.1 Chief complaints

An 82-year-old female patient was referred to our department complaining of chest tightness and abdominal fullness for 8 months, with massive pericardial effusion for 2 months.

2.2 History of present illness

Eight months prior, the patient developed chest tightness and abdominal distension, which worsened over time. She was admitted to the gastroenterology ward of our hospital. Chest CT showed a large amount of pericardial effusion and a small amount of bilateral pleural effusion. Then, the patient was transferred to the cardiology department for further treatment. Relevant laboratory tests and inspections were performed, but no cause was found. After diuretic treatment, the patient's symptoms were gradually relieved, and echocardiography showed that pericardial effusion slightly decreased, and she was discharged. The patient underwent an FDG-PETCT examination at Shibo High Tech Hospital, which showed that pericardial effusion might be related to IgG4-RD. The patient was given an over-the-counter diuretic that contained furosemide and spironolactone. Later, the above symptoms reappeared and gradually worsened, and the patient attended our department for further treatment.

2.3 History of past illness

She had binocular cataract surgery one year ago.

2.4 Physical examination

The patient had a temperature of 36.5°C, a blood pressure of 128/84 mmHg, a pulse of 95 beats per minute, a respiratory rate of 18 breaths per minute, and a finger oxygen saturation of 95%. Cardiac percussion (cardiac dullness) revealed an enlarged area, and a low and dull sound was heard on auscultation. The patient also showed mild pretibial pitting edema. The rest of the physical examination was unremarkable.

2.5 Laboratory examinations

In the department of gastroenterology of our hospital, the results of the patient's laboratory tests showed that the erythrocyte sedimentation rate (ESR) was 67.0 mm/h, D-dimer was 6.42mg/L FEU, brain natriuretic peptide (BNP) was 649ng/ml, total protein was 72.6 g/L, globulin was 35.3g/L, albumin was 35.3 g/L, and immunoglobulin (IgG) was 19.0 g/L. Blood cultures, PPD, T-spot, antinuclear antibody, and extractable nuclear antigen antibody spectrum were all negative. Routine blood tests, routine biochemical tests, thyroid function, tumor markers, coagulation series, pre-transfusion tests, myocardial markers, and routine and urinary tests revealed no significant abnormality.

Some investigations were repeated while the patient was admitted to the rheumatology and immunology department of our hospital. ESR was 29.0 mm/h, D-dimer was 1.86mg/L FEU, BNP was 486ng/ml, total protein was 74.6 g/L, globulin was 35.9g/L, albumin was 38.7 g/L, IgG was 17.2g/L, immunoglobulin subtype 4 (IgG4) was 14.0g/L, complement C3, complement C4, C-reactive protein (CRP), and rheumatoid factors were normal. Antinuclear antibody, antineutrophil cytoplasmic antibody, anti-cyclic citrate peptide antibody, and anti-phospholipid antibody were all negative.

2.6 Imaging examinations

In the department of gastroenterology of our hospital, chest computed tomography (CT) showed a large amount of pericardial effusion and a small amount of bilateral pleural effusion, with multiple small nodules in both lungs (Figures 1A, C). Echocardiography revealed a large amount of fluid in the pericardial cavity. The depth of the posterior wall of the left ventricle was 16mm, the depth of the anterior wall of the right ventricle was 14mm, the depth of the left ventricle wall was 17mm, and the depth of the right atrial roof was 16mm. Thyroid ultrasound showed multiple thyroid nodules TI-RADS-3, swollen lymph nodes on the right side of the neck. Submandibular gland ultrasound showed that large low echo nodules can be detected in the submandibular gland, with clear boundaries, less uniform internal echoes, and blood flow signals. (Figure 2). Abdominal ultrasound displayed no obvious abnormalities. Echocardiography showed moderate fluid accumulation in the pericardial cavity. The depth of the posterior wall of the left ventricle was 11.9mm, and the depth of the left ventricle wall was 14mm. Furthermore, PETCT showed moderate pericardial effusion, which was in accordance with the increased area of FDG uptake, with a maximum SUV of 5.04mm. Bilateral pharyngeal tonsils and submandibular glands manifested symmetrically increased FDG uptake. Moreover, small lymph nodes were observed at the right side of the sternal bone, and the

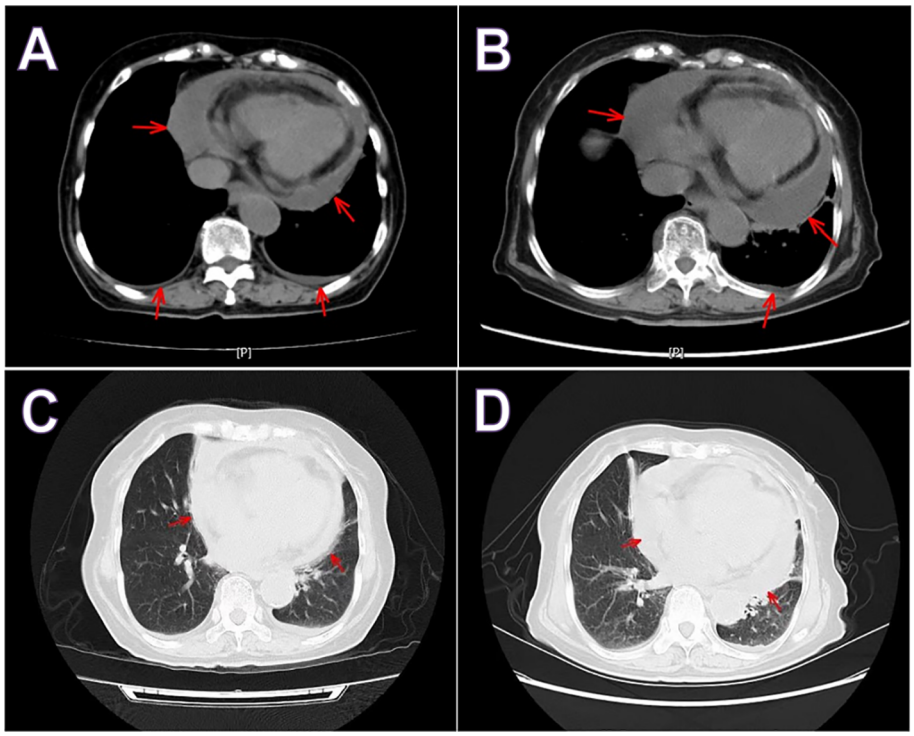

FIGURE 1
Chest computed tomography hospitalizations in gastroenterology **(A, C)** and rheumatology **(B, D)**. Both showed a large amount of pericardial effusion and a small amount of pleural effusion. Red arrow indicate pericardial effusion.

mediastinum and the wall of the ascending aorta all showed increased metabolism (Figure 3).

In the rheumatology department, chest CT showed a large amount of pericardial effusion and a small amount of left pleural effusion, multiple small nodules in both lungs, and disseminated inflammation of the middle lobe of the right lung and the lower lobes of both lungs (Figures 1B, D). The electrocardiogram showed a sinus rhythm, low T-wave, and increased left atrial load. Echocardiography showed a large amount of fluid in the pericardial cavity. The depth of the posterior wall of the left ventricle was 13mm, the depth of the anterior wall of the right ventricle was 10mm, the depth of the left ventricle wall was 10mm, the depth of the apex was 13mm, and the depth of the right atrial roof was 11mm. Three days after admission, a biopsy of the right submandibular gland was performed (Figure 4).

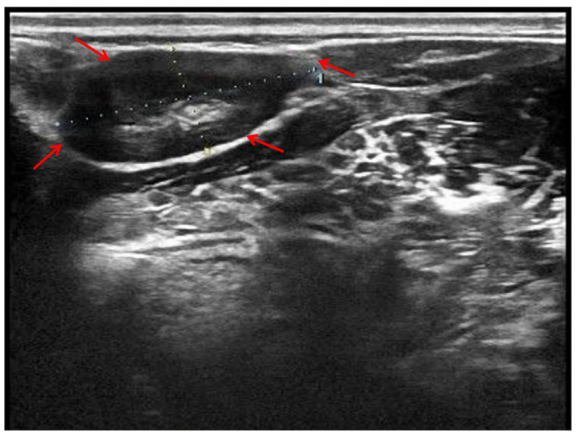

FIGURE 2
Submandibular gland ultrasound showed that large low echo nodules can be detected, with clear boundaries, less uniform internal echoes, and blood flow signals. Red arrow indicates the submandibular gland nodules.

3 Final diagnosis

The final diagnosis of the presented case was IgG4-RD.

4 Treatment

Treatment with 40 mg methylprednisolone and 1000 mg mycophenolate mofetil per day was initiated. After 2 weeks, pericardial effusion was significantly reduced, ESR, BNP, IgG, and IgG4 were decreased. 13 days after admission, echocardiography showed a small amount of fluid in the pericardial cavity. the depth of the anterior wall of the right ventricle was 4mm, the depth of the apex was 5mm. The patient's condition gradually improved.

5 Outcome and follow-up

She did regular outpatient review after discharge. Echocardiography showed that pericardial effusion was

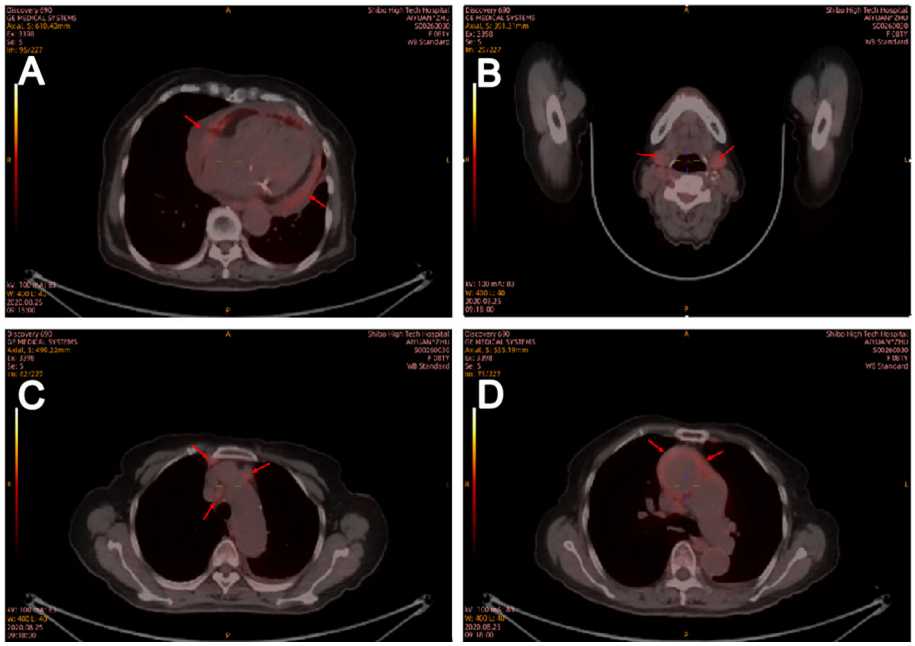

FIGURE 3
Positron emission tomography computed tomography on August 25, 2020. Positron emission tomography computed tomography showed that medium pericardial effusion which corresponding to an increased area of FDG uptake **(A)**. Bilateral pharyngeal tonsil, submandibular gland **(B)**, small lymph nodes in the right side of sternal bone and mediastinum **(C)** and the wall of ascending aorta **(D)** all showed increased metabolism. Red arrow indicates positron emission tomography (CT) scans showing an increase in FDG uptake area in the central envelope effusion.

significantly reduced on 15 days after discharge, and completely absorbed on 2 months after discharge. We reduced the amount of prednisone acetate progressively, and the serum levels of IgG4 gradually decreased. No recurrence of pericardial effusion has been observed in the past year. At present, she was treated with 2.5 mg prednisone per day.

6 Discussion

IgG4-RD is a systemic autoimmune-mediated fibroinflammatory disorder. In 2001, Hamano et al. (8) reported elevated levels of serum IgG4 in patients with autoimmune sclerosing pancreatitis, and the concept of IgG4-related disease was proposed. Subsequently, Yamamoto et al. (9) identified elevated concentrations of serum IgG4 and the prominent infiltration of IgG4-bearing plasma cells into lacrimal and salivary glands in Mikulicz's disease (MD), which differed from Sjögren syndrome. Therefore, MD and autoimmune pancreatitis are believed to be related. Then, IgG4-related disease was found to cause inflammation and fibrosis in many other organs (4, 10). In 2012, the first comprehensive clinical diagnostic criteria of IgG4-RD was published (11): ① one or more characteristic diffuse/localized swellings or masses in organs. ② elevated serum IgG4 concentrations (>135mgdl). ③ marked lymphocyte and plasma cell infiltration and fibrosis, infiltration of IgG4+ plasma cells, and IgG4+/IgG+ cell ratio of >40%, and>10 IgG4+ plasma cells/HPF in histopathological examination. Patients who meet the above conditions can be diagnosed as IgG4-RD. For patients with① and ②, or ① and ③, there is a possibility of IgG4-RD. Our case mainly manifested with massive pericardial effusion, showing a serum IgG4 concentration of 14.0g/L. Considering pathological and immunohistochemical results, the patient was diagnosed with IgG4-RD.

Previously, IgG4-RD was believed to be caused by T helper (Th) 2 cells, but this theory has been completely disproved (12, 13). Only IgG4-RD patients with atopic syndrome have circulating Th2 memory cells (14). The discovery of CD4+ cytotoxic T cells in IgG4-RD may be a major breakthrough in pathophysiological research. CD4+T cells are widely distributed in IgG4-RD lesions and constitute the most common cells in the affected tissues. Clonal expansion of CD4+ cytotoxic T cells is found in the peripheral blood and fibrotic lesions of IgG4-RD patients, indicating that these cells play a crucial role in its pathogenesis (15). In addition, these cells produce IL-1, transforming growth factor (TGF-β), and interferon-gamma, which are all important mediators of fibrosis, constituting the main histopathological manifestation of IgG4-RD. The signaling lymphocytic activation module F7(SLAMF7) is expressed on the surface of CD4+ cytotoxic T cells and has not been previously identified on CD4+T cells (16). After glucocorticoid-induced remission of IgG4-RD, such CD4+ cytotoxic T cells were also reduced (17). In addition, Tfh cells mainly exist in and around the germinal centers of lymph nodes and are also increased in the peripheral blood and affected tissues of IgG4-RD patients. Meanwhile, Tfh cells promote the proliferation and differentiation of B cells (18). Follicular regulatory T cells and Tfh cells regulate germinal center formation and B-cell class conversion (19).

IgG4-RD occurs in a variety of organs, including the pancreas, bile duct, retroperitoneum, lacrimal gland, salivary gland, pituitary gland, prostate, lung, heart, kidney, aorta, and thyroid gland. The

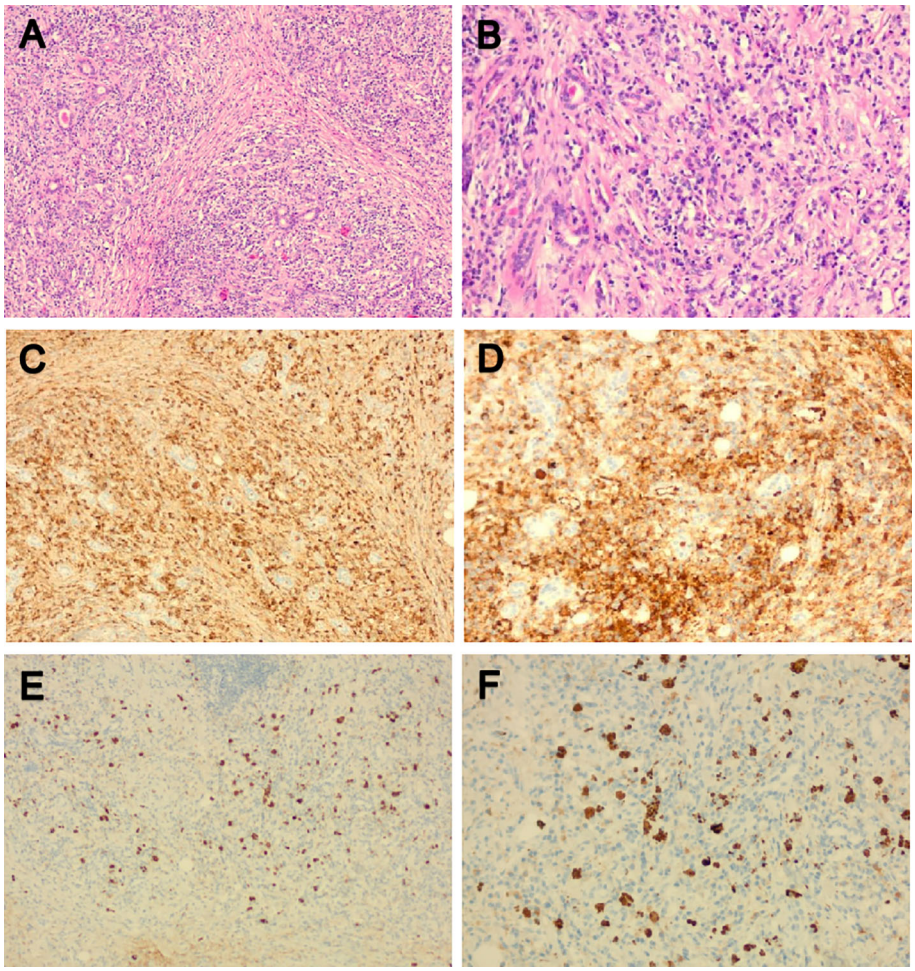

FIGURE 4
Pathological morphology and immunohistochemistry of the right submandibular gland. **(A, B)** HE showed hyperplasia of interstitial fibrous tissue and lymphoid tissue hyperplasia, formation of lymphoid follicle, infiltration of a large amount of lymphocyte and scattered plasma cells and eosinophils; **(C, D)** Immunoglobulin (Ig) G positive plasma cells could be seen by immunohistochemical staining; **(E, F)** IgG4-positive plasma cells could be seen by immunohistochemical staining; The IgG4/IgG ratio was greater than 40%. HE, Hematoxylin and eosin stain; Ig, Immunoglobulin.

condition may be misdiagnosed as malignancy, infection, inflammatory disorders, or other immune-mediated disease (20). IgG4-related cardiovascular lesions include aortitis, arteritis, periaortitis, periarteritis, pericarditis, and inflammatory aneurysm (21). To our knowledge, only a few reports have described concurrent IgG4-RD and pericardial effusion. Generally, patients with acute massive pericardial effusion show hemodynamic changes. However, patients with chronic pericardial effusion have relatively stable vital signs (22). Similar to previous case reports, our patient showed no obvious hemodynamic abnormalities, despite a large amount of pericardial effusion. However, this patient's blood pressure and heart rate were normal and the main symptoms were chest tightness and abdominal fullness. Therefore, pericardial effusion can be the initial presentation in IgG4-RD, and IgG4-associated pericarditis is mostly followed by a chronic course. Nevertheless, the atypical presentation with cardiac and pleural effusion might have led to a misdiagnosis, and failure to administer timely treatment might have resulted in a fatal outcome due to respiratory insufficiency (23).

FDG-PETCT is a commonly used auxiliary diagnostic method for cases with challenging diagnoses. Ozaki et al. revealed that the maximum standardized uptake value (SUV) did not differ significantly in either the early or delayed phase between AIP and pancreatic cancer, but they found multifocal inflammation of the pancreas in AIP, and uptake of FDG by the lacrimal gland, salivary gland, biliary duct, retroperitoneal space, and prostate, which could not be attributed to pancreatic cancer (15). Zhang J et al. (16) reported that FDG-PETCT allowed the detection of the involvement of a greater number of organs compared to conventional evaluations such as physical examination, ultrasonography, and CT. Furthermore, FDG-PETCT demonstrated specific image characteristics and patterns of IgG4-RD. Berti et al. (17) observed that circulating plasmablasts in the serum of IgG4-RD were positively correlated with SUV corrected for partial volume effect (PVC-SUV) and inversely correlated with the total lesion glycolysis (TLG), and found a corresponding reduction in circulating plasmablasts, PVC-SUV, and TLG after immunosuppressive therapies. In the present case, FDG-PETCT

indicated that the pericardial effusion of the patient might be due to IgG4-RD. Due to advanced age, the patient refused to perform pericardiocentesis. FDG-PETCT also showed a high uptake of the submandibular gland in the patient, and submandibular gland ultrasound showed that large low echo nodules can be detected, with clear boundaries, less uniform internal echoes, and blood flow signals, which was consistent with diffuse low-echo areas (rock type) multiple low-echoic nodules surrounded by high-echoic linear shadows (cobblestone pattern)reported in previous studies (24, 25). Finally, the patient was diagnosed with IgG4-RD and received the appropriate treatment. Therefore, FDG-PETCT assists in the detection of the extent of organ involvement and the selection of the biopsy site. Moreover, it can also monitor the treatment efficacy in IgG4-RD (18).

Previous literature has also shown that imaging is beneficial in the diagnosis of IgG4-RD-related diseases with pericardial effusion (5, 26, 27). One study reported the case of a 73-year-old Asian man with progressive forced dyspnea, systemic edema, and pericardial effusion. Positron emission tomography and FDG-PETCT revealed an inflammatory focus in the pericardium. Pericardial biopsy revealed IgG4-RD pericarditis (26). Another case report described a 53-year-old woman who attended the hospital due to general discomfort for 6 months, exhibiting significant weight loss and chest discomfort. The patient then underwent cardiac MRI (CMRI) for further evaluation. This shows a marked thickening of the pericardium and active inflammation. The late gadolinium enhancement (LGE) showed extensive circumferential LGE in the pericardium and non-coronary distribution of the left ventricle with subendocardial linear LGE. The final diagnosis was myocardial infarction caused by IgG4-RD (27). The study by Seshika Ratwatte et al. (5) focused on three patients who demonstrated cardiovascular manifestations of IgG4-RD, as well as the shortcomings and importance of early diagnosis. Two cases developed cardiac manifestations before more typical organ systems were affected, leading to delayed diagnosis. Case 1 presented with acute myocardial infarction secondary to IgG4-RD, with CT coronary angiography revealing that the surrounding soft tissue mass involved the anterior descending and left anterior descending branches. In case 2, pericarditis progressed to pericardium contraction due to IgG4-RD. CT coronary angiography showed significant pericardium thickening, but no obstructive coronary artery stenosis or coronary artery wall thickening. However, CMRI showed pericardium thickening and increased T2-weighted imaging signals, suggesting active inflammation with edema. PET imaging indicated pericardial uptake. Collectively, these cases suggest that identifying the cardiac manifestations of IgG4-RD on cardiac imaging can enhance clinical suspicion and facilitate a definitive diagnosis.

The goal of treatment is to control inflammation, achieve and maintain remission, and protect organ function (28). To date, glucocorticoids remain the accepted first-line drug for the treatment of IgG4-RD, which can be used in the induced remission and maintenance phases of the disease. Usually, the treatment with glucocorticoids has a rapid effect and can be improved within a few days to a few weeks. The effective rate of the hormone is more than 90% (29). The specific dosage of the hormone should be individualized and can be adjusted according to age and condition. Gradually decrease to the minimum maintenance dose after disease control. Due to the high recurrence rate of IgG4-RD after discontinuation, it is necessary for doctors to make a long-term maintenance or discontinuation plan according to the situation of each patient (30).

In recent years, traditional immunosuppressants have been increasingly used in the treatment of IgG4-RD as hormone-reducing agents combined with glucocorticoids. Many studies (31) have shown that hormone combined immunosuppressive therapy is more effective than glucocortixxcoids alone in controlling disease and reducing recurrence in IgG4-RD patients. A combination of hormones and immunosuppressants is recommended when the disease is not adequately controlled by hormone therapy alone and glucocorticoid side effects are evident. Among them, mycophenolate and azathioprine are the most widely used in clinical practice. Because of the slow onset of traditional immunosuppressants, immunosuppressant therapy alone is not recommended in patients with acute activity. For patients who have failed conventional therapy, relapsed during hormone reduction, and have hormone resistance or intolerance, rituximab may be considered, but care should be taken to prevent infection after the use of this drug.

Seshika Ratwatte reported two cases of IgG4-RD with pericardial effusium, one of which was treated with glucocorticoid and azathioprine. The other case was treated with glucocorticoid and rituximab, and the effect was good (27). A case of IgG4-RD woman with pericardial effusion, in which rituximab alone also responded favorably (5). For this patient, the patient is old and long-term use of glucocorticoids is prone to side effects such as hypertension, diabetes and osteoporosis, and the combination of immunosuppressants is helpful to stabilize the condition when hormone reduction is achieved. Considering the high price of rituximab, rituximab was not selected in the treatment of this patient. Mycophenolate was used to control the disease.

7 Conclusion

We herein reported a case who mainly manifested as massive pericardical effusion, and FDG-PETCT imaging revealed FDG accumulation in the pericardium and pericardial fluid, then suggested IgG4-RD. When the patient referred to our department we found IgG4 markedly elevated, and treatment with 40 mg methylprednisolone and 1000 mg mycophenolate mofetil per day was initiated. Finally, pericardial effusion was completely absorbed. For patients with massive pericardial effusion of unknown cause, early detection of IgG4 is recommended, and FDG-PETCT may be helpful for obtaining the diagnosis. The patient is currently still being followed up.

Data availability statement

The original contributions presented in the study are included in the article/supplementary material. Further inquiries can be directed to the corresponding author.

Ethics statement

The studies involving humans were approved by Zibo Central Hospital Medical Ethics Expert Committee. The studies were conducted in accordance with the local legislation and institutional requirements. Written informed consent for participation in this study was provided by the participants' legal guardians/next of kin. Written informed consent was obtained from the individual(s), and minor(s)' legal guardian/next of kin, for the publication of any potentially identifiable images or data included in this article.

Author contributions

QW: Formal Analysis, Investigation, Methodology, Resources, Writing – review & editing. HQ: Software, Supervision, Validation, Writing – original draft. HW: Formal Analysis, Software, Supervision, Validation, Writing – original draft. XW: Conceptualization, Methodology, Project administration, Writing – review & editing. HZ: Conceptualization, Data curation, Funding acquisition, Validation, Visualization, Writing – original draft.

Funding

The author(s) declare that no financial support was received for the research, authorship, and/or publication of this article.

Conflict of interest

The authors declare that the research was conducted in the absence of any commercial or financial relationships that could be construed as a potential conflict of interest.

Publisher's note

References

1. Lanzillotta M, Mancuso G, Della-Torre E. Advances in the diagnosis and management of IgG4 related disease. *Bmj.* (2020) 369:m1067. doi: 10.1136/bmj.m1067

2. Löhr JM, Vujasinovic M, Rosendahl J, Stone JH, Beuers U. IgG4-related diseases of the digestive tract. *Nat Rev Gastroenterol Hepatol* (2022) 19:185–97. doi: 10.1038/s41575-021-00529-y

3. Liu J, Yin W, Westerberg LS, Lee P, Gong Q, Chen Y, et al. Immune dysregulation in igG(4)-related disease. *Front Immunol* (2021) 12:738540. doi: 10.3389/fimmu.2021.738540

4. Maehara T, Moriyama M, Nakamura S. Review of a novel disease entity, immunoglobulin G4-related disease. *J Korean Assoc Oral Maxillofac Surg* (2020) 46:3–11. doi: 10.5125/jkaoms.2020.46.1.3

5. Gorecka MM, Armstrong R, Daly C. Unusual cause of pericardial effusion: IgG4-related disease. *BMJ Case Rep* (2019) 12:e230505. doi: 10.1136/bcr-2019-230505

6. Tello-Sánchez M, Rodríguez-Duque MS, Loidi-López C, Martín-Arroyo J, González-Gay M, Fernández-Ayala Novo M. Pleural and pericardial effusion as the only manifestation of igG4-related disease. *Arch Bronconeumol (Engl Ed).* (2020) 56:597–9. doi: 10.1016/j.arbres.2020.04.013

7. Arao K, Mase T, Iwanami K, Nakai M, Sekiguchi H, Abe Y, et al. IgG4-related pericarditis in which oral corticosteroid therapy was effective. *Intern Med* (2019) 58:1119–22. doi: 10.2169/internalmedicine.1403-18

8. Hamano H, Kawa S, Horiuchi A, Unno H, Furuya N, Akamatsu T, et al. High serum IgG4 concentrations in patients with sclerosing pancreatitis. *N Engl J Med* (2001) 344:732–8. doi: 10.1056/nejm200103083441005

9. Yamamoto M, Takahashi H, Sugai S, Imai K. Clinical and pathological characteristics of Mikulicz's disease (IgG4-related plasmacytic exocrinopathy). *Autoimmun Rev* (2005) 4:195–200. doi: 10.1016/j.autrev.2004.10.005

10. Yamamoto M, Takahashi H, Ohara M, Suzuki C, Naishiro Y, Yamamoto H, et al. A new conceptualization for Mikulicz's disease as an IgG4-related plasmacytic disease. *Mod Rheumatol* (2006) 16:335–40. doi: 10.1007/s10165-006-0518-Y

11. Umehara H, Okazaki K, Masaki Y, Kawano M, Yamamoto M, Saeki T, et al. Comprehensive diagnostic criteria for IgG4-related disease (IgG4-RD), 2011. *Mod Rheumatol* (2012) 22:21–30. doi: 10.1007/s10165-011-0571-z

12. Tajima M, Nagai R, Hiroi Y. IgG4-related cardiovascular disorders. *Int Heart J* (2014) 55:287–95. doi: 10.1536/ihj.13-321

13. Ishiguro N, Moriyama M, Furusho K, Furukawa S, Shibata T, Murakami Y, et al. Activated M2 macrophages contribute to the pathogenesis of igG4-related disease via toll-like receptor 7/interleukin-33 signaling. *Arthritis Rheumatol* (2020) 72:166–78. doi: 10.1002/art.41052

14. Della Torre E, Mattoo H, Mahajan VS, Carruthers M, Pillai S, Stone JH. Prevalence of atopy, eosinophilia, and IgE elevation in IgG4-related disease. *Allergy.* (2014) 69:269–72. doi: 10.1111/all.12320

15. Mattoo H, Mahajan VS, Maehara T, Deshpande V, Della-Torre E, Wallace ZS, et al. Clonal expansion of CD4(+) cytotoxic T lymphocytes in patients with IgG4-related disease. *J Allergy Clin Immunol* (2016) 138:825–38. doi: 10.1016/j.jaci.2015.12.1330

16. Della-Torre E, Bozzalla-Cassione E, Sciorati C, Ruggiero E, Lanzillotta M, Bonfiglio S, et al. A CD8α- subset of CD4+SLAMF7+ Cytotoxic T cells is expanded in patients with igG4-related disease and decreases following glucocorticoid treatment. *Arthritis Rheumatol* (2018) 70:1133–43. doi: 10.1002/art.40469

17. Perugino CA, Kaneko N, Maehara T, Mattoo H, Kers J, Allard-Chamard H, et al. CD4(+) and CD8(+) cytotoxic T lymphocytes may induce mesenchymal cell apoptosis in IgG(4)-related disease. *J Allergy Clin Immunol* (2021) 147:368–82. doi: 10.1016/j.jaci.2020.05.022

18. Chen Y, Lin W, Yang H, Wang M, Zhang P, Feng R, et al. Aberrant expansion and function of follicular helper T cell subsets in igG4-related disease. *Arthritis Rheumatol* (2018) 70:1853–65. doi: 10.1002/art.40556

19. Ito F, Kamekura R, Yamamoto M, Takano K, Takaki H, Yabe H, et al. IL-10(+) T follicular regulatory cells are associated with the pathogenesis of IgG4-related disease. *Immunol Lett* (2019) 207:56–63. doi: 10.1016/j.imlet.2019.01.008

20. Cai S, Hu Z, Chen Y, Zhong J, Dong L. Potential roles of non-lymphocytic cells in the pathogenesis of IgG4-related disease. *Front Immunol* (2022) 13:940581. doi: 10.3389/fimmu.2022.940581

21. Peyronel F, Fenaroli P, Maritati F, Schleinitz N, Vaglio A. IgG4-related disease: advances in pathophysiology and treatment. *Expert Rev Clin Immunol* (2023) 19:537–47. doi: 10.1080/1744666x.2023.2195627

22. Jacob S, Sebastian JC, Cherian PK, Abraham A, John SK. Pericardial effusion impending tamponade: a look beyond Beck's triad. *Am J Emerg Med* (2009) 27:216–9. doi: 10.1016/j.ajem.2008.01.056

23. Sakamoto A, Nagai R, Saito K, Imai Y, Takahashi M, Hosoya Y, et al. Idiopathic retroperitoneal fibrosis, inflammatory aortic aneurysm, and inflammatory pericarditis–retrospective analysis of 11 case histories. *J Cardiol* (2012) 59:139–46. doi: 10.1016/j.jjcc.2011.07.014

24. Shimizu M, Okamura K, Kise Y, Takeshita Y, Furuhashi H, Weerawanich W, et al. Effectiveness of imaging modalities for screening IgG4-related dacryoadenitis and sialadenitis (Mikulicz's disease) and for differentiating it from Sjögren's syndrome (SS), with an emphasis on sonography. *Arthritis Res Ther* (2015) 17:223. doi: 10.1186/s13075-015-0751-x

25. Komori T, Inoue D, Izumozaki A, Sugiura T, Terada K, Yoneda N, et al. Ultrasonography of IgG4-related dacryoadenitis and sialadenitis: Imaging features and clinical usefulness. *Mod Rheumatol* (2022) 32:986–93. doi: 10.1093/mr/roab063

26. Horie K, Tada N, Yamaguchi K, Inazawa K, Endo M, Inoue N. Immunoglobulin G4-related constrictive pericarditis identified by cytological examination of pericardial effusion: a case report. *J Med Case Rep* (2016) 10:359. doi: 10.1186/s13256-016-1159-1

27. Ratwatte S, Day M, Ridley LJ, Fung C, Naoum C, Yiannikas J. Cardiac manifestations of IgG4-related disease: a case series. *Eur Heart J Case Rep* (2022) 6: ytac153. doi: 10.1093/ehjcr/ytac153

28. Wallace ZS, Khosroshahi A, Carruthers MD, Perugino CA, Choi H, Campochiaro C, et al. An international multispecialty validation study of the igG4-related disease responder index. *Arthritis Care Res (Hoboken).* (2018) 70:1671–8. doi: 10.1002/acr.23543

29. Raina A, Yadav D, Krasinskas AM, McGrath KM, Khalid A, Sanders M, et al. Evaluation and management of autoimmune pancreatitis: experience at a large US center. *Am J Gastroenterol* (2009) 104:2295–306. doi: 10.1038/ajg.2009.325

30. Goyal J, Barkin JA, Barkin JS. Randomised controlled trial of long-term maintenance corticosteroid therapy in patients with autoimmune pancreatitis. *Gut.* (2018) 67:591. doi: 10.1136/gutjnl-2017-314460

31. Omar D, Chen Y, Cong Y, Dong L. Glucocorticoids and steroid sparing medications monotherapies or in combination for IgG4-RD: a systematic review and network meta-analysis. *Rheumatol (Oxford).* (2020) 59:718–26. doi: 10.1093/rheumatology/kez380

frontiers | Frontiers in Immunology

TYPE Original Research
PUBLISHED 25 January 2024
DOI 10.3389/fimmu.2023.1251134

OPEN ACCESS

EDITED BY
Charles J. Dimitroff,
Florida International University, United States

REVIEWED BY
Jun Deng,
Shanghai Jiao Tong University, China
Inga Koneczny,
Medical University of Vienna, Austria

*CORRESPONDENCE
Ulrich Beuers
u.h.beuers@amsterdamumc.nl

†These authors contributed equally to this work and share first authorship

RECEIVED 30 June 2023
ACCEPTED 15 December 2023
PUBLISHED 25 January 2024

CITATION
Kersten R, Trampert DC, Hubers LM, Tolenaars D, Vos HR, van de Graaf SFJ and Beuers U (2024) Galectin-3 and prohibitin 1 are autoantigens in IgG4-related cholangitis without clear-cut protective effects against toxic bile acids. *Front. Immunol.* 14:1251134. doi: 10.3389/fimmu.2023.1251134

Galectin-3 and prohibitin 1 are autoantigens in IgG4-related cholangitis without clear-cut protective effects against toxic bile acids

Remco Kersten[1†], David C. Trampert[1†], Lowiek M. Hubers[1], Dagmar Tolenaars[1], Harmjan R. Vos[2], Stan F. J. van de Graaf[1] and Ulrich Beuers[1*]

[1]Tytgat Institute for Liver and Intestinal Research, Department of Gastroenterology and Hepatology, Amsterdam Gastroenterology Endocrinology Metabolism (AGEM), Amsterdam University Medical Center (UMC), University of Amsterdam, Amsterdam, Netherlands, [2]Oncode Institute and Molecular Cancer Research, Center for Molecular Medicine, University Medical Center Utrecht, Utrecht, Netherlands

Background and aims: IgG4-related cholangitis (IRC) is the hepatobiliary manifestation of IgG4-related disease, a systemic B cell-driven fibro-inflammatory disorder. Four autoantigens have recently been described in IgG4-RD: annexin A11, galectin-3, laminin 511-E8, and prohibitin 1. We have previously reported a protective role of annexin A11 and laminin 511-E8 in human cholangiocytes against toxic bile acids. Here, we explored the potentially protective role of the carbohydrate-binding lectin galectin-3 and the scaffold proteins prohibitins 1 and 2.

Methods: Anti-galectin-3, anti-prohibitin 1 and 2 autoantibody positivity in IRC and healthy and disease (primary sclerosing cholangitis (PSC)) control sera was assessed by ELISA/liquid chromatography–tandem mass spectrometry (LC-MS/MS). Human H69 cholangiocytes were subjected to short hairpin RNA (shRNA) knockdown targeting galectin-3 (*LGALS3*), prohibitin 1 (*PHB1*), and prohibitin 2 (*PHB2*). H69 cholangiocytes were also exposed to recombinant galectin-3, the inhibitor GB1107, recombinant prohibitin 1, and the pan-prohibitin inhibitor rocaglamide. Protection against bile acid toxicity was assessed by intracellular pH (pH_i) measurements using BCECF-AM, 22,23-^{3}H-glycochenodeoxycholic acid (^{3}H-GCDC) influx, and GCDC-induced apoptosis using Caspase-3/7 assays.

Results: Anti-galectin-3 autoantibodies were detected in 13.5% of individuals with IRC but not in PSC. Knockdown of *LGALS3* and galectin-3 inhibition with GB1107 did not affect pH_i, whereas recombinant galectin-3 incubation lowered pH_i. *LGALS3* knockdown increased GCDC-influx but not GCDC-induced apoptosis. GB1107 reduced GCDC-influx and GCDC-induced apoptosis. Recombinant galectin-3 tended to decrease GCDC-influx and GCDC-induced apoptosis. Anti-prohibitin 1 autoantibodies were detected in 61.5% and 35.7% of individuals with IRC and PSC, respectively. Knockdown of *PHB1*, combined *PHB1/2* KD, treatment with rocaglamide, and recombinant prohibitin 1 all lowered pH_i. Knockdown of *PHB1*, *PHB2*, or combined *PHB1/2* did not alter GCDC-influx, yet knockdown of *PHB1* increased GCDC-induced apoptosis. Conversely,

10.3389/fimmu.2023.1251134

rocaglamide reduced GCDC-influx but did not attenuate GCDC-induced apoptosis. Recombinant prohibitin 1 did not affect GCDC-influx or GCDC-induced apoptosis. Finally, anti-galectin-3 and anti-prohibitin 1 autoantibody pretreatment did not lead to increased GCDC-influx.

Conclusions: A subset of individuals with IRC have autoantibodies against galectin-3 and prohibitin 1. Gene-specific knockdown, pharmacological inhibition, and recombinant protein substitution did not clearly disclose a protective role of these autoantigens in human cholangiocytes against toxic bile acids. The involvement of these autoantibodies in processes surpassing epithelial secretion remains to be elucidated.

KEYWORDS

biliary bicarbonate umbrella, cholangiopathy, cholestasis, IgG4-related systemic disease, immune-mediated disease, secretory organs

1 Introduction

IgG4-related disease (IgG4-RD) is a systemic fibroinflammatory disorder that can affect many different organs, with the pancreatic and hepatobiliary manifestations being the most common, termed type 1 autoimmune pancreatitis (AIP) and IgG4-related cholangitis (IRC) (1). Serum IgG4 levels are often elevated in individuals with IRC (70%–90%) (1–3), and affected tissues are characterized by typical histopathological findings such as storiform fibrosis, obliterative phlebitis, and a predominantly lymphoplasmacytic infiltrate enriched with $IgG4^+$ B cells.

The clinical presentation and management of IRC have several challenges. First, IRC is often misdiagnosed for either primary sclerosing cholangitis (PSC) or cholangiocarcinoma (CCA), leading to unjustified major hepatobiliary surgeries in up to 30% of individuals with IRC (4). Although an elevated level of serum IgG4 can aid in making the diagnosis of IRC, it is hampered by a lack of sensitivity and specificity (5). Second, subjects with IRC often require long-term corticosteroid therapy, as relapse occurs often upon steroid withdrawal (6). A better understanding of the pathophysiology of IRC would aid in both the diagnosis and treatment of individuals with IRC.

Currently, the pathophysiology of IRC remains unresolved. Our group and others have previously demonstrated the presence of dominant affinity matured $IgG4^+$ B-cell receptor clones and clonally expanded plasmablasts in people with IRC and multiorgan IgG4-RD (7–9). These findings were highly suggestive of the presence of specific autoantigens in IgG4-RD and indeed were followed by the discovery of the autoantigens annexin A11, laminin 511-E8, galectin-3, and prohibitin 1 in people with IgG4-RD (10–13). The presence of autoantibodies against more than one of these four antigens has been demonstrated to correlate with disease severity, and autoantibody titers decreased upon successful treatment (11, 12, 14). Autoantibodies directed against these antigens were mainly of the IgG4 and IgG1 subclasses, but the potential pathogenicity of individual IgG1 or IgG4 autoantibodies in IgG4-RD has not been fully clarified. Mice exposed to isolated IgG1 or IgG4 from people with IgG-RD developed typical organ lesions (15). Notably, IgG1 was shown to be more destructive than IgG4, and the pathogenicity of patient IgG1 was reduced by simultaneous injection of patient IgG4 in a pre-clinical model system. In line with these findings, we have previously shown that two linear epitopes on the autoantigen annexin A11 were recognized by both IgG1 and IgG4 autoantibodies and that IgG4 competitively blocked the binding of IgG1 to these epitopes on annexin A11 (10). These findings indicate that IgG4 could potentially repress an IgG1-driven immune response in IgG4-RD, as also seen in other inflammatory conditions (16). At present, it is unclear whether autoantibodies detected in IgG4-RD are the main driver of IgG4-RD, make up additional pathogenic pathways, or just represent a non-pathogenic epiphenomenon. Nevertheless, there are autoimmune diseases where IgG4 autoantibodies are directly pathogenic (17–21). The potential pathogenicity of IgG1 or IgG4 autoantibodies in IRC could be driven by two mechanisms: i) via a direct functional effect of autoantibodies on the targeted autoantigens, or ii) via an indirect mechanism where autoantibody binding elicits an excessive immune response that would lead to obstructive cholestasis.

To address the potential direct pathogenicity of IgG1 and IgG4 autoantibodies in IRC, an in-depth understanding of the four targeted antigens is essential. To this end, our group has previously demonstrated that annexin A11 is involved in bicarbonate-rich fluid secretion (22). Annexin A11 was demonstrated to facilitate the trafficking of ANO1, a calcium-sensitive chloride channel, to the apical cholangiocyte membrane. This process was inhibited by incubating cholangiocytes with patient serum containing both IgG1 and IgG4 autoantibodies directed against annexin A11. ANO1 establishes a chloride gradient necessary for chloride/bicarbonate exchangers to secrete

bicarbonate into the bile duct lumen at the juxta-apical surface of cholangiocytes. The formed apical alkaline layer, known as the biliary bicarbonate umbrella, keeps bile salts in their deprotonated, membrane-impermeable, and non-toxic state (23, 24). Dysfunction of the biliary bicarbonate umbrella leads to bile acids penetrating cholangiocytes and inducing cholangiocellular damage and death (24). Recent data on the role of the autoantigen laminin 511-E8 in cholangiocytes, among cell barrier functions, point toward the protection of cholangiocytes from toxic bile acids, potentially by stabilizing the biliary bicarbonate umbrella (25). The present work investigates the potential protective effect of the remaining autoantigens in IRC, galectin-3, and prohibitin 1.

Galectin-3 is a β-galactoside-binding lectin that forms pentamers. These pentamers facilitate extracellular matrix (ECM)–cell interactions and cell–cell interactions and form lattices at the plasma membrane of cells, followed by invagination and endosomal transport (Figure 1A) (26). Notably, galectin-3 is required for apical protein sorting, which takes place in a pH-dependent manner (27, 28). Autoantibodies directed against galectin-3 were first described in people with multiorgan IgG4-RD who predominantly presented with type 1 AIP and IgG4-related sialadenitis, two glandular organs that secrete bicarbonate-rich fluids (11). As the adequate formation of the biliary bicarbonate umbrella relies on the presence of various transporters and channels involved in bicarbonate secretion at the apical cholangiocyte membrane and a stable glycocalyx (23, 24), we speculated that galectin-3 could exert a protective effect against toxic bile acids in human cholangiocytes as previously described for the IRC autoantigens annexin A11 and laminin 511-E8 and that galectin-3 autoantibodies could antagonize this protective effect.

Prohibitins (PHBs) are scaffold proteins predominantly located in the inner mitochondrial membrane, where prohibitin 1 and prohibitin 2 together form a ring-like multimeric complex. Prohibitins also localize to the cytosol, nucleus, and plasma membrane, where they interact with cell membrane receptors, cytoskeletal transport systems, and transcription factors (Figure 1B) (29). Autoantibodies against prohibitin 1 were first described in people with dacryosialoadenopathy (Mikulicz's disease), type 1 AIP, and retroperitoneal fibrosis, with predominant manifestations of IgG4-RD in bicarbonate-secreting glands (13). Notably, prohibitin 1 is downregulated in the liver tissue of people with primary biliary cholangitis (PBC) (30), an immune-mediated cholestatic liver disease where defective biliary bicarbonate secretion may play a pathogenic role (24, 31).

The present work first analyzed the presence of IgG4-RD autoantibodies against galectin-3 and prohibitins 1 and 2 in individuals with IRC in comparison to those with PSC (cholestatic disease control) and healthy volunteers. Second, the present work investigated the potential role of the autoantigens galectin-3 and prohibitins 1 and 2 in protecting human cholangiocytes against bile acid-induced toxicity.

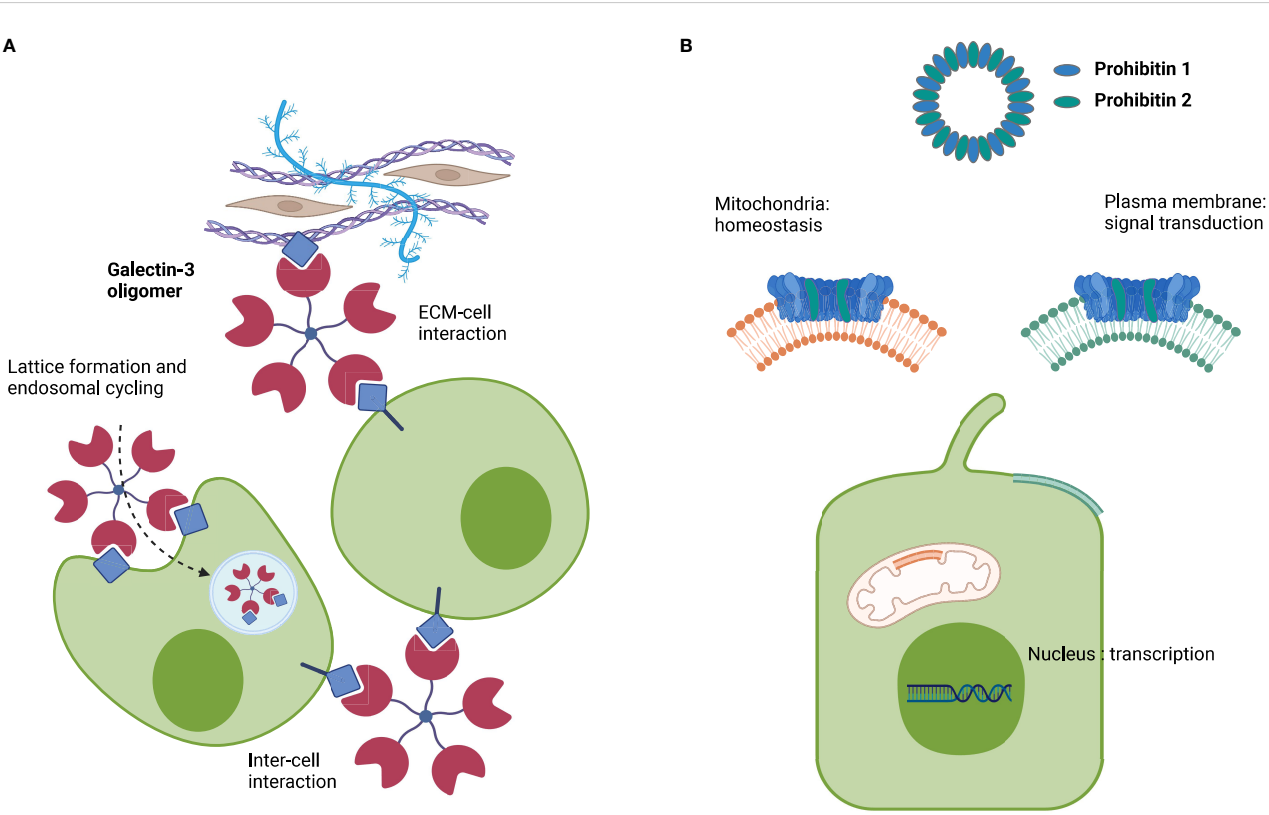

FIGURE 1
Schematic roles of galectin-3 and prohibitins 1 and 2. **(A)** Representation of the multifaceted roles of galectin-3. **(B)** Representation of the multifaceted roles of prohibitins 1 and 2 as a multimeric complex. Image created with BioRender.com.

2 Materials and methods

2.1 Human ethics statement

The use of patient serum samples and human liver tissue was approved by the local medical ethical committee in Amsterdam (MEC 10/007, 2022.0144, and 2020.081). Participants gave written informed consent prior to inclusion in the study.

2.2 Patients

Serum samples were obtained from people with IRC (n = 52), PSC (n = 15), CCA (n = 14), and healthy volunteers (n = 14). Diagnosis of IRC was made according to HISORt criteria (1, 6), whereas diagnosis of PSC was made according to the European Association for the Study of the Liver (EASL) clinical practice guidelines on sclerosing cholangitis (32). The diagnosis of CCA was made based on histological confirmation after suggestive imaging findings.

2.3 ELISA

Alternating rows of 96-well ELISA plates were coated with 100 µl of recombinant galectin-3 (5 µg/ml) (PeproTech #450-38), recombinant prohibitin 1 (1 µg/ml) (FineTest #P5113), recombinant annexin A11 (1 µg/ml) (Abcam #ab101050), or equivalent concentrations of bovine serum albumin (BSA) in phosphate-buffered saline (PBS) and incubated at 4°C overnight (11, 13). Wells were washed seven times with TBST pH 8.0 and subsequently blocked for 1 hour with 1% BSA/TBS pH 8.0 at room temperature. Wells were again washed seven times with TBST pH 8.0. Sera from people with IRC, PSC, CCA, or healthy controls were centrifuged at 9000 rcf for 20 minutes before wells were incubated with diluted serum (1:200 for galectin-3 or 1:20 for prohibitin 1 in 1% BSA/TBS pH 8.0) for 30 minutes at room temperature. After seven washes with TBST pH 8.0, wells were incubated with 100 µl of rabbit anti-human total IgG (Dako #P0214) antibody at 1:2000 dilution for 1 hour at room temperature. IgG4 (Southern Biotech #9200-05) and IgG1 (Southern Biotech #9052-05) specific autoantibodies were detected using secondary mouse anti-human antibodies directed at human IgG4 and human IgG1 at 1:2000 dilution. After seven washes, bound reactants were detected by incubation using 100 µl of 3,3′,5,5′-tetramethylbenzidine (TMB) chromogenic substrate (Merck #CL07). The reaction was subsequently stopped with 100 µl of stop solution (Thermo Scientific #N600), and absorbance was determined at 450 nm using the CLARIOstar (BMG LABTECH, Ortenberg, Germany). Samples were considered positive for autoantibodies against galectin-3, prohibitin 1, or annexin A11 when absorbance values were greater than the mean plus two standard deviations of the healthy control group as previously described (11, 14).

2.4 Immunoprecipitation and liquid chromatography–tandem mass spectrometry analysis

Immunoprecipitation and liquid chromatography–tandem mass spectrometry (LC-MS/MS) was performed as described previously (10). IgG4 high-affinity beads were washed two times with 0.1% NP-40/PBS and subsequently incubated with patient serum containing 600 µg of IgG4 for 1 hour at room temperature. The beads were then washed five times with 0.1% NP-40/PBS and transferred to new Eppendorf tubes. IgG4 antibodies were eluted twice for 10 minutes with citrate buffer pH 3.0. After centrifugation, the supernatant with eluted IgG4 was transferred and neutralized by 0.5 M borate buffer pH 8.8. Purified IgG4 was then covalently bound to tosyl-activated magnetic beads (Dynabeads M-280, Thermo Fisher Scientific) by incubating the beads overnight at 37°C in 125 µl of 3.6 M $(NH_4)_2SO_4$/0.1 M borate buffer pH 8.8. Subsequently, beads were washed with 50 mM Tris pH 7.4, 1 M NaCl, and 1% NP-40 (w/v); blocked for 1 hour in 1 M Tris pH 7.4; washed again four times; and transferred to new Eppendorf tubes. Beads at a volume of 50 µl were then incubated overnight at 4°C with 1200 µl of H69 cytosolic cell lysate with the addition of 1 M NaCl and 1% (w/v) NP-40. Unbound proteins were removed by washing three times with 50 mM Tris pH 7.4, 1 M NaCl, and 1% NP-40 (w/v) and three times with PBS. During the washing process, the beads were transferred twice to a new Eppendorf tube. After washing, the supernatant was discarded, and the beads were frozen for LC-MS/MS analysis. Precipitated proteins were denatured using 8 M urea in 1 M NH_4HCO_3 reduced with 10 mM tris(2-carboxyethyl)phosphine at room temperature for 30 minutes. Hereafter, cysteines were alkylated with 40 mM chloroacetamide for 30 minutes. After diluting four times with 1 M ammonium bicarbonate, proteins were digested by 150 ng of Trypsin/LysC (Promega, Madison, Wisconsin, USA), on-bead overnight at room temperature. Peptides were then bound to an in-house-made C18 stage tip, washed with 0.1% formic acid, and stored at 4°C until LC-MS/MS analysis. After elution from the stage tips, samples were centrifuged in a SpeedVac to remove the acetonitrile. The peptide solution was then diluted with 0.1% formic acid before loading onto the column. Peptides were separated on a 30 cm pico-tip column (50 µm ID, New Objective/Ms Wil, Zurich, Switzerland) packed in-house with 3µm aquapur gold C18 material (Dr Maisch, Ammerbuch, Germany) using a 140- or 200-minute gradient (7% to 80% acetonitrile, 0.1% formic acid), delivered by an easy-nLC 1000 (Thermo Fisher Scientific), and electro-sprayed directly into an Orbitrap Fusion Tribrid Mass Spectrometer (Thermo Fisher Scientific). The data-dependent top-speed mode with a 1-second cycle time was used, in which a full scan over the 400–1500 mass range was performed at 240,000 resolution. The most intense ions (threshold of 5000 ions) were isolated by the quadrupole and fragmented with a higher-energy collisional dissociation collision of 30%. The maximum injection time of the ion trap was set at 35 milliseconds. The raw data matrix containing all proteins identified from immunoprecipitated cholangiocyte cell lysates with IgG4-RD or PSC IgG4 autoantibodies was imported into the proteomics analysis software Perseus (v1.5.5.3, MaxQuant, Max-Planck Institute of Biochemistry). Four technical

replicates were used per patient sample. Data were log2-transformed and filtered for proteins only identified by site, reverse, or potential contaminants. In the obtained data matrix, proteins were annotated by NCBI gene names and full protein names. Log2 peptide intensities for annexin A11 (positive control), RPL22 (loading control), and prohibitins 1 and 2 were plotted for all individual patients. The mass spectrometry proteomics data have been deposited with the ProteomeXchange Consortium via the PRIDE partner repository with the dataset identifier PXD042856 (33).

2.5 Immunohistochemistry on human liver tissue

Sequentially sliced sections of paraffin-embedded human liver tissue were rehydrated by passing through xylene (three times, 7 min) followed by stepwise ethanol washing from 100% to 50%, each for 1 minute. After a wash in MQ, antigen retrieval was performed using 10 mM sodium citrate (Sigma Aldrich #C9999) at pH 6 at 98° C for 20 minutes. Subsequently, peroxidase blocking was performed using 0.3% hydrogen peroxide (VWR #8.22287.1000) for 30 minutes. Aspecific protein blocking was performed using Ultra V (Thermo Scientific #TA-125-UB). Incubation with primary antibodies against galectin-3 (Santa Cruz, raised in mouse), prohibitin 1 (Santa Cruz, raised in mouse), and cytokeratin 19 (Abcam, raised in rabbit) took place overnight at 4°C in a 1:100 dilution. The following day, the slides were washed three times in TBS. Slides were incubated with ready-to-use secondary horseradish peroxidase (HRP)-conjugated anti-rabbit/mouse IgG (BrightVision Immunologic #VWRKDPVO110HRP) for 1 hour at room temperature. The slides were washed three times in TBS. As a substrate, Vector NovaRed (HRP) (Vector Laboratories #SK-4800) was added to the slides for 40 min, after which the reaction was stopped in MQ. Counterstaining was performed by submerging the slides in hematoxylin for 2 min, after which the slides were washed in water for 10 min, followed by a single 3 min wash in MQ. Slides were briefly dried on a heater plate, after which they were mounted using Vectamount (Vector Laboratories #H-5000). Images were assessed and acquired on the Olympus BX51 brightfield microscope using the cellSens Entry software.

2.6 RNA-sequencing datasets

Count files of bulk RNA-sequenced human cholangiocyte models were obtained from Gene Expression Omnibus (GEO), GEO accession GSE156519, and our own dataset GSE221746, and imported into the R2 genomics analysis and visualization platform (http://r2.amc.nl/). Expression values were log2-transformed for each dataset and presented as individual heatmaps. Hepatocyte markers (*ALB* and *ASGR1*) and cholangiocyte markers (*EPCAM* and *KRT19*) were included as a phenotypic reference in the heatmaps.

2.7 Cell culture

H69 cholangiocytes were kindly provided by Dr. Douglas Jefferson (Tufts University, Boston, MS, USA). H69 cells were cultured in a 5% CO_2 incubator as previously described and were passaged twice per week (34). The H69 cell culture medium composition can be found in Supplementary Table S1. Mycoplasma contamination tests were carried out every 3 months, with negative results throughout.

2.8 Lentivirus generation and transduction of shRNA-mediated knockdown

Short hairpin RNA (shRNA) constructs were purchased from the MISSION® TRC version 1 shRNA library (Sigma-Aldrich, St. Louis, MO, USA): *LGALS3* (TRCN0000029305), *PHB1* (TRCN0000029207), *PHB2* (TRCN0000060922), and the non-targeting shRNA control (SHC002). The shRNAs against *LGALS3*, *PHB1*, and *PHB2* all targeted the coding sequence. Lentivirus was produced as previously described in an ML-2/BSL-2 facility (35). In brief, bacterial cultures were grown from which plasmid DNA was isolated using Midiprep kits (Genomed, LabNed). HEK 293T cells were plated in culture dishes and transfected the following day using polyethylenimine (PEI) with a mixture containing the plasmid of interest and the plasmids containing the lentiviral backbone. One day post-transfection, cell media was refreshed, and 72 hours after transfection, cell media containing lentivirus was harvested and stored appropriately. For the lentiviral transduction, H69 cholangiocytes were seeded in 6-well plates and transduced the following day using DEAE dextran and the harvested lentivirus. Six hours post-transduction, cell media was refreshed. After 1 day of recovery, the transduced H69 cholangiocytes were selected with 1 μg/ml puromycin to obtain stable *LGALS3*, *PHB1*, *PHB2*, and combined *PHB1/2* knockdown cholangiocytes.

2.9 RNA isolation, cDNA synthesis, and real-time quantitative PCR

H69 cholangiocytes were cultured in 12-well plates until confluency. Total RNA was isolated with a TRIzol reagent (Sigma #T9424). The RNA-containing phase was isolated with chloroform (Merck #2445) and centrifugation. RNA was recovered by precipitating with isopropyl alcohol (Merck #1040). Pellets were washed with 70% ethanol and resuspended in water treated with diethylpyrocarbonate (DEPC) (Sigma #D5757). Quality (A260/A280 > 1.8) and concentration of RNA samples were checked by spectrophotometry using the NanoDrop 1000 (Thermo Scientific, Waltham, MS, USA). Total RNA with 2 μg of input was treated with DNase I (Promega #M6101), followed by reverse transcription into cDNA using Random Hexamer primers (Promega #SO142), Oligo-dT primers (Invitrogen), and Revertaid transcriptase (Fermentas,

#EP0442), resulting in a total volume of 20 µl cDNA. The cDNA was diluted to 100 µl, after which 2 µl of diluted cDNA served as a template for real-time quantitative PCR (RT-qPCR) with the SensiFAST SYBR No-ROX kit (Bioline). Primers were self-designed to cover all transcript variants of the gene of interest (Supplementary Material and Supplementary Table S2 contain a list of methods and primer sequences). RT-qPCR plates were run on the Bio-Rad CXF96. Raw fluorescent values were exported, and starting concentration (N0) and cycle quantification (Cq) values were obtained using LinRegPCR (version 2013.0, Academic Medical Center, Amsterdam) (36). Expression levels were graphed relative to the geomean of human 36B4 (*RPLP0*) and *HPRT* reference genes, and normalized to the control condition.

2.10 Western blotting

Cells were lysed in radioimmunoprecipitation assay (RIPA) buffer, and lysate samples were prepared in Laemmli sample buffer. After running the samples on sodium dodecyl sulfate–polyacrylamide gel electrophoresis (SDS-PAGE) gels (10% Tris-Glycine), proteins were transferred by semi-dry blotting to polyvinylidene difluoride membranes (Millipore, Burlington, VT, USA), blocked for 2 hours at room temperature in 5% non-fat milk/TBST, and probed overnight at 4°C using the respective primary antibody in 5% non-fat milk/TBST (Supplementary Table S3 for list of antibodies and dilutions). Immune complexes were detected using HRP-conjugated secondary antibodies and visualized using an enhanced chemiluminescence detection reagent (Lumi-light, Roche Diagnostics, Rotkreuz, Switzerland) and ImageQuant LAS 4000 (GE Healthcare, Chicago, IL, USA). Protein bands were quantified using ImageJ 1.50i (Wayne Rasband, National Institutes of Health, Bethesda, MD, USA). Results were presented as fold changes of sham (SHC002)-transduced H69 cells, normalized per experiment.

2.11 Bile acid permeation assay

Bile acid permeation assays were performed as previously described (22). H69 cholangiocytes were cultured until confluence in 24-well plates. Cells were refreshed with new culture medium 24 hours before the experiment. At the start of the experiment, cells were washed once with 500 µl of 20 mM HEPES-buffered Hank's balanced salt solution (HBSS) pH 7.4 (Lonza #BE10-527F, Basel, Switzerland) and equilibrated for 30 minutes with HEPES-buffered HBSS pH 7.4 at 37°C in ambient air. HBSS was removed; 200 µl per well HEPES-buffered HBSS pH 7.4 with 2.87 kBq per well 22,23-^{3}H-glycochenodeoxycholic acid (^{3}H-GCDC), kindly provided by the late Dr. Alan Hofmann (University of California, San Diego, CA, USA), and 750 µM unlabeled GCDC (Sigma-Aldrich #G0759, St. Louis, MO, USA) were added. Excess bile acids were removed after 1, 4, 16, and 64 minutes to obtain kinetic readouts. Cells were washed once with ice-cold PBS and once with 200 µl of ice-cold PBS containing 2% fatty acid-free BSA (Sigma-Aldrich #A6003, St. Louis, MO, USA) to remove potentially membrane-bound GCDC. Cells were incubated with 50 µg/ml of digitonin (Merck, Kenilworth, NJ, USA) in ice-cold PBS to permeabilize the plasma membrane and extract the cytosolic fraction. Radioactivity in the cytosolic fraction was detected using the liquid scintillation counter Tri-carb 2900TR apparatus (PerkinElmer, Groningen, the Netherlands). Cells were then washed with ice-cold PBS and shaken in 0.05% SDS in MQ for 60 minutes on a plate shaker at room temperature. Bicinchoninic acid (BCA) assays were performed on both the cytosolic and membrane fractions to correct ^{3}H-GCDC bile acid permeation values for total protein content per well. Experimental conditions tested in bile acid permeation experiments were as follows: GB1107, 10 µM, 24-hour pretreatment; recombinant galectin-3, 2.5 µg/ml, 24-hour pretreatment; rocaglamide, 100 nM, acute treatment; recombinant prohibitin 1, 0.25 µg/ml and 0.5 µg/ml, 24-hour pretreatment; patient-derived IgG preincubation, 50 µg IgG per 48 well, 48-hour pretreatment.

2.12 Caspase-3/7 assay

H69 cholangiocytes were plated in 96-well culture plates and grown until confluency. In parallel, an identical plate was seeded from the same cell suspensions and used for BCA assays to correct for potential differences in cell counts between shRNA control sham H69 cholangiocytes and *LGALS3*, *PHB1*, *PHB2*, and *PHB1/2* knockdown (KD) H69 cholangiocytes. The culture media were set to pH 6.9 and placed in a 5% CO_2 incubator overnight. The following day, three conditions were set up, consisting of 1500 µM GCDC, 10 µM raptinal as a positive control of apoptosis induction, and an untreated negative control. pH was checked for all solutions and, where necessary, set back at pH 6.9. After the addition of the experimental solutions to the 96-well plate, cells were checked hourly for the initiation of apoptosis under a bright-field microscope. After 3–4 hours, 1500 µM GCDC with media set at pH 6.9 consistently induced rounding of the cells. For measuring Caspase-3/7 activity, the SensoLyte® Homogeneous Rh110 Caspase-3/7 Assay Kit (AnaSpec #AS-71141) was used. Pre-warmed assay buffer at a volume of 5 ml was diluted with 5 ml of pre-warmed MQ and 200 µl of 0.5 M EDTA-NaOH pH 8.0, 200 µl of 1 M DTT, and, finally, 50 µl of (Z-DEVD)2-Rh110 as the fluorogenic indicator was added. Upon Caspase-3/7 cleavage, (Z-DEVD)2-Rh110 generates the Rh110 fluorophore, which was excited and detected at λEx = 496 nm/λEm = 520 nm on the CLARIOstar set at 37°C. Plates were read for 30 minutes. For analysis, slope values in the linear phase were obtained for each well. After assessing successful Caspase-3/7 induction by the positive control raptinal, Caspase-3/7 values were corrected for protein concentration and normalized to the untreated control sham condition. Experimental conditions tested in Caspase-3/7 experiments were as follows: GB1107, 10 µM; recombinant galectin-3, 2.5 and 5 µg/ml; rocaglamide, 100 nM; recombinant prohibitin 1, 0.25 µg/ml and 0.5 µg/ml. All treatments were added in the experimental solutions, i.e., GCDC, raptinal, or negative control.

2.13 Patient-derived IgG isolation

IgGs were isolated from human sera (healthy control, negative for anti-galectin-3 and anti-prohibitin 1 autoantibodies, and IRC patient #21, positive for anti-galectin-3 and anti-prohibitin 1 autoantibodies). In short, 350 µl of PureProteome beads (Millipore #LSKMAGAG10) were washed twice with wash buffer (PBS 0.01% Tween 20) and subsequently incubated with 350 µl of human serum in 1000 µl of wash buffer. Beads were then incubated for 30 minutes at room temperature, undergoing end-over-end mixing. Hereafter, beads were washed three times with wash buffer, and IgGs were subsequently eluted with 0.2 M glycine HCl pH 2.5 and neutralized with 1 M Tris pH 9. BCA assays were performed to determine the IgG content.

2.14 Statistical analysis

Experimental data are presented as means with standard deviations. Clinical data are represented as the median with an interquartile range. Statistical analyses were performed using GraphPad Prism 9 (GraphPad, La Jolla, CA, USA). The distribution of the data was assessed using the Kolmogorov–Smirnov test. For experimental data, the results of the two groups were compared with a paired or unpaired t-test where appropriate. A one-way ANOVA was used when comparing multiple groups. Outliers for RT-qPCR data were detected using the ROUT method. For clinical data, the Kruskal–Wallis test (for non-normally distributed data), one-way ANOVA (for normally distributed data), and the chi-square test (for categorical data) were used. Correlations were performed using Spearman's rank correlation (for non-normally distributed data) or Pearson's correlation (for normally distributed data). p-values <0.05 were considered statistically significant.

3 Results

3.1 Autoantibodies against galectin-3 and prohibitin 1 are present in a subset of people with IRC

First, autoantibody positivity directed against galectin-3 or prohibitin 1 was assessed in people with IRC (n = 52). Individuals with PSC (n = 14 and 15, resp.) and CCA (n = 14) were used as disease controls and healthy controls (n = 13 and 14, resp.). ELISAs for galectin-3 autoantibodies demonstrated that seven out of 52 people (13.5%) with IRC were positive, no people with PSC were positive, three out of 14 (21.4%) with CCA were positive, and one healthy control out of 14 (7.1%) was positive for galectin-3 autoantibodies, indicating that anti-galectin-3 autoantibodies are not specific for IRC (Figure 2A). Three of the people with IRC had specific IgG1 autoantibodies, and five had specific IgG4 autoantibodies directed against galectin-3 (Figures 2B, C). For prohibitin 1, 32 out of 52 people with IRC (61.5%) were positive for autoantibodies. In people with PSC, five out of 14 (35.7%) had autoantibodies against prohibitin 1, whereas, in people with CCA, eight out of 14 (57.1%) had autoantibodies against prohibitin 1, indicating that anti-prohibitin 1 autoantibodies are also not specific for IRC (Figure 2D). Furthermore, one healthy control was positive for anti-prohibitin 1 autoantibodies (7.1%). Fifteen of the people with IRC were positive for specific IgG1 autoantibodies, whereas eight were positive for specific IgG4 autoantibodies directed against prohibitin 1 (Figures 2E, F). Notably, neither IgG nor IgG1 or IgG4 autoantibody titers against galectin-3 or prohibitin 1 correlated with serum liver tests (total bilirubin, alkaline phosphatase (ALP), and gamma-glutamyl transferase (gGT)) when patients tested positive for autoantibodies (Supplementary Figures S1, S2). In a parallel approach, LC-MS/MS was performed on H69 cholangiocyte cell lysates after immunoprecipitation with patient-derived IgG4 coupled to sepharose beads. In line with previous findings, immunoprecipitation of annexin A11 was detected in three out of 16 individuals (19%) (Figure 3). An ELISA for anti-annexin A11 IgG4 autoantibodies detected annexin A11 in three out of 16 (19%) patients (Supplementary Figure S3). These results are similar to our previous findings and validate the LC-MS/MS approach. In this dataset, we did not detect peptides originating from galectin-3. Interestingly, one IgG4-RD patient (#081) with type 1 AIP demonstrated a pulldown of prohibitin 1.

Since prohibitin 1 and prohibitin 2 form a functional complex, we reasoned that prohibitin 2 could also be an autoimmune antigen. However, prohibitin 2 displays a detection pattern (although much less intense) that reflects background binding to the beads, as is illustrated by the ribosomal protein RPL22, which is present in all samples and serves as a loading control. This apparent aspecific binding makes it unfeasible to identify prohibitin 2 as an autoimmune antigen, although prohibitin 2 is detected at the highest intensity in the same patient (#81) who demonstrated prohibitin 1 pulldown, most likely indicating the pulldown of the functional prohibitin 1/2 complex. Thus, autoantibodies against galectin-3, but not against prohibitin 1, may be specific for a subgroup of people with IRC among those with fibrosing cholangiopathies, such as PSC.

People with IRC who were positive for anti-galectin-3 and anti-prohibitin 1 autoantibodies presented with (a tendency of) lower serum bilirubin, ALP, gGT, aspartate aminotransferase (AST), and alanine aminotransferase (ALT) levels (Table 1). Notably, people with IRC who were positive for anti-galectin-3 and anti-prohibitin 1 autoantibodies had high occurrences of major hepatopancreatobiliary (HPB) surgery in the past, possibly explaining in part the mild biochemical alterations after surgical removal of diseased tissue. People with anti-prohibitin 1 autoantibodies less frequently experienced multiorgan involvement. Other affected organs were most often secretory glands (Supplementary Tables S4, S5). Most patients were elderly men and had a history of blue-collar work, which we have previously identified as a risk factor for developing IRC (37). Four patients were positive for both galectin-3 and prohibitin 1 autoantibodies (Supplementary Tables S4, S5; patients #21, #160, #257, and #268). These patients did not have a more severe disease course (Supplementary Figure S4). In general, people with IRC were treated with standard immunosuppressive regimens with varying rates of clinical and biochemical responses (see Supplementary Figure

10.3389/fimmu.2023.1251134

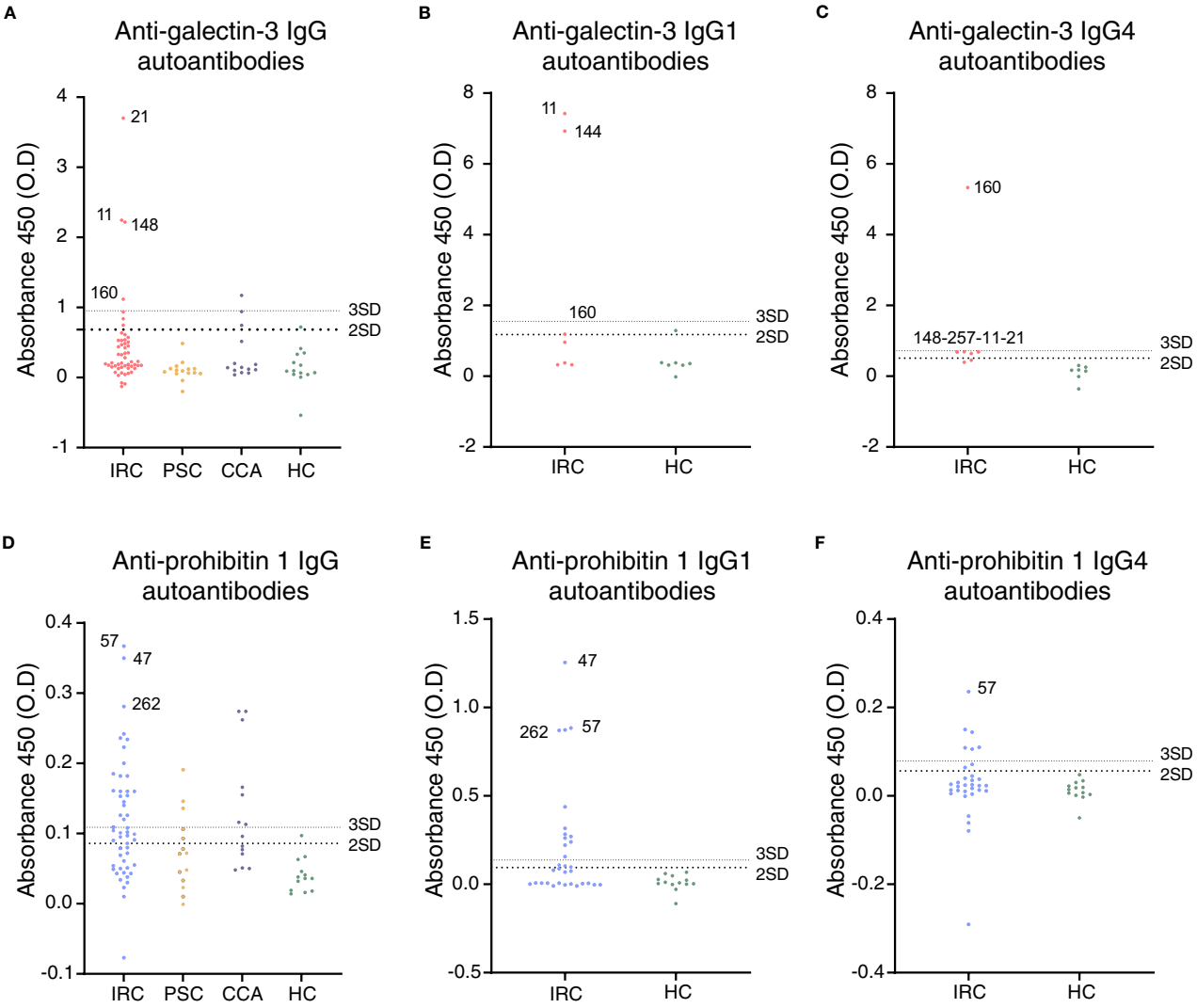

FIGURE 2
Galectin-3 and prohibitin 1 autoantibodies are present in a subset of people with IRC. **(A)** Anti-galectin-3 IgG, **(B)** IgG1, and **(C)** IgG4 autoantibody positivity in people with IRC, PSC, CCA, and healthy controls. Positive patients are annotated, and their further clinical details are presented in Supplementary Table S4. **(D)** Anti-prohibitin 1 IgG, **(E)** IgG1, and **(F)** IgG4 autoantibody positivity in people with IRC, PSC, CCA, and healthy controls. Further clinical details of positive patients are presented in Supplementary Table S5. **(A–F)** Data are represented as individual data points. Levels of significance: the cut-off for autoantibody positivity is defined as the mean plus two times the standard deviation of healthy controls (large dotted line); positivity based on the mean plus three times the standard deviation of healthy controls (small dotted line) is provided per patient in Supplementary Tables S4, S5. Autoantibody titer differences between groups. **(A)** HC *vs.* IRC, ns p = 0.1444; HC *vs.* PSC, ns p = 0.9879; HC *vs.* CCA, ns p = 0.6676; one-way ANOVA. **(B)** HC *vs.* IRC, ns p = 0.1161. **(C)** HC *vs.* IRC, ns p = 0.1124; unpaired t-tests. **(D)** HC *vs.* IRC, ** p = 0.0029; HC *vs.* PSC, ns p = 0.4550; HC *vs.* CCA, ** p = 0.0059; one-way ANOVA. **(E)** HC *vs.* IRC, * p = 0.0306. **(F)** HC *vs.* IRC, ns p = 0.4720; unpaired t-tests. CCA, cholangiocarcinoma; ELISA, enzyme-linked immunosorbent assay; HC, healthy control; IRC, IgG4-related cholangitis; PSC, primary sclerosing cholangitis; O.D., optical density.

S4 for individual cases with high IgG1/IgG4 titer positivity and Supplementary Tables S4, S5 for the complete overview). Thus, people with autoantibodies against galectin-3 or prohibitin 1 did not demonstrate a clinically more severe disease course compared to patients who were negative for these autoantibodies.

3.2 Galectin-3, prohibitin 1, and prohibitin 2 are expressed in human cholangiocyte models

As galectin-3 and prohibitin 1 autoantibodies can be detected in people with IRC, we assessed the cholangiocellular expression of these proteins in control human liver tissue by immunohistochemistry. Galectin-3 staining resulted in a cholangiocellular signal in the bile ducts, and prohibitin 1 staining demonstrated positivity in both cholangiocytes and hepatocytes (Figure 4A). Furthermore, the expression of galectin-3 and prohibitins 1 and 2 was assessed in various human cholangiocyte models at the transcriptional level (Figure 4B). To this end, a publicly available bulk RNA-sequencing dataset on four types of human cholangiocyte organoids was assessed (GEO: GSE156519). In addition, RNA sequencing on human H69 cholangiocytes was performed (GEO: GSE221746). A distinct cholangiocyte phenotype was demonstrated in all cholangiocyte

10.3389/fimmu.2023.1251134

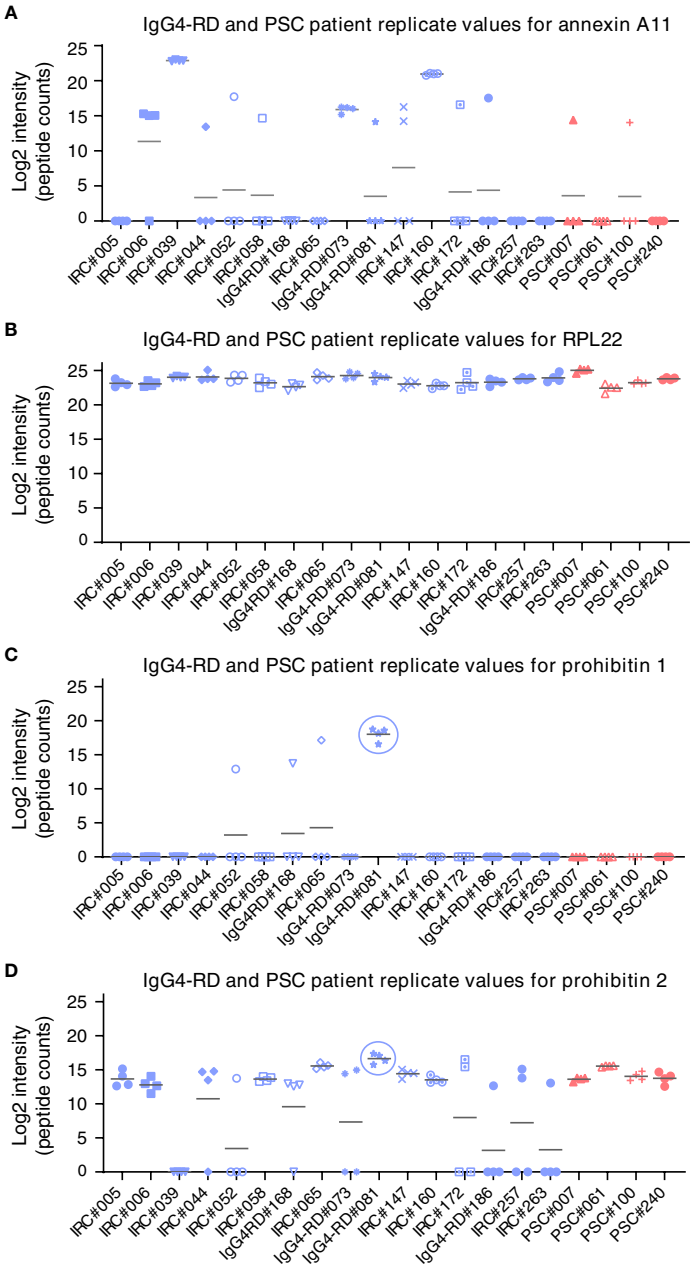

FIGURE 3
LC-MS/MS analysis of target antigens immunoprecipitated by patient-derived IgG4 autoantibodies. Label-free protein intensities (log2) were detected after immunoprecipitation by immobilized patient-derived IgG4 from human H69 cholangiocyte lysates. Four independent replicates were analyzed. **(A)** Annexin A11, **(B)** RPL22, **(C)** prohibitin 1, and **(D)** prohibitin 2. Gray bars represent the average values of four replicate measurements. IgG4-RD, IgG4-related disease; IRC, IgG4-related cholangitis; RPL22, ribosomal protein L22; PSC, primary sclerosing cholangitis; LC-MS/MS, liquid chromatography–tandem mass spectrometry.

organoids and human H69 cholangiocytes by high expression of the cholangiocellular markers *EPCAM* and *KRT19*, while the expression of hepatocyte markers *ALB* and *ASGR1* was low. Expression at the mRNA level of *LGALS3*, *PHB1*, and *PHB2* was evident across all types of cholangiocyte organoids (endoscopic retrograde cholangiopancreatography (ERCP)-derived, bile-collected, extrahepatic, and intrahepatic) and in human H69 cholangiocytes (Figure 4B). Thus, galectin-3 and prohibitins 1 and 2 are abundantly expressed in cholangiocytes, the major cell type affected in IRC.

To investigate the cellular roles of galectin-3, prohibitin 1, and prohibitin 2 in cholangiocytes, stable knockdown cell lines were generated (Figures 4C, D). In addition to single gene knockdown cell lines, as prohibitin 1 and prohibitin 2 form a multimeric complex and can likely be immunoprecipitated as a complex by patient-derived IgG4, both proteins were simultaneously knocked down in a combined *PHB1/2* knockdown cell line. Knockdown efficiency was assessed by Western blotting and qPCR analysis (*LGALS3* 83% KD on Western blotting (WB), 76% KD on RT-qPCR; *PHB1* 67% KD on WB, 52% KD on RT-qPCR; *PHB2* 47% KD on RT-qPCR; Figures 4C, D).

10.3389/fimmu.2023.1251134

TABLE 1 Clinical differences between people with IRC positive and negative for anti-galectin-3 and prohibitin 1 autoantibodies.

	Galectin-3	Prohibitin 1	Negative	P value
Number of IRC patients	7 (13.5%)	32 (61.5%)	17 (32.7%)	
Sex (male subjects/female subjects)	7/0	28/4	14/2	0.6120
Age (years)	60 (48–72)	62 (51–67)	66 (60–71)	0.2258
Blue collar work (%)	5 (71.4%)	22 (68.8%)	12 (70.6%)	0.8974
Multiorgan(%)	6 (86%)	20 (62.5%)	15 (88.2%)	**0.0494**
Malignancy (%)	2 (29%)	13 (40.6%)	5 (29.4%)	0.7568
Major HPB surgery (%)	3 (75%)	14 (43.8%)	1 (5.9%)	**0.0233**
Bilirubin (µmol/L)	35 (18–74)	53 (17–122)	104 (41–187)	0.1464
ALP (IU/L)	232 (141–344)	294 (190–505)	402 (300–760)	**0.0436**
gGT (IU/L)	284 (101–1455)	423 (219–669)	621 (400–1026)	0.1318
AST (IU/L)	83 (36–144)	82 (40–132)	190 (72–306)	**0.0441**
ALT (IU/L)	117 (60–169)	110 (61–187)	350 (87–480)	0.0790
CA19.9 (kU/L)	60 (12–160)	135 (23–221)	412 (22–12836)	0.5651
CRP (mg/L)	1.1 (0.4–325)	23 (5.3–104)	28 (7.5–43)	0.5558
ESR (mm/hour)	30 (11.5–76)	48 (21–67)	65 (22–94)	0.5540

Data are presented as medians with an interquartile range. Normal distributed data were assessed by one-way ANOVA, and non-normal distributed data were assessed by the Kruskal–Wallis test. Bold font indicates statistical significance ($p<0.05$).

3.3 Galectin-3 knockdown, pharmacological inhibition, and recombinant protein substitution do not demonstrate a clear-cut protective effect against toxic bile acids in human cholangiocytes

Based on the role of galectin-3 in the apical sorting of membrane proteins, we hypothesized that galectin-3 could exert a protective effect against toxic bile acids in human cholangiocytes by strengthening the biliary bicarbonate umbrella. Therefore, we used three parallel *in vitro* approaches, namely, stable *LGALS3* knockdown, galectin-3 inhibition by GB1107, and recombinant galectin-3 treatment. We assessed the effects of these parallel approaches by three assays that touch on the stability of the biliary bicarbonate umbrella: i) intracellular pH (pH_i) measurements using BCECF AM; ii) radioactive bile acid influx by measuring 22,23-^{3}H-glycochenodeoxycholic acid (^{3}H-GCDC) permeation; and iii) GCDC-induced apoptosis determined by Caspase-3/7 assays (22, 24). Neither stable knockdown of *LGALS3* nor galectin-3 inhibition with GB1107 induced alterations in pH_i, whereas recombinant galectin-3 treatment lowered the intracellular pH of human cholangiocytes (Supplementary Figure S5). To assess the role of galectin-3 in protecting cholangiocytes against toxic bile acids, we performed radioactive bile acid permeation assays. Stable *LGALS3* knockdown led to slightly increased toxic bile acid permeation after 1, 4, 16, and 64 minutes. In contrast, its acute counterpart—GB1107 treatment—conflictingly lowered toxic bile acid permeation at 4 and 16 minutes. Treatment with recombinant galectin-3 led to a slightly decreased toxic bile acid permeation at 4 and 16 minutes (Figures 5A–F). An increased rate of toxic bile acid permeation into cholangiocytes is expected to eventually induce cholangiocyte apoptosis. To assess this final downstream pathway, we performed Caspase-3/7 assays after exposure to GCDC. Stable *LGALS3* knockdown did not result in an increased rate of apoptosis, despite the increased toxic bile acid permeation. Acute inhibition of galectin-3 by GB1107 strongly reduced GCDC-induced apoptosis. Nevertheless, recombinant galectin-3 treatment only reduced apoptosis at a lower dose of 2.5 µg/ml, but not at a higher dose of 5 µg/ml (Figures 5G–I). Thus, our data do not indicate a clear role for galectin-3 in cholangiocyte protection against toxic bile acids under the experimental conditions chosen.

3.4 Prohibitin knockdown, pharmacological inhibition and recombinant protein substitution do not disclose a role of prohibitins in the human cholangiocyte defense against toxic bile acids

We hypothesized that prohibitins—in analogy with the IRC autoantigens annexin A11 and laminin 511-E8 and consideration of a potential pathogenetic role of prohibitin 1 in PBC (30)—could contribute to the protection of human cholangiocytes against toxic bile acid influx and stabilization of the biliary bicarbonate umbrella. As for galectin-3 (see above), we used three parallel *in vitro* approaches: i) stable *PHB1* or *PHB2* knockdown and combined *PHB1/2* knockdown; ii) pan-prohibitin inhibition by rocaglamide;

10.3389/fimmu.2023.1251134

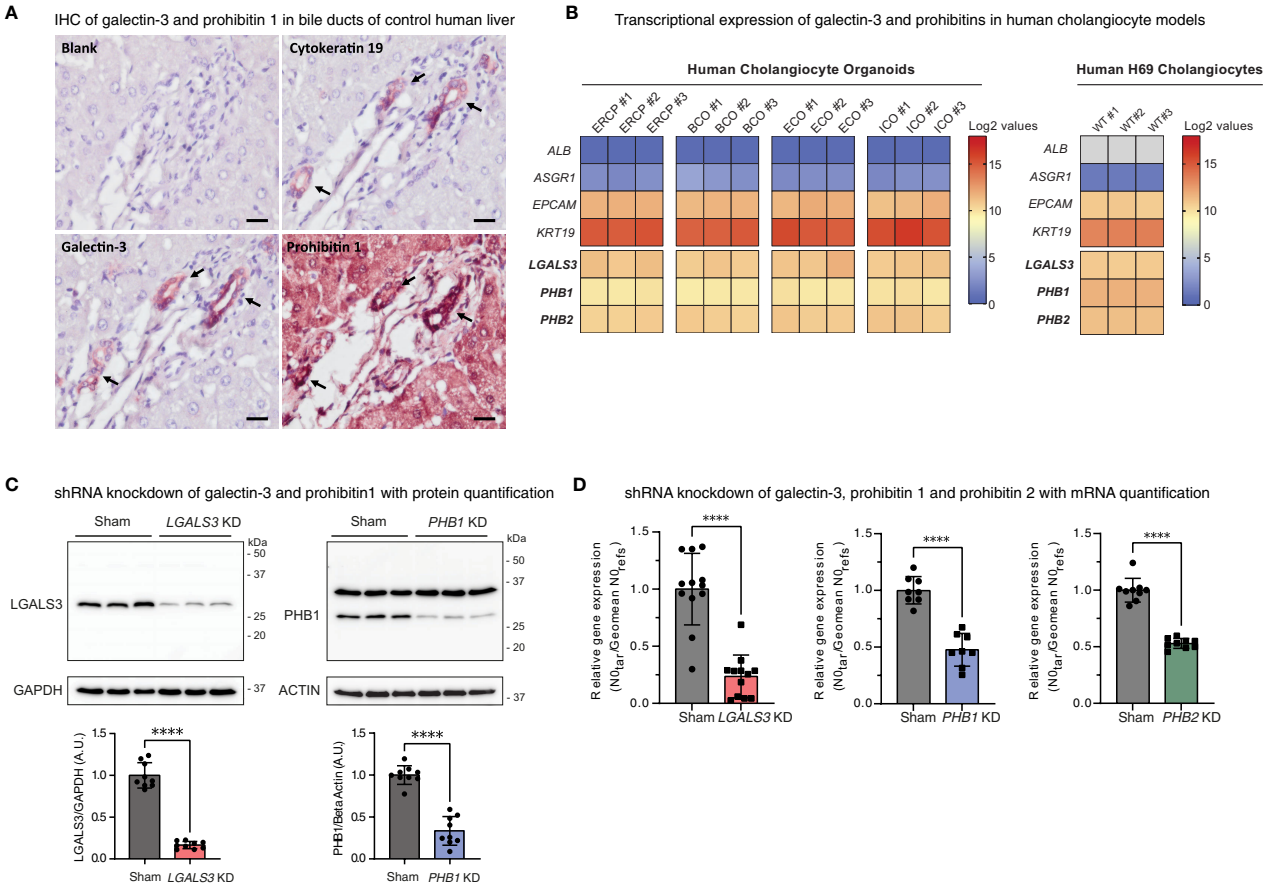

FIGURE 4
Galectin-3, prohibitin 1, and prohibitin 2 are abundantly expressed in human cholangiocyte models. **(A)** Immunohistochemical staining of galectin-3 and prohibitin 1 in control human liver sections with sequential cytokeratin 19 staining as a positive control for bile ducts (annotated by arrows) (scale bar, 20 µm). **(B)** Heatmaps depicting expression levels of galectin-3 and prohibitins 1 and 2 in human cholangiocyte models (positive for *EPCAM* and *KRT19* and negative for hepatocyte markers *ALB* and *ASGR1*). The left shows log2-transformed expression values of four different derivations of human cholangiocyte organoids (ERCP, BCO, ECO, and ICO). The right shows log2-transformed expression values of human H69 cholangiocytes. **(C)** LGALS3 (26 kDa) and PHB1 (30 kDa) expression and knockdown quantification in H69 sham transduced and respective shRNA knockdown cell lines. *LGALS3* KD is normalized by GAPDH (37 kDa) (9 cell samples from n = 3 independent experiments). *PHB1* KD is normalized by beta-actin (42 kDa) (9 cell samples from n = 3 independent experiments). Data are represented as means with standard deviations. **(D)** Relative mRNA expression of *LGALS3*, *PHB1*, and *PHB2* in H69 sham transduced and respective shRNA knockdown cell lines (9–12 cell samples from n = 3–4 independent experiments, 1 outlier value excluded from the sham and *PHB1* dataset). Data are represented as the starting concentration (N0) of target genes over the geomean of the reference genes *36B4* (*RPLP0*) and *HPRT* N0 values normalized to sham. Levels of significance: **(C)** *LGALS3* KD **** $p < 0.0001$ and *PHB1* KD **** $p < 0.0001$, unpaired t-tests. **(D)** *LGALS3* KD **** $p < 0.0001$, *PHB1* KD **** $p < 0.0001$, *PHB2* KD **** $p < 0.0001$, unpaired t-tests. *ALB*, albumin; A.U, arbitrary units; *ASGR1*, asialoglycoprotein receptor 1; BCO, bile-collected organoid (from resected gallbladders and PTC drainage); ECO, extrahepatic cholangiocyte organoid; *EPCAM*, epithelial cell adhesion molecule; ERCP, ERCP-derived cholangiocyte organoid; *GAPDH*, glyceraldehyde-3-phosphate dehydrogenase; ICO, intrahepatic cholangiocyte organoid; IHC, immunohistochemistry; kDa, kilodalton; KD, knockdown; *KRT19*, cytokeratin 19; *LGALS3*, galectin-3; N0, starting concentration; *PHB1*, prohibitin 1; *PHB2*, prohibitin 2; WT, wild type.

and iii) recombinant prohibitin 1 treatment. We assessed the effects of these parallel approaches using the three above-described assays that touch on the stability of the biliary bicarbonate umbrella. Stable knockdown of *PHB1* and combined knockdown of *PHB1/2* showed a decrease in the pH_i of human cholangiocytes (Supplementary Figure S6). To assess whether prohibitins protect cholangiocytes against toxic bile acid influx, we performed radioactive bile acid permeation assays. Under stable knockdown conditions, only the combined *PHB1/2* knockdown showed a slight increase in toxic bile acid permeation after 4 minutes, but not at other time points (Figures 6A, B). Assessment of the final downstream apoptotic pathway showed a slight increase in GCDC-induced apoptosis in the *PHB1* knockdown cell line (Figure 6C).

In line with results after the stable knockdown of *PHB1* and combined knockdown of *PHB1/2*, the pan-prohibitin inhibitor rocaglamide induced a decrease in pH_i in human cholangiocytes (Supplementary Figure S7) and markedly reduced toxic bile acid influx (Figures 7A, C). However, treatment with recombinant prohibitin 1 conflictingly also showed a decrease in pH_i (Supplementary Figure S7) but did not affect toxic bile acid influx in human cholangiocytes (Figures 7B, D) or GCDC-induced apoptosis (Figures 7E, F). Thus, our data do not show evidence

10.3389/fimmu.2023.1251134

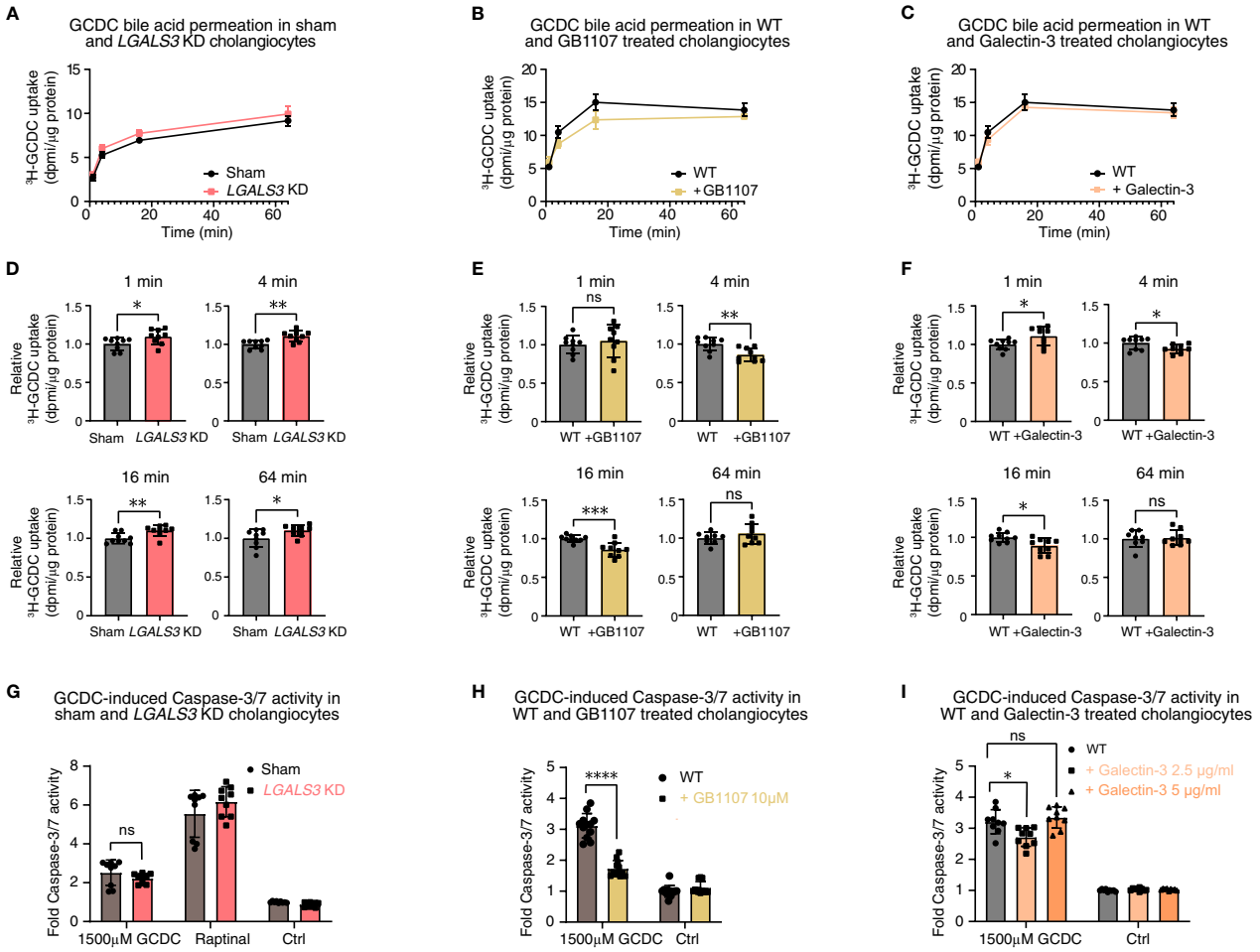

FIGURE 5
Galectin-3 knockdown, pharmacological inhibition, and recombinant protein substitution do not demonstrate a clear damaging or protective effect against toxic bile acids in human cholangiocytes. 22,23-^{3}H-GCDC permeation assay in **(A)** sham and *LGALS3* KD cholangiocytes, **(B)** WT and GB1107-treated cholangiocytes, and **(C)** WT and recombinant galectin-3-treated cholangiocytes (representative experiments of n = 3). Relative quantification of 22,23-^{3}H-GCDC permeation per time point in **(D)** sham and *LGALS3* KD cholangiocytes, **(E)** WT and GB1107-treated cholangiocytes, and **(F)** WT and recombinant galectin-3-treated cholangiocytes (8–9 samples from n = 3 independent experiments). GCDC-induced Caspase-3/7 activity in **(G)** sham and *LGALS3* KD cholangiocytes, **(H)** WT and GB1107-treated cholangiocytes, and **(I)** WT and recombinant galectin-3 treated cholangiocytes (9–12 samples from n = 3–4 independent experiments). Data are represented as means with standard deviations. Levels of significance: **(D)** 1 min: * p = 0.0353. 4 min: ** p = 0.0023. 16 min: ** p = 0.0070. 64 min: * p = 0.0365, unpaired t-tests. **(E)** 1 min: ns, p = 0.5371. 4 min: ** p = 0.0034. 16 min: *** p = 0.0007. 64 min: ns, p = 0.2797, unpaired t-tests. **(F)** 1 min: * p = 0.0311. 4 min: * p = 0.0321. 16 min: * p = 0.0104. 64 min: ns, p = 0.8328, unpaired t-tests. **(G)** ns, p = 0.2204, unpaired t-test. **(H)** **** p < 0.0001, unpaired t-test. **(I)** In order of sham to 2.5 µg/ml, to 5 µg/ml: * p = 0.0103, ns, p = 0.6212, one-way ANOVA. Ctrl, control; DPMI, disintegrations per minute; GCDC, glycochenodeoxycholic acid; KD, knockdown; *LGALS3*, galectin-3; ns, not significant; WT, wild type.

for a potentially relevant protective effect of prohibitins against human toxic bile acids in human cholangiocytes *in vitro*.

3.5 Pretreatment of cholangiocytes with patient-derived IgG positive for anti-galectin-3 and anti-prohibitin 1 autoantibodies does not lead to increased toxic bile acid permeation

As a final experiment, IgGs were isolated from one healthy control (negative for anti-galectin-3 and anti-prohibitin 1 autoantibodies) and one IRC patient (#21) who was positive for anti-galectin-3 and anti-prohibitin 1 autoantibodies (see Figure 2A and Supplementary Tables S4, 5). Pretreatment with patient-derived IgG for 48 hours did not lead to increased GCDC-influx after 16 minutes of incubation (Figure 8).

4 Discussion

The current study is the first to demonstrate that a subset of people with IRC form autoantibodies directed against galectin-3 or prohibitin 1. Autoantibodies against galectin-3 were detected in people with IRC (13.5%) and CCA (21.4%) but not in people with PSC and were of both the IgG1 and IgG4 subclasses. Prohibitin 1 autoantibodies occurred frequently (61.5%) in people with IRC but were also frequently detected in people with PSC (35.7%) and were

10.3389/fimmu.2023.1251134

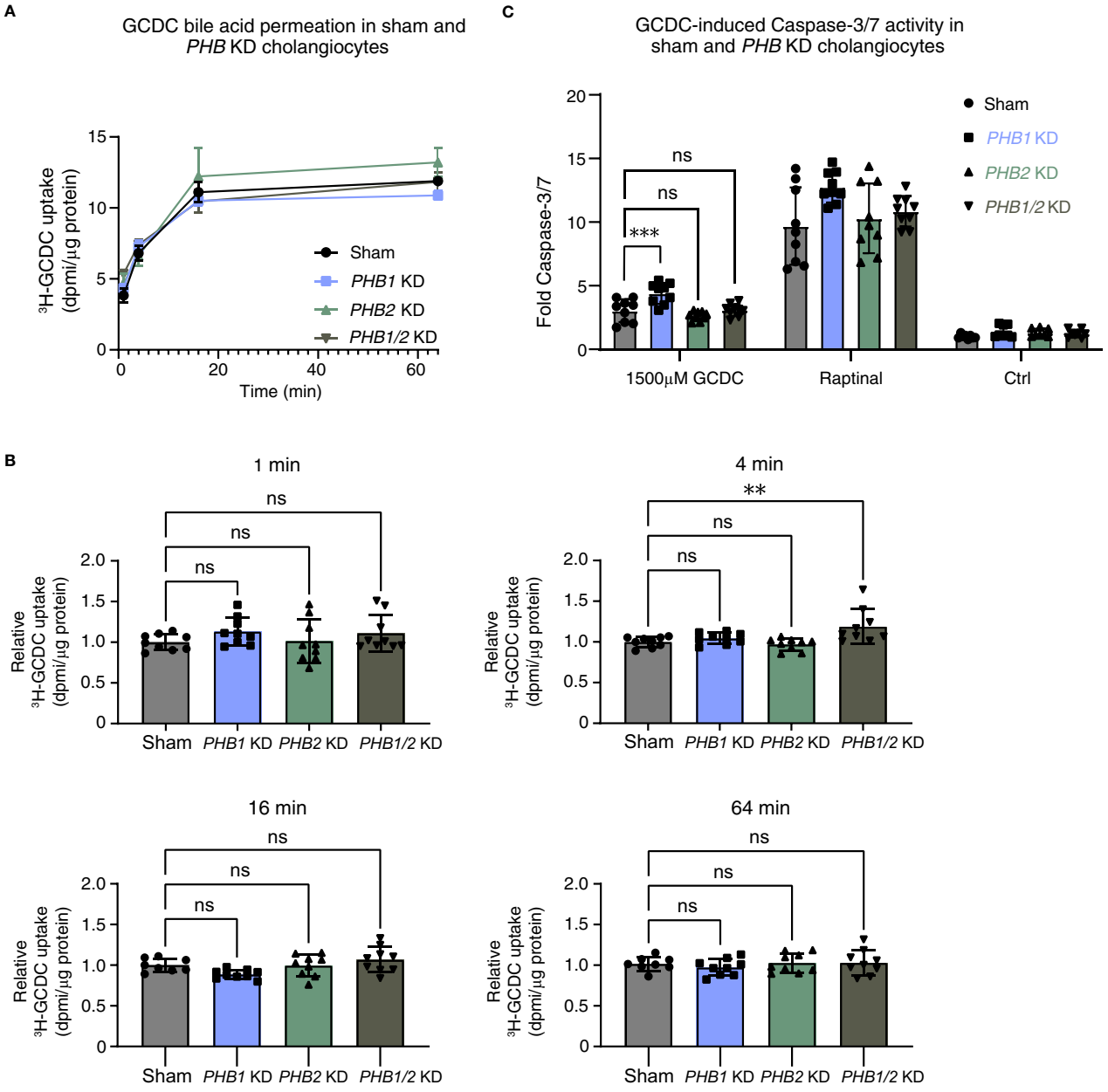

FIGURE 6
Single lentiviral shRNA knockdown of *PHB1* or *PHB2* or double *PHB1/2* knockdown demonstrates a clear damaging effect against toxic bile acids in human cholangiocytes. 22,23-^{3}H-GCDC permeation assay in **(A)** sham, *PHB1* KD, *PHB2* KD, and combined *PHB1/2* KD cholangiocytes (representative experiments of n = 3). Relative quantification of 22,23-^{3}H-GCDC permeation per time point in **(B)** sham, *PHB1* KD, *PHB2* KD, and combined *PHB1/2* KD cholangiocytes (8–9 samples from n = 3 independent experiments). GCDC-induced Caspase-3/7 activity in **(C)** sham, *PHB1* KD, *PHB2* KD, and combined *PHB1/2* KD cholangiocytes (9–12 samples from n = 3–4 independent experiments). Data are represented as means with standard deviations. Levels of significance: **(B)** in order of sham to *PHB1* KD, to *PHB2* KD, to *PHB1/2* KD: 1 min: ns, p = 0.3731, ns, p = 0.9966, ns, p = 0.5143. 4 min: ns, p = 0.7795, ns, p = 0.9155, ** p = 0.0060. 16 min: ns, p = 0.1287, ns, p = 0.9999, ns, p = 0.4846. 64 min: ns, p = 0.7828, ns, p = 0.9940, ns, p = 0.9902, one-way ANOVA. **(C)** In order of sham to *PHB1* KD, to *PHB2* KD, to *PHB1/2* KD: *** p = 0.0005, ns, p = 0.4392, ns, p = 0.9985, one-way ANOVA. Ctrl, control; DPMI, disintegrations per minute; GCDC, glycochenodeoxycholic acid; KD, knockdown; ns, not significant; *PHB1*, prohibitin 1; *PHB2*, prohibitin 2; WT, wild type.

partly of the IgG1 or IgG4 subclass. Neither IgG nor IgG1 or IgG4 titers against galectin-3 or prohibitin 1 correlated with patients' serum liver parameters.

Furthermore, the potential role of galectin-3 and prohibitins 1 and 2 in protecting cholangiocytes against toxic bile acids as previously reported by us for the IRC autoantigens annexin A11 (22) and laminin 511-E8 (25) was assessed in the current study *in vitro* by parallel approaches of stable gene knockdown, pharmacological inhibition, and recombinant galectin-3 or prohibitin 1 treatment. These parallel approaches did not demonstrate clear-cut protective effects in three assays that touch on the functionality of the biliary bicarbonate umbrella (23, 24), including intracellular pH measurements, toxic bile acid permeation studies, and experiments determining GCDC-induced

10.3389/fimmu.2023.1251134

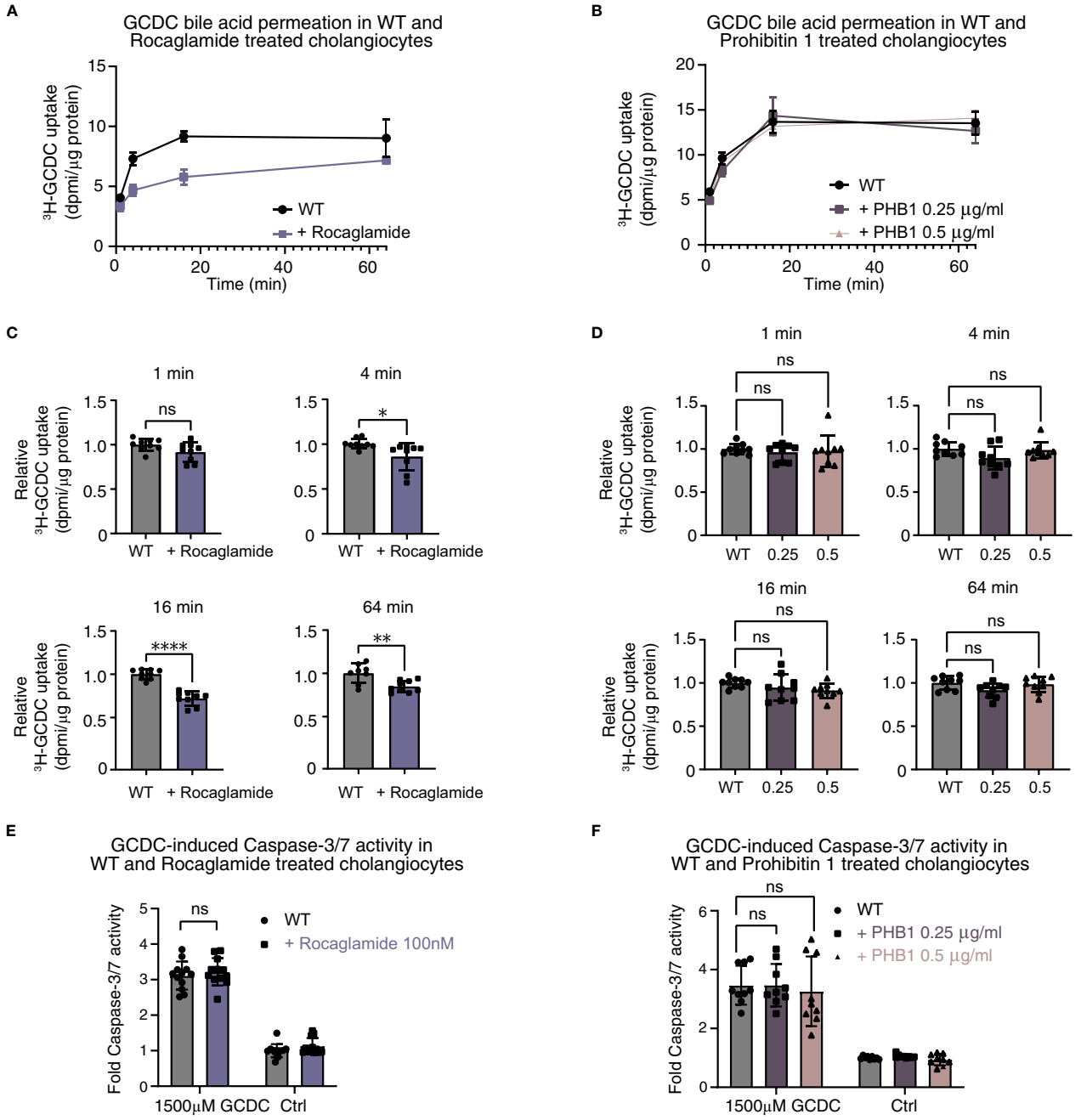

FIGURE 7
Pharmacological inhibition of prohibitins and recombinant protein substitution of prohibitin 1 do not demonstrate a clear damaging or protective effect against toxic bile acids in human cholangiocytes. 22,23-^{3}H-GCDC permeation assay in **(A)** WT and rocaglamide-treated cholangiocytes; **(B)** WT, recombinant low-dose prohibitin 1 0.25 µg/ml, and recombinant high-dose 0.5 µg/ml-treated cholangiocytes (representative experiments of n = 3). Relative quantification of 22,23-^{3}H-GCDC permeation per time point in **(C)** WT and rocaglamide-treated cholangiocytes, and **(D)** WT, recombinant low-dose prohibitin 1 0.25 µg/ml and recombinant high-dose 0.5 µg/ml-treated cholangiocytes (8–9 samples from n = 3 independent experiments). GCDC-induced Caspase-3/7 activity in **(E)** WT and rocaglamide-treated cholangiocytes, and **(F)** WT, recombinant low-dose prohibitin 1 0.25 µg/ml and recombinant high-dose 0.5 µg/ml-treated cholangiocytes (9–12 samples from n = 3–4 independent experiments). Data are represented as means with standard deviations. Levels of significance: **(C)** 1 min: ns, not significant p = 0.0634. 4 min: * p = 0.0167. 16 min: **** p < 0.0001. 64 min: ** p = 0.0041, unpaired t-tests. **(D)** In order of sham to 0.25 µg/ml, to 0.5 µg/ml: 1 min: ns, p = 0.7354, ns, p = 0.8690. 4 min: ns, p = 0.0737, ns, p = 0.9288. 16 min: ns, p = 0.4439, ns, p = 0.1545. 64 min: ns, p = 0.0791, ns, p = 0.9104, one-way ANOVA. **(E)** ns, p = 0.5108, unpaired t-test. **(F)** In order of sham to 0.25 µg/ml, to 0.5 µg/ml: ns, p > 0.9999, ns, p = 0.8369, one-way ANOVA. Ctrl, control; DPMI, disintegrations per minute; GCDC, glycochenodeoxycholic acid; KD, knockdown; ns, not significant; PHB1, prohibitin 1; WT, wild type.

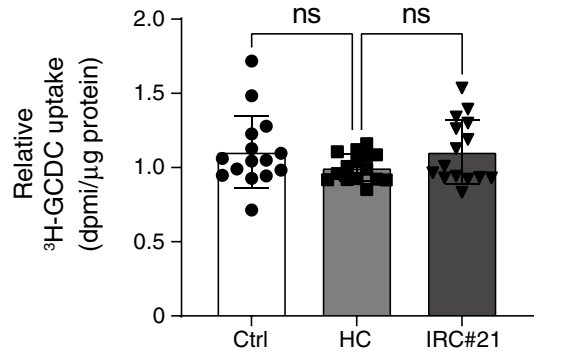

FIGURE 8
Pretreatment of cholangiocytes with patient-derived IgG positive for anti-galectin-3 and anti-prohibitin 1 autoantibodies does not lead to increased toxic bile acid permeation. Relative quantification of 22,23-^{3}H-GCDC permeation into vehicle control cholangiocytes (Ctrl, white), cholangiocytes treated with IgG from a healthy control negative for anti-galectin-3 and anti-prohibitin 1 autoantibodies (HC, light gray), cholangiocytes treated with IgGs isolated from an IRC patient (#21, dark gray), and positive for anti-galectin-3 and anti-prohibitin 1 autoantibodies. The time point is 16 min incubation with 22,23-^{3}H-GCDC (15 samples from n = 5 independent experiments). Levels of significance: HC vs Ctrl ns, p = 0.2474. HC vs IRC#21 ns, p = 0.2410. One-way ANOVA. Ctrl, vehicle control; HC, healthy control; IRC#21, IgG4-related cholangitis patient #21.

cholangiocyte apoptosis. In line with these findings, pretreatment with IgGs isolated from an IRC patient with anti-galectin-3 and anti-prohibitin 1 autoantibodies did not lead to increased GCDC permeation into cholangiocytes.

Galectin-3 and prohibitin 1 autoantibody positivity have previously been assessed in more clinically diverse cohorts of people with IgG4-RD who had multiorgan manifestations. Galectin-3 and prohibitin 1 autoantibodies were detected at higher rates (28% and 73.5%, respectively) than in our IRC-specific cohort (11, 13). This difference in autoantibody positivity could potentially arise from differences in the genetic backgrounds of the cohorts, differences in toxin exposure (37), or differences in disease severity. It should be noted that the recombinant galectin-3 and prohibitin 1 proteins used in these studies and our ELISA experiments were produced in *Escherichia coli*, which lack post-translational modifications such as glycosylation (38). This could potentially lead to false-positive or false-negative results, as glycosylation could affect (auto)antibody binding (39).

As an alternative approach to detecting autoantibodies against galectin-3 and prohibitin 1, we made use of a limited cohort of people with IgG4-RD, where LC-MS/MS was performed after patient-derived IgG4 had been immobilized to immunoprecipitate antigenic targets from H69 cholangiocyte lysates. In this dataset, galectin-3 was not detected, in contrast to the identification of five IgG4 anti-galectin-3-positive patients detected by our ELISA. This difference could potentially be explained by the different techniques (ELISA *vs.* LC-MS/MS), as this has previously been shown to affect antigen detection in IgG4-RD (12), by the sensitivity of the LC-MS/MS, the small group size of the LC-MS/MS cohort, or the fact that only one positive patient (#160) was analyzed in both cohorts. Patient-derived IgG4 beads pulled down prohibitin 1 in one patient with type 1 AIP but not in patients with IRC, which is in line with our ELISA data demonstrating scarce and low titer positivity of IgG4 subclass autoantibodies against prohibitin 1 in people with IRC. In the same patient with type 1 AIP where prohibitin 1 was detected, prohibitin 2 could reliably be detected by MS2 identification, most likely as a consequence of the pulldown of the functional prohibitin 1/2 complex. Whether prohibitin 2 can be a genuine autoantigen remains to be resolved, as prohibitin 2 displays aspecific binding in our assay. We validated our LC-MS/MS approach by performing an ELISA for the previously identified autoantigen annexin A11 (10). It is noteworthy that two IRC patients were assessed positively by both methods: one patient was only detected by LC-MS/MS, and one patient was only detected by ELISA. The diverging results when applying these two methods could potentially arise from false-positive or false-negative findings in our ELISA, as our approach with recombinant proteins derived from *Escherichia coli* could affect autoantibody binding.

Notably, in the clinically diverse galectin-3 IgG4-RD cohort, only 15% of the people who were positive for galectin-3 autoantibodies had a history of IRC, indicating that galectin-3 positivity in IgG4-RD does not de facto lead to the development of IRC. The frequent detection of prohibitin 1 autoantibodies in people with PSC and CCA indicates that anti-prohibitin 1 autoantibodies are aspecific and occur in other immune-mediated cholestatic liver diseases. Although complicated by retrospective analysis, our other clinical data question the direct role of galectin-3 and prohibitin 1 autoantibodies in affecting cholangiocyte defense against toxic bile acids, as i) autoantibody titers against galectin-3 and prohibitin 1 do not correlate with cholestatic serum markers, and ii) patients positive for galectin-3 and prohibitin 1 autoantibodies had (a tendency of) lower cholestatic serum markers compared to patients without galectin-3 and prohibitin 1 autoantibodies. If galectin-3 and prohibitins were to protect cholangiocytes against bile acid toxicity, direct inhibition of their endogenous function by autoantibodies would most likely result in higher cholestatic serum markers, and positive correlations between autoantibody titers and cholestatic serum markers would be expected. Indeed, pretreatment with IgGs isolated from a patient with anti-galectin-3 and anti-prohibitin-1 autoantibodies did not lead to an increase in toxic bile acid permeation into cholangiocytes.

Our *in vitro* experiments, which assess the function of galectin-3 through parallel approaches (stable *LGALS3* knockdown, galectin-3 inhibition with GB1107, and recombinant galectin-3 treatment) have to be interpreted in light of the ubiquitous roles of galectin-3, which strongly depend on its localization (extracellular versus intracellular) (26). Galectin-3 is secreted from epithelial cells to subsequently undergo endosomal uptake and regulate the apical sorting of membrane proteins (27, 28, 40–43). As a robust expression of ion transporters on the apical cholangiocyte membrane is essential for the formation of a protective biliary bicarbonate umbrella (22–24), we investigated the possibility that galectin-3 could be involved in the apical sorting of membrane proteins that stabilize the biliary bicarbonate umbrella. As the transporters involved in stabilizing the biliary

bicarbonate umbrella regulate the secretion of bicarbonate and hydrogen ions, intracellular pH measurements were performed after stable *LGALS3* knockdown, galectin-3 inhibition by the membrane permeable inhibitor GB1107, and recombinant galectin-3 treatment. Neither *LGALS3* knockdown nor GB1107 treatment affected the intracellular pH of human cholangiocytes. Although recombinant galectin-3 treatment did result in a decreased intracellular pH, this was not accompanied by a clear-cut reduction in toxic bile acid permeation after recombinant galectin-3 treatment. Additionally, if galectin-3 were to stabilize the biliary bicarbonate umbrella, *LGALS3* knockdown and GB1107 treatment would be expected to lead to increased toxic bile acid permeation. However, stable *LGALS3* knockdown only slightly increased toxic bile acid permeation, whereas GB1107 treatment conversely reduced toxic bile acid permeation after early time points. These findings indicate that galectin-3 is most likely not involved in the regulation of cholangiocellular bicarbonate secretion, which is in line with the finding that galectin-3 knockout mice only demonstrate increased chloride excretion but no changes in bicarbonate secretion (44).

The interpretation of the results on GCDC-induced apoptosis is complicated by the fact that both pro- and anti-apoptotic roles have been demonstrated for galectin-3. Whether galectin-3 exerts a pro- or anti-apoptotic effect is mostly dependent on the cellular localization of galectin-3, with anti-apoptotic effects described for intracellular galectin-3 and pro-apoptotic effects demonstrated for extracellular galectin-3. Although the role of extracellular galectin-3 has been described as pro-apoptotic (45), overexpression of galectin-3 has been shown to increase cell adhesion to the extracellular matrix, thereby conferring resistance to various apoptotic stimuli (46). Of particular interest here is the role of galectin-3 in promoting cell adhesion to laminin 511, another autoantigen in IRC for which a protective role in cholangiocytes against toxic bile acids has been described (25, 47). These opposing mechanisms of extracellular galectin-3 and the balance with its anti-apoptotic intracellular counterpart could potentially explain the diverging results seen in GCDC-induced apoptosis after *LGALS3* knockdown, galectin-3 inhibition with GB1107, and recombinant galectin-3 treatment in varying doses.

Similar to our studies on the role of galectin-3 in cholangiocytes, three approaches were chosen to assess the role of prohibitins 1 and 2, including stable *PHB1*, *PHB2*, and combined *PHB1/2* knockdown, pan-prohibitin inhibition by rocaglamide, and recombinant prohibitin 1 treatment. Remarkably, all interventions except *PHB2* knockdown led to a decrease in intracellular pH. Although hard evidence is lacking, prohibitins and proteins with prohibitin domains have been suggested to regulate the activity of ion channels by altering the local lipid environment in the plasma membrane (48, 49). Alternatively, prohibitin 1 is a known binding partner to the ion channel regulator annexin A2 (50). This decrease in intracellular pH did not translate into an attenuated toxic bile acid permeation except after rocaglamide treatment. Rocaglamide is a natural prohibitin 1 and 2 ligand that blocks the downstream effects of these proteins. However, as rocaglamide's mechanisms of action are vast and also include translational inhibition (51, 52), the experiments performed in human H69 cholangiocytes exposed to rocaglamide must be interpreted with caution. Just like galectin-3, prohibitins 1 and 2 also have a complex role in apoptosis, and their pro- or anti-apoptotic effects depend on the cell type, their subcellular localization, and post-translational modifications (53). In our experiments, only isolated *PHB1* knockdown led to an increased rate of GCDC-induced apoptosis.

Although our experimental and clinical data do not point to a role for galectin-3 and prohibitins in protecting cholangiocytes against toxic bile acids, galectin-3 and prohibitins could still be involved in the pathogenesis of IRC via other mechanisms. IRC is characterized by aberrant B- and T-cell responses, which can be observed as a lymphoplasmacytic tissue infiltrate and lead to the formation of storiform fibrosis in and around the bile ducts. Notably, galectin-3 plays an important role in regulating B- and T-cell function. Galectin-3 has been shown to inhibit the differentiation of B cells into plasma cells, and galectin-3 knockout mice show increased numbers of plasma cells and develop hypergammaglobulinemia upon infection (54, 55). In addition, spontaneous anti-laminin-secreting plasma cells have been detected in galectin-3 knockout mice (56). These findings are of interest in the context of IgG4-RD's pathogenesis, as affinity-matured B-cell receptor clones have been identified by us and others in people with IgG4-RD (7–9). With regard to T cells, galectin-3 has been shown to induce T-cell apoptosis (57, 58) and negatively regulate TCR-mediated $CD4^+$ T-cell activation (59). Furthermore, galectin-3 plays a relevant role in the formation of (liver) fibrosis (60, 61), and specific galectin-3 inhibitors have been developed to target this process (62).

Also, prohibitins play an apparent role in the regulation of B- and T-cell function and the formation of fibrosis. In B cells, prohibitins 1 and 2 regulate IgG1 production, which is of interest as people with IRC frequently have targeted autoantibodies of the IgG1 subclasses (63). In activated T cells, prohibitin 1 and prohibitin 2 are upregulated (64), with proteomics data showing that prohibitins are particularly expressed on the cell surface of human Th17 cells, where they maintain the stability of Th17 cells (65). This is relevant as IgG4-RD, but other immune-mediated cholestatic liver diseases, such as PSC, are associated with an increased Th17 response (66, 67). Furthermore, prohibitin 1 plays an important role in the formation of fibrosis, as liver-specific $Phb1^{-/-}$ mice spontaneously develop liver fibrosis (68).

Collectively, as we have recently demonstrated that the IRC autoantigens annexin A11 and laminin 511-E8 both display a protective role in human cholangiocytes against toxic bile acids, we hypothesized a similar common role for galectin-3 and prohibitins. Despite the literature supporting this hypothesis and our clinical data demonstrating that galectin-3 and prohibitin 1 are autoantigens in people with IRC, our experimental *in vitro* data did not demonstrate a clear-cut protective role of galectin-3 and prohibitins in human cholangiocytes against toxic bile acids. In addition, pretreatment with autoantibodies directed against galectin-3 and prohibitin 1 did not lead to increased toxic bile acid permeation into cholangiocytes. It is, therefore, unlikely that autoantibodies directed against galectin-3 and prohibitin 1 would directly lead to cholangiocyte damage by interfering with the cholangiocellular functions of galectin-3 and prohibitins. However, as both galectin-3 and prohibitins are involved in pathophysiological processes that are implicated in IRC, such as

regulation of B- and T-cell function and the formation of fibrosis, direct autoantibody-induced functional impairment of galectin-3 and prohibitin 1 could still play a role in the pathogenesis of IRC. Alternatively, autoantibody binding to galectin-3 or prohibitin 1 could elicit an excessive immune response that could lead to the obstructive cholestasis seen in IRC. Thus, our studies on the role of the autoantigens galectin-3 and prohibitin 1 in IRC did not clearly disclose a protective function of these autoantigens in human cholangiocytes against toxic bile acids.

Data availability statement

The mass spectrometry proteomics data have been deposited with the ProteomeXchange Consortium via the PRIDE partner repository with the dataset identifier PXD042856. The RNA sequencing dataset of human H69 cholangiocytes used for this study has been deposited in the R2 genomics analysis and visualization platform and the Gene Expression Omnibus (GEO) and can be openly accessed under GEO accession GSE221746.

Ethics statement

The studies involving humans were approved by the Medical Ethics Committee of Amsterdam University Medical Centers (formerly Academic Medical Center Amsterdam). The studies were conducted in accordance with local legislation and institutional requirements. The participants provided their written informed consent to participate in this study.

Author contributions

RK, DCT, SG, and UB conceived the experiments. RK, DCT, and DT performed the experiments. RK, DCT, DT, HV, SG, and UB analyzed the data. The original draft of the manuscript was written by RK, DCT, and UB, after which reviewing and editing was done by all authors. The final manuscript was approved by all authors.

Funding

This study was supported by a ZonMw Open Competition grant (#09120012010109 to UB), a South African PSC patient foundation grant (Stichting AMC Foundation #20837 to UB), an Amsterdam UMC/AMC PhD Scholarship (to DCT), a Gastrostart grant from the Netherlands Society of Gastroenterology (to RK and DCT), and the X-omics initiative (NWO, project 184.034.019 to HV).

Acknowledgments

Publicly available and our own RNA-sequencing datasets were analyzed and graphically displayed in collaboration with the Department of Epidemiology and Data Science, Bioinformatics Laboratory of Amsterdam UMC, Academic Medical Center. Specifically, we wish to express our gratitude toward Dr. Aldo Jongejan for his recommendations on the analysis of the datasets obtained from Gene Expression Omnibus (GEO) and Dr. Jan Koster for making use of the R2 genomics analysis and visualization platform (http://r2.amc.nl/). In addition, we would like to thank F. Roos, H. Wu, M. Verstegen, and L. van der Laan (GEO accession GSE156519) for depositing their RNA-sequencing dataset in GEO available to the public.

Conflict of interest

The authors declare that the research was conducted in the absence of any commercial or financial relationships that could be construed as a potential conflict of interest.

Publisher's note

Supplementary material

The Supplementary Material for this article can be found online at: https://www.frontiersin.org/articles/10.3389/fimmu.2023.1251134/full#supplementary-material

References

1. Löhr JM, Vujasinovic M, Rosendahl J, Stone JH, Beuers U. IgG4-related diseases of the digestive tract. *Nat Rev Gastroenterol Hepatol* (2022) 19(3):185–97. doi: 10.1038/s41575-021-00529-y

2. Culver EL, Sadler R, Simpson D, Cargill T, Makuch M, Bateman AC, et al. Elevated serum igg4 levels in diagnosis, treatment response, organ involvement, and relapse in a prospective IgG4-related disease UK cohort. *Am J Gastroenterol* (2016) 111 (5):733–43. doi: 10.1038/ajg.2016.40

3. Boonstra K, Culver EL, de Buy Wenniger LM, van Heerde MJ, van Erpecum KJ, Poen AC, et al. Serum immunoglobulin G4 and immunoglobulin G1 for distinguishing immunoglobulin G4-associated cholangitis from primary sclerosing cholangitis. *Hepatol* (2014) 59(5):1954–63. doi: 10.1002/hep.26977

4. Roos E, Hubers LM, Coelen RJS, Doorenspleet ME, de Vries N, Verheij J, et al. IgG4-associated cholangitis in patients resected for presumed perihilar cholangiocarcinoma: a 30-year tertiary care experience. *Am J Gastroenterol* (2018) 113(5):765–72. doi: 10.1038/s41395-018-0036-5

5. Oseini AM, Chaiteerakij R, Shire AM, Ghazale A, Kaiya J, Moser CD, et al. Utility of serum immunoglobulin G4 in distinguishing immunoglobulin G4-associated cholangitis from cholangiocarcinoma. *Hepatol* (2011) 54(3):940–8. doi: 10.1002/hep.24487

6. Ghazale A, Chari ST, Zhang L, Smyrk TC, Takahashi N, Levy MJ, et al. Immunoglobulin G4-associated cholangitis: clinical profile and response to therapy. *Gastroenterol* (2008) 134(3):706–15. doi: 10.1053/j.gastro.2007.12.009

7. Maillette de Buy Wenniger LJ, Doorenspleet ME, Klarenbeek PL, Verheij J, Baas F, Elferink RP, et al. Immunoglobulin G4+ clones identified by next-generation sequencing dominate the B cell receptor repertoire in immunoglobulin G4 associated cholangitis. *Hepatol* (2013) 57(6):2390–8. doi: 10.1002/hep.26232

8. Wallace ZS, Mattoo H, Carruthers M, Mahajan VS, Della Torre E, Lee H, et al. Plasmablasts as a biomarker for IgG4-related disease, independent of serum IgG4 concentrations. *Ann Rheum Dis* (2015) 74(1):190–5. doi: 10.1136/annrheumdis-2014-205233

9. Mattoo H, Mahajan VS, Della-Torre E, Sekigami Y, Carruthers M, Wallace ZS, et al. *De novo* oligoclonal expansions of circulating plasmablasts in active and relapsing IgG4-related disease. *J Allergy Clin Immunol* (2014) 134(3):679–87. doi: 10.1016/j.jaci.2014.03.034

10. Hubers LM, Vos H, Schuurman AR, Erken R, Oude Elferink RP, Burgering B, et al. Annexin A11 is targeted by IgG4 and IgG1 autoantibodies in IgG4-related disease. *Gut* (2018) 67(4):728–35. doi: 10.1136/gutjnl-2017-314548

11. Perugino CA, AlSalem SB, Mattoo H, Della-Torre E, Mahajan V, Ganesh G, et al. Identification of galectin-3 as an autoantigen in patients with IgG4-related disease. *J Allergy Clin Immunol* (2019) 143(2):736–45.e6. doi: 10.1016/j.jaci.2018.05.011

12. Shiokawa M, Kodama Y, Sekiguchi K, Kuwada T, Tomono T, Kuriyama K, et al. Laminin 511 is a target antigen in autoimmune pancreatitis. *Sci Transl Med* (2018) 10 (453). doi: 10.1126/scitranslmed.aaq0997

13. Du H, Shi L, Chen P, Yang W, Xun Y, Yang C, et al. Prohibitin is involved in patients with igG4 related disease. *PloS One* (2015) 10(5):e0125331. doi: 10.1371/journal.pone.0125331

14. Liu H, Perugino CA, Ghebremichael M, Wallace ZS, Montesi SB, Stone JH, et al. Disease severity linked to increase in autoantibody diversity in igG4-related disease. *Arthritis Rheumatol* (2020) 72(4):687–93. doi: 10.1002/art.41140

15. Shiokawa M, Kodama Y, Kuriyama K, Yoshimura K, Tomono T, Morita T, et al. Pathogenicity of IgG in patients with IgG4-related disease. *Gut* (2016) 65(8):1322–32. doi: 10.1136/gutjnl-2015-310336

16. Trampert DC, Hubers LM, van de Graaf SFJ, Beuers U. On the role of IgG4 in inflammatory conditions: lessons for IgG4-related disease. *Biochim Biophys Acta Mol Basis Dis* (2018) 1864(4 Pt B):1401–9. doi: 10.1016/j.bbadis.2017.07.038

17. Huijbers MG, Zhang W, Klooster R, Niks EH, Friese MB, Straasheijm KR, et al. MuSK IgG4 autoantibodies cause myasthenia gravis by inhibiting binding between MuSK and Lrp4. *Proc Natl Acad Sci USA* (2013) 110(51):20783–8. doi: 10.1073/pnas.1313944110

18. Niks EH, van Leeuwen Y, Leite MI, Dekker FW, Wintzen AR, Wirtz PW, et al. Clinical fluctuations in MuSK myasthenia gravis are related to antigen-specific IgG4 instead of IgG1. *J Neuroimmunol* (2008) 195(1-2):151–6. doi: 10.1016/j.jneuroim.2008.01.013

19. Rispens T, Huijbers MG. The unique properties of IgG4 and its roles in health and disease. *Nat Rev Immunol* (2023) 23(11):763–78. doi: 10.1038/s41577-023-00871-z

20. Huijbers MG, Plomp JJ, van der Maarel SM, Verschuuren JJ. IgG4-mediated autoimmune diseases: a niche of antibody-mediated disorders. *Ann N Y Acad Sci* (2018) 1413(1):92–103. doi: 10.1111/nyas.13561

21. Koneczny I, Yilmaz V, Lazaridis K, Tzartos J, Lenz TL, Tzartos S, et al. Common denominators in the immunobiology of igG4 autoimmune diseases: what do glomerulonephritis, pemphigus vulgaris, myasthenia gravis, thrombotic thrombocytopenic purpura and autoimmune encephalitis have in common? *Front Immunol* (2020) 11:605214. doi: 10.3389/fimmu.2020.605214

22. Herta T, Kersten R, Chang JC, Hubers L, Go S, Tolenaars D, et al. Role of the IgG4-related cholangitis autoantigen annexin A11 in cholangiocyte protection. *J Hepatol* (2022) 76(2):319–31. doi: 10.1016/j.jhep.2021.10.009

23. Beuers U, Hohenester S, de Buy Wenniger LJ, Kremer AE, Jansen PL, Elferink RP. The biliary HCO(3)(-) umbrella: a unifying hypothesis on pathogenetic and therapeutic aspects of fibrosing cholangiopathies. *Hepatol* (2010) 52(4):1489–96. doi: 10.1002/hep.23810

24. Hohenester S, Wenniger LM, Paulusma CC, van Vliet SJ, Jefferson DM, Elferink RP, et al. A biliary HCO3- umbrella constitutes a protective mechanism against bile acid-induced injury in human cholangiocytes. *Hepatol* (2012) 55(1):173–83. doi: 10.1002/hep.24691

25. Trampert D, Kersten R, Tolenaars D, Oude-Elferink R, van de Graaf S, Beuers U. The IgG4-related cholangitis autoantigen laminin 511-E8 stabilizes the biliary bicarbonate umbrella in human cholangiocytes. *J Hepatol* (2022) 77:S603–S4. doi: 10.1016/S0168-8278(22)01523-9

26. Dumic J, Dabelic S, Flögel M. Galectin-3: an open-ended story. *Biochim Biophys Acta* (2006) 1760(4):616–35. doi: 10.1016/j.bbagen.2005.12.020

27. Delacour D, Cramm-Behrens CI, Drobecq H, Le Bivic A, Naim HY, Jacob R. Requirement for galectin-3 in apical protein sorting. *Curr Biol* (2006) 16(4):408–14. doi: 10.1016/j.cub.2005.12.046

28. Straube T, von Mach T, Honig E, Greb C, Schneider D, Jacob R. pH-dependent recycling of galectin-3 at the apical membrane of epithelial cells. *Traffic* (2013) 14 (9):1014–27. doi: 10.1111/tra.12086

29. Thuaud F, Ribeiro N, Nebigil CG, Désaubry L. Prohibitin ligands in cell death and survival: mode of action and therapeutic potential. *Chem Biol* (2013) 20(3):316–31. doi: 10.1016/j.chembiol.2013.02.006

30. Barbier-Torres L, Beraza N, Fernández-Tussy P, Lopitz-Otsoa F, Fernández-Ramos D, Zubiete-Franco I, et al. Histone deacetylase 4 promotes cholestatic liver injury in the absence of prohibitin-1. *Hepatol* (2015) 62(4):1237–48. doi: 10.1002/hep.27959

31. Erice O, Munoz-Garrido P, Vaquero J, Perugorria MJ, Fernandez-Barrena MG, Saez E, et al. MicroRNA-506 promotes primary biliary cholangitis-like features in cholangiocytes and immune activation. *Hepatol* (2018) 67(4):1420–40. doi: 10.1002/hep.29533

32. Chazouilleres O, Beuers U, Bergquist A, Karlsen TH, Levy C, Samyn M, et al. EASL Clinical Practice Guidelines on sclerosing cholangitis. *J hepatol* (2022) 77(3):761–806. doi: 10.1016/j.jhep.2022.05.011

33. Perez-Riverol Y, Bai J, Bandla C, García-Seisdedos D, Hewapathirana S, KamatChinathan S, et al. The PRIDE database resources in 2022: a hub for mass spectrometry-based proteomics evidences. *Nucleic Acids Res* (2022) 50(D1):D543–d52. doi: 10.1093/nar/gkab1038

34. Grubman SA, Perrone RD, Lee DW, Murray SL, Rogers LC, Wolkoff LI, et al. Regulation of intracellular pH by immortalized human intrahepatic biliary epithelial cell lines. *Am J Physiol* (1994) 266(6 Pt 1):G1060–70. doi: 10.1152/ajpgi.1994.266.6.G1060

35. Seppen J, Rijnberg M, Cooreman MP, Oude Elferink RP. Lentiviral vectors for efficient transduction of isolated primary quiescent hepatocytes. *J Hepatol* (2002) 36 (4):459–65. doi: 10.1016/S0168-8278(01)00308-7

36. Ramakers C, Ruijter JM, Deprez RH, Moorman AF. Assumption-free analysis of quantitative real-time polymerase chain reaction (PCR) data. *Neurosci Lett* (2003) 339 (1):62–6. doi: 10.1016/S0304-3940(02)01423-4

37. Hubers LM, Schuurman AR, Buijs J, Mostafavi N, Bruno MJ, Vermeulen RCH, et al. Blue-collar work is a risk factor for developing IgG4-related disease of the biliary tract and pancreas. *JHEP Rep* (2021) 3(6):100385. doi: 10.1016/j.jhepr.2021.100385

38. Berlec A, Strukelj B. Current state and recent advances in biopharmaceutical production in Escherichia coli, yeasts and mammalian cells. *J Ind Microbiol Biotechnol* (2013) 40(3-4):257–74. doi: 10.1007/s10295-013-1235-0

39. Lisowska E. The role of glycosylation in protein antigenic properties. *Cell Mol Life Sci* (2002) 59(3):445–55. doi: 10.1007/s00018-002-8437-3

40. Hönig E, Schneider K, Jacob R. Recycling of galectin-3 in epithelial cells. *Eur J Cell Biol* (2015) 94(7-9):309–15. doi: 10.1016/j.ejcb.2015.05.004

41. Hönig E, Ringer K, Dewes J, von Mach T, Kamm N, Kreitzer G, et al. Galectin-3 modulates the polarized surface delivery of β1-integrin in epithelial cells. *J Cell Sci* (2018) 131(11). doi: 10.1242/jcs.213199

42. Liu W, Hsu DK, Chen HY, Yang RY, Carraway KL 3rd, Isseroff RR, et al. Galectin-3 regulates intracellular trafficking of EGFR through Alix and promotes keratinocyte migration. *J Invest Dermatol* (2012) 132(12):2828–37. doi: 10.1038/jid.2012.211

43. Delacour D, Greb C, Koch A, Salomonsson E, Leffler H, Le Bivic A, et al. Apical sorting by galectin-3-dependent glycoprotein clustering. *Traffic* (2007) 8(4):379–88. doi: 10.1111/j.1600-0854.2007.00539.x

44. Bichara M, Attmane-Elakeb A, Brown D, Essig M, Karim Z, Muffat-Joly M, et al. Exploring the role of galectin 3 in kidney function: a genetic approach. *Glycobiol* (2006) 16(1):36–45. doi: 10.1093/glycob/cwj035

45. Nakahara S, Oka N, Raz A. On the role of galectin-3 in cancer apoptosis. *Apoptosis* (2005) 10(2):267–75. doi: 10.1007/s10495-005-0801-y

46. Matarrese P, Fusco O, Tinari N, Natoli C, Liu FT, Semeraro ML, et al. Galectin-3 overexpression protects from apoptosis by improving cell adhesion properties. *Int J Cancer* (2000) 85(4):545–54. doi: 10.1002/(SICI)1097-0215(20000215)85:4<545::AID-IJC17>3.0.CO;2-N

47. Margadant C, van den Bout I, van Boxtel AL, Thijssen VL, Sonnenberg A. Epigenetic regulation of galectin-3 expression by β1 integrins promotes cell adhesion and migration. *J Biol Chem* (2012) 287(53):44684–93. doi: 10.1074/jbc.M112.426445

48. Huber TB, Schermer B, Müller RU, Höhne M, Bartram M, Calixto A, et al. Podocin and MEC-2 bind cholesterol to regulate the activity of associated ion channels. *Proc Natl Acad Sci USA* (2006) 103(46):17079–86. doi: 10.1073/pnas.0607465103

49. Nadimpalli R, Yalpani N, Johal GS, Simmons CR. Prohibitins, stomatins, and plant disease response genes compose a protein superfamily that controls cell proliferation, ion channel regulation, and death. *J Biol Chem* (2000) 275(38):29579–86. doi: 10.1074/jbc.M002339200

50. Bacher S, Achatz G, Schmitz ML, Lamers MC. Prohibitin and prohibitone are contained in high-molecular weight complexes and interact with alpha-actinin and annexin A2. *Biochimie* (2002) 84(12):1207–20. doi: 10.1016/s0300-9084(02)00027-5

51. Wang D, Tabti R, Elderwish S, Abou-Hamdan H, Djehal A, Yu P, et al. Prohibitin ligands: a growing armamentarium to tackle cancers, osteoporosis, inflammatory, cardiac and neurological diseases. *Cell Mol Life Sci* (2020) 77 (18):3525–46. doi: 10.1007/s00018-020-03475-1

52. Li-Weber M. Molecular mechanisms and anti-cancer aspects of the medicinal phytochemicals rocaglamides (=flavaglines). *Int J Cancer* (2015) 137(8):1791–9. doi: 10.1002/ijc.29013

53. Peng YT, Chen P, Ouyang RY, Song L. Multifaceted role of prohibitin in cell survival and apoptosis. *Apoptosis* (2015) 20(9):1135–49. doi: 10.1007/s10495-015-1143-z

54. Acosta-Rodríguez EV, Montes CL, Motrán CC, Zuniga EI, Liu FT, Rabinovich GA, et al. Galectin-3 mediates IL-4-induced survival and differentiation of B cells: functional cross-talk and implications during Trypanosoma cruzi infection. *J Immunol* (2004) 172(1):493–502. doi: 10.4049/jimmunol.172.1.493

55. Oliveira FL, Frazão P, Chammas R, Hsu DK, Liu FT, Borojevic R, et al. Kinetics of mobilization and differentiation of lymphohematopoietic cells during experimental murine schistosomiasis in galectin-3 -/- mice. *J Leukoc Biol* (2007) 82(2):300–10. doi: 10.1189/jlb.1206747

56. Clark AG, Weston ML, Foster MH. Lack of galectin-1 or galectin-3 alters B cell deletion and anergy in an autoantibody transgene model. *Glycobiol* (2013) 23(7):893–903. doi: 10.1093/glycob/cwt026

57. Fukumori T, Takenaka Y, Yoshii T, Kim HR, Hogan V, Inohara H, et al. CD29 and CD7 mediate galectin-3-induced type II T-cell apoptosis. *Cancer Res* (2003) 63 (23):8302–11.

58. Stillman BN, Hsu DK, Pang M, Brewer CF, Johnson P, Liu FT, et al. Galectin-3 and galectin-1 bind distinct cell surface glycoprotein receptors to induce T cell death. *J Immunol* (2006) 176(2):778–89. doi: 10.4049/jimmunol.176.2.778

59. Chen HY, Fermin A, Vardhana S, Weng IC, Lo KF, Chang EY, et al. Galectin-3 negatively regulates TCR-mediated CD4+ T-cell activation at the immunological synapse. *Proc Natl Acad Sci USA* (2009) 106(34):14496–501. doi: 10.1073/pnas.0903497106

60. Li LC, Li J, Gao J. Functions of galectin-3 and its role in fibrotic diseases. *J Pharmacol Exp Ther* (2014) 351(2):336–43. doi: 10.1124/jpet.114.218370

61. Henderson NC, Mackinnon AC, Farnworth SL, Poirier F, Russo FP, Iredale JP, et al. Galectin-3 regulates myofibroblast activation and hepatic fibrosis. *Proc Natl Acad Sci USA* (2006) 103(13):5060–5. doi: 10.1073/pnas.0511167103

62. Slack RJ, Mills R, Mackinnon AC. The therapeutic potential of galectin-3 inhibition in fibrotic disease. *Int J Biochem Cell Biol* (2021) 130:105881. doi: 10.1016/j.biocel.2020.105881

63. Lucas CR, Cordero-Nieves HM, Erbe RS, McAlees JW, Bhatia S, Hodes RJ, et al. Prohibitins and the cytoplasmic domain of CD86 cooperate to mediate CD86 signaling in B lymphocytes. *J Immunol* (2013) 190(2):723–36. doi: 10.4049/jimmunol.1201646

64. Ross JA, Nagy ZS, Kirken RA. The PHB1/2 phosphocomplex is required for mitochondrial homeostasis and survival of human T cells. *J Biol Chem* (2008) 283 (8):4699–713. doi: 10.1074/jbc.M708232200

65. Buehler U, Schulenburg K, Yurugi H, Šolman M, Abankwa D, Ulges A, et al. Targeting prohibitins at the cell surface prevents Th17-mediated autoimmunity. *EMBO J* (2018) 37(16). doi: 10.15252/embj.201899429

66. Grados A, Ebbo M, Piperoglou C, Groh M, Regent A, Samson M, et al. T cell polarization toward T(H)2/T(FH)2 and T(H)17/T(FH)17 in patients with igG4-related disease. *Front Immunol* (2017) 8:235. doi: 10.3389/fimmu.2017.00235

67. Katt J, Schwinge D, Schoknecht T, Quaas A, Sobottka I, Burandt E, et al. Increased T helper type 17 response to pathogen stimulation in patients with primary sclerosing cholangitis. *Hepatol* (2013) 58(3):1084–93. doi: 10.1002/hep.26447

68. Ko KS, Tomasi ML, Iglesias-Ara A, French BA, French SW, Ramani K, et al. Liver-specific deletion of prohibitin 1 results in spontaneous liver injury, fibrosis, and hepatocellular carcinoma in mice. *Hepatol* (2010) 52(6):2096–108. doi: 10.1002/hep.23919

10.3389/fimmu.2023.1251134

Glossary

6-MP	6-mercaptopurine
6-TG	6-thioguanine
36B4 (RPLP0)	ribosomal protein lateral stalk subunit P0
AIP	autoimmune pancreatitis
ANO1	anoctamin 1
ANOVA	analysis of variance
ALB	albumin
ALP	alkaline phosphatase
ALT	alanine aminotransferase
ASGR1	asialoglycoprotein receptor 1
AST	aspartate aminotransferase
AZA	azathioprine
BCA	bicinchoninic acid
BCECF AM	2′ 7′-bis-(2-carboxyethyl)-5-(and-6)-carboxyfluorescein acetoxymethyl ester
BCO	bile-collected cholangiocyte organoid
BSA	bovine serum albumin
CA19.9	cancer antigen 19.9
CCA	cholangiocarcinoma
Cq	cycle quantification
CRP	C-reactive protein
DEAE	diethylaminoethyl
DEPC	diethylpyrocarbonate
DPMI	disintegrations per minute
DTT	dithiothreitol
ECM	extracellular matrix
ECO	extrahepatic cholangiocyte organoid
EDTA	ethylenediaminetetraacetic acid
ELISA	enzyme-linked immunosorbent assay
EPCAM	epithelial cell adhesion molecule
ERCP	endoscopic retrograde cholangiopancreatography
ESR	erythrocyte sedimentation rate
GAPDH	glyceraldehyde-3-phosphate dehydrogenase
GCDC	glycochenodeoxycholic acid
GEO	Gene Expression Omnibus
gGT	gamma-glutamyl transferase
GIST	gastrointestinal stromal tumor
HBSS	Hank's balanced salt solution

(Continued)

Continued

HEPES	4-(2-hydroxyethyl)-1-piperazineethanesulfonic acid
HISORt	Histology, imaging, serology, other organ involvement, response to therapy
HPB	hepatopancreatobiliary
HPF	high-power field
HPRT	hypoxanthine phosphoribosyltransferase 1
HRP	horseradish peroxidase
ICO	intrahepatic cholangiocyte organoid
IHC	immunohistochemistry
IgG4-RD	IgG4-related disease
IRC	IgG4-related cholangitis
KD	knockdown
kDa	kilodalton
KRT19	cytokeratin 19
LC-MS/MS	liquid chromatography with tandem mass spectrometry
LGALS3	galectin-3
MMF	mycophenolate mofetil
mRNA	messenger ribonucleic acid
N0	starting concentration
ns	not significant
PBC	primary biliary cholangitis
PBS	phosphate-buffered saline
PEI	polyethylenimine
PHB1	prohibitin 1
PHB2	prohibitin 2
pHi	intracellular pH
PSC	primary sclerosing cholangitis
PTC	percutaneous transhepatic cholangiography
RIPA	radioimmunoprecipitation assay
RPL22	ribosomal protein L22
RT-qPCR	real-time quantitative polymerase chain reaction
SDS-PAGE	sodium dodecyl sulfate–polyacrylamide gel electrophoresis
shRNA	short hairpin ribonucleic acid
TMB	3, 3′, 5, 5′-tetramethylbenzidine
TBS	tris-buffered saline
TBST	tris-buffered saline tween
TCR	T-cell receptor
Th17	T helper 17 cell

(Continued)

10.3389/fimmu.2023.1251134

Continued

TRC	the RNAi consortium
UDCA	ursodeoxycholic acid
WT	wild type

frontiers | Frontiers in Immunology

TYPE Original Research
PUBLISHED 02 February 2024
DOI 10.3389/fimmu.2024.1347948

OPEN ACCESS

EDITED BY
Luis Querol,
Hospital de la Santa Creu i Sant Pau, Spain

REVIEWED BY
Frank Leypoldt,
University Medical Center Schleswig-Holstein, Germany
Sergio Muñiz-Castrillo,
Stanford Center for Sleep Sciences and Medicine, United States

*CORRESPONDENCE
Lidia Sabater
lisabate@recerca.clinic.cat

†These authors share first authorship

RECEIVED 01 December 2023
ACCEPTED 09 January 2024
PUBLISHED 02 February 2024

CITATION
Landa J, Serafim AB, Alba M, Maudes E, Molina-Porcel L, Garcia-Serra A, Mannara F, Dalmau J, Graus F and Sabater L (2024) IgLON5 deficiency produces behavioral alterations in a knockout mouse model. *Front. Immunol.* 15:1347948. doi: 10.3389/fimmu.2024.1347948

IgLON5 deficiency produces behavioral alterations in a knockout mouse model

Jon Landa[1†], Ana Beatriz Serafim[1†], Mercedes Alba[1], Estibaliz Maudes[1], Laura Molina-Porcel[2,3], Anna Garcia-Serra[1], Francesco Mannara[1], Josep Dalmau[1,4,5,6], Francesc Graus[1] and Lidia Sabater[1,5*]

[1]Neuroimmunology Program, Fundació de Recerca Clínic Barcelona-Institut d'Investigacions Biomédiques August Pi i Sunyer-Caixa Research Institute (CRI), Universitat de Barcelona, Barcelona, Spain, [2]Alzheimer's Disease and Other Cognitive Disorders Unit, Neurology Service, Hospital Clínic, Institut d'Investigacions Biomèdiques August Pi i Sunyer (IDIBAPS), Barcelona, Spain, [3]Neurological Tissue Bank, Biobanc, Hospital Clínic, Institut d'Investigacions Biomèdiques August Pi i Sunyer (IDIBAPS), Barcelona, Spain, [4]Department of Neurology, University of Pennsylvania, Philadelphia, PA, United States, [5]Centro de Investigación Biomédica en Red, Enfermedades Raras (CIBERER), Madrid, Spain, [6]Catalan Institution for Research and Advanced Studies (ICREA), Barcelona, Spain

Background: Anti-IgLON5 disease is a neurological disorder characterized by autoantibodies against IgLON5 and pathological evidence of neurodegeneration. IgLON5 is a cell adhesion molecule of unknown function that is highly expressed in the brain. Our aim was to investigate the impact of IgLON5 loss-of-function in evaluating brain morphology, social behavior, and the development of symptoms observed in an IgLON5 knockout (IgLON5-KO) mouse model.

Methods: The IgLON5-KO mice were generated using CRISPR-Cas9 technology. Immunohistochemistry on fixed sagittal brain sections and Western blotting brain lysates were used to confirm IgLON5 silencing and to evaluate the presence of other cell surface proteins. Two- month-old IgLON5-KO and wild-type (WT) mice underwent a comprehensive battery of behavioral tests to assess 1) locomotion, 2) memory, 3) anxiety, 4) social interaction, and 5) depressive-like behavior. Brain sections were examined for the presence of anatomical abnormalities and deposits of hyperphosphorylated tau in young adult (2-month-old) and aged (22-month-old) mice.

Results: Mice did not develop neurological symptoms reminiscent of those seen in patients with anti-IgLON5 disease. Behavioral testing revealed that 2-month-old IgLON5-KO mice showed subtle alterations in motor coordination and balance. IgLON5-KO females exhibited hyperactivity during night and day. Males were observed to have depressive-like behavior and excessive nest-building behavior. Neuropathological studies did not reveal brain morphological alterations or hyperphosphorylated tau deposits.

Conclusion: IgLON5-KO mice showed subtle alterations in behavior and deficits in fine motor coordination but did not develop the clinical phenotype of anti-IgLON5 disease.

KEYWORDS

Iglon5, animal model, knockout, behavior (mice), anti-IgLON5 antibody encephalopathy

1 Introduction

Anti-IgLON5 disease is a neurological disorder characterized by the presence in serum, and >90% of cases are in cerebrospinal fluid (CSF), with IgG antibodies targeting IgLON5, a neuronal cell adhesion molecule of unknown function. The clinical manifestations of anti-IgLON5 disease are heterogeneous, and most patients present a combination of symptoms that include a sleep disorder with non-rapid eye movement (REM) and REM parasomnias, stridor or obstructive sleep apnea, gait instability, abnormal movements, bulbar symptoms, and cognitive impairment (1–3). Motor neuron disease-like phenotype, mimicking amyotrophic lateral sclerosis, has been also recently described in some patients with anti-IgLON5 disease (4, 5).

In at least 75% of patients, symptoms progress slowly for months or years, a feature that is unusual in other autoimmune encephalitis with antibodies against surface antigens, which often develop in a matter of a few weeks (6). Initial neuropathological findings revealed features of neurodegeneration with deposits of hyperphosphorylated tau in the neurons of the hypothalamus and tegmentum of the brainstem with a rostro-caudal gradient of severity (1, 7). Although the pathogenesis of anti-IgLON5 disease remains unclear, there is strong evidence that it has an autoimmune origin: 1) anti-IgLON5 disease has a robust genetic association with HLA-DRB1*10:01-DQB1*05:01 haplotype (8).; 2) some autopsy studies have not shown abnormal deposits of hyperphosphorylated tau in all patients, suggesting that this is a late event in the disease and not the primary cause (9, 10); 3) *in vitro* experiments of cultured rat brain neurons demonstrated that IgLON5 antibodies produce an irreversible reduction of membrane IgLON5 clusters (11), in addition to cytoskeletal lesions, such as dystrophic neurites and axonal swellings (12).

IgLON5 is the fifth member of the IgLON family, which belongs to the immunoglobulin superfamily of cell adhesion molecules. IgLONs are involved in several physiological processes, including cell adhesion, migration, and neurite outgrowth (13–17). In addition to IgLON5, other members of the IgLON family include the opioid-binding cell adhesion molecule (OBCAM/IgLON1), neurotrimin (NTM/IgLON2), limbic system-associated member protein (LSAMP/IgLON3), and neural growth regulator 1 (NEGR1/IgLON4). IgLONs have three immunoglobulin-like domains in the extracellular region (ectodomain), which are attached to the membrane by a glycosylphosphatidylinositol (GPI) anchor. IgLON5, like the other IgLON family members, is secreted by ectodomain shedding, an important post-translational mechanism involved in neuronal plasticity, axonal guidance, and cell migration. IgLON5 predominantly establishes homomeric and heteromeric *cis*- (within the cell) and *trans*- (between cells) interactions with other IgLON family members that can be disturbed by IgLON5 antibodies (18–20).

Despite the *in vitro* effects of IgLON5 antibodies, passive transfer experiments using cerebroventricular infusion or intracerebral injection of IgLON5-IgG have failed to reproduce the most characteristic symptoms of the disease and have been unable to demonstrate *in vivo* the pathogenic effects described *in vitro* (21, 22).

The limited knowledge of the physiological function of IgLON5 represents a major drawback to studying the pathogenic mechanisms of IgLON5 antibodies and the relation with the tauopathy observed in some patients. Knockout (KO) mice are a powerful tool for understanding the physiologic mechanisms of the suppressed protein and the symptoms derived from its loss. The aim of this study was to investigate the impact of IgLON5 loss-of-function on brain morphology, social behavior, and the development of clinical symptoms observed in anti-IgLON5 disease in an IgLON5-KO mouse model.

2 Materials and methods

2.1 Animals

IgLON5 KO mice C57BL/6NCrl-Iglon5em1(IMPC)Mbp/Mmucd (IgLON5-KO) were generated using CRISPR-Cas9 system at the Mutant Mouse Resource and Research Center (MMRRC; https://www.mmrrc.org/catalog/sds.php?mmrrc_id=50638) in the University of California, Davis (UCD). Exon 3 was deleted using two guide RNA sequences (CTGGAAGCTAGACTTCTGAGGGG and GTGCCCTGCTGAATACCATAAGG) and Cas9 nuclease, introducing a frameshift and creating a premature stop codon. A colony of IgLON5-KO and heterozygous IgLON5−/+ (IgLON5-HET) mice was established locally from the founders. Wild-type (WT) mice with the same genetic background (C57BL/6N) were used as controls and for crossing back with IgLON5-KO to breed IgLON5-HET. Aged IgLON5-KO animals (22-month-old) were used to determine the presence of neurodegenerative features. A maximum of five animals were housed per cage. The room was maintained at controlled temperature (21°C) and humidity (55% ± 10%) with illumination at 12-h cycles; food and water were available *ad libitum*. All procedures were conducted in accordance with standard ethical guidelines and approved by the local ethics committee of the University of Barcelona (procedure code: 10903).

2.2 Behavioral studies

Behavioral testing was performed in 8-week-old female and male mice (25–30 g; KO, n = 27 (16 male and 11 female); WT, n = 24 animals (10 male and 14 female)) to study the following: 1) locomotion (beam balance test, gait analysis, and locomotor activity in activity boxes during 24 hours), 2) memory (novel object location), 3) anxiety (black and white and open field test), 4) social interaction (social interaction test and nest building), and 5) depressive-like behavior (anhedonia and tail suspension test). Prior to the testing period, all mice were handled and acclimated to the experimental room for 1 week. Animals' weight was registered every week during the behavioral evaluation. Non-significant behavioral results are summarized in Table 1. IgLON5-HET animals (n = 20 animals) had no differences from WT animals in behavioral studies (data not shown).

10.3389/fimmu.2024.1347948

TABLE 1 Non-significant behavioral test results.

Parameter	WT male (n = 10)	WT female (n = 14)	KO male (n = 16)	KO female (n = 11)	Statistics (genotype)
Weight (g)	27.43 ± 0.502	23.57 ± 0.312	29.19 ± 0.679	24.04 ± 0.704	p = 0.1103
Brain weight (g)	0.468 ± 0.017	0.471 ± 0.016	0.477 ± 0.015	0.477 ± 0.020	p = 0.1524
Novel object location (NOL)					
Exploration time (s)	32.03 ± 13.081	26.3 ± 15.477	23.14 ± 11.514	16.74 ± 7.018	p = 0.0629
NOL index	0.100 ± 0.155	0.240 ± 0.090	0.214 ± 0.113	0.167 ± 0.168	p = 0.6698
Gait analysis					
Right forelimb stride (cm)	8.24 ± 1.384	7.566 ± 0.706	8.169 ± 0.779	7.941 ± 0.495	p = 0.5470
Left forelimb stride (cm)	8.293 ± 1.314	7.564 ± 0.646	8.298 ± 0.879	7.921 ± 0.509	p = 0.4731
Right hind limb stride (cm)	8.118 ± 1.373	7.541 ± 0.671	8.041 ± 0.798	7.868 ± 0.58	p = 0.6223
Left hind limb stride (cm)	8.161± 1.287	7.576 ± 0.491	8.029 ± 0.897	7.689 ± 0.762	p = 0.9706
Forelimb stride width (cm)	1.433 ± 0.116	1.422 ± 0.141	1.435 ± 0.105	1.363 ± 0.09	p = 0.3935
Hind limb stride width (cm)	2.729 ± 0.21	2.623 ± 0.243	2.755 ± 0.297	2.578 ± 0.197	p = 0.8986
Black and white					
Entries in white	8.333 ± 4	11.846 ± 3.436	7.933 ± 4.511	11.714 ± 4.151	p = 0.8363
Entries in distal white	5.777 ± 3.032	9.076 ± 3.546	8.066 ± 3.411	8.571 ± 3.552	p = 0.4108
Time in white (%)	25.966 ± 11.861	30.421 ± 12.765	33.998 ± 15.833	30.396 ± 7.074	p = 0.3391
Time in distal white (%)	7.995 ± 3.828	9.921 ± 6.466	11.4 ± 6.082	9.791 ± 5.094	p = 0.3686
Open field					
Entries to medial	20.1 ± 7.622	20.9 ± 10.514	23.812 ± 9.224	21.909 ± 7.674	p = 0.3756
Entries to central	4.6 ± 2.319	5.7 ± 4.347	5.312 ± 2.725	5.454 ± 3.615	p = 0.8114
Time out of peripheral (%)	12.767 ± 9.1	10.034 ± 7.477	15.896 ± 6.31	9.68 ± 3.965	p = 0.4976
Social interaction test					
Trial 1 (s)	46.028 ± 9.916	48.417 ± 10.152	46.645 ± 9.545	43.688 ± 12.619	p = 0.3317
Trial 2 (s)	43.546 ± 13.321	45.811 ± 13.859	38.921 ± 15.671	38.43 ± 14.924	
Trial 3 (s)	29.22 ± 18.08	41.332 ± 17.532	34.265 ± 17.312	31.095 ± 15.497	
Trial 4 (s)	30.177 ± 27.804	35.679 ± 18.793	44.206 ± 11.141	29.068 ± 18.199	
Trial 5 (s)	45.535 ± 11.828	41.38 ± 20.58	38.145 ± 25.539	37.151 ± 12.056	
Tail suspension test					
Immobility time (s)	60.34 ± 34.278	134.264 ± 41.748	66.118 ± 40.957	133.4 ± 32.639	p = 0.8230
Energy (unit)	31,889.79 ± 16,486.651	11,527.914 ± 6,410.089	34,514.793 ± 19,148.298	12,493.654 ± 6,083.17	p = 0.6483
Power (unit)	403.58 ± 231.086	203.107 ± 135.828	425.031 ± 221.444	173.436 ± 74.365	p = 0.9362

WT, wild type; KO, knockout.

2.2.1 Novel object location

Animals were habituated to an empty, square arena (25 × 25 cm) with visual cues for 10 minutes twice daily for 4 days. On the day of the test, the animals were placed in the arena with two equal objects in two opposite corners, and they were allowed to explore the objects for 9 minutes (familiarization phase). After 3 hours, the animals were reintroduced to the arena, where one of the objects had been relocated to a different corner. The animal was given 9 minutes to explore the objects (test phase), and the time spent exploring each object was recorded. The following formula was used to compute a discrimination index (novel object location (NOL) index): time of exploration of the moved object minus the

time of exploration of the not moved object, divided by the total time of exploration of both objects. A higher discrimination index indicates a better memory of the position of both objects.

2.2.2 Gait assessment

Animals were trained to run through a 50 × 8 cm corridor with a box in the end. The procedure was repeated twice to habituate the mice to the environment and avoid anxiety. The following day, filter paper was placed on the corridor, and animal paws were painted with non-toxic paint to identify footstep positions. Distance traveled for each paw and distance between opposite paws were measured for each animal. A minimum of four consecutive strides per animal were recorded.

2.2.3 Beam balance test

A 1-m beam with a flat surface of 12-mm width was placed on two poles resting 50 cm above the tabletop. On one pole, a lamp was used as an aversive stimulus (starting point), while food pellets in a black box were placed on the other pole to attract mice (endpoint). For habituation, animals were placed in the middle of the beam and left to cross half the beam. If animals performed the task correctly, they were placed further from the endpoint until they learned to cross the whole beam. Once they performed the task correctly a minimum of three times, the beam was substituted with a 6-mm-wide round beam, and animals performed the task twice. The next day, animals were submitted to the test and placed on the aversive pole, and the time to cross the beam and the number of slips were measured.

2.2.4 Black and white test

The black and white test box was composed of two compartments (20 cm wide, 20 cm long, and 30 cm high) connected by a tunnel that was 6 cm wide and 6 cm high. One compartment was painted black and kept at 10 lux, while the other was painted white, brightly illuminated (500 lux), and subdivided into three sections based on distance from the tunnel (distal, medial, and proximal). Animals were initially placed in the black compartment, creating a conflict between the natural tendency of rodents to explore new environments and the tendency to avoid brightly illuminated areas. Anxiety levels were automatically measured using SMART software (Panlab, Harvard Apparatus, Barcelona, Spain), quantified as the percentage of time spent in the light box and the number of entries made into each section.

2.2.5 Locomotor activity

Spontaneous locomotor activity was automatically analyzed using activity boxes (9 × 20 × 11 cm; Imetronic, Pessac, France) equipped with two rows of photocell detectors. Animals' locomotion was evaluated over 24 hours, divided into 12 hours of light and 12 hours of darkness. Activity was quantified by counting the number of times the animal crossed the detector. Day and night cycles were analyzed separately.

2.2.6 Open field test

Animals were placed in a brightly illuminated (500 lux) round arena of 25-cm diameter, divided into three concentric circles (peripheral, medial, and central). Mice were free to explore the arena for 5 minutes. Anxiety levels were determined based on the time spent in the peripheral zone, as well as the number of entries made into each section. Tracking of the mice was automatically measured using SMART software (Panlab, Harvard Apparatus).

2.2.7 Sucrose preference test

Anhedonia was measured by the preference for sucrose. Two bottles containing water that were swapped positions daily were placed in the cage, one with 2% sucrose and one without. The consumption from each bottle was recorded over 5 days. On the fifth day, the mice's sucrose preference was calculated as the ratio of water with sucrose consumed to the total liquid (water with and without sucrose) consumed. A lower ratio is indicative of depressive-like behavior (23).

2.2.8 Social interaction test

Individualized mice (1-week minimum) were exposed to a mouse of the same sex and similar age for 1 minute and then removed from the interaction cage. The same intruder was introduced four times separated by intervals of 10 minutes. In the fifth trial, the intruder was changed to a different mouse. Trials were recorded, and the total time that the experimental mouse interacted with the intruder mouse was measured. Development of social memory was indicated by a reduction of exploration time with the same animal (trials 1–4) and increased exploration time during the interaction with a new animal.

2.2.9 Nest-building test

A nest-building test was performed by introducing 9 g of Nestlets material (Ancare, Bellmore, NY, USA) overnight in the cage of individualized mice. The following day, the nest was scored using a previously described scale, and unused Nestlets material was weighted (24).

2.2.10 Tail suspension test

Mice were suspended by adhesive tape applied to the tail in an automatic system for 6 minutes (BIO-TST, Bioseb, Vitrolles, France). The total periods of immobility, energy, and power were automatically recorded during the experimental period. Prolonged periods of immobility are indicators of helplessness, a characteristic of depressive-like behavior (25).

2.3 Brain tissue processing

Animals were deeply anesthetized with isoflurane and perfused with phosphate-buffered saline (PBS) after the last behavioral test. Brains were removed and weighed. For analysis of membrane proteins, brains were cut sagittally. One hemisphere was dissected to obtain protein extracts of the hippocampus, cerebellum, and brainstem; the other was processed for the immunohistochemistry analysis of cell surface proteins following previously described protocols (26). To investigate the presence of signs of neurodegeneration in aged animals, 22-

month-old mice (IgLON5-KO, IgLON5-HET, and WT) underwent trans-cardiac perfusion with PBS fixed in 4% paraformaldehyde (PFA) for 12 hours, cut into 2-mm coronal sections, and incubated in increasing concentrations of alcohol (70% for 3 hours twice, 96% overnight, and 100% for 3 hours); after an additional 3 hours in xylene, tissue was embedded in paraffin and kept at room temperature until used.

2.4 Immunohistochemistry

Immunohistochemistry to detect neuronal cell-surface proteins was performed using a standard avidin–biotin–peroxidase method as previously described on 7-µm frozen sagittal rat brain sections post-fixed with PFA. The following commercial antibodies were used: 1:500 diluted IgLON5 (ab122763, abcam, Cambridge, UK), IgLON1 (STJ94590), IgLON2 (STJ94442), IgLON3 (STJ116461), IgLON4 (STJ94394, St. John's Laboratory, London, UK), KIDINS220 (21856-1-AP, Proteintech, Rosemont, IL, USA), IGSF21 (21465-1-AP; Proteintech), and CACNA2D2 (SAB1401461, Sigma-Aldrich, Darmstadt, Germany); serum (1:200 diluted) or CSF (1:5 diluted) from patients containing IgLON5, NMDAR, GABABR, and GABAAR antibodies was used also to investigate their presence in IgLON5-KO brains.

To study the brain structure and presence of tau hyperphosphorylation in aged animals, 4-µm-thick coronal sections were deparaffinized in xylene, rehydrated in alcohol, washed in tap water, and heated for 2 min in a pressure cooking oven in 0.1 M sodium citrate buffer (pH 6.0). Sections were then stained with hematoxylin and eosin or processed for immunohistochemistry. Phospho-tau (ser202, Thr205) monoclonal antibodies (AT8, MN1020, Thermo Fisher Scientific, Waltham, MA, USA) or neurofilament medium staining (ab7794, abcam, 1:5,000 diluted) was incubated overnight at 4°C (1:1,000 diluted) followed by goat anti-mouse biotinylated as secondary antibody (1:1,000 diluted), revealed by a standard avidin–biotin–peroxidase method and visualization by diaminobenzidine. A section of the prefrontal cortex from an Alzheimer's disease patient was included as a positive control of tau hyperphosphorylation and incubated with AT8 antibody as described above.

2.5 Western blotting

Dissected brain regions were homogenized in standard lysis buffer (Tris-HCl 50 mM, NaCl 150 mM, EDTA 5 mM, 1% triton X-100, and protease inhibitor cocktail 1:50 diluted) by sonication. Lysates were centrifuged at 16,100 *g* for 15 minutes, and the supernatant was kept. The concentration of protein was determined using a standard bicinchoninic acid (BCA) assay, and 10 µg of protein was loaded into a gel and, after electrophoresis, transferred to a nitrocellulose membrane (1704158, Bio-Rad, Hercules, CA, USA). Anti-IgLON5 (abcam), beta-actin (Sigma-Aldrich), IgLON5 (ab122763, abcam, Cambridge, UK), IgLON1 (STJ94590), IgLON2 (STJ94442), IgLON3 (STJ116461), and IgLON4 (STJ94394) were incubated in 1/1,000 dilution overnight at 4°C followed by the appropriate secondary antibody (anti-rabbit-horseradish peroxidase (HRP) or anti-mouse-HRP) and were revealed following a standard enhanced chemiluminescence developing kit (RPN2108, GE Healthcare, Chicago, IL, USA).

2.6 Statistical analysis

Statistical analyses were performed using GraphPad Prism 7. Results are expressed as mean values ± SD and outliers (Table 1). To analyze data from behavioral studies, a two-way ANOVA model with Sidak's multiple comparison tests was performed including the between-subjects factors experimental group and sex. If the test had multiple time points, a three-way ANOVA model with Tukey's multiple comparisons was applied to observe only robust differences.

3 Results

3.1 IgLON5-KO mouse phenotype description and histological studies

IgLON5 protein was undetectable by immunohistochemistry on IgLON5-KO brain sections (Figures 1A–C) when incubated with IgLON5-abs from patients (sera or CSF) or with IgLON5 commercial antibody. IgLON5-HET showed weaker reactivity than WT mice by immunohistochemistry (Figures 1D–F) but depicts the typical IgLON5 staining pattern identical to that of WT mice (Figures 1G–I). IgLON5 was also not detected by Western blotting in tissue lysates obtained from the brainstem, cerebellum, or hippocampus of the IgLON5-KO mice (Figure 2A). The other IgLON family members were not upregulated in IgLON5-KO mouse brains (Figure 2B). In terms of expression of synaptic receptors, NMDAR, GABABR, or binding partners previously described (CACN2D2A, IGSF21, and KIDINS220) (20) were not altered in IgLON5-KO mice either (data not shown).

IgLON5-KO mice were viable and fertile and did not exhibit any evident body morphological alterations. Offspring followed Mendelian sex segregation (100 births). There were no differences in weight between IgLON5-KO and WT animals ($p = 0.6927$) or in the brain weight at sacrifice ($p = 0.1658$) in either young animals or those aged 22 months (Table 1). We observed no brain abnormalities by conventional hematoxylin and eosin or neurofilament staining of the fiber tracts. Similarly, the area of the ventricles was also similar in IgLON5-KO and WT mice (Figure 3). We investigated the presence of phospho-tau deposits in nine 22-month-old IgLON5-KO and nine WT mice (five females and four males). We did not observe tau deposits in IgLON5-deficient animals or controls (Figure 4).

3.2 IgLON5-KO mice have motor and balance deficits

An extensive battery of tests was applied to investigate behavioral deficits in 2-month-old IgLON5-KO in comparison

10.3389/fimmu.2024.1347948

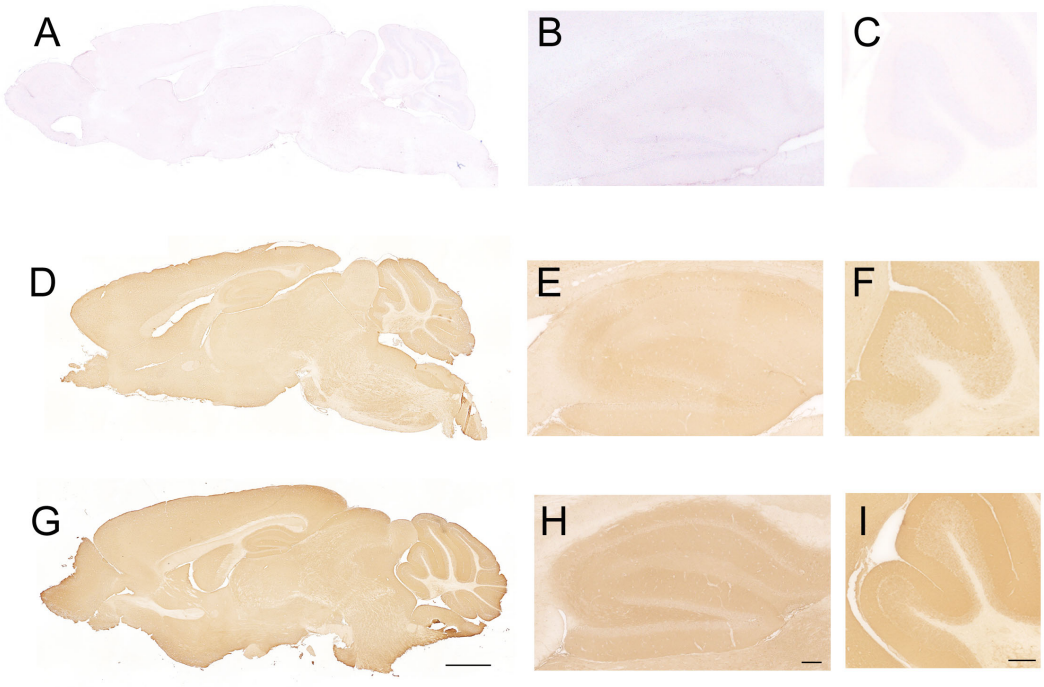

FIGURE 1
Immunohistochemistry on sagittal sections of mouse brain fixed tissue and stained with cerebrospinal fluid (CSF) containing anti-IgLON5 antibodies from a patient. **(A–C)** Incubation of IgLON5-knockout (KO) mouse brain tissue with antibodies against IgLON5 shows no reactivity against IgLON5, demonstrating that KO mice do not express detectable IgLON5 protein. **(B)** Magnification of the hippocampus of IgLON5-KO stained with anti-IgLON5 antibodies. **(C)** Magnification of the cerebellum showing no reactivity against IgLON5. **(D–F)** Brain tissue from IgLON5-HET mice showed weaker reactivity than wild-type (WT), as expected, when stained with CSF containing IgLON5 antibodies but reproduced the typical diffuse staining of the neuropil produced by IgLON5 antibodies shown in WT mice **(G–I)**. **(G)** WT mice stained with IgLON5 antibodies depicting the typical pattern of staining of IgLON5 antibodies. **(H)** Magnification of the staining of IgLON5 antibodies in WT mouse hippocampus. **(I)** Magnification of staining pattern of anti-IgLON5 antibodies in WT mouse cerebellum. Immunohistochemistry was counterstained with hematoxylin. Scale bars: mice hippocampus **(G)** 2 mm, **(H)** 250 µm, and **(I)** 250 µm.

with WT mice (Figure 5A). IgLON5-KO mice showed a greater number of slips in the beam balance test, which assesses fine motor coordination, balance, and vestibulomotor function (genotype: $F(1, 98) = 8.867$; $p = 0.0037$). IgLON5-KO males lost their balance significantly more times than WT mice ($p = 0.03$). Although IgLON5-KO females displayed also more slips than WT females, statistical significance was not reached in the *post-hoc* test ($p = 0.08$) (Figure 5B). Time spent to cross the beam was not different between genotypes (KO-WT), indicating that the observed loss of balance cannot be attributed to deficits in muscle strength (Figure 5C).

During the daytime, when mice are expected to rest because they are nocturnal, IgLON5-KO female mice exhibited hyperactive behavior. This was evidenced by a consistent increase of back-and-forth movements across the box compared with WT females ($p < 0.0001$) (Figure 5D). The increase in back-and-forth movements of IgLON5-KO females was accompanied by a higher number of daytime rearing ($p = 0.0006$) (Figure 5E). Males did not show statistically significant differences in this test during daytime (Figures 5D, E).

During the nighttime, when mice are expected to be more active, IgLON5-KO females crossed the sensor of the activity box more times compared to female WT ($p = 0.02$), maintaining the hyperactivity condition seen during daytime. IgLON5-KO males showed the same tendency to hyperactivity as females, and more back-and-forth movements were observed during the night compared with WT mice ($p = 0.03$) (Figure 5F). In this case, the number of rearing was not significantly different between males and females (Figure 5G).

3.3 Male IgLON5-KO mice presented depressive-like and excessive nesting behaviors

Male IgLON5-KO mice manifested lower sucrose preference compared to WT mice ($p = 0.0487$) (Figure 5H). In addition to this depressive-like behavior, male KO mice showed excessive nest-building activity. They built significantly better and larger nests ($p = 0.0115$) (Figure 5I) and used more material compared to WT male littermates ($p \leq 0.0001$) (Figure 5J). We did not observe differences in the behavior of females.

Overall, these results indicate that IgLON5-KO mice have subtle deficits in fine motor coordination hyper-locomotion activity and

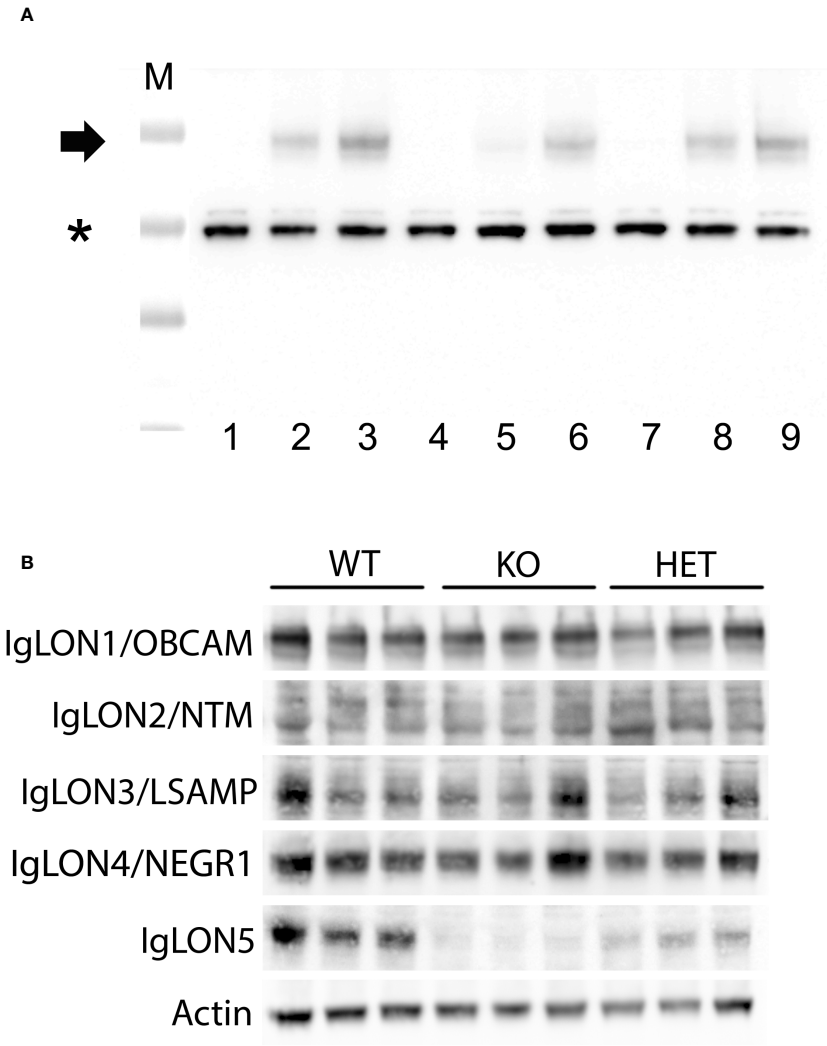

FIGURE 2
(A) Western blotting of lysates from tissue of different mouse brain areas showing the absence of IgLON5 in the IgLON5 knockout mice; cerebellum (lanes 1–3), hippocampus (lanes 4–6), and brainstem (lanes 7–9). Lysates from IgLON5 knockout mice correspond to lanes 1, 4, and 7; lysates from IgLON5-HET mice correspond to lanes 2, 5, 8; lysates from wild-type (WT) mice correspond to lanes 3, 6, and 9. M indicates the molecular weight marker, * indicates band of beta-actin, and the arrow indicates the glycosylated IgLON5 molecular weight. **(B)** Western blotting analysis of mouse cerebellum lysates showing that there is no compensatory effect of the other members of the IgLON family in the absence of IgLON5. Three different mice of each genotype (WT, knockout (KO), and HET) are shown for every antibody incubated (rows, antibodies against IgLON1 to IgLON5 proteins).

depressive-like behavior and that these deficits were sex-dependent. Whereas male IgLON5-KO mice showed more problems with motor coordination and depressive-like behavior, females showed hyper-locomotion activity.

4 Discussion

We present the initial characterization of the phenotype and behavior of an IgLON5-KO mouse model.

IgLON5-KO mice showed only subtle abnormalities in the behavioral studies, and results differed between males and females. First, IgLON5-KO males had an increase in slips in the beam balance test, which assesses motor and vestibular function by quantifying the ability to balance on a narrow wooden beam. Although statistical analyses did not reach significance in the female IgLON5-KOs, they showed the same trend as in males. Our results suggest that IgLON5 has a physiological role in fine motor coordination and balance; these findings support the possibility that IgLON5 autoantibodies can interfere with IgLON5's function and may be pathogenically involved in the gait instability frequently noted in this disorder. This is also consistent with the results of a recent study of passive antibody transfer where intracerebral injections of IgLON5-IgG from patients into the nigrostriatal dopaminergic pathway of mice produced sustained motor impairment (22). Behavioral studies reported in KOs of other IgLON family members did not describe deficits in balance or motor coordination (27–30) (Table 2).

Second, female IgLON5-KOs showed hyperactivity during darkness and also during the light phase when mice are

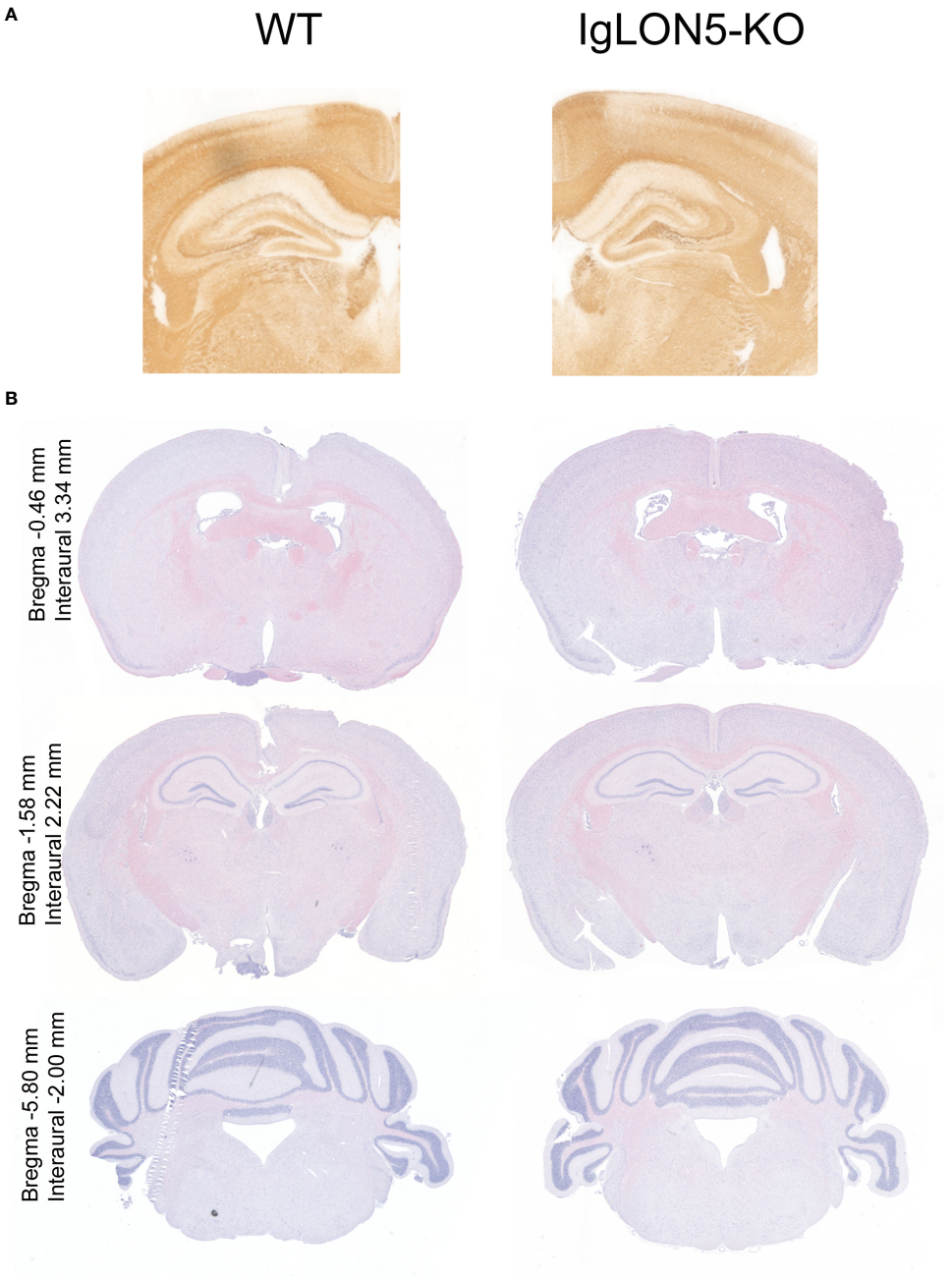

FIGURE 3
Brain morphology showed no major alterations of IgLON5-knockout (KO) compared to age-matched wild-type (WT) mice (22-month-old). **(A)** Neurofilament immunostaining showed no alteration in the gross cytoarchitecture of the major fiber tracks. **(B)** Histological staining with hematoxylin and eosin of 22-month-old mouse IgLON5-KO tissue compared to age-matched WT mouse tissue also showed no abnormalities in coronal sections of comparable paraffin-embedded brain areas.

supposed to be resting. Deletion of the other IgLONs in mouse models also showed hyperactivity, especially in stressful conditions (23, 27) (Table 2). This phenotypic feature together with a depressive-like behavior and an obsessive nest-building activity observed in IgLON5-KO males could indicate a role of IgLON5 deficiency in psychiatric-related symptoms (32).

Our results on the behavior of IgLON5-KO mice are similar to those reported in other IgLON-KO mouse models, which also showed subtle behavioral abnormalities, related to social behavior, learning, and locomotor activity (Table 2). These behavioral alterations have suggested that IgLONs are implicated in the pathogenesis of psychiatric disorders. However, psychiatric symptoms are not a major complaint in anti-IgLON5 disease. In a series of 53 patients with anti-IgLON5 disease, only nine (17%) developed psychosis or hallucinations (33). However, the two IgLON family members, Negr1 (IgLON4) and LSAMP

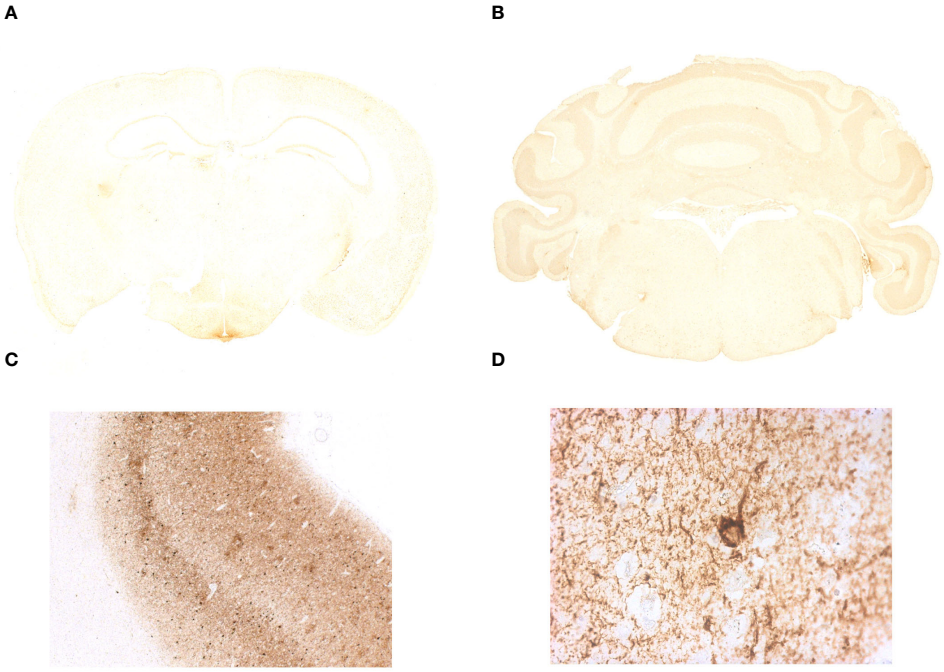

FIGURE 4
Immunohistochemistry on coronal sections of paraffin-embedded mouse brain tissue did not show the presence of abnormal tau phosphorylation in IgLON5-knockout (KO) mice. **(A, B)** Brain tissue IgLON5-KO mice immunostained with AT8 antibody shows no specific binding to neuropil threads or abnormal tau deposition described in anti-IgLON5 tauopathy. Hippocampus, tegmentum of the brainstem, and hypothalamus show no evidence of pathological changes in IgLON5-KO mice. **(C)** Immunostaining of the prefrontal cortex of a patient with Alzheimer's disease was run in parallel and serves as positive control. **(D)** Magnification of a positive area for AT8 antibody staining of the Alzheimer's disease patient tissue showing a neuron with tau aggregation in neurofibrillary tangles.

(IgLON3), which showed more behavioral alterations in the KO mouse model, have been implicated in several psychiatric disorders (23, 27, 34). Recent meta-analyses using the Genome-Wide Association Study (GWAS) have identified a single-nucleotide polymorphism (SNP) of Negr1 gene associated with the diagnosis of major depression (35). Also, Negr1 has been proposed as a biomarker of major depression because CSF Negr1 levels were elevated in patients with this disorder (36). Similarly, SNPs in LSAMP gene have been associated with major depression and panic disorders (37). In contrast, NTM (IgLON2) KO mice only showed minor emotional-related learning deficiencies in the active avoidance test, and in human genetic studies, NTM has not been identified as a risk for psychiatric diseases (30).

IgLON5-KO mice were viable and fertile and did not show any appreciable morphologic or cerebral alterations. Gross and microscopic neuroanatomy examination of IgLON5-KO and WT mice did not reveal differences regarding principal fiber tracks or volume of the ventricles, in either young adult or older mice. Studies of KOs of other IgLONs reported also no major abnormalities except for Negr1, which showed substantial volumetric alterations in the ventricular space (23). Although ventriculomegaly was observed in a patient with anti-IgLON5 disease (38), the brain MRI of most (>90%) patients showed a similar degree of atrophy as that of age-matched controls or only a mild atrophy of the brainstem (38, 39).

Finally, we investigated whether aged IgLON5-KO mice developed signs of neurodegeneration. In these mice, the deficiency in IgLON5 did not lead to distinct pathological signs such as neuronal loss or tau hyperphosphorylation, which have been reported in the autopsies of some patients (1, 7). This observation suggests that other factors in addition to IgLON5 loss, for example, inflammatory changes associated with IgLON5 autoimmunity, may be important in the development of the neurodegenerative alterations observed in some patients. Therefore, it is possible that the antibody effects observed *in vitro* are necessary to cause the disease; thus, IgG1-dependent cross-linking and internalization of IgLON5 clusters would be followed by alteration of the cytoskeletal architecture and would lead ultimately to tau aggregation and phosphorylation through common pathways described for neurodegenerative diseases. The role of IgG4 IgLON5 antibodies in the disease is less clear because *in vitro* studies have shown that alteration of the interactions of the IgLON5 protein with its binding partners, which is the main pathogenic mechanism described for IgG4 antibodies, was not specific to a subclass. However, IgG4 antibodies may be relevant to the pathogenesis of the disease because a recent autopsy study has reported the presence of abundant IgG4 deposits in areas of the brain where IgLON5 is highly expressed and whose dysfunction may explain the clinical symptoms (10). Our study has limitations because we have not conducted a detailed sleep evaluation, and the

10.3389/fimmu.2024.1347948

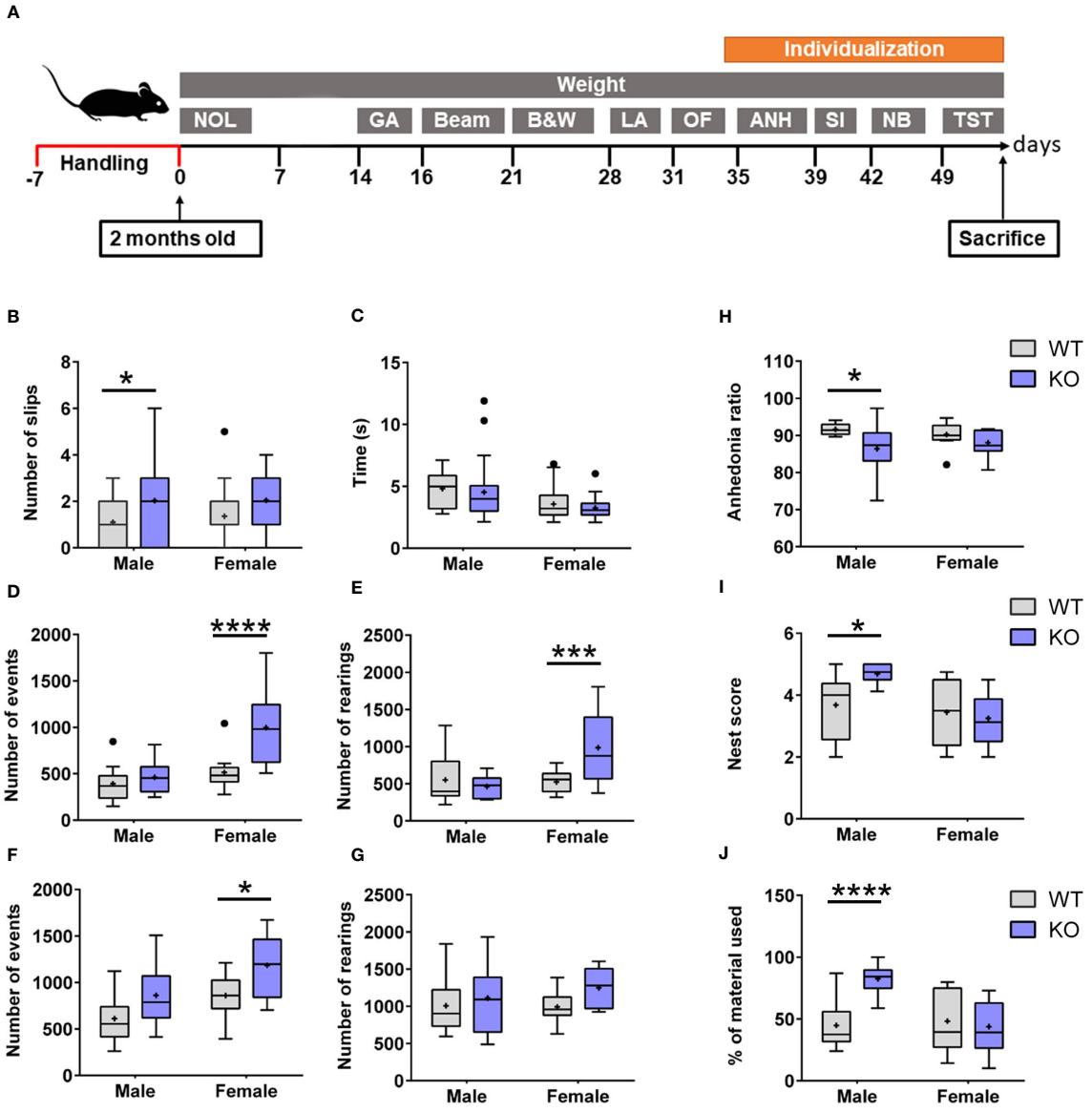

FIGURE 5
(A) Experimental design of the behavioral testing in 2-month-old IgLON5-KO and WT mice to assess the following: 1) Hippocampal-dependent spatial memory: novel object location (NOL). 2) Balance and locomotion: gait analysis (GA), beam balance test (Beam), and locomotor activity (LA). 3) Anxiety: black and white (B&W) and open field (OF). 4) Depressive-like behavior: anhedonia (ANH) and tail suspension test (TST). 5) Social interaction (SI). 6) Nest building (NB). To perform social depressive-like behaviors, nest-building animals were individualized. **(B)** Graphical representation of the quantification of slips in beam balance test separated by sexes and genotypes. IgLON5-KO males exhibited significantly more slips (purple) compared with male WT mice (gray) (*p = 0.03). Although females showed the same trend, they did not reach statistical significance (p = 0.08). **(C)** Time spent to cross the beam was not different between sexes or genotypes. **(D, E)** Spontaneous locomotor activity during daytime measured in activity boxes evidenced hyper-locomotion activity in KO females with an increase in the number of events (genotype, p = 0.0003; *post-hoc* test females, ****p < 0.0001; males, not significant) **(D)** and rearings (genotype, p = 0.026; *post-hoc* test females, ***p = 0.0006) **(E)**. This behavior was not observed in males. **(F, G)** Locomotor activity during nighttime showed similar results to those observed during daytime in IgLON5-KO females with more movement events (genotype, p = 0.0014; *post-hoc* test females, *p = 0.02) **(F)**, and rearing measurements were not significant **(G)**. **(H)** IgLON5-KO males showed less sucrose preference, which is indicative of depressive-like behavior (genotype, p = 0.01; *post-hoc* test males, *p = 0.0487). **(I, J)** Nest-building analyses revealed that IgLON5-KO males built more elaborate nests (genotype, p = 0.01; *post-hoc* test males, *p = 0.0115) **(I)** and used more material (genotype, p = 0.005; *post-hoc* males, **** p < 0.0001) **(J)**. WT, wild type; KO, knockout.

clinical phenotype of IgLON5 deficiency is not fully coincident with the core of symptoms of the disease; however, these symptoms are also variable among patients. Another limitation is that we focused our studies on the behavior and brain of mice, but IgLON5 is also present in systemic tissues like muscle fibers, which were not investigated and should be explored in future studies.

To summarize, our model of IgLON5-KO shows subtle deficits in fine motor coordination, balance, and behavioral alterations similar to those seen in KOs of other IgLON

TABLE 2 Comparison of the behavior of IgLON5-KO with five studies reported on NMT-KO, LSAMP-KO, and NEGR1-KO.

	IgLON5-KO female	IgLON5-KO male	NTM-KO (30)	LSAMP-KO (27, 28)	NEGR1-KO (23, 31)
Behavior					
Anxiety				* ↓	↑[¶]
Depressive-like behavior		↑	ND	ND	↑[¶]
Social interaction				↓	↓
Motor activity	↑	↑[&]		*↑	
Memory/learning			↓ **	↓[$]	↓
Motor coordination		↓	ND		

Green cells indicate no differences between KO and WT mice and red cells indicate some disparity in results.
WT, wild type; KO, knockout.
[&]Increased motor activity observed only at night.
*In response to novel environments.
**Mild deficits in cognitive challenging emotional learning tasks.
[$]Impaired spatial memory in one study (Qiu, 2010) (28).
[¶]Abnormal (Noh, 2019) (31).
↑, increased.
↓, decreased.
ND, not determined.

family members. These changes were in part sex-dependent. However, the IgLON5-KO mouse model does not reproduce the clinical phenotype or the tauopathy reported in anti-IgLON5 disease.

Data availability statement

The original contributions presented in the study are included in the article/supplementary material. Further inquiries can be directed to the corresponding author.

Ethics statement

The animal study was approved by Comitè Ètic d'Experimentació Animal, Universidad de Barcelona. The study was conducted in accordance with the local legislation and institutional requirements.

Author contributions

JL: Conceptualization, Investigation, Methodology, Writing – review & editing. AS: Investigation, Methodology, Writing – review & editing. MA: Methodology, Writing – review & editing, Investigation. EM: Investigation, Methodology, Writing – review & editing. LM-P: Conceptualization, Methodology, Writing – review & editing, Investigation. AG-S: Investigation, Methodology, Writing – review & editing. FM: Methodology, Writing – review & editing, Investigation. JD: Writing – review & editing, Investigation, Methodology. FG: Investigation, Supervision, Writing – review & editing, Methodology. LS: Conceptualization, Funding acquisition, Investigation, Methodology, Supervision, Writing – original draft, Writing – review & editing.

Funding

The author(s) declare financial support was received for the research, authorship, and/or publication of this article. This study has been funded by Instituto de Salud Carlos III through the project PI18/00067, PI21/00165 (co-funded by the European Regional Development Fund "Investing in your future"). We want to thank the European Joint Programme on Rare Diseases (EJPRD) for funding a Networking event contract number: 463001015. This project has received funding from the European Union's Horizon 2020 research and innovation programme under the EJP RD COFUND-EJP N° 825575. IDIBAPS belongs to CERCA (Centres de recerca de Calalunya). ABS thanks Fundação para a Ciência e Tecnologia (FCT) of Portugal for the doctoral fellowship grant number 2022.13121.BD. EM is a recipient of a Doctoral Fellowship grant from the Basque Government (PREDOC).

Acknowledgments

We thank FCT for the doctoral fellowship grant number 2022.13121.BD recipient Ana Beatriz Serafim. We thank the animal facility of Universitat de Barcelona for the management of the mouse colony of IgLON5-KO. We are indebted to the Biobanc-Hospital Clinic-FRCB-IDIBAPS for samples and data procurement.

Conflict of interest

FG: royalties, Euroimmun for the use of IgLON5 as an autoantibody test; JD: royalties, Athena Diagnostic for use of Ma2 as an autoantibody test; royalties and Euroimmun for use of NMDA receptor, GABAB receptor, GABAA receptor, DPPX, and IgLON5 as autoantibody tests.

The remaining authors declare that the research was conducted in the absence of any commercial or financial relationships that could be construed as a potential conflict of interest.

The handling editor LQ declared a past co-authorship with the author JD and LS.

The author(s) declared that they were an editorial board member of Frontiers, at the time of submission. This had no impact on the peer review process and the final decision.

Publisher's note

References

1. Sabater L, Gaig C, Gelpi E, Bataller L, Lewerenz J, Torres-Vega E, et al. A novel non-rapid-eye movement and rapid-eye-movement parasomnia with sleep breathing disorder associated with antibodies to IgLON5: A case series, characterisation of the antigen, and post-mortem study. *Lancet Neurol* (2014) 13:575–86. doi: 10.1016/S1474-4422(14)70051-1

2. Gaig C, Graus F, Compta Y, Högl B, Bataller L, Brüggemann N, et al. Clinical manifestations of the anti-IgLON5 disease. *Neurology* (2017) 88:1736–43. doi: 10.1212/WNL.0000000000003887

3. Gaig C, Compta Y, Heidbreder A, Marti MJ, Titulaer MJ, Crijnen Y, et al. Frequency and characterization of movement disorders in anti-igLON5 disease. *Neurology* (2021) 97:e1367. doi: 10.1212/WNL.0000000000012639

4. Tao QQ, Wei Q, Song SJ, Yin XZ. Motor neuron disease-like phenotype associated with anti-IgLON5 disease. *CNS Neurosci Ther* (2018) 24:1305–8. doi: 10.1111/cns.13038

5. Sista SR, Crum B, Aboseif A, Devine MF, Zekeridou A, Hammami MB, et al. Motor-neuron-disease-like phenotype associated with IgLON5 disease. *J Neurol* (2022) 269(11):6139–44. doi: 10.1007/s00415-022-11262-0

6. Dalmau J, Graus F. Antibody-mediated encephalitis. *New Engl J Med vol* (2018) 378:840–51. doi: 10.1056/NEJMra1708712

7. Gelpi E, Höftberger R, Graus F, Ling H, Holton JL, Dawson T, et al. Neuropathological criteria of anti-IgLON5-related tauopathy. *Acta Neuropathol.* (2016) 132:531–43. doi: 10.1007/s00401-016-1591-8

8. Gaig C, Ercilla G, Daura X, Ezquerra M, Fernández-Santiago R, Palou E, et al. HLA and microtubule-associated protein tau H1 haplotype associations in anti-IgLON5 disease. *Neurol - Neuroimmunol. Neuroinflamm* (2019) 6:e605. doi: 10.1212/NXI.0000000000000605

9. Erro ME, Sabater L, Martínez L, Herrera M, Ostolaza A, García de Gurtubay I, et al. Anti-IGLON5 disease A new case without neuropathologic evidence of brainstem tauopathy. *Neurol Neuroimmunol Neuroinflamm* (2019) 7(2):e651. doi: 10.1212/NXI.0000000000000651

10. Berger-Sieczkowski E, Endmayr V, Haider C, Ricken G, Jauk P, Macher S, et al. Analysis of inflammatory markers and tau deposits in an autopsy series of nine patients with anti-IgLON5 disease. *Acta Neuropathol* (2023) 146(4):631–45. doi: 10.1007/s00401-023-02625-6

11. Sabater L, Planagumà J, Dalmau J, Graus F. Cellular investigations with human antibodies associated with the anti-IgLON5 syndrome. *J Neuroinflamm* (2016) 13:226. doi: 10.1186/s12974-016-0689-1

12. Landa J, Gaig C, Plagumà J, Saiz A, Antonell A, Sanchez-Valle R, et al. Effects of igLON5 antibodies on neuronal cytoskeleton: A link between autoimmunity and neurodegeneration. *Ann Neurol* (2020) 88:1023–7. doi: 10.1002/ana.25857

13. Hashimoto T, Yamada M, Maekawa S, Nakashima T, Miyata S. IgLON cell adhesion molecule Kilon is a crucial modulator for synapse number in hippocampal neurons. *Brain Res* (2008) 1224:1–11. doi: 10.1016/j.brainres.2008.05.069

14. Pischedda F, Piccoli G. The IgLON family member negr1 promotes neuronal arborization acting as soluble factor via FGFR2. *Front Mol Neurosci* (2016) 8. doi: 10.3389/fnmol.2015.00089

15. Reed J, McNamee C, Rackstraw S, Jenkins J, Moss D. Diglons are heterodimeric proteins composed of IgLON subunits, and Diglon-CO inhibits neurite outgrowth from cerebellar granule cells. *J Cell Sci* (2004) 117:3961–73. doi: 10.1242/jcs.01261

16. Gil OD, Zhang L, Chen S, Ren YQ, Pimenta A, Zanazzi G, et al. Complementary expression and heterophilic interactions between igLON family members neurotrimin and LAMP. *J Neurobiol* (2002) 51:190–204. doi: 10.1002/neu.10050

17. Akeel M, McNamee CJ, Youssef S, Moss D. DIgLONs inhibit initiation of neurite outgrowth from forebrain neurons via an IgLON-containing receptor complex. *Brain Res* (2011) 1374:27–35. doi: 10.1016/j.brainres.2010.12.028

18. Malinverno M, Carta M, Epis R, Marcello E, Verpelli C, Cattabeni F, et al. Cellular/Molecular Synaptic Localization and Activity of ADAM10 regulate excitatory synapses through N-Cadherin cleavage. *J Neurosci* (2010) 30(48):16343–55. doi: 10.1523/JNEUROSCI.1984-10.2010

19. Sanz R, Ferraro GB, Fournier AE. IgLON cell adhesion molecules are shed from the cell surface of cortical neurons to promote neuronal growth *. *J Biol Chem* (2014) 290(7):4330–42. doi: 10.1074/jbc.M114.628438

20. Landa J, Serafim AB, Gaig C, Saiz A, Koneczny I, Hoftberger R, et al. Patients' IgLON5 autoantibodies interfere with IgLON5-protein interactions. *Front Immunol* (2023) 14:1151574. doi: 10.3389/fimmu.2023.1151574

21. Alvente S, Matteoli G, Molina-Porcel L, Landa J, Alba M, Bastianini S, et al. Pilot study of the effects of chronic intracerebroventricular infusion of human Anti-IgLON5 disease antibodies in mice. *Cells* (2022) 11(6):1024. doi: 10.3390/cells11061024

22. Gao Y, Li H, Luo H, Ni Y, Feng Y, He L, et al. Purified serum IgG from a patient with Anti-IgLON5 antibody cause long-term movement disorders with impaired dopaminergic pathways in mice. *Biomedicines* (2023) 11:2483. doi: 10.3390/biomedicines11092483

23. Singh K, Jayaram M, Kaare M, Leidmaa E, Jagomäe T, Heinla I, et al. Neural cell adhesion molecule Negr1 deficiency in mouse results in structural brain endophenotypes and behavioral deviations related to psychiatric disorders. *Sci Rep* (2019) 9(1):5457. doi: 10.1038/s41598-019-41991-8

24. Neely CLC, Pedemonte KA, Boggs KN, Flinn JM. Nest building behavior as an early indicator of behavioral deficits in mice. *J Vis Exp* (2019) 19(152). doi: 10.3791/60139

25. Can A, Dao DT, Terrillion CE, Piantadosi SC, Bhat S, Gould TD. The tail suspension test. *J Vis Exp* (2012) 28(59):3769. doi: 10.3791/3769

26. Ances BM, Vitaliani R, Taylor RA, Liebeskind DS, Voloschin A, Houghton DJ, et al. Treatment-responsive limbic encephalitis identified by neuropil antibodies: MRI and PET correlates. *Brain* (2005) 128:1764. doi: 10.1093/brain/awh526

27. Catania EH, Pimenta A, Levitt P. Genetic deletion of lsamp causes exaggerated behavioral activation in novel environments. *Behav Brain Res* (2008) 188(2):380–90. doi: 10.1016/j.bbr.2007.11.022

28. Qiu S, Champagne DL, Peters M, Catania EH, Weeber EJ, Levitt P, et al. Loss of limbic system-associated membrane protein leads to reduced hippocampal mineralocorticoid receptor expression, impaired synaptic plasticity, and spatial memory deficit. *Biol Psychiatry* (2010) 68:197–204. doi: 10.1016/j.biopsych.2010.02.013

29. Singh K, Loreth D, Pöttker B, Hefti K, Innos J, Schwald K, et al. Neuronal growth and behavioral alterations in mice deficient for the psychiatric disease-associated negr1 gene. *Front Mol Neurosci* (2018) 11. doi: 10.3389/fnmol.2018.00030

30. Mazitov T, Bregin A, Philips MA, Innos J, Vasar E. Deficit in emotional learning in neurotrimin knockout mice. *Behav Brain Res* (2017) 317:311–8. doi: 10.1016/j.bbr.2016.09.064

31. Noh K, Lee H, Choi TY, Joo Y, Kim SJ, Kim H, et al. Negr1 controls adult hippocampal neurogenesis and affective behaviors. *Mol Psychiatry* (2019) 24(8):1189–205. doi: 10.1038/s41380-018-0347-3

32. Wolmarans DW, Stein DJ, Harvey BH. Excessive nest building is a unique behavioural phenotype in the deer mouse model of obsessive–compulsive disorder. *J Psychopharmacol* (2016) 30:867–74. doi: 10.1177/0269881116645554

33. Grüter T, Möllers FE, Tietz A, Dargvainiene J, Melzer N, Heidbreder A, et al. Clinical, serological and genetic predictors of response to immunotherapy in anti-IgLON5 disease. *Brain* (2022) 146(2):600–11. doi: 10.1093/brain/awac090

34. Szczurkowska J, Pischedda F, Pinto B, Managò F, Haas CA, Summa M, et al. NEGR1 and FGFR2 cooperatively regulate cortical development and core behaviours related to autism disorders in mice. *Brain* (2018) 141(9):2772. doi: 10.1093/brain/awy190

35. Wang X, Cheng W, Zhu J, Yin H, Chang S, Yue W, et al. Integrating genome-wide association study and expression quantitative trait loci data identifies NEGR1 as a causal risk gene of major depression disorder. *J Affect. Disord* (2020) 265:679–86. doi: 10.1016/j.jad.2019.11.116

36. Carboni L, Pischedda F, Piccoli G, Lauria M, Musazzi L, Popoli M, et al. Depression-Associated gene Negr1-Fgfr2 Pathway is altered by antidepressant treatment. *Cells* (2020) 9(8):1818. doi: 10.3390/cells9081818

37. Koido K, Traks T, Balõtšev R, Eller T, Must A, Koks S, et al. Associations between LSAMP gene polymorphisms and major depressive disorder and panic disorder. *Transl Psychiatry* (2012) 2:152. doi: 10.1038/tp.2012.74

38. Urso D, De Blasi R, Anastasia A, Gnoni V, Rizzo V, Nigro S, et al. Neuroimaging findings in a patient with Anti-IgLON5 Disease: Cerebrospinal fluid dynamics abnormalities. *Diagnostics* (2022) 12:849. doi: 10.3390/diagnostics12040849

39. Honorat JA, Komorowski L, Josephs KA, Fechner K, St Louis EK, Hinson SR, et al. IgLON5 antibody. *Neurol Neuroimmunol. Neuroinflamm* (2017) 4(5):e385. doi: 10.1212/NXI.0000000000000385

frontiers | Frontiers in Immunology

TYPE Review
PUBLISHED 16 February 2024
DOI 10.3389/fimmu.2024.1272084

OPEN ACCESS

EDITED BY
Hani S. Mousa,
University of Cambridge, United Kingdom

REVIEWED BY
Maartje G. Huijbers,
Leiden University Medical Center (LUMC), Netherlands
Marco Lanzillotta,
Vita-Salute San Raffaele University, Italy
Inga Koneczny,
Medical University of Vienna, Austria

*CORRESPONDENCE
Emma L. Culver
emma.culver@nhs.net

RECEIVED 03 August 2023
ACCEPTED 25 January 2024
PUBLISHED 16 February 2024

CITATION
Motta RV and Culver EL (2024) IgG4 autoantibodies and autoantigens in the context of IgG4-autoimmune disease and IgG4-related disease.
Front. Immunol. 15:1272084.
doi: 10.3389/fimmu.2024.1272084

IgG4 autoantibodies and autoantigens in the context of IgG4-autoimmune disease and IgG4-related disease

Rodrigo V. Motta[1] and Emma L. Culver[1,2]*

[1]Translational Gastroenterology and Liver Unit, Nuffield Department of Medicine, University of Oxford, Oxford, United Kingdom, [2]Department of Gastroenterology and Hepatology, Oxford University Hospitals NHS Foundation Trust, Oxford, United Kingdom

Immunoglobulins are an essential part of the humoral immune response. IgG4 antibodies are the least prevalent subclass and have unique structural and functional properties. In this review, we discuss IgG4 class switch and B cell production. We review the importance of IgG4 antibodies in the context of allergic responses, helminth infections and malignancy. We discuss their anti-inflammatory and tolerogenic effects in allergen-specific immunotherapy, and ability to evade the immune system in parasitic infection and tumour cells. We then focus on the role of IgG4 autoantibodies and autoantigens in IgG4-autoimmune diseases and IgG4-related disease, highlighting important parallels and differences between them. In IgG4-autoimmune diseases, pathogenesis is based on a direct role of IgG4 antibodies binding to self-antigens and disturbing homeostasis. In IgG4-related disease, where affected organs are infiltrated with IgG4-expressing plasma cells, IgG4 antibodies may also directly target a number of self-antigens or be overexpressed as an epiphenomenon of the disease. These antigen-driven processes require critical T and B cell interaction. Lastly, we explore the current gaps in our knowledge and how these may be addressed.

KEYWORDS

IgG4, IgG4-RD, autoantibody, antigen, autoimmunity

1 Introduction

Antibodies are the fundamental component of humoral immune responses, also known as antibody-dependent responses. These molecules can recognise and neutralise pathogens, either by binding to molecular antigens and directly preventing their pathogenic effect, or by opsonising these pathogens and triggering effector functions, such as the complement system, antibody-dependent cell-mediated cytotoxicity and antibody-dependent cellular phagocytosis.

Five different classes of antibodies, or immunoglobulins (Ig) are found in humans, namely IgM, IgD, IgA, IgE and IgG. IgM and IgD are involved in primary adaptive humoral immunity and can be found in mature naïve B cells (1), which undergo specialisation and a class switch towards long lived B cells and plasmablasts that produce IgA, IgE and IgG (2, 3). IgA is mainly involved in mucosal humoral immunity. IgE is one of the main components of allergic reactions. IgG is part of several different processes both in health and disease.

IgG has four subclasses (i.e., IgG1, IgG2, IgG3 and IgG4) which form part of the immune response. Under normal conditions, IgG1-3 can fixate complement and opsonise pathogens, whilst IgG4 only activates complement under special circumstances, at high antibody and antigen concentrations. IgG and its subclasses are involved in autoimmune processes, such as rheumatoid arthritis, systemic lupus erythematous, ANCA-associated vasculitides, as well as IgG4-autoimmune diseases (IgG4-AID) and IgG4-related disease (IgG4-RD).

In this review, we describe the structure and function of IgG4 antibodies, discuss the role of this class in allergy, helminth infections, malignancies, and autoimmune diseases. A greater emphasis is placed on IgG4-related disease and the role of IgG4 antibodies in the pathogenesis of the disease.

2 Structure and function of IgG4 antibodies

Immunoglobulin G has four subclasses, with IgG4 representing up to 5% of the total IgG concentration (4). Their structure is based on 2 heavy and 2 light chains bound together by disulphide bridges. There are interactions between the light and heavy chains, as well as a connection between the two heavy chains at the hinge region. This region is important because it gives structural flexibility to the molecule. Both the light and heavy chains have antigen-binding sites, the variable region (V_L and V_H), and areas responsible for the effector function of the antibodies, called constant region (C_L and C_H1, C_H2, C_H3, C_H4). Furthermore, these molecules can be divided by function, the "Fragment, antigen binding" (Fab) region and the "Fragment, crystallised" (Fc) region, which is responsible for the effector function (5). In the CH2 domain, a switch of proline to serine at position 228 in the hinge of IgG4 facilitates Fab-arm exchange (Figure 1). Schuurman, Aalberse and colleagues observed that this phenomenon is marked by the dissociation of the two heavy chains and recombination of two random IgG4 monomers (heavy and light chains) to form a bispecific dimer (6). Even though this new molecule might recognise two different antigens, it is functionally monovalent, and cannot form large immune complexes (7–9). The Fc portion in IgG4 antibodies have a high affinity for antigens and FcγIIb receptors but low affinity for Fcγ stimulatory receptors and cannot tipically activate the classical complement pathway (10). These characteristics hinder Fc mediated effector functions and prevent further sensitisation of the immune system (8, 11–13). There are, however, situations where IgG4 molecules can activate the complement pathway. The first is via recruiting mannose-binding lectins and activating the lectin pathway, which has been observed in anti-PLA2R membranous nephropathy (14). The second is through mutations of the Fc region, enabling these molecules to form hexamers and

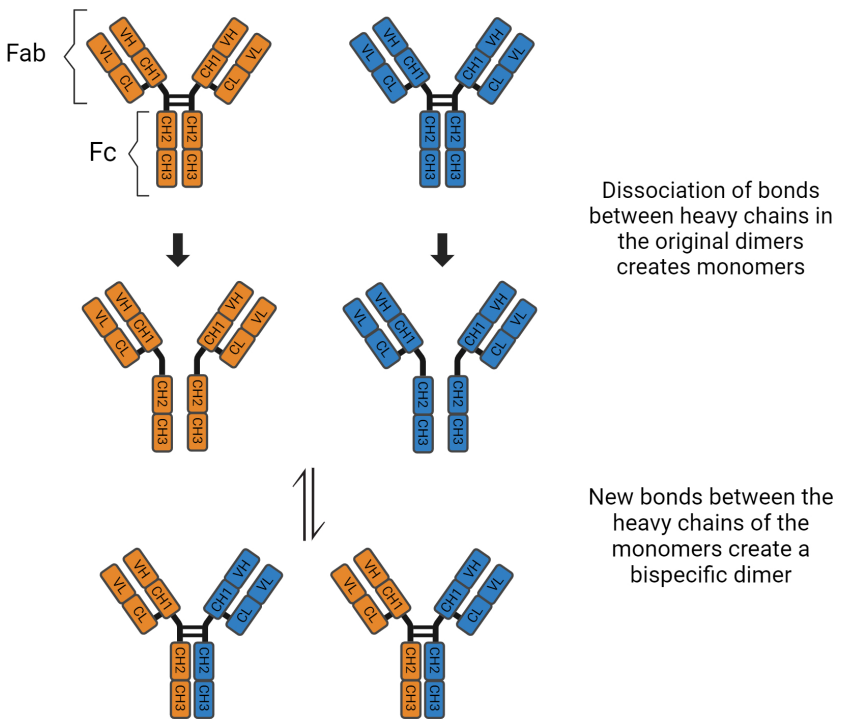

FIGURE 1
Fab arm exchange in IgG4 antibodies.

bind to C1q (15). These molecules can also activate the complement system using the classical pathway when there is high antigen density and high antibody concentration (16). Finally, Oskam, Rispens and collaborators showed that in opposition to previous evidence, the heavy chains of IgG4 molecules can dissociate and interact with the Fc region of other IgGs. It is not clear whether this mechanism plays a role in the pathogenesis of autoimmune diseases, but it modulates the affinity of IgG1 and IgG2 for C1q (17). Hence, IgG4 has anti-inflammatory properties, and it is involved both in health, such as the development of tolerance in allergies (18), as well as disease, such as curbing immune responses against helminth infections (19) (Table 1).

3 Class switch recombination and somatic hypermutation

When exposed to antigens, naïve B cells become antibody secreting B cells via the extrafollicular and follicular pathways, which are complementary. The initial response to antigens is predominantly driven by the extrafollicular path (20, 21). It involves T follicular helper (Tfh) cells driving the differentiation of naïve B cells into short lived plasmablasts, which will maintain an immune response for up to a week after the trigger (20, 22).

To create an immune response based on IgG4, B cells must undergo class switch recombination (CSR) and somatic hypermutation (SHM) (11, 23, 24). These processes are hallmarks of follicular responses, which take part in germinal centres (GC) of lymph nodes and the spleen. In the follicular pathway, antibody secreting B cells develop high affinity and specificity and become either memory B cells or long-lived plasma cells (LLPC). The GCs are divided in dark and light zones, with functional differences. The dark zone promotes proliferation of B cells, as well as CSR and SHM (25). CSR is marked by deletional recombination in the heavy chain gene that leads to a change in Ig class, thus changing effector functions of the antibodies, while preserving the affinity for specific antigens. Given its mechanism, switch in Ig class follows a sequential pattern from IgM/IgD to IgG3, IgG1 and IgA1, called proximal classes. A secondary switch then gives rise to distal classes such as IgG2, IgG4 and IgA2 (23, 26, 27) and has been attributed to stimuli from T helper 2 (Th2) cells. Interleukin (IL) 4 and IL-13 are responsible for skewing the antibody production to IgG4 and stimuli involving IL-10 and/or IL-21 lead to selection of IgG1 antibodies (28). After these clones have developed high-affinity and specificity, they migrate into the light zone. There, they will undergo a selection according to interactions with Tfh cells and follicular dendritic cells (29). Once the highly specific clones are selected, they leave the GC and become LLPC or migrate to the bone marrow as memory B cells.

TABLE 1 IgG4 antibodies: structural characteristics and functional consequences.

Molecule structure	Function
Change of proline (IgG1) to serine (IgG4) at position 228 in the core hinge region	Asymmetry in the structure with different Fab arms. The final antibody is functionally monovalent. **IgG4 cannot bind to two different antigens neither form large immune complexes.**
CH2 domain amino acid substitutions - L234F and P331S	Low-affinity to FcγRIIa and FcγRIIIa. **Weak ability to bind to FcγRI compared with IgG1**
CH2 domain amino acid substitution - P331S	Negligible binding to the C1q protein complex. **Cannot trigger the classical complement pathway**
Constant domain links with Fc portion of other IgG molecules	Compete with other antibodies and impairs IgG1 ability to activate complement or form immune complexes. **Anti-inflammatory function**

In the function column, the bold values represent the functional outcomes.

4 IgG4 in allergic reactions

IgG4 antibodies have an important role in the development of tolerance in atopic patients. It has been extensively shown that beekeepers develop an IgG4-based response to bee venom associated with reduction of symptoms after exposure to the toxin (30, 31), and the same event has been described in other cases of occupational exposure (32, 33). Furthermore, allergen-specific immunotherapy is based on the development of IgG4 antibodies against allergens through regular and incremental exposure to allergenic antigens (34). IgG4 competitively binds to allergens, thus hindering the formation of IgE-antigen immune complexes (35, 36). Furthermore, it also binds to FcγRIIb, an inhibitory Fcγ receptor, preventing the degranulation of mast cells and the cascade that would lead to allergic responses (37–39).

On the other hand, IgG4 antibodies are also involved in the maintenance of the disease in cases of eosinophilic oesophagitis (EoE) and eosinophilic chronic rhinosinusitis (40–42). The most robust evidence that this class is involved in disease comes from studies associating it with symptoms in patients with EoE. During food avoidance tests, patients referred less symptoms and biopsies showed reduction of IgG4 deposition (43). In addition, histological levels of IgG4 were found to be significantly lower during remission when compared to samples collected during disease activity (44). For a detailed review on the topic, please see (45).

5 IgG4 in helminthic infections

Helminthic infections are another scenario where IgG4 antibodies show their tolerogenic effects. Patients with acute parasitic infection usually show a balanced Th1/Th2 immune response, with a predominance of IFN-γ over IL-10, and a higher count of peripheral eosinophils (46). If the pathogen fails to evade the host response, this leads to parasite clearance and termination of the infection.

Individuals with chronic infection, however, show an immune response with a Th2 profile, where IL-10 plays a critical modulatory role in skewing antibody production towards IgG4 (46). A response based on parasite-specific IgG4 antibodies, then, dampens IgE-

mediated immune response and perpetuates the infection. Asymptomatic patients show a restricted response to parasite antigens, while those with severe chronic disease have lower levels of serum IgG4 antibodies and show signs of organ damage (46). Studies also show that individuals with a high parasite burden have higher levels of parasite-specific IgG4 than patients with a lower parasite burden (47, 48). The immunomodulatory effects of helminthic infections are also seen in the response to allergens, where patients with chronic parasitic infection show lower levels of IgE-reactivity to dust antigens (49).

6 IgG4 in malignancies

Antitumour humoral responses can prevent malignancies from developing further and even annihilate them by triggering humoral and cell-mediated immune responses. Some neoplasms induce class switch of anti-tumour antibodies to the IgG4 class, leading to immune escape and IgG4-mediated tumour-tolerogenic responses (50). Melanoma and pancreatic ductal adenocarcinoma cells induce a modified Th2 immune response around their microenvironment, triggering B cells to undergo antibody class switch towards IgG4 (51, 52). These antibodies will then competitively bind to cancer antigens and damp anti-tumour immune responses. Higher serum levels of IgG4 are associated with fewer cytotoxic T cells (53) and with a worse prognosis in patients with cholangiocarcinoma and melanoma (50, 54).

A meta-analysis reported that patients with IgG4-RD have an increased risk of clonal B cell lymphoma and pancreatic malignancy when compared with a matched general population (55). The mechanisms driving this increased risk remain speculative and include 1) chronic inflammation-induced carcinogenesis; 2) IgG4-related tumour-induced immune escape; 3) paraneoplastic phenomenon, as most malignancies detected distant from the site of disease activity. The class switch towards IgG4 induced by some malignancies may also play a role in the initiation of IgG4-RD. K-ras codon gene mutations associated with gastrointestinal cancer have been reported in patients with IgG4-related pancreatitis (56). These mutations are also associated with cellular transformation and genetic instability (57, 58).

7 IgG4 in IgG4-autoimmune diseases

Huijbers et al. were the first to collectively describe IgG4 autoimmune diseases (IgG4-AID) as a spectrum of conditions characterised by autoantibody responses against a known antigen (59). Evidence shows that these diseases are caused by IgG4 antibodies recognising autoantigens, although not all antigens have been validated. The diagnosis of IgG4-AID depends on high level of suspicion and identification of IgG4 autoantibodies against the antigen(s) specific to each disease (60). Koneczny proposed a classification system based on evidence of antibodies against extracellular antigens, and direct pathogenic mechanism of IgG4 antibodies observed *in vitro* and validated in animal models through passive transfer (61). Although 29 antigens have been described in IgG4-AID (Table 2), only the six antigens have met all three Koneczny criteria of IgG4 pathogenicity (61). For a thorough review on IgG4-AID and autoantigens involved in these disorders, please read (62).

7.1 Desmoglein 1 (Dsg1) and 3 (Dsg3):

Desmoglein 1 and 3 are transmembrane proteins found in keratinocytes. Anti-Dsg1 IgG4 is responsible for the development of pemphigus foliaceous (PF), while anti-Dsg3 IgG4 antibodies, and in some cases anti-Dsg1 IgG4, cause pemphigus vulgaris. These antibodies target epitopes in EC1 and EC2 domains, including in fogo selvagem (FS), an endemic PF specific to Brazil (63), and in the endemic PF found in Tunisia (64). Qian and Peng observed a cross-link between anti-LJM11, a protein present in the saliva of sand flies (*L. longipalpis*), and anti-Dsg1 antibodies in patients with FS and healthy controls from the same region (65, 66). The difference being that antibodies from the healthy population recognised the EC5 domain of Dsg1 rather than EC1 and EC2 (63, 65–67). Studies investigating the Tunisian population found that endemic PF patients and healthy controls from the same area had anti-Dsg1 IgG and demonstrated a cross-link between these antibodies and the salivary extract from *P. papatasi* (68–70). The antibodies in healthy Tunisians, instead of targeting the epitopes involved in endemic PF, bound to epitopes in the EC3, EC4 and EC5 of Dsg1 (64) and were mostly IgG1, IgG2 and IgG3 (71)

7.2 Muscle-specific kinase (MuSK):

MuSK is a tyrosine kinase involved in the transduction of electrical signals at the neuromuscular junction and is involved in MuSK myasthenia gravis (MG) (72). Anti-MuSK IgG4 antibodies often target the Ig-like 1 domain of the protein (73–75), which has important functional implications. This region contains the site where lipoprotein receptor-related protein 4 (Lrp4) binds to MuSK and activates the kinase, which causes clustering of acetylcholine receptors (AchR) at the synapse. By competitively binding to that domain, IgG4 antibodies block Lrp4-dependent activation of MuSK (76, 77), thus impairing migration of AchR to the neuromuscular junction. Other IgG subclasses might also be involved in MuSK MG. Huijbers et al. observed that valency affects the outcomes of antibody binding to MuSK and may, in fact, lead to activation of the kinase (78). Furthermore, patients with MuSK-MG have higher levels of IgG4, but they also have higher levels of IgG1 when compared to controls, which does not corroborate the theory that these patients have overall responses biased towards IgG4 (79).

7.3 Contactin 1 (CNTN1):

Contactin 1 binds with CNTN1-associated protein 1 (Caspr1) and neurofascin 155 (NF155), forming an axo-glial complex that is involved in paranode architecture and maintenance of myelin in axons (80). Chronic inflammatory demyelinating

TABLE 2 Comparison between antigens, symptoms, animal models, HLA associations and responsiveness to immunosuppression between IgG4-AID and IgG4-RD.

Antigen	Localisation of antigen	Disease	Symptoms	Organ affected	Evidence of passive transfer	Evidence through active immunisation	Ig type	Response to immunosuppressants	HLA associations
Carbonic anhydrase II	Cytoplasm	IgG4-RD	Pseudotumours, fibrosis. Varies according to organ affected.	Pancreas, bile ducts, sallivary and lacrimal glands, kidneys, retroperitoneum, aorta, orbits	No	Yes	IgG4	Yes	HLA-DQB1*0401, HLA-DRB1*0405, HLA-DRB1*16, FCGR2B
Plasminogen binding protein type A/UBR2	Cytoplasm and nucleus				No	No	Total IgG		
Lactoferrin	Pancreatic juice				No	No	Total IgG		
Pancreatic secretory trypsinogen inhibitor (SPINK1)	Pancreatic juice				No	No	Total IgG		
Trypsinogens	Pancreatic juice				No	No	Total IgG		
Annexin A11	Cytoplasm, cell membrane				Yes	No	IgG1 and IgG4		
Laminin 511-E8	Extracellular matrix				Yes	Yes	IgG1 and IgG4		
Galectin 3	Extracellular matrix, cytosol and nucleus				No	No	IgG4 and IgE		
Prohibitin	Nucleus, cytoplasm and mitochondria				No	No	IgG4		
Desmoglein 1	Cell membrane	Pemphigous foliaceous	Blistering lesions	Skin	Yes	Yes	IgG4 and IgG1	Yes	HLA-DRB1*0404, *1402, *1406, or *0102
Desmoglein 3	Cell membrane	Pemphigus vulgaris	Blistering lesions	Skin	Yes	No	IgG4 and IgG1	Yes	HLA-DRB1*14, HLA-DRB1*04:02, HLA-B*38, HLA-B*55

(Continued)

10.3389/fimmu.2024.1272084

TABLE 2 Continued

Antigen	Localisation of antigen	Disease	Symptoms	Organ affected	Evidence of passive transfer	Evidence through active immunisation	Ig type	Response to immunosuppressants	HLA associations
Muscle-specific kinase	Cell membrane	MuSK myasthenia gravis	Weakness and atrophy of neck, tongue, shoulder and bulbar muscles.	Muscles (Motoneural junction)	Yes	Yes	IgG4	Yes	HLA-DQB1*05, HLA-DRB1*13, HLA-DRB1*16
Contactin 1	Cell membrane	Chronic inflammatory demyelinating polyradiculoneuropathy	Subacute neuropathy, sensory ataxia and tremor.	CNS and PNS	Yes	No	IgG4	Variable	HLA-DQB1*02
Neurofascin 155	Cell membrane				Yes	No	IgG4	Variable	
CASPR1	Cell membrane				No	No	IgG4	Variable	
Neurofascin 140/186	Cell membrane				No	No	IgG4	Variable	
ADAMTS13	Blood circulation	Thrombotic thrombocytopenic purpura	Thrombotic events	Blood	Yes	No	IgG1 and IgG4	Yes	HLA-DRB1*11, HLA-DRB1*08:03
CASPR2	Cell membrane	Isaac's syndrome, Morvan's syndrome, limbic encephalitis	Epilepsy, behavioural and mental abnormalities, autonotmic instability, motor and sensory neuropathy.	CNS and PNS	Yes***	No	IgG4	Variable	HLA-DRB1*11:01
LGI1	Cell membrane	LGI1-associated limbic encephalitis, Isaac's syndrome	Epilepsy, behavioural and mental abnormalities, seizures, dystonia, sensory and motor neuropathy.	CNS and PNS	Yes***	No	IgG4	Variable	HLA-DRB1*07:01
PLA2R	Cell membrane	Membranous nephropathy	Oedema, fatigue, changes in urine	Kidneys	Yes	Yes****	IgG4	Yes	HLA-DQA1, HLA-DRB1*1501, HLA-DRB1*0301
THSD7A	Cell membrane				Yes	No	IgG4	Yes	
Alfa-enolase	Cell membrane				No	No	IgG4 and IgG1	Yes	
Superoxide dismutase 2 (SOD2)	Mitochondria				No	No	IgG4 and IgG1	Yes	
Aldose reductase	Cytoplasm				No	No	IgG4 and IgG1	Yes	
GPIHBP1	Cell membrane	GPIHBP1 autoantibody syndrome	Severe hypertriglyceridemia	Blood	No	No	IgG4	Needs more studies	

(Continued)

10.3389/fimmu.2024.1272084

TABLE 2 Continued

Antigen	Localisation of antigen	Disease	Symptoms	Organ affected	Evidence of passive transfer	Evidence through active immunisation	Ig type	Response to immunosuppressants	HLA associations
Laminin 332	Cell membrane	Mucous membrane pemphigoid	Blistering mucosal lesions, mainly in the oral cavity and conjunctivae	Mucosa	Yes	No	IgG4	Yes	HLA-DQB1*0301
Type IV Collagen	Extracellular matrix	Goodpasture syndrome, epidermolysis bullosa acquisita (EBA)	Haemoptysis, changes in urine/blistering lesions	Lungs and kidneys, skin	Yes	Yes	IgG1 and IgG2	Yes	HLA-DRB1*1501/ HLA-DR15, HLA-DRB1*15:03
IgLON5	Extracellular matrix	IgLON5 parasomnia	gait instability, non-REM and REM parasomnia, cognitive decline, movement disorders.	CNS	No	No	IgG1	Variable	HLA-DRB1*10:01-DQB1*05:01
DPPX	Cell membrane	Anti-DPPX encephalitis	Weight loss, gastrointestinal symptoms, cognitive-mental dysfunction, tremor, seizures, autonomic dysfunction.	CNS	No	No	IgG4 and IgG1	Variable	
ANCA	Cytoplasm	ANCA-related vasculitides	Fatigue, haemoptysis, muscle pain, changes in urine	Blood vessels, kidneys	Yes	Yes	IgG1, IgG3, IgG4	Yes	HLA-DRB1*04, HLA-DRB1*07, HLA-DRB1*09, HLA-DRB3, HLA-DRB1*13, HLA-DQ
Bullous pemphigoid antigen 180	Cell membrane	Bullous pemphigoid	Blistering lesions	Skin	Yes	Yes	IgG1	Yes	HLA-DQB1*0301
Bullous pemphigoid antigen 230	Cytoplasm	Bullous pemphigoid	Blistering lesions	Skin	Yes	Yes	IgG1	Yes	HLA-DQB1*0301
IFN 1, IL-17A, IL-22	Extracellular matrix	Autoimmune polyendocrinopathy-candidiasis-ectodermal dystrophy	Chronic candidiasis, hypothyroidism, hypogonadism	Skin, mucosa, endocrine organs, lungs, bowels	No	No	IgG1 and IgG4	Yes*/**	
P200 (laminin gamma1)	Cell membrane	Anti-p200 pemphigoid	Blistering lesions	Skin	No	No	IgG4	Needs more studies	

*Only the autoimmune manifestations respond to immunosuppressants.
** Ruxolitinib might be effective in the treatment of chronic mucocutaneous candidiasis in patients with STAT1 gain-of-function mutations.
***Did not trigger all the symptoms observed in patients.
****Knock-in PLA2R mice spontaneously developed MN.

10.3389/fimmu.2024.1272084

polyradiculoneuropathy (CIDP) is a IgG4-AID, and one of the possible antigens in this disorder is CNTN1. Anti-CNTN1 IgG4 antibodies recognise the IgC2 domains of CNTN1 and block its interaction with NF155, which leads to impaired cell aggregation and changes in paranodal architecture (81). Patients may present with other autoantibodies and have different clinical syndromes. Those presenting antibodies against neurofascin 186 (NF186), for instance, may present with renal impairment given both CNTN1 and NF186 are found in podocytes (62, 82).

7.4 Neurofascin 155 (NF155):

Neurofascin 155 is expressed by myelinating glial cells and, alongside Caspr1 and CNTN1, is part of the septate-like junction in paranodes found both in the central and peripherical nervous systems. Animal studies have confirmed the pathogenicity of anti-NF155 antibodies. Manso and colleagues demonstrated that intrathecal infusion of IgG4 from anti-NF155 CIDP patients induced similar symptoms in previously healthy mice (83). Early studies identified that these antibodies recognise the Fn3 and Fn4 domains of NF155, which does not participate in the interaction with CNTN1, and suggested a possible blocking mechanism that would cause the clinical presentation (84). Nevertheless, Manso et al. found that anti-NF155 IgG4 is associated with aggregation of the antigen and induces its depletion. They could not determine which mechanism was responsible for the depletion of surface NF155 and suggested that it might have to do with proteolysis of the antigen or molecular instability (83, 85).

7.5 ADAMTS13:

ADAM metallopeptidase with thrombospondin type 1 motif 13 (ADAMTS13) is a protease found in the blood circulation. It is responsible for the proteolytic cleavage of the multimeric form of von Willebrand factor (vWf) and ensuring normal haemostasis (86). Anti-ADAMTS13 IgG4 antibodies and vWf recognise the spacer-domain of the antigen, thus creating a competition for binding with ADAMTS13 (87). Autoimmune thrombotic thrombocytopenic purpura (TTP) is marked by an initial response based on IgG1 antibodies against ADAMTS13. The chronic antigenic stimulation then promotes class switch towards IgG4, which perpetuates the disease (88). The accumulation of vWf causes platelet aggregation and formation of microthrombi, which leads to the characteristic phenotype of microangiopathic haemolytic anaemia.

8 IgG4 in IgG4-related disease

IgG4-related disease (IgG4-RD) is a chronic relapsing immune-mediated fibro-inflammatory disorder and its hallmark is the presence of IgG4 antibodies in the sites affected (89). The diverse organ involvement in this disease is linked by a unique histopathology; a lymphoplasmacytic infiltrate rich in IgG4+ plasma blasts and $CD4^+$ T cells, storiform fibrosis, and obliterative phlebitis (90).

There are currently three theories on the role of IgG4 antibodies in IgG4-RD: 1) IgG4 antibodies directly cause the disease by targeting self-antigens; 2) IgG4-RD patients have an immune response inherently biased towards production of IgG4 antibodies to any stimulus; 3) IgG4 is only present to modulate an immune response based on different pathways. It continues to be elusive whether the overexpression of these antibodies is an epiphenomenon of the inflammatory reaction or has a causal role in disease pathology.

8.1 Do IgG4 antibodies directly cause disease by targeting self-antigens?

Next-generation sequencing studies yield evidence to support that the pathogenesis of IgG4-RD is an antigen-driven process mediated by B and T cell interactions (91). Circulating B cells are predominantly $IgG4^+$ B cells with extensive V-region mutations affecting both hypervariable and framework regions, suggesting signs of antibody maturation (91, 92). Mattoo et al. observed expansion of $CD19^+CD27^+CD20^-CD38^{hi}$ plasmablasts, which are oligoclonally restricted as shown by analysis of immunoglobulin heavy V and J regions (92). Naïve B cells then undergo *de novo* recruitment during disease relapse. In patients who have a disease flare after treatment with rituximab, activated B cells and plasmablasts have increased somatic hypermutation when compared to before B cell depleting therapy, suggesting a possible driver for the autoreactive pathogenic process (92).

Differences in B cell phenotypes may be clinically important, as demonstrated by Li and colleagues (93). Patients with active IgG4-RD had increased plasmablasts ($CD19^+CD24^-CD38^{hi}$, $CD19^+CD27^{hi}CD38^{hi}$, and $CD19^+IgD^-CD38^{hi}$) and reduced numbers of $CD19^+$ B cells, $IgD^+CD38^{+/-}$ naïve B cells and $CD24^{hi}CD38^{hi}$ B regulatory cells (Breg) when compared to controls (93). Cluster analysis revealed that patients with a high count of plasmablast and memory B cells, low count of naïve B cells and Bregs had a higher disease burden and were predominantly male (93). This highlights the importance of antigen-specific LLPC in the pathogenesis of IgG4-RD. Whilst Rituximab (anti-CD20) reduces the number of short-lived B cells expressing CD20, memory B cells and LLPC lack this surface protein and can evade depletion, contributing to the relapse of disease.

Analysis of IgG4-RD lesions showed that tissue $CD4^+$ T cells are clonally expanded with a cytolytic phenotype, expressing granzyme A, perforin and $SLAMF7^+$ (SLAM family member 7) (94), and secreting IL-1β, TGF-β and IFN-γ, cytokines associated with fibrosis (94, 95). Drugs that deplete B cells lead to profound clinical remission and significantly reduce serum plasmablasts and $CD4^+$ cytotoxic cell populations. Therefore, the excellent response to B cell depletion support that these cells are involved in the pathophysiology of IgG4-RD (93, 96, 97). Overall, this evidence suggests that T-dependent B cell activation is essential in the pathogenesis of IgG4-RD. For a thorough review of the roles of different T cells in IgG4-RD, please see (91).

HLA-mediated antigen presentation occurs in a number of autoimmune diseases, such as DRB1*15 in multiple sclerosis, DRB1*04 in rheumatoid arthritis and DQB1*02 and DQB1*03 in coeliac disease. A genome-wide association study in 857 Japanese IgG4-RD patients suggested that the HLA-DRB1*04:05 allele was important in the development of IgG4-RD (98). Indeed, mice expressing this risk allele develop autoimmune pancreatitis (99). This allele is also associated with type 1 diabetes and Crohn's disease (100, 101). Furthermore, the single nucleotide polymorphism (SNP) rs134097 found in FcγRIIb was strongly associated with IgG4-RD, as well as with two phenotypes of the disease (pancreato-biliary and Mikulicz), number of swollen organs and serum IgG4 level at diagnosis. This SNP might play a critical role in IgG4-RD because its locus directly impacts on the expression of FcyRIIb, a receptor involved in the elimination of self-reactive B cells.

8.1.1 Autoantigens in IgG4-RD

Many studies suggest a role of autoantigens in patients with IgG4-RD. Neonatal mice that received passive transfer of purified IgG1 and IgG4 from patients with active IgG4-RD showed evidence of damage to salivary glands and the pancreas (102). Several autoantibodies have been identified in the context of IgG4-related autoimmune pancreatitis, such as lactoferrin, carbonic anhydrase, pancreas secretory trypsin inhibitor, amylase-alpha, heat shock protein and plasminogen-binding protein. However, many of these lacked sensitivity and specificity for those with other organ manifestations (103).

8.1.1.1 *Helicobacter pylori* antigens

Human carbonic anhydrase II (CAII) is an enzyme found in the cytoplasm of pancreatic ductal epithelial cells, as well as in kidney tubules, gallbladder and glial cells. Given the discovery of antibodies against *H. pylori* in the sera of patients with IgG4-related pancreatitis and Sjogren's syndrome (104–106), it was proposed that *H. pylori* infection could be driving the disease through molecular mimicry with CAII (107). Frulloni and colleagues identified that, in fact, immunoglobulins from IgG4-RD patients targeted plasminogen-binding protein type A (PBP), also an antigen found in *H. pylori*. This protein shares sequence homology with a human protein, ubiquitin protein ligase E3 component n-recognin 2 (UBR2). The group proceeded to show that 19 (95%) of their patients with IgG4-related pancreatitis had antibodies against PBP and similar results were replicated with UBR2 (108). A large study by Culver et al., however, did not replicate the findings. Among 69 IgG4-RD patients and 51 controls with autoimmune or inflammatory diseases, authors found similar T and B cell reactivity against PBP between groups (109). Jesnowski and colleagues investigated the presence of conserved sequences of H. pylori in the pancreatic tissue and juice of patients with IgG4-related pancreatitis and pancreatic cancer via nested PCR and couldn't identify any signal of H. pylori DNA (110), corroborating previous findings that the bacterium is unlikely to be directly involved in the pathogenesis of IgG4-related pancreatitis.

8.1.1.2 Acinar antigens

Lactoferrin (LF), pancreatic secretory trypsinogen inhibitor (SPINK1) and trypsinogens have been identified as possible antigens in IgG4-related pancreatitis (111, 112) and antibodies against the last two proteins have been reported in different cohorts of patients with the disease. Löhr and colleagues showed that patients with chronic IgG4-related pancreatitis have a severely reduced population of acinar cells in histopathological studies. The presence of antibodies against trypsinogens was replicated in an animal model of the disease, thus corroborating this finding (112). Nevertheless, they could not differentiate between subtypes of autoimmune pancreatitis and could not explain why acinar cells resume production of digestive enzymes during remission of IgG4-related pancreatitis.

8.1.1.3 Annexin A11

Annexin A11 is part of a family of calcium-dependent phospholipid-binding proteins. It is found in the cytosol of cholangiocytes, pancreatic duct cells and islands of Langerhans as well as other tissues. Hubers and colleagues (113) identified IgG4 antibodies against annexin A11 in 9 (18%) patients with IgG4-related pancreatitis and cholangitis, whilst not in controls with other pancreatobiliary diseases, including malignancies. Reinforcing this finding, the location where this antigen was identified corresponded to the pattern of injury in pancreatobiliary disease (114). It was also found in patients with IgG4-related salivary involvement, suggesting that annexin A11 is not specific to pancreatobiliary involvement.

The 'biliary bicarbonate umbrella' is responsible for protecting human cholangiocytes from hydrophobic bile acid influx (115). Herta et al. reported that annexin A11 is necessary so that this defensive mechanism can be adequate. Antibodies against annexin A11 inhibited the function of this self-antigen, thus the authors speculate that this may impair the biliary bicarbonate umbrella and facilitate bile duct damage in patients with IgG4-related cholangitis (116).

Lastly, Hubers et al. demonstrated that IgG4 antibodies isolated from patients with IgG4-RD compete with IgG1 for binding to annexin A11, thus reinforcing that the first has an anti-inflammatory role in the disease pathogenesis (113). These results have been replicated in the passive transfer experiment with neonatal mice, where IgG from IgG4-RD patients induced a similar pattern of pancreatic and salivary lesion. Shiokawa and colleagues observed that both IgG1 and IgG4 antibodies could trigger the injury. The first, however, had its activity dampened by simultaneous injection of IgG4 antibodies (117).

8.1.1.4 Laminin 511-E8

Laminin is a component of the extracellular matrix (ECM) of tissues, and integrin alfa-6-beta-4 is a cellular adhesion molecule that binds to laminins in the ECM. A Japanese group identified antibodies against laminin 511-E8 in 51% (26/51) of patients with IgG4-related pancreatitis and in only 1.6% of healthy volunteers (118). Sixteen percent (4/25) of those who did not have antibodies

to laminin, had antibodies against its ligand, integrin alpha-6-beta-1.

Passive transfer and active immunisation animal models confirmed that mice that received human sera from patients with IgG4-related pancreatitis and those immunized with human laminin 511-E8 developed an immune response responsible for injury in pancreatic tissue and salivary glands in the same pattern as observed in IgG4-RD (119). Regardless of serum concentration of IgG4, half of these patients had specific IgG1 antibodies whilst only one patient had IgG4 against laminin 511-E8. Furthermore, only pancreatic and salivary gland injury was demonstrated.

Shiokawa observed that anti-laminin 511-E8 antibodies decreased upon treatment with glucocorticoids in an equivalent manner as other biomarkers of activity (119) (e.g., serum IgG4 concentration and pancreatic imaging). These results have not been validated externally. In contrast, In a US IgG4-RD cohort, the positivity rate for laminin 511-E8 antibody was similar between IgG4-RD (7%), disease controls, and healthy volunteers (118).

8.1.1.5 Galectin-3

Galectin-3 is a cytoplasmatic b-galactoside-binding lectin identified in systemic fibroproliferative conditions, such as systemic sclerosis and pulmonary fibrosis (120). In a US cohort of 121 IgG4-RD patients, using immunoaffinity chromatography and mass spectrometry of plasmablast clones, 34 (28%) were positive for IgG4-specific anti-galectin-3 antibody while almost none of the 45 disease controls with interstitial pulmonary fibrosis and 50 healthy volunteers showed similar results (121). Furthermore, IgE-specific anti-galectin-3 antibodies were also detected but other IgG subclasses had little to no reactivity among the participants (121).

Perugino et al. used a galectin level threshold above 10.25ng/mL, which is independently associated with all-cause mortality in systemic sclerosis (122), to divide their cohort into two groups; those with higher levels had 64% positivity for IgG4 anti-galectin-3 antibodies, whilst those with lower levels had 23% positivity (121). Moreover, the authors reported a correlation between the presence of these antibodies and lymphadenopathy in IgG4-RD, as well as a trend between higher serum concentration of galectin-3 and increased IgG4-RD Responder Index of disease activity, number of organs and multi-organ involvement.

A Japanese group used proteomic analysis to demonstrate a 13-fold increased expression of galectin-3 in the pancreas of patients with IgG4-related pancreatitis compared with heathy pancreatic tissue (123). Galectin-3 is expressed by different cell lines in affected organs in IgG4-RD, including pancreas, bile ducts, salivary glands, kidney, lung, aorta and retroperitoneum, supporting a role in tissue fibrosis in IgG4-RD (124).

8.1.1.6 Prohibitin

Prohibitins are ubiquitously expressed and are important in critical cell processes. Prohibitin 1 is involved in transcription, apoptosis and mitochondrial protein folding (125), while prohibitin 2 is essential in mitochondrial homeostasis and autophagy (126). Du and colleagues identified a protein that has 8 unique peptides matched to human prohibitin, and also shares 40% of sequence similarity, using affinity purification of patient serum and mass spectrometry (127). Seventy-three percent (65/89) of patients with IgG4-RD had antibodies against prohibitin, whilst only 13% with Sjogren's syndrome and 1.4% of healthy volunteers showed positivity. Moreover, the anti-prohibitin antibody was observed in patients with IgG4-related pancreatic disease, salivary disease, retroperitoneal fibrosis, and other organ involvement (127).

8.1.2 Role of autoantigens as biomarkers in IgG4-RD

Currently, there is no evidence that measuring autoantigens can help to diagnose IgG4-RD, detect response to treatment or predict early signs of a disease flare. There are discrepancies between cohorts on the relative frequency of each autoantigen; Liu and colleagues assessed for the presence of autoantigens in a US IgG4-RD cohort and found 7% positivity for laminin 511-E8, 10% for prohibitin, 12% for annexin A11 and 28% for galectin-3 (118). The authors also observed that there was no clinically meaningful difference between patients with and without the presence of one autoantibody. Nevertheless, patients with positivity for more than one antibody had a more severe presentation, usually with higher levels of inflammatory biomarkers (e.g., total IgG and subclasses, C-reactive protein, and complement consumption) as well as greater risk of visceral organ involvement (118). This is in keeping with findings in other autoimmune diseases.

We can speculate that it is not just one autoantigen that dominates in IgG4-RD, and that the presence of multiple autoantigens may promote a larger breach of B cell tolerance and correlate with a more aggressive inflammatory disease phenotype. Another possible explanation for the wide variety of autoantibodies found in IgG4-RD might be that, in fact, it is not a single disease, but rather a spectrum of disorders characterised by a similar response to different stimuli. Further studies need to demonstrate a single trigger for the disease and/or identify mechanisms to justify why an autoantigen is not involved in all four phenotypes of the disease.

8.2 Do patients with IgG4-RD have a biased immune response towards the production of IgG4 against any stimulus?

Another theory behind the development of IgG4-RD is that patients have an inherently biased immune response and preferentially produce IgG4. IgG4 antibody has an important role in the development of tolerance after chronic exposure to allergens (34), and an association between allergy and/or atopy and IgG4-RD has been described by many groups (128–133). There are different definitions for allergy and atopy, which creates a variance in the prevalence of these conditions reported in patients with IgG4-RD (134). Studies observed between 18 and 76% of patients with IgG4-RD have allergy (130–133) and between 14 and 46% have atopy (129, 135, 136). A predominance of type 2 immunity has been reported in such patients. There is an abundance of IL-4 and IL-13, which drive CSR towards IgG4 and IgE production, as well as activation of eosinophils (137). Some studies have suggested a phenotype that is more treatment refractory and aggressive in

those with allergy/atopy, higher IgE and IgG4 level and peripheral blood eosinophil counts.

Our group has shown that antigens derived from food and animals elicited a polyclonal IgG4 response in patients with IgG4-RD. These food antigens included egg white and yolk, milk, banana, peanut, rice, wheat, and animal cat dander. Indeed, high serum levels of IgG4 in this setting may reflect a defective regulation of the overall immune response (138).

We have also shown that IgG4-RD may be associated with prolonged contact with occupational antigens. Exposure to solvents, industrial and metal dusts, automotive's pigments and oils was described in up to 61% of patients in two independent cohorts of IgG4-related sclerosing cholangitis in the Netherlands and the UK (139). Blue collar workers were further identified as a risk factor for developing disease in a case-controlled study (140). No single contaminant was identified, which raises the question whether prolonged contact with a number of environmental antigens trigger the disease and drive the IgG4 response. There is also emerging data on the role of asbestos in IgG4-related retroperitoneal fibrosis, and tobacco smoking conferring an increased risk of developing the disease.

An IgG4 class switch response and production of excessive IgG4 antibodies in the disease is likely determined by the immune cell milieu. During active IgG4-RD, restricted clones of B cells and plasmablasts proliferate through a Tfh2 cell-dependent pathway. Interleukin (IL)-21 producing Tfh2 lymphocytes promote somatic hypermutation in B cells inside GC, while IL-4 producing Tfh2 cells are involved in CSR (141–143). Regulatory T cells and IL-10 are also involved in the making of an IgG4-based response (144, 145).

8.3 Are IgG4 antibodies trying to curb an overactive inflammation caused by a different trigger in IgG4-RD?

Finally, we need to consider whether IgG4 antibodies are an epiphenomenon and actually are trying to control inflammation based on a different mechanism. Mouse models confirmed that total IgG from patients with IgG4-RD caused a similar pancreatic injury in the animals (113, 117). Shiokawa and colleagues analysed differences between the pathogenic effect of IgG1 and IgG4 of patients with IgG4-RD when these antibodies were injected in mice (117). When injected separately, both classes caused pancreatic injury and IgG4 also caused salivary damage, but interestingly, when these antibodies were injected simultaneously, IgG4 competed with IgG1 and significantly reduced its binding to pancreatic tissue. Thus, there may be a competitive effect of producing excess IgG4 anitbodies to dampen an inflammatory process that precedes them.

Against this theory is the evidence that IgG4 antibodies in patients with IgG4-RD are highly specific and have high affinity for their target given that circulating B cells are in their majority $IgG4^+$ B cells with extensive V-region mutations (91, 92). These findings suggest that these antibodies come from B cells/plasma cells that have undergone rounds of maturation rather than an inflammatory response, thus making the case that IgG4-RD behaves more like an autoimmune disease instead of an inflammatory disorder.

9 Parallels between IgG4-AID and IgG4-RD

The antigens proposed for IgG4-RD are ubiquitous and found both in the cytosol and the extra cellular matrix. Nevertheless, with the exception of laminin 511-E8, they fall short of meeting either Witebsky or Koneczny criteria for autoimmunity (61, 146). This brings into question whether these antibodies are the drivers of IgG4-RD. There is evidence that antibodies can penetrate the plasma membrane and recognise intracellular antigens (147–149). In fact, many entry mechanisms have been studied, such as interaction of basic residues with a negatively charged cell membrane (150), Fc-receptor mediated entry (151), endocytosis (147, 152, 153), and nucleoside transporters (154). Among the six IgG4-AID that meet IgG4 autoimmunity criteria, however, all the antigens involved in their pathogenesis are found in the cell membrane or free in the blood circulation (62).

Another important consideration when analysing the role of autoantigens in IgG4-RD is the clinical presentation of the disease. Regardless of phenotype (i.e., pancreatobiliary, head and neck, retroperitoneum and aorta, and systemic), the hallmarks of IgG4-RD are proliferative and/or fibrotic lesions in the organs affected. These findings are diametrically opposed to those from IgG4-AID, where symptoms are driven by IgG4 antibodies blocking antigen function, such as in CNTN1-associated CIDP (155). Histological examination of IgG4-RD lesions shows a massive invasion of $IgG4^+$ B cells and plasmablasts and extensive (storiform) fibrosis (156). Furthermore, $CD4^+$ and $CD8^+$ cytotoxic T lymphocytes are also part of the immune response found in organs with active inflammation and peripheral blood (157), suggesting that the interaction between T and B cells play a critical role in the damage caused by IgG4-RD.

10 Current research gaps in IgG4-RD

Despite recent developments in IgG4-RD research, there are essential questions without an answer. One of the most important ones is why and how patients develop it. Previous studies reported an association of HLA-DRB1 and FCGR2B with IgG4-RD, including with phenotypical characteristics (98), and two studies observed a relation between HLA genes, particularly HLA-DQB1*04:01", HLA-DRB1*04:05 and HLA-DRB1*16 in patients with autoimmune pancreatitis type 1 and 2 (158, 159). Moreover, it is also important to look at B cell specialisation and how it can impact humoral immune responses favouring IgG4 expression. As in IgG4-AID, it is paramount to identify whether naturally occurring antigen(s) is(are) driving the immune response in IgG4-RD and the evidence surrounding self-antigens needs to be validated in external cohorts. We must consider the possibility that, such as IgG4-AID, IgG4-RD is a spectrum of diseases rather than a single entity. Finally, the increased expression of IgG4 antibodies and the presence of $IgG4^+$ plasma cells in sites with IgG4-RD inflammation highlights the importance of clarifying the mechanisms that favour class switch

towards IgG4 rather than other IgG subclasses. This knowledge is crucial to understand the pathogenesis of IgG4-RD (160).

Author contributions

RVM: Conceptualization, Data curation, Writing – original draft, Writing – review & editing. EC: Conceptualization, Data curation, Supervision, Writing – original draft, Writing – review & editing.

Funding

The author(s) declare that no financial support was received for the research, authorship, and/or publication of this article.

Acknowledgments

The National Institute for Health Research (NIHR) Biomedical Research Centre (BRC) Oxford supports ELC for work in inflammation and cancer.

Conflict of interest

EC: consults for Horizon Therapeutics, Zenus BioPharma and Sanofi for IgG4-RD. EC receives funding from the National Institute for Health Research NIHR Biomedical Research Centre BRC Oxford, Oxford Hospitals Charitable Grant and Research Capability Fund.

The remaining author declares that the research was conducted in the absence of any commercial or financial relationships that could be construed as a potential conflict of interest.

Publisher's note

References

1. Klein U, Rajewsky K, Küppers R. Human immunoglobulin (Ig)M+IgD+ peripheral blood B cells expressing the CD27 cell surface antigen carry somatically mutated variable region genes: CD27 as a general marker for somatically mutated (memory) B cells. *J Exp Med* (1998) 188:1679–89. doi: 10.1084/jem.188.9.1679

2. Brinkmann V, Müller S, Heusser CH. T cell dependent differentiation of human B cells: direct switch from IgM to IgE, and sequential switch from IgM via IgG to IgA production. *Mol Immunol* (1992) 29:1159–64. doi: 10.1016/0161-5890(92)90051-x

3. Dogan I, Bertocci B, Vilmont V, Delbos F, Mégret J, Storck S, et al. Multiple layers of B cell memory with different effector functions. *Nat Immunol* (2009) 10:1292–9. doi: 10.1038/ni.1814

4. Stone JH, Zen Y, Deshpande V. IgG4-related disease. *N Engl J Med* (2012) 366:539–51. doi: 10.1056/NEJMra1104650

5. Schroeder HW, Cavacini L. Structure and function of immunoglobulins. *J Allergy Clin Immunol* (2010) 125:S41–52. doi: 10.1016/j.jaci.2009.09.046

6. Schuurman J, Van Ree R, Perdok GJ, Van Doorn HR, Tan KY, Aalberse RC. Normal human immunoglobulin G4 is bispecific: it has two different antigen-combining sites. *Immunology* (1999) 97:693–8. doi: 10.1046/j.1365-2567.1999.00845.x

7. van der Neut Kolfschoten M, Schuurman J, Losen M, Bleeker WK, Martínez-Martínez P, Vermeulen E, et al. Anti-inflammatory activity of human IgG4 antibodies by dynamic Fab arm exchange. *Science* (2007) 317:1554–7. doi: 10.1126/science.1144603

8. Aalberse RC, Stapel SO, Schuurman J, Rispens T. Immunoglobulin G4: an odd antibody. *Clin Exp Allergy* (2009) 39:469–77. doi: 10.1111/j.1365-2222.2009.03207.x

9. Angal S, King DJ, Bodmer MW, Turner A, Lawson AD, Roberts G, et al. A single amino acid substitution abolishes the heterogeneity of chimeric mouse/human (IgG4) antibody. *Mol Immunol* (1993) 30:105–8. doi: 10.1016/0161-5890(93)90432-b

10. Bruhns P, Iannascoli B, England P, Mancardi DA, Fernandez N, Jorieux S, et al. Specificity and affinity of human Fcgamma receptors and their polymorphic variants for human IgG subclasses. *Blood* (2009) 113:3716–25. doi: 10.1182/blood-2008-09-179754

11. James LK, Bowen H, Calvert RA, Dodev TS, Shamji MH, Beavil AJ, et al. Allergen specificity of IgG(4)-expressing B cells in patients with grass pollen allergy undergoing immunotherapy. *J Allergy Clin Immunol* (2012) 130:663–670.e3. doi: 10.1016/j.jaci.2012.04.006

12. Van der Zee S, Aalberse RC. IgG4 and hyposensitization. *N Engl Reg Allergy Proc* (1987) 8:389–91. doi: 10.2500/108854187778999667

13. van der Zee JS, van Swieten P, Aalberse RC. Inhibition of complement activation by IgG4 antibodies. *Clin Exp Immunol* (1986) 64:415–22.

14. Yang Y, Wang C, Jin L, He F, Li C, Gao Q, et al. IgG4 anti-phospholipase A2 receptor might activate lectin and alternative complement pathway meanwhile in idiopathic membranous nephropathy: an inspiration from a cross-sectional study. *Immunol Res* (2016) 64:919–30. doi: 10.1007/s12026-016-8790-1

15. Diebolder CA, Beurskens FJ, de Jong RN, Koning RI, Strumane K, Lindorfer MA, et al. Complement is activated by IgG hexamers assembled at the cell surface. *Science* (2014) 343:1260–3. doi: 10.1126/science.1248943

16. Prodjinotho UF, Hoerauf A, Adjobimey T. IgG4 antibodies from patients with asymptomatic bancroftian filariasis inhibit the binding of IgG1 and IgG2 to C1q in a Fc-Fc-dependent mechanism. *Parasitol Res* (2019) 118:2957–68. doi: 10.1007/s00436-019-06451-2

17. Oskam N, Damelang T, Streutker M, Ooijevaar-de Heer P, Nouta J, Koeleman C, et al. Factors affecting IgG4-mediated complement activation. *Front Immunol* (2023) 14:1087532. doi: 10.3389/fimmu.2023.1087532

18. Navas A, Ruiz-Leon B, Serrano P, Martí M, Espinazo ML, Blanco N, et al. Natural and induced tolerance to hymenoptera venom: A single mechanism? *Toxins (Basel)* (2022) 14:426. doi: 10.3390/toxins14070426

19. Hagel I, Cabrera M, Buvat E, Gutiérrez L, Santaella C, Borges R, et al. Antibody responses and resistance against Ascaris lumbricoides infection among Venezuelan rural children: the influence of ethnicity. *J Trop Pediatr* (2008) 54:354–6. doi: 10.1093/tropej/fmn032

20. Elsner RA, Shlomchik MJ. Germinal center and extrafollicular B cell responses in vaccination, immunity, and autoimmunity. *Immunity* (2020) 53:1136–50. doi: 10.1016/j.immuni.2020.11.006

21. Weisel F, Shlomchik M. Memory B cells of mice and humans. *Annu Rev Immunol* (2017) 35:255–84. doi: 10.1146/annurev-immunol-041015-055531

22. Wrammert J, Smith K, Miller J, Langley WA, Kokko K, Larsen C, et al. Rapid cloning of high-affinity human monoclonal antibodies against influenza virus. *Nature* (2008) 453:667–71. doi: 10.1038/nature06890

23. Stavnezer J, Guikema JEJ, Schrader CE. Mechanism and regulation of class switch recombination. *Annu Rev Immunol* (2008) 26:261–92. doi: 10.1146/annurev.immunol.26.021607.090248

24. Aalberse RC, van der Gaag R, van Leeuwen J. Serologic aspects of IgG4 antibodies. I. Prolonged immunization results in an IgG4-restricted response. *J Immunol* (1983) 130:722–6. doi: 10.4049/jimmunol.130.2.722

25. Muramatsu M, Kinoshita K, Fagarasan S, Yamada S, Shinkai Y, Honjo T. Class switch recombination and hypermutation require activation-induced cytidine deaminase (AID), a potential RNA editing enzyme. *Cell* (2000) 102:553–63. doi: 10.1016/s0092-8674(00)00078-7

26. Jackson KJL, Wang Y, Collins AM. Human immunoglobulin classes and subclasses show variability in VDJ gene mutation levels. *Immunol Cell Biol* (2014) 92:729–33. doi: 10.1038/icb.2014.44

27. Kitaura K, Yamashita H, Ayabe H, Shini T, Matsutani T, Suzuki R. Different somatic hypermutation levels among antibody subclasses disclosed by a new next-

generation sequencing-based antibody repertoire analysis. *Front Immunol* (2017) 8:389. doi: 10.3389/fimmu.2017.00389

28. Unger P-PA, Lighaam LC, Vermeulen E, Kruithof S, Makuch M, Culver EL, et al. Divergent chemokine receptor expression and the consequence for human IgG4 B cell responses. *Eur J Immunol* (2020) 50:1113–25. doi: 10.1002/eji.201948454

29. Victora GD, Dominguez-Sola D, Holmes AB, Deroubaix S, Dalla-Favera R, Nussenzweig MC. Identification of human germinal center light and dark zone cells and their relationship to human B-cell lymphomas. *Blood* (2012) 120:2240–8. doi: 10.1182/blood-2012-03-415380

30. Matysiak J, Matysiak J, Bręborowicz A, Kycler Z, Dereziński P, Kokot ZJ. Immune and clinical response to honeybee venom in beekeepers. *Ann Agric Environ Med* (2016) 23:120–4. doi: 10.5604/12321966.1196866

31. García-Robaina JC, de la Torre-Morín F, Vazquez-Moncholi C, Fierro J, Bonnet-Moreno C. The natural history of Apis-specific IgG and IgG4 in beekeepers. *Clin Exp Allergy* (1997) 27:418–23. doi: 10.1111/j.1365-2222.1997.tb00727.x

32. Matsui EC, Diette GB, Krop EJM, Aalberse RC, Smith AL, Curtin-Brosnan J, et al. Mouse allergen-specific immunoglobulin G and immunoglobulin G4 and allergic symptoms in immunoglobulin E-sensitized laboratory animal workers. *Clin Exp Allergy* (2005) 35:1347–53. doi: 10.1111/j.1365-2222.2005.02331.x

33. Jones M, Jeal H, Schofield S, Harris JM, Shamji MH, Francis JN, et al. Rat-specific IgG and IgG_4 antibodies associated with inhibition of IgE-allergen complex binding in laboratory animal workers. *Occup Environ Med* (2014) 71:619–23. doi: 10.1136/oemed-2014-102119

34. Jarkvist J, Salehi C, Akin C, Gülen T. Venom immunotherapy in patients with clonal mast cell disorders: IgG4 correlates with protection. *Allergy* (2020) 75:169–77. doi: 10.1111/all.13980

35. James LK, Shamji MH, Walker SM, Wilson DR, Wachholz PA, Francis JN, et al. Long-term tolerance after allergen immunotherapy is accompanied by selective persistence of blocking antibodies. *J Allergy Clin Immunol* (2011) 127:509–16. doi: 10.1016/j.jaci.2010.12.1080

36. Shamji MH, Kappen J, Abubakar-Waziri H, Zhang J, Steveling E, Watchman S, et al. Nasal allergen-neutralizing IgG4 antibodies block IgE-mediated responses: Novel biomarker of subcutaneous grass pollen immunotherapy. *J Allergy Clin Immunol* (2019) 143:1067–76. doi: 10.1016/j.jaci.2018.09.039

37. Burton OT, Logsdon SL, Zhou JS, Medina-Tamayo J, Abdel-Gadir A, Noval Rivas M, et al. Oral immunotherapy induces IgG antibodies that act through FcγRIIb to suppress IgE-mediated hypersensitivity. *J Allergy Clin Immunol* (2014) 134:1310–1317.e6. doi: 10.1016/j.jaci.2014.05.042

38. Uermösi C, Zabel F, Manolova V, Bauer M, Beerli RR, Senti G, et al. IgG-mediated down-regulation of IgE bound to mast cells: a potential novel mechanism of allergen-specific desensitization. *Allergy* (2014) 69:338–47. doi: 10.1111/all.12327

39. Kanagaratham C, Derakhshan T, El Ansari YS, Furiness KN, Hollers E, Keldsen M, et al. IgG:FcγRIIb signals block effector programs of IgE:FcεRI-activated mast cells but spare survival pathways. *J Allergy Clin Immunol* (2023) 152:453–68. doi: 10.1016/j.jaci.2023.03.027

40. Clayton F, Fang JC, Gleich GJ, Lucendo AJ, Olalla JM, Vinson LA, et al. Eosinophilic esophagitis in adults is associated with IgG4 and not mediated by IgE. *Gastroenterology* (2014) 147:602–9. doi: 10.1053/j.gastro.2014.05.036

41. Koyama T, Kariya S, Sato Y, Gion Y, Higaki T, Haruna T, et al. Significance of IgG4-positive cells in severe eosinophilic chronic rhinosinusitis. *Allergol Int* (2019) 68:216–24. doi: 10.1016/j.alit.2018.09.002

42. Rosenberg CE, Mingler MK, Caldwell JM, Collins MH, Fulkerson PC, Morris DW, et al. Esophageal IgG4 levels correlate with histopathologic and transcriptomic features in eosinophilic esophagitis. *Allergy* (2018) 73:1892–901. doi: 10.1111/all.13486

43. Hoofien A, Papadopoulou A, Gutiérrez-Junquera C, Martínez Gómez MJ, Domínguez-Ortega G, Oudshoorn J, et al. Sustained remission of eosinophilic esophagitis following discontinuation of dietary elimination in children. *Clin Gastroenterol Hepatol* (2020) 18:249–251.e1. doi: 10.1016/j.cgh.2019.03.008

44. Quinn L, Nguyen B, Menard-Katcher C, Spencer L. IgG4+ cells are increased in the gastrointestinal tissue of pediatric patients with active eosinophilic gastritis and duodenitis and decrease in remission. *Dig Liver Dis* (2023) 55:53–60. doi: 10.1016/j.dld.2022.08.020

45. Qin L, Tang L-F, Cheng L, Wang H-Y. The clinical significance of allergen-specific IgG4 in allergic diseases. *Front Immunol* (2022) 13:1032909. doi: 10.3389/fimmu.2022.1032909

46. Caldas IR, Campi-Azevedo AC, Oliveira LFA, Silveira AMS, Oliveira RC, Gazzinelli G. Human schistosomiasis mansoni: immune responses during acute and chronic phases of the infection. *Acta Trop* (2008) 108:109–17. doi: 10.1016/j.actatropica.2008.05.027

47. Figueiredo JP, Oliveira RR, Cardoso LS, Barnes KC, Grant AV, Carvalho EM, et al. Adult worm-specific IgE/IgG4 balance is associated with low infection levels of Schistosoma mansoni in an endemic area. *Parasite Immunol* (2012) 34:604–10. doi: 10.1111/pim.12001

48. Adjobimey T, Hoerauf A. Induction of immunoglobulin G4 in human filariasis: an indicator of immunoregulation. *Ann Trop Med Parasitol* (2010) 104:455–64. doi: 10.1179/136485910X12786389891407

49. Resende SD, Magalhães FC, Rodrigues-Oliveira JL, Castro VN, Souza CSA, Oliveira EJ, et al. Modulation of allergic reactivity in humans is dependent on schistosoma mansoni parasite burden, low levels of IL-33 or TNF-α and high levels of IL-10 in serum. *Front Immunol* (2018) 9:3158. doi: 10.3389/fimmu.2018.03158

50. Harada K, Shimoda S, Kimura Y, Sato Y, Ikeda H, Igarashi S, et al. Significance of immunoglobulin G4 (IgG4)-positive cells in extrahepatic cholangiocarcinoma: molecular mechanism of IgG4 reaction in cancer tissue. *Hepatology* (2012) 56:157–64. doi: 10.1002/hep.25627

51. Karagiannis P, Gilbert AE, Josephs DH, Ali N, Dodev T, Saul L, et al. IgG4 subclass antibodies impair antitumor immunity in melanoma. *J Clin Invest* (2013) 123:1457–74. doi: 10.1172/JCI65579

52. Hinz S, Pagerols-Raluy L, Oberg H-H, Ammerpohl O, Grüssel S, Sipos B, et al. Foxp3 expression in pancreatic carcinoma cells as a novel mechanism of immune evasion in cancer. *Cancer Res* (2007) 67:8344–50. doi: 10.1158/0008-5472.CAN-06-3304

53. Kimura Y, Harada K, Nakanuma Y. Pathologic significance of immunoglobulin G4-positive plasma cells in extrahepatic cholangiocarcinoma. *Hum Pathol* (2012) 43:2149–56. doi: 10.1016/j.humpath.2012.03.001

54. Karagiannis P, Villanova F, Josephs DH, Correa I, Van Hemelrijck M, Hobbs C, et al. Elevated IgG4 in patient circulation is associated with the risk of disease progression in melanoma. *Oncoimmunology* (2015) 4:e1032492. doi: 10.1080/2162402X.2015.1032492

55. Yu T, Wu Y, Liu J, Zhuang Y, Jin X, Wang L. The risk of Malignancy in patients with IgG4-related disease: a systematic review and meta-analysis. *Arthritis Res Ther* (2022) 24:14. doi: 10.1186/s13075-021-02652-2

56. Kamisawa T, Horiguchi S-I, Hayashi Y, Yun X, Yamaguchi T, Tsuruta K, et al. K-ras mutation in the major duodenal papilla and gastric and colonic mucosa in patients with autoimmune pancreatitis. *J Gastroenterol* (2010) 45:771–8. doi: 10.1007/s00535-010-0211-y

57. Jinesh GG, Sambandam V, Vijayaraghavan S, Balaji K, Mukherjee S. Molecular genetics and cellular events of K-Ras-driven tumorigenesis. *Oncogene* (2018) 37:839–46. doi: 10.1038/onc.2017.377

58. Zhao B, Kimura W, Futakawa N, Muto T, Kubota K, Harihara Y, et al. p53 and p21/Waf1 protein expression and K-ras codon 12 mutation in carcinoma of the papilla of Vater. *Am J Gastroenterol* (1999) 94:2128–34. doi: 10.1111/j.1572-0241.1999.01309.x

59. Huijbers MG, Querol LA, Niks EH, Plomp JJ, van der Maarel SM, Graus F, et al. The expanding field of IgG4-mediated neurological autoimmune disorders. *Eur J Neurol* (2015) 22:1151–61. doi: 10.1111/ene.12758

60. Rispens T, Huijbers MG. The unique properties of IgG4 and its roles in health and disease. *Nat Rev Immunol* (2023) 23(11):763–78. doi: 10.1038/s41577-023-00871-z

61. Koneczny I. A new classification system for igG4 autoantibodies. *Front Immunol* (2018) 9:97. doi: 10.3389/fimmu.2018.00097

62. Koneczny I. Update on IgG4-mediated autoimmune diseases: New insights and new family members. *Autoimmun Rev* (2020) 19:102646. doi: 10.1016/j.autrev.2020.102646

63. Li N, Aoki V, Hans-Filho G, Rivitti EA, Diaz LA. The role of intramolecular epitope spreading in the pathogenesis of endemic pemphigus foliaceus (fogo selvagem). *J Exp Med* (2003) 197:1501–10. doi: 10.1084/jem.20022031

64. Toumi A, Saleh MA, Yamagami J, Abida O, Kallel M, Masmoudi A, et al. Autoimmune reactivity against precursor form of desmoglein 1 in healthy Tunisians in the area of endemic pemphigus foliaceus. *J Dermatol Sci* (2013) 70:19–25. doi: 10.1016/j.jdermsci.2013.02.002

65. Qian Y, Jeong JS, Maldonado M, Valenzuela JG, Gomes R, Teixeira C, et al. Cutting Edge: Brazilian pemphigus foliaceus anti-desmoglein 1 autoantibodies cross-react with sand fly salivary LJM11 antigen. *J Immunol* (2012) 189:1535–9. doi: 10.4049/jimmunol.1200842

66. Peng B, Temple BR, Yang J, Geng S, Culton DA, Qian Y. Identification of a primary antigenic target of epitope spreading in endemic pemphigus foliaceus. *J Autoimmun* (2021) 116:102561. doi: 10.1016/j.jaut.2020.102561

67. Diaz LA, Prisayanh P, Qaqish B, Temple BR, Aoki V, Hans-Filho G, et al. A lutzomyia longipalpis salivary protein induces cross-reactive antibodies to pemphigus autoantigen desmoglein 1. *J Invest Dermatol* (2020) 140:2332–2342.e10. doi: 10.1016/j.jid.2020.02.041

68. Kallel Sellami M, Ben Ayed M, Mouquet H, Drouot L, Zitouni M, Mokni M, et al. Anti-desmoglein 1 antibodies in Tunisian healthy subjects: arguments for the role of environmental factors in the occurrence of Tunisian pemphigus foliaceus. *Clin Exp Immunol* (2004) 137:195–200. doi: 10.1111/j.1365-2249.2004.02493.x

69. Abida O, Kallel-Sellami M, Joly P, Ben Ayed M, Zitouni M, Masmoudi A, et al. Anti-desmoglein 1 antibodies in healthy related and unrelated subjects and patients with pemphigus foliaceus in endemic and non-endemic areas from Tunisia. *J Eur Acad Dermatol Venereol* (2009) 23:1073–8. doi: 10.1111/j.1468-3083.2009.03265.x

70. Zaraa I, Boussoffara T, Ben Ahmed M, Marzouki S, Ben Hassouna N, Sellami MK, et al. Exposure to Phlebotomus papatasi and/or Leishmania major: possible etiologic link to Tunisian pemphigus. *J Invest Dermatol* (2012) 132:479–82. doi: 10.1038/jid.2011.291

71. Kallel Sellami M, Zitouni M, Tombari W, Ben Ayed M, Abida O, Laadhar L, et al. Anti-desmoglein-1 antibodies are prevalent in Tunisian patients with hydatidosis and leishmaniasis. *Br J Dermatol* (2007) 156:591–3. doi: 10.1111/j.1365-2133.2006.07687.x

72. Hoch W, McConville J, Helms S, Newsom-Davis J, Melms A, Vincent A. Auto-antibodies to the receptor tyrosine kinase MuSK in patients with myasthenia gravis without acetylcholine receptor antibodies. *Nat Med* (2001) 7:365–8. doi: 10.1038/85520

73. McConville J, Farrugia ME, Beeson D, Kishore U, Metcalfe R, Newsom-Davis J, et al. Detection and characterization of MuSK antibodies in seronegative myasthenia gravis. *Ann Neurol* (2004) 55:580–4. doi: 10.1002/ana.20061

74. Huijbers MG, Vink A-FD, Niks EH, Westhuis RH, van Zwet EW, de Meel RH, et al. Longitudinal epitope mapping in MuSK myasthenia gravis: implications for disease severity. *J Neuroimmunol* (2016) 291:82–8. doi: 10.1016/j.jneuroim.2015.12.016

75. Takamori M, Nakamura T, Motomura M. Antibodies against Wnt receptor of muscle-specific tyrosine kinase in myasthenia gravis. *J Neuroimmunol* (2013) 254:183–6. doi: 10.1016/j.jneuroim.2012.09.001

76. Koneczny I, Cossins J, Waters P, Beeson D, Vincent A. MuSK myasthenia gravis IgG4 disrupts the interaction of LRP4 with MuSK but both IgG4 and IgG1-3 can disperse preformed agrin-independent AChR clusters. *PloS One* (2013) 8:e80695. doi: 10.1371/journal.pone.0080695

77. Huijbers MG, Zhang W, Klooster R, Niks EH, Friese MB, Straasheijm KR, et al. MuSK IgG4 autoantibodies cause myasthenia gravis by inhibiting binding between MuSK and Lrp4. *Proc Natl Acad Sci U.S.A.* (2013) 110:20783–8. doi: 10.1073/pnas.1313944110

78. Huijbers MG, Vergoossen DL, Fillié-Grijpma YE, van Es IE, Koning MT, Slot LM, et al. MuSK myasthenia gravis monoclonal antibodies: Valency dictates pathogenicity. *Neurology(R) neuroimmunology Neuroinflamm* (2019) 6:e547. doi: 10.1212/NXI.0000000000000547

79. Vergoossen DLE, Ruiter AM, Keene KR, Niks EH, Tannemaat MR, Strijbos E, et al. Enrichment of serum IgG4 in MuSK myasthenia gravis patients. *J Neuroimmunol* (2022) 373:577978. doi: 10.1016/j.jneuroim.2022.577978

80. Faivre-Sarrailh C, Devaux JJ. Neuro-glial interactions at the nodes of Ranvier: implication in health and diseases. *Front Cell Neurosci* (2013) 7:196. doi: 10.3389/fncel.2013.00196

81. Labasque M, Hivert B, Nogales-Gadea G, Querol L, Illa I, Faivre-Sarrailh C. Specific contactin N-glycans are implicated in neurofascin binding and autoimmune targeting in peripheral neuropathies. *J Biol Chem* (2014) 289:7907–18. doi: 10.1074/jbc.M113.528489

82. Sistani L, Rodriguez PQ, Hultenby K, Uhlen M, Betsholtz C, Jalanko H, et al. Neuronal proteins are novel components of podocyte major processes and their expression in glomerular crescents supports their role in crescent formation. *Kidney Int* (2013) 83:63–71. doi: 10.1038/ki.2012.321

83. Manso C, Querol L, Lleixà C, Poncelet M, Mekaouche M, Vallat J-M, et al. Anti-Neurofascin-155 IgG4 antibodies prevent paranodal complex formation. *vivo. J Clin Invest* (2019) 129:2222–36. doi: 10.1172/JCI124694

84. Ng JKM, Malotka J, Kawakami N, Derfuss T, Khademi M, Olsson T, et al. Neurofascin as a target for autoantibodies in peripheral neuropathies. *Neurology* (2012) 79:2241–8. doi: 10.1212/WNL.0b013e31827689ad

85. Dutta DJ, Woo DH, Lee PR, Pajevic S, Bukalo O, Huffman WC, et al. Regulation of myelin structure and conduction velocity by perinodal astrocytes. *Proc Natl Acad Sci U.S.A.* (2018) 115:11832–7. doi: 10.1073/pnas.1811013115

86. Zheng XL. ADAMTS13 and von Willebrand factor in thrombotic thrombocytopenic purpura. *Annu Rev Med* (2015) 66:211–25. doi: 10.1146/annurev-med-061813-013241

87. Ferrari S, Mudde GC, Rieger M, Veyradier A, Kremer Hovinga JA, Scheiflinger F. IgG subclass distribution of anti-ADAMTS13 antibodies in patients with acquired thrombotic thrombocytopenic purpura. *J Thromb Haemost* (2009) 7:1703–10. doi: 10.1111/j.1538-7836.2009.03568.x

88. Sinkovits G, Szilágyi Á, Farkas P, Inotai D, Szilvási A, Tordai A, et al. Concentration and subclass distribution of anti-ADAMTS13 igG autoantibodies in different stages of acquired idiopathic thrombotic thrombocytopenic purpura. *Front Immunol* (2018) 9:1646. doi: 10.3389/fimmu.2018.01646

89. Masaki Y, Umehara H. [IgG4-related disease-the diagnostic confusion and how to avoid it]. *Nihon Rinsho Meneki Gakkai Kaishi* (2009) 32:478–83. doi: 10.2177/jsci.32.478

90. Khosroshahi A, Wallace ZS, Crowe JL, Akamizu T, Azumi A, Carruthers MN, et al. International consensus guidance statement on the management and treatment of igG4-related disease. *Arthritis Rheumatol* (2015) 67:1688–99. doi: 10.1002/art.39132

91. Maillette de Buy Wenniger LJ, Doorenspleet ME, Klarenbeek PL, Verheij J, Baas F, Elferink RPO, et al. Immunoglobulin G4+ clones identified by next-generation sequencing dominate the B cell receptor repertoire in immunoglobulin G4 associated cholangitis. *Hepatology* (2013) 57:2390–8. doi: 10.1002/hep.26232

92. Mattoo H, Mahajan VS, Della-Torre E, Sekigami Y, Carruthers M, Wallace ZS, et al. *De novo* oligoclonal expansions of circulating plasmablasts in active and relapsing IgG4-related disease. *J Allergy Clin Immunol* (2014) 134:679–87. doi: 10.1016/j.jaci.2014.03.034

93. Li J, Liu Z, Zhang P, Lin W, Lu H, Peng Y, et al. Peripheral B-cell immunophenotyping identifies heterogeneity in igG4-related disease. *Front Immunol* (2021) 12:747076. doi: 10.3389/fimmu.2021.747076

94. Mattoo H, Mahajan VS, Maehara T, Deshpande V, Della-Torre E, Wallace ZS, et al. Clonal expansion of CD4(+) cytotoxic T lymphocytes in patients with IgG4-related disease. *J Allergy Clin Immunol* (2016) 138:825–38. doi: 10.1016/j.jaci.2015.12.1330

95. Maehara T, Mattoo H, Ohta M, Mahajan VS, Moriyama M, Yamauchi M, et al. Lesional CD4+ IFN-γ+ cytotoxic T lymphocytes in IgG4-related dacryoadenitis and sialoadenitis. *Ann Rheum Dis* (2017) 76:377–85. doi: 10.1136/annrheumdis-2016-209139

96. Carruthers MN, Topazian MD, Khosroshahi A, Witzig TE, Wallace ZS, Hart PA, et al. Rituximab for IgG4-related disease: a prospective, open-label trial. *Ann Rheum Dis* (2015) 74:1171–7. doi: 10.1136/annrheumdis-2014-206605

97. Lanzillotta M, Della-Torre E, Wallace ZS, Stone JH, Karadag O, Fernández-Codina A, et al. Efficacy and safety of rituximab for IgG4-related pancreato-biliary disease: A systematic review and meta-analysis. *Pancreatology* (2021) 21:1395–401. doi: 10.1016/j.pan.2021.06.009

98. Terao C, Ota M, Iwasaki T, Shiokawa M, Kawaguchi S, Kuriyama K, et al. IgG4-related disease in the Japanese population: a genome-wide association study. *Lancet Rheumatol* (2019) 1:e14–22. doi: 10.1016/S2665-9913(19)30006-2

99. Freitag TL, Cham C, Sung H-H, Beilhack GF, Durinovic-Belló I, Patel SD, et al. Human risk allele HLA-DRB1*0405 predisposes class II transgenic Ab0 NOD mice to autoimmune pancreatitis. *Gastroenterology* (2010) 139:281–91. doi: 10.1053/j.gastro.2010.03.038

100. Thomson G, Valdes AM, Noble JA, Kockum I, Grote MN, Najman J, et al. Relative predispositional effects of HLA class II DRB1-DQB1 haplotypes and genotypes on type 1 diabetes: a meta-analysis. *Tissue Antigens* (2007) 70:110–27. doi: 10.1111/j.1399-0039.2007.00867.x

101. Arimura Y, Isshiki H, Onodera K, Nagaishi K, Yamashita K, Sonoda T, et al. Characteristics of Japanese inflammatory bowel disease susceptibility loci. *J Gastroenterol* (2014) 49:1217–30. doi: 10.1007/s00535-013-0866-2

102. Overdijk MB, Verploegen S, Ortiz Buijsse A, Vink T, Leusen JHW, Bleeker WK, et al. Crosstalk between human IgG isotypes and murine effector cells. *J Immunol* (2012) 189:3430–8. doi: 10.4049/jimmunol.1200356

103. Smyk DS, Rigopoulou EI, Koutsoumpas AL, Kriese S, Burroughs AK, Bogdanos DP. Autoantibodies in autoimmune pancreatitis. *Int J Rheumatol* (2012) 2012:940831. doi: 10.1155/2012/940831

104. Nishimori I, Yamamoto Y, Okazaki K, Morita M, Onodera M, Kino J, et al. Identification of autoantibodies to a pancreatic antigen in patients with idiopathic chronic pancreatitis and Sjögren's syndrome. *Pancreas* (1994) 9:374–81. doi: 10.1097/00006676-199405000-00015

105. Kountouras J, Zavos C, Chatzopoulos D. A concept on the role of Helicobacter pylori infection in autoimmune pancreatitis. *J Cell Mol Med* (2005) 9:196–207. doi: 10.1111/j.1582-4934.2005.tb00349.x

106. Guarneri F, Guarneri C, Benvenga S. Helicobacter pylori and autoimmune pancreatitis: role of carbonic anhydrase via molecular mimicry? *J Cell Mol Med* (2005) 9:741–4. doi: 10.1111/j.1582-4934.2005.tb00506.x

107. Kountouras J, Zavos C, Gavalas E, Tzilves D. Challenge in the pathogenesis of autoimmune pancreatitis: potential role of helicobacter pylori infection via molecular mimicry. *Gastroenterology* (2007) 133:368–9. doi: 10.1053/j.gastro.2007.05.044

108. Frulloni L, Lunardi C, Simone R, Dolcino M, Scattolini C, Falconi M, et al. Identification of a novel antibody associated with autoimmune pancreatitis. *N Engl J Med* (2009) 361:2135–42. doi: 10.1056/NEJMoa0903068

109. Culver EL, Smit WL, Evans C, Sadler R, Cargill T, Makuch M, et al. No evidence to support a role for Helicobacter pylori infection and plasminogen binding protein in autoimmune pancreatitis and IgG4-related disease in a UK cohort. *Pancreatology* (2017) 17:395–402. doi: 10.1016/j.pan.2017.04.002

110. Jesnowski R, Isaksson B, Möhrcke C, Bertsch C, Bulajic M, Schneider-Brachert W, et al. Helicobacter pylori in autoimmune pancreatitis and pancreatic carcinoma. *Pancreatology* (2010) 10:462–6. doi: 10.1159/000264677

111. Asada M, Nishio A, Uchida K, Kido M, Ueno S, Uza N, et al. Identification of a novel autoantibody against pancreatic secretory trypsin inhibitor in patients with autoimmune pancreatitis. *Pancreas* (2006) 33:20–6. doi: 10.1097/01.mpa.0000226881.48204.fd

112. Löhr J-M, Faissner R, Koczan D, Bewerunge P, Bassi C, Brors B, et al. Autoantibodies against the exocrine pancreas in autoimmune pancreatitis: gene and protein expression profiling and immunoassays identify pancreatic enzymes as a major target of the inflammatory process. *Am J Gastroenterol* (2010) 105:2060–71. doi: 10.1038/ajg.2010.141

113. Hubers LM, Vos H, Schuurman AR, Erken R, Oude Elferink RP, Burgering B, et al. Annexin A11 is targeted by IgG4 and IgG1 autoantibodies in IgG4-related disease. *Gut* (2018) 67:728–35. doi: 10.1136/gutjnl-2017-314548

114. Zamboni G, Lüttges J, Capelli P, Frulloni L, Cavallini G, Pederzoli P, et al. Histopathological features of diagnostic and clinical relevance in autoimmune pancreatitis: a study on 53 resection specimens and 9 biopsy specimens. *Virchows Arch* (2004) 445:552–63. doi: 10.1007/s00428-004-1140-z

115. Hohenester S, Wenniger LM de B, Paulusma CC, van Vliet SJ, Jefferson DM, Elferink RPO, et al. A biliary HCO3- umbrella constitutes a protective mechanism against bile acid-induced injury in human cholangiocytes. *Hepatology* (2012) 55:173–83. doi: 10.1002/hep.24691

116. Herta T, Kersten R, Chang J-C, Hubers L, Go S, Tolenaars D, et al. Role of the IgG4-related cholangitis autoantigen annexin A11 in cholangiocyte protection. *J Hepatol* (2022) 76:319–31. doi: 10.1016/j.jhep.2021.10.009

117. Shiokawa M, Kodama Y, Kuriyama K, Yoshimura K, Tomono T, Morita T, et al. Pathogenicity of IgG in patients with IgG4-related disease. *Gut* (2016) 65:1322–32. doi: 10.1136/gutjnl-2015-310336

118. Liu H, Perugino CA, Ghebremichael M, Wallace ZS, Montesi SB, Stone JH, et al. Disease severity linked to increase in autoantibody diversity in igG4-related disease. *Arthritis Rheumatol* (2020) 72:687–93. doi: 10.1002/art.41140

119. Shiokawa M, Kodama Y, Sekiguchi K, Kuwada T, Tomono T, Kuriyama K, et al. Laminin 511 is a target antigen in autoimmune pancreatitis. *Sci Transl Med* (2018) 10 (453):eaaq0997. doi: 10.1126/scitranslmed.aaq0997

120. Hirani N, MacKinnon AC, Nicol L, Ford P, Schambye H, Pedersen A, et al. Target inhibition of galectin-3 by inhaled TD139 in patients with idiopathic pulmonary fibrosis. *Eur Respir J* (2021) 57(5):2002559. doi: 10.1183/13993003.02559-2020

121. Perugino CA, AlSalem SB, Mattoo H, Della-Torre E, Mahajan V, Ganesh G, et al. Identification of galectin-3 as an autoantigen in patients with IgG4-related disease. *J Allergy Clin Immunol* (2019) 143:736–745.e6. doi: 10.1016/j.jaci.2018.05.011

122. Faludi R, Nagy G, Tőkés-Füzesi M, Kovács K, Czirják L, Komócsi A. Galectin-3 is an independent predictor of survival in systemic sclerosis. *Int J Cardiol* (2017) 233:118–24. doi: 10.1016/j.ijcard.2016.12.140

123. Salah A, Yoshifuji H, Ito S, Kitagori K, Kiso K, Yamada N, et al. High expression of galectin-3 in patients with igG4-related disease: A proteomic approach. *Patholog Res Int* (2017) 2017:9312142. doi: 10.1155/2017/9312142

124. Li L, Li J, Gao J. Functions of galectin-3 and its role in fibrotic diseases. *J Pharmacol Exp Ther* (2014) 351:336–43. doi: 10.1124/jpet.114.218370

125. Liu H, Fan H, He P, Zhuang H, Liu X, Chen M, et al. Prohibitin 1 regulates mtDNA release and downstream inflammatory responses. *EMBO J* (2022) 41:e111173. doi: 10.15252/embj.2022111173

126. Xu Y, Shen J, Ran Z. Emerging views of mitophagy in immunity and autoimmune diseases. *Autophagy* (2020) 16:3–17. doi: 10.1080/15548627.2019.1603547

127. Du H, Shi L, Chen P, Yang W, Xun Y, Yang C, et al. Prohibitin is involved in patients with igG4 related disease. *PloS One* (2015) 10:e0125331. doi: 10.1371/journal.pone.0125331

128. Culver EL, Sadler R, Bateman AC, Makuch M, Cargill T, Ferry B, et al. Increases in igE, eosinophils, and mast cells can be used in diagnosis and to predict relapse of igG4-related disease. *Clin Gastroenterol Hepatol* (2017) 15:1444–1452.e6. doi: 10.1016/j.cgh.2017.02.007

129. Della Torre E, Mattoo H, Mahajan VS, Carruthers M, Pillai S, Stone JH. Prevalence of atopy, eosinophilia, and IgE elevation in IgG4-related disease. *Allergy* (2014) 69:269–72. doi: 10.1111/all.12320

130. Gao Y, Zheng M, Cui L, Chen N, Wang Y-N, Zhan Y-T, et al. IgG4-related disease: association between chronic rhino-sinusitis and systemic symptoms. *Eur Arch Otorhinolaryngol* (2018) 275:2013–9. doi: 10.1007/s00405-018-5013-5

131. Zhang X, Zhang P, Li J, He Y, Fei Y, Peng L, et al. Different clinical patterns of IgG4-RD patients with and without eosinophilia. *Sci Rep* (2019) 9:16483. doi: 10.1038/s41598-019-52847-6

132. Saeki T, Kobayashi D, Ito T, Tamura M, Yoshikawa S, Yamazaki H. Comparison of clinical and laboratory features of patients with and without allergic conditions in IgG4-related disease: A single-center experience in Japan. *Mod Rheumatol* (2018) 28:845–8. doi: 10.1080/14397595.2017.1416891

133. Sanders S, Fu X, Zhang Y, Perugino CA, Wallwork R, Della-Torre E, et al. Lifetime allergy symptoms in igG4-related disease: A case-control study. *Arthritis Care Res (Hoboken)* (2022) 74:1188–95. doi: 10.1002/acr.24545

134. D'Astous-Gauthier K, Ebbo M, Chanez P, Schleinitz N. Implication of allergy and atopy in IgG4-related disease. *World Allergy Organ J* (2023) 16:100765. doi: 10.1016/j.waojou.2023.100765

135. Della-Torre E, Germanò T, Ramirez GA, Dagna L, Yacoub MR. IgG4-related disease and allergen-specific immunotherapy. *Ann Allergy Asthma Immunol* (2020) 124:631–3. doi: 10.1016/j.anai.2020.03.024

136. Mattoo H, Della-Torre E, Mahajan VS, Stone JH, Pillai S. Circulating Th2 memory cells in IgG4-related disease are restricted to a defined subset of subjects with atopy. *Allergy* (2014) 69:399–402. doi: 10.1111/all.12342

137. Michailidou D, Schwartz DM, Mustelin T, Hughes GC. Allergic aspects of igG4-related disease: implications for pathogenesis and therapy. *Front Immunol* (2021) 12:693192. doi: 10.3389/fimmu.2021.693192

138. Culver EL, Vermeulen E, Makuch M, van Leeuwen A, Sadler R, Cargill T, et al. Increased IgG4 responses to multiple food and animal antigens indicate a polyclonal expansion and differentiation of pre-existing B cells in IgG4-related disease. *Ann Rheum Dis* (2015) 74:944–7. doi: 10.1136/annrheumdis-2014-206405

139. de Buy Wenniger LJM, Culver EL, Beuers U. Exposure to occupational antigens might predispose to IgG4-related disease. *Hepatology* (2014) 60:1453–4. doi: 10.1002/hep.26999

140. Hubers LM, Schuurman AR, Buijs J, Mostafavi N, Bruno MJ, Vermeulen RCH, et al. Blue-collar work is a risk factor for developing IgG4-related disease of the biliary tract and pancreas. *JHEP Rep* (2021) 3:100385. doi: 10.1016/j.jhepr.2021.100385

141. Cargill T, Makuch M, Sadler R, Lighaam LC, Peters R, van Ham M, et al. Activated T-follicular helper 2 cells are associated with disease activity in igG4-related sclerosing cholangitis and pancreatitis. *Clin Transl Gastroenterol* (2019) 10:e00020. doi: 10.14309/ctg.0000000000000020

142. Bélanger S, Crotty S. Dances with cytokines, featuring TFH cells, IL-21, IL-4 and B cells. *Nat Immunol* (2016) 17:1135–6. doi: 10.1038/ni.3561

143. Weinstein JS, Herman EI, Lainez B, Licona-Limón P, Esplugues E, Flavell R, et al. TFH cells progressively differentiate to regulate the germinal center response. *Nat Immunol* (2016) 17:1197–205. doi: 10.1038/ni.3554

144. Lighaam LC, Rispens T. The immunobiology of immunoglobulin G4. *Semin Liver Dis* (2016) 36:200–15. doi: 10.1055/s-0036-1584322

145. Akiyama M, Suzuki K, Yasuoka H, Kaneko Y, Yamaoka K, Takeuchi T. Follicular helper T cells in the pathogenesis of IgG4-related disease. *Rheumatol (Oxford)* (2018) 57:236–45. doi: 10.1093/rheumatology/kex171

146. Witebsky E, Rose NR, Terplan K, Paine JR, Egan RW. Chronic thyroiditis and autoimmunization. *J Am Med Assoc* (1957) 164:1439–47. doi: 10.1001/jama.1957.02980130015004

147. Douglas J N. Antibodies to an intracellular antigen penetrate neuronal cells and cause deleterious effects. *J Clin Cell Immunol* (2013) 04:157ra142. doi: 10.4172/2155-9899.1000134

148. Hansen JE, Chan G, Liu Y, Hegan DC, Dalal S, Dray E, et al. Targeting cancer with a lupus autoantibody. *Sci Transl Med* (2012) 4(157):157ra142. doi: 10.1126/scitranslmed.3004385

149. Noble PW, Young MR, Bernatsky S, Weisbart RH, Hansen JE. A nucleolytic lupus autoantibody is toxic to BRCA2-deficient cancer cells. *Sci Rep* (2014) 4:5958. doi: 10.1038/srep05958

150. Song Y-C, Sun G-H, Lee T-P, Huang JC, Yu C-L, Chen C-H, et al. Arginines in the CDR of anti-dsDNA autoantibodies facilitate cell internalization via electrostatic interactions. *Eur J Immunol* (2008) 38:3178–90. doi: 10.1002/eji.200838678

151. Lisi S, Sisto M, Soleti R, Saponaro C, Scagliusi P, D'Amore M, et al. Fcgamma receptors mediate internalization of anti-Ro and anti-La autoantibodies from Sjögren's syndrome and apoptosis in human salivary gland cell line A-253. *J Oral Pathol Med* (2007) 36:511–23. doi: 10.1111/j.1600-0714.2007.00563.x

152. Choi D-K, Bae J, Shin S-M, Shin J-Y, Kim S, Kim Y-S. A general strategy for generating intact, full-length IgG antibodies that penetrate into the cytosol of living cells. *MAbs* (2014) 6:1402–14. doi: 10.4161/mabs.36389

153. Jang JY, Jeong JG, Jun HR, Lee SC, Kim JS, Kim YS, et al. A nucleic acid-hydrolyzing antibody penetrates into cells via caveolae-mediated endocytosis, localizes in the cytosol and exhibits cytotoxicity. *Cell Mol Life Sci* (2009) 66:1985–97. doi: 10.1007/s00018-009-9179-2

154. Hansen JE, Tse C-M, Chan G, Heinze ER, Nishimura RN, Weisbart RH. Intranuclear protein transduction through a nucleoside salvage pathway. *J Biol Chem* (2007) 282:20790–3. doi: 10.1074/jbc.C700090200

155. Endmayr V, Tunc C, Ergin L, De Rosa A, Weng R, Wagner L, et al. Anti-neuronal igG4 autoimmune diseases and igG4-related diseases may not be part of the same spectrum: A comparative study. *Front Immunol* (2021) 12:785247. doi: 10.3389/fimmu.2021.785247

156. Chari ST, Smyrk TC, Levy MJ, Topazian MD, Takahashi N, Zhang L, et al. Diagnosis of autoimmune pancreatitis: the Mayo Clinic experience. *Clin Gastroenterol Hepatol* (2006) 4:1010–6. doi: 10.1016/j.cgh.2006.05.017

157. Lu C, Li S, Qing P, Zhang Q, Ji X, Tang Z, et al. Single-cell transcriptome analysis and protein profiling reveal broad immune system activation in IgG4-related disease. *JCI Insight* (2023) 8(17):e167602. doi: 10.1172/jci.insight.167602

158. Ota M, Katsuyama Y, Hamano H, Umemura T, Kimura A, Yoshizawa K, et al. Two critical genes (HLA-DRB1 and ABCF1)in the HLA region are associated with the susceptibility to autoimmune pancreatitis. *Immunogenetics* (2007) 59:45–52. doi: 10.1007/s00251-006-0178-2

159. Goni E, Regel I, Mahajan UM, Amodio A, De Marchi G, Beyer G, et al. HLA-DRB1∗16 and -DQB1∗05 alleles are strongly associated with autoimmune pancreatitis in a cohort of hundred patients. *Pancreatology* (2022) 22:466–71. doi: 10.1016/j.pan.2022.03.015

160. Umehara H, Okazaki K, Nakamura T, Satoh-Nakamura T, Nakajima A, Kawano M, et al. Current approach to the diagnosis of IgG4-related disease – Combination of comprehensive diagnostic and organ-specific criteria. *Mod Rheumatol* (2017) 27:381–91. doi: 10.1080/14397595.2017.1290911

frontiers | Frontiers in Immunology

TYPE Review
PUBLISHED 18 April 2024
DOI 10.3389/fimmu.2024.1346671

OPEN ACCESS

EDITED BY
Inga Koneczny,
Medical University of Vienna, Austria

REVIEWED BY
Michelangelo Maestri,
University of Pisa, Italy
Anna Punga,
Uppsala University, Sweden
Vuslat Yilmaz,
Istanbul University, Türkiye

*CORRESPONDENCE
Miriam L. Fichtner
miriam.fichtner@charite.de

RECEIVED 29 November 2023
ACCEPTED 29 February 2024
PUBLISHED 18 April 2024

CITATION
Ünlü S, Sánchez Navarro BG, Cakan E, Berchtold D, Meleka Hanna R, Vural S, Vural A, Meisel A and Fichtner ML (2024) Exploring the depths of IgG4: insights into autoimmunity and novel treatments. *Front. Immunol.* 15:1346671. doi: 10.3389/fimmu.2024.1346671

Exploring the depths of IgG4: insights into autoimmunity and novel treatments

Selen Ünlü[1,2], Blanca G. Sánchez Navarro[3], Elif Cakan[4], Daniel Berchtold[3], Rafael Meleka Hanna[3], Secil Vural[1,5], Atay Vural[1,6], Andreas Meisel[3] and Miriam L. Fichtner[1,3]*

[1]Koç University Research Center for Translational Medicine (KUTTAM), İstanbul, Türkiye, [2]Koç University School of Medicine, Istanbul, Türkiye, [3]Department of Neurology with Experimental Neurology, Integrated Myasthenia Gravis Center, Neuroscience Clinical Research Center, Charité Universitätsmedizin Berlin, Berlin, Germany, [4]Ragon Institute of Massachusetts General Hospital, Massachusetts Institute of Technology and Harvard University, Cambridge, MA, United States, [5]Department of Dermatology and Venereology, Koç University School of Medicine, İstanbul, Türkiye, [6]Department of Neurology, Koç University School of Medicine, İstanbul, Türkiye

IgG4 subclass antibodies represent the rarest subclass of IgG antibodies, comprising only 3-5% of antibodies circulating in the bloodstream. These antibodies possess unique structural features, notably their ability to undergo a process known as fragment-antigen binding (Fab)-arm exchange, wherein they exchange half-molecules with other IgG4 antibodies. Functionally, IgG4 antibodies primarily block and exert immunomodulatory effects, particularly in the context of IgE isotype-mediated hypersensitivity reactions. In the context of disease, IgG4 antibodies are prominently observed in various autoimmune diseases combined under the term IgG4 autoimmune diseases (IgG4-AID). These diseases include myasthenia gravis (MG) with autoantibodies against muscle-specific tyrosine kinase (MuSK), nodo-paranodopathies with autoantibodies against paranodal and nodal proteins, pemphigus vulgaris and foliaceus with antibodies against desmoglein and encephalitis with antibodies against LGI1/CASPR2. Additionally, IgG4 antibodies are a prominent feature in the rare entity of IgG4 related disease (IgG4-RD). Intriguingly, both IgG4-AID and IgG4-RD demonstrate a remarkable responsiveness to anti-CD20-mediated B cell depletion therapy (BCDT), suggesting shared underlying immunopathologies. This review aims to provide a comprehensive exploration of B cells, antibody subclasses, and their general properties before examining the distinctive characteristics of IgG4 subclass antibodies in the context of health, IgG4-AID and IgG4-RD. Furthermore, we will examine potential therapeutic strategies for these conditions, with a special focus on leveraging insights gained from anti-CD20-mediated BCDT. Through this analysis, we aim to enhance our understanding of the pathogenesis of IgG4-mediated diseases and identify promising possibilities for targeted therapeutic intervention.

KEYWORDS

IgG4, IgG4-AID, IgG4-RD, immunotherapies, antibodies

1 Introduction

A prerequisite for selecting effective therapies is a profound understanding of the underlying (immuno-) pathology. Many existing therapies, while exhibiting efficacy, are often expensive and may induce side effects that significantly compromise the overall quality of life for patients (1). Therefore, a deeper understanding of the immunopathology is necessary to make informed treatment decisions and to identify therapies that are both effective and efficient in a personal-tailored manner. To gain deeper insights into immunopathology, a valuable approach is to employ reverse translational medicine. In reverse translational medicine, scientific discoveries are informed by clinical observations (2). The clinical observation this review is based on is the remarkable effect of anti-CD20-mediated B cell depletion therapy (BCDT) in disorders with a prevalence of IgG4 subclass antibodies (3–12). This effect is not exclusive for IgG4-mediated diseases where antibodies are the major effectors of pathology like in IgG4 autoimmune diseases (IgG4-AID); IgG4-related disease (IgG4-RD) also responds well to anti-CD20-mediated BCDT (13). In this review will first explore B cells, antibody subclasses, and their properties in general, before we specifically highlight the unique features of IgG4 subclass antibodies in the context of IgG4-AID and IgG4-RD. In the concluding segment of this review, we will examine potential therapies for these diseases, with a particular focus on exploring insights derived from anti-CD20-mediated BCDT.

2 Insights into B cell functions and antibody diversity

In autoimmune diseases, the immune system malfunctions, targeting the body's own structures. While the immune response involves a variety of cells, some of these autoimmune diseases are characterized by a prominent role of B cells and their effector molecules - the autoantibodies. B cells originate in the bone marrow and undergo several stages of development before maturing into antibody-secreting cells (ASCs), namely plasmablasts and plasma cells (14, 15). The distinct developmental stages of B cell subsets can be identified by surface markers that are expressed at varying levels throughout the maturation process (16). These surface markers are the basis for several B cell targeting therapies, which we will further explore in the section on therapeutic interventions.

In addition to their function as ASCs, B cells play diverse roles in the immune system. They contribute to antigen presentation, cytokine secretion, and the regulation of immune responses (17–19). B cells play a crucial role in modulating T cell responses in both health and disease. Both B and T cells originate from common precursors in the bone marrow, but T cells undergo their final maturation in the thymus (20). B and T cells constitute the adaptive immune system. While B cells contribute to the humoral immune response, T cells serve as the effectors of the cellular response (15). Through antigen presentation, B cells contribute to the negative selection of autoreactive T cells in the thymus, regulate the extent of primary CD4+ T cell responses, and contribute to T cell memory generation (21–23). Antigen presentation by B cells contributes to the immunopathology in several T cell-mediated diseases, including autoimmune hepatitis, rheumatoid arthritis and multiple sclerosis (24–28). Furthermore, B cells are essential for the formation and maintenance of humoral immunological memory, which is crucial for a rapid and effective response upon re-exposure to pathogens (29–31). These memory B cells constitute a crucial reservoir for the generation of ASCs and the corresponding antibody repertoire (14, 31). Throughout the progression of an immune response to an external antigen, B cells undergo affinity maturation, enhancing the affinity of antibodies they produce (32–34). This heightened affinity arises from the interplay of clonal selection and the somatic hypermutation (SHM) process, leading to the gradual accumulation of antibodies with successively greater affinities.

Within the human serum, there is a constant presence of approximately ≈ 9-15 g/L of various IgG subclass antibodies circulating throughout the body (35). These antibodies are polyclonal which means they display diverse specificities, recognizing individual distinct antigens. The interaction between an antibody and its corresponding antigen is highly specific. The segment of the antibody directly involved in this antibody-antigen interaction is termed the variable region (Figure 1A), whereas the constant region - the basis for the categorization of antibodies into isotypes and subclasses - is linked to the antibody's effector and pathogenic function as well as maturation state (Figures 1B, C) (36). Antibodies are categorized into IgD, IgM, IgE, IgA, and IgG isotypes (37). IgD and IgM are primarily linked to B cells during the naive stage, while antigen-experienced B cells predominantly employ the other isotypes (38).

3 The divergent properties of IgG1-4 subclass autoantibodies and unique features of IgG4

The diseases highlighted in this review predominantly involve autoantibodies belonging to the IgG subclass, which can be further divided into IgG1, IgG2, IgG3 and IgG4 (37). Each subclass has distinct structural and functional properties, leading to varied effector functions including complement activation, opsonization (= presenting antigens to phagocytes), antibody-dependent cell-mediated cytotoxicity (ADCC) and neutralization of toxins (37). The most abundant subclass is IgG1 (≈ 65-70%) (39); opsonization, ADCC and complement activation are among the predominant effector functions of IgG1 antibodies (37, 40). IgG2 (≈ 20-25%) antibodies, in contrast, are less effective in complement activation, but potent in opsonization of encapsulated bacteria (39–41). The third most common subclass is IgG3 (≈ 5-8%); IgG3 antibodies are very potent effectors of the immune system and activate the complement cascade, induce ADCC and neutralize toxins (39, 41, 42).

Notably, the least common subclass IgG4 (≈ 3-5%) stands out among these subclasses due to its unique ability to undergo the process of fragment antigen binding (Fab)-arm exchange (39, 43). IgG subclass antibodies are normally dimers with two identical

10.3389/fimmu.2024.1346671

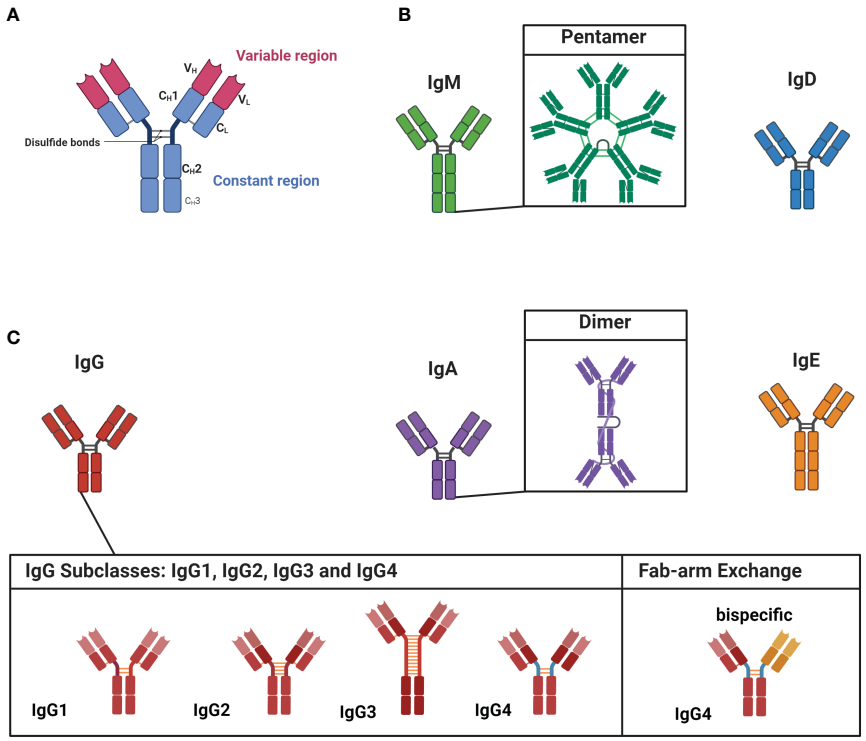

FIGURE 1
Structure of antibodies, isotypes and IgG subclasses. **(A)** Antibodies are dimeric structures that consist of two identical antigen-binding sites, known as the variable region (VH and VL). This region, called the fragment-antigen binding (Fab) region, is formed by the combination of the light chain and the heavy chain and is the antigen binding site of the antibody. The hinge region connects the Fab region to the constant region (Fc region, CH1-CH3), which determines the antibody's isotype and function. **(B)** The isotypes of IgM and IgD are associated with less experienced, or "naïve," cells. IgM is found as a pentamer. **(C)** IgG, IgA, and IgE are linked to more matured antibodies. IgA has the ability to form dimeric structures, while IgG has four subclasses: IgG1, IgG2, IgG3, and IgG4. IgG4 subclass antibodies can undergo Fab-arm exchange, allowing them to become bispecific. Figure created with Biorender.com.

binding sites (Figure 1A). Fab-arm exchange enables IgG4 subclass antibodies to exchange (half)-molecules with other IgG4 antibodies, resulting in bispecific antibodies with two distinct variable regions (Figure 1C; on the left). Fab-arm exchange requires the CH3-domain of the IgG4 antibody (see Figure 1A) and a reducing environment. As this reaction does not require any additional proteins or co-factors, it results in a highly dynamic process during which IgG4 antibodies constantly exchange arms *in vivo* which generates an ever-changing repertoire of hetero-bivalent IgG4 antibodies (43). Fab-arm exchanged-bispecific IgG4 antibodies cannot cross-link antigens and do not form immune complexes (37). In addition, structural differences in the CH2 domain of IgG4 antibodies are responsible for its low affinity toward C1q from the complement cascade and activating Fcγ receptors (44, 45). However, a recent study revealed that elevated levels of IgG4 antibodies can activate the complement cascade (46). Both variable and constant region glycosylation were found to influence this process. Nonetheless, the biological relevance of this finding remains uncertain. Thus, IgG4 subclass antibodies are generally considered immunomodulatory and referred to as 'blocking antibodies' and might function as 'antigen sink' (45, 47–49). The blocking function is evident in the context of insect venom or house dust mite hypersensitivity. Antigen-specific IgG4 block the binding of sensitizing IgE to the allergens and consequently prevent allergic symptoms (50). In a similar manner, IgG4 can also prevent hypersensitivity reactions during chronic helminth infections (51, 52). The role of IgG4 subclass antibodies in IgG4-AID and IgG4-RD is further delineated for each specific condition in the subsequent chapter.

The generation of IgG4 most frequently occurs in situations of chronic antigen exposure and might be associated with a continuous germinal center reaction and consecutive rounds of class switch recombination that eventually terminates with a class switch toward IgG4 (53–55). This distinctive property renders IgG4 antibodies particularly prevalent in conditions involving recurrent antigen exposure, as evident in beekeepers and antibodies recognizing bee-related toxins (47, 56–59). The process of class switch to IgG4, similar to the generation of IgE, is regulated by the cytokines IL-4 and IL-13 and necessitates co-stimulation by CD40 (60). Importantly, IL-10 has been shown to reduce IgE secretion and increase IgG4 production and might be directly involved in regulating class switch recombination toward IgG4 (60). More recently, a specialized subset of follicular T helper (Tfh) cells was discovered in tertiary lymphoid tissues of patients suffering from IgG4-related disease. These Tfh cells express the markers BCL6, CXCR5, and ICOS as well as the cytokines IL-4, IL-21, and IL-10 and therefore might crucially regulate the switch to IgG4 (61).

4 Features of autoantibodies in IgG4-mediated diseases

IgG4 subclass antibodies are notably predominant in IgG4-AID and IgG4-RD (3–10). A summary of the clinical and epidemiological characteristics of the diseases can be found in Table 1. This review focuses on the immunopathology of these diseases and the properties of the corresponding antibodies in the context of disease.

4.1 MuSK myasthenia gravis

The autoantibodies in myasthenia gravis (MG) target structures at the muscle endplate of the neuromuscular junction (NMJ) hindering neuromuscular transmission (100, 101). These autoantibodies disrupt the interaction between the ligand acetylcholine and the acetylcholine receptor (AChR) at the NMJ. They achieve this by directly targeting the AChR or structures within the muscle-specific tyrosine kinase (MuSK)/Low Density

TABLE 1 Comparison of characteristics of IgG4 subtypes of MG, CIDP, Pemphigus and IgG4-RD.

	MG	Nodo-paranodopathies	Pemphigus	Encephilits	IgG4-RD
Antigenic Target of IgG4 Subclass Autoantibodies	MuSK	Neurofascin-155, contactin-1/caspr-1, pan-neurofascins	PV: Desmoglein 1, Desmoglein 3 PF: Desmoglein 1	LGI1, CASPR2	–
Relevance of Fab-arm exchange	Increases pathogenicity of autoantibodies	Decreases pathogenicity of autoantibodies	PF: Increase of pathogenic effect PV: monovalent autoantibodies are pathogenic, pathogenic capacity most likely not influenced by valency	–	most likely present; disease not autoantibody-mediated
Prevalence (per 100,000)	2.2 to 36.7 (62, 63)	0.8 to 8.9 (64)	0.4 to 30 (65)	LIG1: 8.3 (66) CASPR2: -	0.8 to 1.4 (67)
Age of Onset	before the age of 40 (68, 69)	40-60 (70, 71)	PV: 40-60 (72, 73) PF: 50-60 (74)	40-60 (mean age of 43-44) (75, 76)	50-60 (mean age of onset 56,5) (67)
Male to Female Ratio	Predominantly female (68, 69)	Predominantly male (64, 77–79)	Predominantly female (PV) (80, 81) Equally distributed (PF) (74)	Predominantly male (75, 82)	58% female (67)
Genetic Factors	HLA class II genes: HLA DQB1*05, DRB1*14 and DRB1*16 (83–89)	No clear genetic predisposition 90)	HLA class II genes (72, 91–95)	LIG1: HLA-DRB1*07:01, DQA1*02:01, DQB1*02:02 (96, 97) CASPR2: HLA-DRB1*11:01, DQA1*05:01, DQB1*03:01 (97, 98)	HLA-DRB1 and FCGR2B regions (99)
Location of Pathology	Neuromuscular junction	Axon of nerves at the Nodes of Ranvier	Skin and mucous membranes	Brain	No specific site; Autoimmune-mediated fibroinflammatory lesions
Clinical Presentation	Muscle weakness, increased fatigability	Progressive Weakness, Numbness	Skin Blisters, Lesions, Rash	LGI1: limbic encephalitis with faciobrachial dystonic seizures CASPR2: limbic encephalitis, Morvan's syndrome, peripheral nerve hyperexcitability syndrome, ataxia and distinct movement disorders	Organ-specific and Systemic Involvement
Therapy	Corticosteroids, PE, iVIG, Immuno-suppressants, RTX	Corticosteroids, PE, iVIG, Immunosuppressants, RTX	Corticosteroids, Immunosuppressants, RTX	Corticosteroids, PE, iVIG, Immuno-suppressants, RTX	Corticosteroids, RTX

MuSK, muscle-specific tyrosine kinase; PF, pemphigus foliaceus; PV, pemphigus vulgaris; PE, plasma exchange; iVIG, intravenous Immunoglobulin; RTX, Rituximab.

Lipoprotein Receptor-Related Protein 4 (LRP4) pathway, critical for the proper clustering and functionality of AChRs (102). The consequence of this interference is the disruption of signaling from nerves to muscles and patients present clinically with increased fatigability and muscle weakness (100, 101). MG is a very heterogeneous disease consisting of several different subtypes. These subtypes are partly categorized by the target antigen that the antibodies detect. So far, three main target antigens have been identified and validated: AChR (103, 104), MuSK (105), and LRP4 (106, 107). Although all of these subtypes are unified under the term MG, each disease has distinct clinical and immunological features (59). The immunological differences are further apparent in the subclass usage of each subtype. While AChR, and LRP4 autoantibodies are mostly of the IgG1, IgG2 and IgG3 subclass (59, 106, 108), MuSK is predominantly IgG4 (4–6). Interestingly, antibodies of the IgG1-3 subclasses in MuSK MG impact the clustering of AChRs (109, 110), resulting in a reduction of clustered AChRs. The precise mechanism underlying this effect remains to be fully elucidated and seems to be divergent from IgG4 MuSK autoantibodies (110).

The isolation and characterization of monoclonal autoantibodies (mAbs) against MuSK has significantly advanced our understanding of MuSK-MG (12, 111–114). The knowledge that plasmablasts are a source for MuSK autoantibodies and the development of mechanisms for the enrichment of this specific B cell population (111–114), were instrumental for the generation of MuSK mAbs (111, 113, 114). The ectodomain of MuSK consists of three Ig-like (Ig1-3) domains and a frizzled domain (115, 116). Previous findings revealed that the majority of MuSK autoantibodies recognize the Ig-like domain 1 on the MuSK receptor, as observed with human polyclonal sera (117). These polyclonal autoantibodies were proven to be pathogenic *in vitro* and *in vivo* via passive transfer (118–120), directly inhibiting the interaction between MuSK and LRP4 (109, 117). More recently, mAbs detecting the Ig-like domain 2 were also shown to have pathogenic capacities (113). The impact of valency on the pathogenicity after Fab-arm exchange of MuSK autoantibodies was initially demonstrated in sera-based experiments (121) and subsequently confirmed with human MuSK mAbs (112, 122, 123). It has further been shown that affinity maturation plays a crucial role in the pathogenic development of MuSK mAbs and that a high affinity coupled with monovalency is essential to reach a pathogenic threshold necessary for the potent disruption of AChR clusters at the NMJ (122). MuSK autoantibody titer correlates well with disease severity in MuSK MG (5, 6, 124–126), might be a potential biomarker to detect relapse in MuSK MG (114, 127) and treatment success with BCDT (114, 124).

4.2 Nodo-paranodopathies with autoantibodies targeting NF155, CNTN1, and CASPR1

Chronic inflammatory demyelinating polyradiculoneuropathy (CIDP) is a progressive autoimmune peripheral neuropathy, where the main target is the myelin sheath of peripheral nerves (128, 129). Over the last decade, antibodies targeting the proteins located in the nodes of Ranvier and the paranodal region have been identified and reported to be present in 2-15% of patients clinically diagnosed with CIDP (10, 130). Although these patients are generally diagnosed clinically as CIDP, there is a growing consensus on classifying seropositive CIDP patients under nodo-paranodopathies instead of CIDP, as there are distinct immunopathological and clinical characteristics between IgG4-mediated nodo-paranodopathies and CIDP (131–133).

These antibodies target mainly neurofascin 155 (NF155), neurofascin 186 (NF186), neurofascin 140 (NF140), contactin-1 (CNTN1), and contactin-associated protein 1 (CASPR1) (8, 10, 134–138). In the majority of patients with nodo-paranodopathy, the dominant immunoglobulin subclass is IgG4, particularly for anti-NF155, anti-CNTN1, and anti-CASPR1 (8, 10). These proteins function as cell adhesion molecules. NF155 proteins are located mainly on the myelin loops of Schwann cells and bind to the CNTN1-CASPR1 complexes that are found on the axolemma. The resulting tripartite protein complexes attach the myelin loops strongly to the axon in the paranodes, resulting in formation of the largest junctions known in the body. Antibodies against CNTN1 and CASPR1 bind to the epitopes found in domains that interact with the partner proteins, therefore abolishing the formation of tripartite complexes and leading to disruption of paranodal junctions, resulting in conduction deficits (10, 139). A distinguished feature of anti-NF155 IgG4 antibodies is that these antibodies do not prevent the interaction of its target protein with its partners. Instead, binding of these antibodies leads to the formation of NF155 clusters on Schwann cell surface, resulting in depletion of proteins necessary for the formation of the paranodal complex (140). In summary, unlike classical CIDP, IgG4 antibodies against paranodal antigens do not cause inflammation or demyelination, but rather cause paranodal detachment and disturbance of nodal electrophysiology leading to conduction blocks and potentially axonal degeneration.

Further examination of patient sera with anti-NF155 antibodies revealed that pathogenic monospecific bivalent IgG4 antibodies are present in the sera. The effect of monovalency on pathogenicity is variable in nodo-paranodopathies. In contrast to MuSK MG, the decreased valency of anti–Neurofascin-155 IgG4 subclass autoantibodies resulting from Fab-arm exchange strongly diminished the effect of pathogenic antibodies (141). In CNTN1 autoantibodies, however, monovalency showed similar pathogenic capacities in comparison to their divalent counterparts (142). Similar to MuSK MG, the autoantibodies titers in nodo-paranodopathies correlate well with clinical diseases severity (137, 143, 144).

4.3 Pemphigus with autoantibodies targeting Dsg1 and Dsg2

Pemphigus is a group of autoimmune bullous diseases characterized by a pathogenic autoimmune response, primarily driven by autoantibodies targeting two key desmosomal adhesion proteins (145). Desmogleins are Ca^{2+}-dependent transmembrane proteins situated in keratinocyte desmosomes and play a crucial role

in maintaining the integrity and cohesion of keratinocytes within the epidermis (146). Dsg1 is primarily located in superficial layers, while Dsg3 is found in basal and parabasal layers of the skin (147). The two main subgroups of pemphigus are pemphigus vulgaris (PV) and pemphigus foliaceus (PF), the latter being less common (3, 7, 9).

Pathogenic autoantibodies in pemphigus are of the IgG1 and IgG4 sublcass. These antibodies specifically identify epitopes situated within the EC1 and EC2 domains of Dsg1 and Dsg3 (148). The interaction of these autoantibodies results in the obstruction of cell-cell adhesion, leading to the development of skin blisters (3, 149). This pathological mechanism has been substantiated *in vitro*, wherein the antibodies prompt the separation of cell sheets in cultured human keratinocytes and human skin explants (150–152). Clinical evidence underscores the pathogenicity of IgG4 in comparison to other serum IgG fractions, as eliminating IgG4 from PV sera has been observed to lead to a 81% reduction in dissociation in keratinocyte assays (7). In cases of active disease, both PV and PF patients typically manifest enriched desmoglein reactive IgG4 and IgG1, while individuals in remission and certain healthy relatives of pemphigus patients may solely exhibit IgG1 (149, 153–155). Additionally, the passive transfer of maternal antibodies to the fetus induces a transient neonatal form of pemphigus [201]. Polyclonality and epitope specificity affect the pathogenic effect of autoantibodies in PV (156). Beyond impeding cell-cell adhesion, the autoantibodies can also modulate signal transduction pathways that influence cytoskeleton rearrangement and cell adhesion in keratinocytes (152, 157, 158) For instance, the activation of p38 mitogen-activated protein kinase (p38MAPK) plays a vital role in causing the loss of cell cohesion. Blocking p38MAPK in the human epidermis has been shown to prevent blistering. Therefore, the specific morphological alterations induced by pathogenic IgG in mucocutaneous PV such as widening between desmosomes and the decrease in desmosome size are at least partially associated with p38MAPK signaling (152, 157). Monovalency resulting from Fab-arm exchange was shown to increase the pathogenic effect of patient-derived autoantibodies in PF (159). The effect of valency in PV seems less pronounced (160, 161). Monovalent single-chain variable-region fragments of autoantibodies derived from PV patients' demonstrated pathogenic capacity *in vivo* (151) as well as Fabs of patient-derived mAbs (161). In pemphigus, there is no direct correlation of autoantibody titer to disease severity and as such, the titer cannot be used to monitor disease activity directly (162, 163).

4.4 LGI1/CASPR2-antibody Encephalitis

Antibody-mediated encephalitis is a heterogeneous group of disorders caused by more than 21 different antibodies (164). Among these, anti-LGI1 and anti-CASPR2 encephalitis are related to IgG4 as the dominant immunoglobulin subtype (165). LGI1 is a synaptic protein that binds to presynaptic metalloproteinase domain-containing protein 23 (ADAM23) and postsynaptic ADAM22. ADAM23 positions voltage-gated potassium channels in the presynaptic terminal and AMPA receptor in the postsynaptic membrane. Antibody binding disrupts LGI1-ADAM22/ADAM23 complexes on the cell surface leading to diminished AMPAR and voltage-gated potassium channel (VGKC) clusters. Loss of inhibitory VGKC complexes heightens neuron excitability, while AMPAR loss impairs long-term potentiation. The AMPAR loss is believed to directly contribute to the memory deficits observed in individuals with anti-LGI1 encephalitis (166, 167). CASPR2 serves as a transmembrane cell adhesion protein that interacts with Kv1.1 and Kv1.2 VGKCs in the juxtaparanodal region of myelinated peripheral nerves. In addition to its distribution in the nodes of Ranvier across the central and peripheral nervous systems, CASPR2 is also found in the synapses of the limbic system and basal ganglia (164). In mice, intrathecal infusion of anti-CNTN2 IgG, comprising a mixture of IgG1 and IgG4, purified from individuals with anti-CASPR2 encephalitis, were observed to induce memory deficits. This effect was attributed to hindering CASPR2/TAG1 interaction and reducing the surface levels of CASPR2, Kv1.1, and AMPAR, similar to LGI1 antibodies (168). CASPR2 antibodies exert their pathogenicity mainly through blocking (169), while studies showing the effect of monovalency on pathogenicity are currently missing. In LGI1 encephalitis the effect of valency on the pathogenic capacity has also not been investigated in detail yet. Similarly, the correlation of the autoantibody titer in the bloodstream with clinical disease severity is unknown. Levels of autoantibodies found in the cerebrospinal fluid might serve as a more accurate indicator in these pathologies of the central nervous system.

4.5 IgG4-RD

IgG4-RD is an immune-mediated systemic condition characterized by fibroinflammatory lesions in various organs; these lesions can mimic malignancies, infections, and inflammatory disorders, often accompanied by elevated IgG4 levels, though not always (170, 171). Recognized as a distinct disease only since 2003, early diagnoses of IgG4-related disease were often incidental findings during surgical resections of lesions initially suspected to be malignant (172, 173). IgG4-RD is characterized by three major histopathological findings: a dense lymphoplasmacytic infiltrate, fibrosis, at least focally in a storiform pattern, and obliterative phlebitis. Additionally, a diagnosis requires an increased number of IgG4 plasma cells in the tissue (174). The 2019 American College of Rheumatology/European League Against Rheumatism (ACR/EULAR) established comprehensive criteria for diagnosing and investigating IgG4-RD. These criteria include: (1) involvement of at least one of 11 possible organs, (2) a total of 32 exclusion criteria, and (3) eight weighted inclusion criteria (175).

Regarding the underlying immunopathology, CD4+ cytotoxic T lymphocytes play a pivotal role, constituting a major subset in both tissue and circulation. These cells secrete pro-fibrotic cytokines such as IL-1β, TGF-β1, and IFN-γ, along with cytolytic molecules like granzymes (176, 177). Among this population, the dominant effector subset is characterized by CD27lo CD28lo CD57hi cells with clonal expansion, and activated CD8+ T cells expressing granzyme-A are also observed (178). A recent study on tertiary lymphoid organs in IgG4-RD revealed a significant infiltration of a Tfh subset that is LAG3 and IL-10 positive (61). Activated B cells

and plasmablasts may interact with these CD4+ T cell subsets, contributing to fibrosis and inflammation in IgG4-RD (176). Notably, a study highlighting dominant plasmablast clones identified galectin-3 autoantibodies, present in a subset of patients and correlated with galectin-3 plasma levels (179). Unlike autoantibody-mediated autoimmune disorders, the direct involvement of B cells in IgG4-RD pathology remains unclear and requires further investigation. The circulating IgG4 antibodies in IgG4-RD most likely are predominantly monovalent due to Fab-arm exchange. Interestingly, the levels of IgG4 subclass antibodies is not always elevated in these patients (170, 171).

5 Therapeutic Interventions

The standard treatment for autoimmune diseases previously involved broad immunosuppressive drugs (180). While these therapies improve symptoms, their effectiveness is often limited by adverse side effects. Moreover, not all patients respond to these conventional treatments. Interestingly, patients who do not respond to standard therapies have shown positive responses to treatments originally used in B cell malignancies, such as anti-CD20 mediated BCDT (3–12). Studying the efficacy of anti-CD20 mediated BCDT has provided valuable insights into potential therapies for B cell pathologies. Additionally, distinct therapies influence the B cell repertoire differently as observed in patients that received mycophenolate mofetil and anti-CD20-mediated BCDT (181), highlighting the potential benefits of combination therapy. In this chapter, we will first examine anti-CD20 mediated BCDT and then explore new therapeutic approaches.

5.1 Anti-CD20-mediated BCDT

Originally developed for treating B cell malignancies, anti-CD20 mediated BCDT has proven effective in managing diverse autoimmune conditions, including multiple sclerosis, PV, rheumatoid arthritis, CIDP, and MuSK MG (124, 135, 182–184). Anti-CD20 mediated BCDT exhibits remarkable efficiency in IgG4-AID and IgG4-RD (3–12).

Many MuSK MG patients enter stable remission for several years following anti-CD20 mediated BCDT, with significantly reduced or non-detectable MuSK autoantibody titers (124, 125, 185). However, relapses can occur in some patients over time (68, 185–187). In these cases, the MuSK autoantibody titer may increase months before clinical-detectable relapse (114, 125, 127). During relapse, frequencies of plasmablasts and memory B cells are elevated, with disease-related autoantibody-expressing B cells identified within these populations (111, 113, 114, 188–190). Consequently, MuSK MG patients treated with anti-CD20 mediated BCDT undergo cycles of remission followed by phases of clinical relapse. Most patients with IgG4-mediated nodo-paranodopathies are unresponsive to IVIg and steroids, unlike classical CIDP. As such, IVIg and steroid unresponsiveness should lead to antibody testing in CIDP patients. Anti-CD20 mediated BCDT shows beneficial effects in the majority of patients with IgG4-mediated nodo-paranodopathies, particularly those refractory to other therapies (191–195). In a large cohort of anti-NF155 antibody positive patients, 77% of patients responded to anti-CD20 mediated BCDT (194). In addition, serum neurofilament light chain (NfL) levels which are an indicator for axonal damage and anti-NF155 antibody titers were also decreased after therapy. Similar positive outcomes have been observed in pemphigus (196–198). High-dose anti-CD20 mediated BCDT therapy extended remission duration, although it did not impact the relapse rate (40%) compared to a low-dose regimen (197). Furthermore, treatment response to anti-CD20-mediated BCDT is good in LGI1/CASPR2-antibody encephalitis (11, 199). Interestingly, anti-CD20-mediated BCDT has emerged as a highly effective therapy option in IgG4-RD, underscoring the potential involvement of B cells in the pathophysiology (13).

However, it is crucial to emphasize that the response to anti-CD20 mediated BCDT varies and not all patients achieve remission (125, 197, 200, 201). In MuSK MG, non-response in patients might be associated with a prevalence of pathogenic IgG1-3 subclass antibodies (110). Additionally, in AChR MG, which was previously considered a less favorable target for anti-CD20 mediated BCDT, a small subset of patients' benefits from anti-CD20 mediated BCDT. These positive responses have been observed in cases of severe refractory AChR MG (200, 202). Anti-CD20 mediated BCDT appears to yield better results when initiated during the early stages of AChR MG (203, 204). This variability in response is likely due to the heterogeneity of the underlying immunopathologies (59) and an increasing significance of long-lived plasma cells in the immunopathogenesis as the disease progresses over time. In some instances, disease progression occurred post-anti-CD20 mediated BCDT administration (205), potentially linked to the presence of anti-RTX antibodies, known to impede responsiveness of anti-CD20 mediated BCDT in IgG4-mediated nodo-paranodopathies (206). Ocrelizumab, another BCDT targeting CD19 with lower immunogenic potential, has proven to be a successful alternative in patients developing anti-RTX mAbs (207). The variation in response may, to some extent, be associated with IgG subclasses other than IgG4 playing significant roles in the immunopathology of these patients (110).

However, the complexity of CD20 expression should be acknowledged, extending beyond B cells to include T cells (Figure 2). Thus, anti-CD20 mediated BCDT does not exclusively affect B cells; subsets of T cells expressing CD20 on their surface are also impacted by this therapy (208–210). This depletion of CD20-expressing T cells has been observed in multiple sclerosis (208, 211). For B cells, CD20 is expressed at nearly all stages of B cell differentiation, excluding plasma cells, Pro-B-cells, and Pre-B-I (Figure 2) (16). The initial report of T cells with CD20dim expression (208, 212), was first widely considered a flow cytometry artifact (213). Subsequently, this population was identified as a distinct T cell subset with both immune-regulatory and proinflammatory activities (208, 214). The frequency of CD20+ T cells in the peripheral blood of healthy individuals is relatively low (1-4%). However, these cells are increased under inflammatory

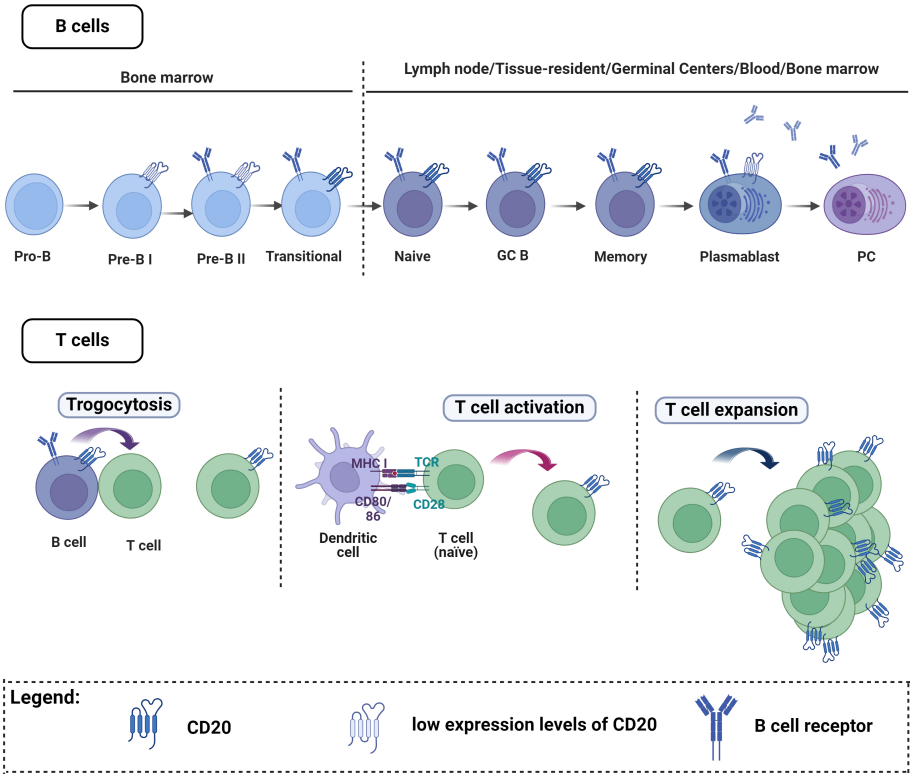

FIGURE 2
CD20 expression on B cells and T cells. B cells. CD20 is expressed at almost all stages of B cell maturation, with the exception of plasma cells, Pro-B cells, and Pre-B-I cells. T cells. A small number of T cells express CD20, and there are three main theories explaining how these cells acquire CD20: One explanation proposes that T cells may acquire CD20 through trogocytosis, involving simultaneous transfer from B cells. Alternatively, CD20 acquisition might occur during T cell activation or result from the clonal expansion of CD20-expressing T cells. Figure created with Biorender.com.

conditions and enriched in tissues including tonsils, thymus, bone marrow, and cerebrospinal fluid compared to the peripheral blood (208, 210, 215, 216). The origin of CD20-expressing T cells remains unclear (Figure 2). One proposed explanation is that T cells acquire CD20 through the process of trogocytosis, involving the simultaneous transfer of HLA-DR and CD20 from B cells (210, 216–218). However, the low expression of HLA-DR on T cells suggests that trogocytosis may not fully elucidate the origin of this subset (208, 217). Additionally, CD8+ T cells are known to interact mainly with cross-presenting dendritic cells during conditions such as viral infection, rather than B cells. As dendritic cells are not known to express CD20 on cell surface, the acquisition of CD20 by CD8+ T cells through trogocytosis remains questionable. Moreover, *MS4A1*, the gene that encodes CD20, was shown to be transcribed in T cells (208). Therefore, CD20 acquisition may occur during T cell activation (217, 219) or result from clonal expansion of CD20-expressing T cells (217, 220). Myelin-specific CD8+ CD20+ T cells were shown to be depleted together with B cells after CD20 monoclonal therapies (221). The major T cell subtypes that were lost included memory CD8+CD20+ and central memory CD8+ T cells but not CD4+CD20+ T cells and this may contribute to increased infection rate seen in these patients (222). Another study found that pretreatment levels of CD8+CD20+ T cells that have a proinflammatory phenotype have a significant inverse relationship with disease burden before treatment. Additionally, these cells were predictive of early disease activity following the initiation of anti-CD20 therapy (223). Therefore, RTX's effectiveness in these autoimmune diseases may not only be the consequence of RTX's effect on B cells.

B cell depletion by anti-CD20 mediated BCDT is further limited, as disease-relevant B cells persist even after treatment (114, 190). The persistence of these B cell clones is not unique to MuSK MG; this phenomenon extends to various autoimmune disorders, including Sjögren's syndrome, SLE, systemic sclerosis, and ANCA-associated vasculitis (181, 224, 225). These persistent B cells were found to reemerge in MuSK MG months before clinical detectable relapse simultaneously with an increase of autoantibody titer (114). Several characteristics distinguish persistent B cell clones. CD20 expression is crucial for the efficacy of anti-CD20-mediated B cell depletion therapy. Both persistent memory B cells and antibody-secreting cells (ASCs) express low CD20 levels (114, 190). Furthermore, persistent memory B cell subsets express genes associated with previous tissue homing (114, 188, 190, 226–228). Additionally, B cell memory clones that are highly expanded show a higher rates of persistence (190, 229–231). Alterations in the BAFF/APRIL system, including reduced BAFF-R expression and elevated TACI and BCMA levels, are observed in persistent clones and plasmablasts at the time of relapse (114, 190, 232). Nevertheless, it is evident that the remarkable effect of anti-CD20 mediated BCDT in IgG4-associated disorders suggests a direct impact on the reservoir of pathogenic cells in these diseases.

5.2 New therapeutic approaches

5.2.1 Anti-CD19 mediated BCDT

CD19 is a transmembrane glycoprotein from the immunoglobulin superfamily (233) and it is functionally associated with modulation of antigen-independent B cell differentiation and immunoglobulin-induced B cell activation (234). The expression profile of CD19 is broader than that of CD20, starting earlier at the stage of pro-B cells and extending into plasmablasts and plasma cells beyond the expression of CD20 (234, 235). Two anti-CD19 mAbs have reached clinical trials: XmAb5871 and Inebilizumab (236, 237). XmAb5871 is currently investigated in a phase II clinical trial (ClinicalTrials.gov Identifier: NCT02725476) and Inebilizumab (ClinicalTrials.gov Identifier: NCT04540497) in ongoing phase III clinical trials for patients with IgG4-RD. Inebilizumab is further tested in MG (MINT; ClinicalTrials.gov Identifier: NCT04524273). CD19 has gained attention in recent years as an alternative therapy to anti-CD20 mediated BCDT. Given its broader expression profile, especially in ASCs. Besides, it could be an interesting alternative for patients developing resistance to CD20 therapies, as it has already been reported in some non-responders (207).

5.2.2 Anti-CD38 mediated BCDT

The main expression of CD38 is observed in hematopoietic cells. It was first identified as a lymphocyte specific antigen, but current studies revealed that it is ubiquitously expressed (238, 239). Plasma cells and memory B cells express high levels of CD38, while it is expressed at low levels in normal lymph and bone marrow cells (240). CD38 is also expressed in B cell precursors, germinal center B cells, and plasma cells and in other immune cells like NK cells, neutrophils and myeloid cells (239). CD38 is a multifunctional, membrane-bound protein that serves as an antigen and as an enzyme. It catalyzes the metabolism of cyclic ADP-ribose (cADPR) and nicotinic acid adenine dinucleotide phosphate (NAADP). These are two different calcium second messengers, involved in several cell functions (238, 239). Besides this enzymatic function, CD38 can also act as a receptor for CD31, acting as an adhesion molecule for mediating selectin-like binding of hematopoietic cells to endothelial cells and facilitating their transmigration to tissue (239). The role of CD38 in immune cells ranges from immunomodulation to effector functions during inflammation, where it could regulate cell recruitment, cytokine release and NAD availability. This expression profile of CD38, together with its role in inflammatory processes, make CD38 an interesting target in the context of autoimmune diseases (239, 240). Antibodies targeting CD38 have been proposed as a potential therapeutic approach to eliminate plasma cells that produce autoantibodies. Daratumab and Isatuximab have already been established as an important therapeutic target for Multiple Myeloma (MM) (241). Isatuximab binds to an epitope that partially covers the catalytic site of CD38, without changing its configuration, while Daratumumab is binding outside the catalytic site (242). In SLE patients, Daratumumab was found to restore NK cytotoxic function which promoted the elimination of circulating plasma cells (240). Thus, anti-CD38 might be a potent drug to reduce the levels of ASCs.

5.2.3 Anti-CD40 mediated BCDT

CD40 is constitutively expressed on B lymphocytes, and CD40L is mainly expressed in the surface of activated CD4+ T cells, inducing activation, proliferation and cytokine production. Besides, they are found in other hematopoietic cells such as monocytes and dendritic cells as well as non-hematopoietic cells like mast cells, basophils, NK cells, macrophages, megakaryocytes and platelets (243). CD40 is a receptor of the TNF superfamily (243) and together with its ligand, CD40L (CD154), they form an important stimulatory immune checkpoint (244). CD40/CD40L interaction is essential for the formation of germinal centers and the production of class-switched antibodies. It is also important in humoral and cellular immunity, being involved in the activation of innate and adaptative immune cells, regulation of B cell, T cell and APC activation and immunological memory (243, 244).

This role in activation of immune responses makes it an attractive target for potential therapies, and recently, it has been the subject of multiple studies with this aim (244). Iscalimab is a human anti-CD40 monoclonal antibody (244) and it has been recently evaluated for safety and efficacy in moderate to severe symptomatic MG in a phase II clinical trial (245). Previously, a therapeutic benefit had been reported in patients with other autoimmune diseases such as Sjörgen Syndrome (246) and Graves´disease (247). In the case of Pemphigus, the interaction between CD40 and its ligand is important for the induction of pathogenic anti-Dsg3 IgG antibodies (248). Therefore, anti CD40L could be a potential therapeutic approach for Pemphigus (249). In summary, antibodies directed against the CD40/CD40L axis constitute a novel target with potential benefits for patients with autoimmune diseases, by targeting plasma cells involved in the production of pathogenic autoantibodies.

5.2.4 Targeting the BAFF/APRIL-system

The BAFF/APRIL-system plays a crucial role in regulating the survival and maintenance of B cells. This system consists of two key ligands, B-cell activating factor (BAFF) and a proliferation-inducing ligand (APRIL), along with three receptors: the transmembrane activator and calcium modulator and cyclophilin ligand interactor (TACI), B cell maturation antigen (BCMA), and B-cell activating factor receptor (BAFF-R) (250). BAFF and APRIL ligands are primarily produced by myeloid and stromal cells, while their corresponding receptors are found on circulating B cells. These receptors are expressed at various stages of B cell development, suggesting a dynamic regulation of B cell survival and maintenance throughout maturation (16). Dysregulation within the BAFF/APRIL-system is associated with autoimmune diseases as well as cancer, allergies, transplants, infections, and immunodeficiencies (251). Elevated levels of BAFF/APRIL soluble receptors and ligands are linked to B cell pathologies, observed in conditions like MG, SLE, Sjögren´s syndrome, and RA, among others (251–255).

This pivotal role in autoimmune diseases suggests that targeting components of this system may offer a potential therapeutic avenue (251). Belimumab (GSK1550188), a recombinant monoclonal antibody targeting soluble BAFF, was the first FDA-approved biologic for SLE treatment, following positive safety and efficacy outcomes in phase III clinical trials (ClinicalTrials.gov Identifier: NCT00424476; ClinicalTrials.gov Identifier: NCT00410384) (251). Unexpectedly, Belimumab did not demonstrate significant efficacy in a phase II clinical trial for Myasthenia Gravis (AChR and MuSK) (ClinicalTrials.gov Identifier: NCT01480596) (256). Other BAFF-targeting agents such as Blisibimod and Tabalumab have undergone phase II/III clinical trials for diseases like SLE and MM (257–259). In recent years, research has focused on dual inhibitor agents, like Atacicept, which inhibit both BAFF and APRIL simultaneously. Atacicept is designed as the extracellular domain of the receptor TACI fused to the human Fc domain (260, 261). Atacicept has shown beneficial effects in SLE and RA patients by significantly depleting plasma cells (262–266) and Telitacicept, another dual inhibitor, has also demonstrated positive effects in autoimmune diseases (259). In a phase II clinical trial for SLE, Telitacicept exhibited beneficial effects (267). Additionally, there is an ongoing phase III clinical trial in China to evaluate the efficacy and safety of Telitacicept in the treatment of MG, currently recruiting (ClinicalTrials.gov Identifier: NCT04660565). Another ongoing phase IV clinical trial in China is assessing the use of Belimumab for the treatment of IgG4-RD, with results pending (ClinicalTrials.gov Identifier: NCT04660565). Although dual inhibtion of BAFF and APRIL seems to have beneficial effects in some autoimmune disorder, in multiple sclerosis a trial for atacicept had to be halted due to increased disease activity in patients compared to placebo (268–270). Thus, the complexity of the BAFF/APRIL-system has to be further investigated to better understand how therapy influences the underlying immunopathology of individual diseases.

5.2.5 Proteasome inhibitors

The ubiquitin/proteasome system constitutes one of the main pathways for intracellular protein degradation (271, 272). Therefore, it is a key component for maintaining a dynamic control over key signaling components of the immune response, as well as overall cell homeostasis. Malfunctioning of the proteasome system is associated with pathological conditions, like cancer or autoimmune disorders (272). Proteasome inhibition results in the accumulation of defective immunoglobulin chains, leading to stress in the endoplasmic reticulum, misfolding of proteins and ultimately cell apoptosis (271, 273). It has been proven to be critical for plasma cell function due to their high rate of antibody synthesis. Inhibiting the proteasome results in the apoptosis of plasma cells and a consequent decrease in antibody production. Besides, proteasome inhibition also hinders the production of pro-inflammatory cytokines (273). This makes the proteasome a promising novel target for antibody mediated autoimmune diseases, involving long-lived plasma cells, like SLE (273) or AChR-MG (59).

Bortezomib, initially approved for MM, is a dipeptide boronic acid derivative, that binds to the catalytic site of the proteasome with high affinity on plasma cells (272, 273). There have been several clinical trials for Bortezomib in SLE patients, that probe a remarkable efficacy of Bortezomib, especially in SLE patients that had been refractory to prior immunosuppression therapies (271, 274). Bortezomib and other proteasome inhibitors have shown beneficial effect in EAMG, a mouse model of MG (275, 276). *In-vitro* studies of thymic cell cultures derived from AChR-MG patients with Bortezomib could eliminate thymus-derived plasma cells and reduce IgG levels (277). A phase 2 clinical trial (ClinicalTrials.gov Identifier: NCT02102594) to investigate the use of Bortezomib on patients with therapy-refractory Myasthenia Gravis (generalized) or SLE or RA is currently still ongoing (278). Thus, Bortezomib is another good potential candidate for a more targeted immunotherapy in B cell pathologies.

5.2.6 FcRn inhibitors

Human IgG is one of the most abundant proteins in serum, probably because of the uniquely long half-life, for which neonatal fragment crystallizable (Fc) receptor (FcRn) plays an essential role (279, 280). The FcRn is a multifunctional atypical form of Fc-gamma receptor. It was first identified as the responsible of transporting IgG from the maternal to the fetal circulation. Later it was found that, among other functions, it plays an essential role in IgG recycling, by protecting IgG from intracellular degradation, therefore, expanding the half-life (280, 281). FcRn inhibitors enhance the catabolism of IgG by blocking the FcRn-mediated IgG recycling pathway leading to reduced IgG levels in serum and a decrease in pathogenic autoantibodies (282).

In recent years, FcRn inhibitors have emerged as promising targets for autoantibody-mediated autoimmune diseases. Efgartigimod (ARGX-113) binds to FcRn, preventing IgG recycling (282). A phase III trial in MG showed efficacy and tolerability (283) and an ongoing trial for pediatric MG patients is currently recruiting (ClinicalTrials.gov Identifier: NCT05374590), alongside a phase III trial assessing different dosing regimens (ClinicalTrials.gov Identifier: NCT04980495). SYNT001, another FcRn inhibitor, demonstrated efficacy in a phase I/II trial for Pemphigus (284). Rozanolixizumab, also an anti-FcRn monoclonal antibody, showed positive results in MG clinical trials (285). Several trials are ongoing for Rozanolixizumab in MG treatment, including a phase III trial (ClinicalTrials.gov Identifier: NCT04650854) and a self-administration study (ClinicalTrials.gov Identifier: NCT05681715). Additionally, a phase II/III trial for pediatric MG patients is ongoing (ClinicalTrials.gov Identifier: NCT06149559). Other FcRn inhibitors like Batoclimab are also in clinical trials, including a phase III trial for generalized MG (ClinicalTrials.gov Identifier: NCT05403541) and testing in patients with active CIDP (ClinicalTrials.gov Identifier: NCT05581199). Overall, FcRn inhibitors hold promise as therapy for IgG-driven autoimmune diseases like MG, offering targeted treatment with potentially fewer side effects than nonspecific therapies.

5.2.7 Complement inhibitors

The complement system comprises a network of over 30 proteins, which interact in a sequential and regulated manner, culminating in the formation of the membrane attack complex

(MAC). The MAC inserts into cell membranes, leading to pore formation and cell damage (286). The classical complement pathway is activated by antibody-antigen complexes (see chapter 3). Not all antibody isotypes are capable of activating the complement cascade. Targeting the complement system in diseases with autoantibodies that are mainly of the IgG1 or IgG3 subclass has shown remarkable efficacy, especially in the context of AChR MG. AChR autoantibodies are mainly of the subclass IgG1 (287). Eculizumab, inhibiting complement activation by targeting C5, demonstrated beneficial outcomes in phase III trials (ClinicalTrials.gov Identifier: NCT02301624; ClinicalTrials.gov Identifier: NCT01997229) and is approved for treating AChR+ MG patients (288). Ravulizumab, another C5 inhibitor, is currently in phase III trials (ClinicalTrials.gov Identifier: NCT03920293) (289). However, complement inhibition may not provide clinical benefits for patients suffering from IgG4 mediated diseases.

5.2.8 BTK inhibitors

Bruton´s tyrosine kinase (BTK) is a multifunctional cytoplasmic protein member of the TEC kinase family (290), crucial in B-cell biology, involved in maintaining B-cell survival, proliferation, differentiation and activation (291). Apart from B cells, it is also expressed in mast cells, NK cells, T cells, macrophages, neutrophils, monocytes and basophils (291), highlighting its multifaceted role in the immune system. Among the functions of BTK, it integrates signaling to regulate B cell development through BCR (290). Besides it is also involved in TLR-mediated signaling, chemokine mediated homing of pre-B cells into lymphoid organs and mediates in inflammatory processes driven by IgG complexes (291). Due to its central role in B cell immunity, BTK inhibition therapies have been gaining attention as first-line therapy for B cell malignancies (292). Its involvement in B cell survival and differentiation has also linked BTK with autoimmune diseases (291). Indeed, studies have shown increased levels of BTK expression in B cells from patients suffering from autoimmune diseases, which appears to be correlated with autoantibody production (293). Therefore, BTK inhibitors represent a promising therapeutic strategy for autoimmune diseases. BTK inhibitors are small molecules that are able to downregulate various B cell functions like cell proliferation, differentiation, maturation and survival overall. Besides, they can inhibit the activity of macrophages, mast cells and eosinophils (249). Currently, inhibition of BTK is being investigated for SLE (271). Fenebrutinib, a BTK inhibitor, was investigated in a phase II clinical trial in SLE (ClinicalTrials.gov Identifier: NCT02908100). Despite effectively targeting the BTK pathway, it did not meet the trial's primary endpoint for efficacy (294). In pemphigus, the BTK inhibitor PRN1008 has been studied in a phase III clinical trial (ClinicalTrials.gov Identifier: NCT03762265), but it was terminated based on lack of efficacy. Although, the efficacy of BTK inhibitors as standalone treatments is limited, it might still hold potential in combination therapies.

5.2.9 CAR and CAAR T cells

Chimeric antigen (CAR)-T cell therapies, initially designed for targeting tumor cells, involve priming T cells with anti-tumor activity and then reintroducing them into the patient (295–297). These modified T cells express chimeric antigen receptors (CARs), genetically engineered to have tumor antigen-specific binding sites and a T cell activating domain (298). This allows them to recognize and kill cells expressing the target antigen.

Anti-CD19 CAR T cell therapy gained FDA approval in 2017 for treating B cell malignancies (299), sparking interest in expanding CAR T cell applications beyond cancer, particularly in autoimmune therapies (300). CAR-T therapies aim to redirect T cells against autoantibody-secreting B cells. In addition to CAR T cells, chimeric autoantibody (CAAR) receptor T cell therapies were developed (301–305). CAAR T-cells, distinct from CAR T-cells, express chimeric autoantibody receptors targeting pathogenic antibodies from autoreactive B cells (306). These include anti-BCMA (301–304), investigated in the context of MG (ClinicalTrials.gov identifier: NCT04146051), anti-CD19 (303) (ClinicalTrials.gov identifier: NCT03030976), and most recently, anti-MuSK and anti-NMDA, which have shown initial beneficial effects in a mouse models (305, 307). Another phase I trial (ClinicalTrials.gov Identifier: NCT04422912) is assessing Dsg3-CAAR T cells in Pemphigus vulgaris (308). CAR and CAAR T-cell therapies constitute a promising approach for a more selective and personalized treatment of autoimmune diseases.

6 Conclusion and outlook

The reason why some autoimmune diseases are predominantly IgG4 and not another subclass is still not completely understood. Despite the shared characteristic of having autoantibodies belonging to the IgG4 subclass, these diseases exhibit numerous differences. No discernible pattern emerges concerning the site of pathology, age of onset, or specific genetic predispositions (Table 1). Generally, the pathogenesis of autoimmune disorders is the result of a combination of defects in the immune system together with environmental, and genetic factors similar to the observed pathogenesis of multiple sclerosis, SLE, and type 1 diabetes (309–313). Given the rarity of some of these diseases, our current understanding may be limited. Thus, it is highly probable that clear patterns are not yet discernible. Future investigations are likely to provide more clarity.

IgG4 antibodies play dual roles in health and disease (49). In health, they serve protective and regulatory functions by predominantly inhibiting the actions of IgE antibodies (45, 47–49). However, in autoimmune conditions, where IgE antibodies are not the primary effectors, IgG4 antibodies contribute directly to immunopathology. Similarly, Fab-arm exchange seems to be a coincidental aspect of IgG4-mediated diseases. Fab-arm exchange enhances the diversity of IgG4 antibodies and increases their potential to engage with antigens (45, 47–49). This intrinsic property of IgG4 antibodies can either enhance the pathogenicity of autoantibodies, as observed with MuSK autoantibodies (112, 121–123), without significantly affecting their effects as seen in CNTN1 autoantibodies and pemphigus (142, 151, 161) or diminish their pathogenic potential as seen with anti-Neurofascin-155 IgG4 (141). Therefore, there is a variability in the relevance of Fab-arm

exchange for pathogenic capacity in these diseases. Nevertheless, the underlying immunopathology in these IgG4-mediated diseases appears to share similarities, as seen by the overall positive response to anti-CD20-mediated BCDT in these diseases (3–12). Hence, it is probable that comparable treatments will yield similar outcomes in these conditions.

Author contributions

SÜ: Writing – review & editing, Writing – original draft, Conceptualization. BS: Writing – review & editing. EÇ: Writing – review & editing, Writing – original draft, Conceptualization. DB: Writing – review & editing. RMH: Writing – review & editing. SV: Writing – review & editing, Writing – original draft, Conceptualization. AV: Writing – review & editing, Writing – original draft, Conceptualization. AM: Writing – review & editing, Writing – original draft, Conceptualization. MF: Writing – review & editing, Writing – original draft, Visualization, Supervision, Conceptualization.

Funding

The author(s) declare financial support was received for the research, authorship, and/or publication of this article. MF has received a pilot grant from the DGM (Deutsche Gesellschaft für Muskelkranke e.V. (DGM) and a DFG Research Fellowship (FI 2471/2-1).

Acknowledgments

The figures were created with biorender.com by MF.

Conflict of interest

MF has further received speaker honoraria from Alexion Pharmaceuticals and is a member of the Alexion-Akademie based in Germany. AM has received speaker or consultancy honoraria or financial research support (paid to his institution) from Alexion Pharmaceuticals, argenx, Axunio, Desitin, Grifols, Hormosan Pharma, Janssen, Merck, Octapharma, UCB, and Xcenda. He serves as medical advisory board chairman of the German Myasthenia Gravis Society.

The remaining authors declare that the research was conducted in the absence of any commercial or financial relationships that could be construed as a potential conflict of interest.

Publisher's note

References

1. Anand U, Dey A, Chandel AKS, Sanyal R, Mishra A, Pandey DK, et al. Cancer chemotherapy and beyond: Current status, drug candidates, associated risks and progress in targeted therapeutics. *Genes Dis.* (2023) 10:1367–401. doi: 10.1016/j.gendis.2022.02.007

2. Ledford H. Translational Research: The full cycle. *Nature.* (2008) 453:843–5. doi: 10.1038/453843a

3. Futei Y, Amagai M, Ishii K, Kuroda-Kinoshita K, Ohya K, Nishikawa T. Predominant IgG4 subclass in autoantibodies of pemphigus vulgaris and foliaceus. *J Dermatol Sci.* (2001) 26:55–61. doi: 10.1016/S0923-1811(00)00158-4

4. Mcconville J, Farrugia ME, Beeson D, Kishore U, Metcalfe R, Newsom-Davis J, et al. Detection and characterization of MuSK antibodies in seronegative myasthenia gravis. *Ann Neurol.* (2004) 55:580–4. doi: 10.1002/ana.20061

5. Ohta K, Shigemoto K, Fujinami A, Maruyama N, Konishi T, Ohta M. Clinical and experimental features of MuSK antibody positive MG in Japan. *Eur J Neurol.* (2007) 14:1029–34. doi: 10.1111/j.1468-1331.2007.01870.x

6. Niks EH, Van Leeuwen Y, Leite MI, Dekker FW, Wintzen AR, Wirtz PW, et al. Clinical fluctuations in MuSK myasthenia gravis are related to antigen-specific IgG4 instead of IgG1. *J Neuroimmunol.* (2008) 195:151–6. doi: 10.1016/j.jneuroim.2008.01.013

7. Funakoshi T, Lunardon L, Ellebrecht CT, Nagler AR, O'leary CE, Payne AS. Enrichment of total serum IgG4 in patients with pemphigus. *Br J Dermatol.* (2012) 167:1245–53. doi: 10.1111/j.1365-2133.2012.11144.x

8. Ng JK, Malotka J, Kawakami N, Derfuss T, Khademi M, Olsson T, et al. Neurofascin as a target for autoantibodies in peripheral neuropathies. *Neurology.* (2012) 79:2241–8. doi: 10.1212/WNL.0b013e31827689ad

9. Lo AS, Mao X, Mukherjee EM, Ellebrecht CT, Yu X, Posner MR, et al. Pathogenicity and epitope characteristics do not differ in igG subclass-switched anti-desmoglein 3 igG1 and igG4 autoantibodies in pemphigus vulgaris. *PloS One.* (2016) 11:e0156800. doi: 10.1371/journal.pone.0156800

10. Vural A, Doppler K, Meinl E. Autoantibodies against the node of ranvier in seropositive chronic inflammatory demyelinating polyneuropathy: diagnostic, pathogenic, and therapeutic relevance. *Front Immunol.* (2018) 9:1029. doi: 10.3389/fimmu.2018.01029

11. Dalakas MC. Autoimmune neurological disorders with igG4 antibodies: a distinct disease spectrum with unique igG4 functions responding to anti-B cell therapies. *Neurotherapeutics.* (2022) 19:741–52. doi: 10.1007/s13311-022-01210-1

12. Oconnor K, Fichtner M. The mechanisms of immunopathology underlying B cell depletion therapy-mediated remission and relapse in patients with MuSK MG: Immune mechanisms of MuSK MG. *RRNMF Neuromuscular J.* (2023) 4(12):e127167. doi: 10.17161/rrnmf.v4i3

13. Carruthers MN, Topazian MD, Khosroshahi A, Witzig TE, Wallace ZS, Hart PA, et al. Rituximab for IgG4-related disease: a prospective, open-label trial. *Ann Rheum Dis.* (2015) 74:1171–7. doi: 10.1136/annrheumdis-2014-206605

14. Nutt SL, Hodgkin PD, Tarlinton DM, Corcoran LM. The generation of antibody-secreting plasma cells. *Nat Rev Immunol.* (2015) 15:160–71. doi: 10.1038/nri3795

15. Janeway C. *Immunobiology : the immune system in health and disease; Chapter 8 The Development of B and T Lymphocytes.* 9th ed. (2017) New York: Garland Science.

16. Krumbholz M, Derfuss T, Hohlfeld R, Meinl E. B cells and antibodies in multiple sclerosis pathogenesis and therapy. *Nat Rev Neurol.* (2012) 8:613–23. doi: 10.1038/nrneurol.2012.203

17. Mauri C, Bosma A. Immune regulatory function of B cells. *Annu Rev Immunol.* (2012) 30:221–41. doi: 10.1146/annurev-immunol-020711-074934

18. Shen P, Fillatreau S. Antibody-independent functions of B cells: a focus on cytokines. *Nat Rev Immunol.* (2015) 15:441–51. doi: 10.1038/nri3857

19. Ghosh D, Jiang W, Mukhopadhyay D, Mellins ED. New insights into B cells as antigen presenting cells. *Curr Opin Immunol.* (2021) 70:129–37. doi: 10.1016/j.coi.2021.06.003

20. Kumar BV, Connors TJ, Farber DL. Human T cell development, localization, and function throughout life. *Immunity*. (2018) 48:202–13. doi: 10.1016/j.immuni.2018.01.007

21. Bradley LM, Harbertson J, Biederman E, Zhang Y, Bradley SM, Linton PJ. Availability of antigen-presenting cells can determine the extent of CD4 effector expansion and priming for secretion of Th2 cytokines in *vivo*. *Eur J Immunol*. (2002) 32:2338–46. doi: 10.1002/1521-4141(200208)32:83.0.CO;2-R

22. Yamano T, Nedjic J, Hinterberger M, Steinert M, Koser S, Pinto S, et al. Thymic B cells are licensed to present self antigens for central T cell tolerance induction. *Immunity*. (2015) 42:1048–61. doi: 10.1016/j.immuni.2015.05.013

23. Adler LN, Jiang W, Bhamidipati K, Millican M, Macaubas C, Hung SC, et al. The other function: class II-restricted antigen presentation by B cells. *Front Immunol*. (2017) 8:319. doi: 10.3389/fimmu.2017.00319

24. Nakken B, Munthe LA, Konttinen YT, Sandberg AK, Szekanecz Z, Alex P, et al. B-cells and their targeting in rheumatoid arthritis–current concepts and future perspectives. *Autoimmun Rev*. (2011) 11:28–34. doi: 10.1016/j.autrev.2011.06.010

25. Molnarfi N, Schulze-Topphoff U, Weber MS, Patarroyo JC, Prod'homme T, Varrin-Doyer M, et al. MHC class II-dependent B cell APC function is required for induction of CNS autoimmunity independent of myelin-specific antibodies. *J Exp Med*. (2013) 210:2921–37. doi: 10.1084/jem.20130699

26. Béland K, Marceau G, Labardy A, Bourbonnais S, Alvarez F. Depletion of B cells induces remission of autoimmune hepatitis in mice through reduced antigen presentation and help to T cells. *Hepatology*. (2015) 62:1511–23. doi: 10.1002/hep.27991

27. Jackson SW, Kolhatkar NS, Rawlings DJ. B cells take the front seat: dysregulated B cell signals orchestrate loss of tolerance and autoantibody production. *Curr Opin Immunol*. (2015) 33:70–7. doi: 10.1016/j.coi.2015.01.018

28. Fraussen J, Claes N, Van Wijmeersch B, Van Horssen J, Stinissen P, Hupperts R, et al. B cells of multiple sclerosis patients induce autoreactive proinflammatory T cell responses. *Clin Immunol*. (2016) 173:124–32. doi: 10.1016/j.clim.2016.10.001

29. Kurosaki T, Kometani K, Ise W. Memory B cells. *Nat Rev Immunol*. (2015) 15:149–59. doi: 10.1038/nri3802

30. Akkaya M, Kwak K, Pierce SK. B cell memory: building two walls of protection against pathogens. *Nat Rev Immunol*. (2020) 20:229–38. doi: 10.1038/s41577-019-0244-2

31. Inoue T, Kurosaki T. Memory B cells. *Nat Rev Immunol*. (2024) 24:5–17. doi: 10.1038/s41577-023-00897-3

32. Sarvas H, Makela O. Haptenated bacteriophage in the assay of antibody quantity and affinity: maturation of an immune response. *Immunochemistry*. (1970) 7:933–43. doi: 10.1016/0019-2791(70)90054-6

33. Rajewsky K. Clonal selection and learning in the antibody system. *Nature*. (1996) 381:751–8. doi: 10.1038/381751a0

34. Neuberger MS. Novartis Medal Lecture. Antibodies: a paradigm for the evolution of molecular recognition. *Biochem Soc Trans*. (2002) 30:341–50. doi: 10.1042/bst0300341

35. Oyeyinka GO, Salimonu LS, Williams AI, Johnson AO, Ladipo OA, Osunkoya BO. Range of normal serum immunoglobulin (IgG, IgA and IgM) values in Nigerians. *Afr J Med Med Sci*. (1984) 13:169–76.

36. Janeway C. *Immunobiology : the immune system in health and disease; Chapter 4 Antigen Recognition by B-cell and T-cell Receptors*. 9th ed. (2017) New York: Garland Science.

37. Vidarsson G, Dekkers G, Rispens T. IgG subclasses and allotypes: from structure to effector functions. *Front Immunol*. (2014) 5:520. doi: 10.3389/fimmu.2014.00520

38. Volkov M, Coppola M, Huizinga R, Eftimov F, Huizinga TWJ, van der Kooi AJ, et al. Comprehensive overview of autoantibody isotype and subclass distribution. *J Allergy Clin Immunol*. (2022) 150:999–1010. doi: 10.1016/j.jaci.2022.05.023

39. Hjelholt A, Christiansen G, Sørensen US, Birkelund S. IgG subclass profiles in normal human sera of antibodies specific to five kinds of microbial antigens. *Pathog Dis*. (2013) 67:206–13. doi: 10.1111/2049-632X.12034

40. De Taeye SW, Rispens T, Vidarsson G. The ligands for human igG and their effector functions. *Antibodies (Basel)*. (2019) 8. doi: 10.3390/antib8020030

41. Thomson CA. IgG structure and function. In: Ratcliffe MJH, editor. *Encyclopedia of immunobiology*, vol. 15-22 . Academic Press, Oxford (2016).

42. Damelang T, Rogerson SJ, Kent SJ, Chung AW. Role of igG3 in infectious diseases. *Trends Immunol*. (2019) 40:197–211. doi: 10.1016/j.it.2019.01.005

43. Van Der Neut Kolfschoten M, Schuurman J, Losen M, Bleeker WK, Martinez-Martinez P, Vermeulen E, et al. Anti-inflammatory activity of human IgG4 antibodies by dynamic Fab arm exchange. *Science*. (2007) 317:1554–7. doi: 10.1126/science.1144603

44. Chappel MS, Isenman DE, Everett M, Xu YY, Dorrington KJ, Klein MH. Identification of the Fc gamma receptor class I binding site in human IgG through the use of recombinant IgG1/IgG2 hybrid and point-mutated antibodies. *Proc Natl Acad Sci U.S.A*. (1991) 88:9036–40. doi: 10.1073/pnas.88.20.9036

45. Pillai S. Is it bad, is it good, or is IgG4 just misunderstood? *Sci Immunol*. (2023) 8: eadg7327. doi: 10.1126/sciimmunol.adg7327

46. Oskam N, Damelang T, Streutker M, Ooijevaar-De Heer P, Nouta J, Koeleman C, et al. Factors affecting IgG4-mediated complement activation. *Front Immunol*. (2023) 14:1087532. doi: 10.3389/fimmu.2023.1087532

47. Nakagawa T, Miyamoto T. The role of IgG4 as blocking antibodies in asthmatics and in bee keepers. *Int Arch Allergy Appl Immunol*. (1985) 77:204–5. doi: 10.1159/000233787

48. James LK, Till SJ. Potential mechanisms for igG4 inhibition of immediate hypersensitivity reactions. *Curr Allergy Asthma Rep*. (2016) 16:23. doi: 10.1007/s11882-016-0600-2

49. Rispens T, Huijbers MG. The unique properties of IgG4 and its roles in health and disease. *Nat Rev Immunol*. (2023) 23:763–78. doi: 10.1038/s41577-023-00871-z

50. Vercelli D, De Monte L, Monticelli S, Di Bartolo C, Agresti A. To E or not to E? Can an IL-4-induced B cell choose between IgE and IgG4? *Int Arch Allergy Immunol*. (1998) 116:1–4. doi: 10.1159/000023918

51. Hussain R, Ottesen EA. IgE responses in human filariasis. IV. Parallel antigen recognition by IgE and IgG4 subclass antibodies. *J Immunol*. (1986) 136:1859–63. doi: 10.4049/jimmunol.136.5.1859

52. Rihet P, Demeure CE, Dessein AJ, Bourgois A. Strong serum inhibition of specific IgE correlated to competing IgG4, revealed by a new methodology in subjects from a S. mansoni endemic area. *Eur J Immunol*. (1992) 22:2063–70. doi: 10.1002/eji.1830220816

53. Aalberse RC, van der Gaag R, Van Leeuwen J. Serologic aspects of IgG4 antibodies. I. Prolonged immunization results in an IgG4-restricted response. *J Immunol*. (1983) 130:722–6. doi: 10.4049/jimmunol.130.2.722

54. Van Der Zee JS, Van Swieten P, Aalberse RC. Serologic aspects of IgG4 antibodies. II. IgG4 antibodies form small, nonprecipitating immune complexes due to functional monovalency. *J Immunol*. (1986) 137:3566–71. doi: 10.4049/jimmunol.137.11.3566

55. Irrgang P, Gerling J, Kocher K, Lapuente D, Steininger P, Habenicht K, et al. Class switch toward noninflammatory, spike-specific IgG4 antibodies after repeated SARS-CoV-2 mRNA vaccination. *Sci Immunol*. (2023) 8:eade2798. doi: 10.1126/sciimmunol.ade2798

56. Garcia-Robaina JC, de la Torre-Morin F, Vazquez-Moncholi C, Fierro J, Bonnet-Moreno C. The natural history of Apis-specific IgG and IgG4 in beekeepers. *Clin Exp Allergy*. (1997) 27:418–23. doi: 10.1046/j.1365-2222.1997.1350806.x

57. Varga EM, Kausar F, Aberer W, Zach M, Eber E, Durham SR, et al. Tolerant beekeepers display venom-specific functional IgG4 antibodies in the absence of specific IgE. *J Allergy Clin Immunol*. (2013) 131:1419–21. doi: 10.1016/j.jaci.2012.08.037

58. Trampert DC, Hubers LM, Van De Graaf SFJ, Beuers U. On the role of IgG4 in inflammatory conditions: lessons for IgG4-related disease. *Biochim Biophys Acta Mol Basis Dis*. (2018) 1864:1401–9. doi: 10.1016/j.bbadis.2017.07.038

59. Fichtner ML, Jiang R, Bourke A, Nowak RJ, O'connor KC. Autoimmune pathology in myasthenia gravis disease subtypes is governed by divergent mechanisms of immunopathology. *Front Immunol*. (2020) 11:776. doi: 10.3389/fimmu.2020.00776

60. Jeannin P, Lecoanet S, Delneste Y, Gauchat JF, Bonnefoy JY. IgE versus IgG4 production can be differentially regulated by IL-10. *J Immunol*. (1998) 160:3555–61. doi: 10.4049/jimmunol.160.7.3555

61. Munemura R, Maehara T, Murakami Y, Koga R, Aoyagi R, Kaneko N, et al. Distinct disease-specific Tfh cell populations in 2 different fibrotic diseases: IgG(4)-related disease and Kimura disease. *J Allergy Clin Immunol*. (2022) 150:440–455.e417. doi: 10.1016/j.jaci.2022.03.034

62. Phillips LH. The epidemiology of myasthenia gravis. *Semin Neurol*. (2004) 24:17–20. doi: 10.1055/s-2004-829593

63. Bubuioc AM, Kudebayeva A, Turuspekova S, Lisnic V, Leone MA. The epidemiology of myasthenia gravis. *J Med Life*. (2021) 14:7–16. doi: 10.25122/jml-2020-0145

64. Broers MC, Bunschoten C, Nieboer D, Lingsma HF, Jacobs BC. Incidence and prevalence of chronic inflammatory demyelinating polyradiculoneuropathy: A systematic review and meta-analysis. *Neuroepidemiology*. (2019) 52:161–72. doi: 10.1159/000494291

65. Rosi-Schumacher M, Baker J, Waris J, Seiffert-Sinha K, Sinha AA. Worldwide epidemiologic factors in pemphigus vulgaris and bullous pemphigoid. *Front Immunol*. (2023) 14:1159351. doi: 10.3389/fimmu.2023.1159351

66. Muñoz-Sánchez G, Planagumà J, Naranjo L, Couso R, Sabater L, Guasp M, et al. The diagnosis of anti-LGI1 encephalitis varies with the type of immunodetection assay and sample examined. *Front Immunol*. (2022) 13:1069368. doi: 10.3389/fimmu.2022.1069368

67. Wallace ZS, Miles G, Smolkina E, Petruski-Ivleva N, Madziva D, Cook C, et al. Incidence, prevalence and mortality of IgG4-related disease in the USA: a claims-based analysis of commercially insured adults. *Ann Rheum Dis*. (2023) 82:957–62. doi: 10.1136/ard-2023-223950

68. Guptill JT, Sanders DB, Evoli A. Anti-MuSK antibody myasthenia gravis: clinical findings and response to treatment in two large cohorts. *Muscle Nerve*. (2011) 44:36–40. doi: 10.1002/mus.22006

69. Rodolico C, Bonanno C, Toscano A, Vita G. MuSK-associated myasthenia gravis: clinical features and management. *Front Neurol*. (2020) 11:660. doi: 10.3389/fneur.2020.00660

70. Vallat JM, Sommer C, Magy L. Chronic inflammatory demyelinating polyradiculoneuropathy: diagnostic and therapeutic challenges for a treatable condition. *Lancet Neurol*. (2010) 9:402–12. doi: 10.1016/S1474-4422(10)70041-7

71. Kieseier BC, Mathey EK, Sommer C, Hartung HP. Immune-mediated neuropathies. *Nat Rev Dis Primers*. (2018) 4:31. doi: 10.1038/s41572-018-0027-2

72. Meyer N, Misery L. Geoepidemiologic considerations of auto-immune pemphigus. *Autoimmun Rev*. (2010) 9:A379–382. doi: 10.1016/j.autrev.2009.10.009

73. Kasperkiewicz M, Ellebrecht CT, Takahashi H, Yamagami J, Zillikens D, Payne AS, et al. Pemphigus. *Nat Rev Dis Primers*. (2017) 3:17026. doi: 10.1038/nrdp.2017.26

74. Lepe K, Yarrarapu SNS, Zito PM. Pemphigus foliaceus. In: *StatPearls*. StatPearls Publishing Copyright © 2023, StatPearls Publishing LLC, Treasure Island (FL) (2023).

75. Ghimire P, Khanal UP, Gajurel BP, Karn R, Rajbhandari R, Paudel S, et al. Anti-LGI1, anti-GABABR, and Anti-CASPR2 encephalitides in Asia: A systematic review. *Brain Behav*. (2020) 10:e01793. doi: 10.1002/brb3.1793

76. Guo K, Liu X, Lin J, Gong X, Li A, Liu Y, et al. Clinical characteristics, long-term functional outcomes and relapse of anti-LGI1/Caspr2 encephalitis: a prospective cohort study in Western China. *Ther Adv Neurol Disord*. (2022) 15:17562864211073203. doi: 10.1177/17562864211073203

77. Chiò A, Cocito D, Bottacchi E, Buffa C, Leone M, Plano F, et al. Idiopathic chronic inflammatory demyelinating polyneuropathy: an epidemiological study in Italy. *J Neurol Neurosurg Psychiatry*. (2007) 78:1349–53. doi: 10.1136/jnnp.2007.114868

78. Rajabally YA, Simpson BS, Beri S, Bankart J, Gosalakkal JA. Epidemiologic variability of chronic inflammatory demyelinating polyneuropathy with different diagnostic criteria: study of a UK population. *Muscle Nerve*. (2009) 39:432–8. doi: 10.1002/mus.21206

79. Hafsteinsdottir B, Olafsson E. Incidence and natural history of idiopathic chronic inflammatory demyelinating polyneuropathy: A population-based study in Iceland. *Eur Neurol*. (2016) 75:263–8. doi: 10.1159/000445884

80. Kridin K. Pemphigus group: overview, epidemiology, mortality, and comorbidities. *Immunol Res*. (2018) 66:255–70. doi: 10.1007/s12026-018-8986-7

81. Kridin K, Schmidt E. Epidemiology of pemphigus. *JID Innov*. (2021) 1:100004. doi: 10.1016/j.xjidi.2021.100004

82. Binks SNM, Klein CJ, Waters P, Pittock SJ, Irani SR. LGI1, CASPR2 and related antibodies: a molecular evolution of the phenotypes. *J Neurol Neurosurg Psychiatry*. (2018) 89:526–34. doi: 10.1136/jnnp-2017-315720

83. Niks EH, Kuks JB, Roep BO, Haasnoot GW, Verduijn W, Ballieux BE, et al. Strong association of MuSK antibody-positive myasthenia gravis and HLA-DR14-DQ5. *Neurology*. (2006) 66:1772–4. doi: 10.1212/01.wnl.0000218159.79769.5c

84. Bartoccioni E, Scuderi F, Augugliaro A, Chiatamone Ranieri S, Sauchelli D, Alboino P, et al. HLA class II allele analysis in MuSK-positive myasthenia gravis suggests a role for DQ5. *Neurology*. (2009) 72:195–7. doi: 10.1212/01.wnl.0000339103.08830.86

85. Alahgholi-Hajibehzad M, Yilmaz V, Gülsen-Parman Y, Aysal F, Oflazer P, Deymeer F, et al. Association of HLA-DRB1∗14, -DRB1∗16 and -DQB1∗05 with MuSK-myasthenia gravis in patients from Turkey. *Hum Immunol*. (2013) 74:1633–5. doi: 10.1016/j.humimm.2013.08.271

86. Ehsan S, Amirzargar A, Yekaninejad MS, Mahmoudi M, Mehravar S, Moradi B, et al. Association of HLA class II (DRB1, DQA1, DQB1) alleles and haplotypes with myasthenia gravis and its subgroups in the Iranian population. *J Neurol Sci*. (2015) 359:335–42. doi: 10.1016/j.jns.2015.11.021

87. Nikolic AV, Andric ZP, Simonovic RB, Rakocevic Stojanovic VM, Basta IZ, Bojic SD, et al. High frequency of DQB1*05 and absolute absence of DRB1*13 in muscle-specific tyrosine kinase positive myasthenia gravis. *Eur J Neurol*. (2015) 22:59–63. doi: 10.1111/ene.12525

88. Kanai T, Uzawa A, Kawaguchi N, Sakamaki T, Yoshiyama Y, Himuro K, et al. HLA-DRB1*14 and DQB1*05 are associated with Japanese anti-MuSK antibody-positive myasthenia gravis patients. *J Neurol Sci*. (2016) 363:116–8. doi: 10.1016/j.jns.2016.02.031

89. Hong Y, Li HF, Romi F, Skeie GO, Gilhus NE. HLA and MuSK-positive myasthenia gravis: A systemic review and meta-analysis. *Acta Neurol Scand*. (2018) 138:219–26. doi: 10.1111/ane.2018.138.issue-3

90. Blum S, Mccombe PA. Genetics of Guillain-Barré syndrome (GBS) and chronic inflammatory demyelinating polyradiculoneuropathy (CIDP): current knowledge and future directions. *J Peripher Nerv Syst*. (2014) 19:88–103. doi: 10.1111/jns5.12074

91. Moraes ME, Fernandez-Vina M, Lazaro A, Diaz LA, Filho GH, Friedman H, et al. An epitope in the third hypervariable region of the DRB1 gene is involved in the susceptibility to endemic pemphigus foliaceus (fogo selvagem) in three different Brazilian populations. *Tissue Antigens*. (1997) 49:35–40. doi: 10.1111/j.1399-0039.1997.tb02707.x

92. Loiseau P, Lecleach L, Prost C, Lepage V, Busson M, Bastuji-Garin S, et al. HLA class II polymorphism contributes to specify desmoglein derived peptides in pemphigus vulgaris and pemphigus foliaceus. *J Autoimmun*. (2000) 15:67–73. doi: 10.1006/jaut.2000.0388

93. Vodo D, Sarig O, Sprecher E. The genetics of pemphigus vulgaris. *Front Med (Lausanne)*. (2018) 5:226. doi: 10.3389/fmed.2018.00226

94. Schmidt E, Kasperkiewicz M, Joly P. Pemphigus. *Lancet*. (2019) 394:882–94. doi: 10.1016/S0140-6736(19)31778-7

95. Petzl-Erler ML. Beyond the HLA polymorphism: A complex pattern of genetic susceptibility to pemphigus. *Genet Mol Biol*. (2020) 43:e20190369. doi: 10.1590/1678-4685-gmb-2019-0369

96. Kim TJ, Lee ST, Moon J, Sunwoo JS, Byun JI, Lim JA, et al. Anti-LGI1 encephalitis is associated with unique HLA subtypes. *Ann Neurol*. (2017) 81:183–92. doi: 10.1002/ana.24860

97. Binks S, Varley J, Lee W, Makuch M, Elliott K, Gelfand JM, et al. Distinct HLA associations of LGI1 and CASPR2-antibody diseases. *Brain*. (2018) 141:2263–71. doi: 10.1093/brain/awy109

98. Muñiz-Castrillo S, Joubert B, Elsensohn MH, Pinto AL, Saint-Martin M, Vogrig A, et al. Anti-CASPR2 clinical phenotypes correlate with HLA and immunological features. *J Neurol Neurosurg Psychiatry*. (2020) 91:1076–84. doi: 10.1136/jnnp-2020-323226

99. Terao C, Ota M, Iwasaki T, Shiokawa M, Kawaguchi S, Kuriyama K, et al. IgG4-related disease in the Japanese population: a genome-wide association study. *Lancet Rheumatol*. (2019) 1:e14–22. doi: 10.1016/S2665-9913(19)30006-2

100. Vincent A. Unravelling the pathogenesis of myasthenia gravis. *Nat Rev Immunol*. (2002) 2:797–804. doi: 10.1038/nri916

101. Gilhus NE. Myasthenia gravis. *N Engl J Med*. (2016) 375:2570–81. doi: 10.1056/NEJMra1602678

102. Glass DJ, Bowen DC, Stitt TN, Radziejewski C, Bruno J, Ryan TE, et al. Agrin acts via a MuSK receptor complex. *Cell*. (1996) 85:513–23. doi: 10.1016/S0092-8674(00)81252-0

103. Lindstrom JM, Engel AG, Seybold ME, Lennon VA, Lambert EH. Pathological mechanisms in experimental autoimmune myasthenia gravis. II. Passive transfer of experimental autoimmune myasthenia gravis in rats with anti-acetylcholine recepotr antibodies. *J Exp Med*. (1976) 144:739–53. doi: 10.1084/jem.144.3.739

104. Lindstrom JM, Seybold ME, Lennon VA, Whittingham S, Duane DD. Antibody to acetylcholine receptor in myasthenia gravis. Prevalence, clinical correlates, and diagnostic value. *Neurology*. (1976) 26:1054–9. doi: 10.1212/WNL.26.11.1054

105. Hoch W, Mcconville J, Helms S, Newsom-Davis J, Melms A, Vincent A. Auto-antibodies to the receptor tyrosine kinase MuSK in patients with myasthenia gravis without acetylcholine receptor antibodies. *Nat Med*. (2001) 7:365–8. doi: 10.1038/85520

106. Higuchi O, Hamuro J, Motomura M, Yamanashi Y. Autoantibodies to low-density lipoprotein receptor-related protein 4 in myasthenia gravis. *Ann Neurol*. (2011) 69:418–22. doi: 10.1002/ana.22312

107. Pevzner A, Schoser B, Peters K, Cosma NC, Karakatsani A, Schalke B, et al. Anti-LRP4 autoantibodies in AChR- and MuSK-antibody-negative myasthenia gravis. *J Neurol*. (2012) 259:427–35. doi: 10.1007/s00415-011-6194-7

108. Lazaridis K, Tzartos SJ. Autoantibody specificities in myasthenia gravis; implications for improved diagnostics and therapeutics. *Front Immunol*. (2020) 11. doi: 10.3389/fimmu.2020.00212

109. Koneczny I, Cossins J, Waters P, Beeson D, Vincent A. MuSK myasthenia gravis IgG4 disrupts the interaction of LRP4 with MuSK but both IgG4 and IgG1-3 can disperse preformed agrin-independent AChR clusters. *PloS One*. (2013) 8:e80695. doi: 10.1371/journal.pone.0080695

110. Cao M, Liu WW, Maxwell S, Huda S, Webster R, Evoli A, et al. IgG1-3 muSK antibodies inhibit AChR cluster formation, restored by SHP2 inhibitor, despite normal muSK, DOK7, or AChR subunit phosphorylation. *Neurol Neuroimmunol Neuroinflamm*. (2023) 10(6):e200147. doi: 10.1212/NXI.0000000000200147

111. Stathopoulos P, Kumar A, Nowak RJ, O'connor KC. Autoantibody-producing plasmablasts after B cell depletion identified in muscle-specific kinase myasthenia gravis. *JCI Insight*. (2017) 2:e94263–75. doi: 10.1172/jci.insight.94263

112. Huijbers MG, Vergoossen DL, Fillie-Grijpma YE, Van Es IE, Koning MT, Slot LM, et al. MuSK myasthenia gravis monoclonal antibodies: Valency dictates pathogenicity. *Neurol Neuroimmunol Neuroinflamm*. (2019) 6:e547. doi: 10.1212/NXI.0000000000000547

113. Takata K, Stathopoulos P, Cao M, Mane-Damas M, Fichtner ML, Benotti ES, et al. Characterization of pathogenic monoclonal autoantibodies derived from muscle-specific kinase myasthenia gravis patients. *JCI Insight*. (2019) 4. doi: 10.1172/jci.insight.127167

114. Fichtner ML, Hoehn KB, Ford EE, Mane-Damas M, Oh S, Waters P, et al. Reemergence of pathogenic, autoantibody-producing B cell clones in myasthenia gravis following B cell depletion therapy. *Acta Neuropathol Commun*. (2022) 10:154. doi: 10.1186/s40478-022-01454-0

115. Jennings CG, Dyer SM, Burden SJ. Muscle-specific trk-related receptor with a kringle domain defines a distinct class of receptor tyrosine kinases. *Proc Natl Acad Sci United States America*. (1993) 90:2895–9. doi: 10.1073/pnas.90.7.2895

116. Otsuka K, Ito M, Ohkawara B, Masuda A, Kawakami Y, Sahashi K, et al. Collagen Q and anti-MuSK autoantibody competitively suppress agrin/LRP4/MuSK signaling. *Sci Rep*. (2015) 5:13928. doi: 10.1038/srep13928

117. Huijbers MG, Zhang W, Klooster R, Niks EH, Friese MB, Straasheijm KR, et al. MuSK IgG4 autoantibodies cause myasthenia gravis by inhibiting binding between MuSK and Lrp4. *Proc Natl Acad Sci U.S.A*. (2013) 110:20783–8. doi: 10.1073/pnas.1313944110

118. Cole RN, Reddel SW, Gervásio OL, Phillips WD. Anti-MuSK patient antibodies disrupt the mouse neuromuscular junction. *Ann Neurol*. (2008) 63:782–9. doi: 10.1002/ana.21371

119. Klooster R, Plomp JJ, Huijbers MG, Niks EH, Straasheijm KR, Detmers FJ, et al. Muscle-specific kinase myasthenia gravis IgG4 autoantibodies cause severe neuromuscular junction dysfunction in mice. *Brain*. (2012) 135:1081–101. doi: 10.1093/brain/aws025

120. Plomp JJ, Huijbers MG, van der Maarel SM, Verschuuren JJ. Pathogenic IgG4 subclass autoantibodies in MuSK myasthenia gravis. *Ann N Y Acad Sci*. (2012) 1275:114–22. doi: 10.1111/j.1749-6632.2012.06808.x

121. Koneczny I, Stevens JA, De Rosa A, Huda S, Huijbers MG, Saxena A, et al. IgG4 autoantibodies against muscle-specific kinase undergo Fab-arm exchange in myasthenia gravis patients. *J Autoimmun*. (2017) 77:104–15. doi: 10.1016/j.jaut.2016.11.005

122. Fichtner ML, Vieni C, Redler RL, Kolich L, Jiang R, Takata K, et al. Affinity maturation is required for pathogenic monovalent IgG4 autoantibody development in myasthenia gravis. *J Exp Med*. (2020) 217(12):e20200513. doi: 10.1084/jem.20200513

123. Vergoossen DLE, Plomp JJ, Gstöttner C, Fillié-Grijpma YE, Augustinus R, Verpalen R, et al. Functional monovalency amplifies the pathogenicity of anti-MuSK IgG4 in myasthenia gravis. *Proc Natl Acad Sci U.S.A*. (2021) 118(13):e2020635118. doi: 10.1073/pnas.2020635118

124. Diaz-Manera J, Martinez-Hernandez E, Querol L, Klooster R, Rojas-Garcia R, Suarez-Calvet X, et al. Long-lasting treatment effect of rituximab in MuSK myasthenia. *Neurology*. (2012) 78:189–93. doi: 10.1212/WNL.0b013e3182407982

125. Marino M, Basile U, Spagni G, Napodano C, Iorio R, Gulli F, et al. Long lasting rituximab-induced reduction of specific - but not of total- IgG4 in MuSK-positive myasthenia gravis. *Front Immunol*. (2020) 11:2020. doi: 10.3389/fimmu.2020.00613

126. Berger B, Schröter N. Changes in antibody titers and clinical course in myasthenia gravis retrospective study. *Prog Neurol Psychiatry*. (2022) 26:28–33. doi: 10.1002/pnp.738

127. Triplett JD, Hardy TA, Riminton DS, Chu SYK, Reddel SW. Association between musk antibody concentrations and the myasthenia gravis composite score in 3 patients: A marker of relapse? *Muscle Nerve*. (2019) 60:307–11. doi: 10.1002/mus.26609

128. Dyck PJB, Tracy JA. History, diagnosis, and management of chronic inflammatory demyelinating polyradiculoneuropathy. *Mayo Clin Proc*. (2018) 93:777–93. doi: 10.1016/j.mayocp.2018.03.026

129. Stino AM, Naddaf E, Dyck PJ, Dyck PJB. Chronic inflammatory demyelinating polyradiculoneuropathy-Diagnostic pitfalls and treatment approach. *Muscle Nerve*. (2021) 63:157–69. doi: 10.1002/mus.27046

130. Stathopoulos P, Alexopoulos H, Dalakas MC. Autoimmune antigenic targets at the node of Ranvier in demyelinating disorders. *Nat Rev Neurol*. (2015) 11:143–56. doi: 10.1038/nrneurol.2014.260.

131. Uncini A, Vallat JM. Autoimmune nodo-paranodopathies of peripheral nerve: the concept is gaining ground. *J Neurol Neurosurg Psychiatry*. (2018) 89:627–35. doi: 10.1136/jnnp-2017-317192

132. Khadilkar SV, Kamat S, Patel R. Nodo-paranodopathies: concepts, clinical implications, and management. *Ann Indian Acad Neurol*. (2022) 25:1001–8. doi: 10.4103/aian.aian_382_22

133. Uncini A. Autoimmune nodo-paranodopathies 10 years later: Clinical features, pathophysiology and treatment. *J Peripher Nerv Syst*. (2023) 28 Suppl 3:S23–s35. doi: 10.1111/jns.12569

134. Mathey EK, Derfuss T, Storch MK, Williams KR, Hales K, Woolley DR, et al. Neurofascin as a novel target for autoantibody-mediated axonal injury. *J Exp Med*. (2007) 204:2363–72. doi: 10.1084/jem.20071053

135. Querol L, Nogales-Gadea G, Rojas-Garcia R, Martinez-Hernandez E, Diaz-Manera J, Suarez-Calvet X, et al. Antibodies to contactin-1 in chronic inflammatory demyelinating polyneuropathy. *Ann Neurol*. (2012) 73(3):370–80. doi: 10.1002/ana.23794

136. Doppler K, Appeltshauser L, Villmann C, Martin C, Peles E, Krämer HH, et al. Auto-antibodies to contactin-associated protein 1 (Caspr) in two patients with painful inflammatory neuropathy. *Brain*. (2016) 139:2617–30. doi: 10.1093/brain/aww189

137. Delmont E, Manso C, Querol L, Cortese A, Berardinelli A, Lozza A, et al. Autoantibodies to nodal isoforms of neurofascin in chronic inflammatory demyelinating polyneuropathy. *Brain*. (2017) 140:1851–8. doi: 10.1093/brain/awx124

138. Querol L, Siles AM, Alba-Rovira R, Jáuregui A, Devaux J, Faivre-Sarrailh C, et al. Antibodies against peripheral nerve antigens in chronic inflammatory demyelinating polyradiculoneuropathy. *Sci Rep*. (2017) 7:14411. doi: 10.1038/s41598-017-14853-4

139. Manso C, Querol L, Mekaouche M, Illa I, Devaux JJ. Contactin-1 IgG4 antibodies cause paranode dismantling and conduction defects. *Brain*. (2016) 139:1700–12. doi: 10.1093/brain/aww062

140. Manso C, Querol L, Lleixà C, Poncelet M, Mekaouche M, Vallat JM, et al. Anti-Neurofascin-155 IgG4 antibodies prevent paranodal complex formation in *vivo*. *J Clin Invest*. (2019) 129:2222–36. doi: 10.1172/JCI124694

141. Jentzer A, Attal A, Roué C, Raymond J, Lleixà C, Illa I, et al. IgG4 valency modulates the pathogenicity of anti–neurofascin-155 igG4 in autoimmune nodopathy. *Neurol - Neuroimmunology Neuroinflamm*. (2022) 9:e200014. doi: 10.1212/NXI.0000000000200014

142. Taieb G, Jentzer A, Vegezzi E, Lleixà C, Illa I, Querol L, et al. Effect of monovalency on anti-contactin-1 IgG4. *Front Immunol*. (2023) 14:1021513. doi: 10.3389/fimmu.2023.1021513

143. Appeltshauser L, Junghof H, Messinger J, Linke J, Haarmann A, Ayzenberg I, et al. Anti-pan-neurofascin antibodies induce subclass-related complement activation and nodo-paranodal damage. *Brain*. (2023) 146:1932–49. doi: 10.1093/brain/awac418

144. Bresciani L, Salvalaggio A, Vegezzi E, Visentin A, Fortuna A, Anglani M, et al. Caspr1 antibodies autoimmune paranodopathy with severe tetraparesis: Potential relevance of antibody titers in monitoring treatment response. *J Peripher Nerv Syst*. (2023) 28:522–7. doi: 10.1111/jns.12565

145. Malik AM, Tupchong S, Huang S, Are A, Hsu S, Motaparthi K. An updated review of pemphigus diseases. *Medicina (Kaunas)*. (2021) 57(10):1080. doi: 10.3390/medicina57101080

146. Fuchs M, Kugelmann D, Schlegel N, Vielmuth F, Waschke J. Desmoglein 2 can undergo Ca2+-dependent interactions with both desmosomal and classical cadherins including E-cadherin and N-cadherin. *Biophys J*. (2022) 121:1322–35. doi: 10.1016/j.bpj.2022.02.023

147. Amagai M. Autoimmune and infectious skin diseases that target desmogleins. *Proc Jpn Acad Ser B Phys Biol Sci*. (2010) 86:524–37. doi: 10.2183/pjab.86.524

148. Di Zenzo G, Di Lullo G, Corti D, Calabresi V, Sinistro A, Vanzetta F, et al. Pemphigus autoantibodies generated through somatic mutations target the desmoglein-3 cis-interface. *J Clin Invest*. (2012) 122:3781–90. doi: 10.1172/JCI64413

149. Rock B, Martins CR, Theofilopoulos AN, Balderas RS, Anhalt GJ, Labib RS, et al. The pathogenic effect of IgG4 autoantibodies in endemic pemphigus foliaceus (fogo selvagem). *N Engl J Med*. (1989) 320:1463–9. doi: 10.1056/NEJM198906013202206

150. Ishii K, Harada R, Matsuo I, Shirakata Y, Hashimoto K, Amagai M. *In vitro* keratinocyte dissociation assay for evaluation of the pathogenicity of anti-desmoglein 3 IgG autoantibodies in pemphigus vulgaris. *J Invest Dermatol*. (2005) 124:939–46. doi: 10.1111/j.0022-202X.2005.23714.x

151. Payne AS, Ishii K, Kacir S, Lin C, Li H, Hanakawa Y, et al. Genetic and functional characterization of human pemphigus vulgaris monoclonal autoantibodies isolated by phage display. *J Clin Invest*. (2005) 115:888–99. doi: 10.1172/JCI24185

152. Saito M, Stahley SN, Caughman CY, Mao X, Tucker DK, Payne AS, et al. Signaling dependent and independent mechanisms in pemphigus vulgaris blister formation. *PloS One*. (2012) 7:e50696. doi: 10.1371/journal.pone.0050696

153. Bhol K, Natarajan K, Nagarwalla N, Mohimen A, Aoki V, Ahmed AR. Correlation of peptide specificity and IgG subclass with pathogenic and nonpathogenic autoantibodies in pemphigus vulgaris: a model for autoimmunity. *Proc Natl Acad Sci U.S.A*. (1995) 92:5239–43. doi: 10.1073/pnas.92.11.5239

154. Kricheli D, David M, Frusic-Zlotkin M, Goldsmith D, Rabinov M, Sulkes J, et al. The distribution of pemphigus vulgaris-IgG subclasses and their reactivity with desmoglein 3 and 1 in pemphigus patients and their first-degree relatives. *Br J Dermatol*. (2000) 143:337–42. doi: 10.1046/j.1365-2133.2000.03659.x

155. Warren SJ, Arteaga LA, Rivitti EA, Aoki V, Hans-Filho G, Qaqish BF, et al. The role of subclass switching in the pathogenesis of endemic pemphigus foliaceus. *J Invest Dermatol*. (2003) 120:104–8. doi: 10.1046/j.1523-1747.2003.12017.x

156. Yamamoto Y, Aoyama Y, Shu E, Tsunoda K, Amagai M, Kitajima Y. Anti-desmoglein 3 (Dsg3) monoclonal antibodies deplete desmosomes of Dsg3 and differ in their Dsg3-depleting activities related to pathogenicity. *J Biol Chem*. (2007) 282:17866–76. doi: 10.1074/jbc.M607963200

157. Egu DT, Walter E, Spindler V, Waschke J. Inhibition of p38MAPK signalling prevents epidermal blistering and alterations of desmosome structure induced by pemphigus autoantibodies in human epidermis. *Br J Dermatol*. (2017) 177:1612–8. doi: 10.1111/bjd.15721

158. Yoshida K, Ishii K, Shimizu A, Yokouchi M, Amagai M, Shiraishi K, et al. Non-pathogenic pemphigus foliaceus (PF) IgG acts synergistically with a directly pathogenic PF IgG to increase blistering by p38MAPK-dependent desmoglein 1 clustering. *J Dermatol Sci*. (2017) 85:197–207. doi: 10.1016/j.jdermsci.2016.12.010

159. Rock B, Labib RS, Diaz LA. Monovalent Fab' immunoglobulin fragments from endemic pemphigus foliaceus autoantibodies reproduce the human disease in neonatal Balb/c mice. *J Clin Invest*. (1990) 85:296–9. doi: 10.1172/JCI114426

160. Mascaró JM Jr., España A, Liu Z, Ding X, Swartz SJ, Fairley JA, et al. Mechanisms of acantholysis in pemphigus vulgaris: role of IgG valence. *Clin Immunol Immunopathol*. (1997) 85:90–6. doi: 10.1006/clin.1997.4408

161. Tsunoda K, Ota T, Saito M, Hata T, Shimizu A, Ishiko A, et al. Pathogenic relevance of IgG and IgM antibodies against desmoglein 3 in blister formation in pemphigus vulgaris. *Am J Pathol*. (2011) 179:795–806. doi: 10.1016/j.ajpath.2011.04.015

162. Bhol K, Tyagi S, Natarajan K, Nagarwalla N, Ahmed AR. Use of recombinant pemphigus vulgaris antigen in development of ELISA and IB assays to detect pemphigus vulgaris autoantibodies. *J Eur Acad Dermatol Venereol*. (1998) 10:28–35. doi: 10.1111/j.1468-3083.1998.tb00924.x

163. Bracke S, Speeckaert R, Van Geel N, De Bacquer D, Lambert J. Evaluation of commercially available ELISA assays as a tool for monitoring and managing pemphigus patients: a prospective study. *Eur J Dermatol*. (2013) 23:33–9. doi: 10.1684/ejd.2012.1901

164. Ryding M, Mikkelsen AW, Nissen MS, Nilsson AC, Blaabjerg M. Pathophysiological effects of autoantibodies in autoimmune encephalitides. *Cells*. (2024) 13(1):15. doi: 10.3390/cells13010015

165. Seery N, Butzkueven H, O'brien TJ, Monif M. Contemporary advances in antibody-mediated encephalitis: anti-LGI1 and anti-Caspr2 antibody (Ab)-mediated encephalitides. *Autoimmun Rev*. (2022) 21:103074. doi: 10.1016/j.autrev.2022.103074

166. Toshika O, Yuko F, Miwako Y, Taisuke M, Norihiko Y, Hiroshi T, et al. Autoantibodies to epilepsy-related LGI1 in limbic encephalitis neutralize LGI1-ADAM22 interaction and reduce synaptic AMPA receptors. *J Neurosci*. (2013) 33:18161. doi: 10.1523/JNEUROSCI.3506-13.2013

167. Petit-Pedrol M, Sell J, Planagumà J, Mannara F, Radosevic M, Haselmann H, et al. LGI1 antibodies alter Kv1.1 and AMPA receptors changing synaptic excitability, plasticity and memory. *Brain*. (2018) 141:3144–59. doi: 10.1093/brain/awy253

168. Joubert B, Petit-Pedrol M, Planagumà J, Mannara F, Radosevic M, Marsal M, et al. Human CASPR2 antibodies reversibly alter memory and the CASPR2 protein complex. *Ann Neurol*. (2022) 91:801–13. doi: 10.1002/ana.26345

169. Patterson KR, Dalmau J, Lancaster E. Mechanisms of Caspr2 antibodies in autoimmune encephalitis and neuromyotonia. *Ann Neurol*. (2018) 83:40–51. doi: 10.1002/ana.25120

170. Kamisawa T, Zen Y, Pillai S, Stone JH. IgG4-related disease. *Lancet*. (2015) 385:1460–71. doi: 10.1016/S0140-6736(14)60720-0

171. Perugino CA, Stone JH. IgG4-related disease: an update on pathophysiology and implications for clinical care. *Nat Rev Rheumatol*. (2020) 16:702–14. doi: 10.1038/s41584-020-0500-7

172. Kamisawa T, Funata N, Hayashi Y, Eishi Y, Koike M, Tsuruta K, et al. A new clinicopathological entity of IgG4-related autoimmune disease. *J Gastroenterol*. (2003) 38:982–4. doi: 10.1007/s00535-003-1175-y

173. Stone JH, Zen Y, Deshpande V. IgG4-related disease. *New Engl J Med*. (2012) 366:539–51. doi: 10.1056/NEJMra1104650

174. Deshpande V, Zen Y, Chan JK, Yi EE, Sato Y, Yoshino T, et al. Consensus statement on the pathology of IgG4-related disease. *Mod Pathol*. (2012) 25:1181–92. doi: 10.1038/modpathol.2012.72

175. Wallace ZS, Naden RP, Chari S, Choi H, Della-Torre E, Dicaire JF, et al. The 2019 american college of rheumatology/european league against rheumatism classification criteria for igG4-related disease. *Arthritis Rheumatol*. (2020) 72:7–19. doi: 10.1002/art.41120

176. Mattoo H, Stone JH, Pillai S. Clonally expanded cytotoxic CD4+ T cells and the pathogenesis of IgG4-related disease. *Autoimmunity*. (2017) 50:19–24. doi: 10.1080/08916934.2017.1280029

177. Pillai S, Perugino C, Kaneko N. Immune mechanisms of fibrosis and inflammation in IgG4-related disease. *Curr Opin Rheumatol*. (2020) 32:146–51. doi: 10.1097/BOR.0000000000000686

178. Perugino CA, Kaneko N, Maehara T, Mattoo H, Kers J, Allard-Chamard H, et al. CD4(+) and CD8(+) cytotoxic T lymphocytes may induce mesenchymal cell apoptosis in IgG(4)-related disease. *J Allergy Clin Immunol*. (2021) 147:368–82. doi: 10.1016/j.jaci.2020.05.022

179. Perugino CA, Alsalem SB, Mattoo H, Della-Torre E, Mahajan V, Ganesh G, et al. Identification of galectin-3 as an autoantigen in patients with IgG(4)-related disease. *J Allergy Clin Immunol*. (2019) 143:736–745.e736. doi: 10.1016/j.jaci.2018.05.01

180. Fugger L, Jensen LT, Rossjohn J. Challenges, progress, and prospects of developing therapies to treat autoimmune diseases. *Cell*. (2020) 181:63–80. doi: 10.1016/j.cell.2020.03.007

181. Bashford-Rogers RJM, Bergamaschi L, Mckinney EF, Pombal DC, Mescia F, Lee JC, et al. Analysis of the B cell receptor repertoire in six immune-mediated diseases. *Nature*. (2019) 574:122–6. doi: 10.1038/s41586-019-1595-3

182. Edwards JC, Szczepanski L, Szechinski J, Filipowicz-Sosnowska A, Emery P, Close DR, et al. Efficacy of B-cell-targeted therapy with rituximab in patients with rheumatoid arthritis. *N Engl J Med*. (2004) 350:2572–81. doi: 10.1056/NEJMoa032534

183. Hauser SL, Waubant E, Arnold DL, Vollmer T, Antel J, Fox RJ, et al. B-cell depletion with rituximab in relapsing-remitting multiple sclerosis. *N Engl J Med*. (2008) 358:676–88. doi: 10.1056/NEJMoa0706383

184. Joly P, Maho-Vaillant M, Prost-Squarcioni C, Hebert V, Houivet E, Calbo S, et al. First-line rituximab combined with short-term prednisone versus prednisone alone for the treatment of pemphigus (Ritux 3): a prospective, multicentre, parallel-group, open-label randomised trial. *Lancet*. (2017) 389:2031–40. doi: 10.1016/S0140-6736(17)30070-3

185. Nowak RJ, Dicapua DB, Zebardast N, Goldstein JM. Response of patients with refractory myasthenia gravis to rituximab: a retrospective study. *Ther Adv Neurol Disord*. (2011) 4:259–66. doi: 10.1177/1756285611411503

186. Blum S, Gillis D, Brown H, Boyle R, Henderson R, Heyworth-Smith D, et al. Use and monitoring of low dose rituximab in myasthenia gravis. *J Neurol Neurosurg Psychiatry*. (2011) 82:659–63. doi: 10.1136/jnnp.2010.220475

187. Robeson KR, Kumar A, Keung B, Dicapua DB, Grodinsky E, Patwa HS, et al. Durability of the rituximab response in acetylcholine receptor autoantibody-positive myasthenia gravis. *JAMA Neurol*. (2016) 74(1):60–6. doi: 10.1001/jamaneurol.2016.4190

188. Anolik JH, Barnard J, Owen T, Zheng B, Kemshetti S, Looney RJ, et al. Delayed memory B cell recovery in peripheral blood and lymphoid tissue in systemic lupus erythematosus after B cell depletion therapy. *Arthritis Rheum*. (2007) 56:3044–56. doi: 10.1002/art.22810

189. Adlowitz DG, Barnard J, Biear JN, Cistrone C, Owen T, Wang W, et al. Expansion of activated peripheral blood memory B cells in rheumatoid arthritis, impact of B cell depletion therapy, and biomarkers of response. *PloS One*. (2015) 10:e0128269. doi: 10.1371/journal.pone.0128269

190. Jiang R, Fichtner ML, Hoehn KB, Pham MC, Stathopoulos P, Nowak RJ, et al. Single-cell repertoire tracing identifies rituximab-resistant B cells during myasthenia gravis relapses. *JCI Insight*. (2020) 5(14):e136471. doi: 10.1172/jci.insight.136471

191. Querol L, Rojas-García R, Diaz-Manera J, Barcena J, Pardo J, Ortega-Moreno A, et al. Rituximab in treatment-resistant CIDP with antibodies against paranodal proteins. *Neurol Neuroimmunol Neuroinflamm*. (2015) 2:e149. doi: 10.1212/NXI.0000000000000149

192. Roux T, Debs R, Maisonobe T, Lenglet T, Delorme C, Louapre C, et al. Rituximab in chronic inflammatory demyelinating polyradiculoneuropathy with associated diseases. *J Peripheral Nervous Syst*. (2018) 23:235–40. doi: 10.1111/jns.12287

193. Jiao L, Xiang Y, Li S, Zhang F, Ruan X, Guo S. Efficacy of low dose rituximab in treatment-resistant CIDP with antibodies against NF-155. *J Neuroimmunol*. (2020) 345:577280. doi: 10.1016/j.jneuroim.2020.577280

194. Martín-Aguilar L, Lleixà C, Pascual-Goñi E, Caballero-Ávila M, Martínez-Martínez L, Díaz-Manera J, et al. Clinical and laboratory features in anti-NF155 autoimmune nodopathy. *Neurol Neuroimmunol Neuroinflamm*. (2022) 9(1):e1098. doi: 10.1212/NXI.0000000000001098

195. Wang W, Liu C, Li W, Zhang D, Shan Y, Zheng J, et al. Clinical and diagnostic features of anti-neurofascin-155 antibody-positive neuropathy in Han Chinese. *Ann Clin Trans Neurol*. (2022) 9:695–706. doi: 10.1002/acn3.51550

196. Leuci S, Levine D, Zhang J, Razzaque Ahmed A. Response in patients with pemphigus vulgaris to rituximab therapy. Basis of the biology of B cells. *G Ital Dermatol Venereol*. (2009) 144:379–409.

197. Wang HH, Liu CW, Li YC, Huang YC. Efficacy of rituximab for pemphigus: a systematic review and meta-analysis of different regimens. *Acta Derm Venereol*. (2015) 95:928–32. doi: 10.2340/00015555-2116

198. Mahmoudi H, Tavakolpour S, Balighi K, Farid AS, Nili A, Jan D, et al. Rituximab in practice: Clinical evaluation of patients with pemphigus after rituximab administration. *Dermatologic Ther*. (2021) 34:e14633. doi: 10.1111/dth.14633

199. Thaler FS, Zimmermann L, Kammermeier S, Strippel C, Ringelstein M, Kraft A, et al. Rituximab treatment and long-term outcome of patients with autoimmune encephalitis: real-world evidence from the GENERATE registry. *Neurol Neuroimmunol Neuroinflamm*. (2021) 8(6):e1088. doi: 10.1212/NXI.0000000000001088

200. Bastakoti S, Kunwar S, Poudel S, Quinonez J, Bista S, Singh N, et al. Rituximab in the management of refractory myasthenia gravis and variability of its efficacy in anti-muSK positive and anti-AChR positive myasthenia gravis. *Cureus*. (2021) 13:e19416. doi: 10.7759/cureus.19416

201. Chaganti S, Hannaford A, Vucic S. Rituximab in chronic immune mediated neuropathies: a systematic review. *Neuromuscul Disord*. (2022) 32:621–7. doi: 10.1016/j.nmd.2022.05.013

202. Landon-Cardinal O, Friedman D, Guiguet M, Laforêt P, Heming N, Salort-Campana E, et al. Efficacy of rituximab in refractory generalized anti-AChR myasthenia gravis. *J Neuromuscul Dis*. (2018) 5:241–9. doi: 10.3233/JND-180300

203. Brauner S, Eriksson-Dufva A, Hietala MA, Frisell T, Press R, Piehl F. Comparison between rituximab treatment for new-onset generalized myasthenia gravis and refractory generalized myasthenia gravis. *JAMA Neurol*. (2020) 77:974–81. doi: 10.1001/jamaneurol.2020.0851

204. Piehl F, Eriksson-Dufva A, Budzianowska A, Feresiadou A, Hansson W, Hietala MA, et al. Efficacy and safety of rituximab for new-onset generalized myasthenia gravis: the RINOMAX randomized clinical trial. *JAMA Neurol*. (2022) 79:1105–12. doi: 10.1001/jamaneurol.2022.2887

205. Mahmoudi H, Balighi K, Tavakolpour S, Daneshpazhooh M. Unexpected worsening of pemphigus vulgaris after rituximab: A report of three cases. *Int Immunopharmacol*. (2019) 71:40–2. doi: 10.1016/j.intimp.2019.02.037

206. Bai Y, Li W, Yan C, Hou Y, Wang Q. Anti-rituximab antibodies in patients with refractory autoimmune nodopathy with anti-neurofascin-155 antibody. *Front Immunol*. (2023) 14. doi: 10.3389/fimmu.2023.1121705

207. Casertano S, Signoriello E, Rossi F, Di Pietro A, Tuccillo F, Bonavita S, et al. Ocrelizumab in a case of refractory chronic inflammatory demyelinating polyneuropathy with anti-rituximab antibodies. *Eur J Neurol*. (2020) 27:2673–5. doi: 10.1111/ene.14498

208. Schuh E, Berer K, Mulazzani M, Feil K, Meinl I, Lahm H, et al. Features of human CD3+CD20+ T cells. *J Immunol*. (2016) 197:1111–7. doi: 10.4049/jimmunol.1600089

209. Vlaming M, Bilemjian V, Freile J.Á., Lourens HJ, Van Rooij N, Huls G, et al. CD20 positive CD8 T cells are a unique and transcriptionally-distinct subset of T cells with distinct transmigration properties. *Sci Rep*. (2021) 11:20499. doi: 10.1038/s41598-021-00007-0

210. Lee AYS. CD20(+) T cells: an emerging T cell subset in human pathology. *Inflammation Res*. (2022) 71:1181–9. doi: 10.1007/s00011-022-01622-x

211. Palanichamy A, Jahn S, Nickles D, Derstine M, Abounasr A, Hauser SL, et al. Rituximab efficiently depletes increased CD20-expressing T cells in multiple sclerosis patients. *J Immunol*. (2014) 193:580–6. doi: 10.4049/jimmunol.1400118

212. Hultin LE, Hausner MA, Hultin PM, Giorgi JV. CD20 (pan-B cell) antigen is expressed at a low level on a subpopulation of human T lymphocytes. *Cytometry*. (1993) 14:196–204. doi: 10.1002/cyto.990140212

213. Henry C, Ramadan A, Montcuquet N, Pallandre JR, Mercier-Letondal P, Deschamps M, et al. CD3+CD20+ cells may be an artifact of flow cytometry: comment on the article by Wilk et al. *Arthritis Rheum*. (2010) 62:2561–2563; author reply 2563-2565. doi: 10.1002/art.27527

214. Pavlasova G, Mraz M. The regulation and function of CD20: an "enigma" of B-cell biology and targeted therapy. *Haematologica*. (2020) 105:1494–506. doi: 10.3324/haematol.2019.243543

215. Wilk E, Witte T, Marquardt N, Horvath T, Kalippke K, Scholz K, et al. Depletion of functionally active CD20+ T cells by rituximab treatment. *Arthritis Rheum*. (2009) 60:3563–71. doi: 10.1002/art.24998

216. De Bruyn M, Wiersma VR, Wouters MC, Samplonius DF, Klip HG, Helfrich W, et al. CD20(+) T cells have a predominantly Tc1 effector memory phenotype and are expanded in the ascites of patients with ovarian cancer. *Oncoimmunology*. (2015) 4: e999536. doi: 10.1080/2162402X.2014.999536

217. Chen Q, Yuan S, Sun H, Peng L. CD3(+)CD20(+) T cells and their roles in human diseases. *Hum Immunol*. (2019) 80:191–4. doi: 10.1016/j.humimm.2019.01.001

218. Ochs J, Nissimov N, Torke S, Freier M, Grondey K, Koch J, et al. Proinflammatory CD20(+) T cells contribute to CNS-directed autoimmunity. *Sci Transl Med*. (2022) 14:eabi4632. doi: 10.1126/scitranslmed.abi4632

219. Murayama Y, Mukai R, Sata T, Matsunaga S, Noguchi A, Yoshikawa Y. Transient expression of CD20 antigen (pan B cell marker) in activated lymph node T cells. *Microbiol Immunol*. (1996) 40:467–71. doi: 10.1111/j.1348-0421.1996.tb01096.x

220. Takami A, Saito M, Nakao S, Asakura H, Nozue T, Onoe Y, et al. CD20-positive T-cell chronic lymphocytic leukaemia. *Br J Haematol*. (1998) 102:1327–9. doi: 10.1046/j.1365-2141.1998.00884.x

221. Sabatino JJ Jr., Wilson MR, Calabresi PA, Hauser SL, Schneck JP, Zamvil SS. Anti-CD20 therapy depletes activated myelin-specific CD8(+) T cells in multiple sclerosis. *Proc Natl Acad Sci U.S.A*. (2019) 116:25800–7. doi: 10.1073/pnas.1915309116

222. Mathias A, Pantazou V, Perriot S, Canales M, Jones S, Oberholster L, et al. Ocrelizumab impairs the phenotype and function of memory CD8(+) T cells: A 1-year longitudinal study in patients with multiple sclerosis. *Neurol Neuroimmunol Neuroinflamm*. (2023) 10(2):e200084. doi: 10.1212/NXI.0000000000200084

223. Shinoda K, Li R, Rezk A, Mexhitaj I, Patterson KR, Kakara M, et al. Differential effects of anti-CD20 therapy on CD4 and CD8 T cells and implication of CD20-expressing CD8 T cells in MS disease activity. *Proc Natl Acad Sci U.S.A*. (2023) 120: e2207291120. doi: 10.1073/pnas.2207291120

224. Hershberg U, Meng W, Zhang B, Haff N, St Clair EW, Cohen PL, et al. Persistence and selection of an expanded B-cell clone in the setting of rituximab therapy for Sjögren's syndrome. *Arthritis Res Ther*. (2014) 16:R51. doi: 10.1186/ar4481

225. De Bourcy CFA, Dekker CL, Davis MM, Nicolls MR, Quake SR. Dynamics of the human antibody repertoire after B cell depletion in systemic sclerosis. *Sci Immunol*. (2017) 2(15):eaan8289. doi: 10.1126/sciimmunol.aan8289

226. Leandro MJ, Cambridge G, Ehrenstein MR, Edwards JCW. Reconstitution of peripheral blood B cells after depletion with rituximab in patients with rheumatoid arthritis. *Arthritis Rheumatism*. (2006) 54:613–20. doi: 10.1002/art.21617

227. Mamani-Matsuda M, Cosma A, Weller S, Faili A, Staib C, Garçon L, et al. The human spleen is a major reservoir for long-lived vaccinia virus–specific memory B cells. *Blood*. (2008) 111:4653–9. doi: 10.1182/blood-2007-11-123844

228. Ramwadhdoebe TH, Van Baarsen LGM, Boumans MJH, Bruijnen STG, Safy M, Berger FH, et al. Effect of rituximab treatment on T and B cell subsets in lymph node biopsies of patients with rheumatoid arthritis. *Rheumatology*. (2019) 58:1075–85. doi: 10.1093/rheumatology/key428

229. Nakou M, Katsikas G, Sidiropoulos P, Bertsias G, Papadimitraki E, Raptopoulou A, et al. Rituximab therapy reduces activated B cells in both the peripheral blood and bone marrow of patients with rheumatoid arthritis: depletion of memory B cells correlates with clinical response. *Arthritis Res Ther*. (2009) 11:R131. doi: 10.1186/ar2798

230. Colliou N, Picard D, Caillot F, Calbo S, Le Corre S, Lim A, et al. Long-term remissions of severe pemphigus after rituximab therapy are associated with prolonged failure of desmoglein B cell response. *Sci Transl Med*. (2013) 5:175ra130. doi: 10.1126/scitranslmed.3005166

231. Maurer MA, Tuller F, Gredler V, Berger T, Lutterotti A, Lünemann JD, et al. Rituximab induces clonal expansion of IgG memory B-cells in patients with inflammatory central nervous system demyelination. *J Neuroimmunol*. (2016) 290:49–53. doi: 10.1016/j.jneuroim.2015.11.006

232. Becerra E, de la Torre I, Leandro MJ, Cambridge G. B cell phenotypes in patients with rheumatoid arthritis relapsing after rituximab: expression of B cell-activating factor-binding receptors on B cell subsets. *Clin Exp Immunol*. (2017) 190:372–83. doi: 10.1111/cei.13024

233. Wang K, Wei G, Liu D. CD19: a biomarker for B cell development, lymphoma diagnosis and therapy. *Exp Hematol Oncol*. (2012) 1:36. doi: 10.1186/2162-3619-1-36

234. Forsthuber TG, Cimbora DM, Ratchford JN, Katz E, Stüve O. B cell-based therapies in CNS autoimmunity: differentiating CD19 and CD20 as therapeutic targets. *Ther Adv Neurol Disord*. (2018) 11:1756286418761697. doi: 10.1177/1756286418761697

235. Hofmann K, Clauder AK, Manz RA. Targeting B cells and plasma cells in autoimmune diseases. *Front Immunol*. (2018) 9:835. doi: 10.3389/fimmu.2018.00835

236. Chu SY, Yeter K, Kotha R, Pong E, Miranda Y, Phung S, et al. Suppression of rheumatoid arthritis B cells by XmAb5871, an anti-CD19 antibody that coengages B cell antigen receptor complex and Fcγ receptor IIb inhibitory receptor. *Arthritis Rheumatol*. (2014) 66:1153–64. doi: 10.1002/art.38334

237. Cree BA, Bennett JL, Sheehan M, Cohen J, Hartung HP, Aktas O, et al. Placebo-controlled study in neuromyelitis optica-Ethical and design considerations. *Mult Scler*. (2016) 22:862–72. doi: 10.1177/1352458515620934

238. Lee HC. Structure and enzymatic functions of human CD38. *Mol Med*. (2006) 12:317–23. doi: 10.2119/2006-00086.Lee

239. Piedra-Quintero ZL, Wilson Z, Nava P, Guerau-De-Arellano M. CD38: an immunomodulatory molecule in inflammation and autoimmunity. *Front Immunol*. (2020) 11:597959. doi: 10.3389/fimmu.2020.597959

240. Ye X, Zhao Y, Ma W, Ares I, Martínez M, Lopez-Torres B, et al. The potential of CD38 protein as a target for autoimmune diseases. *Autoimmun Rev*. (2023) 22:103289. doi: 10.1016/j.autrev.2023.103289

241. Bisht K, Fukao T, Chiron M, Richardson P, Atanackovic D, Chini E, et al. Immunomodulatory properties of CD38 antibodies and their effect on anticancer efficacy in multiple myeloma. *Cancer Med*. (2023) 12:20332–52. doi: 10.1002/cam4.6619

242. Leleu X, Martin T, Weisel K, Schjesvold F, Iida S, Malavasi F, et al. Anti-CD38 antibody therapy for patients with relapsed/refractory multiple myeloma: differential mechanisms of action and recent clinical trial outcomes. *Ann Hematol*. (2022) 101:2123–37. doi: 10.1007/s00277-022-04917-5

243. Karnell JL, Rieder SA, Ettinger R, Kolbeck R. Targeting the CD40-CD40L pathway in autoimmune diseases: Humoral immunity and beyond. *Adv Drug Delivery Rev*. (2019) 141:92–103. doi: 10.1016/j.addr.2018.12.005

244. Tang T, Cheng X, Truong B, Sun L, Yang X, Wang H. Molecular basis and therapeutic implications of CD40/CD40L immune checkpoint. *Pharmacol Ther*. (2021) 219:107709. doi: 10.1016/j.pharmthera.2020.107709

245. Gomezmancilla B, Meriggioli MN, Genge A, Roubenoff R, Espié P, Dupuy C, et al. Efficacy and safety of iscalimab, a novel anti-CD40 monoclonal antibody, in moderate-to-severe myasthenia gravis: A phase 2 randomized study. *J Clin Neurosci*. (2024) 119:76–84. doi: 10.1016/j.jocn.2023.11.013

246. Fisher BA, Szanto A, Ng WF, Bombardieri M, Posch MG, Papas AS, et al. Assessment of the anti-CD40 antibody iscalimab in patients with primary Sjögren's syndrome: a multicentre, randomised, double-blind, placebo-controlled, proof-of-concept study. *Lancet Rheumatol*. (2020) 2:e142–52. doi: 10.1016/S2665-9913(19)30135-3

247. Kahaly GJ, Stan MN, Frommer L, Gergely P, Colin L, Amer A, et al. A novel anti-CD40 monoclonal antibody, iscalimab, for control of graves hyperthyroidism-A proof-of-concept trial. *J Clin Endocrinol Metab*. (2020) 105(3):dgz013. doi: 10.1210/clinem/dgz013

248. Aoki-Ota M, Kinoshita M, Ota T, Tsunoda K, Iwasaki T, Tanaka S, et al. Tolerance induction by the blockade of CD40/CD154 interaction in pemphigus vulgaris mouse model. *J Invest Dermatol*. (2006) 126:105–13. doi: 10.1038/sj.jid.5700016

249. Bilgic Temel A, Murrell DF. Pharmacological advances in pemphigus. *Curr Opin Pharmacol*. (2019) 46:44–9. doi: 10.1016/j.coph.2019.01.001

250. Cancro MP. *BLyS ligands and receptors*. Totowa, NJ: Humana Press (2010). doi: 10.1007/978-1-60327-013-7

251. Vincent FB, Saulep-Easton D, Figgett WA, Fairfax KA, Mackay F. The BAFF/APRIL system: emerging functions beyond B cell biology and autoimmunity. *Cytokine Growth Factor Rev*. (2013) 24:203–15. doi: 10.1016/j.cytogfr.2013.04.003

252. Kim JY, Yang Y, Moon JS, Lee EY, So SH, Lee HS, et al. Serum BAFF expression in patients with myasthenia gravis. *J Neuroimmunol*. (2008) 199:151–4. doi: 10.1016/j.jneuroim.2008.05.010

253. Guptill JT, Yi JS, Sanders DB, Guidon AC, Juel VC, Massey JM, et al. Characterization of B cells in muscle-specific kinase antibody myasthenia gravis. *Neurol Neuroimmunol Neuroinflamm*. (2015) 2:e77. doi: 10.1212/NXI.0000000000000077

254. Kang SY, Kang CH, Lee KH. B-cell-activating factor is elevated in serum of patients with myasthenia gravis. *Muscle Nerve*. (2016) 54:1030–3. doi: 10.1002/mus.25162

255. Samy E, Wax S, Huard B, Hess H, Schneider P. Targeting BAFF and APRIL in systemic lupus erythematosus and other antibody-associated diseases. *Int Rev Immunol*. (2017) 36:3–19. doi: 10.1080/08830185.2016.1276903

256. Hewett K, Sanders DB, Grove RA, Broderick CL, Rudo TJ, Bassiri A, et al. Randomized study of adjunctive belimumab in participants with generalized myasthenia gravis. *Neurology*. (2018) 90:e1425–34. doi: 10.1212/WNL.0000000000005323

257. Raje NS, Moreau P, Terpos E, Benboubker L, Grząśko N, Holstein SA, et al. Phase 2 study of tabalumab, a human anti-B-cell activating factor antibody, with bortezomib and dexamethasone in patients with previously treated multiple myeloma. *Br J Haematol*. (2017) 176:783–95. doi: 10.1111/bjh.14483

258. Merrill JT, Shanahan WR, Scheinberg M, Kalunian KC, Wofsy D, Martin RS. Phase III trial results with blisibimod, a selective inhibitor of B-cell activating factor, in subjects with systemic lupus erythematosus (SLE): results from a randomised, double-blind, placebo-controlled trial. *Ann Rheum Dis*. (2018) 77:883–9. doi: 10.1136/annrheumdis-2018-213032

259. Shi F, Xue R, Zhou X, Shen P, Wang S, Yang Y. Telitacicept as a BLyS/APRIL dual inhibitor for autoimmune disease. *Immunopharmacol Immunotoxicol*. (2021) 43:666–73. doi: 10.1080/08923973.2021.1973493

260. Gross JA, Johnston J, Mudri S, Enselman R, Dillon SR, Madden K, et al. TACI and BCMA are receptors for a TNF homologue implicated in B-cell autoimmune disease. *Nature*. (2000) 404:995–9. doi: 10.1038/35010115

261. Gross JA, Dillon SR, Mudri S, Johnston J, Littau A, Roque R, et al. TACI-Ig neutralizes molecules critical for B cell development and autoimmune disease. impaired B cell maturation in mice lacking BLyS. *Immunity*. (2001) 15:289–302. doi: 10.1016/S1074-7613(01)00183-2

262. Dall'era M, Chakravarty E, Wallace D, Genovese M, Weisman M, Kavanaugh A, et al. Reduced B lymphocyte and immunoglobulin levels after atacicept treatment in patients with systemic lupus erythematosus: results of a multicenter, phase Ib, double-blind, placebo-controlled, dose-escalating trial. *Arthritis Rheum*. (2007) 56:4142–50. doi: 10.1002/art.23047

263. Tak PP, Thurlings RM, Rossier C, Nestorov I, Dimic A, Mircetic V, et al. Atacicept in patients with rheumatoid arthritis: results of a multicenter, phase Ib, double-blind, placebo-controlled, dose-escalating, single- and repeated-dose study. *Arthritis Rheum*. (2008) 58:61–72. doi: 10.1002/art.23178

264. Cogollo E, Silva MA, Isenberg D. Profile of atacicept and its potential in the treatment of systemic lupus erythematosus. *Drug Des Devel Ther*. (2015) 9:1331–9. doi: 10.2147/DDDT

265. Isenberg D, Gordon C, Licu D, Copt S, Rossi CP, Wofsy D. Efficacy and safety of atacicept for prevention of flares in patients with moderate-to-severe systemic lupus erythematosus (SLE): 52-week data (APRIL-SLE randomised trial). *Ann Rheum Dis*. (2015) 74:2006–15. doi: 10.1136/annrheumdis-2013-205067

266. Stohl W. Inhibition of B cell activating factor (BAFF) in the management of systemic lupus erythematosus (SLE). *Expert Rev Clin Immunol*. (2017) 13(6):623–33. doi: 10.1080/1744666X.2017.1291343

267. Di W, Jing L, Dong X, Joan TM, Ronald FVV, Yi L, et al. Telitacicept in patients with active systemic lupus erythematosus: results of a phase 2b, randomised, double-blind, placebo-controlled trial. *Ann Rheumatic Dis*. (2023). doi: 10.1136/ard-2023-224854

268. Hartung HP. [Atacicept: a new B lymphocyte-targeted therapy for multiple sclerosis]. *Nervenarzt*. (2009) 80:1462–72. doi: 10.1007/s00115-009-2838-6

269. Hartung HP, Kieseier BC. Atacicept: targeting B cells in multiple sclerosis. *Ther Adv Neurol Disord*. (2010) 3:205–16. doi: 10.1177/1756285610371146

270. Kappos L, Hartung HP, Freedman MS, Boyko A, Radu EW, Mikol DD, et al. Atacicept in multiple sclerosis (ATAMS): a randomised, placebo-controlled, double-blind, phase 2 trial. *Lancet Neurol*. (2014) 13:353–63. doi: 10.1016/S1474-4422(14)70028-6

271. Bag-Ozbek A, Hui-Yuen JS. Emerging B-cell therapies in systemic lupus erythematosus. *Ther Clin Risk Manag*. (2021) 17:39–54. doi: 10.2147/TCRM.S252592

272. Wang J, Fang Y, Fan RA, Kirk CJ. Proteasome inhibitors and their pharmacokinetics, pharmacodynamics, and metabolism. *Int J Mol Sci*. (2021) 22 (21):11595. doi: 10.3390/ijms222111595

273. Parodis I, Gatto M, Sjöwall C. B cells in systemic lupus erythematosus: Targets of new therapies and surveillance tools. *Front Med (Lausanne)*. (2022) 9:952304. doi: 10.3389/fmed.2022.952304

274. Alexander T, Cheng Q, Klotsche J, Khodadadi L, Waka A, Biesen R, et al. Proteasome inhibition with bortezomib induces a therapeutically relevant depletion of plasma cells in SLE but does not target their precursors. *Eur J Immunol*. (2018) 48:1573–9. doi: 10.1002/eji.201847492

275. Gomez AM, Vrolix K, Martinez-Martinez P, Molenaar PC, Phernambucq M, van der Esch E, et al. Proteasome inhibition with bortezomib depletes plasma cells and autoantibodies in experimental autoimmune myasthenia gravis. *J Immunol*. (2011) 186:2503–13. doi: 10.4049/jimmunol.1002539

276. Liu R-T, Zhang P, Yang C-L, Pang Y, Zhang M, Zhang N, et al. ONX-0914, a selective inhibitor of immunoproteasome, ameliorates experimental autoimmune myasthenia gravis by modulating humoral response. *J Neuroimmunology*. (2017) 311:71–8. doi: 10.1016/j.jneuroim.2017.08.005

277. Gomez AM, Willcox N, Vrolix K, Hummel J, Nogales-Gadea G, Saxena A, et al. Proteasome inhibition with bortezomib depletes plasma cells and specific autoantibody production in primary thymic cell cultures from early-onset myasthenia gravis patients. *J Immunol*. (2014) 193:1055–63. doi: 10.4049/jimmunol.1301555

278. Kohler S, Märschenz S, Grittner U, Alexander T, Hiepe F, Meisel A. Bortezomib in antibody-mediated autoimmune diseases (TAVAB): study protocol for a unicentric, non-randomised, non-placebo controlled trial. *BMJ Open*. (2019) 9:e024523. doi: 10.1136/bmjopen-2018-024523

279. Simister NE, Story CM, Chen HL, Hunt JS. An IgG-transporting Fc receptor expressed in the syncytiotrophoblast of human placenta. *Eur J Immunol*. (1996) 26:1527–31. doi: 10.1002/eji.1830260718

280. Patel DD, Bussel JB. Neonatal Fc receptor in human immunity: Function and role in therapeutic intervention. *J Allergy Clin Immunol*. (2020) 146:467–78. doi: 10.1016/j.jaci.2020.07.015

281. Burmeister WP, Gastinel LN, Simister NE, Blum ML, Bjorkman PJ. Crystal structure at 2.2 A resolution of the MHC-related neonatal Fc receptor. *Nature*. (1994) 372:336–43. doi: 10.1038/372336a0

282. Zuercher AW, Spirig R, Baz Morelli A, Rowe T, Kasermann F. Next-generation Fc receptor-targeting biologics for autoimmune diseases. *Autoimmun Rev*. (2019) 18:102366. doi: 10.1016/j.autrev.2019.102366

283. Howard JFJr., Bril V, Vu T, Karam C, Peric S, Margania T, et al. Safety, efficacy, and tolerability of efgartigimod in patients with generalised myasthenia gravis (ADAPT): a multicentre, randomised, placebo-controlled, phase 3 trial. *Lancet Neurol*. (2021) 20:526–36. doi: 10.1212/WNL.96.15_supplement.4520

284. Werth VP, Culton DA, Concha JSS, Graydon JS, Blumberg LJ, Okawa J, et al. Safety, tolerability, and activity of ALXN1830 targeting the neonatal fc receptor in chronic pemphigus. *J Invest Dermatol*. (2021) 141:2858–2865.e2854. doi: 10.1016/j.jid.2021.04.031

285. Bril V, Drużdż A, Grosskreutz J, Habib AA, Mantegazza R, Sacconi S, et al. Safety and efficacy of rozanolixizumab in patients with generalised myasthenia gravis (MycarinG): a randomised, double-blind, placebo-controlled, adaptive phase 3 study. *Lancet Neurol*. (2023) 22:383–94. doi: 10.1016/S1474-4422(23)00077-7

286. Kareem S, Jacob A, Mathew J, Quigg RJ, Alexander JJ. Complement: Functions, location and implications. *Immunology*. (2023) 170:180–92. doi: 10.1111/imm.13663

287. Rodgaard A, Nielsen FC, Djurup R, Somnier F, Gammeltoft S. Acetylcholine receptor antibody in myasthenia gravis: predominance of IgG subclasses 1 and 3. *Clin Exp Immunol*. (1987) 67:82–8.

288. Howard JF, Utsugisawa K, Benatar M, Murai H, Barohn RJ, Illa I, et al. Safety and efficacy of eculizumab in anti-acetylcholine receptor antibody-positive refractory generalised myasthenia gravis (REGAIN): a phase 3, randomised, double-blind, placebo-controlled, multicentre study. *Lancet Neurol*. (2017) 16:976–86. doi: 10.1016/S1474-4422(17)30369-1

289. Vu T, Ortiz S, Katsuno M, Annane D, Mantegazza R, Beasley KN, et al. Ravulizumab pharmacokinetics and pharmacodynamics in patients with generalized myasthenia gravis. *J Neurol*. (2023) 270:3129–37. doi: 10.1007/s00415-023-11617-1

290. Zarrin AA, Bao K, Lupardus P, Vucic D. Kinase inhibition in autoimmunity and inflammation. *Nat Rev Drug Discovery*. (2021) 20:39–63. doi: 10.1038/s41573-020-0082-8

291. Mendes-Bastos P, Brasileiro A, Kolkhir P, Frischbutter S, Scheffel J, Moñino-Romero S, et al. Bruton's tyrosine kinase inhibition-An emerging therapeutic strategy in immune-mediated dermatological conditions. *Allergy*. (2022) 77:2355–66. doi: 10.1111/all.15261

292. Mcdonald C, Xanthopoulos C, Kostareli E. The role of Bruton's tyrosine kinase in the immune system and disease. *Immunology*. (2021) 164:722–36. doi: 10.1111/imm.13416

293. Rip J, van der Ploeg EK, Hendriks RW, Corneth OBJ. The role of bruton's tyrosine kinase in immune cell signaling and systemic autoimmunity. *Crit Rev Immunol*. (2018) 38:17–62. doi: 10.1615/CritRevImmunol.v38.i1

294. Isenberg D, Furie R, Jones NS, Guibord P, Galanter J, Lee C, et al. Efficacy, safety, and pharmacodynamic effects of the bruton's tyrosine kinase inhibitor fenebrutinib (GDC-0853) in systemic lupus erythematosus: results of a phase II, randomized, double-blind, placebo-controlled trial. *Arthritis Rheumatol*. (2021) 73:1835–46. doi: 10.1002/art.41811

295. Irving BA, Weiss A. The cytoplasmic domain of the T cell receptor zeta chain is sufficient to couple to receptor-associated signal transduction pathways. *Cell*. (1991) 64:891–901. doi: 10.1016/0092-8674(91)90314-O

296. Kalos M, Levine BL, Porter DL, Katz S, Grupp SA, Bagg A, et al. T cells with chimeric antigen receptors have potent antitumor effects and can establish memory in patients with advanced leukemia. *Sci Transl Med*. (2011) 3:95ra73. doi: 10.1126/scitranslmed.3002842

297. Ellebrecht CT, Bhoj VG, Nace A, Choi EJ, Mao X, Cho MJ, et al. Reengineering chimeric antigen receptor T cells for targeted therapy of autoimmune disease. *Science*. (2016) 353:179–84. doi: 10.1126/science.aaf6756

298. Labanieh L, Mackall CL. CAR immune cells: design principles, resistance and the next generation. *Nature*. (2023) 614:635–48. doi: 10.1038/s41586-023-05707-3

299. Sterner RC, Sterner RM. CAR-T cell therapy: current limitations and potential strategies. *Blood Cancer J*. (2021) 11:69. doi: 10.1038/s41408-021-00459-7

300. Blache U, Tretbar S, Koehl U, Mougiakakos D, Fricke S. CAR T cells for treating autoimmune diseases. *RMD Open*. (2023) 9(4):e002907. doi: 10.1136/rmdopen-2022-002907

301. Lee L, Draper B, Chaplin N, Philip B, Chin M, Galas-Filipowicz D, et al. An APRIL-based chimeric antigen receptor for dual targeting of BCMA and TACI in multiple myeloma. *Blood*. (2018) 131:746–58. doi: 10.1182/blood-2017-05-781351

302. Raje N, Berdeja J, Lin Y, Siegel D, Jagannath S, Madduri D, et al. Anti-BCMA CAR T-cell therapy bb2121 in relapsed or refractory multiple myeloma. *N Engl J Med*. (2019) 380:1726–37. doi: 10.1056/NEJMoa1817226

303. Ying Z, Huang XF, Xiang X, Liu Y, Kang X, Song Y, et al. A safe and potent anti-CD19 CAR T cell therapy. *Nat Med*. (2019) 25:947–53. doi: 10.1038/s41591-019-0421-7

304. Zhang W, Feng J, Cinquina A, Wang Q, Xu H, Zhang Q, et al. Treatment of systemic lupus erythematosus using BCMA-CD19 compound CAR. *Stem Cell Rev Rep*. (2021) 17:2120–3. doi: 10.1007/s12015-021-10251-6

305. Oh S, Mao X, Manfredo-Vieira S, Lee J, Patel D, Choi EJ, et al. Precision targeting of autoantigen-specific B cells in muscle-specific tyrosine kinase myasthenia gravis with chimeric autoantibody receptor T cells. *Nat Biotechnol*. (2023) 41:1229–38. doi: 10.1038/s41587-022-01637-z

306. Menon D, Bril V. Pharmacotherapy of generalized myasthenia gravis with special emphasis on newer biologicals. *Drugs*. (2022) 82:865–87. doi: 10.1007/s40265-022-01726-y

307. Reincke SM, Von Wardenburg N, Homeyer MA, Kornau HC, Spagni G, Li LY, et al. Chimeric autoantibody receptor T cells deplete NMDA receptor-specific B cells. *Cell*. (2023) 186:5084–5097.e5018. doi: 10.1016/j.cell.2023.10.001

308. Lee J, Lundgren DK, Mao X, Manfredo-Vieira S, Nunez-Cruz S, Williams EF, et al. Antigen-specific B cell depletion for precision therapy of mucosal pemphigus vulgaris. *J Clin Invest*. (2020) 130:6317–24. doi: 10.1172/JCI138416

309. Mok CC, Lau CS. Pathogenesis of systemic lupus erythematosus. *J Clin Pathol*. (2003) 56:481–90. doi: 10.1136/jcp.56.7.481

310. Dendrou CA, Fugger L, Friese MA. Immunopathology of multiple sclerosis. *Nat Rev Immunol*. (2015) 15:545–58. doi: 10.1038/nri3871

311. Phillips WD, Vincent A. Pathogenesis of myasthenia gravis: update on disease types, models, and mechanisms. *F1000Res*. (2016) 5:F1000 Faculty Rev-1513. doi: 10.12688/f1000research

312. Paschou SA, Papadopoulou-Marketou N, Chrousos GP, Kanaka-Gantenbein C. On type 1 diabetes mellitus pathogenesis. *Endocr Connect*. (2018) 7:R38–r46. doi: 10.1530/EC-17-0347

313. Yi JS, Guptill JT, Stathopoulos P, Nowak RJ, O'connor KC. B cells in the pathophysiology of myasthenia gravis. *Muscle Nerve*. (2018) 57:172–84. doi: 10.1002/mus.25973

frontiers | Frontiers in Immunology

TYPE Original Research
PUBLISHED 23 April 2024
DOI 10.3389/fimmu.2024.1325171

OPEN ACCESS

EDITED BY
Chris Wincup,
King's College Hospital NHS Foundation Trust, United Kingdom

REVIEWED BY
Abhishek Saxena,
Shenzhen Bay Laboratory, China
Laurent Paardekooper,
Leiden University Medical Center (LUMC), Netherlands
Paola Cavalcante,
IRCCS Carlo Besta Neurological Institute Foundation, Italy

*CORRESPONDENCE
Pilar Martinez-Martinez
p.martinez@maastrichtuniversity.nl
Mario Losen
m.losen@maastrichtuniversity.nl

†These authors have contributed equally to this work

‡These authors have contributed equally to this work and share last authorship

RECEIVED 23 October 2023
ACCEPTED 25 March 2024
PUBLISHED 23 April 2024

CITATION
Koneczny I, Mané-Damas M, Zong S, De Haas S, Huda S, van Kruining D, Damoiseaux J, De Rosa A, Maestri M, Guida M, Molenaar P, Van Damme P, Fichtenbaum A, Perkmann T, De Baets M, Lazaridis K, Zouvelou V, Tzartos S, Ricciardi R, Losen M and Martinez-Martinez P (2024) A retrospective multicenter study on clinical and serological parameters in patients with MuSK myasthenia gravis with and without general immunosuppression.
Front. Immunol. 15:1325171.
doi: 10.3389/fimmu.2024.1325171

A retrospective multicenter study on clinical and serological parameters in patients with MuSK myasthenia gravis with and without general immunosuppression

Inga Koneczny[1,2], Marina Mané-Damas[1†], Shenghua Zong[1†], Sander De Haas[1†], Saif Huda[3,4], Daan van Kruining[5], Jan Damoiseaux[6], Anna De Rosa[7], Michelangelo Maestri[7], Melania Guida[7], Peter Molenaar[1], Philip Van Damme[8,9], Andreas Fichtenbaum[2,10], Thomas Perkmann[10], Marc De Baets[1], Konstantinos Lazaridis[11], Vasiliki Zouvelou[12], Socrates Tzartos[11,13], Roberta Ricciardi[7,14], Mario Losen[1*‡] and Pilar Martinez-Martinez[1*‡]

[1]Research Group Neuroinflammation and Autoimmunity, Department of Psychiatry and Neuropsychology, School for Mental Health and Neuroscience, Maastricht University, Maastricht, Netherlands, [2]Division of Neuropathology and Neurochemistry, Department of Neurology, Medical University of Vienna, Vienna, Austria, [3]Neurosciences Group, Nuffield Department of Clinical Neurosciences, Weatherall Institute of Molecular Medicine, University of Oxford, Oxford, United Kingdom, [4]Department of Neurology, Walton Centre National Health Service (NHS) Foundation Trust, Liverpool, United Kingdom, [5]Department of Psychiatry and Neuropsychology, Maastricht University, Maastricht, Netherlands, [6]Central Diagnostic Laboratory, Maastricht University Medical Center, Maastricht, Netherlands, [7]Department of Clinical and Experimental Medicine, Neurology Unit, University of Pisa, Pisa, Italy, [8]Neurology Department, University Hospital, Leuven, Belgium, [9]Department of Neurosciences, Center for Brain & Disease Research, VIB, Leuven, Belgium, [10]Department of Laboratory Medicine, Medical University of Vienna, Vienna, Austria, [11]Department of Immunology, Hellenic Pasteur Institute, Athens, Greece, [12]1st Neurology Department, National and Kapodistrian University of Athens, Athens, Greece, [13]Department of Neuroimmunology, Tzartos NeuroDiagnostics, Athens, Greece, [14]Cardio Thoracic and Vascular Surgery Department, University of Pisa, Pisa, Italy

Introduction: Muscle-specific kinase (MuSK)- myasthenia gravis (MG) is caused by pathogenic autoantibodies against MuSK that correlate with disease severity and are predominantly of the IgG4 subclass. The first-line treatment for MuSK-MG is general immunosuppression with corticosteroids, but the effect of treatment on IgG4 and MuSK IgG4 levels has not been studied.

Methods: We analyzed the clinical data and sera from 52 MuSK-MG patients (45 female, 7 male, median age 49 (range 17–79) years) from Italy, the Netherlands, Greece and Belgium, and 43 AChR-MG patients (22 female, 21 male, median age 63 (range 2–82) years) from Italy, receiving different types of immunosuppression, and sera from 46 age- and sex-matched non-disease controls (with no diagnosed diseases, 38 female, 8 male, median age 51.5 (range 20–68) years) from the Netherlands. We analyzed the disease severity (assessed by MGFA or QMG score), and measured concentrations of MuSK IgG4, MuSK IgG, total IgG4 and total IgG in the sera by ELISA, RIA and nephelometry.

Results: We observed that MuSK-MG patients showed a robust clinical improvement and reduction of MuSK IgG after therapy, and that MuSK IgG4 concentrations, but not total IgG4 concentrations, correlated with clinical severity. MuSK IgG and MuSK IgG4 concentrations were reduced after immunosuppression in 4/5 individuals with before-after data, but data from non-linked patient samples showed no difference. Total serum IgG4 levels were within the normal range, with IgG4 levels above threshold (1.35g/L) in 1/52 MuSK-MG, 2/43 AChR-MG patients and 1/45 non-disease controls. MuSK-MG patients improved within the first four years after disease onset, but no further clinical improvement or reduction of MuSK IgG4 were observed four years later, and only 14/52 (26.92%) patients in total, of which 13 (93.3%) received general immunosuppression, reached clinical remission.

Discussion: We conclude that MuSK-MG patients improve clinically with general immunosuppression but may require further treatment to reach remission. Longitudinal testing of individual patients may be clinically more useful than single measurements of MuSK IgG4. No significant differences in the serum IgG4 concentrations and IgG4/IgG ratio between AChR- and MuSK-MG patients were found during follow-up. Further studies with larger patient and control cohorts are necessary to validate the findings.

KEYWORDS

MuSK myasthenia gravis, IgG4, corticosteroids, prednisolone, prednisone, IgG4 autoimmune disease

1 Introduction

Muscle-specific kinase (MuSK)-myasthenia gravis (MuSK-MG) is a severe autoimmune disease of the neuromuscular junction (NMJ) (1, 2). This condition is characterized by autoantibodies targeting MuSK, a pivotal tyrosine kinase crucial for NMJ development and maintenance (3). MuSK autoantibodies belong predominantly (approximately 90%) to the IgG4 subclass (4–8) that blocks the binding of MuSK to its direct binding partner, low-density lipoprotein receptor-related protein 4 (Lrp4), thereby interrupting a vital signal transduction pathway essential for the maintenance of the NMJ architecture (6, 9). MuSK-MG belongs to the IgG4 autoimmune diseases (IgG4-AIDs) (10, 11), which share common features such as low disease prevalence, predominance of IgG4 subclass antibodies with blocking as a pathogenic mechanism, and HLA associations (12–14).

The first-line treatment of patients with MuSK-MG consists of general immunosuppression with corticosteroids such as prednisone, often in combination with azathioprine. Even though it has been generally accepted to be a reliable treatment, a fraction of patients with MG remains treatment resistant and more difficult to manage clinically. Recent literature suggested general immunosuppression to be a less efficient treatment for MuSK-MG compared to AChR-MG (15, 16). B-cell depletion with rituximab has shown clinical benefit in MuSK-MG and other IgG4-AIDs (13, 17–21), and led to the reduction of MuSK IgG4 (22), but there is a lack of studies analyzing total IgG4 and MuSK IgG4 levels in patients with general immunosuppression.

In this study, we analyzed disease severity [assessed by Myasthenia Gravis Foundation of America (MGFA) or quantitative myasthenia gravis (QMG) score] in relation to MuSK IgG4, MuSK IgG, total IgG4, and total IgG concentrations in serum or plasma from patients with MuSK or AChR MG with and without immunosuppression and non-disease individuals, measured by enzyme-linked immunosorbent assay (ELISA), radioimmunoassay (RIA), and nephelometry.

Abbreviations: AChR, Acetylcholine receptor; ECD, Extracellular domain; ELISA, Enzyme-linked immunosorbent assay; IgG, Immunglobulin G; IgG1–3, Immunoglobulin G1, G2, and G3; IgG4, Immunoglobulin G4; IVIG, Intravenous immunoglobulin; Lrp4, Low-density lipoprotein receptor-related protein 4; MG, Myasthenia gravis; MGFA score, Myasthenia Gravis Foundation of America clinical classification score; MuSK, Muscle-specific (tyrosine) kinase; NMJ, Neuromuscular junction; QMG score, Quantitative myasthenia gravis score; RIA, Radioimmunoassay.

2 Materials and methods

2.1 Patients

The study had a cross-sectional design, as the patient samples were taken at the same time as the clinical scoring. We also had additional

follow-up serum of five patients from Greece available. All patient material was obtained with approval from the relevant ethical boards and after informed consent of the patients. We used serum or plasma from 52 patients with MuSK-MG: 45 female and 7 male patients; median age of onset, 43 years (range, 10–79 years); median age at sample, 49 years (Table 1 and Data Table 1). Among these, 13 sera were from treatment-naïve patients with MuSK-MG (1 from the Netherlands, 1 from Belgium, 6 from Italy, and 5 from Greece) and 44 samples were from patients with MuSK-MG receiving general immunosuppression (36 from Italy, 2 from Belgium, 1 from the Netherlands, and 5 from Greece). The five patients from Greece had samples before and after long-term immunosuppression and were therefore included in both groups (for each of the five different patients, we included one sample in the before treatment group and one sample in the after treatment group; Table 1 and Data Tables 1 and 2). The patients received immune therapy consisting of prednisone, azathioprine, intravenous immunoglobulins (IVIGs), cyclosporine, or combinations thereof (Data Table 1); these treatments are collectively referred to as "general immunosuppression". This term was chosen to highlight the distinction from the more specific B-cell depletion therapy involving rituximab. At the time of sample collection, we included all patients with MuSK-MG, but rituximab was not established for the treatment of MuSK-MG at the clinic in Pisa. We observed that from other clinical centers (the Netherlands and Belgium), two patients receiving rituximab were in the cohort; this sample size was considered insufficient for a meaningful statistical analysis and were therefore excluded from the study. Five patients with MuSK-MG received IVIG in combination with other treatments (three in combination with prednisone and two in combination with cyclosporine and prednisone, all in intervals of 1–3 months; Data Table 1), which theoretically could affect serum IgG levels, but in all cases, blood sampling was prior to the IVIG infusion. The MGFA scores of the patients were between I and V, or they were in clinical remission. In tables and figures requiring numerical values, patients in clinical remission were represented as "0" to ensure their inclusion in the datasets. We defined a clinical improvement as a reduction of the MGFA score by a minimum of one point, and patients with unchanged or increased MGFA as not improved. The absence of AChR antibodies was confirmed by RIA. The clinical information is summarized in Data Table 1. Sera from 45 age- and sex-matched non-disease controls (Sanquin, Amsterdam) were used as controls: 38 female and 8 male controls; median age at sample, 51.5 years (range, 20–68 years). Furthermore, sera from 43 patients with AChR-MG (all from Italy), namely, 22 female and 21 male patients, with a median age of 63 years (range, 2–82 years) were used. Of these, 15 patients were untreated and 28 patients received general immunosuppression (summary in Table 1 and details in Data Table 1). Clinical data were collected at the same time as blood samples during routine clinical checkups by the treating physician. The serum/plasma samples were analyzed using the tests outlined below. Owing to unavailable or low serum/plasma volumes or missing clinical data in a subset of samples, not all sera could be analyzed for every parameter.

TABLE 1 Summarized clinical information (details in Supplementary Table 1).

	MuSK-MG	AChR-MG	Non-disease controls
Female, n (%)	45 (86.54%)	22 (51.16%)	38 (82.61%)
Male, n (%)	7 (13.46%)	21 (48.84%)	8 (17.39%)
Age at sample, median (range)	49 (17–79)	63 (2–82)	47.8 (20–68)
Age of onset, median (range)	43 (10–79)	62 (1–82)	
General immune therapy, n (%)	39 (75%)/44 84.62%)*	28 (65.1%)	
Oral corticosteroids (prednisone, dexamethasone)	26 (50%)	19 (44.19%)	
Prednisone and azathioprine	7 (13.46%)	6 (13.95%)	
Prednisone and IVIG	3 (5.77%)	0	
Prednisone, plasmapheresis	2 (3.85%)	0	
Azathioprine only	1 (1.92%)	0	
Other combinations (see Supplementary Table 1)	5 (9.62%)	3 (6.98%)	
Thymectomy	5 (9.61%)	7 (16.28%)	

*Five patients with MuSK-MG from Greece had samples before and after treatment (details in Table 2).

2.2 MuSK IgG and MuSK IgG4 measurement

Total MuSK autoantibody levels were assessed by RIA (RSR, UK) according to the manufacturer's instructions. MuSK IgG4 levels were measured by ELISA. To this end, ELISA plates (Microlon, catalog number 655092, Greiner, Austria) were coated with 1 µg/mL MuSK extracellular domain (ECD) produced in mammalian cells (a kind gift of Dr. Bernard Rees-Smith, RSR, UK). Bound MuSK antibodies were detected with mouse anti-human IgG4:HRP (1:3,500, catalog number MCA2098P, AbD Serotec, Germany). Samples were incubated with substrate containing 3,3′,5,5′-tetramethylbenzidine, and absorbance at 450 nm was measured using a VictorX3 plate reader (PerkinElmer, USA).

2.3 IgG quantification

IgG levels in patient sera were analyzed by ELISA, an immunoassay readily available in our research laboratory. ELISA plates (Microlon, catalog number 655092, Greiner, Austria) were coated with goat $F(ab)_2$ anti-human IgG Fcγ (1:200, catalog number 109-006-008, Jackson ImmunoResearch, USA). Samples were added together with a standard dilution series of mAb-637 IgG1 (23). Bound antibodies were detected with goat F(ab)2 anti-human IgG Fcγ conjugated to HRP (1:20,000, catalog number 109-036-008, Jackson ImmunoResearch, USA). Samples were incubated with substrate containing 3,3′,5,5′-tetramethylbenzidine, and absorbance at 450 nm was measured using a VictorX3 plate reader (PerkinElmer, USA). IgG concentrations were verified using nephelometry.

2.4 IgG4 quantification

Human IgG4 serum/plasma concentrations were determined using particle-enhanced immune nephelometry with the BN II System (BN II Nephelometer, Siemens, Germany). Quantification of IgG4 levels by ELISA was not established. Hence, the methodology of the routine clinical laboratory was chosen after establishing that there was a good correlation between ELISA and nephelometry for total IgG (Supplementary Figure 2A).

2.5 Statistics

Statistical analyses were conducted using GraphPad Prism software version 9. Data were analyzed by normality and lognormality tests. In graphs with three or more datasets and Gaussian distribution, one-way analysis of variance (ANOVA) with Tukey post-hoc test was used. When data failed the normality test, nonparametric Kruskal–Wallis test and Dunn's multiple comparisons test were used instead, and data were presented with median. In graphs with two datasets that showed a normal distribution, two-tailed *t*-test was used. Datasets without normal distribution and unmatched samples were analyzed using the Mann–Whitney test and datasets without normal distribution and paired data were analyzed with the Wilcoxon matched-pair signed-rank test. XY data were analyzed by linear regression followed by correlation analysis using the Pearson correlation efficient in case of normally distributed data, or the Spearman correlation coefficient in case the data did not show Gaussian distribution.

MuSK IgG4 and total IgG4 data were checked for normality, log-transformed, and analyzed using RStudio (version RStudio 2023.06.0 + 421). Linear regression models were constructed to assess the relationship ($\alpha = 0.05$) between receiving immunosuppressive therapy and MuSK IgG4 levels. Additionally, age, sex, and MGFA scores were included as covariates. Furthermore, the association between immunosuppressive therapy and total IgG4 levels was investigated, and the same covariates were analyzed. Finally, the relationship between disease status (MuSK/AChR-MG) and total IgG4 levels was assessed, and the covariates age, sex, and immunosuppressive therapy were included in the model. An alpha level of 0.05 was used as the threshold for statistical significance.

3 Results

3.1 Immune therapy with clinical improvement was associated with reduced MuSK IgG levels

First, we assessed whether patients with MuSK-MG showed a clinical benefit from treatment with general immunosuppression. MGFA data from two time points (onset: before immunosuppression and follow-up: after immunosuppression) of 37 patients (36 Italy and 1 Belgium) receiving general immunosuppression were available. Following the diagnosis, where the patients were treatment naïve, the patients received immunosuppressive and immunomodulatory treatments, including oral corticosteroids alone (26 patients) or prednisone in combination with further treatments [azathioprine, IVIG, plasmapheresis, mycophenolate mofetil, or cyclosporine (11 patients)] (see Data Table 1 for details). A significant reduction in MGFA scores after treatment was found (Figure 1A, $p < 0.0001$, Wilcoxon matched-pair signed-rank test). An absence of symptoms at follow-up was only observed in 10 out of 37 patients. When analyzing all patients with MuSK-MG, independent of their treatment, only 14/52 patients (26.9%) reached clinical remission (Data Table 1 and Table 1). Additionally, MuSK IgG levels, as reported by the local diagnostic centers, demonstrated a decrease in patients undergoing immunosuppression (Figure 1B, $p < 0.0001$, Wilcoxon matched-pair signed-rank test) and MuSK IgG levels correlated with the MGFA scores of the patients (Supplementary Figure 1). When analyzing clinical severity after different immunosuppressive treatments, prednisone or dexamethasone alone ($p < 0.0001$) or in combination with other immunosuppressive treatment ($p=0.0103$) led to significant reductions in the MGFA score (Figure 1C). Treatment with prednisone or dexamethasone alone also led to a significant reduction of MuSK IgG levels ($p= 0.0013$, Kruskal Wallis test and Dunn's multiple comparison test, Figure 1D).

3.2 Clinical improvement was not significantly associated with reduced MuSK IgG4 or total IgG4 concentrations

Next, we analyzed whether MuSK IgG4, total IgG4, and total IgG levels were similarly reduced in patients with MuSK-MG. In the Italian/Belgian cohort, before–after immunomodulatory treatment sera/plasma were not available to assess these parameters. However, matched pairs of serum/plasma from individual patients before and after treatment were available from five patients from Greece (see summarized clinical information in Table 2).

The before–after treatment samples indicated a clinical improvement in QMG scores (Figure 2A), which did not correlate with a consistent reduction in the total IgG levels (Figure 2B) or total IgG4 levels (Figure 2C), but with clinical change assessed by MGFA scores (Figure 2D), a reduction of MuSK IgG levels in three of four patients (Figure 2E) and MuSK IgG4 levels in four of five patients (Figure 2F).

However, unlike for MuSK IgG4, total serum IgG4 concentrations (Figure 2C) and total IgG levels were not consistently reduced after treatment. Due to the low number of patients, we assessed whether these results could also be reproduced in the larger patient cohort with additional samples from non-matched patients with and without immunosuppression from Italy, the Netherlands, and Belgium.

To this aim, we measured MuSK IgG4 concentrations from 44 patients with MuSK-MG (including the five Greek patients in the before treatment group) by ELISA. MuSK IgG4 levels correlated

10.3389/fimmu.2024.1325171

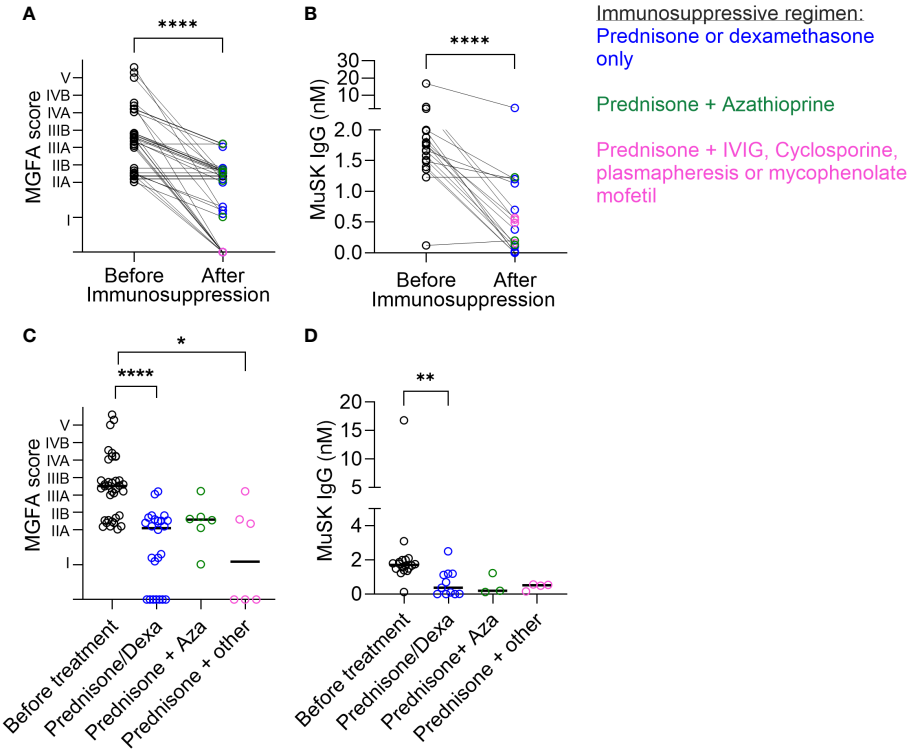

FIGURE 1
Disease severity and MuSK IgG levels were reduced after immunosuppression. **(A)** MGFA scores of patients with MuSK-MG at onset and at follow-up time after receiving immunosuppression. ****$p < 0.0001$, Wilcoxon matched-pair signed-rank test. To increase visibility, the lines of the MGFA scores were nudged slightly up or down. **(B)** MuSK IgG levels (determined at the time of diagnosis and the last follow-up) were reduced after receiving immunosuppressive treatment. Wilcoxon matched-pair signed-rank test, ****$p < 0.0001$. Comparison of **(C)** MGFA scores and **(D)** MuSK IgG titers (nM) before and after distinct treatments. Treatment is indicated as follows: blue = prednisone or dexamethasone, green = prednisone in combination with azathioprine, and pink = prednisone in combination with IVIG, cyclophosphamide, plasmapheresis, or mycophenolate mofetil. Kruskal–Wallis with Dunn's post test. ****$p < 0.0001$, **$p = 0.0013$, *$p = 0.0103$. To include samples from patients with clinical remission in the graphs, these were given a value of "MGFA = 0".

TABLE 2 Clinical data of five Greek patients with MuSK-MG before and after immunosuppressive treatment.

Patient code	Sex	Age at diagnosis	Duration of treatment (months)	Treatment status	MuSK Ab concentration (nM, cutoff for positivity: >0.030)	Time treatment started after onset	QMG	Treatment (immunosuppression, IS)
G1	M	79	54 months	Before	27	0.6 months (20 days)	4	No IS
				After	21		0	Prednisone
G2	F	17	60 months	Before	11	2 months	2	No IS
				After	5.5		0	Prednisone
G3	F	45	6 months	Before	0.045	1 month	3	No IS
				After	0.1		1	Prednisone
G4	F	47	39 months	Before	n.a.	6 months	8	No IS
				After	1.8		4	Prednisone/Cyclosporine
G5	F	49	33 months	Before	13	3 months	9	No IS
				After	4.5		3	Prednisone/ Mycophenolate mofetil

IS, immunosuppression.

10.3389/fimmu.2024.1325171

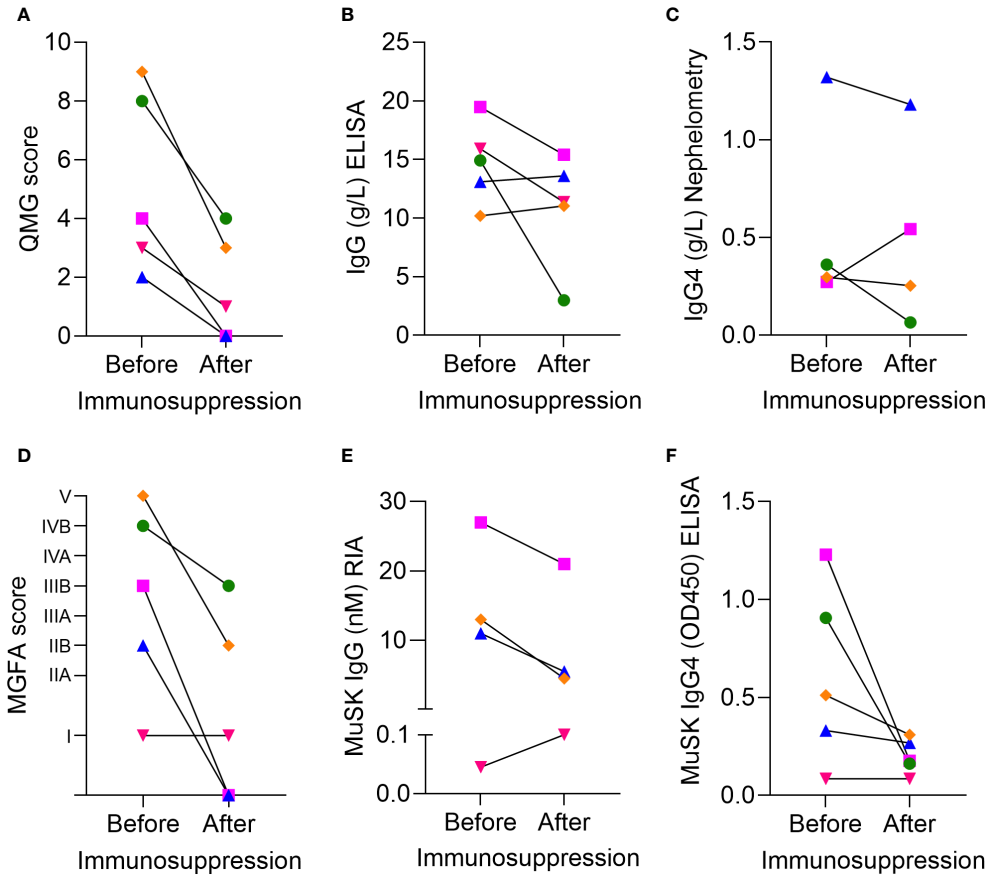

FIGURE 2
Clinical severity and serological data of five patients with MuSK-MG from Greece before and after immunosuppressive treatment. **(A)** Clinical severity by QMG score, **(B)** IgG concentrations measured by ELISA, **(C)** IgG4 concentrations measured by nephelometry, **(D)** MGFA scores. Pharmacological remission is indicated as 0. **(E)** MuSK IgG concentration assessed by RIA, **(F)** MuSK IgG4 levels measured by ELISA. Colors indicate individual patients: pink = G1, blue = G2, red = G3, green = G4, and orange =G5. Because of the limited serum volume, the IgG4 of patient G3 and the MuSK IgG of patient G4 could not be assessed. Statistical analysis was not considered appropriate due to the low sample number.

significantly with the MuSK IgG levels ($p = 0.0011$, linear regression, Spearman correlation, Supplementary Figure 2B) and MGFA scores ($p = 0.026$, linear regression, Spearman correlation, Figure 3A). However, no significant difference between treated and untreated patients was found ($p = 0.96$, Mann–Whitney test, Figure 3B). We hypothesized that the cause of this unexpected finding could result from the heterogeneity of the untreated patients' cohort. We further analyzed the group and defined two subgroups: patients with MuSK-MG at onset (≤6 months after onset) and patients with MuSK-MG later in the disease course (>6 months after onset, Supplementary Figure 3A). At disease onset, the patients had a trend for higher MuSK IgG4 levels and more severe disease manifestations (Supplementary Figures 3A, B), with significantly higher MGFA compared to the scores from patients included later during disease ($p = 0.040$, Mann–Whitney test, Supplementary Figure 3C). Furthermore, disease severity significantly correlated with MuSK IgG4 levels in these patients ($p = 0.022$, linear regression, Pearson correlation coefficient, Supplementary Figure 3D).

We were uncertain whether the apparent lack of reduction in MuSK IgG4 levels in patients undergoing immune therapy stemmed from a less aggressive treatment approach or if, in fact, there was a reduction but from much higher initial antibody levels following clinical improvement. Therefore, we compared MuSK IgG4 and total IgG4 concentrations in patients with MuSK-MG from Italy, Belgium, and the Netherlands with and without clinical improvement. We did not see a significant difference in MuSK IgG4 or IgG4 levels between the groups (Figures 4A, B). However, we observed a trend for higher MuSK IgG4 (but not total IgG4) levels in patients without clinical improvement. The data exhibited substantial variability, and the low sample size might have obscured any underlying effect.

Linear regression models assessing the relationship between immunosuppressive therapy and MuSK IgG4 levels revealed no significant association ($\beta = 0.017$, $p = 0.951$; Supplementary Table 1a and Supplementary Figure 7). The addition of covariates sex, age, and MGFA scores did not change this relationship (Supplementary Table 1b).

Taken together, this implies that the variability of MuSK IgG4 levels among different patients is more pronounced than changes within individual patients. Consequently, performing longitudinal

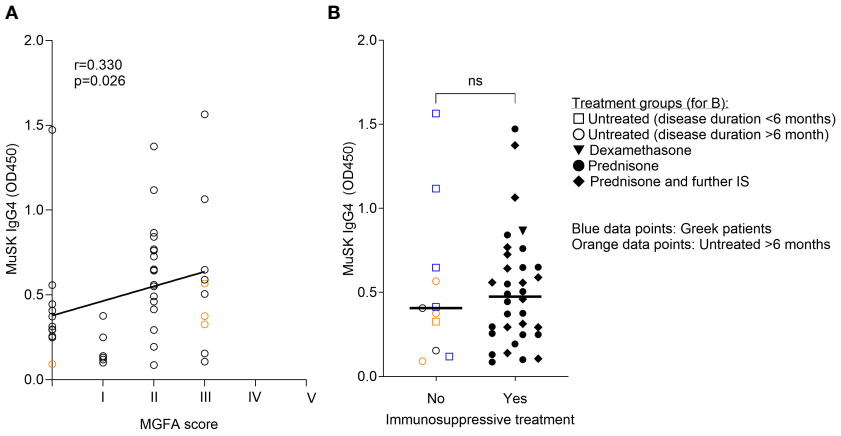

FIGURE 3
MuSK IgG4 levels correlated with clinical severity, but not with treatment status. MuSK IgG4 concentrations were measured by ELISA. **(A)** MuSK IgG4 concentrations (OD450) correlated with clinical severity (MGFA score). Linear regression followed by correlation with Spearman correlation coefficient. **(B)** MuSK IgG4 concentrations in patients with and without immunosuppressive treatments. Patients from Greece are indicated by blue symbols. Patients who remained untreated >6 months after disease onset are indicated by orange symbols. ns= non-significant. *N* = 3. Mann–Whitney test.

testing on individual patients might offer more valuable insights for prognosis compared to comparing sera across different patients.

3.3 IgG and IgG4 concentrations in patients with and without immune therapy

Next, we assessed IgG and IgG4 concentrations in patients with MuSK-MG and AChR-MG in comparison to non-disease controls.

As expected, patients with AChR-MG receiving immunosuppressive treatment had lower IgG concentrations than untreated patients with AChR-MG (p = 0.036). Compared to non-disease controls, IgG concentrations were lower in patients with MuSK-MG with immunosuppression (p = 0.025) and patients with AChR-MG with immunosuppression (p = 0.025). Treated patients with MuSK-MG had lower IgG levels than untreated patients, but the difference did not reach statistical significance (Figure 5, Kruskal–Wallis test with Dunn's multiple comparisons test). Five of the patients with MuSK underwent thymectomy prior to diagnosis of MuSK MG (patients indicated in teal symbols in Figure 5), and histology showed that all had a normal or atrophic thymus.

Next, we assessed total IgG4 concentrations in sera from non-disease controls and patients with AChR-MG and MuSK-MG and observed no significant correlation between IgG4 concentrations and disease severity in patients with MuSK-MG (Supplementary Figure 4A) or in total IgG4 concentrations between patients with MuSK-MG and those with AChR-MG with and without immunosuppressive treatment (Figure 6A). Additionally, total IgG4 serum concentrations did not correlate with the MuSK IgG concentration measured by RIA (Supplementary Figure 4C). Total IgG4 levels were not significantly different between patients with MG and non-disease controls (Supplementary Figure 4B). Overall IgG4 concentrations only exceptionally exceed the threshold value of 1.35 g/L (indicated as a horizontal dotted line, Figure 6A), which is used to indicate elevated serum IgG4 levels in patients with IgG4-related diseases. We also observed that, intriguingly, both patients

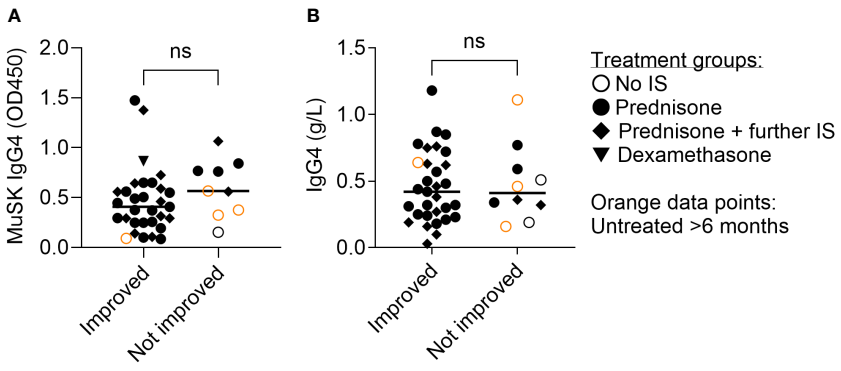

FIGURE 4
Clinical improvement was not associated with significantly reduced MuSK IgG4 **(A)** or total IgG4 concentrations **(B)**. Average disease duration: 10.3 years (range, 0–34 years, details in Supplementary Table 1). ns= non-significant. Mann–Whitney test.

10.3389/fimmu.2024.1325171

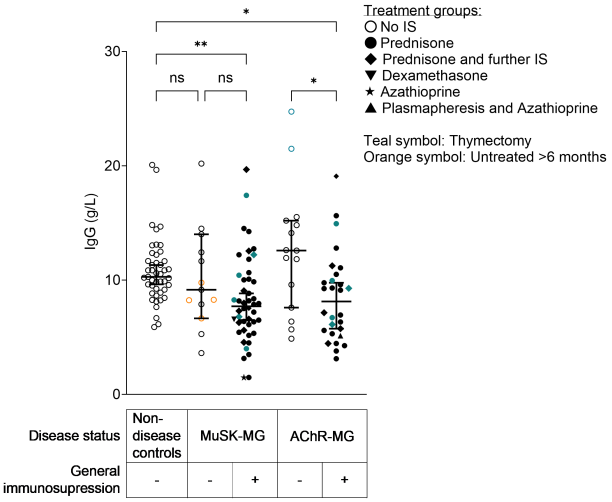

FIGURE 5
IgG concentrations in patients with MuSK-MG and AChR-MG with and without immunosuppressive treatment and non-disease controls. IgG concentrations were measured by IgG ELISA. **Non-disease control vs. MuSK-MG with immunosuppression: p = 0.025. *AChR-MG without vs. AChR-MG with immunosuppression: p = 0.036. *Non-disease control vs. AChR-MG with immunosuppression: p = 0.025. Kruskal–Wallis test with Dunn's multiple comparisons test. ns= non-significant.

with AChR-MG and those with MuSK-MG showed an enrichment of IgG4 (Figure 6B, fold change of mean IgG4/IgG ratio in patients compared to non-disease controls: AChR = 2.58; AChR + IS = 2.17; MuSK = 2.91; MuSK + IS = 2.40), with no significant difference between MuSK-MG and AChR-MG. We also analyzed whether age and sex affected the IgG4 concentrations but found no correlation between age and IgG4 concentrations in patients with MuSK-MG or non-disease controls (Supplementary Figure 5). We observed, as expected, a trend for higher IgG4 levels in male patients in most groups (Supplementary Figure 6), though interestingly the three patients with MG (two with AChR-MG and one with MuSK-MG) with elevated IgG4 were women (Supplementary Figure 6B).

Furthermore, when linear regression models were used, no statistically significant relationship was identified between immunosuppressive therapy and total IgG4 levels (β = 0.023, p = 0.897; Supplementary Table 2a and Supplementary Figure 8). The association remained statistically insignificant when sex, age, and MGFA were introduced as covariates (Supplementary Table 2b). Furthermore, linear regression models assessing the relationship between total IgG4 levels and disease status compared to non-disease controls showed no significant association with either AChR-MG (β = 0.282, p = 0.256) or MuSK-MG (β = 0.331, p = 0.140; Supplementary Table 3a and Supplementary Figure 9). Moreover, the addition of the covariates age, sex, and immunosuppressant therapy did not change this relationship (Supplementary Table 3b).

3.4 Clinical severity over long disease duration

The Pisa cohort included patients with follow-up times of over 30 years. We therefore wanted to investigate how disease duration affected the clinical severity, MuSK IgG4, and total IgG4 concentrations. We observed that there was a significant reduction of MGFA scores in patients in the first 1–4 years after onset (Figure 7A), which remained stable with no further improvement afterwards. MuSK IgG4 (Figure 7B) and IgG4 concentrations (Figure 7C) also did not significantly change over time.

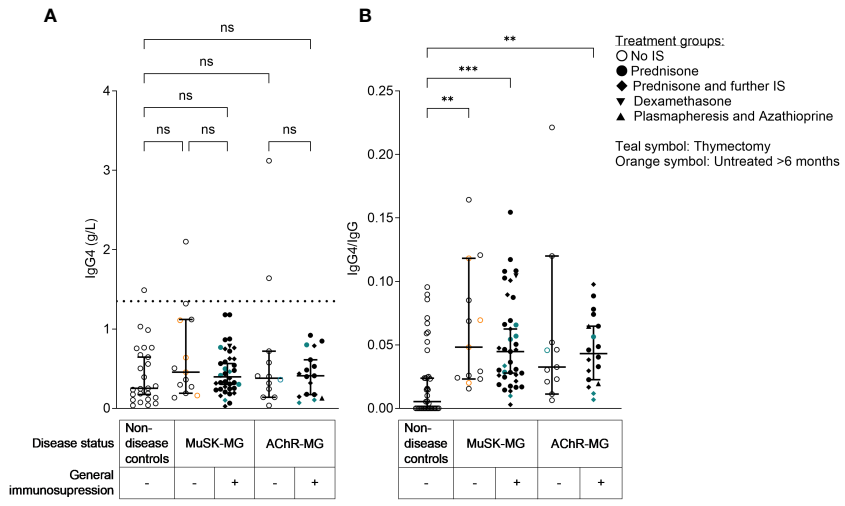

FIGURE 6
Serum IgG4 concentrations in patients with MG were, with a few exceptions, within the normal range, while relative IgG4 levels (IgG4/IgG) were enriched in patients with AChR-MG and MuSK-MG. **(A)** IgG4 serum concentrations in patients with MG and controls, Kruskal-Wallis test with Dunn's multiple comparisons test. The dotted line indicates the cut-off for elevated IgG4 levels (defined as 1.35 g/L). **(B)** Relative IgG4 levels (IgG4/IgG), Kruskal–Wallis test with Dunn's multiple comparisons test. **Non-disease controls vs. MuSK-MG untreated: p = 0.0038; ***non-disease controls vs. MuSK treated: p = 0.0002; **non-disease controls vs. AChR-MG treated: p = 0.0051. ns= non-significant.

10.3389/fimmu.2024.1325171

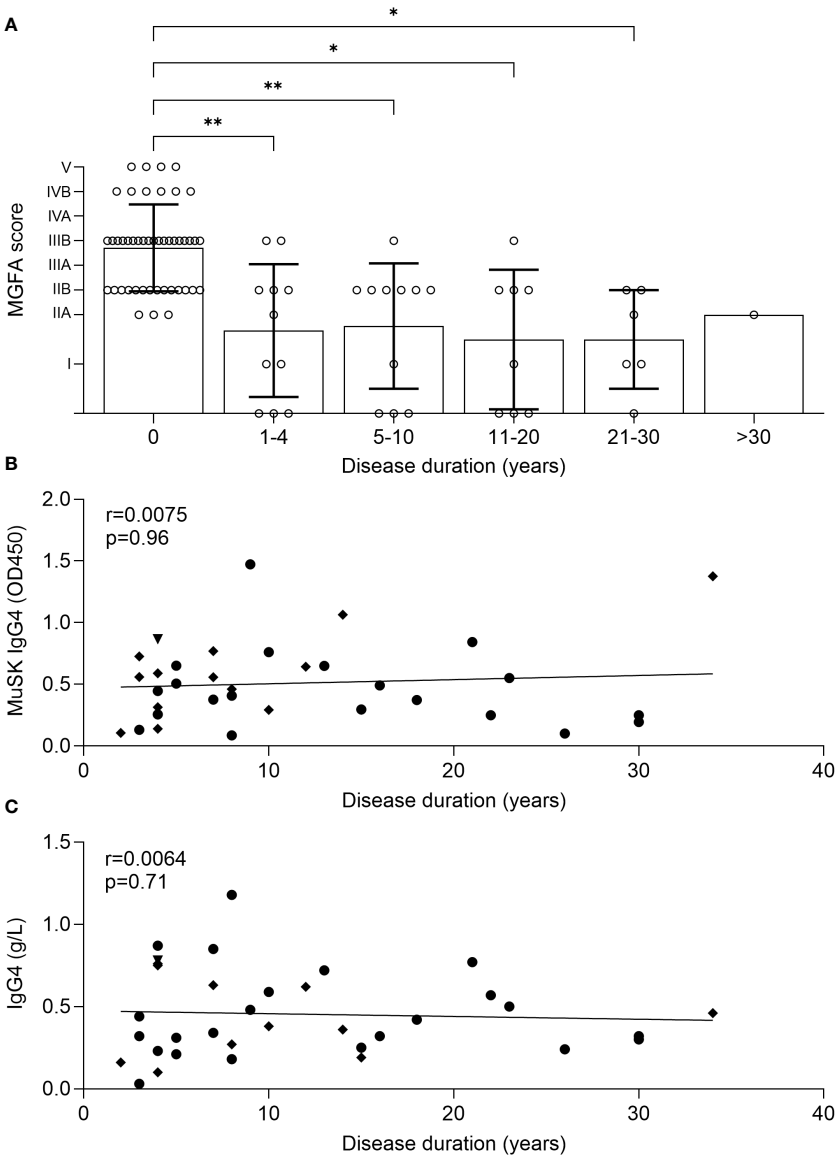

FIGURE 7
Analysis of MGFA scores showed a significant clinical improvement in the first 4 years of disease, but no further improvement afterwards **(A)**, Kruskal–Wallis test (adjusted *p*-values: 0 vs. 1–4: $p = 0.005$ (**); 0 vs. 5–10: $p = 0.0094$(**); 0 vs. 11–20: $p = 0.013$ (*); 0 vs. 21–30: $p = 0.01$ (*). Clinical remission was indicated by an MGFA score of "0" to allow inclusion in the dataset. Simple linear regression with Spearman correlation. No significant reduction of MuSK IgG4 and IgG4 levels over time **(B, C)**.

4 Discussion

MuSK-MG is caused by pathogenic IgG4 autoantibodies (6, 9), and MuSK antibody levels correlate with disease severity (24). Patients with MuSK-MG are often treated with general immunosuppression (mostly with prednisone and azathioprine), but the total IgG4 and MuSK IgG4 levels in patients with general immunosuppression had not yet been studied.

In this cross-sectional study, we investigated disease severity, MuSK IgG and IgG4 levels, as well as total IgG and IgG4 concentrations in patients at disease onset and during follow-up with and without immunosuppression. We made five main observations: (1) Patients with MuSK-MG showed a robust clinical improvement and reduction of MuSK IgG after therapy (average treatment time: 11.5 years, range: 0–34 years), but only 14/52 patients (26.9%) were in remission at the time of the analysis; (2) MuSK IgG4 concentrations, but not total IgG4 concentrations, correlated with clinical severity and total MuSK IgG levels; (3) MuSK IgG4 concentrations were reduced after immunosuppression in four out of five individuals with before–after data, but data from non-linked patients showed that inter-patient variability is greater than the effect in individual patients; (4) total IgG4 levels were within the normal range in all patients with MG, with few exceptions from all groups, with a relative enrichment of IgG4/IgG in both patients with AChR-MG and those with MuSK-MG; and (5) patients improved within the first 4 years after disease onset and remained stable with no further clinical improvement or MuSK IgG4 reduction.

Based on our observations, we hypothesize that (1) patients with MuSK-MG improved clinically with general immunosuppression especially during the first 4 years of treatment, but the majority did not reach clinical remission and therefore may require treatment alternatives; (2) longitudinal testing of MuSK-IgG4 in individual patients may have greater merit than comparing single-time-point measurements across patients; and (3) further studies with larger cohorts are necessary to assess serum IgG4 concentrations in patients with MuSK-MG and enrichment of total IgG4/IgG since these were not significantly different between patients with AChR-MG and those with MuSK-MG in our study.

4.1 Clinical response and MuSK IgG4 concentrations after immunosuppression

While it has been described that treatment with rituximab has greater clinical benefit for patients with MuSK-MG than general immunosuppression (15, 16), studies investigating the effect of general immunosuppression, particularly on MuSK IgG4 levels, are lacking. We observed a significant clinical improvement after general immunosuppression, indicated as reduction in the MGFA score, in our patient cohort. Nevertheless, clinical remission was only achieved in 12/42 treated patients with available before–after treatment data (10/36 from Italy, 0/1 from Belgium, and 2/5 from Greece), and clinical improvement was mostly observed within the first 4 years of disease duration, suggesting that a substantial fraction of patients might benefit from additional treatment.

We expected to see lower MuSK IgG4 levels in patients receiving treatment compared to untreated patients because (1) IgG4 is the predominant subclass of MuSK autoantibodies that directly cause the disease (6–9); (2) in line with previous publications (6, 24), MuSK IgG correlated with disease severity; (3) and so did MuSK IgG4 in our study; and finally (4) treatment led to clinical improvement and reduction of MuSK IgG. Upon analyzing four patients with MuSK-MG from Greece before and after receiving immunosuppression, we noted a tendency towards decreased MuSK IgG4 levels alongside clinical improvement. However, this trend could not be replicated in a more extensive cohort with cross-sectional data. Subsequent examination of untreated patients with MuSK-MG unveiled substantial heterogeneity within this group. Coupled with a notable inter-patient variability in treatment responses, these factors have influenced the data, underscoring the notion that longitudinally testing MuSK IgG4 in individual patients might offer greater clinical insights than analyzing a single measurement per patient. This is in line with a recent study investigating the effects of rituximab on MuSK IgG4 concentrations with longitudinal sampling, where a substantial inter-patient variability in MuSK IgG4 concentrations was overcome with normalization to individual patient baseline levels (22). The study also showed a correlation between MuSK IgG4 levels and clinical response to rituximab, which, together with our findings in the Greek patients, suggests that MuSK IgG4 is a suitable prognostic biomarker when used for intra-patient analysis.

4.2 Enrichment of IgG4 is not associated with IgG4 autoimmunity

MuSK-MG is an IgG4-AID (11, 25); therefore, the study of IgG4 serum levels may give valuable insights into the immunopathogenesis and etiology (13). An open question in the field is why the autoantibodies in these diseases are mainly of the IgG4 subclass, and one hypothesis is that an immune dysregulation may lead to a skewed IgG subclass profile and increased production of IgG4 and total IgG (13). No indication for increased IgG production could be found in our study, as there was no significant difference in total IgG between non-disease controls and untreated patients with MuSK-MG, which is in line with previous studies (26, 27).

In contrast, a recent study showed an inverse correlation between AChR autoantibody levels and clinical improvement in patients with AChR-MG over time (28). The authors highlight the potential of measuring AChR autoantibody levels as an objective measurement to evaluate treatment efficacy and allow timely changes in the immunosuppressive treatment selected to prevent unnecessary delays in individual patients. It is also essential, for the accurate quantification of the autoantibodies, to include a serial dilution of the patient's serum or plasma. The lack of these or other controls makes it difficult to draw a conclusion on the impact of IgG and antigen-specific autoantibody levels in the pathology across the literature.

We next studied whether IgG4 levels were increased in patients with MuSK-MG. In our study, four samples were above the threshold of 1.35 g/L: 1/52 (1.9%) patients with MuSK-MG [1/13 (7.7%) untreated patients with MuSK-MG], 2/43 (4.6%) patients with AChR-MG [2/15 (13.3%) untreated], and 1/45 (2.22%) non-disease controls. This is in contrast to a recent study by Vergoossen et al. where 22% of 28 untreated patients with MuSK-MG showed above-threshold IgG4 concentrations (26). Both studies had low numbers of patients due to the rarity of disease, and this may account for the variation. Furthermore, we also did not observe a correlation between total IgG4 and disease severity, while MuSK IgG and disease severity correlated. We then explored the possibility of a relative enrichment of IgG4, combining reduced total IgG levels with stable/higher total IgG4, and observed a significant IgG4/IgG enrichment, which is in line with one previous study (26), but in contrast to another study with no enrichment (27). It is tempting to speculate that differences in IgG1–IgG3 versus IgG4 expression may be influenced by a different inflammation status in IgG4 autoimmunity in contrast to classic IgG1 autoimmunity. In line with this hypothesis, the Vergoossen study observed a relative IgG4 enrichment specific for MuSK-MG that was not observed in AChR-MG. Nonetheless, we and others found elevated serum IgG4 levels and enrichment of IgG4/IgG in patients with AChR-MG (29). We observed a trend for a sub-threshold (<1.35 g/L) increase of total IgG4 levels in both patients with AChR-MG and those with MuSK-MG with and without immunosuppression, and an enrichment of IgG4/IgG in both patients with AChR-MG and those with MuSK-MG, which is in line with the study of Liu and colleagues (29). However, it is possible with the data at hand to agree with the main conclusions of the abovementioned studies (26, 30), that a

significant elevation of serum IgG4, as observed as in IgG4-related diseases, is not observed in MuSK-MG.

What may have caused the discrepant results? Different geographic regions, and thus different genetic backgrounds, as well as technical differences in the determination of IgG and MuSK-specific IgG concentrations may also play a role. Immunosuppression may have affected IgG4 levels, but we also included untreated patients and covariate analysis did not show an effect of treatment on IgG4 levels. The discrepancy in data interpretation is also likely to derive from the data transformation that was applied. Since our data were not normally distributed, we log-transformed the data before regression analyses. When the analyses were performed without the log transformation, the results resembled the Vergoossen study more (26), indicating that differences in the statistical approach may have caused the differences. The enrichment of serum IgG4 in AChR-MG and MuSK-MG is interesting, as mild elevation of IgG4 could be a characteristic of MG in general, as it is also in a range of disorders from cancer to allergy and rheumatoid arthritis (31–35). However, we observed that IgG4 concentrations did not correlate with MuSK IgG concentrations, disease severity, or disease duration in patients with MuSK-MG. Therefore, we conclude that aberrant IgG4 production is unlikely to be the main driver of immunopathogenesis and that MuSK IgG4 only comprises a minor fraction of the total IgG4 antibody repertoire. Furthermore, the presence of individuals with elevated IgG4 (>1.35 g/L) may be common across populations, as IgG4 is known to be highly variable in healthy individuals, ranging between 0.01 and 1.4 mg/mL, dependent on age, sex, and ethnicity, and may seasonally change, e.g., during allergy/infection seasons (36–39). Interestingly, a recent study showed that tobacco smoking is associated in a dose-dependent manner with elevated serum IgG4 levels (40). Smoking after disease onset is associated with an increase in disease severity and the progression towards generalized muscle weakness (41–43), but to date, the effect of smoking on IgG4 in MuSK-MG has not been investigated, and it is possible that tobacco use is a confounding factor for the analysis of serum IgG4.

4.3 Limitations

A key limitation of our study is the fluctuating nature of MuSK-MG, with clinical severity changing over time. Moreover, MG has a low disease prevalence, and therefore, sample numbers were limited. This is a limitation of the study, and findings require to be validated with larger patient numbers in the future. A further limitation of the study is that the clinical severity was assessed only via MGFA scores and not by a more quantitative score such as QMG. Furthermore, owing to technical reasons, MuSK IgG levels assessed at the local diagnostic centers in Pisa and the Neuroimmunology group in Oxford differed from each other (Supplementary Tables). The RIA measurements from Oxford of the patients from Pisa correlated well with the results from our ELISA, suggesting a higher accuracy of the RIA. Therefore, quantitative analyses used the measurements by the RIA measurements from Oxford. The local measurements from Pisa were only used in Figure 1 to investigate the overall change in MuSK IgG levels over time (Figure 1B).

5 Conclusion

General immunosuppression had a clinical benefit for patients with MuSK-MG during the first 4 years of disease duration, but only 13/44 patients with general immunosuppression or 14/52 patients with MuSK-MG in total reached clinical remission, suggesting that other or more intense treatments may be necessary for a substantial fraction of patients with MuSK-MG to reach remission. The immunosuppressive treatment also led to a reduction of MuSK IgG4 in four out of five individual patients, but could not be observed across patients, probably due to inter-patient variability. Serum IgG4 was within the normal range, but relatively enriched (IgG4/IgG) in both patients with AChR-MG and those with MuSK-MG. Owing to the low sample size, further studies with larger cohorts and longitudinal sampling are required to validate these findings.

Data availability statement

The original contributions presented in the study are included in the article/Supplementary Material. Further inquiries can be directed to the corresponding authors.

Ethics statement

The studies involving humans were approved by Institutional Review Boards of the Medical University of Vienna, Austria (EK 1442/2017). The studies were conducted in accordance with the local legislation and institutional requirements. Written informed consent for participation in this study was provided by the participants' legal guardians/next of kin.

Author contributions

IK: Conceptualization, Data curation, Formal analysis, Funding acquisition, Investigation, Methodology, Resources, Supervision, Validation, Visualization, Writing – original draft, Writing – review & editing. MMD: Data curation, Investigation, Methodology, Writing – review & editing. SZ: Data curation, Investigation, Methodology, Writing – review & editing. SDH: Data curation, Investigation, Methodology, Writing – review & editing. SH: Writing – review & editing. DVK: Formal analysis, Validation, Visualization, Writing – original draft, Writing – review & editing. JD: Data curation, Supervision, Writing – review & editing. ADR: Writing – review & editing, Resources. MM: Resources, Writing – review & editing. MG: Resources, Writing – review & editing. PM: Writing – review & editing. PVD: Writing – review & editing, Resources. AF: Writing – review & editing, Data curation, Supervision. TP: Supervision, Writing – review & editing. MDB: Writing – review & editing, Supervision. KL: Resources, Writing – review & editing. VZ: Writing – review & editing, Resources. ST: Resources, Writing – review & editing. RR:

Resources, Writing – review & editing. ML: Resources, Writing – review & editing, Conceptualization, Data curation, Formal analysis, Methodology, Supervision, Validation, Visualization, Writing – original draft. PMM: Conceptualization, Supervision, Writing – original draft, Writing – review & editing, Investigation, Project administration.

Funding

The author(s) declare financial support was received for the research, authorship, and/or publication of this article. We are grateful for financial support offered by the following funding agencies: IK was supported by a Hertha Firnberg project grant by the Austrian Science Fund (FWF): T996-B30. PD holds a senior clinical investigatorship from FWO-Vlaanderen and is supported by the ALS Liga België. PMM was supported by an Aspasia/NWO grant (015.011.033), and SZ and MMD were supported by Kootstra Talent Fellowships.

Acknowledgments

We thank Amelia Evoli for the inclusion of one MuSK-MG patient from Rome.

Conflict of interest

PD participated in advisory board meetings for Pfizer, Biogen, Cytokinetics, CSL Behring, Alexion Pharmaceuticals, argenx, UCB, Muna Therapeutics, Alector, QurAlis and Ferrer. Author ST was employed by company Tzartos NeuroDiagnostics.

The remaining authors declare that the research was conducted in the absence of any commercial or financial relationships that could be construed as a potential conflict of interest.

The author(s) declared that they were an editorial board member of Frontiers, at the time of submission. This had no impact on the peer review process and the final decision.

Publisher's note

Supplementary material

The Supplementary Material for this article can be found online at: https://www.frontiersin.org/articles/10.3389/fimmu.2024.1325171/full#supplementary-material

References

1. Cao M, Koneczny I, Vincent A. Myasthenia gravis with antibodies against muscle specific kinase: an update on clinical features, pathophysiology and treatment. *Front Mol Neurosci.* (2020) 13:159. doi: 10.3389/fnmol.2020.00159

2. Koneczny I, Herbst R. Myasthenia gravis: pathogenic effects of autoantibodies on neuromuscular architecture. *Cells.* (2019) 8. doi: 10.3390/cells8070671

3. DeChiara TM, Bowen DC, Valenzuela DM, Simmons MV, Poueymirou WT, Thomas S, et al. The receptor tyrosine kinase MuSK is required for neuromuscular junction formation in vivo. *Cell.* (1996) 85:501–12. doi: 10.1016/S0092-8674(00)81251-9

4. Hoch W, McConville J, Helms S, Newsom-Davis J, Melms A, Vincent A. Auto-antibodies to the receptor tyrosine kinase MuSK in patients with myasthenia gravis without acetylcholine receptor antibodies. *Nat Med.* (2001) 7:365–8. doi: 10.1038/85520

5. Koneczny I, Cossins J, Vincent A. The role of muscle-specific tyrosine kinase (MuSK) and mystery of MuSK myasthenia gravis. *J anatomy.* (2014) 224:29–35. doi: 10.1111/joa.12034

6. Koneczny I, Cossins J, Waters P, Beeson D, Vincent A. MuSK myasthenia gravis IgG4 disrupts the interaction of LRP4 with MuSK but both IgG4 and IgG1-3 can disperse preformed agrin-independent AChR clusters. *PloS One.* (2013) 8:e80695. doi: 10.1371/journal.pone.0080695

7. McConville J, Farrugia ME, Beeson D, Kishore U, Metcalfe R, Newsom-Davis J, et al. Detection and characterization of MuSK antibodies in seronegative myasthenia gravis. *Ann Neurol.* (2004) 55:580–4. doi: 10.1002/ana.20061

8. Klooster R, Plomp JJ, Huijbers MG, Niks EH, Straasheijm KR, Detmers FJ, et al. Muscle-specific kinase myasthenia gravis IgG4 autoantibodies cause severe neuromuscular junction dysfunction in mice. *Brain.* (2012) 135:1081–101. doi: 10.1093/brain/aws025

9. Huijbers MG, Zhang W, Klooster R, Niks EH, Friese MB, Straasheijm KR, et al. MuSK IgG4 autoantibodies cause myasthenia gravis by inhibiting binding between MuSK and Lrp4. *Proc Natl Acad Sci U S A.* (2013) 110:20783–8. doi: 10.1073/pnas.1313944110

10. Huijbers MG, Querol LA, Niks EH, Plomp JJ, van der Maarel SM, Graus F, et al. The expanding field of IgG4-mediated neurological autoimmune disorders. *Eur J Neurol.* (2015) 22:1151–61. doi: 10.1111/ene.12758

11. Koneczny I. Update on IgG4-mediated autoimmune diseases: New insights and new family members. *Autoimmun Rev.* (2020) 19:102646. doi: 10.1016/j.autrev.2020.102646

12. Panhuber A, Lamorte G, Bruno V, Cetin H, Bauer W, Hoftberger R, et al. A systematic review and meta-analysis of HLA class II associations in patients with IgG4 autoimmunity. *Sci Rep.* (2022) 12:9229. doi: 10.1038/s41598-022-13042-2

13. Koneczny I, Tzartos J, Mane-Damas M, Yilmaz V, Huijbers MG, Lazaridis K, et al. IgG4 autoantibodies in organ-specific autoimmunopathies: reviewing class switching, antibody-producing cells, and specific immunotherapies. *Front Immunol.* (2022) 13:834342. doi: 10.3389/fimmu.2022.834342

14. Koneczny I, Yilmaz V, Lazaridis K, Tzartos J, Lenz TL, Tzartos S, et al. Common denominators in the immunobiology of igG4 autoimmune diseases: what do glomerulonephritis, pemphigus vulgaris, myasthenia gravis, thrombotic thrombocytopenic purpura and autoimmune encephalitis have in common? *Front Immunol.* (2021) 11. doi: 10.3389/fimmu.2020.605214

15. Suh J, Goldstein JM, Nowak RJ. Clinical characteristics of refractory myasthenia gravis patients. *Yale J Biol Med.* (2013) 86:255–60.

16. Baggi F, Andreetta F, Maggi L, Confalonieri P, Morandi L, Salerno F, et al. Complete stable remission and autoantibody specificity in myasthenia gravis. *Neurology.* (2013) 80:188–95. doi: 10.1212/WNL.0b013e31827b907b

17. Evoli A, Alboini PE, Damato V, Iorio R, Provenzano C, Bartoccioni E, et al. Myasthenia gravis with antibodies to MuSK: an update. *Ann N Y Acad Sci.* (2018) 1412:82–9. doi: 10.1111/nyas.13518

18. Gilhus NE, Tzartos S, Evoli A, Palace J, Burns TM, Verschuuren J. Myasthenia gravis. *Nat Rev Dis primers.* (2019) 5:30. doi: 10.1038/s41572-019-0079-y

19. Evoli A, Bianchi MR, Riso R, Minicuci GM, Batocchi AP, Servidei S, et al. Response to therapy in myasthenia gravis with anti-MuSK antibodies. *Ann N Y Acad Sci.* (2008) 1132:76–83. doi: 10.1196/annals.1405.012

20. Diaz-Manera J, Martinez-Hernandez E, Querol L, Klooster R, Rojas-Garcia R, Suarez-Calvet X, et al. Long-lasting treatment effect of rituximab in MuSK myasthenia. *Neurology.* (2012) 78:189–93. doi: 10.1212/WNL.0b013e3182407982

21. Tomschik M, Hilger E, Rath J, Mayer EM, Fahrner M, Cetin H, et al. Subgroup stratification and outcome in recently diagnosed generalized myasthenia gravis. *Neurology.* (2020) 95:e1426–e36. doi: 10.1212/WNL.0000000000010209

22. Marino M, Basile U, Spagni G, Napodano C, Iorio R, Gulli F, et al. Long-lasting rituximab-induced reduction of specific-but not total-igG4 in muSK-positive myasthenia gravis. *Front Immunol*. (2020) 11:613. doi: 10.3389/fimmu.2020.00613

23. Graus YF, de Baets MH, van Breda Vriesman PJ, Burton DR. Anti-acetylcholine receptor Fab fragments isolated from thymus-derived phage display libraries from myasthenia gravis patients reflect predominant specificities in serum and block the action of pathogenic serum antibodies. *Immunol Lett*. (1997) 57:59–62. doi: 10.1016/S0165-2478(97)00046-1

24. Bartoccioni E, Scuderi F, Minicuci GM, Marino M, Ciaraffa F, Evoli A. Anti-MuSK antibodies: correlation with myasthenia gravis severity. *Neurology*. (2006) 67:505–7. doi: 10.1212/01.wnl.0000228225.23349.5d

25. Huijbers MG, Plomp JJ, van der Maarel SM, Verschuuren JJ. IgG4-mediated autoimmune diseases: a niche of antibody-mediated disorders. *Ann N Y Acad Sci*. (2018) 1413:92–103. doi: 10.1111/nyas.13561

26. Vergoossen DLE, Ruiter AM, Keene KR, Niks EH, Tannemaat MR, Strijbos E, et al. Enrichment of serum IgG4 in MuSK myasthenia gravis patients. *J Neuroimmunol*. (2022) 373:577978. doi: 10.1016/j.jneuroim.2022.577978

27. Endmayr V, Tunc C, Ergin L, de Rosa A, Weng R, Wagner L, et al. Anti-neuronal IgG4 autoimmune diseases and IgG4-related diseases may not be part of the same spectrum: a comparative study. *medRxiv*. (2021). doi: 10.1101/2021.09.30.21264258

28. Marcuse F, Brandts L, Moens D, Damoiseaux J, Hochstenbag M, Hoeijmakers JGJ, et al. The association between anti-acetylcholine receptor antibody level and clinical improvement in myasthenia gravis. *Eur J Neurol*. (2022) 29:1187–97. doi: 10.1111/ene.15238

29. Liu Y, Wang W, Li J. Evaluation of serum IgG subclass concentrations in myasthenia gravis patients. *Int J Neurosci*. (2011) 121:570–4. doi: 10.3109/00207454.2011.596293

30. Endmayr V, Tunc C, Ergin L, De Rosa A, Weng R, Wagner L, et al. Anti-neuronal igG4 autoimmune diseases and igG4-related diseases may not be part of the same spectrum: A comparative study. *Front Immunol*. (2021) 12:785247. doi: 10.3389/fimmu.2021.785247

31. Chen LF, Mo YQ, Ma JD, Luo L, Zheng DH, Dai L. Elevated serum IgG4 defines specific clinical phenotype of rheumatoid arthritis. *Mediators inflammation*. (2014) 2014:635293. doi: 10.1155/2014/635293

32. Wang Z, Zhu M, Luo C, Zhen Y, Mu J, Zhang W, et al. High level of IgG4 as a biomarker for a new subset of inflammatory bowel disease. *Sci Rep*. (2018) 8:10018. doi: 10.1038/s41598-018-28397-8

33. Ryu JH, Horie R, Sekiguchi H, Peikert T, Yi ES. Spectrum of disorders associated with elevated serum igG4 levels encountered in clinical practice. *Int J Rheumatol*. (2012) 2012:232960. doi: 10.1155/2012/232960

34. Boonstra K, Culver EL, de Buy Wenniger LM, van Heerde MJ, van Erpecum KJ, Poen AC, et al. Serum immunoglobulin G4 and immunoglobulin G1 for distinguishing immunoglobulin G4-associated cholangitis from primary sclerosing cholangitis. *Hepatology*. (2014) 59:1954–63. doi: 10.1002/hep.26977

35. Ebbo M, Grados A, Bernit E, Vely F, Boucraut J, Harle JR, et al. Pathologies associated with serum igG4 elevation. *Int J Rheumatol*. (2012) 2012:602809. doi: 10.1155/2012/602809

36. Nirula A, Glaser SM, Kalled SL, Taylor FR. What is IgG4? A review of the biology of a unique immunoglobulin subtype. *Curr Opin Rheumatol*. (2011) 23:119–24. doi: 10.1097/BOR.0b013e3283412fd4

37. French M. Serum IgG subclasses in normal adults. *Monogr Allergy*. (1986) 19:100–7.

38. Aucouturier P, Danon F, Daveau M, Guillou B, Sabbah A, Besson J, et al. Measurement of serum IgG4 levels by a competitive immunoenzymatic assay with monoclonal antibodies. *J Immunol Methods*. (1984) 74:151–62. doi: 10.1016/0022-1759(84)90376-4

39. Harkness T, Fu X, Zhang Y, Choi HK, Stone JH, Blumenthal KG, et al. Immunoglobulin G and immunoglobulin G subclass concentrations differ according to sex and race. *Ann allergy Asthma immunology: Off Publ Am Coll Allergy Asthma Immunol*. (2020) 125:190–5 e2. doi: 10.1016/j.anai.2020.03.018

40. Tsuji Y, Koga T, Nonaka F, Nobusue K, Kawashiri SY, Yamanashi H, et al. Identification of risk factors for elevated serum IgG4 levels in subjects in a large-scale health checkup cohort study. *Front Immunol*. (2023) 14:1124417. doi: 10.3389/fimmu.2023.1124417

41. Gratton SM, Herro AM, Feuer WJ, Lam BL. Cigarette smoking and activities of daily living in ocular myasthenia gravis. *J neuro-ophthalmology: Off J North Am Neuro-Ophthalmology Society*. (2016) 36:37–40. doi: 10.1097/WNO.0000000000000306

42. Miyazaki Y, Niino M, Sakushima K, Takahashi E, Naganuma R, Amino I, et al. Association of smoking and generalized manifestations of myasthenia gravis. *Intern Med*. (2022) 61:1693–8. doi: 10.2169/internalmedicine.8460-21

43. Apinyawasisuk S, Chongpison Y, Thitisaksakul C, Jariyakosol S. Factors affecting generalization of ocular myasthenia gravis in patients with positive acetylcholine receptor antibody. *Am J Ophthalmol*. (2020) 209:10–7. doi: 10.1016/j.ajo.2019.09.019

frontiers | Frontiers in Immunology

TYPE Original Research
PUBLISHED 16 May 2024
DOI 10.3389/fimmu.2024.1376456

OPEN ACCESS

EDITED BY
Jakob Nilsson,
University Hospital Zürich, Switzerland

REVIEWED BY
Ilijas Jelcic,
Neurozentrum Bellevue AG, Switzerland
Amanda Piquet,
University of Colorado Anschutz Medical Campus, United States

*CORRESPONDENCE
Romana Höftberger
romana.hoeftberger@meduniwien.ac.at

†These authors have contributed equally to this work

RECEIVED 25 January 2024
ACCEPTED 15 April 2024
PUBLISHED 16 May 2024

CITATION
Koneczny I, Macher S, Hutterer M, Seifert-Held T, Berger-Sieczkowski E, Blaabjerg M, Breu M, Dreyhaupt J, Dutra LA, Erdler M, Fae I, Fischer G, Frommlet F, Heidbreder A, Högl B, Klose V, Klotz S, Liendl H, Nissen MS, Rahimi J, Reinecke R, Ricken G, Stefani A, Süße M, Teive HAG, Weis S, Berger T, Sabater L, Gaig C, Lewerenz J and Höftberger R (2024) HLA dependency and possible clinical relevance of intrathecally synthesized anti-IgLON5 IgG4 in anti-IgLON5 disease. *Front. Immunol.* 15:1376456. doi: 10.3389/fimmu.2024.1376456

HLA dependency and possible clinical relevance of intrathecally synthesized anti-IgLON5 IgG4 in anti-IgLON5 disease

Inga Koneczny[1], Stefan Macher[2], Markus Hutterer[3,4], Thomas Seifert-Held[5,6], Evelyn Berger-Sieczkowski[2], Morten Blaabjerg[7], Markus Breu[2], Jens Dreyhaupt[8], Livia Almeida Dutra[9], Marcus Erdler[10], Ingrid Fae[11], Gottfried Fischer[11], Florian Frommlet[12], Anna Heidbreder[3,13], Birgit Högl[13], Veronika Klose[14], Sigrid Klotz[1], Herburg Liendl[6], Mette S. Nissen[7], Jasmin Rahimi[10], Raphael Reinecke[1], Gerda Ricken[1], Ambra Stefani[13], Marie Süße[15], Helio A. G. Teive[16], Serge Weis[17], Thomas Berger[2,18], Lidia Sabater[19,20], Carles Gaig[20,21], Jan Lewerenz[14†] and Romana Höftberger[1,18*†]

[1]Division of Neuropathology and Neurochemistry, Department of Neurology, Medical University of Vienna, Vienna, Austria, [2]Department of Neurology, Medical University of Vienna, Vienna, Austria, [3]Department of Neurology, Johannes Kepler University Linz, Linz, Austria, [4]Department of Neurology with Stroke Unit and Acute Geriatrics, Saint John of God Hospital Linz, Linz, Austria, [5]Department of Neurology, Medical University of Graz, Graz, Austria, [6]Department of Neurology, Landeskrankenhaus (LKH) Murtal, Standort Knittelfeld, Austria, [7]Department of Neurology, Odense University Hospital, Odense, Denmark, [8]Institute for Epidemiology and Medical Biometry, Ulm University, Ulm, Germany, [9]Brain Institute, Hospital Israelita Albert Einstein, São Paulo, Brazil, [10]Department of Neurology and Karl Landsteiner Institute for Neuroimmunological and Neurodegenerative Disorders Klinik Donaustadt, Vienna, Austria, [11]Department of Blood Group Serology and Transfusion Medicine, Medical University of Vienna, Vienna, Austria, [12]Center of Medical Data Science, Medical University of Vienna, Vienna, Austria, [13]Department of Neurology, Medical University of Innsbruck, Innsbruck, Austria, [14]Department of Neurology, University Hospital Ulm, Ulm, Germany, [15]Department of Neurology, University Medicine Greifswald, Greifswald, Germany, [16]Movement Disorders Unit, Neurology Service, Internal Medicine Department, Hospital de Clínicas, Federal University of Paraná, Curitiba, PR, Brazil, [17]Division of Neuropathology, Department of Pathology and Molecular Pathology, Johannes Kepler University Linz, Linz, Austria, [18]Comprehensive Center for Clinical Neurosciences and Mental Health, Medical University of Vienna, Vienna, Austria, [19]Fundació de recerca clínic-Institut d'Investigacions Biomèdiques August Pi i Sunyer (FCRB-IDIBAPS), Caixa Research Institute (CRI), Universitat de Barcelona, Barcelona, Spain, [20]Centro de Investigación Biomédica en Red de Enfermedades Raras (CIBERER), Madrid, Spain, [21]Department of Neurology, Hospital Clínic, Barcelona, Spain

Background: Anti-IgLON5 disease is a rare chronic autoimmune disorder characterized by IgLON5 autoantibodies predominantly of the IgG4 subclass. Distinct pathogenic effects were described for anti-IgLON5 IgG1 and IgG4, however, with uncertain clinical relevance.

Methods: IgLON5-specific IgG1-4 levels were measured in 46 sera and 20 cerebrospinal fluid (CSF) samples from 13 HLA-subtyped anti-IgLON5 disease patients (six females, seven males) using flow cytometry. Intervals between two consecutive serum or CSF samplings (31 and 10 intervals, respectively) were categorized with regard to the immunomodulatory treatment active at the end of

the interval, changes of anti-IgLON5 IgG1 and IgG4 levels, and disease severity. Intrathecal anti-IgLON5 IgG4 synthesis (IS) was assessed using a quantitative method.

Results: The median age at onset was 66 years (range: 54–75), disease duration 10 years (range: 15–156 months), and follow-up 25 months (range: 0–83). IgLON5-specific IgG4 predominance was observed in 38 of 46 (83%) serum and 11 of 20 (55%) CSF samples. Anti-IgLON5 IgG4 levels prior clinical improvement in CSF but not serum were significantly lower than in those prior stable/progressive disease. Compared to IgLON5 IgG4 levels in serum, CSF levels in HLA-DRB1*10:01 carriers were significantly higher than in non-carriers. Indeed, IgLON5-specific IgG4 IS was demonstrated not only in four of five HLA-DRB1*10:01 carriers but also in one non-carrier. Immunotherapy was associated with decreased anti-IgGLON5 IgG serum levels. In CSF, lower anti-IgLON5 IgG was associated with immunosuppressive treatments used in combination, that is, corticosteroids and/or azathioprine plus intravenous immunoglobulins or rituximab.

Conclusion: Our findings might indicate that CSF IgLON5-specific IgG4 is frequently produced intrathecally, especially in HLA-DRB1*10:01 carriers. Intrathecally produced IgG4 may be clinically relevant. While many immunotherapies reduce serum IgLON5 IgG levels, more intense immunotherapies induce clinical improvement and may be able to target intrathecally produced anti-IgLON5 IgG. Further studies need to confirm whether anti-IgLON5 IgG4 IS is a suitable prognostic and predictive biomarker in anti-IgLON5 disease.

KEYWORDS

IgLON5, IgG4, HLA, cerebrospinal fluid, intrathecal synthesis, therapy

Introduction

Anti-IgLON5 disease is a rare chronic autoimmune disorder hallmarked by antineuronal surface autoantibodies against IgLON5, an immunoglobulin superfamily cell-adhesion molecule with high expression in the central nervous system (CNS). The clinical presentation of anti-IgLON5 disease is quite heterogeneous with patients presenting with distinct rapid eye movement (REM) and non-REM parasomnias, obstructive sleep apnea and stridor, variable features of gait instability, movement disorders, and brainstem symptoms (1). Anti-IgLON5 disease is typically chronically progressive. Depending on which symptoms predominate, four different phenotypes have been delineated which are dominated by either (1): the sleep disorder with parasomnia and sleep apnea (2); bulbar dysfunction with dysarthria, dysphagia, sialorrhea, stridor, or acute respiratory insufficiency (3); a progressive supranuclear palsy (PSP)–like movement disorder; or (4) cognitive decline (1). Rare phenotypes mimic motor neuron disease or acute encephalitis (2, 3). The typically insidious clinical course and neuronal tau aggregates predominantly involving the brainstem and hypothalamus (4) suggest an underlying neurodegenerative process. However, tauopathy may be absent in some patients (5). In turn, a strong association with HLA-DRB1*10:01 and HLA-DQB1*05:01 alleles and the observations that IgLON5-specific IgG1 may cause IgLON5 protein internalization and subsequent cytoskeletal changes *in vitro* (6) point to a primary autoimmune process. Indeed, patients with anti-IgLON5 disease may benefit from early immunotherapy (7). The anti-IgLON5 antibodies are predominantly of the IgG4 subclass (followed by IgG1) in most patients (4). Anti-IgLON5 IgG1 induced irreversible IgLON5 internalization (8), whereas IgG4 interfered with IgLON5 protein interactions (9) *in vitro*. However, their individual contributions to disease *in vivo* and their prognostic/predictive relevance remain unclear.

Autoimmune encephalitis (AIE) with neuronal surface autoantibodies are heterogenous (10) but may be grouped according to the IgG1 or IgG4 predominance of their target-specific antineuronal antibodies (10). CSF inflammation in IgG4-predominant AIEs is typically less prominent than in IgG1-predominant AIEs (11). AIE associated with NMDAR antibodies is a prototypical IgG1-predominant AIE. Herein, prominent intrathecal

synthesis (IS) of the total and target-specific IgG is well established (12). Surprisingly, in LGI1-antibody AIE (which is the most common IgG4-associated AIE), the otherwise non-inflammatory CSF contains many target-specific B cells. B cells and plasma cells also occur frequently in the largely non-inflammatory CSF in anti-IgLON5 disease (13, 14). Thus, target-specific IgG IS may also play a role in IgG4-predominant autoimmune disorders, including anti-IgLON5 disease. Of note, antigen-specific IgG IS is much more difficult to target therapeutically than systemic antibody production (15, 16).

Here, we longitudinally investigate the changes in individual anti-IgLON5 IgG subclass profiles in serum and CSF of 13 anti-IgLON5 disease patients in association with short- and long-term treatment follow-up. In addition, we established a method to quantify IS of anti-IgLON5 IgG4. Our aim was to delineate factors contributing to disease progression and characterize candidate biomarkers for therapeutic response.

Methods

Patients

Longitudinal serum and CSF of 13 patients with anti-IgLON5 disease were included in this study. The samples were referred to the Division of Neuropathology and Neurochemistry at the Department of Neurology, Medical University of Vienna for diagnostic testing between October 2014 and December 2022. The clinical information was obtained by the investigators. Four patients were previously published (17–21). The disease severity was estimated as functional impairment using the modified Rankin scale (mRS) at the different sample time points.

Flow cytometry analysis of IgG subclasses

The analysis of IgG subclasses was adapted from our previously published method (22, 23). Briefly, HEK293T cells were transfected with plasmid DNA encoding full-length human IgLON5 fused to Turbo GFP (tGFP, derived from Origene, Rockville, Maryland, USA, RG22549). Each 2×10^5 cells were incubated with a 1:40 dilution of patient serum or 1:10 dilution of CSF in incubation medium (DMEM supplemented with 1% penicillin/streptomycin, 1% BSA, 20mM HEPES, and 10% donkey serum) for 20 min at 4°C. The cells then were washed, fixed for 10 min using 4% paraformaldehyde, washed, and incubated with 1:500 biotinylated mouse anti-human IgG1 (B6775), IgG2 (B3398), IgG3 (B3523), or IgG4 (B3648, all by Sigma-Aldrich, St Louis, Missouri, USA) in incubation medium for 30 min at 4°C. The cells were again washed, and bound biotinylated IgG was visualized by incubating cells with Cy3-streptavidin (434315, Invitrogen, Waltham, Massachusetts, USA) diluted 1:750 in incubation medium for 30 min at 4°C in the dark. The cells were washed and resuspended in phosphate-buffered saline with 2.5 mM ethylenediaminetetraacetic acid, pH 8.0 before analysis with a Cytoflex LX flow cytometer (Beckman Coulter Brea, California, USA). tGFP-positive and -negative cells were gated, respectively, and their median fluorescence intensity (MFI) for Cy3 was measured in the phytoerythrin channel (Supplementary Methods Figure S1), the value of tGFP-negative cells was subtracted from tGFP-positive cells to account for unspecific binding of antibodies to the cells (ΔMFI). Depending on serum/CSF availability, the measurements were repeated in independent experiments (N = 1–5). Four reference samples were measured in every experiment and used to normalize the results of individual experiments (Supplementary Methods). These assay conditions resulted in a largely linear correlation of ΔMFI with antibody levels. At very high levels, ΔMFI reached the nonlinear range (Supplementary Methods). While technical limitations (the use of different subclass-specific antibodies) did not permit the calculation of absolute percentages of anti-IgLON5 IgG1, 2, 3, and 4 and total anti-IgLON5 IgG, the sum of anti-IgLON5 IgG1 + 2+3 + 4 ΔMFI was used as a surrogate marker for total anti-IgLON5 IgG ("total" anti-IgLON5 IgG), which was used to determine relative percentages of anti-IgLON5-IgG1, 2, 3, and 4. IgG4 predominance was defined as anti-IgLON5 IgG4 exceeding 66% of "total" anti-IgLON5 IgG. Anti-IgLON5 IgG4/IgG1 ratios were calculated for every sample. All analyses were made for anti-IgLON5 IgG1-4. Thus, all references to IgG1-4 always refer to anti-IgLON5 IgG1-4.

Interval analysis

Each interval flanked by either two subsequent serum or CSF samplings was characterized in four dimensions: (1) duration, (2) immunosuppressive treatment regimen at the end of the interval, (3) changes in disease severity, and (4) anti-IgLON5 IgG levels. We defined the following time spans for the treatment effects, which include one additional month as buffer: 4 months for intravenous immunoglobulins (IVIG) (24), 7 months for rituximab, 4 months for corticosteroids >5 mg, 5 months for cyclophosphamide, 5 months for azathioprine. For acute therapies, immunoadsorption (IA) and plasmapheresis were considered active for 1 month (Figure 1). Clinical improvement was defined as a decrease and clinical worsening as an increase in the mRS. In mildy affected patients (mRS always 1), descriptions of clinical improvements or worsening were taken into account. A >25% increase in antibody levels during the interval was defined as increased, a change of ±25% as unchanged, and >25% decrease as decreased levels. We defined IgG4/IgG1 ratio during sampling intervals as lower (>20% less), stable (0 ± 20%), or increased (>20% higher) ratios.

HLA genotyping

Genotyping of HLA-DRB1 and -DQB1 was performed as described (25). We used HLA-genotyping data from the 11 Austrian patients (Supplementary Table S3) and HLA data from a cohort of 200 Austrian individuals from the database of the Allele Frequency Network (26) to calculate the relative frequency of distinct HLA alleles as odds ratio (OR, Supplementary Table S4).

10.3389/fimmu.2024.1376456

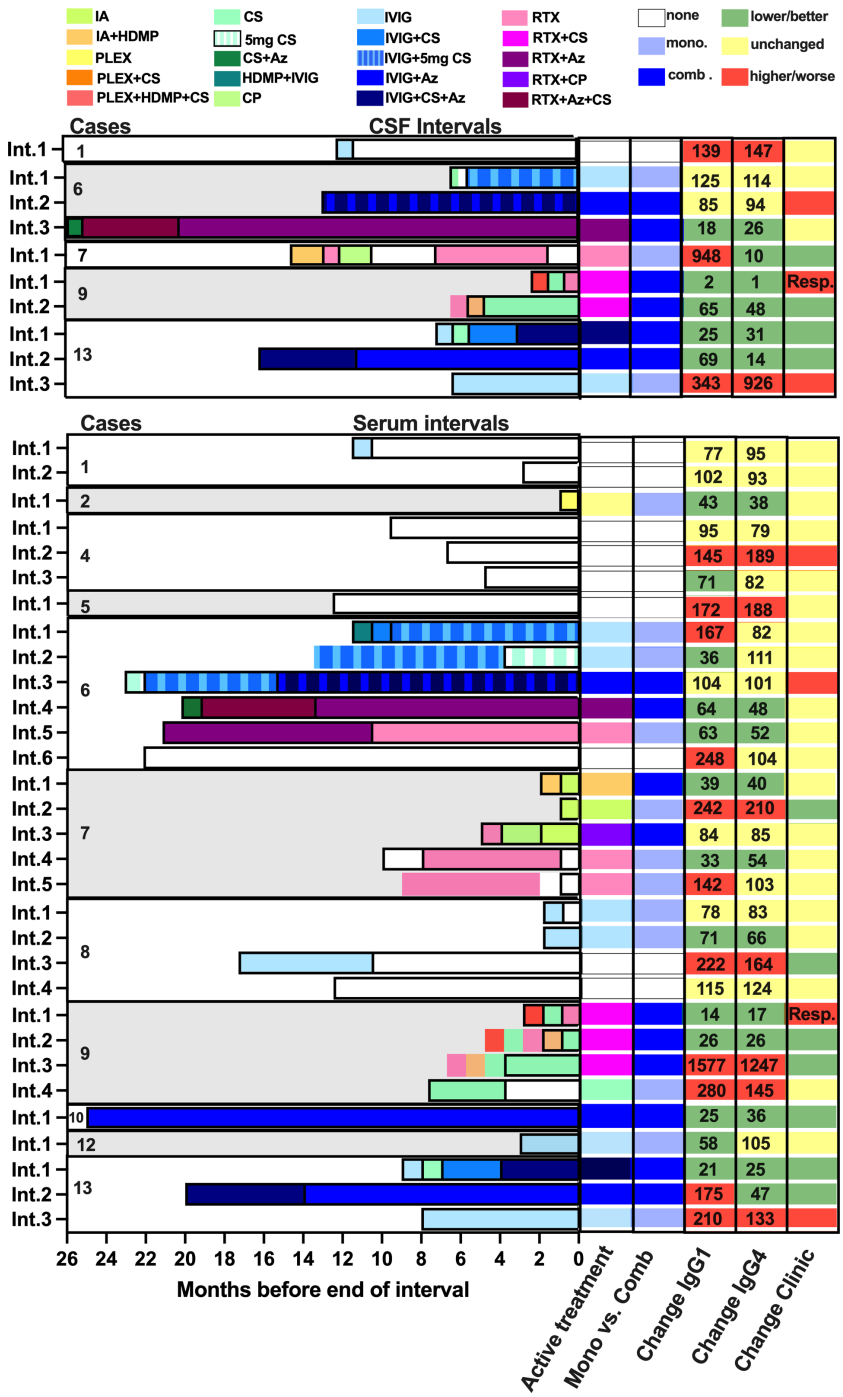

FIGURE 1
Graphical summary of serum and cerebral spinal fluid intervals including immunomodulatory treatments, changes in anti-IgLON5 IgG1 and IgG4 levels, as well as clinical changes. Treatments were color-coded as indicated. The last active treatment was assessed as described in the Methods sections. Two long-active treatment in parallel (with corticosteroids >5 mg/day) were categorized as combination treatment. The numbers in the columns for changes in IgG1 and IgG4 indicate the percentage change at the end of each interval compared to the start. Resp = patient responded well to rituximab 1 month after first treatment, but the interval terminated 1 week before manifestation of clinical improvement.

Intrathecal IgLON5 antibody synthesis

Anti-IgLON5 IgG4 IS was assessed in anti-IgLON5-disease CSF/serum pairs with routine data for the total CSF/serum IgG ratio (Q_{IgG}) and CSF/serum albumin ratio (Q_{Alb}) available. No IS of total IgG was reported for the serum/CSF pairs utilized. To calculate CSF/serum ratios, data points need to be in the absolutely linear range of the assay, and matrix effects must be absent. To generate suitable raw data, anti-IgLON5 IgG4 levels were measured in sera and CSF following dilution to identical IgG concentrations, to ensure ΔMFI intensities in a similar range in the absence of IS and strictly within the linear range of the assay (see Supplementary Methods).

The CSF/serum ΔMFI intensity ratio obtained by this approach is identical to the CSF/serum antibody index (AI) as reported by Reiber and Lange (27). The CSF/serum anti-IgLON5 IgG4 ratio was then obtained by multiplying the CSF and serum ΔMFI by the respective dilution factors. Z scores for anti-IgLON5 IgG4 IS and total IgG IS were calculated as described recently (28). Control CSF/serum pairs without IS ("control AI 1," IgLON5-antibody-negative CSF/serum pairs spiked with high-titer IgLON5-IgG4 sera to obtain a $Q_{IgLON5\text{-}IgG4}$ identical to the Q_{IgG}) and 10-fold IS ("control AI 10," IgLON5-antibody-negative CSF/serum pairs spiked with high-titer IgLON5-IgG4 sera to obtain a $Q_{IgLON5\text{-}IgG4}$ 10-fold higher than the Q_{IgG}) were used to successfully validate the assay (Supplementary Methods).

Statistical analysis

The OR and 95% confidence intervals (95% CI) for individual HLA alleles of Austrian patients were calculated using Episheet[1] (29). Unless stated otherwise, descriptive statistics of ordinal- and interval-scaled variables are given as median and interquartile range (IQR). The statistical analysis was done with GraphPad Prism 9.0 software, using either Fisher's exact test, Mann–Whitney, Kruskal–Wallis test or linear regression with Pearson correlation as appropriate. Statistical significance was determined as $p \leq 0.05$. Due to the low number of patients, data points and the retrospective nature, the statistical analysis had to be categorized as exploratory and merely hypothesis-generating. Consequently, a one-sided testing strategy was applied if not stated otherwise.

Standard protocol approvals, registrations, and patient consents

The study was approved by the Ethics Committee of the Medical University of Vienna (EK 1442/2017, 1636/19, and 1123/15).

Results

Patients

Twenty CSF and 46 serum samples (in total 66 samples) were available from 13 patients with positive results in the IgLON5 cell-based assay (six females, seven males, 11 from Austria, one from Denmark, and one from Germany). The median age at onset was 66 years (range: 54–75) with a follow-up time of 25 months (range: 0–83). Longitudinal sampling was available from 11 patients with a median number of four serum samples (range: 0–7) and one CSF sample (range: 0–4). Among these, five patients with matching serum/CSF pairs with routine data for Q_{Alb} and Q_{IgG} were still available after initial measurements. The disease duration between disease onset and the last serum/CSF sample analyzed was 10 years (range: 1.25–13 years).

Nine of the 13 patients (69%) exhibited one of the phenotypes characterized by Gaig et al. (1). However, only one patient (8%) presented with the prototypical sleep disorder. A bulbar syndrome found in four patients (31%) was most common. A PSP-like phenotype was also common (3 of 13, 23%). One patient (8%) presented with a cognitive phenotype. Four patients (31%) could not be classified according to Gaig et al. (1). Two (15%) predominantly exhibited peripheral hyperexcitability. One of the two remaining patients' phenotype clinically resembled Parkinson's disease in combination with peripheral hyperexcitability. The other remaining patient showed gait instability, mild cognitive impairment, sensory hyperexcitability as well as transient choreoathetosis of the left arm (Supplementary Tables S1/S2, see Appendix for detailed case descriptions).

Median mRS at first presentation was 3 (range: 1–5). Three (23%) patients improved by at least one mRS point during follow-up, six (46%) worsened and died during follow-up after a disease duration of 124 (120–147) months compared to seven (54%) surviving patients with a disease duration at last follow-up of 85 (48–128) months ($p = 0.08$). The patients who died had significantly higher mRS (median: 3.5, range: 3–5) at time of diagnosis than surviving patients (median: 2, range: 1–3; $p = 0.006$, Supplementary Figure S1). Nine of 13 (69%) patients received eight different therapeutic regimens [IVIG, plasmapheresis (PLEX), oral corticosteroids (CS), intravenous high-dose methylprednisolone, azathioprine (Aza), rituximab (RTX), cyclophosphamide (CP), immunoadsorption (IA) alone or in combination]. Four patients (31%) carried both HLA-DRB1*10:01 and HLA-DQB1*05:01 risk alleles, six (46%) carried one risk allele (one HLA-DRB1*10:01 only, five HLA-DQB1*05:01 only), while three (23%) carried none (Supplementary Table S3). Compared to an Austrian reference population, the allele frequency for both HLA-DRB1*10:01 and HLA-DQB1*05:01 was significantly increased in the 11 Austrian patients [OR (95%CI): HLA-DRB1*10:01 75 (5–3933), $p < 0.001$; HLA-DQB1*05:01 8 (2–51), $p < 0.01$, Supplementary Table S4]. Presence of the HLA-DRB1*10:01 risk allele did not affect age of onset or sex distribution (Supplementary Figure S2A). However, DRB1*10:01-negative patients at clinical presentation tended to be slightly less functionally impaired [median mRS (IQR): DRB1*10:01-negative 2.5 (2.0–3.0), DRB1*10:01-positive 3.0 (3.0–4.5); $p = 0.1974$] associated with a tendency to more frequent clinical stability [negative: five of eight (63%), positive: one of five (20%); $p = 0.1795$, Supplementary Figure S2B]; however, these effects were not statistically significant. All three patients with a PSP-like phenotype were DRB1*10:01-negative [PSP-like/total with specificDRB1*10:01 carrier status: negative 3/8 (38%), positive 0/5, $p = 0.0435$], two other DRB1*10:01-negative cases presented with atypical phenotypes with peripheral hyperexcitability (one resembling Parkinson's disease, and the other non-classifiable, Supplementary Figure S2C and Supplementary Tables S1/S2). Interestingly, median CSF cell count was sevenfold higher in DRB1*10:01-positive compared to negative cases [positive: 7 (2.5–36) leukocytes/µl; negative: 1 (0–3.5) leukocytes/µl; $p = 0.0101$, Supplementary Figure 2D].

1 http://www.epidemiolog.net/studymat/.

Changes in CSF anti-IgLON5 IgG4 coincide with changes in disease severity

Next, we assessed anti-IgLON5 IgG1-4 levels in serum and CSF (Supplementary Figures S3/S4). The relative variability in serum anti-IgLON5 IgG1 was higher than for IgG4 (Supplementary Figure S5). Anti-IgLON5 IgG4 predominated in 38 of 46 (83%) serum, but only 11 of 20 (55%) CSF samples ($p = 0.022$), IgG1 in one of 46 (2%) serum and one of 20 (5%) CSF samples. Interestingly, IgG4 predominance of anti-IgLON5 IgG was due to higher anti-IgLON5 IgG4 levels but not lower anti-IgLON5 IgG1 levels in both serum and CSF (Supplementary Figure S6). Then, we analyzed whether either anti-IgLON5 IgG1 and 4 levels in serum and CSF preceded future clinical changes or whether changes in antibody levels were paralleled by changes in symptoms severity in the various intervals between CSF and serum samplings with different treatments considered active at the end ot the interval (Figure 1). In contrast to serum (Figures 2A/2C, left panels), CSF anti-IgLON5 IgG1 tended to be and IgG4 levels were significantly lower prior to improvement compared to stable or worsening disease (IgG1: $p = 0.09$, IgG4: $p = 0.04$, Figures 2B, D, left panels). During the intervals, no association with changes in serum anti-IgLON5 IgG1/4 levels nor CSF anti-IgLON5 IgG1 levels was found (Figures 2A–C, right panels). However, in four of six (66%) intervals with decreased CSF anti-IgLON5 IgG4 levels clinical improvement was noted but, in none of the intervals in stable or increased CSF anti-IgON5 IgG4 levels, a finding not statistically significant due to the low number of data points ($p = 0.08$, Figure 2D, right panel). Of note, no systematic changes of interval length correlated with changes in IgG4, IgG1, IgG4/IgG1 ratio, or functional impairment (Supplementary Figure S7). Q_{Alb}, available for seven of 13 (54%) measurements preceding stable disease or worsening and two of three (67%) preceding improvement, was not lower in the group experiencing future improvement than in those with less good outcome (Supplementary Figure S8). Thus, it seems highly unlikely that the low CSF IgG4 levels prior to improvement are explained by better blood/CSF-barrier function resulting in less filtration of blood anti-IgLON5 IgG4 into the CSF.

CSF anti-IgLON5 IgG4 is synthesized intrathecally especially in HLA-DRB*10:01 carriers

Plotting CSF against serum anti-IgLON5 IgG4 levels in all first CSF/serum pairs showed considerably higher relative CSF anti-IgLON5 levels in patients carrying the DRB1*10:01 allele compared to non-carriers (Figure 3A, left panel). When filtrated into the CSF from plasma, IgG levels are usually 100- to 1,000-fold lower compared to serum levels corresponding to CSF-to-serum ratios of $1–10 \times 10^{-3}$ (30). CSF levels in three of four DRB1*10:01-negative patients were 292- to 433-fold lower than serum levels (Supplementary Table S2), thus, in the expected range when explained by filtration into the CSF only. CSF anti-IgLON5 IgG4 in the fourth non-carrier, patient 12, was only 32-fold lower. In the five DRB1*10:01 carriers, CSF anti-IgLON5 levels were only fourfold to 23-fold lower than the respective serum levels. This resulted in 26-fold higher CSF/serum IgG4 ratios in DRB1*10:01 carriers [75 (59–153) $\times 10^{-3}$] compared to non-carriers [2.9 (2.3–24) $\times 10^{-3}$, $p = 0.008$, Figure 3A, right panel]. Of note, this effect seems to be independent of a simultaneous DQB1*05:01 carriership (Supplementary Figure S9). Thus, we hypothesized that, especially in DRB1*10:01 carriers, anti-IgLON5 IgG4 may be synthesized intrathecally. Of note, a similar, but less robust, threefold increase in the CSF/serum anti-IgLON5 IgG1 ratio was found in DRB1*10:01 carriers (Figure 3B, left panel), while anti-IgLON5 IgG2 and IgG3 CSF/serum ratios tended to be higher in non-carriers (Figure 3B, middle/right panels). These findings strongly suggest anti-IgLON5 IgG4 IS, especially in DRB1*10:01 carriers.

To exactly quantify the IS of anti-IgLON5 IgG4 ($zQ_{IgLON5\text{-}IgG4}$) in comparison to total IgG IS ($zQ_{Total\ IgG}$) in CSF/serum pairs with available data for Q_{Alb} and Q_{IgG} and remaining sample volume, we employed an innovative and sensitive strategy using IS *z* scores (see Supplementary Methods). Overall, a strong correlation the $zQ_{IgLON5\text{-}IgG4}$ with the anti-IgLON5 IgG4 serum-CSF ratio was observed (Supplementary Figure S10), indicating that the mere ratios analyzed for their dependency on the HLA genotype (Figure 3) represent a good surrogate parameter of anti-IgLON5 IgG4 IS.

In all five patients, four DRB1*10:01 carriers (Pat 1/9/6/13) and the non-carrier patient 12, definite anti-IgLON5 IgG4 IS ($zQ_{IgLON5\text{-}IgG4} \geq 3$) could be demonstrated at least at one-time point (Figure 4A). Of note, $zQ_{IgLON5\text{-}IgG4}$ dropped in patients 9 and 13 after treatment with either RTX+CS (patient 9) or IVIG+CS+Az (patient 13) and again increased in patient 13 after stopping Aza and reducing IVIG frequency, which was associated with clinical relapse. In addition, the median $zQ_{IgLON5\text{-}IgG4}$ (20.0, 6.0–25.7) exceeded the $zQ_{IgG\text{-}total}$ (1.1, 0.5–2.3, $p = 0.004$) 18-fold with $zQ_{IgG\text{-}total}$ being never ≥3 (Figure 4B). When changes $zQ_{IgLON5\text{-}IgG4}$ during all available intervals were analyzed, $zQ_{IgLON5\text{-}IgG4}$ changes only tended to change in the same direction as $zQ_{IgG\text{-}total}$ or serum anti-IgGLON5 IgG4 levels (Figure 4C, left and middle panels). However, a similar association with changes in CSF anti-IgLON5 IgG4 was highly significant ($p = 0.008$, Figure 4C, right panel), confirming CSF anti-IgLON5 IgG as the major influence on $zQ_{IgLON5\text{-}IgG4}$. Most importantly, clinical deterioration or improvement during an interval was significantly associated with either an increase or decrease in $zQ_{IgLON5\text{-}IgG4}$, respectively($p = 0.017$, Figures 4C, D).

In summary, we could confirm that, in a subset of patients with anti-IgLON5 disease, and likely in those carrying the HLA-DRB1*10:01 allele, anti-IgLON5 IgG4 is synthesized intrathecally and this may be pathophysiologically relevant.

Combination therapy reduces CSF anti-IgLON5 IgG4 and leads to clinical improvement

Next, we analyzed how different treatment strategies during the intervals affected anti-IgLON5 IgG1/4 levels. Treatments were

10.3389/fimmu.2024.1376456

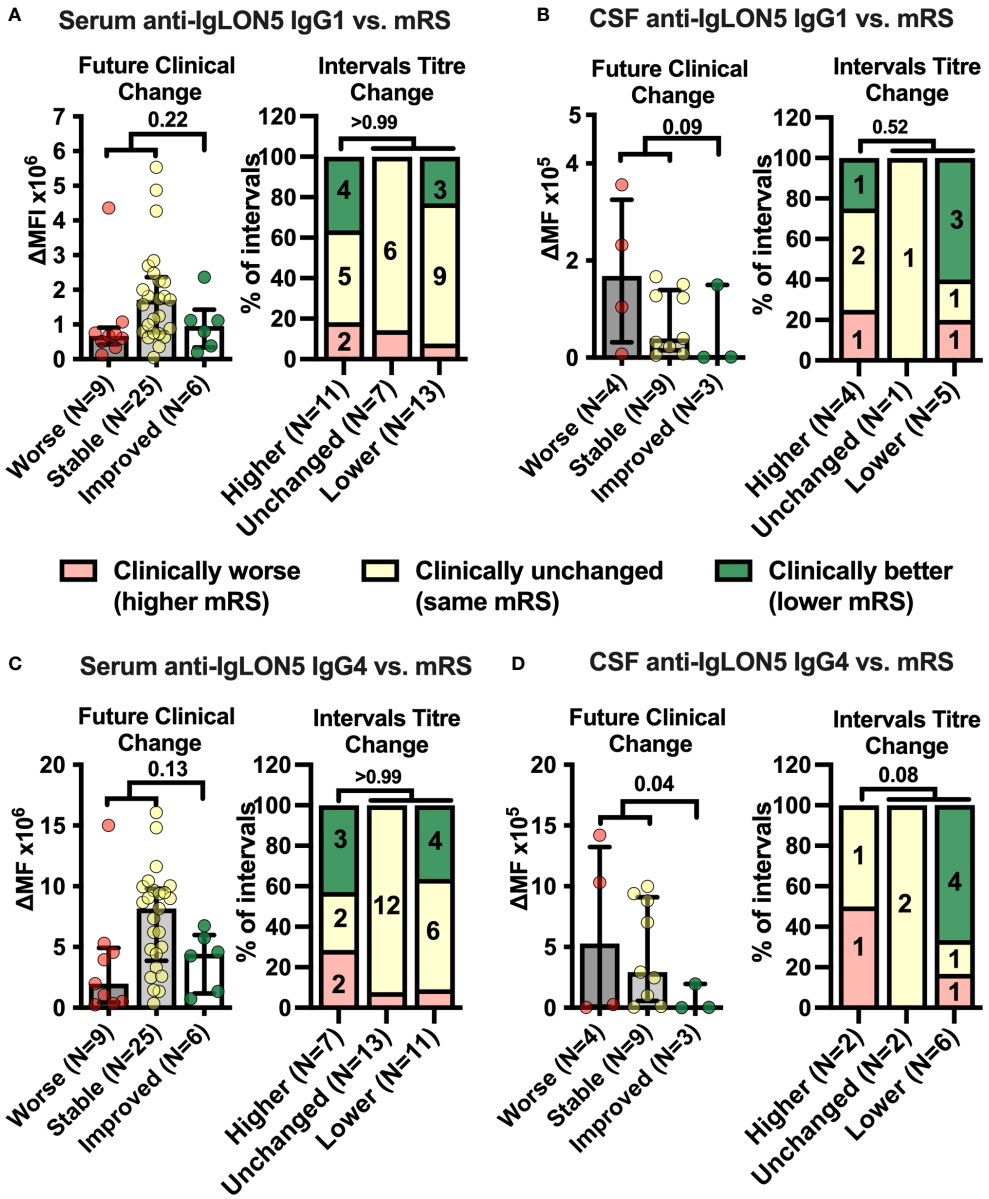

FIGURE 2
Cerebrospinal fluid anti-IgLON5 IgG1 and IgG4 levels and their changes over time correspond better with disease severity than serum levels. **(A–D)** Left graphs: IgLON5 IgG1 (**A, B** left) or IgG4 (**C, D** left) levels (bars + error bars = mean ± SEM) in serum (**A, C** left) and cerebrospinal fluid (CSF, **B, D** left) measured by flow cytometry and expressed as mean fluorescence intensity above background (ΔMFI) as in Figure 1 were grouped according to future clinical change at the next follow-up visit categorized as clinically worsened (≥ +1 mRS point, red), unchanged (mRS unchanged, yellow) or improved (≤ −1 mRS point, green). If the mRS was 1 (no functional impairment), changes of reported symptoms were used to categorize intervals. **(A–D)** Right graphs: The clinical change between two consecutive serum (A, C, right) or CSF (B, D, right) sampling intervals was categorized as clinically worse (≥ +1 mRS point, or worsening of symptoms if mRS = 1, red), unchanged (mRS unchanged, or unchanged symptoms if mRS =1, yellow) or improved (≤ −1 mRS point, or improvement of symptoms if mRS =1, green) and changes of anti-IgLON5 IgG1 (**A, B** right) or IgG4 (**C, D** right) levels during these intervals were categorized as higher (+ ≥ 20%), unchanged (± 20%), or lower (−≥ 20%). Bars show the percentage of intervals with one of the three clinical change categories when grouped according to the antibody change category. Numbers in stacked bar graphs indicate the number of intervals. Numbers in column titles indicate the numbers of measurements (left graphs) or intervals (right graphs). For statistical analysis, data were dichotomized into clinically worse/stable versus improved (left graphs) or higher levels versus unchanged or lower levels (right graphs) before testing using one-tailed Mann–Whitney *U* (left graphs) or Fisher's exact tests (right graphs). The *p*-values are indicated.

categorized either as monotherapies (or combination of short-lived therapies), and combinations of RTX and IVIG with other therapies (for details, see Figure 1 and Appendix). While there was only a tendency of more frequent decreases in serum anti-IgLON5 IgG1 in intervals with immunotherapy compared to those without therapy [no therapy: one of nine (11%), any therapy: 10 of 22 (46%), p = 0.07, Figure 5A, left panel, additional information regarding the length of the intervals can be found in Supplementary Figure S11], this association was highly significant for anti-IgLON5 IgG4 [no therapy: zero of nine (0%), any therapy: 11 of 22 (50%), p = 0.008, Figure 5A, middle panel. Interestingly, decreased serum anti-IgLON5 IgG4 was observed in seven of 10 (70%) intervals with

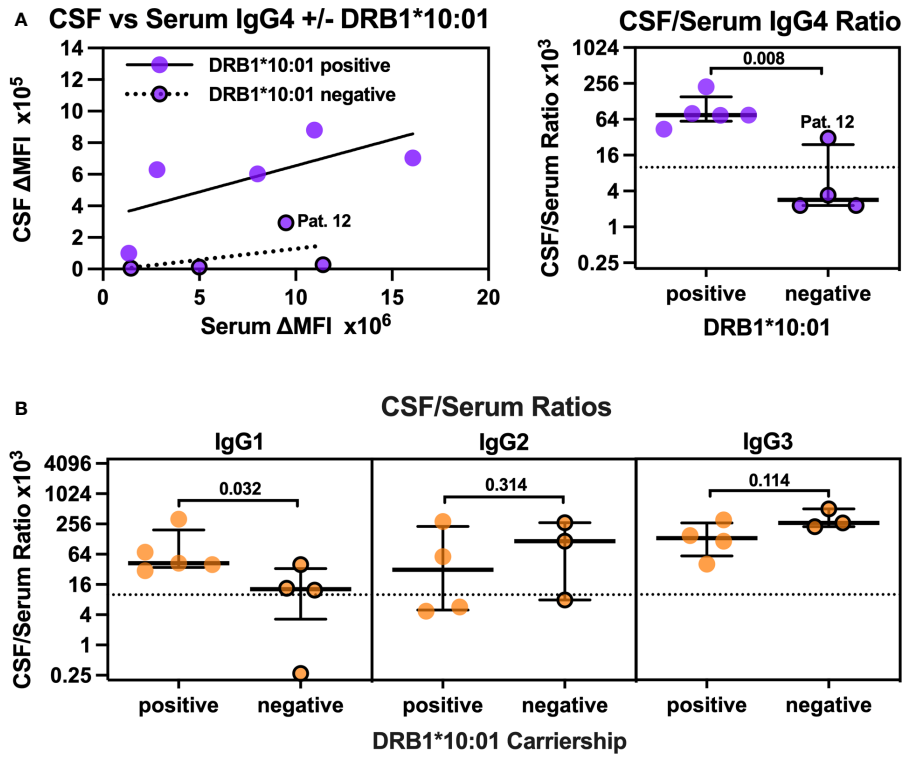

FIGURE 3
CSF/Serum ratios for anti-IgLON5 IgG4 but also IgG1 are higher in DRB1*10:01 carriers compared to non-carriers. (**A**, left panel) The mean fluorescence intensity above background (ΔMFI) for anti-IgLON5 IgG4 in CSF was plotted against serum anti-IgLON5 IgG4 ΔMFI separatedly for DRB1*10:01 carriers (circles without borders) and non-carriers (circles with black borders). The results of linear regression (carriers: R^2 = 0.47, p = 0.1984, non-carriers R^2 0.21, p = 0.5466) and the non-carrier with the higher CSF/serum ratio (patient 12) are indicated. (**A**, right panel, **B**): CSF/serum ratios for anti-IgLON4 IgG4 (**A**, right panel), IgG1–3 **(B)** of DRB1*10:01 carriers compared to non-carriers. Statistical analysis in the right panel of **(A, B)** was performed using one-sided Mann–Whitney *U* tests. The *p*-values are indicated. A comparison of anti-IgLON5 IgG4 CSF/serum ratios in association with of DRB1*10:01 and DQB1*05:01 carriership can be found in Supplementary Figure S13.

combination immunotherapy, but in only four of 12 (33%) with monotherapy. However, due to the low number of data points, this difference failed to reach statistical significance (p = 0.09, Figure 5A, right panel). In CSF, no treatment (one of one interval, 100%) and immunotherapy with IVIG or RTX alone (three of three intervals, 100%) did not lead to reduced anti-IgLON5 IgG1 levels, but a reduction was found in five of six intervals (83%) with combination therapy (p = 0.02 no/mono- compared to combined therapy, Figure 5B, left panel). Furthermore, anti-IgLON5 IgG4 levels decreased in one of four intervals (25%) with no or monotherapy (decrease in one interval with RTX only) but in five of six (83%) intervals with combination therapy (six of 10 intervals with any therapy, Figure 5B right panels). Due to one interval with response to RTX only, these differences failed to reach statistical significance (no/mono- vs. combination therapy p = 0.11, mono- vs. combination therapy, p = 0.22).

Next, we investigated clinical responses to different immunotherapy regimens. The frequency of clinical improvement was comparably low during serum intervals with any treatment regimen [six of 22 (27%)] and those without [one of nine (11%), p = 0.32, Figure 6A]. In contrast, in five of 10 (50%) intervals with combination immunotherapy including either RTX or IVIG but only one of 12 (8%) with monotherapy clinical improvement was observed [Figure 6B, p = 0.04]. With regard to the combination, in five of 10 intervals with RTX- or IVIG-containing combination immunotherapy (50%) Aza was added. Clinical improvement was observed in three of five (60%) serum intervals with Aza but in only four of 26 (15%) without (p = 0.03, Figure 6C). Thus, the pattern of clinical improvement in response to therapy closely resembled the decrease in CSF but not serum anti-IgLON5 IgG4 levels.

Discussion

In this retrospective longitudinal study, we investigated IgLON5 IgG subclass profiles in serum and CSF in 13 IgLON5 patients in the context of the patients' HLA alleles, clinical presentation, disease severity, and immunotherapy. Our strategy was to analyze all parameters or their change at the beginning and end of each clinical follow-up interval that included sampling of biofluids for assessment of anti-IgLON5 subclass levels, using flow cytometry along with an innovative quantitative technique to quantify the IS of anti-IgLON5 IgG4.

Although the results of our exploratory study often did not meet criteria of statistical significance, they yielded a coherent picture, allowing to generate new hypotheses of the biology of anti-IgLON5 disease, particularly (A) that intrathecally produced CSF IgLON5 IgG4 as well as the cellular inflammatory response may depend on

10.3389/fimmu.2024.1376456

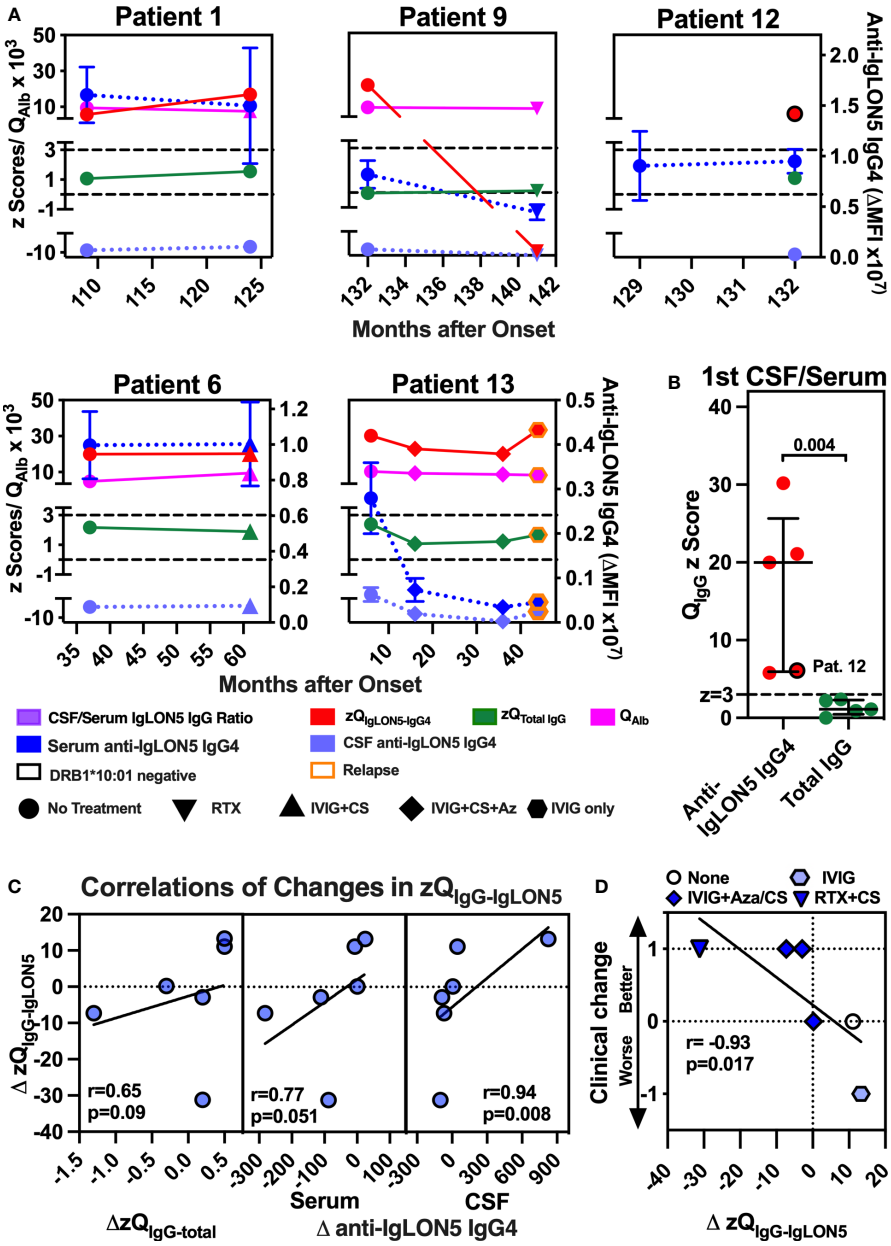

FIGURE 4
Robust intrathecal synthesis of anti-IgLON5 IgG4 was observed in five of five patients, and change in clinical severity and CSF IgLON5 IgG4 correlate with changes in the IgLON5-IgG4–specific IS (zQIgG-IgLON5). (**A**, left panel) The mean fluorescence intensity above background (ΔMFI) for anti-IgLON5 IgG4 in CSF of each first CSF/serum pair available was plotted against the anti-IgLON5 IgG4 ΔMFI in serum for five DRB1*10:01 carriers (no border) and four non-carriers (black border). Patient 12 is indicated. The lines represent simple linear regression. (**A**, right panel) CSF/serum ratios of DRB1*10:01 carriers compared to non-carriers. **(B)** Precise quantification of intrathecal anti-IgLON5 IgG4 synthesis using CSF/serum pairs with corresponding data for CSF/serum IgG (Q_{IgG}) and albumin ratio (Q_{Alb}) from patients 1, 6, 9, 12, and 13 still available following the initial measurements. Results from repeat flow cytometry performed after dilution to equal concentrations of total IgG in CSF and serum were converted to z-scores for anti-IgLON5 IgG4 ($zQ_{IgLON5-IgG4}$) $_{IgG4}$ and total IgG ($zQ_{Total\ IgG}$) as described in the methods and Supplementary Methods. Results for $zQ_{IgLON5-IgG4}$ (red) and $zQ_{Total\ IgG}$ (green) were plotted against the disease duration using the left *y*-axis. The corresponding Q_{Alb} (pink, left *y*-axis) and serum and CSF anti-IgLON5 IgG4 mean ± SEM levels dark blue and light blue, respectively, right *y*-axis) are shown for comparison. The cutoff above which definite intrathecal synthesis ($z = 3$) can be assumed and z-score without intrathecal synthesis ($z = 0$) are indicated as black dashed lines. A black border indicates DRB*10:01 non-carriers, orange border clinical relapse. Circle: no treatment in the preceeding interval, upright triangle: Rituximab (RTX), hexagon: IVIG only, inverse triangle: IVIG + corticosteroids (CS), diamond: IVIG + CS + azathioprine (Az) **(B)** $zQ_{IgLON5-IgG4}$s of the first CSF/serum pair of all five patients compared to the respective z $zQ_{Total\ IgG}$s. Again, patient 12 is marked by a black border. Statistical comparisons were performed using two-tailed Mann–Whitney *U* test. **(C, D)** The change of the z score for the CSF/serum IgG4 ratio ($\Delta zQ_{IgG4-IgLON5}$) in all six intervals with $zQ_{IgG4-IgLON5}$ available at both start and end was plotted against the changes in total IgG IS ($zQ_{IgG-total}$, **C**, left panel), change in serum IgG4 (**C**, middle panel), CSF IgG4 (**C**, right panel), and clinical change **(D)**. Clinical change was defined as –1 = worse (indicated by clinical deterioration and/or increase in mRS), 0 = stable (clinically stable, no change in mRS), 1 = better (clinical improvement and/or reduction of mRS). The results of simple linear regression are depicted. The correlation coefficients obtained by with Pearson correlation and their *p*-values are indicated.

10.3389/fimmu.2024.1376456

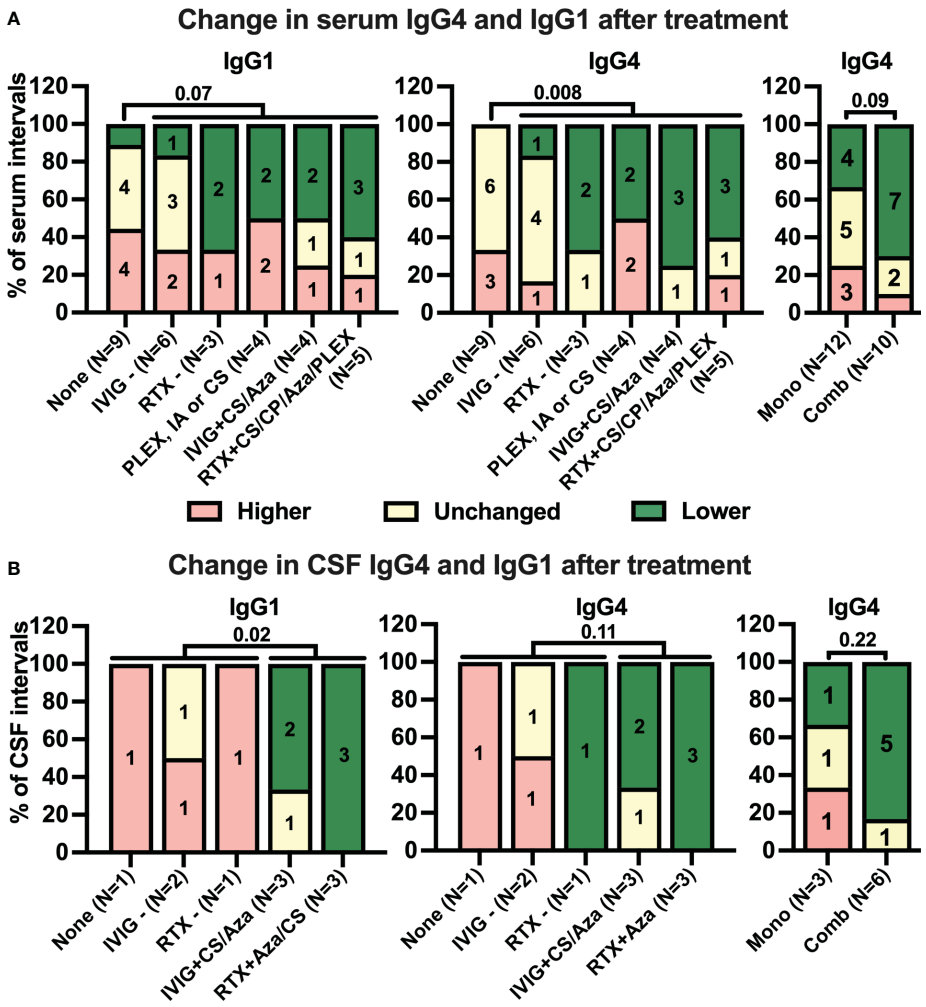

FIGURE 5
While many treatments tend to reduce serum anti-IgLON5 levels, only combination immunotherapy coincides with reduction of anti-IgLON5 levels in cerebrospinal fluid. Intervals between two consecutive serum **(A)** and cerebrospinal fluid (CSF, **B**) samplings were categorized according to the immunotherapy administrated during the interval as described in the methods sections (None = no treatment, IVIG– = intravenous immunoglobulins only, RTX– = rituximab only, PLEX or CS = plasma exchange or corticosteroids, IVIG +CS/Aza = IVIG + corticosteroids or azathioprine, RTX + CS/CP/Aza/PLEX= rituximab in combination with corticosteroids, cyclophosphamide, azathioprine, or plasmapheresis). The number of intervals is indicated below the bars. Antibody level changes during these intervals were categorized as higher (+> 20%, red), unchanged (± 20%, yellow), or lower (–> 20%, green). Bars show the percentage of intervals assigned to the three antibody levels change categories for anti-IgLON5 IgG1 (left graphs) and IgG4 (middle and right graphs) when grouped according to the treatment regimen. For the right graphs, treatments were dichotomized as monotherapy (Mono) or combination therapy (Comb). In addition, for statistical analysis treatments during the intervals were dichotomized into absence of treatment versus any treatment for serum (**A**, left and middle graph) or no or monotherapy versus combination therapy for CSF (**B**, left and middle graphs). A statistical comparison was performed by one-sided Fisher's exact test. The *p*-values are indicated above the graphs.

the HLA genotype and, if present, (B) may represent a marker of clinical and prognostic relevance in a subset of patients, and (C) that patients may be more likely to benefit from immunosuppressive treatment in combination. Our main findings that support these hypotheses are that (1) DRB1*10:01 non-carriers show lower CSF-to-serum anti–IgLON5-IgG4 levels and CSF leukocytes when compared to carriers of this risk allele, (2) anti-IgLON5 IgG4 IS was observed not only in all analyzed DRB1*10:01 carriers but also in one non-carrier, (3) the reduction in anti-IgLON5-IgG4 IS correlated with reduced CSF anti-IgLON5 IgG4 and clinical improvement, and (4) low CSF IgG4 levels were associated with future clinical improvement. Further, (5) although many treatments could reduce serum anti-IgLON5 IgG1/4 levels, clinical improvementwas more frequently observed after intense immunotherapy, often containing combinations of either RTX or IVIG with CS, but especially Aza. Taken together these findings led us to form a new hypothesis: that intrathecal anti-IgLON5 IgG synthesis, especially of IgG4, could potentially represent a surrogate marker for disease activity in a subset of patients and may thus be a promising prognostic and/or predictive biomarker. With the limitation that these are preliminary data of a small patient cohort that warrant further studies with larger patient cohorts to validate, we cautiously suggest that both CSF and serum anti-IgLON5 should be monitored. Before becoming available as routine diagnostic tests, the performance of quantitative assays for IgLON5 IgG1 and IgG4 levels along with new strategies to

10.3389/fimmu.2024.1376456

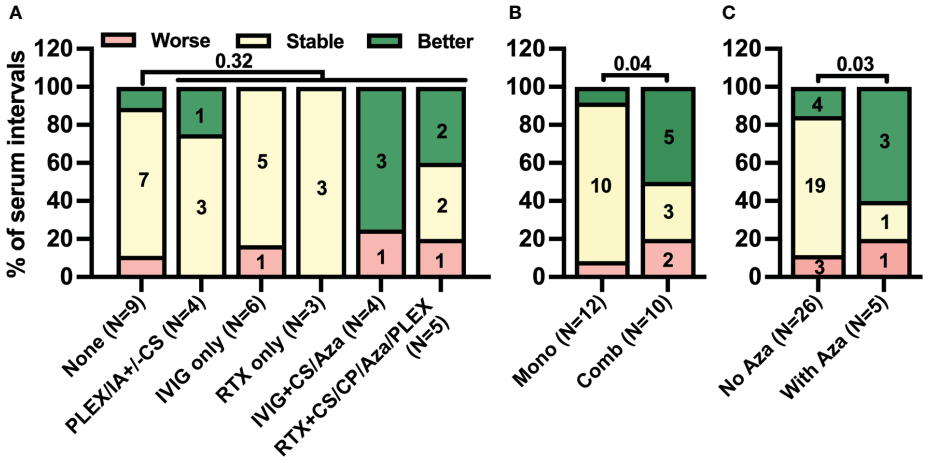

FIGURE 6
Combination treatment rather than only immunomodulatory treatment is associated with clinical improvement. Intervals between two consecutive serum samplings were categorized according to the immunotherapy administrated during the interval as described in the methods sections (**A**: None = no treatment, IVIG ± CS/Aza = intravenous immunoglobulins with or without corticosteroids or azathioprine, RTX ± CS/Aza/CP/Plex = rituximab with or without CS, Aza, cyclophosphamide or plasma exchange, PLEX or CS = plasma exchange or corticosteroids, **B**: No/Mono = no treatment or monotherapy; **C**: No Aza = without azathioprine, With Aza = with azathioprine). The number of intervals is indicated below the bars. Changes in clinical severity during these intervals were categorized as worse (red), stable (yellow), or better (green) as described in the Materials & Methods section. A statistical comparison was performed by one-sided Fisher's exact test. The *p*-values are indicated above the graphs.

calculate their IS will have to be validated more extensively. Currently, IS of target-specific antibodies is most frequently presented as AI calculated according to Reiber and Lange (31). However, this procedure has two major disadvantages. First, in the AI formula the denominator for the target-specific antibody CSF/serum ratio switches from the actual Q_{IgG} to the 99.5% percentile reference value (Q_{lim}) in case the actual Q_{IgG} is higher than Q_{lim}. Thus, in cohorts of individuals with and without proven quantitatively relevant intrathecal IgG synthesis according to Reiber ($Q_{IgG}>Q_{lim}$) (32), the AIs are calculated by different formulas prohibiting quantitative statistical analysis. Second, when patient in a cohort do not exhibit proven quantitatively relevant IgG synthesis according to Reiber ($Q_{IgG}\leq Q_{lim}$) but the actual Q_{IgG} is above the 50th percentile of the reference range (as in our cohort), the AI formula tends to underestimate IS as the actual Q_{IgG} (which might indicate a 90% likelihood of IS if, e.g., it is located at the level of the 90th percentile) but not the estimated Q_{IgG} in the absence of IgG IS as the denominator. Both disadvantaged do not occur using the approach suggested by Brauchle et al. and employed in our manuscript, which, in addition, is based on a considerably higher number of data points (27).

Our study shows a predominance of IgG4 in 88% of patients. This is in line with a previous study (25) but in contrast to an earlier study with a lower frequency (33%) (1). The IgG4 predominance in our study was largely due to higher IgG4 levels in IgG4-predominant patients but not lower antibody levels of other subclasses, especially IgG1. Furthermore, in our cohort, which showed the expected high frequency of the known risk alleles HLA-DQB1*05:01 and DRB1*10:01, a higher number of risk alleles seemed to coincide with higher anti-IgLON5 IgG4 levels in serum and CSF. The HLA-DQB1*05 allele has been associated with other IgG4-predominant autoimmune diseases (33–36). Recent data supports the view that HLA-DQ containing a β-subunit encoded by the HLA-DQB1*05:01 anti-IgLON5 disease risk allele plays a pivotal role in the presentation of IgLON5 peptides to T-helper cells and initiation of the anti-IgLON5 immune response (37). The authors suggested that any association of anti-IgLON5 disease with HLA-DRB1*10:01 risk allele may be merely indirect due to its linkage disequilibrium with HLA-DQB1*05:01. Nevertheless, our observations suggest that the presence of HLA-DRB1*10:01 may contribute to disease, as the association of HLA-DRB1*10:01 risk allele with proportionally highly CSF anti-IgLON5 IgG levels most likely representing IS described herein seems to be directly mediated by the HLA-DR genotype. Replicating this observation in larger cohorts might yield relevant insight into the pathoimmunobiology of anti-IgLON5 disease.

Notably, it has been consistently reported that about 10% of anti-IgLON5 disease patients test negative for anti-IgLON5 IgG in CSF [e.g. (38, 39)]. These probably correspond to those with low CSF levels in our cohort when using flow cytometry. In turn, many patients reported to be CSF anti–IgLON5-positive may have target-specific IgG IS. Indeed, one patient each with anti-IgLON5 in CSF only (18) and higher anti-IgLON5 IgG levels in CSF compared to serum have been reported (40). Do these two groups represent different immunological and clinical phenotypes? In the initial description by Sabater et al., one patient with the clinical diagnosis of PSP and anti-IgLON5 IgG in serum only was reported but at this time due to the negative CSF tests it was doubted whether this actually was anti-IgLON5 disease (4). However, later Gaig et al. reported that in anti-IgLON5 disease with PSP-like phenotype CSF may test negative for anti-IgLON5 IgG in 50% of the patients (1). Interestingly, these patients were threefold less likely to carry the DRB1*10:01 risk allele. In our study, only one of four patients with PSP-like anti-IgLON5 disease was DRB1*10:01 carrier. Perhaps the presence of the risk allele predisposes for more robust immigration of antigen-specific B-

cells into the intrathecal compartment or brain. Moreover, low intrathecal anti-IgLON5 IgG production may also evade detection in CSF as anti-IgLON5 IgG may be adsorbed in brain tissue due to binding to the membrane-bound and/or shedded antigen (9).

Although clinically distinct from anti-IgLON5 disease, anti-LGI1 AIE equally presents with IgG4 predominance of the target-specific IgG, low titers of target-specific antibodies in CSF compared to serum and largely non-inflammatory CSF results (14, 41, and 42) (41). Of note, not only could clonal expansion of B cells in anti-LGI1 AIE be demonstrated but also that B cells producing LGI1-specific antibodies are present in the CSF (42, 43). Correspondingly, abundant CSF B cells and even plasma cells have been found in most cases with anti-IgLON5 disease (13). These observations might indicate that target-specific recruitment of B cells to the intrathecal compartment with subsequent expansion might be a characteristic of IgG4-predominant autoimmune disorders. In contrast, recruitment of unspecific B cells with production of polyspecific antibodies including multiple anti-viral specificities associated with a robust quantitative IS of total IgG was demonstrated to be a hallmark of AIE with NMDAR antibodies (14, 44), which are largely of the IgG1 and IgG3 subclass. Thus, future experiments should focus on the comparative studies of peripheral and CSF B cells as well as the binding specificity, avidity, affinity and post-translational modifications of target-specific IgG4 produced in both compartments to unravel the relevance of intrathecally produced anti-IgLON5 IgG4.

Which is the best treatment choice for anti-IgLON5 disease? In our small cohort, we observed favorable outcomes mostly after immunosuppressive treatment in combination, which consisted of RTX or IVIG in combination with Aza or CS, or combinations including Aza. However, the number of study participants was low; therefore, further studies are necessary to confirm this observation. Taken together, our findings clearly indicate an urgent need for further studies to investigate the efficacy of combination therapies, particularly involving IVIG or RTX in combination with Aza and CS.

Limitations

Anti-IgLON5 disease is rare and no guidelines for treatment of anti-IgLON5 disease exist. Thus, our cohort included a limited number of patients with heterogenous treatment regimens. This limits the conclusions that can be drawn from our data. Flow cytometry is a quantitative method, and individual titrations showed linearity of the assay in general, but a high degree of inter-assay variability could not be entirely overcome by normalization. We used four different IgG-subclass–specific secondary antibodies, but these were also used successfully in diseases with IgG1 predominance (45, 46). We decided to measure anti-IgLON5 IgG1/4 at a low dilution to allow detection of low antibody levels, accepting that in exceptional cases with very high antibody levels serum anti-IgLON5 IgG4 levels may exceed the linear range of the assay. We thus optimized the assay to allow a direct comparison of CSF and serum antibody levels and demonstrated that this approach is quantitative, though sensitivity was reduced in patients with very low antibody levels.

Conclusion

Although anti-IgLON5 disease is rare and the retrospective nature of our study made it difficult to compare results, we present several important findings and hypotheses: (1) intrathecal synthesis of anti-IgLON5 IgG4 may be of clinical and prognostic relevance, as we observed IgLON5-specific IS in all five tested patients (of which four were DRB1*10:01 positive). Further, CSF (but not serum) anti-IgLON5 IgG4 levels correlated with clinical outcomes whereby low CSF levels preceded clinical improvement. (2) Initial observations suggest a potential clinical benefit from combined immunotherapy, as we found that immunotherapy was associated with reduced anti-IgLON5 antibody levels, and combination therapy had greater effect on clinical outcomes. Further studies will be necessary to ascertain our observations in a larger patient cohort.

Data availability statement

The original contributions presented in the study are included in the article/Supplementary Material. Further inquiries can be directed to the corresponding author.

Ethics statement

The studies involving humans were approved by Ethikkommission Medizinische Universität Wien, Vienna, Austria. The studies were conducted in accordance with the local legislation and institutional requirements. The participants provided their written informed consent to participate in this study.

Author contributions

IK: Conceptualization, Data curation, Formal analysis, Funding acquisition, Investigation, Methodology, Project administration, Validation, Visualization, Writing – original draft, Writing – review & editing. SM: Resources, Writing – review & editing. MH: Resources, Writing – review & editing. TS-H: Resources, Writing – review & editing. EB-S: Resources, Writing – review & editing. MBl: Resources, Writing – review & editing. MBr: Resources, Writing – review & editing. JD: Resources, Writing – review & editing. LD: Resources, Writing – review & editing. ME: Resources, Writing – review & editing. IF: Resources, Writing – review & editing, Investigation. GF: Investigation, Resources, Writing – review & editing. FF: Methodology, Writing – review & editing. AH: Resources, Writing – review & editing. BH: Resources, Writing – review & editing. VK: Writing – review & editing. SK: Resources, Writing – review & editing. HL: Resources, Writing – review & editing. MN: Resources, Writing – review & editing. JR: Resources, Writing – review & editing.

RR: Resources, Writing – review & editing. GR: Writing – review & editing. AS: Writing – review & editing. MS: Writing – review & editing. HT: Writing – review & editing. SW: Resources, Writing – review & editing. TB: Resources, Writing – review & editing. LS: Resources, Writing – review & editing. CG: Resources, Writing – review & editing. JL: Conceptualization, Formal analysis, Resources, Supervision, Validation, Writing – original draft, Writing – review & editing. RH: Data curation, Funding acquisition, Investigation, Resources, Supervision, Validation, Writing – review & editing.

Funding

The author(s) declare financial support was received for the research, authorship, and/or publication of this article. This work was supported by the Austrian Science Fund (FWF), project number T996-B30, I6565-B (SYNABS), and the Austrian Society of Neurology (Österreichische Gesellschaft für Neurologie). This study was supported in part by ISCIII—Subdirección General de Evaluación y Fomento de la Investigación Sanitaria—and the Fondo Europeo de Desarrollo Regional (ISCIII-FEDER; PI21/00165, LS and CG) and the Germany Ministry for Education and Research (BMBF; 01GM2208B, JL).

Acknowledgments

We are grateful for the assistance of Andreas Spittler from the Core Facility Flow Cytometry at the Medical University of Vienna. We thank Johanna Wachutka, Katrin Köbl, and Sophie Nitsch for excellent technical assistance. The IgLON5-GFP plasmid was kindly provided by Francesc Graus.

Conflict of interest

TS-H reports travel grants and speaker honoraria from Roche. MBr has received honoraria for speaking from Sanofi. No conflict of interest with respect to the present study. AH reports speaker honoraria for UCB, Bioprojet, Servier, Medice, Jazz Pharmaceuticals BH reports speaker honoraria Jazz and Abbvie and advisor feed from Lundbeck. MS reports personal fees and grants from Merck Healthcare Deutschland and Bayer Vital GmbH and grant support from the University of Greifswald Gerhard-Domagk fellowship. HT reports speaker honoraria from Jansen, UCB and Zambon. TB has participated in meetings sponsored by and received honoraria lectures, advisory boards, consultations from pharmaceutical companies marketing treatments for MS: Allergan, Biogen, Biologix, Bionorica, BMS/Celgene, Eisei, Janssen-Cilag, MedDay, Merck, Novartis, Roche, Sandoz, Sanofi-Genzyme, Teva, UCB. His institution has received financial support in the past 12 months by unrestricted research grants Bayer, Biogen, BMS/Celgene, Merck, Novartis, Roche, Sanofi-Genzyme, Teva and for participation in clinical trials in multiple sclerosis sponsored by Alexion, Bayer, Biogen, BMS/Celgene, Merck, Novartis, Roche, Sanofi-Aventis, Teva. JL reports travel honoraria and speakers fees from the Cure Huntington's Disease Initiative CHDI, the Movement Disorders Society as the German Society for Cerebrospinal Fluid Diagnostic and Clinical Neurochemistry DGLN. His institution received financial compensation for clinical trials with JL as principal investigator from CHDI. He is member of the executive board of the DGLN. He received research funding from the German Federal Ministry of Education and Research BMBF. RH reports speaker honoraria from UCB and Biogen. The Medical University of Vienna Austria; employer of RH receives payment for antibody assays and for antibody validation experiments organized by Euroimmun Lübeck, Germany.

The remaining authors declare that the research was conducted in the absence of any commercial or financial relationships that could be construed as a potential conflict of interest.

The author(s) declared that they were an editorial board member of Frontiers, at the time of submission. This had no impact on the peer review process and the final decision.

Publisher's note

Supplementary material

The Supplementary Material for this article can be found online at: https://www.frontiersin.org/articles/10.3389/fimmu.2024.1376456/full#supplementary-material

References

1. Gaig C, Graus F, Compta Y, Hogl B, Bataller L, Bruggemann N, et al. Clinical manifestations of the anti-IgLON5 disease. *Neurology*. (2017) 88:1736–43. doi: 10.1212/WNL.0000000000003887

2. Werner J, Jelcic I, Schwarz EI, Probst-Muller E, Nilsson J, Schwizer B, et al. Anti-igLON5 disease: A new bulbar-onset motor neuron mimic syndrome. *Neurology(R) Neuroimmunol Neuroinflamm*. (2021) 8. doi: 10.1212/NXI.0000000000000962

3. Montagna M, Amir R, De Volder I, Lammens M, Huyskens J, Willekens B. IgLON5-associated encephalitis with atypical brain magnetic resonance imaging and cerebrospinal fluid changes. *Front Neurol*. (2018) 9:329. doi: 10.3389/fneur.2018.00329

4. Sabater L, Gaig C, Gelpi E, Bataller L, Lewerenz J, Torres-Vega E, et al. A novel non-rapid-eye movement and rapid-eye-movement parasomnia with sleep breathing disorder associated with antibodies to IgLON5: a case series, characterisation of the

antigen, and post-mortem study. *Lancet Neurol*. (2014) 13:575–86. doi: 10.1016/S1474-4422(14)70051-1

5. Erro ME, Sabater L, Martinez L, Herrera M, Ostolaza A, Garcia de Gurtubay I, et al. Anti-IGLON5 disease: A new case without neuropathologic evidence of brainstem tauopathy. *Neurology(R) Neuroimmunol Neuroinflamm*. (2020) 7. doi: 10.1212/NXI.0000000000000651

6. Landa J, Gaig C, Plaguma J, Saiz A, Antonell A, Sanchez-Valle R, et al. Effects of igLON5 antibodies on neuronal cytoskeleton: A link between autoimmunity and neurodegeneration. *Ann Neurol*. (2020) 88:1023–7. doi: 10.1002/ana.25857

7. Gruter T, Mollers FE, Tietz A, Dargvainiene J, Melzer N, Heidbreder A, et al. Clinical, serological and genetic predictors of response to immunotherapy in anti-IgLON5 disease. *Brain*. (2023) 146:600–11. doi: 10.1093/brain/awac090

8. Sabater L, Planaguma J, Dalmau J, Graus F. Cellular investigations with human antibodies associated with the anti-IgLON5 syndrome. *J Neuroinflamm*. (2016) 13:226. doi: 10.1186/s12974-016-0689-1

9. Landa J, Serafim AB, Gaig C, Saiz A, Koneczny I, Hoftberger R, et al. Patients' IgLON5 autoantibodies interfere with IgLON5-protein interactions. *Front Immunol*. (2023) 14:1151574. doi: 10.3389/fimmu.2023.1151574

10. Dalmau J, Graus F. Antibody-mediated encephalitis. *N Engl J Med*. (2018) 378:840–51. doi: 10.1056/NEJMra1708712

11. Blinder T, Lewerenz J. Cerebrospinal fluid findings in patients with autoimmune encephalitis-A systematic analysis. *Front Neurol*. (2019) 10:804. doi: 10.3389/fneur.2019.00804

12. Leypoldt F, Hoftberger R, Titulaer MJ, Armangue T, Gresa-Arribas N, Jahn H, et al. Investigations on CXCL13 in anti-N-methyl-D-aspartate receptor encephalitis: a potential biomarker of treatment response. *JAMA Neurol*. (2015) 72:180–6. doi: 10.1001/jamaneurol.2014.2956

13. Strippel C, Heidbreder A, Schulte-Mecklenbeck A, Korn L, Warnecke T, Melzer N, et al. Increased intrathecal B and plasma cells in patients with anti-igLON5 disease: A case series. *Neurology(R) Neuroimmunol Neuroinflamm*. (2022) 9. doi: 10.1212/NXI.0000000000001137

14. Durr M, Nissen G, Suhs KW, Schwenkenbecher P, Geis C, Ringelstein M, et al. CSF findings in acute NMDAR and LGI1 antibody-associated autoimmune encephalitis. *Neurology(R) Neuroimmunol Neuroinflamm*. (2021) 8. doi: 10.1212/NXI.0000000000001086

15. Ruiz-López E, Schuhmacher AJ. Transportation of single-domain antibodies through the blood–brain barrier. *Biomolecules*. (2021) 11:1131. doi: 10.3390/biom11081131

16. Batchelor TT, Grossman SA, Mikkelsen T, Ye X, Desideri S, Lesser GJ. Rituximab monotherapy for patients with recurrent primary CNS lymphoma. *Neurology*. (2011) 76:929–30. doi: 10.1212/WNL.0b013e31820f2d94

17. Berger-Sieczkowski E, Endmayr V, Haider C, Ricken G, Jauk P, Macher S, et al. Analysis of inflammatory markers and tau deposits in an autopsy series of nine patients with anti-IgLON5 disease. *Acta Neuropathol*. (2023) 146:631–45. doi: 10.1007/s00401-023-02625-6

18. Hogl B, Heidbreder A, Santamaria J, Graus F, Poewe W. IgLON5 autoimmunity and abnormal behaviours during sleep. *Lancet*. (2015) 385:1590. doi: 10.1016/S0140-6736(15)60445-7

19. Nissen MS, Blaabjerg M. Anti-igLON5 disease: A case with 11-year clinical course and review of the literature. *Front Neurol*. (2019) 10:1056. doi: 10.3389/fneur.2019.01056

20. Gruter T, Mollers FE, Tietz A, Dargvainiene J, Melzer N, Heidbreder A, et al. Clinical, serological and genetic predictors of response to immunotherapy in anti-IgLON5 disease. *Brain*. (2022) 146(2):600–11. doi: 10.1093/brain/awac090

21. Gaig C, Compta Y, Heidbreder A, Marti MJ, Titulaer MJ, Crijnen Y, et al. Frequency and characterization of movement disorders in anti-igLON5 disease. *Neurology*. (2021) 97:e1367–81. doi: 10.1212/WNL.0000000000012639

22. De Simoni D, Ricken G, Winklehner M, Koneczny I, Karenfort M, Hustedt U, et al. Antibodies to nodal/paranodal proteins in paediatric immune-mediated neuropathy. *Neurology(R) Neuroimmunol Neuroinflamm*. (2020) 7. doi: 10.1212/NXI.0000000000000763

23. Koneczny I, Cossins J, Waters P, Beeson D, Vincent A. MuSK myasthenia gravis IgG4 disrupts the interaction of LRP4 with MuSK but both IgG4 and IgG1-3 can disperse preformed agrin-independent AChR clusters. *PloS One*. (2013) 8:e80695. doi: 10.1371/journal.pone.0080695

24. Jacob S, Rajabally YA. Current proposed mechanisms of action of intravenous immunoglobulins in inflammatory neuropathies. *Curr Neuropharmacol*. (2009) 7:337–42. doi: 10.2174/157015909790031166

25. Gaig C, Ercilla G, Daura X, Ezquerra M, Fernandez-Santiago R, Palou E, et al. HLA and microtubule-associated protein tau H1 haplotype associations in anti-IgLON5 disease. *Neurol Neuroimmunol Neuroinflamm*. (2019) 6. doi: 10.1212/NXI.0000000000000605

26. Gonzalez-Galarza FF, McCabe A, Santos E, Jones J, Takeshita L, Ortega-Rivera ND, et al. Allele frequency net database (AFND) 2020 update: gold-standard data classification, open access genotype data and new query tools. *Nucleic Acids Res*. (2020) 48:D783–D8. doi: 10.1093/nar/gkz1029

27. Reiber H, Peter JB. Cerebrospinal fluid analysis: disease-related data patterns and evaluation programs. *J Neurol Sci*. (2001) 184:101–22. doi: 10.1016/S0022-510X(00)00501-3

28. Brauchle F, Rapp D, Senel M, Huss A, Dreyhaupt J, Klose V, et al. Clinical associations and characteristics of the polyspecific intrathecal immune response in elderly patients with non-multiple sclerosis chronic autoimmune-inflammatory neurological diseases - a retrospective cross-sectional study. *Front neurol*. (2023) 14:1193015. doi: 10.3389/fneur.2023.1193015

29. Rothman KJ GS, Lash T. *Modern epidemiology. 3 ed*. New York: Lippincott, Williams & Wilkins (2008).

30. Reiber H. Cerebrospinal fluid–physiology, analysis and interpretation of protein patterns for diagnosis of neurological diseases. *Mult Scler*. (1998) 4:99–107. doi: 10.1177/135245859800400302

31. Reiber H, Lange P. Quantification of virus-specific antibodies in cerebrospinal fluid and serum: sensitive and specific detection of antibody synthesis in brain. *Clin Chem*. (1991) 37:1153–60. doi: 10.1093/clinchem/37.7.1153

32. Reiber H. Flow rate of cerebrospinal fluid (CSF)–a concept common to normal blood-CSF barrier function and to dysfunction in neurological diseases. *J Neurol Sci*. (1994) 122:189–203. doi: 10.1016/0022-510X(94)90298-4

33. Panhuber A, Lamorte G, Bruno V, Cetin H, Bauer W, Hoftberger R, et al. A systematic review and meta-analysis of HLA class II associations in patients with IgG4 autoimmunity. *Sci Rep*. (2022) 12:9229. doi: 10.1038/s41598-022-13042-2

34. Hong Y, Li HF, Romi F, Skeie GO, Gilhus NE. HLA and MuSK-positive myasthenia gravis: A systemic review and meta-analysis. *Acta Neurol Scand*. (2018) 138:219–26. doi: 10.1111/ane.2018.138.issue-3

35. Li S, Zhang Q, Wang P, Li J, Ni J, Wu J, et al. Association between HLA-DQB1 polymorphisms and pemphigus vulgaris: A meta-analysis. *Immunol Invest*. (2018) 47:101–12. doi: 10.1080/08820139.2017.1385622

36. Koneczny I, Yilmaz V, Lazaridis K, Tzartos J, Lenz TL, Tzartos S, et al. Common denominators in the immunobiology of igG4 autoimmune diseases: what do glomerulonephritis, pemphigus vulgaris, myasthenia gravis, thrombotic thrombocytopenic purpura and autoimmune encephalitis have in common? *Front Immunol*. (2021) 11. doi: 10.3389/fimmu.2020.605214

37. Yogeshwar SM, Muniz-Castrillo S, Sabater L, Peris-Sempere V, Mallajosyula V, Luo G, et al. HLA-DQB1*05 subtypes and not DRB1*10:01 mediates risk in anti-IgLON5 disease. *Brain*. (2024). doi: 10.1093/brain/awae048

38. Bruggemann N, Wandinger KP, Gaig C, Sprenger A, Junghanns K, Helmchen C, et al. Dystonia, lower limb stiffness, and upward gaze palsy in a patient with IgLON5 antibodies. *Move Disord*. (2016) 31:762–4. doi: 10.1002/mds.26608

39. Tagliapietra M, Frasson E, Cardellini D, Mariotto S, Ferrari S, Zanusso G, et al. Hypothalamic-bulbar MRI hyperintensity in anti-igLON5 disease with serum-restricted antibodies: A case report and systematic review of literature. *J Alzheimer's dis: JAD*. (2021) 79:683–91. doi: 10.3233/JAD-201105

40. Hansen N, Hirschel S, Stocker W, Manig A, Falk HS, Ernst M, et al. Figural memory impairment in conjunction with neuropsychiatric symptoms in igLON5 antibody-associated autoimmune encephalitis. *Front Psychiatry*. (2020) 11:576. doi: 10.3389/fpsyt.2020.589466

41. Muniz-Castrillo S, Haesebaert J, Thomas L, Vogrig A, Pinto AL, Picard G, et al. Clinical and prognostic value of immunogenetic characteristics in anti-LGI1 encephalitis. *Neurology(R) Neuroimmunol Neuroinflamm*. (2021) 8. doi: 10.1212/NXI.0000000000000974

42. Kornau HC, Kreye J, Stumpf A, Fukata Y, Parthier D, Sammons RP, et al. Human cerebrospinal fluid monoclonal LGI1 autoantibodies increase neuronal excitability. *Ann Neurol*. (2020) 87:405–18. doi: 10.1002/ana.25666

43. Lehmann-Horn K, Irani SR, Wang S, Palanichamy A, Jahn S, Greenfield AL, et al. Intrathecal B-cell activation in LGI1 antibody encephalitis. *Neurology(R) neuroimmunol Neuroinflamm*. (2020) 7. doi: 10.1212/NXI.0000000000000669

44. Schwenkenbecher P, Skripuletz T, Lange P, Durr M, Konen FF, Mohn N, et al. Intrathecal antibody production against epstein-barr, herpes simplex, and other neurotropic viruses in autoimmune encephalitis. *Neurology(R) Neuroimmunol Neuroinflamm*. (2021) 8. doi: 10.1212/NXI.0000000000001062

45. Spatola M, Petit Pedrol M, Maudes E, Simabukuro M, Muniz-Castrillo S, Pinto AL, et al. Clinical features, prognostic factors, and antibody effects in anti-mGluR1 encephalitis. *Neurology*. (2020) 95:e3012–e25. doi: 10.1212/WNL.0000000000010854

46. Zrzavy T, Endmayr V, Bauer J, Macher S, Mossaheb N, Schwaiger C, et al. Neuropathological variability within a spectrum of NMDAR-encephalitis. *Ann Neurol*. (2021) 90:725–37. doi: 10.1002/ana.26223

frontiers | Frontiers in Immunology

TYPE Original Research
PUBLISHED 20 June 2024
DOI 10.3389/fimmu.2024.1322159

OPEN ACCESS

EDITED BY
Vuslat Yilmaz,
Istanbul University, Türkiye

REVIEWED BY
Yoshiko Matsuda,
National Center for Child Health and Development (NCCHD), Japan
Yoshiro Horai,
Sasebo City General Hospital, Japan

*CORRESPONDENCE
Xiaoming Huang
hxming@mail.sysu.edu.cn
Xiang Liu
liux3@mail.sysu.edu.cn

†These authors have contributed equally to this work

RECEIVED 15 October 2023
ACCEPTED 22 March 2024
PUBLISHED 20 June 2024

CITATION
Lin X, Lin P, Fan J, Zhang B, Liang F, Han P, Liu X and Huang X (2024) IgG4-related disease with nasopharyngeal malignancy-like manifestations.
Front. Immunol. 15:1322159.
doi: 10.3389/fimmu.2024.1322159

IgG4-related disease with nasopharyngeal malignancy-like manifestations

Xijun Lin[1†], Peiliang Lin[1†], Jianming Fan[2†], Biying Zhang[3], Faya Liang[1], Ping Han[1], Xiang Liu[1*] and Xiaoming Huang[1*]

[1]Department of Otolaryngology-Head and Neck Surgery, Sun Yat-sen Memorial Hospital, Sun Yat-sen University, Guangzhou, China, [2]Department of Otolaryngology-Head and Neck Surgery, The Eighth Affiliated Hospital, Sun Yat-sen University, Shenzhen, China, [3]Department of Pathology, Sun Yat-sen Memorial Hospital, Sun Yat-sen University, Guangzhou, China

Background: IgG4-related disease (IgG4-RD) was characterized by single or multiple masses in organs, which may mimic various inflammatory and malignant diseases. Here, we summarize 4 patients with aggressive manifestations of IgG4-RD that mimic nasopharynx cancer to provide some new sights for the diagnosis of IgG4-RD.

Case summary: Four patients were included in our series. The age ranged from 53 to 64 years old, and the duration of the disease ranged from 4 to 6 months. The chief complaints included headache, rhinorrhea, or diplopia. All patients had more than 10 IgG4+ plasma cells/HPF in immunohistochemistry with plasma IgG4 levels ranging from 218 mg/dL to 765 mg/dL. All of them met the diagnostic criteria of IgG4-RD.

Conclusion: The described case is highly similar to the clinical manifestations of nasopharyngeal carcinoma. Although pathology is the gold standard, there are still limitations. Serological IgG4 can help confirm the diagnosis. Timely diagnosis of IgG4-RD is of great significance in preventing secondary organ damage in patients with active diseases.

KEYWORDS

IgG4-related disease, nasopharyngeal mass, diagnosis, case series, Epstein-Barr virus (EBV)

Introduction

IgG4-related disease (IgG4-RD) was first conceptualized as a systemic disease in 2003 (1). Since then, worldwide awareness of IgG4-related diseases has increased, and experts are now familiar with most of its clinical features. The main clinical feature of IgG4-RD is a swollen lesion of the involved organ with typical serological and histological features including lymphoplasmacytic hyperplasia, fibrosis, occlusive phlebitis, and elevated serum IgG4, which can lead to permanent organ damage and death if left untreated (2–4). The disease is

deemed to be the result of plasma immune cell-mediated overproduction of IgG4 from immunoglobulin IgG, since serum IgG4 is significantly elevated in 60-70% of patients with IgG4-RD (5). However, it has also been reported that serum IgG4 within the normal range occurs in about 20% of patients. IgG4-RD mainly influences middle-aged and elderly people, with an incidence ratio of 1.6:1 between men and women (6).

IgG4-RD can involve multiple organs, common in but not limited to the pancreas, orbit, salivary glands, and lymph nodes, and clinical symptoms vary with the organ involved (7). Pancreatic, biliary tract involvement, retroperitoneal aorta, head and neck, and salivary gland involvement are the most common involved organs (8). Incidence ratio is approximately 4:1 between head and neck and other sites of involvement (3). Recently, studies have found that IgG4-RD can also be associated with otorhinopharyngology involvement. Depending on the site of involvement, IgG4-RD occurring in the nasal cavity can accompany with runny nose, nasal congestion, and dull headache (9), and occurring in the throat can exhibit persistent cough, swallowing pain, and dysphonia (10, 11). While otologic symptoms as initial manifestations may reveal tinnitus, progressive sensorineural hearing loss, serous otitis media, and even dizziness (12, 13). Few studies, however, described nasopharyngeal symptoms as individual clinical manifestations.

With the introduction of the diagnostic criteria for IgG4-RD (6), the diagnosis rate of IgG4-RD in otolaryngology has increased, but it is still easily confused with other diseases. In this article, we summarized the clinical features and diagnostic procedures of four patients who were finally diagnosed with IgG4-related disease with nasopharyngeal malignancy-like manifestations to help clinicians understand this entity.

Materials

All patients diagnosed with IgG4-RD in Sun Yat-sen Memorial Hospital from December 2018 to July 2020 were reviewed. Diagnostic criteria for IgG4-RD were as follows (6): 1. Diffuse or limited swelling or mass in one or more organs; 2. Serum IgG4 > 135 mg/dL; 3. IgG4+ plasma cells per high power field (cells/HPF) higher than 10 cells. And the inclusion criteria were as follows: 1. Final diagnosis was IgG4-RD; 2. The lesions involved the nasopharynx at least.

The basic information of patients, including age, gender, symptoms, disease duration, and treatment process, was collected through the electronic case system. Laboratory test data including EBv (Epstein-Barr virus, EBv) level, lgG4 level, C-reactive protein, immunological, rheumatic, lupus erythematosus, vasculitis markers were recorded during hospitalization and outpatient follow-up; CT, MRI, and PET-CT features of patients were summarized and analyzed by imaging physicians, and pathological results of all patients were collected. This study protocol was accepted by the Review Institution of the Sun Yat-sen Memorial Hospital.

Results

Four patients were included in our series. There were 3 males and 1 female. The age ranged from 53 to 64 years old, and the duration of the disease ranged from 4 to 6 months. The chief complaints included headache, rhinorrhea, or diplopia. There were 2 positive and 2 negative serum EBV IgA antibodies, with lgG4 levels ranging from 218 mg/dL to 765 mg/dL. The immunological, rheumatic, lupus erythematosus, and vasculitis markers of the four patients were all within the normal range. The basic information and clinical data of all patients were summarized in Table 1.

All patients underwent fiberoptic endoscope and MR-enhanced examinations suggestive of nasopharyngeal occupying lesions. MRI images resembled nasopharyngeal malignancy and were characterized as follows: Fibroscopy and MRI suggest bulging of the right nasopharynx, disappearance of the crypt, and shallow pharyngeal opening of the eustachian tube. Note the involvement of the fatty gap of the right petrostaphylinus (Figure 1). Whole-body PET-CT showed active FDG metabolism in the center of the lesion, while the rest of the whole-body scans showed no significant abnormalities. Four cases occurred in the nasopharynx and showed shallowing of the pharyngeal fossa, significant thickening of the parietal, posterior, and posterior walls of the nasopharynx, and the lateral wall of the lesion. In the more severe cases, the lesion involved the palatal sail and levator muscles, the internal and external pterygoid muscles, and was accompanied by bone destruction at the skull base.

All patients underwent surgical pathological examination, and pathologic results showed inflammatory granulation tissue and fibrous tissue hyperplasia with more lymphocytes, plasma cells, and neutrophils infiltration. All patients had more than 10 IgG4+ plasma cells/HPF in immunohistochemistry.

All patients had remission of symptoms after glucocorticoid and immunosuppressive treatment after the diagnosis of IgG4-related disease. Headache, diplopia, epistaxis, and dysphagia symptoms were also improved. A good response to glucocorticoid therapy is an effective way to differentiate IgG4-relative disease from pharyngeal malignancy. However, due to the influence of characteristics such as the location of the lesion and the onset of the disease, it was difficult to obtain the pathological samples accurately. Wherein three patients with IgG4 underwent multiple pathological biopsies (up to 8 times) before they were finally confirmed (Patient 2).

Discussion

Patients with IgG4-RD onset at different sites exhibit unique clinical, epidemiological, and serological features. Their clinical symptoms and morbidity manifest differently, and the serologic findings in patients with IgG4-RD are mostly nonspecific, as serum IgG4 is elevated in only some patients, which means that there are still some patients with serum IgG4 below diagnostic criteria levels. Elevated serum IgG4 levels can be caused by a variety of diseases, including Sjogren's syndrome, sarcoidosis, multicentric Castleman's disease, granulomatosis with polyangiitis, eosinophilic granulomatosis with polyangiitis, eosinophilia, malignant lymphoma, cancers, all of which need to be distinguished from IgG4-RD (14–16). And because it can occur in a wide range of neoplastic, infectious, and autoimmune

TABLE 1 Basic information of 4 cases of IgG4-RD in nasopharynx.

Case	Sex	Age	Course	Manifestation	EB virus	IgG4 (mg/dL)	IgG4+ cells/HPF	Site	Treatment	Outcome
1	Male	63	5M	Headache	–	218	22	nasopharynx	MP 40mg qd CTX 0.2g qod	Remission
2	Male	53	5M	Epistaxis, Diplopia	+	324	>10	nasopharynx	MP 40mg qd CTX 50mg qd	Remission
3	Female	64	4M	Headache	+	268	75	nasopharynx	MP 40mg qd CTX 50mg qd	Remission
4	Male	67	6M	Headache	–	765	>10	nasopharynx	MP 40mg qd CTX 50mg qd	Remission

MP, methylprednisolone; CTX, cyclophosphamide.

diseases, elevated serum IgG4 is currently only applied for the initial screening of IgG4-RD. These diseases are not currently considered since the markers of immunological, rheumatic, lupus erythematosus and vasculitis did not exceed the normal range in 4 patients.

Radiological examinations of most of the involved organs are also mostly nonspecific, for example, IgG4-RD is indistinguishable from images of malignant tumors and inflammatory diseases. In the four cases of IgG4-RD, we reported, the imaging presentation was similar to that of pharyngeal malignancy. It also involved the lateral wall of the nasopharynx and the parapharyngeal space, and the surrounding bones such as the occipital slope, the butterfly bone, and the temporal bone were destroyed, and the internal carotid artery canal, the jugular foramen, and the internal auditory canal could be invaded as the disease progressed intensification. It has been reported (17) that PET-CT can diagnose IgG4-RD only in the absence of associated inflammatory episodes, and the reduction of ^{18}F-FDG uptake after treatment can assess the therapeutic effect. Currently, PET-CT is more often used to assess the extent of the lesion and to stage the extent of the disease, and it can assist in localizing the biopsy site to improve the biopsy detection rate.

The definitive diagnosis of IgG4-RD requires strict clinic opathological correlation, as clinical evaluation, laboratory assessment, and imaging studies often do not easily distinguish it from diseases such as tumors and infectious inflammatory diseases. IgG4-RD pathological histological changes are dense lymphoplasmacytic proliferation, tissue fibrosis, and occlusive phlebitis. The literature reports that IgG4-RD includes two stages of pathogenesis with inflammatory episodes and fibrosis as the outcome (2, 18). This may lead to different degrees of lesion tissue fibrosis at the time of biopsy as well as different stages of disease

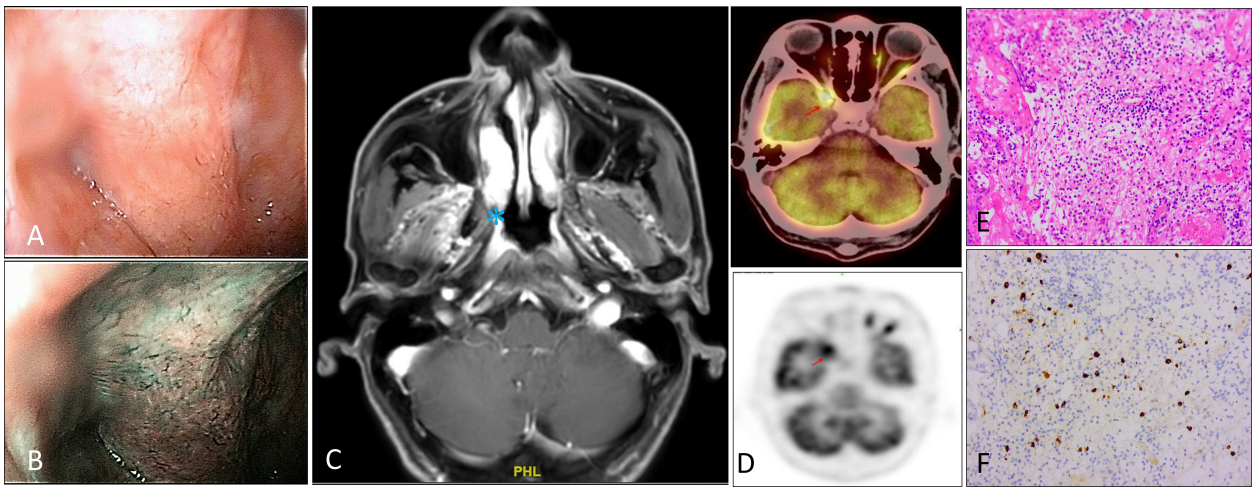

FIGURE 1
Fibroscopy, radiologic, and histologic features of IgG4-RD patient. **(A–C)** Fibroscopy and MRI suggest bulging of the right nasopharynx, disappearance of the crypt, and shallow pharyngeal opening of the eustachian tube. Note the involvement of the fatty gap of the right petrostaphylinus. **(D)** PET-CT showed active FDG metabolism at nasopharynx. **(E, F)** Hematoxylin-eosin staining demonstrating lymphocytes, plasma cells, and a few neutrophils, eosinophils infiltrate, accompanied by fibrous tissue hyperplasia. Immunohistochemical staining showed IgG4-positive cells, greater than 10/HPF. These images are at a 20X original magnification.

progression and different absolute values of IgG4 counts or IgG4 to IgG ratios for each lesion biopsy. The diagnostic criteria for IgG4-RD in lymph node tissue, lacrimal gland, and salivary gland are IgG4-positive cells ≥HPF and IgG4/IgG ratio requirement ≥ 40%, and in retroperitoneal fibrosis or some renal lesions, IgG4+ cells/high power field > 10 are considered positive (19). However, there are no reports about the criteria of IgG4+ cells in nasopharyngeal IgG4-RD. In our reports, four patients had IgG4+ plasma cells higher than 10 cells at high power field, but the IgG4/IgG ratio did not exceed 40%, considering that the lesions were located in deep tissues limiting the acquisition of pathological specimens or the lesions are at different stages of onset.

Although the clinical symptoms and imaging presentation of IgG4-RD with pharyngeal involvement are similar to those of pharyngeal malignancies, the treatment options for the two are different. The preferred treatment modality for nasopharyngeal malignancies is radiation therapy, whereas glucocorticoids are the first-line agents to induce remission in all patients with active IgG4-RD (20). Remission after glucocorticoid therapy is a differentiating point in the treatment of IgG4-RD and malignancy, but glucocorticoids should be used with caution until the diagnosis is clear. In this study, four patients with IgG4-RD were considered malignant lesions due to pharyngeal occupancy. Several times of pathological biopsies were performed, all of which were not malignant and suggested inflammatory tissue containing a large number of plasma cell infiltrates. Combined with the serum IgG4 results, the diagnosis of IgG4-RD could be made, and the diagnostic glucocorticoid treatment could significantly relieve the symptoms.

Inoue was the first to report a case of IgG4-RD that started in one nasal cavity and showed progressive destruction, with loss of intranasal structures and recurrent bleeding from the nasal cavity (21). The presentation of IgG4-RD in the nasopharynx has not been reported in the literature. In our study, IgG4-RD also showed an aggressive presentation on pharyngeal imaging, with nasopharyngeal MR showing significant thickening of soft tissue and soft tissue mass formation in the posterior and parietal walls of the nasopharynx with moderate enhancement on enhanced scans and invasion of the skull base bone; oropharyngeal MR showed an irregular soft tissue mass shadow in the oropharynx and invasion of the surrounding cervical fascial space. One study found that IgG4 plasma cell infiltration was seen in nasal mucosal tissue biopsies in both IgG4-associated chronic sinusitis and common chronic sinusitis, and there was no statistical difference in the number of IgG4 plasma cell infiltrates between the two diseases (22), leading to a possible lack of specificity of nasal tissue biopsy in the diagnosis of IgG4-RD. In addition, the levels of EB virus in two patients have exceeded the normal range which associates with nasopharyngeal malignancy. There have been reports of IgG4 antibodies produced by host B lymphocytes in the Epstein-Barr virus lytic reactivation group (23), which may be the reason why EB virus can be detected in IgG4-RD patients.

A recent publication in the Lancet-Journal of Rheumatology mentioned the classification of IgG4-RD pathology into proliferative and fibrotic types based on the clinical and pathological features of the organs involved in IgG4-RD (24). Proliferative lesions mainly involve glands and epithelial tissues, and this type is characterized by lymphoproliferation and significantly elevated IgG4 levels in serum and focal tissues. The fibrotic lesions often originate outside the glands, and the fibrosis of the involved tissues is more prominent in this type, while the lymphoproliferative degree is lower than that of the proliferative type, and the pathology is often single organ involvement, with significant fibrosis and relatively little lymphoplasmacytic infiltration, which is less likely to form germinal centers and is somewhat aggressive. Four cases of IgG4-related diseases of the nasopharynx were classified as fibrosis type according to the classification: (1) Single site involved, located outside the glandular tissue; (2) patients had mildly elevated serum IgG4 more than 135 mg/dL; (3) Lesions showed significant fibrosis; (4) Pathological tissue had IgG4+ plasma infiltrated. Whether tissue biopsy of the nasopharynx correlates with IgG4-RD still requires more studies to further confirm.

Conclusion

IgG4-RD can involve the nasopharynx as a first and single manifestation, and pharyngeal tissue biopsy and serum IgG4 level testing are currently effective means of diagnosing IgG4-RD. While there is a lack of clear diagnostic criteria. We should distinguish these patients in clinical practice and improve the necessary tests including serum IgG4 testing and histopathological examination of lesions. We expect better serological markers and imaging methods to help identify and clarify the diagnostic direction, differentiate from malignant tumors, avoid misdiagnosis, and improve the detection rate of IgG4-RD.

Author's note

This is a English language translation/reprint of “IgG4-related disease with nasopharyngeal malignancy-like manifestations” originally published in Chinese at 10.13201/j.issn.2096-7993.2022.04.011 (25). Xi-Jun Lin prepared this translation. Permission was granted by Journal of Clinical Otorhinolaryngology Head and Neck Surgery.

Data availability statement

The original contributions presented in the study are included in the article/supplementary material. Further inquiries can be directed to the corresponding author.

Ethics statement

The study was approved by the Ethics Committee of Sun Yat-sen Memorial Hospital, Sun Yat-sen University, Ethics number SYSKY-2022-545-01. The studies were conducted in accordance with the local legislation and institutional requirements. The participants provided their written informed consent to participate in this study. Written informed consent was obtained from the individual(s) for the publication of any potentially identifiable images or data included in this article.

Author contributions

XL: Writing – original draft. PL: Writing – review & editing, Investigation, Visualization. JF: Writing – review & editing, Investigation, Visualization. BZ: Data curation. FL: Writing – review & editing, Data curation. PH: Writing – review & editing, Data curation. XL: Writing – review & editing, Conceptualization, Project administration, Supervision. XH: Writing – review & editing, Conceptualization, Project administration, Supervision.

Funding

The author(s) declare that no financial support was received for the research, authorship, and/or publication of this article.

Conflict of interest

The authors declare that the research was conducted in the absence of any commercial or financial relationships that could be construed as a potential conflict of interest.

Publisher's note

References

1. Kamisawa T, Funata N, Hayashi Y, Eishi Y, Koike M, Tsuruta K, et al. A new clinicopathological entity of IgG4-related autoimmune disease. *J Gastroenterol*. (2003) 38:982–4. doi: 10.1007/s00535-003-1175-y

2. Shimizu Y, Yamamoto M, Naishiro Y, Sudoh G, Ishigami K, Yajima H, et al. Necessity of early intervention for IgG4-related disease–delayed treatment induces fibrosis progression. *Rheumatol (Oxford England)*. (2013) 52:679–83. doi: 10.1093/rheumatology/kes358

3. Della-Torre E, Lanzillotta M, Doglioni C. Immunology of IgG4-related disease. *Clin Exp Immunol*. (2015) 181:191–206. doi: 10.1111/cei.12641

4. Bledsoe JR, Della-Torre E, Rovati L, Deshpande V. IgG4-related disease: review of the histopathologic features, differential diagnosis, and therapeutic approach. *APMIS Acta Pathol Microbiol Immunol Scand*. (2018) 126:459–76. doi: 10.1111/apm.12845

5. Aalberse RC, Stapel SO, Schuurman J, Rispens T. Immunoglobulin G4: an odd antibody. *Clin Exp Allergy*. (2009) 39:469–77. doi: 10.1111/j.1365-2222.2009.03207.x

6. Umehara H, Okazaki K, Masaki Y, Kawano M, Yamamoto M, Saeki T, et al. Comprehensive diagnostic criteria for IgG4-related disease (IgG4-RD), 2011. *MOD Rheumatol*. (2012) 22:21–30. doi: 10.1007/s10165-011-0571-z

7. Celis IM, Kriekaart RL, Aliredjo RP, et al. IgG4-related disease: a disease we probably often overlook. *Netherlands J Med*. (2017) 75:27–31.

8. Lanzillotta M, Mancuso G, Della-Torre E. Advances in the diagnosis and management of IgG4 related disease. *BMJ (Clinical Res ed.)*. (2020) 369:m1067. doi: 10.1136/bmj.m1067

9. Sasaki T, Takahashi K, Mineta M, Fujita T, Aburano T. Immunoglobulin G4-related sclerosing disease mimicking invasive tumor in the nasal cavity and paranasal sinuses. *AJNR Am J Neuroradiol*. (2012) 33:E19–20. doi: 10.3174/ajnr.A2495

10. Völker HU, Scheich M, Zettl A, Hagen R, Müller-Hermelink HK, Gattenlöhner S. Laryngeal inflammatory myofibroblastic tumors: Different clinical appearance and histomorphologic presentation of one entity. *Head Neck*. (2010) 32:1573–8. doi: 10.1002/hed.21232

11. Reder L, Della-Torre E, Stone JH, Mori M, Song P. Clinical manifestations of IgG4-related disease in the pharynx: case series and review of the literature. *Ann Otology Rhinol Laryngol*. (2015) 124:173–8. doi: 10.1177/0003489414549574

12. Cho HK, Lee YJ, Chung JH, Koo JW. Otologic manifestation in IgG4-related systemic disease. *Clin Exp Otorhinolar*. (2011) 4:52–4. doi: 10.3342/ceo.2011.4.1.52

13. Fujimoto S, Kim CH, Green T, Xu H. Otologic manifestations of immunoglobulin G4-related disease. *Ear Nose Throat J*. (2019) 98:630–1. doi: 10.1177/0145561319842852

14. Kamisawa T, Zen Y, Pillai S, et al. IgG4-related disease. *Lancet (London England)*. (2015) 385:1460–71. doi: 10.1016/S0140-6736(14)60720-0

15. Deshpande V, Zen Y, Chan JK, Yi EE, Sato Y, Yoshino T, et al. Consensus statement on the pathology of IgG4-related disease. *Modern Pathol*. (2012) 25:1181–92. doi: 10.1038/modpathol.2012.72

16. Khosroshahi A, Wallace ZS, Crowe JL, Akamizu T, Azumi A, Carruthers MN, et al. International consensus guidance statement on the management and treatment of IgG4-related disease. *Arthritis Rheumatol (Hoboken NJ)*. (2015) 67:1688–99. doi: 10.1002/art.39132

17. Takahashi H, Yamashita H, Morooka M, Kubota K, Takahashi Y, Kaneko H, et al. The utility of FDG-PET/CT and other imaging techniques in the evaluation of IgG4-related disease. *Joint Bone Spine*. (2014) 81:331–6. doi: 10.1016/j.jbspin.2014.01.010

18. Pillai S, Perugino C, Kaneko N. Immune mechanisms of fibrosis and inflammation in IgG4-related disease. *Curr Opin Rheumatol*. (2020) 32:146–51. doi: 10.1097/BOR.0000000000000686

19. Wallace ZS, Naden RP, Chari S, Choi HK, Della-Torre E, Dicaire JF, et al. The 2019 American College of Rheumatology/European League Against Rheumatism classification criteria for IgG4-related disease. *Ann Rheum Dis*. (2020) 79:77–87. doi: 10.1136/annrheumdis-2019-216561

20. Lanzillotta M, Campochiaro C, Mancuso G, Ramirez GA, Capurso G, Falconi M, et al. Clinical phenotypes of IgG4-related disease reflect different prognostic outcomes. *Rheumatol (Oxford England)*. (2020) 59:2435–42. doi: 10.1093/rheumatology/keaa221

21. Inoue A, Wada K, Matsuura K, Osafune H, Ida Y, Kosakai A, et al. IgG4-related disease in the sinonasal cavity accompanied by intranasal structure loss. *Auris nasus larynx*. (2016) 43:100–4. doi: 10.1016/j.anl.2015.05.005

22. Moteki H, Yasuo M, Hamano H, Uehara T, Usami S. IgG4-related chronic rhinosinusitis: a new clinical entity of nasal disease. *Acta Oto-Laryngol*. (2011) 131:518–26. doi: 10.3109/00016489.2010.533699

23. Nagata K, Hara S, Nakayama Y, Higaki K, Sugihara H, Kuwamoto S, et al. Epstein-Barr virus lytic reactivation induces IgG4 production by host B lymphocytes in Graves' Disease patients and controls: A subset of Graves' Disease is an IgG4-related disease-like condition. *Viral Immunol*. (2018) 31:540–7. doi: 10.1089/vim.2018.0042

24. Prof Wen Zhang A, Prof John H. Stone B: management of Igg4-related disease. *Lancet Rheumatol*. (2019) 1:E55–56. doi: 10.1016/S2665-9913(19)30017-7

25. Lin X, Lin P, Liu X. IgG4-related disease with nasopharyngeal Malignancy-like manifestations]. Lin chuang er bi yan hou tou jing wai ke za zhi. *J Clin Otorhinolaryngol Head Neck Surg*. (2022) 36:293–6. doi: 10.13201/j.issn.2096-7993.2022.04.011

frontiers | Frontiers in Immunology

TYPE Review
PUBLISHED 19 September 2024
DOI 10.3389/fimmu.2024.1376723

OPEN ACCESS

EDITED BY
Inga Koneczny,
Medical University of Vienna, Austria

REVIEWED BY
Kazunori Yamada,
Kanazawa Medical University, Japan
Federico Pratesi,
University of Pisa, Italy
Hani S. Mousa,
University of Cambridge, United Kingdom

*CORRESPONDENCE
Maria Maslinska
maslinskam@gmail.com

RECEIVED 26 January 2024
ACCEPTED 26 July 2024
PUBLISHED 19 September 2024

CITATION
Maslinska M and Kostyra-Grabczak K (2024) Immunoglobulin G4 in primary Sjögren's syndrome and IgG4-related disease - connections and dissimilarities.
Front. Immunol. 15:1376723.
doi: 10.3389/fimmu.2024.1376723

Immunoglobulin G4 in primary Sjögren's syndrome and IgG4-related disease - connections and dissimilarities

Maria Maslinska* and Kinga Kostyra-Grabczak

Early Arthritis Clinic, National Institute of Geriatrics, Rheumatology and Rehabilitation, Warsaw, Poland

Primary Sjögren's syndrome (pSS) is an autoimmune disease, with B cell hyperactivation and autoantibody production as its immunological hallmarks. Although the distinction between immunoglobulin G4-related disease (IgG4-RD) and pSS, based on the presence or absence of certain autoantibodies, seems easy to make, possibility of elevated serum IgG4 concentration and often similar organ involvement may lead to a misdiagnosis. The increased serum concentration of IgG4 in IgG4-RD is not clearly linked to the pathogenesis of IgG-RD and it has been suggested that it may constitute just an epiphenomenon. The aim of this article is to discuss the presence of IgG4 in pSS and IgG4-RD and its potential significance for these two diseases.

KEYWORDS

immunoglobulin G4, Sjögren's syndrome, IgG4-related disease, autoimmunity, lymphomas

Introduction

Primary Sjögren's syndrome (pSS) is a chronic autoimmune disease with a dominance of immunological features such as hypergammaglobulinemia, B and T cell activation, autoantibody production mainly against ribonucleoproteins (anti-SSA/Ro and anti-SSB/La antibodies), low levels of C3 and C4 components of the complement system, rheumatoid factor (RF) and cryoglobulin production. The main autoimmune and inflammatory process, with infiltrations of mononuclear cells, takes place in exocrine glands and internal organs. Due to the tropism of exocrine glands, of lacrimal and salivary glands in particular, the dysfunction of those glands is observed, causing dryness - one of the main clinical features of pSS (1).

The presence of anti-Ro/SSA and anti-La/SSB is typical for pSS (1). Less often, immunological tests may reveal anti-centromere B (CENP-B) and anti-citrullinated protein antibodies (ACPA) or antibodies more specific to other connective tissue diseases (2, 3). Rheumatoid factor may also be present in IgM, IgA, and IgG classes of immunoglobulins (4, 5). The association of pSS and primary biliary cholangitis with AMA-

M2 autoantibodies or autoimmune thyroiditis with thyroid peroxidase antibodies (TPOAb) and thyroglobulin antibodies (TgAb) is also well established (6, 7).

Immunoglobulin G4-related disease (IgG4-RD) is another autoimmune disorder, which shares some of its clinical symptoms with pSS, including the presence of the inflammatory and autoimmune process in the salivary and thyroid glands and other similar organs. Its identification underlines the attention paid to immunoglobulin G4 in recent years, its role in the human immune system, and the connection of this antibody to various clinical states.

Interestingly, for years, Mikulicz's disease (MD)—currently recognized as a clinical manifestation of IgG4-RD—was considered a form of pSS. It was described by a Polish surgeon, Jan Mikulicz-Radecki, in 1888 and its symptoms include sialadenitis and dacryoadenitis with salivary and lachrymal gland enlargement (8, 9). Another example of isolated submandibular gland involvement is chronic sclerosing sialadenitis, known as Kutner's tumor (chronic sclerosing sialadenitis), which is also currently classified as a manifestation of IgG4-RD. It occurs without the involvement of other salivary glands, which is one of the elements that distinguishes it from pSS, where the characteristic feature is the involvement of the parotid and submandibular glands (8). The increased serum concentration of IgG4 is a recognized immunological determinant of IgG4-RD, while in the case of pSS, various relationships are presented - both a decrease and, in some studies, an increase in the concentration of this immunoglobulin. The still not fully recognized pathophysiological role of the IgG4, the research, that led to the distinguishing of IgG4-RD, as well as the similarities between this disease and pSS were the inspiration to write the present article.

Overview of the unique role of IgG4

In human serum, the IgG4 class of immunoglobulins is least abundant among other immunoglobulins G and constitutes approximately 5% of IgG (10). Serum IgG4 levels increase gradually from birth and by the age of approximately 10 years they usually reach adult levels, hindering the assessment of IgG4 levels in young children (11). Isolated IgG4 deficiency is very rare and more often occurs in combination with a deficiency of other immunoglobulins (IgG1, IgG2, or IgA). There are observations (mainly in children) indicating that in a case of IgG4 deficiency, recurrent respiratory infections, allergies, candidiasis, and chronic diarrhea occur (12, 13). IgG4 deficiency was also observed in patients with associated inflammatory bowel disease (14). Currently, a lot of attention is being paid to IgG4 hypergammaglobulinemia, which may occur in a healthy population (in ~5%), although increased serum concentration in a healthy population has not yet been proven to have clinical consequences (15).

IgG4 is attributed with an anti-inflammatory role (e.g., response to parasitic infections and allergies) and is also associated with a potentially pathogenic role in autoimmune diseases and with a response to biological treatment or cancer development (16).

Such varied perceptions of the role of IgG4 in immune processes are related to its specific features and abilities, different from other IgG molecules.

In 1997, the structure of an IgG4 Fc fragment was described (17, 18). The structure of human IgG4 is highly homologous (over 90%) to other IgG subclasses, but its unique properties result from specific amino acid differences in the heavy chain, especially in the hinge region, which allows for the phenomenon of fab arm exchange (FAE) (observed *in vitro* only for this subclass of immunoglobulin G) as well as the variability in CH3 domains (19, 20).

The unique property of IgG4 is FAE, which is possible due to relatively labile disulfide bonds between the heavy chains of IgG4 molecules, which allow for the phenomenon of recombination (exchange of half-molecules, each consisting of one heavy chain and one light chain). Such an exchange between two IgG4 molecules allows for the formation of a monovalent (for each antigen)/bispecific antibody, contrary to other IgG monomers, which are bivalent, but monospecific in nature (21, 22). The FAE phenomenon is also favored by a weaker CH3-CH3 interaction in IgG4, caused by the replacement of lysine with arginine (position 409) (19).

In a physiological state, IgG4 is an anti-inflammatory antibody and weakly activates the complement system. Under conditions of increased IgG4 concentration, the consumption of complement components was observed, which indicates such a possibility. It is suggested that special properties of IgG4, such as FAE and glycosylation of Fc fragments, affect complement activation (10, 19). It is also proposed that IgG4 blocks the binding of other immunoglobulin subclasses to the complement component 1q (C1q).

The glycosylation of the Fc IgG4 fragment is another process that plays a role in altering IgG4 effector functions (23). Glycosylation changes the affinity of IgG4 to the different FcγRs (24). Studies on the glycosylation of IgG and IgG4, including in the pathophysiology, (e.g., IgG4 in primary membranous nephropathy causes activation of the lectin pathway and induction of podocyte damage) indicated a pro-inflammatory role of this process and the possibility of the complement activation also by glycoforms of IgG4 (25, 26). Current research indicates that the process of glycosylation of IgG, including IgG4, may have a pro-inflammatory role and is associated with the pathogenesis of various inflammatory diseases. However, the assessment of this phenomenon requires further research.

In Oskam N et al. (27), the authors showed that complement activation by IgG4 is possible, but only at high antigen densities and high antibody concentrations. The researchers managed to demonstrate that such an activation occurred only through the classical pathway. It is possible that these potential pathways are enhanced by galactosylation, while the occurrence of FAE has the opposite effect. However, these findings do not explain the pathogenic role of IgG4 in IgG4-RD or, for example, in primary membranous nephropathy (pMN).

The antigen-specific activity of IgG4 under the influence of chronic antigen stimulation in allergic diseases and in the course of immunotherapy was studied more widely and earlier than the problem of IgG4-related disease (16).

In allergic diseases, as well as in IgG4-RD, T helper type 2 (Th2) cells play an important role associated with interleukin 4 (IL-4) and 13 (IL-13) production (Th2 cytokines). These cytokines stimulate B cells to switch to class IgG4 immunoglobulin production (28).

Because of this stimulation, B cells exposed to an allergen, in addition to producing allergenic IgE, produce IgG4. Immunoglobulin G4 competes with IgE to prevent the activation and the subsequent degranulation of mast cells and basophils. Subsequently, the IgE to IgG4 (IgE/IgG4) ratio decreases. This situation also occurs during allergen-specific immunotherapy. In such circumstances, the persistence of increased IgG4 concentration may be observed for a longer period of time, even up to 3 years (29). Because of the described observations in some diseases with IgE elevation, the protective role of IgG4 has been suggested.

A study on anti-drug antibodies in the biological treatment of RA revealed that adalimumab-treated patients developed antibodies against adalimumab mainly in the IgG4 isotype, rather than in the IgG1 isotype (30). Such observations were associated with longer (3 years in cited study) drug exposition. It was demonstrated that a longer exposition to an antigen (drug) can cause the development of more IgG4 anti-drug-antibodies—a finding which corresponds with other research on time of exposure to allergen/antigen and IgG4 antibodies production.

In summary, it is believed that in the case of allergic diseases and immunotherapy, IgG4 may have a potentially protective effect. A similar increase of both IgG4 and IgE levels is observed in helminth infections (31, 32). Furthermore, beekeepers and laboratory workers may exhibit high serum levels of the allergen-specific IgG4, which protects them from an anaphylactic reaction (20).

However, it is still not clearly established whether increased serum concentration of IgG4 plays an important role in diseases such as IgG4-RD or Crohn's disease (CD) or whether it should be considered an epiphenomenon only (33).

IgG4 detection

In clinical practice, the detection of IgG4 currently is based on different tests, namely, radioimmunoassay (RIA), enzyme-linked immunosorbent assay (ELISA), and immunonephelometry, with two latter ones being most commonly used. In Su et al. (34), a comparison study between these tests proved good compatibility between ELISA and the nephelometric assays. The fact that the costs of performing an ELISA test are lower than immunonephelometry may also be important in planning research.

An antigen-binding radioimmunoassay (RIA) was used particularly in the oldest studies, in which it was used to measure liquid-phase IgG4 antibodies (35).

For years, the problem of establishing a cut-off value for a significant IgG4 concentration, in a way as to maintain the greatest sensitivity and specificity of the tests, has been discussed. Especially since the identification of IgG4-RD, it has become important to determine what value of IgG4 concentration is most likely to be associated with this disease. The classification criteria for IgG4 – RD adopted a value of 1.35 (135 mg/dL) as the cut-off value (36) but in some studies, higher levels were noted as being more specific and sensitive (37, 38).

Carruthers et al. (39) noted that elevated serum IgG4 concentrations had only 60% specificity and a 34% positive predictive value (PPV). Therefore, the authors suggest that a doubled cut-off value may increase the specificity of the test.

In some studies, researchers highlighted that elevated serum concentrations of IgG4 or plasmablasts may be a hallmark of IgG4-RD (40).

This approach is determined by the difficulties in interpreting symptoms and diagnosing IgG4-RD in the presence of a normal/low serum IgG4 concentration. Although such a discussion is currently taking place mainly in relation to IgG4-RD, its outcome may have further consequences, leading to a re-evaluation of diagnostic criteria for other diseases, including pSS, related in various ways to IgG4.

The outline of pSS pathogenesis

The discussion of the potential role of IgG4 in pSS requires a basic understanding of pSS pathogenesis—a problem that still remains not yet fully understood. However, certain factors, such as a breach of immune tolerance, endothelial damage, release of autoantigens, and B cell activation with autoantibody production, were confirmed as immunological features of this chronic autoimmune disease, which is also known under the name of "autoimmune epithelitis" (41).

In recent years, the role of the activity of the interferon pathway in pSS, as well as other autoimmune rheumatic diseases, has been examined. The overexpression of type I IFN is called IFN-I signature (42). Other studies highlighted the significance of T lymphocytes as cells that influence the activation of B lymphocytes with the participation of stimulating factors (CTLA-4) and through the production of B cell stimulating factors such as BAFF/BlySS (43).

Sicca symptoms due to exocrine gland involvement remain the main clinical feature of pSS, although it does not take place in the early stages of pSS. Importantly, in different age groups of patients, we can expect different symptoms as they present with different levels of immune system activity and varied degrees of organ and exocrine gland damage. Several pSS phenotypes have been described and the type designation highlights sicca symptoms, systemic involvement, and organ damage as follows: sicca without organ damage, sicca with glandular involvement/mild systemic involvement, and sicca with severe systemic involvement (44).

The main immunological hallmarks of pSS are anti-ribonucleoprotein antibodies (anti Ro/SSA and anti-La/SSB). They belong to antibodies against extractable nuclear antigens (ENA) which are present in the cell's cytoplasm. Anti-Ro/SSA ab was divided in 1981 by Lerner et al. (45) in two subclasses depending of a molecular weight: anti-Ro52 kDa and anti-Ro60 kDa.

Interestingly, Ro52 and Ro60 antigens are coded on different chromosomes. Ro60 is coded on chromosome 19 and forms complexes with small cytoplasmic RNA (hY-RNA complexes) which may be involved in binding misfolded mRNA and influence its degradation.

Ro52 is coded on chromosome 11, belongs to the tripartite motif protein (TRIM) family, and is involved in inflammation and apoptosis (46).

Some researchers suggest that anti-Ro60 abs are sufficient to diagnose pSS, while anti-La/SSB abs are heterogenous and may be present in other autoimmune diseases, such as systemic lupus erythematosus (SLE), neonatal lupus erythematosus (NLE), and inflammatory myositis as well as pSS. As has been concluded in recent studies, anti-Ro60 abs are considered a triggering factor for autoimmunity (glomerulonephritis, ultraviolet light radiation sensitivity). Anti-Ro52 abs are associated also with other autoimmune diseases, such as systemic sclerosis, rheumatoid arthritis, and primary cholangitis.

However, despite differences between anti-Ro/SSA subclasses, the measurement of anti-Ro/SS-A antibodies as a complex in an ENA panel is sufficient for the determination of their presence for diagnosis according to the current classification criteria of pSS (46).

In the Figure 1, the outline of the recognized pSS pathogenesis is presented.

Diagnosis of primary Sjögren's syndrome

To confirm pSS diagnosis, the European League Against Rheumatism/American College of Rheumatology (EULAR/ACR) classification criteria should be met, and a differential diagnosis should also be performed to exclude other diseases (47). The elements of pSS classification criteria are presented in Table 1.

The classification criteria are met if the final scoring reaches a minimum of four points and the exclusion criteria are not fulfilled.

A short introduction to IgG4-related disease

IgG4-related disease is a chronic autoinflammatory disease of an unknown etiology. The principal symptoms of IgG4-RD include the

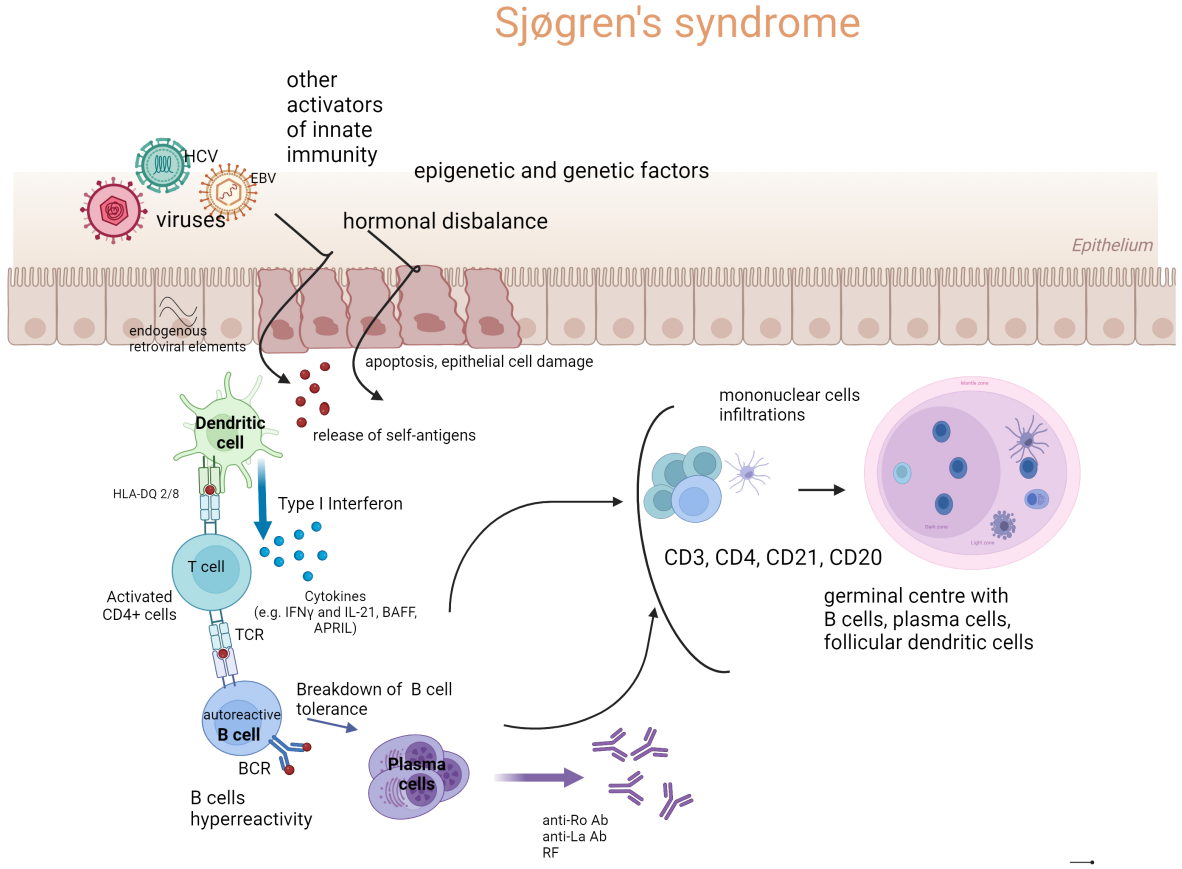

FIGURE 1
The outline of Sjögren's syndrome pathogenesis (Created with BioRender.com). Genetic susceptibility, environmental factors such as mainly viral infections, but also bacterial infections, dysbiosis (microbiome disbalance), endogenous retroviral elements, hormonal disbalance (estrogen deficiency), and ultraviolet radiation (UV) are involved in epithelial cell damage and apoptosis. The endothelial cell damage and release of autoantigens stimulate innate and acquired immunity. The first-line immune response leads to the activation of dendritic cells (DC), especially of a type I signature of the IFN pathway, which releases interferons (IFNs). Subsequently, cross-talk between DC and T cells and their production of B cell stimulating factors (e.g., IFNγ, B cell activating factor (BAFF), a proliferation-inducing ligand (APRIL), and interleukin-21 (IL-21)) cause the activation of B cells and their hyperreactivity. Newly formed plasma cells produce autoantibodies, to ribonucleoproteins in particular, such as anti-Ro/anti-La antibodies and rheumatoid factors (RF) in various classes of immunoglobulins. In target organs (primarily salivary glands), cell infiltrates are formed, consisting of mononuclear cells such as dendritic cells (mainly CD21), T lymphocytes (CD4+, CD3+), CD20 B lymphocytes, and plasma cells. Under the influence of chronic and intense stimulation, tertiary lymphatic structures may be formed—germinal centers (GC), and activation of B cells beyond the control of T lymphocytes may occur. Such stimulation carries the risk of developing a lymphoproliferative process in pSS.

TABLE 1 EULAR/ACR classification criteria for primary Sjogren's syndrome diagnosis (47).

Domain	Parameter	Points	Exclusions
Mouth dryness	Unstimulated salivary flow	1	Active HCV (PCR), confirmed sarcoidosis, GvHD, neck and head radiotherapy, amyloidosis, IgG4-RD, previous lymphoma.
Eye dryness	Schirmer's test ≤ 5mm/5 min	1	
	Ocular Staining Score (OSS) ≥5 or Bijsterveld's test ≥4	1	
Immunological	Anti-SSA/ Ro antibodies	2	
Histopathological	*FS* ≥ 1	2	

To fulfill the classification criteria, the total requested score must be ≥4.
OSS, ocular staining score (48); HCV, hepatitis C virus; GvHD, growth versus host disease; FS, focus score (1 for each mononuclear cell infiltrate, which contains at least 50 inflammatory cells, that is present in a 4 mm^2 of a biopsy section).

elevation of IgG4 serum concentration, characteristic infiltrations of mononuclear cells, fibrosis, and formation of pseudotumors. C-reactive protein elevation and fever are not characteristic of IgG4-RD as for other autoimmune-autoinflammatory diseases, e.g., Castleman's disease, antineutrophil cytoplasmic antibody-associated vasculitis (especially eosinophilic granulomatosis with polyangiitis EGPA)—a phenomenon which should be considered in a differential diagnosis.

A histopathological examination is considered the gold standard of IgG-RD diagnosis, revealing storiform fibrosis, inflammation with infiltration by lymphocyte and plasmatic cells, eosinophilia, and obliterative phlebitis. The formation of germinal centers and lymphoid follicles is also observed.

A storiform pattern of fibrosis (similar to the woven fabric pattern in microscopy assessment) is considered typical for IgG4-RD, however, it can also be observed in neoplastic changes. In the late stage of IgG4-RD, acellular fibrosis dominates (49). Storiform fibrosis is accompanied by dense lymphoplasmacytic infiltrates, often partially eosinophilic infiltrates and obliterative phlebitis.

Obliterative vascular disease is a unique feature of IgG4-RD, not observed in other vasculitis, e.g., granulomatosis with polyangiitis (GPA), polyarteritis nodosa (PN), or microscopic polyangiitis (MPA). In IgG4-RD, vessel wall necrosis is not observed (49).

In infiltrations, IgG4 + plasma cells are dominant (greater than 10 IgG4 + plasma cells/HPF) with a ratio of IgG4 +/IgG + cells greater than 40%.

The current classification criteria for IgG4 - RD diagnosis were established and published in 2019 (36). The verification of whether a patient meets the classification criteria of IgG4-RD is divided into three steps.

The first step is based on the entry criteria (Table 2).

The second step is only possible after meeting the entry criteria. It requires a consideration of possible exclusions, which are listed in Table 3.

In the final step, verification of the inclusion criteria is performed. Inclusion criteria are divided into eight domains. The findings in each domain are weighted, and cases with 20 points or more are classified as IgG4-RD. However, according to the ACR/EULAR IgG4 classification criteria, if any exclusion criterium is met, the patient cannot be further considered as having IgG4 -RD. As a rule, the highest weighted item in each domain is scored (Table 4).

Additional notes: a) in the immunostaining domain biopsies from lymph nodes, mucosal surfaces of the gastrointestinal tract and skin are not acceptable; b) 'Indeterminate' means that a pathologist is unable to clearly quantify the number of positively stained cells within an infiltrate, yet can still ascertain that the number of cells is at least 10/hpf.

The introduction of the 2019 ACR/EULAR IgG4-RD criteria is an attempt to exclude—with the optimal precision in the diagnosis of this multiorgan and multisymptomatic disease—all mimickers and maintain sufficient sensitivity and specificity (the first validation cohort had a specificity of 99.2% and sensitivity of 85.5%, and the second validation a specificity of 97.8% and sensitivity of 82.0%) (36).

Antibodies in the IgG4 subclass

In clinical practice, adverse reactions to food ingredients manifest with symptoms of intolerance as well as with the production of specific antibodies in various classes of immunoglobulins, especially in IgE, IgG, or IgG4. In food intolerance, IgG4 antibodies are associated with basophils and with mastocyte degranulation—elements similarly active in other allergic reactions. In food intolerance, total IgG and IgG4 are significantly increased. While an initial elevation of IgE is observed, a subsequent increase in IgG/IgG4 ratio constitutes a delayed persistent phase (from 24 hours to 5 days) of food intolerance (50). Therefore, for food allergy, diagnostic ELISA tests have been developed for specific IgG4 antibodies against food antigens (50).

In rheumatoid arthritis (RA), specific anti-citrullinated cyclic peptide antibodies (ACPAs) in the IgG4 class of immunoglobulins may occur. Carbone et al. (51) presented a metanalysis from three studies on 328 RA patients in total and concluded that elevated IgG4 ACPA was observed in 35.98% of patients. The Fab segments of RF can react with the Fc part of the IgG molecule and mainly generate IgM (RF)-IgG immune complexes. They can also recognize the Fc domains of IgG4 to form IgG4-RF immune complexes which may activate the complement system and cause synovial injury (52). In patients with RA, increased IgG4 serum concentration was also observed as was the presence of IgG4 in the inflammatory active synovium.

The focus on IgG4 led to the search for connections between this immunoglobulin and other autoimmune diseases. It seems

TABLE 2 Entry criteria for the evaluation for IgG4–RD according to ACR/EULAR classification criteria.

The involvement of organs characteristic/typical in IgG4-RD
Pancreas, salivary glands, bile ducts, orbits, kidney, lung, aorta, retroperitoneum, pachymeninges, and thyroid gland (only Riedel's thyroiditis), as well as evidence of an inflammatory process accompanied by a lymphoplasmacytic infiltrate in one of the listed organs, which cannot be attributed to any other condition.

TABLE 3 List of exclusions (36).

Exclusions
1. Clinical
Documented recurrent fever >38°C (in the absence of any clinical features of infection).
No objective response to glucocorticoids [no response to a treatment with prednisone at a minimum of 40 mg/day (~0.6 mg/kg/day) for 4 weeks]. The decrease of IgG4 serum concentration only is not considered as a response to treatment.
2. Serological
Leukopenia and thrombocytopenia without alternative explanation*
Peripheral eosinophilia >3,000 mm3.
Presence of antineutrophil cytoplasmic antibodies (ANCA)**
Presence of AID antibodies (anti-dsDNA, RNP, SM antibodies)***
Cryoglobulinemia with another explanation for a patient's condition
Other AID-specific antibodies****
3. Radiological
Rapid radiological progression
Long bone abnormalities typical of Erdheim-Chester disease
Splenomegaly
Radiological findings typical or suspected of infection or malignancy
4. Histopathological findings:
Cellular infiltrates suggesting malignancy that has not been sufficiently evaluated
Markers consistent with inflammatory myofibroblastic tumour (IMT)*****
Dominant neutrophilic inflammation
Necrotizing vasculitis
Prominent necrosis
Primarily granulomatous inflammation
Pathologic features of macrophage/histiocytic disorder (hemophagocytic lymphohistiocytosis spectrum diseases, HLH)******
5. Diagnosis with another disease:
Multicentric Castleman's disease
Crohn's disease*******
Ulcerative colitis*******
Hashimoto thyroiditis********

ANCA, antineutrophil cytoplasmic antibody; dsDNA, double-stranded DNA; IgG4-RD, IgG4-related disease; MPO, myeloperoxidase; PR3, proteinase 3; anti-SM antibody, anti-Smith antibody.
*Hematologic features atypical for IgG4-RD.
**Antibodies against proteinase 3 or myeloperoxidase.
***Autoantibodies of low specificity such as RF and ANA do not account for an exclusion and are not clear exclusions.
****Anti-Ro/SSA, anti-La/SSB, double-stranded DNA, RNP, and Sm antibodies in titers greater than normal suggest an alternative diagnosis. Other autoantibodies associated with a high specificity for another immune-mediated condition suggest another diagnosis. Such specific autoantibodies include anti-synthetase antibodies (e.g., anti–Jo-1), anti–topoisomerase III (Scl-70), and anti–phospholipase A2 receptor antibodies.
*****IMT benign tumor consisted with myofibroblastic and fibroblastic cells and lymphocytes and eosinophils.
******HLH haemophagocytic lymphohistiocytosis this is a hyper-inflammatory disease with multiorgan failure, primary (genetic mutations), secondary (triggering by infection, malignancy, autoimmune disorders).
*******If pancreato-biliary disease is present.
********If the thyroid is the only proposed location of disease manifestation.

obvious that, especially in IgG4-RD, various IgG4 associations were analyzed. Kiyama et al. (53) showed that in spite of the elevation of IgG4 in the sera of patients with IgG4-RD, the production of antinuclear antibodies (ANA) antibodies in the IgG4 subclass was not observed. Therefore, the authors suggested that the elevation of IgG4 levels is non-specific (epiphenomenon?) and not pathogenetic, concluding that IgG4-RD is not an autoimmune disease.

Demirci et al. (54) found a significant increase in serum levels of IgG4 in patients with celiac disease (CD) versus the control group and the authors concluded that IgG4 levels can constitute a biochemical marker for CD.

In an animal model in the study by Bi et al. (55), it was found that switching anti – ADAMTS13 (a disintegrin and metalloproteinase with a thrombospondin type 1 motif, member 13) to the IgG4 subclass had a protective effect in a IgG4-mediated disease, thrombotic thrombocytopenic purpura (TTP), in contrast to IgG3 anti-ADAMTS13 antibodies. In pemphigus foliaceus (PF), autoantibodies to desmoglein 1 (anti-Dsg1) in the IgG4 subclass of immunoglobulins played an opposite role by reducing FcγR-binding affinity or ablating FcγRs, which enhanced their pathogenic function. In PF, the IgG1 subclass was revealed to be non-pathogenic (56).

An interesting topic, however beyond the scope of this article, is the existence of IgG4-nervous system dependent diseases including myasthenia with muscle specific tyrosine kinase (MuSK) antibodies or chronic inflammatory demyelinating polyneuropathy (CIDP) with neurofascin-155, contactin-1/CASPR-1 antibodies, and anti-LGI 1 as well as in CASPR2-associated limbic encephalitis, neuromyotonia, and Morvan syndrome (57, 58). The cases of anti-IgLON5 and anti-DPPX-spectrum CNS diseases related to IgG4 were also described (59).

Sjögren's syndrome and antibodies in the immunoglobulin G4 class of immunoglobulins

Primary Sjögren's syndrome is relatively common among systemic diseases of a connective tissue and is associated with the

TABLE 4 Inclusion domains and items included in the IgG4 ACR/EULAR classification criteria (36).

Histology	Uninformative biopsy Dense lymphocytic infiltrate Dense lymphocytic infiltrate and obliterative phlebitis Dense lymphocytic infiltrate and storiform fibrosis with or without obliterative phlebitis	0 4 6 13
Immunostaining	IgG4+:IgG+ ratio is 0%–40% or indeterminate and the number of IgG4 + cells/hpf is 0–9. The IgG4+:IgG+ ratio is ≥41% and the number of IgG4 +cells/hpf is 0–9 or indeterminate or (2) the IgG4 +:IgG+ ratio is 0–40% or indeterminate and the number of IgG4+ cells/hpf is ≥10 or indeterminate. IgG4+:IgG+ ratio is 41%–70% and the number of IgG4 + cells/hpf is ≥10 or the IgG4+:IgG+ ratio is ≥71% and the number of IgG4 + cells/hpf is 10–50. IgG4+:IgG+ ratio is ≥71% and the number of IgG4 + cells/hpf is ≥51	0 7 14 16
IgG4 serum concentration	Normal or not checked >Normal but <2× upper limit of normal 2–5× upper limit of normal ≥>5× upper limit of normal	0 4 6 11
Lacrimal, parotid, sublingual and submandibular glands (bilateral)	No set of glands involved One set of glands involved Two or more sets of glands involved	0 6 14
Chest	Not checked or neither of the items listed is present Peribronchovascular and septal thickening Paravertebral band-like soft tissue in the thorax	0 4 10
Pancreas and biliary tree	Not checked or none of the items are present Diffuse pancreas enlargement (loss of lobulations) Diffuse pancreas enlargement and capsule-like rim with decreased enhancement Pancreas (either of the above) and biliary tree involvement	0 8 11 19
Kidney	Not checked or none of the items listed are present Hypocomplementemia Renal pelvis thickening/soft tissue Bilateral renal cortex low-density areas	0 6 8 10
Retroperitoneum	Not checked or neither of the items listed is present Diffuse thickening of the abdominal aortic wall Circumferential or anterolateral soft tissue around the infrarenal aorta or iliac arteries	0 4 8

hpf/HPF, high-power field.

hyperactivity of B lymphocytes, which increases the possibility of the emergence of autoantibodies.

Antibodies to ribonucleoproteins are characteristic of pSS, but only anti-Ro/SS-A antibodies are included in the current classification criteria for this disease (47). However, antinuclear antibodies are present in the majority of pSS patients. Kiyjama et al.'s work (53) shows that ANA-IgG4 antibodies are rare in rheumatic diseases. Among the patients analyzed in the study only one, with pSS, had ANA-IgG4 antibodies. This patient did not meet the criteria for IgG4-RD. Although he had anti-Ro/Ss-A antibodies, the researchers did not indicate whether those included anti-Ro-IgG4. Antinuclear antibodies are usually present in IgG1-3 subclasses. They can also be present in low titers in IgG4-RD (a higher titer constitutes an exclusion criterion in IgG-RD diagnosis).

Wahren and colleagues (60), in 1994, investigated humoral response to Ro60kDa/SS-A and La/SS-B antigens and found that IgM and IgG (1-4) responses to these antigens coexist, while among IgG antibodies, IgG1 dominates.

In Sjögren's syndrome, polyclonal hypergammaglobulinemia is one of the main laboratory findings and immunoglobulins usually belong to various classes. In pSS, hyperglobulinemia is associated with high serum levels of RF (IgM, IgA, and IgG). In rare cases, immunoglobulins of one class are responsible for the hyperglobulinemia. Liu et al. (61) studied immunoglobulin profiles in pSS and SLE patients. They showed that in pSS, IgG1, IgG2, and IgG3 were usually increased among the subclasses of immunoglobulin G, while there was a visible and significant reduced level of IgG4 in the sera of pSS patients and a decrease of the IgG4 to IgG ratio. Interestingly, in a cited work, the serum concentrations of IgG1-3 immunoglobulins were similar in pSS and SLE patients, however, a difference was observed between pSS and SLE in the IgG4 concentration. The authors did not find an explanation for this fact. In another work, a lower serum concentration of IgG4 in the pSS group ($p=0.0435$) and a significantly lower ($p=0.0035$) ratio of serum IgG4 to total IgG compared to healthy subjects, were confirmed. This study also showed a weak negative correlation ($r= - 0.274$) between C4 component complement levels and IgG4 (62).

There are also studies of pSS patients in which an increase of IgG4 serum concentration was shown, but it should be taken into account that such results concerned a small number of pSS patients, only 7.5% percent (n=10) of the pSS group (63).

The role of IgG4 in a context of the development of lymphomas and sialadenitis in primary Sjögren's syndrome and IgG4-RD

Primary Sjögren's syndrome increases the risk of lymphoma development due to lymphatic organ involvement, especially B cells. In pSS, all elements of the immune response leading to the stimulation of maturation and activation of B lymphocytes and the disruption of the controlling mechanisms (breaching the control of, among others, T lymphocytes) result in the hyperreactivity of B cells.

Mucosa-associated lymphoid tissue (MALT) lymphoma is the most often observed lymphoma emerging during a course of pSS. Its different types are distinguished depending on their localization: gut-associated lymphoid tissue (GALT), bronchus-associated lymphoid tissue (BALT), or nasal-associated lymphoid tissue (NALT) lymphoma. Salivary gland MALT lymphoma is the most frequent localization of the initial lymphoproliferation in pSS (64, 65).

The main risk factors for lymphoma development in pSS are presented in Table 5 (65).

Risk factors for lymphoma development include Fms-like tyrosine kinase 3 ligand (Flt-3L), a type I transmembrane protein activating Flt-3 which stimulates progenitor cells in bone marrow and blood. A study revealed that high levels of Flt-3L were associated with lymphoma (66). The Flt3/Flt3L cascade is responsible for the development and maintenance of DCs (67). Flt3L – IgG4 (modified Fc region) has been investigated as a drug in immunotherapy and adjuvant in vaccines and may potentially become a drug for autoimmune diseases (68).

Lymphomas such as MALT lymphoma and diffuse large B cell lymphoma (DLBCL) can also develop in IgG4-related sialadenitis and orbital IgG4-RD localization (69).

A picture of salivary glands in ultrasonography with a high SGUS score evaluation can be a diagnostic predictor of risk of lymphoma development, particularly when it coincides with a high minor salivary gland biopsy (MSGB) focus score (70). Although this imaging method is not included in pSS classification criteria, its results may suggest a need for further lymphoma diagnostics. Another useful method, which can be used as a second step to better establish a place suspected of tumor development, infiltration, and lymphoproliferation, is magnetic resonance imaging (MRI) (71).

A craniofacial MRI image from a patient with pSS is shown in Figure 2.

IgG4-related sialadenitis is quite often present in this disease and may suggest pSS, particularly in the presence of changes in the major salivary glands. In such instances, the IgG4 concentration in the serum should be determined and an analysis of cells from a biopsy of the minor salivary glands performed. An examination of the material from a biopsy of the major salivary glands is useful both for establishing a diagnosis of IgG4-RD and verifying whether lymphoproliferation occurred.

Pulmonary nodular lymphoid hyperplasia (PNLH, pulmonary pseudolymphoma) is characterized by an increase in IgG4+ plasma cells and a higher IgG4+/IgG+ plasma cell ratio compared to other pulmonary lymphoid proliferations. In contrast, in a low-grade B cell lymphoma and BALT lymphoma, which may be associated with pSS, such a phenomenon was not confirmed (72, 73).

The presence of pSS, as a preexisting autoimmune disorder, was also reported in cases of bronchial-associated lymphoid tissue lymphoma (a relatively rare disease) (74, 75).

There are also various reports of an increased risk of carcinogenesis in IgG4-RD. In Yu et al.'s (76) metanalysis of 10 studies, the overall standardized incidence ratio (SIR) estimated an increased risk of overall cancer in IgG4-RD patients (SIR 2.57 95% CI 1.72–3.84) compared with the general population. This risk was particularly high in cases of pancreatic cancer and lymphoma (SIR 4.07 95% CI 1.04–15.92, SIR 69.17 95% CI 3.91–1223.04, respectively) (76).

In IgG4-RD the main risk factors for malignancy development are currently considered to be (77):

- autoimmune pancreatitis
- eosinophilia

TABLE 5 The risk factors for lymphoma development in pSS. Risk factors confirmed by Fragkioudaki et al.'s study (65) are in blue.

Domain	Feature/parameter
Clinical	Longer duration of pSS (longer time of mainly B cells but also T cells or NK cells stimulation)
	Persistent enlargement of salivary glands
	Lymphadenopathy
	Cryoglobulinemic vasculitis
	Palpable purpura
	Glomerulonephritis
	Raynaud 's phenomenon
	Peripheral neuropathy
	Concurrent chronic infections (*Hepatitis C virus, Helicobacter pylori, Campylobacter jejuni, Borrelia burgdoferi, Chlamydophila psittaci*)
	Moderate/high-disease activity, calculated with ESSDAI or clinESSDAI
Serological	Leukopenia
	Low C4 component of complement
	Monoclonal gammopathy
	Cryoglobulinemia
	Autoantibody positivity (anti-SSA/Ro, anti-SSB/La)
	Rheumatoid factor
	FLT3L*
Histopathological	High focus score (≥3)
	Presence of germinal centers

*Fms-like tyrosine kinase 3 ligand (Flt-3L).

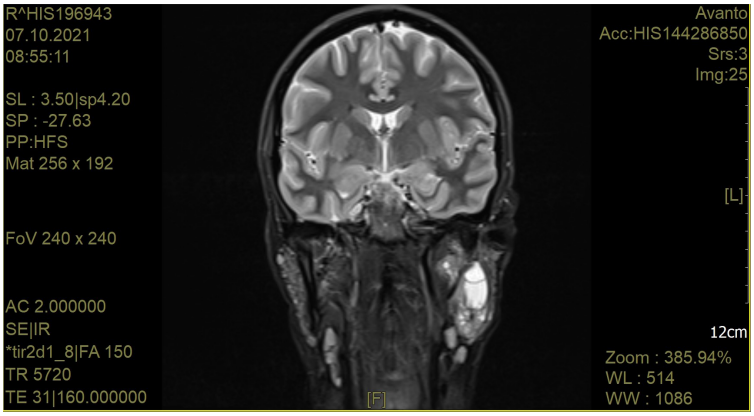

FIGURE 2
A craniofacial magnetic resonance image of a patient with pSS. The left parotid gland is bulging outwards. The right parotid gland is not enlarged. Altered vesicular structure of the parotid and submandibular glands. In the left parotid gland in the deep lobe, cystic lesions are visible. A group of cystic structures is visible in the central part of the left parotid gland. After i. v. contrast administration, no significant signal amplification was observed. Currently, the salivary ducts are not dilated. There are numerous lymphatic nodules in the parotid glands (approx. 6 mm). In the submandibular area, there are single lymph nodes up to 11 mm long. There are numerous lymph nodes in the neck, measuring up to 15 mm.

TABLE 6 Comparison of the selected parameters/features of pSS and IgG4-RD.

Parameter/feature	pSS	IgG4-RD
Median age at diagnosis	>50*	50-60
Sex	F>M	M >F
Autoantibodies/ immunological biomarkers	Anti-Ro antibodies, anti-La antibodies, ANA, RF,	none
IgG4 serum concentration	Normal or decreased	Usually elevated
Hypergammaglobulinemia**		
Mouth/eye dryness	Usually present	May be present
Salivary glands enlargement	Present (risk of MALT lymphoma)	Present (IgG4 related sialadenitis)
Lymphadenopathy	+	+
Cryoglobulins***	Mixed cryoglobulins usually present	Mixed cryoglobulins rarely present
Kidney	Tubulointerstitial nephritis, membranous nephropathy, renal tubular acidosis	Tubulointerstitial nephritis, membranous nephropathy
Retroperitoneum	is not typical, cases of idiopathic retroperitoneal fibrosis (IRF) were described	renal insufficiency due to a retroperitoneal fibrosis, typical periaortitis
Thyroid glands	Hashimoto's disease	Riedel's thyroiditis
Lungs	Interstitial lung disease inflammatory pseudotumor, interstitial pneumonitis, organizing pneumonia, lymphomatoid granulomatosis	Interstitial lung disease: nonspecific interstitial pneumonia, usual interstitial pneumonia lymphocytic interstitial pneumonia, organizing pneumonia
Gastrointestinal	Primary biliary cholangitis (PBC)	AIP type 1
Malignancy	Mainly lymphomas	Higher overall risk of malignancies in comparison to the general population (pancreatic; lymphoma)
Malignancy mimicker****	+	+

*currently, as a result of improved diagnostics and more widespread knowledge of pSS, it is often diagnosed at an earlier stage and in the population younger than >50 years.
**hypergammaglobulinemia.
***In both diseases mixed cryoglobulins can be present, as combination of monoclonal RF IgM and polyclonal IgG (type II) or combination of polyclonal RF IgM and polyclonal IgG (type III).
****Taking into account the clinical course of IgG4-RD with the formation of pseudotumors, organ and extra-organ infiltration (retroperitoneal fibrosis, periorbital infiltration, etc.), it seems that IgG4-RD may more often imitate malignancy, e.g. occurring as a pancreatic tumor in AIP-1.
AIP-1, autoimmune pancreatitis type 1; ANA, antinuclear antibodies; MALT, mucosa-associated lymphoid tissue; PBC, primary biliary cholangitis; RF, rheumatoid factor. + presence/confirmation.

However, the data about eosinophilia are conflicting. In some reports, it is presented as a protective factor (78) while in others, as a risk for cancer development (77).

IgG4-RD lymphadenopathy in some reports was misdiagnosed as Hodgkin's lymphoma (79) but most reported cases indicate that MALT lymphomas more frequently occur in orbital IgG4-RD. The majority of these reports are derived from Asia (76). Further studies and meta-analyses should be performed to reliably assess the actual situation.

Taking into account that the possibility of lymphoma development exists both in pSS and IgG4-RD, but is higher in pSS, the differentiation between these two diseases may, in some especially serologically unclear cases, be crucial for diagnosis, proper treatment, and estimating the risk of lymphoma.

A comparison of the main clinical features of primary Sjogren's syndrome and IgG4-related disease

A summary of the main features of pSS and IgG4-RD is presented in Table 6.

When analyzing organ involvement in pSS compared to IgG4-RD, similarities and tropism of certain organs, e.g., salivary glands, in both diseases should be taken into account. Certain locations and types of lesions may be more indicative of one of these diseases. Thus, changes only in submandibular glands (e.g., Kuttner's tumor, defined as a chronic sclerosing sialadenitis) without parotid gland involvement is a common feature of IgG4-RD and is rarely seen in pSS (8, 80).

Based on the studies indicating a reduction in IgG4 in the serum of patients with pSS (60), in the absence of specific autoantibodies, the assessment of IgG4 concentration may prove vital for the differentiation between pSS and IgG4-RD, with an increased concentration pointing to IgG4-RD and a decreased one indicating pSS.

Despite adopting the presence of several diseases as an exclusion criterium for the IgG4-RD diagnosis, there is an ongoing discussion on the potential possibility of IgG4-RD overlapping or co-existing with other diseases (81, 82). Addressing this problem requires further research and data gathering, which exceed the scope of this work.

Conclusions

The main difference between IgG4-RD and pSS in the context of the presence of IgG4 is that while the serum concentration of IgG4 in IgG4-RD is typically elevated, the same phenomenon does not occur in pSS and some studies indicate a decrease in IgG4 serum level in pSS below its normal range.

This phenomenon may have a diagnostic value—in particular in the context of similar clinical features and affected organs in pSS and IgG4-RD—but its significance is not clear and this issue requires more research.

The role of IgG4 in pSS, as well as in IgG4-RD, is not fully understood and should be a subject of a further research. Currently, the still incomplete understanding of the dual role IgG4 plays in the immune response undermines the proper interpretation of the obtained test results.

Author contributions

MM: Conceptualization, Formal analysis, Supervision, Visualization, Writing – original draft, Writing – review & editing, Data curation, Methodology, Resources. KK: Data curation, Formal analysis, Resources, Writing – original draft, Writing – review & editing.

Funding

The author(s) declare that no financial support was received for the research, authorship, and/or publication of this article

Acknowledgments

We would like to thank Krzysztof Maśliński for the linguistic correction of the text.

Conflict of interest

The authors declare that the research was conducted in the absence of any commercial or financial relationships that could be construed as a potential conflict of interest.

Publisher's note

References

1. Jonsson R, Vogelsang P, Volchenkov R, Espinosa A, Wahren-Herlenius M, Appel S. The complexity of Sjögren's syndrome: novel aspects on pathogenesis. *Immunol Lett*. (2011) 141:1–9. doi: 10.1016/j.imlet.2011.06.007

2. Park Y, Lee J, Koh JH, Choe JY, Sung YK, Lee SS, et al. Clinical influences of anticentromere antibody on primary Sjögren's syndrome in a prospective Korean cohort. *Korean J Intern Med*. (2021) 36:1492–503. doi: 10.3904/kjim.2020.146

3. Gottenberg JE, Mignot S, Nicaise-Rolland P, Cohen-Solal J, Aucouturier F, Goetz J, et al. Prevalence of anti-cyclic citrullinated peptide and anti-keratin antibodies in patients with primary Sjögren's syndrome. *Ann Rheum Dis*. (2005) 64:114–7. doi: 10.1136/ard.2003.019794

4. Maślińska M, Mańczak M, Kwiatkowska B, Ramsperger V, Shen L, Suresh L. IgA immunoglobulin isotype of rheumatoid factor in primary Sjögren's syndrome. *Rheumatol Int*. (2021) 41:643–9. doi: 10.1007/s00296-020-04782-3

5. Meek B, Kelder JC, Claessen AME, van Houte AJ, Ter Borg EJ. Rheumatoid factor isotype and Ro epitope distribution in primary Sjögren syndrome and rheumatoid arthritis with keratoconjunctivitis sicca. *RheumatolInt*. (2018) 38:1487–93. doi: 10.1007/s00296-018-4090-5

6. Deng X, Li J, Hou S, Ci B, Liu B, Xu K. Prevalence and impact of Sjögren's syndrome in primary biliary cholangitis: a systematic review and meta-analysis. *Ann Hepatol*. (2022) 27:100746. doi: 10.1016/j.aohep.2022.100746

7. Baldini C, Ferro F, Mosca M, Fallahi P, Antonelli A. The association of Sjögren syndrome and autoimmune thyroid disorders. *Front Endocrinol (Lausanne)*. (2018) 9:121. doi: 10.3389/fendo.2018.00121

8. Kamiński B, Błochowiak K. Mikulicz's disease and Küttner's tumor as manifestations of IgG4-related diseases: a review of the literature. *Reumatologia*. (2020) 58:243–50. doi: 10.5114/reum.2020.98437

9. Yamamoto M, Harada S, Ohara M, Suzuki C, Naishiro Y, Yamamoto H, et al. Clinical and pathological differences between Mikulicz's disease and Sjögren's syndrome. *Rheumatology*. (2005) 44:227–34. doi: 10.1093/rheumatology/keh447

10. Vidarsson G, Dekkers G, Rispens T. IgG subclasses and allotypes: From structure to effector functions. *Front Immunol*. (2014) 5:520. doi: 10.3389/fimmu.2014.00520

11. Schauer U, Stemberg F, Rieger CH, Borte M, Schubert S, Riedel F, et al. IgG. IgG subclass concentrations in certified reference material 470 and reference values for children and adults determined with the binding site reagents. *Clin Chem*. (2003) 49:1924–9. doi: 10.1373/clinchem.2003.022350

12. Parker AR, Skold M, Ramsden DB, Ocejo-Vinyals JG, López-Hoyos M, Harding S. The clinical utility of measuring IgG subclass immunoglobulins during immunological investigation for suspected primary antibody deficiencies. *Lab Med*. (2017) 48:314–25. doi: 10.1093/labmed/lmx058

13. Moss RB, Carmack MA, Esrig S. Deficiency of IgG4 in children: association of isolated IgG4 deficiency with recurrent respiratory tract infection. *J Pediatr*. (1992) 120:16–21. doi: 10.1016/S0022-3476(05)80590-6

14. Rawat A, Suri D, Gupta A, Saikia B, Minz RW, Singh S. Isolated immunoglobulin G4 subclass deficiency in a child with bronchiectasis. *Indian J Pediatr*. (2014) 81:932–3. doi: 10.1007/s12098-013-1247-9

15. Koutroumpakis F, Evans Phillips A, Yadav D, Machicado JD, Ahsan M, Ramos Rivers A, et al. Serum IgG4 subclass deficiency defines a distinct, commonly encountered, severe inflammatory bowel disease subtype. *Inflammation Bowel Dis*. (2021) 27:855–63. doi: 10.1093/ibd/izaa230

16. Rispens T, Huijbers MG. The unique properties of IgG4 and its roles in health and disease. *Nat Rev Immunol*. (2023) 23:763–78. doi: 10.1038/s41577-023-00871-z

17. Sohi MK, Corper AL, Wan T, Steinitz M, Jefferis R, Beale D, et al. Crystallization of a complex between the Fab fragment of a human immunoglobulin M (IgM) rheumatoid factor (RF-AN) and the Fc fragment of human IgG4. *Immunology*. (1996) 88:636–41. doi: 10.1046/j.1365-2567.1996.d01-692.x

18. Corper AL, Sohi MK, Bonagura VR, Steinitz M, Jefferis R, Feinstein A, et al. Structure of human IgM rheumatoid factor Fab bound to its autoantigen IgG Fc reveals a novel topology of antibody-antigen interaction. *Nat Struct Biol*. (1997) 4:374–81. doi: 10.1038/nsb0597-374

19. Lighaam L, Rispens T. The immunobiology of immunoglobulin G4. *Semin Liver Disease*. (2016) 36:200–15. doi: 10.1055/s-0036-1584322

20. Trampert DC, Hubers LM, van de Graaf SFJ, Beuers U. On the role of IgG4 in inflammatory conditions: lessons for IgG4-related disease. *Biochim Biophys Acta (BBA) - Mol Basis Dis*. (2018) 1864:1401–9. doi: 10.1016/j.bbadis.2017.07.038

21. Schuurman J, Labrijn AF, Parren PW. Fab-arm exchange: what's in a name? *MAbs*. (2012) 4:636. doi: 10.4161/mabs.22075

22. Davies AM, Rispens T, Ooijevaar-de Heer P, Gould HJ, Jefferis R, Aalberse RC, et al. Structural determinants of unique properties of human IgG4-Fc. *J Mol Biol*. (2014) 426:630–44. doi: 10.1016/j.jmb.2013.10.039

23. Kozłowska K, Rydlewska M, Ząbczyńska M, Pocheć E. Glikozylacja IgG w chorobach autoimmunizacyjnych. *Postępy Higieny i Medycyny Doświadczalnej*. (2018) 72:975–90. doi: 10.5604/01.3001.0012.7351

24. Wang TT. IgG fc glycosylation in human immunity. *Curr Top Microbiol Immunol*. (2019) 423:63–75. doi: 10.1007/82_2019_152

25. Konno N, Sugimoto M, Takagi T, Furuya M, Asano T, Sato S, et al. Changes in N-glycans of IgG4 and its relationship with the existence of hypocomplementemia and individual organ involvement in patients with IgG4-related disease. *PLoS One*. (2018) 13:e0196163. doi: 10.1371/journal.pone.0196163

26. Haddad G, Lorenzen JM, Ma H, de Haan N, Seeger H, Zaghrini C, et al. Altered glycosylation of IgG4 promotes lectin complement pathway activation in anti-PLA2R1-associated membranous nephropathy. *J Clin Invest*. (2021) 131:e140453. doi: 10.1172/JCI140453

27. Oskam N, Damelang T, Streutker M, Ooijevaar-de Heer P, Nouta J, Koeleman C, et al. Factors affecting IgG4-mediated complement activation. *Front Immunol*. (2023) 14:1087532. doi: 10.3389/fimmu.2023.1087532

28. Moriyama M, Nakamura S. Th1/Th2 immune balance and other T helper subsets in IgG4-related disease. *Curr Top Microbiol Immunol*. (2017) 401:75–83. doi: 10.1007/82_2016_40

29. Pavón-Romero GF, Parra-Vargas MI, Ramírez-Jiménez F, Melgoza-Ruiz E, Serrano-Pérez NH, Teran LM. Allergen immunotherapy: current and future trends. *Cells*. (2022) 11:212. doi: 10.3390/cells11020212

30. Bartelds GM, Krieckaert CL, Nurmohamed MT, van Schouwenburg PA, Lems WF, Twisk JW, et al. Development of antidrug antibodies against adalimumab and association with disease activity and treatment failure during long-term follow-up. *JAMA*. (2011) 305:1460–8. doi: 10.1001/jama.2011.406

31. Turner JD, Faulkner H, Kamgno J, Kennedy MW, Behnke J, Boussinesq M, et al. Allergen-specific IgE and IgG4 are markers of resistance and susceptibility in a human intestinal nematode infection. *Microbes Infect*. (2005) 7:990–6. doi: 10.1016/j.micinf.2005.03.036

32. Adjobimey T, Hoerauf A. Induction of immunoglobulin G4 in human filariasis: an indicator of immunoregulation. *Ann Trop Med Parasitol*. (2010) 104:455–64. doi: 10.1179/136485910X12786389891407

33. Bushara O, Escobar DJ, Weinberg SE, Sun L, Liao J, Yang GY. The possible pathogenic role of IgG4-producing plasmablasts in stricturing Crohn's disease. *Pathobiology*. (2022) 89:187–97. doi: 10.1159/000521259

34. Xu Wl., Ling Yc., Wang Zk., Deng F. Diagnostic performance of serum IgG4 level for IgG4-related disease: a meta-analysis. *Sci Rep*. (2016) 6:32035. doi: 10.1038/srep32035

35. Rowntree S, Platts-Mills TA, Cogswell JJ, Mitchell EB. A subclass IgG4-specific antigen-binding radioimmunoassay (RIA): comparison between IgG and IgG4 antibodies to food and inhaled antigens in adult atopic dermatitis after desensitization treatment and during development of antibody responses in children. *J Allergy Clin Immunol*. (1987) 80:622–30. doi: 10.1016/0091-6749(87)90017-0

36. Wallace ZS, Naden RP, Chari S, Choi HK, Della-Torre E, Dicaire JF, et al. Members of the ACR/EULAR IgG4-RD classification criteria working group. The 2019 American college of rheumatology/European league against rheumatism classification criteria for IgG4-related disease. *Ann Rheum Dis*. (2020) 79:77–87. doi: 10.1136/annrheumdis-2019-216561

37. Yu KH, Chan TM, Tsai PH, Chen CH, Chang PY. Diagnostic performance of serum IgG4 levels in patients with IgG4-related disease. *Med (Baltimore)*. (2015) 94:e1707. doi: 10.1097/MD.0000000000001707

38. Ebbo M, Grados A, Bernit E, Vély F, Boucraut J, Harlé JR, et al. Pathologies associated with serum IgG4 elevation. *Int J Rheumatol*. (2012) 2012:602809. doi: 10.1155/2012/602809

39. Carruthers M, Khosroshahi A, Augustin T, Deshpande V, Stone JH. The diagnostic utility of serum IgG4 concentrations in IgG4-related disease. *Ann Rheum Dis*. (2015) 74:14–8. doi: 10.1136/annrheumdis-2013-204907

40. Wallace ZS, Mattoo H, Carruthers M, Mahajan VS, Della-Torre E, Lee H, et al. Plasmablasts as a biomarker for IgG4-related disease, independent of serum IgG4 concentrations. *Ann Rheum Dis*. (2015) 74:190–5. doi: 10.1136/annrheumdis-2014-205233

41. Ogawa Y, Takeuchi T, Tsubota K. Autoimmune epithelitis and chronic inflammation in Sjögren's syndrome-related dry eye disease. *Int J Mol Sci*. (2021) 22:11820. doi: 10.3390/ijms222111820

42. Del Papa N, Minniti A, Lorini M, Carbonelli V, Maglione W, Pignataro F, et al. The role of interferons in the pathogenesis of Sjögren's syndrome and future therapeutic perspectives. *Biomolecules*. (2021) 11:251. doi: 10.3390/biom11020251

43. Smulski CR, Eibel H. BAFF and BAFF-receptor in B cell selection and survival. *Front Immunol*. (2018) 9:2285. doi: 10.3389/fimmu.2018.02285

44. Goules AV, Tzioufas AG. Primary Sjögren's syndrome: clinical phenotypes, outcome and the development of biomarkers. *Immunol Res*. (2017) 65:331–44. doi: 10.1007/s12026-016-8844-4

45. Lerner MR, Boyle JA, Hardin JA, Steitz JA. Two novel classes of small ribonucleoproteins detected by antibodies associated with lupus erythematosus. *Science*. (1981) 211:400–2. doi: 10.1126/science.6164096

46. Oke V, Wahren-Herlenius M. The immunobiology of Ro52 (TRIM21) in autoimmunity: a critical review. *J Autoimmun*. (2012) 39:77–82. doi: 10.1016/j.jaut.2012.01.014

47. Shiboski CH, Shiboski SC, Seror R, Criswell LA, Labetoulle M, Lietman TM, et al. 2016 American college of rheumatology/European league against rheumatism classification criteria for primary Sjögren's syndrome: A consensus and data-driven methodology involving three international patient cohorts. *Arthritis Rheumatol*. (2017) 69:35–45. doi: 10.1002/art.39859

48. Whitcher JP, Shiboski CH, Shiboski SC, Heidenreich AM, Kitagawa K, Zhang S, et al. A simplified quantitative method for assessing keratoconjunctivitis sicca from the Sjögren's Syndrome International Registry. *Am J Ophthalmol*. (2010) 149:405–15. doi: 10.1016/j.ajo.2009.09.013

49. Mahajan VS, Mattoo H, Deshpande V, Pillai SS, Stone JH. IgG4-related disease. *Annu Rev Pathol*. (2014) 9:315–47. doi: 10.1146/annurev-pathol-012513-104708

50. Platts-Mills TAE, Keshavarz B, Wilson JM, Li RC, Heymann PW, Gold DR, et al. An overview of the relevance of IgG4 antibodies in allergic disease with a focus on food allergens. *Children (Basel)*. (2021) 8:418. doi: 10.3390/children8050418

51. Carbone G, Wilson A, Diehl SA, Bunn J, Cooper SM, Rincon M. Interleukin-6 receptor blockade selectively reduces IL-21 production by CD4 T cells and IgG4 autoantibodies in rheumatoid arthritis. *Int J Biol Sci*. (2013) 9:279–88. doi: 10.7150/ijbs.5996

52. Sakthiswary R, Shaharir SS, Wahab AA. Frequency and clinical significance of elevated IgG4 in rheumatoid arthritis: A systematic review. *Biomedicines*. (2022) 10:558. doi: 10.3390/biomedicines10030558

53. Kiyama K, Yoshifuji H, Kandou T, Hosono Y, Kitagori K, Nakashima R, et al. Screening for IgG4-type anti-nuclear antibodies in IgG4-related disease. *BMC Musculoskelet Disord*. (2015) 16:129. doi: 10.1186/s12891-015-0584-4

54. Demirci H, Polat Z, Ozturk K, Kekilli M, Kantarcioglu M, Sahiner F, et al. The degree of mucosal damage to the small intestine and serum immunoglobulin G4 levels correlate with celiac disease. *Eur J Gastroenterol Hepatol*. (2015) 27:781–4. doi: 10.1097/MEG.0000000000000362

55. Bi Y, Su J, Zhou S, Zhao Y, Zhang Y, Zhang H, et al. Distinct impact of IgG subclass on autoantibody pathogenicity in different IgG4-mediated diseases. *Elife*. (2022) 11:e76223. doi: 10.7554/eLife.76223

56. Koneczny I. Update on IgG4-mediated autoimmune diseases: New insights and new family members. *Autoimmun Rev*. (2020) 19(10):102646. doi: 10.1016/j.autrev.2020.102646

57. Huijbers MG, Querol LA, Niks EH, Plomp JJ, van der Maarel SM, Graus F, et al. The expanding field of IgG4-mediated neurological autoimmune disorders. *Eur J Neurol*. (2015) 22:1151–61. doi: 10.1111/ene.12758

58. Dalakas MC. Autoimmune neurological disorders with IgG4 antibodies: a distinct disease spectrum with unique IgG4 functions responding to anti-B cell therapies. *Neurotherapeutics*. (2022) 19:741–52. doi: 10.1007/s13311-022-01210-1

59. Fayyaz A, Kurien BT, Scofield RH. Autoantibodies in Sjögren's syndrome. *Rheum Dis Clin North Am*. (2016) 42:419–34. doi: 10.1016/j.rdc.2016.03.002

60. Wahren M, Ringertz NR, Pettersson I. IgM and IgG subclass distribution of human anti-Ro/SSA 60 kDa autoantibodies. *Scandinavian J Immunol*. (1994) 39:179–83. doi: 10.1111/j.1365-3083.1994.tb03357.x

61. Liu Y, Li J. Preferentially immunoglobulin (IgG) subclasses production in primary Sjögren's syndrome patients. *Clin Chem Lab Med (CCLM)*. (2012) 50 (2):345–9. doi: 10.1515/cclm.2011.771

62. Maślińska M, Wojciechowska B, Mańczak M, Kwiatkowska B. Serum immunoglobulin G4 in Sjögren's syndrome: a pilot study. *Rheumatol Int*. (2020) 40:555–61. doi: 10.1007/s00296-020-04529-0

63. Mavragani CP, Fragoulis GE, Rontogianni D, Kanariou M, Moutsopoulos HM. Elevated IgG4 serum levels among primary Sjögren's syndrome patients: do they unmask underlying IgG4-related disease? *Arthritis Care Res (Hoboken)*. (2014) 5:773–7. doi: 10.1002/acr.22216

64. Voulgarelis M, Ziakas PD, Papageorgiou A, Baimpa E, Tzioufas AG, Moutsopoulos HM. Prognosis and outcome of non-Hodgkin lymphoma in primary Sjogren syndrome. *Medicine*. (2012) 91:1–9. doi: 10.1097/MD.0b013e31824125e4

65. Fragkioudaki S, Mavragani CP, Moutsopoulos HM. Predicting the risk for lymphoma development in Sjogren syndrome: An easy tool for clinical use. *Med (Baltimore)*. (2016) 95:25. doi: 10.1097/MD.0000000000003766

66. Tobón GJ, Renaudineau Y, Hillion S, Cornec D, Devauchelle-Pensec V, Youinou P, et al. The Fms-like tyrosine kinase 3 ligand, a mediator of B cell survival, is also a marker of lymphoma in primary Sjögren's syndrome. *Arthritis Rheumatol*. (2010) 1:3447–56. doi: 10.1002/art.27611

67. Wilson KR, Villadangos JA, Mintern JD. Dendritic cell Flt3 - regulation, roles and repercussions for immunotherapy. *Immunol Cell Biol*. (2021) 99:962–71. doi: 10.1111/imcb.12484

68. Ramos MI, Tak PP, Lebre MC. Fms-like tyrosine kinase 3 ligand-dependent dendritic cells in autoimmune inflammation. *Autoimmun Rev*. (2014) 2:117–24. doi: 10.1016/j.autrev.2013.09.010

69. Bledsoe JR, Wallace ZS, Stone JH, Deshpande V, Ferry JA. Lymphomas in IgG4-related disease: clinicopathologic features in a Western population. *Virchows Arch*. (2018) 5:839–52. doi: 10.1007/s00428-017-2286-9

70. Chatzis L, Goules AV, Pezoulas V, Baldini C, Gandolfo S, Skopouli FN, et al. A biomarker for lymphoma development in Sjogren's syndrome: Salivary gland focus score. *J Autoimmun*. (2021) 121:102648. doi: 10.1016/j.jaut.2021.102648

71. Alunno A, Leone MC, Giacomelli R, Gerli R, Carubbi F. Lymphoma and lymphomagenesis in primary Sjögren's syndrome. *Front Med (Lausanne)*. (2018) 5:102. doi: 10.3389/fmed.2018.00102

72. Guinee DG Jr., Franks TJ, Gerbino AJ, Murakami SS, Acree SC, Kross MI. Pulmonary nodular lymphoid hyperplasia (pulmonary pseudolymphoma): the significance of increased numbers of IgG4-positive plasma cells. *Am J Surg Pathol*. (2010) 34:1812–9. doi: 10.1097/PAS.0b013e318282d0fa

73. Nishimura Y, Wien EA, Nishimura MF, Nishikori A, Sato Y, Otsuka F. Clinical characteristics and outcomes of IgG4-positive marginal zone lymphoma: Systematic scoping review. *Pathol Int*. (2022) 72:361–70. doi: 10.1111/pin.13251

74. Yachoui R, Leon C, Sitwala K, Kreidy M. Pulmonary MALT lymphoma in patients with Sjögren's syndrome. *Clin Med Res*. (2017) 15:6–12. doi: 10.3121/cmr.2017.1341e3766

75. Mole EN, Papadakos VT, Sfontouris CI. Bronchus-associated lymphoid tissue lymphoma (BALT) in a patient with primary Sjögren's syndrome. *Mediterr J Rheumatol*. (2017) 28:52–6. doi: 10.31138/mjr.28.1.52

76. Yu T, Wu Y, Liu J, Zhuang Y, Jin X, Wang L. The risk of Malignancy in patients with IgG4-related disease: a systematic review and meta-analysis. *Arthritis Res Ther*. (2022) 24:14. doi: 10.1186/s13075-021-02652-2

77. Liu Y, Fu J, Ning X, Li H, Ma X, Wang K, et al. Malignancy risk of immunoglobin G4-related disease: evidence from a large cohort multicenter retrospective study. *Rheumatol Ther*. (2021) 8:1207–21. doi: 10.1007/s40744-021-00326-8

78. Tang H, Yang H, Zhang P, Wu D, Zhang S, Zho J, et al. Malignancy and IgG4-related disease: the incidence, related factors and prognosis from a prospective cohort study in China. *Sci Rep*. (2020) 10:4910. doi: 10.1038/s41598-020-61585-z

79. Nakayama R, Matsumoto Y, Horiike S, Kobayashi S, Nakao R, Nagoshi H, et al. Close pathogenetic relationship between ocular immunoglobulin G4-related disease (IgG4-RD) and ocular adnexal mucosa-associated lymphoid tissue (MALT) lymphoma. *Leuk Lymphoma*. (2014) 55:1198–202. doi: 10.3109/10428194.2013.823494

80. Putra J, Ornstein DL. Küttner tumor: IgG4-related disease of the submandibular gland. *Head Neck Pathol*. (2016) 10:530–2. doi: 10.1007/s12105-016-0729-2

81. Baisya R, Yerram KV, Baby A, Devarasetti PK, Rajasekhar L. Immunoglobulin G4-related lesions in autoimmune diseases: unusual presentations at atypical sites-A tale of 2 cases with literature review. *Eur J Rheumatol*. (2023) 10:169–75. doi: 10.5152/eurjrheum.2023.23052

82. Kim D, Kim SH, Kim EH. Intracranial tumors associated with IgG4-related disease. *Brain Tumor Res Treat*. (2021) 2:93–9. doi: 10.14791/btrt.2021.9.e17

Frontiers in Immunology

Explores novel approaches and diagnoses to treat immune disorders.

The official journal of the International Union of Immunological Societies (IUIS) and the most cited in its field, leading the way for research across basic, translational and clinical immunology.

Discover the latest Research Topics

See more →

Frontiers

Avenue du Tribunal-Fédéral 34
1005 Lausanne, Switzerland
frontiersin.org

Contact us

+41 (0)21 510 17 00
frontiersin.org/about/contact